2015

Assessing the effects of long-term ocean acidification on benthic communities at CO2 seeps

Baggini, Cecilia

http://hdl.handle.net/10026.1/3321

http://dx.doi.org/10.24382/3890
Plymouth University

ASSESSING THE EFFECTS OF LONG-TERM OCEAN ACIDIFICATION ON BENTHIC COMMUNITIES AT CO_2 SEEPS

by

CECILIA BAGGINI

A thesis submitted to Plymouth University and Bremen University in partial fulfilment for the degree of

DOCTOR OF PHILOSOPHY

and

DOCTOR OF SCIENCE (DR. RER. NAT.)

School of Marine Science and Engineering

Marine Biology & Ecology Research Centre (MBERC)

In collaboration with

Hellenic Centre for Marine Research

University of Palermo

November 2014

Assessing the effects of long-term ocean acidification on benthic communities at CO_2 seeps

Cecilia Baggini

Abstract

Ocean acidification has the potential to profoundly affect marine ecosystems before the end of this century, but there are large uncertainties on its effects on temperate benthic communities. Volcanic CO_2 seeps provide an opportunity to examine and improve our understanding of community responses to ocean acidification. In this thesis, two Mediterranean CO_2 seeps (Methana in Greece and Vulcano in Italy) were used to investigate the responses of macroalgae and their epifaunal communities to increased CO_2. Changes in plant-herbivore interactions at elevated CO_2, as well as adaptation potential of dominant macroalgae and responses of macroalgae and epifauna to concurrent exposure to elevated CO_2 and copper pollution, were also examined. Firstly, I determined that volcanic seeps off Methana (Greece) are suitable for ocean acidification studies as they do not have confounding gradients in temperature, salinity, total alkalinity, nutrients, hydrogen sulphide, heavy metals or wave exposure. Calcifying macroalgae abundance decreased as CO_2 increased both at Methana and at Vulcano, while fucoid algae seemed to benefit from elevated pCO_2 levels. Seasonality greatly affected macroalgal responses to increasing CO_2, according to the annual cycles of dominant species. Epifaunal communities of dominant fucoid algae changed at elevated pCO_2 as well, with calcifying invertebrates decreasing and polychaetes increasing near the seeps. Herbivore control of macroalgal biomass did not greatly change at elevated pCO_2 levels, as limpets had a minor role in controlling macroalgal biomass off

Vulcano (Italy) and sea urchins were replaced by herbivorous fish near seeps off Methana. The two macroalgal species examined for signs of long-term acclimatisation (*Cystoseira corniculata* (Turner) Zanardini and *Jania rubens* (Linnaeus) J.V.Lamouroux) to ocean acidification using reciprocal transplants did not appear to have permanently acclimatised to elevated pCO_2 levels, but changed their physiology in four to nine months depending on the local environment. Furthermore, when exposed to a 36-hour copper pulse at elevated pCO_2 levels both seaweed species accumulated more copper in their tissues compared to those exposed to copper in reference pCO_2 conditions, and this resulted in altered epifaunal assemblages on *C. corniculata*. These observations suggest that benthic communities will significantly change as CO_2 levels increase, and that long-term acclimatisation is not likely to play a significant role; this would have profound consequences for benthic ecosystems and the services they provide.

Untersuchungen zu den Langzeiteffekten der Ozeanversauerung auf benthische Lebensgemeinschaften an natürlichen CO_2-Quellen

Cecilia Baggini

Zusammenfassung

Ozeanversauerung hat das Potenzial, Meeresökosysteme noch vor dem Ende dieses Jahrhunderts nachhaltig zu verändern. Große Unsicherheiten gibt es allerdings bislang über die Auswirkungen auf Benthosgemeinschaften der gemäßigten Breiten. Natürliche vulkanische CO_2-Quellen bieten die Möglichkeit, unser Verständnis der Reaktionen natürlicher Lebensgemeinschaften auf die Versauerung der Ozeane zu erweitern. In dieser Arbeit wurden zwei Standorte natürlicher CO_2-Quellen im Mittelmeer CO_2 untersucht (Methana in Griechenland und Vulcano in Italien), um die Reaktionen von Makroalgen und deren Aufwuchsgemeinschaften auf erhöhte CO_2-Konzentrationen zu untersuchen. Veränderungen von Pflanze/Herbivor-Wechselwirkungen bei erhöhtem CO_2, sowie das Anpassungspotential von dominanten Makroalgen und die Reaktionen von Makroalgen und Epifauna auf die gleichzeitige Exposition unter erhöhtem CO_2 und Kupferverschmutzung wurden erfasst. Zunächst stellte ich fest, dass die natürlichen CO_2-Quellen vor Methana (Griechenland) gut für Versauerungsstudien geeignet sind, da sie nicht wesentlich durch zusätzliche Schwankungen in der Temperatur, im Salz- und Gesamtalkaligehalt, in der Nährstoffverfügbarkeit, im Gehalt von Schwefelwasserstoff und Schwermetallen oder der Wellenexposition beeinflusst sind. An beiden Standorten verringerte sich die Abundanz kalkbildender Makroalgen mit zunehmender CO_2-Konzentration, während fucoide Algen von

einem erhöhten pCO_2 profitierten. Abhängig von den spezifischen Jahreszyklen der jeweils dominanten Arten wurde ein starker saisonaler Einfluss auf die Reaktionen von Makroalgen auf steigende CO_2-Konzentrationen ermittelt. Die Epifauna-Gemeinschaften auf dominanten fucoiden Algen veränderten sich ebenfalls mit steigendem pCO_2, indem die Abundanz kalkbildender Wirbelloser abnahm und Polychaeten in der Nähe der Quellen zunahmen. Die Kontrolle der Großalgen-Biomasse durch Herbivore veränderte sich bei erhöhtem pCO_2 nur unwesentlich: Napfschnecken spielten eine untergeordnete Rolle bei der Kontrolle der Makroalgenbiomasse vor Vulcano (Italien) und am Standort Methana wurden in der Nähe der CO_2-Quellen Seeigel durch herbivore Fische ersetzt. Die beiden Markoalgen-Arten (*Cystoseira corniculata* (Turner) Zanardini und *Jania rubens* (Linnaeus) J.V.Lamouroux), welche mittels reziproker Transplantationen auf Anzeichen langfristiger Anpassungen an Ozeanversauerung untersucht wurden, scheinen sich nicht genetisch an den erhöhten pCO_2 angepasst zu haben, aber änderten ihre Physiologie innerhalb weniger Monate in Abhängigkeit von der lokalen Umgebung. Eine zusätzliche 36-stündige Kupferexposition bei erhöhtem pCO_2 führte in beiden Algenarten zur verstärkten Akkumulation von Kupfer im Gewebe im Vergleich zu den Kontrollbedingungen unter normalem pCO_2. Dieser zusätzliche Faktor führte zu einer Veränderung der Epifauna-Gemeinschaft von *C. corniculata.* Diese Beobachtungen legen nahe, dass sich benthische Lebensgemeinschaften bei einem Anstieg des CO_2-Niveaus deutlich verändern, und dass eine genetische Anpassung vermutlich nicht erfolgt. Daraus könnten sich weitreichende Folgen für benthische Ökosysteme und ihre Dienstleistungen ergeben.

Contents:

List of Figures

List of Tables

Acknowledgements

I would like to thank my supervisory team, Prof. Jason Hall-Spencer, Prof. Kai Bischof, Dr Marco Milazzo, Dr Antonella Pancucci-Papadopoulou and Dr Eva Krasakopoulou, who all helped with this thesis according to their expertise.

I am immensely grateful for all the help I have received during fieldwork, especially from Alessio Deidda, who travelled to Italy and Greece to help me in most of my sampling trip. I also received great help from Maria Salomidi, Laura Bray, Emanuela Voutsinas, Yiannis Issaris and Eva Krasakopoulou from the Hellenic Centre for Marine Research during fieldwork at Methana and from Mariagrazia Graziano, Marco Milazzo, Giuseppe Bruno and Laura Ciriminna at Vulcano. I would also like to thank Kai Bischof for generously loaning me his Diving PAM.

I am extremely grateful to the staff from Bremen University and the Leibniz Center for Tropical Marine Ecology, especially Laurie Hofmann and Mirta Teichberg, for the very enjoyable collaboration and the training during my visit in Bremen. Many people at the Hellenic Centre for Marine Research have helped me in the laboratory analysis, and I especially want to thank Louisa Giannoudi, Alexandra Pavlidou and Eleni Rouselaki. Antonella Pancucci-Papadopoulou from HCMR and Renato Chemello and Annamaria Mannino from University of Palermo greatly helped me to identify invertebrates and macroalgae.

I would also like to thank everyone at the Marine Biology and Ecology Research Centre at Plymouth University for their help during the last three years, especially Balbina Ramsay and Laura Pettit for the precious company during countless hours of microscopy work, and Andy Foggo and Richard Billington for their help with phenols analysis.

AUTHOR'S DECLARATION

At no time during the registration for the degree of Doctor of Philosophy has the author been registered for any other University award without prior agreement of the Graduate Committee. Work submitted for this research degree at the Plymouth University has not formed part of any other degree either at Plymouth University or at another establishment.

This study was financed with the aid of a studentship from the Joint Doctorate programme MARES selected under Erasmus Mundus coordinated by Ghent University (FPA 2011-0016) and carried out in collaboration with Bremen University, University of Palermo and the Hellenic Centre for Marine Research. Additional funding was granted by the EU FP7 project 'Mediterranean Sea Acidification under a changing climate' (grant agreement no. 265103) to fund part of the fieldwork, the EU FP7 European Project on OCean Acidification (EPOCA) funded a research training visit to Bremen University and the British Ecological Society, Plymouth Marine Science and Education Foundation and Plymouth Marine Institute granted me travel bursaries to attend international conferences.

Relevant scientific seminars and conferences were regularly attended at which work was often presented; work from this project and collaborations established during this period lead to a number of publications:

- **C. Baggini**, Y. Issaris, M. Salomidi, J.M. Hall-Spencer (2014). Herbivore diversity improves benthic community resilience to ocean acidification. *Journal of Experimental Marine Biology and Ecology* (accepted pending revisions).

- **C. Baggini**, M. Salomidi, E. Voutsinas, L. Bray, E. Krasakopoulou, J.M. Hall-Spencer (2014). Seasonality affects macroalgal community response to increases in pCO_2. *PLoS ONE*, 9: e106520.
- L.C. Hofmann, K. Bischof, **C. Baggini**, A. Johnson, K. Koop-Jakobsen, M. Teichberg (2014). CO_2 and inorganic nutrient enrichment affect the performance and competitive strength of a calcifying green alga and its non-calcifying epiphyte. *Oecologia* (accepted pending revisions).
- G. Langer., G. Nehrke, **C. Baggini**, R. Rodolfo-Metalpa, J.M. Hall-Spencer, J. Bijma (2014). Limpets counteract ocean acidification induced shell corrosion by thickening of aragonitic shell layers. *Biogeosciences Discussions*, 11: 12571-12590.
- P. Calosi, S.P.S. Rastrick, M. Graziano, S.C. Thomas, **C. Baggini**, H.A. Carter, J. Hall-Spencer, M. Milazzo, J.I. Spicer (2012). Ecophysiology of sea urchins living near shallow water CO_2 vents: Investigations of acid-base balance and ionic regulation using *in-situ* transplantation. *Marine Pollution Bulletin*, 73: 470-484.
- S. Hahn, R. Rodolfo-Metalpa, E. Griesshaber, W.W. Schmahl, D. Buhl, J.M. Hall-Spencer, **C. Baggini**, K.T. Fehr, A. Immenhauser (2012). Marine bivalve shell geochemistry and ultrastructure from modern low pH environments: environmental effect versus experimental bias. *Biogeosciences*, 9: 1897-1914.

Presentations at conferences:

- Using CO_2 vents as a natural analogue for ocean acidification (2011). Oral presentation, 4th Annual Plymouth Marine Science Conference, Plymouth, UK.

- Effects of ocean acidification on *Mytilus galloprovincialis* and *Patella caerulea* at natural CO_2 vents (2012).Poster presentation, Third Symposium on the ocean in a high CO_2 world, Monterrey, California.
- Effects of short-term copper exposure on seaweeds acclimatised to high CO_2 (2013). Pollution Responses in Marine Organisms symposium, Faro, Portugal.
- Greek CO_2 vents show community effects of ocean acidification in the oligotrophic Aegean Sea (2013). INTECOL, London, UK.

List of research chapters and declaration of own contribution

Chapters 2 and 3: the same contributions apply to both chapters

Chapter 2: Assessing the suitability of a volcanic seep area off Methana (Greece) for ocean acidification studies

Chapter 3: Changes in subtidal macroalgal communities along pCO_2 gradients at Mediterranean volcanic seeps

Contributors: Cecilia Baggini, Maria Salomidi, Emanuela Voutsinas, Laura Bray, Eva Krasakopoulou, Jason M. Hall-Spencer

Contributions: I designed and performed the sampling with help from MS, EV, LB and EK; I analysed all samples with help from EK, performed statistical analyses and wrote the manuscript with help from all authors; JMH-S supervised the thesis.

Chapter 4: Canopy algal epifauna changes at elevated pCO_2 at two Mediterranean volcanic seeps

Contributors: Cecilia Baggini, Renato Chemello, Marco Milazzo, Mariagrazia Graziano, Antonella Pancucci-Papadopoulou, Laura Ciriminna, Jason Hall-Spencer

Contributions: I designed the experiment with help from MG, RC and MM, and performed the sampling with help from LC, who also helped processing the samples; I identified all invertebrates with help from RC and AP, performed statistical analyses and wrote the manuscript; JMH-S supervised the thesis.

Chapter 5: Effect of herbivores on benthic communities at different pCO_2 levels

Contributors: Cecilia Baggini, Mariagrazia Graziano, Marco Milazzo, Maria Salomidi, Yiannis Issaris, Marco Franzitta, Giuseppe Bruno, Jason Hall-Spencer

Contributions: I designed the experiment with help from MG and MM, and performed the sampling with help from MM, GB, MS and YI; I processed all samples with help from MF, performed statistical analyses and wrote the manuscript with help from all co-authors; JMH-S supervised the thesis.

Chapters 6 and 7: the same contributions apply to both chapters

Chapter 6: Seaweed acclimatisation to high pCO_2 at volcanic seeps

Chapter 7: A short-term copper pulse affects macroalgal copper accumulation and indirectly alters epifaunal colonisation at elevated pCO_2

Contributors: Cecilia Baggini, Kai Bischof, Murray Brown, Jason Hall-Spencer

Contributions: I designed the experiment with feedback from MB during the transfer process, performed the sampling, processed all samples, performed

statistical analyses and wrote the manuscript; JMH-S and KB supervised the thesis and provided useful feedback on the manuscript.

DECLARATION/ ERKLÄRUNG

Ich erkläre

1. die Arbeit ohne unerlaubte fremde Hilfe angefertigt,
2. keine anderen als die von mir angegebenen Quellen und Hilfsmittel benutzt und
3. die den benutzten Werken wörtlich oder inhaltlich entnommenen Stellen als solche kenntlich gemacht zu haben.

Word count of main body of thesis: 53,331

Signed .....

Date.....

Chapter 1

Community responses to ocean acidification on temperate rocky reefs: possible causes and adaptation potential

1.1 Introduction

Since the beginning of industrial revolution, man has released huge quantities of carbon dioxide to the atmosphere. Atmospheric CO_2 concentrations reached 400 ppmv in April 2014 (NOAA, 2014) and are rising more rapidly than previously thought (Intergovernmental Panel on Climate Change, 2014). This increase is a concern, as atmospheric CO_2 was relatively constant over the last 800.000 years, with values ranging between 172 and 300 ppmv (Lüthi *et al.*, 2008). About one fourth of anthropogenic CO_2 emissions has been absorbed by the oceans, thereby reducing their effects in the atmosphere (Le Quéré *et al.*, 2009), but at the same time increasing the carbon dioxide concentration in seawater. A trend in increasing surface ocean pCO_2 parallel to the increase in atmospheric carbon dioxide is clearly detectable using long-term monitoring stations (Brewer *et al.*, 1997; Hofmann *et al.*, 2011).

Increased seawater pCO_2 causes changes in the ocean carbonate system, a process referred to as 'ocean acidification' (Caldeira and Wickett, 2003). When carbon dioxide dissolves in water it forms carbonic acid (H_2CO_3), a weak acid that is highly unstable in seawater (1). H_2CO_3 readily dissociates to form bicarbonate ions (HCO_3^-) and hydrogen ions (2). Bicarbonate ions can in turn dissociate to produce carbonate ions (CO_3^{2-}) and hydrogen ions. However, increased $[H^+]$ causes reaction (3) to reverse and bicarbonate ions to become more stable in seawater.

$$CO_2 + H_2O \leftrightarrow H_2CO_3 \qquad (1)$$

$$H_2CO_3 \leftrightarrow HCO_3^- + H^+ \qquad (2)$$

$$HCO_3^- \leftrightarrow CO_3^{2-} + H^+ \qquad (3)$$

Overall, ocean acidification causes a decrease in seawater pH (i.e. an increase in $[H^+]$) and carbonate ion concentration and an increase in aqueous CO_2 ($CO_{2(aq)}$), dissolved inorganic carbon and $[HCO_3^-]$, with total alkalinity remaining constant. Decreased carbonate ion concentrations are leading to lower calcium carbonate saturation state (Ω_{CaCO3}) in the world oceans, meaning that $CaCO_3$ is becoming more likely to dissolve. This happens because $[CO_3^{2-}]$ is one of the determinants of calcium carbonate saturation, as shown in equation (4).

$$\Omega_{CaCO3} = [Ca^{2+}]\,[CO_3^{2-}] / K^*_{sp} \qquad (4)$$

There are two forms of calcium carbonate: aragonite and calcite. These have different solubility product constants (K^*_{sp}) and thus different solubility, with aragonite being less stable than calcite in seawater (Tyrrell, 2008). A third form of calcium carbonate, high-magnesium calcite, forms the carbonic skeleton of some organisms and is even more soluble than aragonite. K^*_{sp} varies with pressure and temperature, making calcium carbonate more likely to dissolve at low temperatures and high pressure. Deep polar waters are already undersaturated (i.e. $\Omega_{CaCO3} < 1$) with respect to aragonite, whereas superficial waters are predicted to become undersaturated in the next decades (Orr *et al.*, 2005; Steinacher *et al.*, 2009; Tittensor *et al.*, 2010).

With regards to the global ocean, mean pH has already decreased from ~8.2 to ~8.1 compared to pre-industrial times (Key *et al.*, 2004), probably the lowest value in the last two million years (Hönisch *et al.*, 2009). A further decrease of approximately 0.4 units is projected for the end of this century according to the “business as usual” scenario (Caldeira and Wickett, 2003), which underestimates the present rate of anthropogenic CO_2 release into the atmosphere (IPCC, 2014). For the year 2300, different emission scenarios

depend on improvements in fossil fuel extraction techniques. In the “business as usual” scenario, the mean ocean pH is predicted to reach a value of 7.4, but if mining techniques improve the subsequent increase in anthropogenic emissions could lead to a mean ocean pH of 7.1. Moreover, methane hydrate exploitation could cause ocean pH to reach a minimum of 6.8 (Caldeira and Wickett, 2005). The predicted changes in seawater carbonate chemistry are illustrated in Figure 1.1; these changes will not be permanent, because increased dissolution of deep-sea carbonate sediments and weathering on land will eventually buffer them. Carbonate dissolution from rocks and sediments, however, takes thousands of years to equilibrate the ocean carbonate system (Caldeira and Wickett, 2003), whereas current rates of increase in atmospheric carbon dioxide are already causing dramatic changes in the ocean carbonate chemistry.

In Earth’s geological history, changes in seawater pCO_2 occurred more slowly than today, allowing weathering and sediment carbonate dissolution to raise carbonate saturation states. Therefore, care should be taken when comparing current changes in carbonate chemistry with those geological periods in the past that had high pCO_2. Only periods with a similar rate and magnitude of change can help us predict the long-term effects of ocean acidification. In order to identify relevant episodes, it is necessary to reconstruct at least two seawater carbonate parameters, as high carbon dioxide concentration in seawater does not imply a low calcium carbonate saturation state (Zeebe and Ridgwell, 2011). An example is the Cretaceous, when very high seawater pCO_2 was combined with high saturation state of calcium carbonate. This combination of factors was due to the slower increase of carbon dioxide compared to the current rates of increase and the fact that high concentrations of carbon dioxide were

maintained for millions of years. When changes in marine carbonate chemistry occur at these timescales, they can be buffered by dissolution of carbonate sediments. This situation had thus a lower potential to affect biological calcification than ocean acidification (Zeebe and Westbroek, 2003; Ridgwell and Schmidt, 2010).

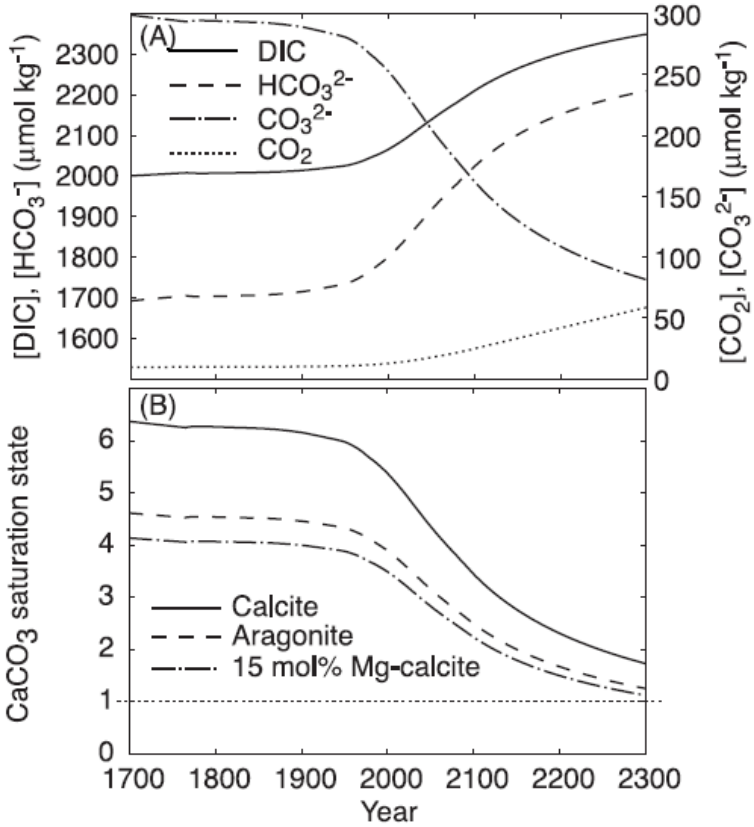

Figure 1.1. Surface water dissolved inorganic carbon chemistry between 1700 and 2300 calculated using a shallow-water ocean carbonate model at 25°C and 35 psu. (A) Total dissolved inorganic carbon concentration [DIC], [CO_2], [HCO_3^-], and [CO_3^{2-}], and (B) surface water saturation state with respect to calcite, aragonite and 15 mol % magnesian calcite (Andersson *et al.,* 2005).

Suitable past ocean acidification analogues are periods of rapid (i.e. less than 10000 years) increase in seawater pCO_2, which would give no time for compensatory mechanisms to act. The best analogue for ocean acidification

with good geological records is probably the Paleocene-Eocene Thermal Maximum (PETM, ~55.8 million years ago). In this period a temperature increase of 5-9°C over a few thousand years was coupled with massive carbon release. The subsequent decline in seawater pH and $CaCO_3$ saturation state is similar to ocean acidification in many aspects, albeit rates of change were still slower than the current ones (Zachos *et al.*, 2005). This event did not appear to have significant effects on superficial nanoplankton (Gibbs *et al.*, 2006), but it caused a dramatic decrease in benthic foraminifera species (e.g. Thomas, 2007) and sediment fauna in general (Rodriguez-Tovar *et al.*, 2011). It is not clear, however, if extinctions were caused by changes in carbonate chemistry, oxygen reduction or temperature increase, although it could have been a combination of the above. All things considered, it seems that ocean acidification is an unprecedented phenomenon in our planet's history (Zeebe and Ridgwell, 2011).

Anthropogenic emissions are currently causing rapid changes in ocean carbonate chemistry that are well known and understood (Doney *et al.*, 2009; Orr, 2011), but ocean acidification also has the potential to affect various physical, biogeochemical and biological processes. Predictions of how these processes will respond to an increase in seawater pCO_2 are much less certain, and are an urgent priority for future research (Gattuso *et al.*, 2011). Ocean acidification can affect nutrient availability (Raven *et al.*, 2005; Doney *et al.*, 2009; Hutchins *et al.*, 2009) and trace metal speciation (Raven *et al.*, 2005; Tyrrell, 2008; Doney *et al.*, 2009; Millero *et al.*, 2009; Breitbarth *et al.*, 2010; Shi *et al.*, 2010), as well as sound wave diffusion through seawater (Hester *et al.*, 2008; Brewer and Hester, 2009). Furthermore, many biological processes may be affected, including all pH-dependent physiological functions (e.g. acid-base balance, protein activity) and those processes that use a carbon species as

substrate (e.g. photosynthesis, calcification) (Fabry *et al.*, 2008). Ocean acidification is then likely to affect benthic communities, but their responses are hard to predict because interspecific interactions can cause unexpected changes at the community level (Hale *et al.*, 2011)

1.2 Community effects of ocean acidification on temperate rocky reefs

Laboratory experiments assessing responses to increased CO_2 determine species' relative sensitivities to high CO_2. They can also reveal threshold tolerance values as well as physiological mechanisms involved in biological responses to ocean acidification. It is difficult, however, to scale up from such studies and predict how whole ecosystems will change as our oceans continue to acidify; this approach does not consider interactions between species, which dramatically influence community structure (Kroeker *et al.*, 2013a). Furthermore, the artificial conditions in a laboratory are probably very stressful for some taxa, and this could alter results (Widdicombe *et al.*, 2010).

Consequently, researchers have begun studying ocean acidification effects on community structure using mesocosm experiments. The need to test results obtained in laboratory conditions with simplified communities, however, has also led researchers to manipulate pCO_2 in the field or study areas with naturally high CO_2 concentrations. Such data are being used to develop models to predict how ecosystems will change as seawater carbon dioxide continues to increase.

1.2.1 Laboratory and mesocosm experiments

A community composed of long-lived organisms usually does not change its composition at the timescale of most laboratory and mesocosm experiments (i.e. days to months, rarely years). Therefore, only responses of single species and their interactions to increased pCO_2 can be observed using this approach. In this context, coral reef ecosystems are the most studied: mesocosm experiments lasting up to ten months reported a decrease in coral and coralline algae calcification and growth (Jokiel *et al.*, 2008; Küffner *et al.*, 2008), sometimes leading to net community $CaCO_3$ loss at low pH (Andersson *et al.*, 2009).

Temperate communities are much less studied, but there is evidence that ocean acidification will cause changes here as well. Macroalgal species show differential sensitivity to increased CO_2; for instance, cover of the calcifying alga *Corallina officinalis* decreased, whereas the non-calcifying *Chondrus crispus* was more abundant as CO_2 increased (Hofmann *et al.*, 2012). Biomass and productivity decreased with increased CO_2 and temperature in communities associated with canopy-forming brown algae, but the invasive *Sargassum muticum* resulted more resistant to both stressors than the native *Cystoseira tamariscifolia* (Olabarria *et al.*, 2013). Community changes are therefore likely even when the dominant species are not calcifiers.

Some macroalgal species seem to be advantaged at elevated CO_2 because they are carbon-limited (Harley *et al.*, 2012). For instance, some turf algae have the potential of outcompeting kelp on Australian rocky shores when CO_2 and nutrients concurrently increase (Falkenberg *et al.*, 2013a). Shading from kelp,

however, reduces turf growth, meaning that a shift from kelp to turf algae is only likely if kelp cover is reduced by other stressors (Falkenberg *et al.*, 2012).

Invertebrate communities have been shown to change as well: for instance, Hale *et al.* (2011) found that organisms associated with turf algae generally reacted to increased pCO_2 consistently with predictions from single species experiments. However, reduced predation rates and competition for space caused nematode abundance to increase unexpectedly. These communities change from being dominated by calcareous organisms to being dominated by non-calcareous organisms at a pH between 7.2 and 7.8 (Christen *et al.*, 2013).

1.2.2 Field pCO_2 manipulation

In recent years, various techniques to increase seawater pCO_2 in the field have been developed for the study of whole communities in their natural environment. In Chesapeake Bay (USA), CO_2 bubbling in open waters was used to assess changes in marine plants chemical defences (Arnold *et al.*, 2012). While this method allows for natural flow conditions, pCO_2 varies with current speed and direction.

Seawater mixed with CO_2 can also be injected into open chambers to better control carbonate chemistry variability while reproducing natural water movement (Campbell and Fourqurean, 2011). This system has been used to test the effects of ocean acidification on the seagrass *Thalassia testudinum*: its growth was not affected by elevated CO_2, whereas nitrogen and phosphorous content significantly decreased with increased CO_2 (Campbell and Fourqurean, 2013). Seagrass epiphytes were more affected by increased CO_2 than by increased nutrients, with calcifying species being substituted by fleshy species (Campbell and Fourqurean, 2014).

A similar system, which uses closed or semi-enclosed chambers, is the Free Ocean Carbon Enrichment system (FOCE); similarly to the previous one, this system can be used to run long term experiments with entire communities exposed to natural levels of light, nutrients and temperature (Waz *et al.*, 2007; Kline *et al.*, 2012). FOCE systems have been successfully used in Australia, where pH was lowered by 0.4 units and dissolution of coralline algae increased at high CO_2 during a short-term experiment (Kline *et al.*, 2012). FOCE systems may be used to assess the effects of ocean acidification on many ecological processes, but are too small to influence some ecosystem properties, such as population connectivity or larval recruitment. So far, no results are available from temperate FOCE systems, even though experiments are being conducted in the Mediterranean Sea using eFOCE (European FOCE) and a shallow water FOCE (swFOCE) system is under development in California (Gattuso *et al.*, 2014).

1.2.3 Areas with naturally elevated pCO_2

Areas with naturally high CO_2 can be used to assess long-term community responses to ocean acidification. Hydrothermal vents are generally characterised by low pH and emit fluids that can contain various gases, especially carbon dioxide, hydrogen sulphide, methane and nitrogen (Tarasov *et al.*, 2005). Increased concentrations of heavy metals in the surrounding sediments are also common (e.g. Dando *et al.*, 2000; Hübner *et al.*, 2004), and macroalgae near such vents can have increased metal concentrations in their tissues (Couto *et al.*, 2010). Vents shallower than 200 m are generally populated by a subset species inhabiting the surrounding area. They are thus very different from deep-sea vents, where chemosynthetic vent-obligated species are abundant (Tarasov *et al.*, 2005).

In shallow areas, usually there is a notable reduction in biodiversity proceeding towards the vents (Melwani and Kim, 2008; Karlen *et al.*, 2010). Here, the most abundant species are those able to resist elevated temperatures and high concentrations of toxic gases and heavy metals. They also have to be resistant to reduced salinity if volcanic emissions are mixed with fresh water (Tarasov *et al.*, 2005). An exception to this trend was reported at vents off Milos (Greece), where sessile macroepibenthos had higher biodiversity near the vents than at the control sites (Morri *et al.*, 1999; Pansini *et al.*, 2000; Bianchi *et al.*, 2011). However, infauna showed an opposite trend, possibly because of the high sulphide concentration in the sediment near the vents (Thiermann *et al.*, 1997). Hot fluid emissions were also indicated as the cause for increased occurrence of warm-water seaweeds near the emissions (De Biasi and Aliani, 2003).

Although many of these areas have high seawater CO_2 concentration, there are very often confounding gradients in temperature, toxic gases, heavy metals or salinity, so their utility to understand community responses to ocean acidification is limited. However, it is possible to find shallow water seeps emitting almost exclusively carbon dioxide without confounding gradients in temperature, salinity, toxic gases and heavy metal contamination. There are only a few published examples of CO_2 seeps at temperate shores used as ocean acidification proxies, such as the two off Italy (Hall-Spencer *et al.*, 2008; Boatta *et al.*, 2013).

There biodiversity, especially that of calcifying taxa, is reduced as pCO_2 increases (Hall-Spencer *et al.* 2008; Martin *et al.*, 2008; Dias *et al.*, 2010; see Figure 1.2) and benthic communities are simpler and more homogeneous as CO_2 increases (Kroeker *et al.*, 2013b). Moreover, shifts in macroalgal dominance along a pCO_2 gradient have been reported (Porzio *et al.*, 2011), and

invertebrate recruitment is heavily influenced as well (Cigliano *et al.*, 2010). Benthic invertebrates also experience a reduction in diversity and biomass, and the community trophic complexity is lower at high CO_2 levels (Kroeker *et al.*, 2011).

Figure 1.2. *Posidonia oceanica* covered in calcareous epiphytes at pH 8.2 at CO_2 vents off Ischia (left) and lacking Corallinaceae at pH 7.6 (right); yellow arrow points to CO_2 bubbles (Hall-Spencer *et al.*, 2008).

Experiments at seeps have revealed different sensitivities of sea urchin species to elevated CO_2: *Paracentrotus lividus*, the main consumer of fleshy algae, is less resistant to elevated carbon dioxide (Calosi *et al.*, 2013a). Changes in herbivore densities have knock-on effects on fleshy macroalgae, such as the calcifying alga *Padina pavonica* (Linnaeus) Thivy. Even though these algae are less calcified at elevated CO_2 levels, their cover in fact increases because they are subject to less herbivore pressure (Johnson *et al.*, 2012). Experiments at seeps can also detect differences in responses to CO_2 as temperature increases: calcification rates in a Mediterranean coral was not affected by pCO_2 in spring, but strongly decreased at elevated CO_2 levels after a very warm summer (Rodolfo-Metalpa *et al.*, 2011).

At volcanic seeps, it is also possible to test differences in ecological processes along pCO_2 gradients. For macroalgal communities, both early recruitment (Porzio *et al.*, 2013) and final community composition after one year (Kroeker *et al.*, 2013c) change greatly with increasing CO_2 due to the direct effects of carbon dioxide and to changes in interspecific interactions. For instance, crustose coralline algae manage to recruit at elevated pCO_2 levels, but their decreased growth rates near the seeps allow fleshy algae to outcompete them (Kroeker *et al.*, 2013c).

Carbon dioxide seeps are proving useful for ocean acidification research because they show us how whole communities change with long-term exposure to high CO_2 levels. They can also be used to test hypotheses developed in laboratory-based experiments. However, seeps are not a perfect reproduction of CO_2-influenced ecosystems, since they are too small to host entire populations. Motile taxa such as fish are not likely to be as heavily influenced by CO_2 as sessile taxa (Riebesell, 2008) and pelagic larvae settling near the seeps can originate from unaffected populations (Cigliano *et al.*, 2010). Moreover, if sites too close to the CO_2 source are chosen, pH can fluctuate rapidly and be very different from what natural ecosystems experience. Hence, care must be taken to select sites appropriately, so that daily and seasonal fluctuations in pH remain as similar as possible to reference sites (Kerrison *et al.*, 2011).

Acidified estuaries are another possibility to study biological responses to ocean acidification in a natural environment. Two types of estuaries have been considered so far, those with high levels of biogenic CO_2 produced by microbial respiration and those exposed to acid sulphate soils runoffs. In the first type pH is lower than in reference estuaries because of increased CO_2 and can cause biological effects such as increased gastropod shell corrosion (Marshall *et al.*,

2008). However, in these areas oxygen levels are generally lower than reference values and nutrients have higher concentrations because of nutrient discharges, potentially confounding the effect of high CO_2 (Mucci *et al.*, 2011). Estuaries can also be subject to acidification episodes if acid sulphate soils are transported by rivers after heavy rainfall events. Although they are not proper ocean acidification analogues, since low pH is episodic and not due to increased CO_2 concentration, hypoxia is not an issue in these sites. Molluscs in these estuaries are less abundant than in control estuaries, although within the natural range of variation reported for that region (Amaral *et al.*, 2011), and mollusc shells are weaker as well (Amaral *et al.*, 2012).

Small-scale analogue systems are very useful to show community effects of ocean acidification, but they cannot be used to assess changes in large scale processes such as population connectivity and larval supply. These processes could be studied in larger high pCO_2 areas, such as upwelling regions, which could be a precious source of information on ecosystems subject to naturally high pCO_2. In temperate regions, undersaturated waters rise from the deep sea along the east coast of USA and Canada and on the Chilean coast (Feely *et al.*, 2008; Mayol *et al.*, 2012). In some cases upwelling waters even penetrate in estuaries, where they have dramatic effects on the pH of waters lacking a carbonate buffer system (Feely *et al.*, 2010). Long-term monitoring of intertidal communities on the Eastern Pacific shores detected a decreased abundance of calcifying organisms when CO_2 is higher (Wootton *et al.*, 2008), and calcifying seaweed epibionts are also less abundant in upwelling areas (Saderne and Wahl, 2013). Elevated CO_2 levels in upwelling waters are compromising oyster aquaculture on eastern US shores (Barton *et al*., 2012) as well as the fitness of other commercial species such as the Atlantic cod (Frommel *et al.*, 2012).

Some calcifying organisms seem to have adapted to the high pCO_2 recorded in upwelling areas: for instance, mussels are dominant in the Kiel fjord, despite being subject to upwelling episodes during their recruitment season (Thomsen *et al.*, 2010). However, at least some of them already live near their tolerance limit, such as sea urchin living on the USA east coast. Although their larval calcification is not impaired in present-day upwelling conditions, larvae are negatively affected by near future conditions (Evans *et al.*, 2013).

Using this approach could improve our understanding of large scale effect of ocean acidification, although with some limitations. In these systems it is often difficult to decide which environmental factor is driving the observed changes, as many factors usually co-vary with seawater CO_2 concentration. For instance, waters off Chile have high pCO_2, but that is correlated with low oxygen concentration, making the effect of these two concurring factors difficult to disentangle and potentially leading to overestimation of high CO_2 negative effects (Mayol *et al.*, 2012). Furthermore, upwelling waters are generally low in temperature and rich in nutrients, whereas climate change scenarios predict opposite trends (Beardall *et al.*, 2009). Lower temperatures and higher food availability compared with future scenarios could reduce the biological effects of high CO_2, thus leading to underestimation of the detrimental effects of ocean acidification (Thomsen *et al.*, 2010; Melzner *et al.*, 2011).

1.2.4 Modelling approach

Integrating results from single organisms and communities on an ecosystem scale could be done using a modelling approach. Models are widely used in climate change research for physical and chemical factors (e.g. Anderssonn *et al.*, 2005; Caldeira and Wickett, 2005; Orr *et al.*, 2005), and models involving

also biological factors are currently being developed. Policy makers need to know how marine ecosystems will react not only to ocean acidification, but to concurrent stressors such as increasing temperature, eutrophication and overfishing (Hilmi *et al.*, 2012). Models predicting ecosystem effects of multiple stressors, however, are more difficult to produce because of the system complexity and data scarcity on many factors, e.g. potential for adaptation (Blackford, 2010).

At the moment, there are only a few studies using models to assess ecosystem effects of ocean acidification, but some work has already been done on coral reefs. For instance, a recent study models the potential reef organisms have to influence carbonate chemistry on a local scale (Anthony *et al.*, 2011a). Their results show that the predicted increase in seaweed dominance could actually help calcification in communities downstream, as macroalgae decrease seawater pCO_2 through photosynthesis. These results are consistent with data from Manzello *et al.* (2012), who reported that seagrass beds in Florida take up carbon dioxide and raise the calcium carbonate saturation experienced by inshore coral reefs to pre-industrial levels, although this effect is seasonal because it depends on seagrass productivity.

Models can also be used to predict how interacting stressors will affect communities; for instance, it has been shown that overfishing and eutrophication will decrease coral reef resilience to ocean acidification and increasing temperature. The reason for this is that corals will be less competitive than macroalgae, which will grow faster and will be favoured by decreased fish grazing (Anthony *et al.*, 2011b). Similar results were obtained using a model to analyse how long-term fisheries exploitation and ocean acidification would interact to affect various functional groups (Griffith *et al.*,

2011). This study showed that increased seawater pCO_2 is likely to influence very heavily overfished areas and cause major regime shifts around 2040. It is already possible to see that although in their infancy, models are a promising approach because they can predict large-scale responses that are difficult to test experimentally.

1.3 Mechanisms driving community changes

Community responses to ocean acidification result from the combination of direct effects of carbon dioxide on single species and indirect effects (i.e. biological interactions). While most ocean acidification research has focused on direct effects of elevated CO_2, there is increasing evidence that indirect effects are extremely important in determining community changes (Alsterberg *et al.*, 2013). In the terrestrial environment, biological interactions have been proven to be more important than direct climate change effects (Ockendon et al., 2014), but there is no such evidence for community responses to ocean acidification.

1.3.1 Changes in organism physiology

Most studies on the biological effects of ocean acidification are laboratory experiments that measure physiological responses, most commonly calcification, of a single species. A recent meta-analysis concluded that overall effects of high pCO_2 on organisms' survival, growth, calcification and reproduction are strong and negative (Kroeker *et al.*, 2013a). Moreover, high CO_2 levels have subtler negative effects, such as those on behaviour (Briffa *et al.*, 2012) and neuroreceptors (Munday *et al.*, 2014). Predictions of future ecosystems conditions are also complicated by high taxonomic variability in biological responses to ocean acidification. For example, Ries *et al.* (2009) measured net calcification rates in 18 animal and algal taxa. Calcification rates

decreased in most species, but a wide range of responses was recorded, from negative to parabolic (i.e. highest calcification rates at intermediate pCO_2 values) to positive.

Responses to ocean acidification will not only vary among taxonomic groups (Kroeker *et al.*, 2013a, see Figure 1.3), but in some cases will be species- (Miller *et al*., 2009), sex- (Holcomb *et al.*, 2011), clone- (Pistevos *et al.*, 2011) or strain-specific (Langer *et al.*, 2009; Hoppe *et al.*, 2011). This high degree of variability in biological responses to ocean acidification has led to conflicting reports: for instance, calcification rates of the coccolithophore *Emiliania huxleyi* have been reported to decrease (De Bodt *et al.*, 2010; Riebesell *et al.*, 2000) or increase (Iglesias-Rodriguez *et al.*, 2008) when exposed to low pH. In the first instance, it was thought that this difference was caused by methodological issues (Iglesias-Rodriguez *et al.*, 2008). However, the two methods used to modify water chemistry in these studies cause very similar changes in the carbonate system (Schulz *et al.*, 2009). Evidence of strain-specific responses was given by Langer *et al.* (2009), and Hoppe *et al.* (2011) confirmed that methodological issues do not cause a variation in *Emiliania huxleyi* responses to ocean acidification.

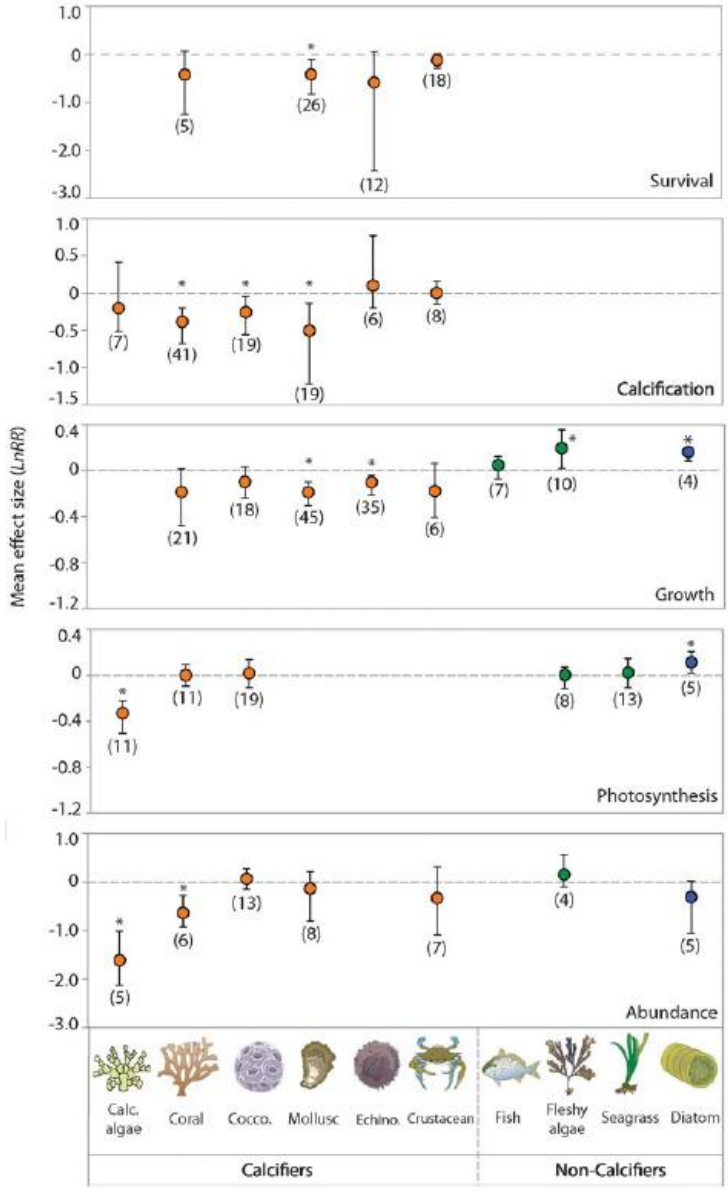

Figure 1.3. Taxonomic variation in effects of ocean acidification. Note the different y-axis scale for growth and photosynthesis. Mean effect size and 95% bias-corrected bootstrapped confidence interval are shown for all organisms combined (overall), calcifiers (orange) and noncalcifiers (green). The calcifiers category includes: calcifying algae, corals, coccolithophores, molluscs, echinoderms and crustaceans. The noncalcifiers category includes: fish, fleshy algae and seagrasses. The number of experiments used to calculate mean effect sizes are shown in parentheses. The mean effect size is significant when the 95% confidence interval does not overlap zero (*); Kroeker *et al.*, 2013a.

Predicting how species and their populations will react to increased CO_2 is complex but necessary if we want to prepare for marine ecosystem changes in the near future. Fortunately, certain traits are proving useful in determining how an organism may respond to ocean acidification. Firstly, very mobile taxa with high metabolic rates usually have efficient mechanisms to regulate pH (Melzner *et al.*, 2009), and are thus likely to be less affected directly by lowered pH compared to non-regulators. A meta-analysis on studies on mobile taxa with good acid-base regulation such as fish and brachyuran crustaceans did not show significant negative responses to high CO_2 levels on survival and growth (Kroeker *et al.*, 2013a), although there is evidence that some tropical fish species have their sensory abilities impaired when carbon dioxide increases (Munday *et al.*, 2014). Negligible effects of elevated CO_2 on growth and calcification were also related to good acid-base regulation in the cephalopod *Sepia officinalis* (Gutowska *et al.*, 2010). In contrast with these results, the giant squid *Dosidicus gigas* has been reported to suffer metabolic depression following short-term exposure to elevated CO_2, possibly because of the very high pH sensitivity of its oxygen-binding pigments (Rosa and Seibel, 2008). Thus, highly pH-sensitive blood pigments insure the rapid oxygen supply necessary to maintain very high metabolic rates, but they could be a disadvantage in a high-CO_2 world if pH regulation is not extremely efficient (Pörtner *et al.*, 2004).

For calcifying organisms, pH regulation at the calcification site will probably determine calcification responses to high CO_2 (Venn *et al.*, 2011). $[H^+]$ regulation at crystallisation sites has been detected in many taxa, including crabs (Cameron, 1985), coralline red and calcareous green algae (Borowitzka, 1987; McConnaughey & Whelan, 1997), foraminifera (Rink *et al.*, 1998) and

scleractinian corals (Al-Horani *et al*., 2003; Venn *et al.*, 2011). Differential efficiency in calcification regulation may be one of the causes for the varied calcification responses to high CO_2 between taxa.

At intermediate pCO_2 levels calcification rates can increase (Wood *et al.* 2008; Gooding *et al.* 2009; McDonald *et al.,* 2009; Ries *et al.*, 2009; Findlay *et al.*, 2011; Rodolfo-Metalpa *et al.*, 2011). These responses may be due to the fact that calcification substrata used by many organisms are bicarbonate ions or aqueous carbon dioxide (Wilbur, 1964; Bubel, 1975; Decker & Lennarz, 1988; Al-Horani *et al*., 2003), both of which will increase following ocean acidification. Alternatively, increased calcification could be a defensive mechanism aiming to compensate for the increased dissolution rates of calcified structures at high CO_2 (McDonald *et al.,* 2009). There are several examples of increased shell dissolution at elevated CO_2 levels in molluscs, echinoderms and corals (Nienhuis *et al.*, 2010; Findlay *et al.*, 2011; Rodolfo-Metalpa *et al.*, 2011). These studies all conclude that the decrease in net calcification rates with increased pCO_2 levels is mostly caused by an increase in dissolution rather than a decrease in the organism's calcification. Organisms that build their skeletons using Mg-calcite, the most soluble form of calcium carbonate, suffer the most from increased dissolution rates as pCO_2 increases (Johnson *et al.*, 2014).

Given the significant increase in carbonate dissolution rates when calcium carbonate saturation state is low, species protecting their shells or skeletons with an organic layer will probably be favoured in an ocean acidification scenario. Rodolfo-Metalpa *et al.* (2011), for instance, showed that coral skeleton and mollusc shells were significantly more damaged in species without or with very limited organic cover. In some cases the organic layer is damaged at high

CO_2 levels, exposing carbonate structures to acidified seawater (Thomsen *et al.*, 2010; Rodolfo-Metalpa *et al.*, 2011)

Even species with very efficient acid-base regulation will require more energy to maintain extracellular pH values in a range compatible with the organism's needs as seawater pH decreases (Thomsen and Melzner, 2010). An organism may manage to maintain most of its physiological functions, but have to down-regulate some others, as reported for the swimming crab *Necora puber* (Small *et al.*, 2010) and in the barnacle *Semibalanus balanoides* (Findlay *et al.*, 2010). In other cases, changes in energy allocation such as compensatory increases in calcification rates could reduce the energy available for other essential physiological processes (Bradassi *et al.*, 2013). Energy can also be allocated depending on the individual; for instance, in the coral *Astrangia poculata* calcification rates decreased with increasing CO_2, but this was more evident in females, probably because they needed energy for egg production (Holcomb *et al.*, 2011). However, up-regulation of physiological processes is not always sustainable in the long term (Lombardi *et al.*, 2011).

Energy availability is extremely important in determining biological responses to ocean acidification, so food supply has an essential role. Increased nutrient or food supply can counter the effects of ocean acidification in corals (Cohen *et al.*, 2009; Holcomb *et al.*, 2010; Chauvin *et al.*, 2011) and molluscs (Thomsen *et al.*, 2010; Thomsen *et al.*, 2013). Increased food availability does not always have a significant effect, but this probably happens when food is not limiting (Holcomb *et al.*, 2011); in some cases, energy supply even outweighs the effects of carbon dioxide (Thomsen *et al.*, 2013).

Photosynthetic organisms could be positively influenced by ocean acidification if they are able to fix more inorganic carbon, and thus have more energy available. Many algal species have carbon concentrating mechanisms (CCMs), so they are less likely to be limited by inorganic carbon concentration (Raven *et al.*, 2012). However, higher seawater pCO_2 would give them a significant advantage, because a greater proportion of their inorganic carbon uptake could derive from passive CO_2 diffusion instead of the energetically expensive CCMs (Cornwall *et al.*, 2012; Harley *et al.*, 2012). The increased energy availability, however, may not be enough to counter the negative effects of ocean acidification in calcifying species faced with the increased energetic costs of calcification at high pCO_2 levels (Bradassi *et al.*, 2013).

The natural pCO_2 variability a species experiences also contributes to its tolerance to ocean acidification. Species exposed to high levels of CO_2 in their habitat could be more resistant to the negative effects of ocean acidification (Maas *et al.*, 2012; Moulin *et al.*, 2011). In addition, short-term experiments are often not representative of the full acclimation potential of a species to ocean acidification. For instance, even a species considered very sensitive to ocean acidification such as the deep-sea coral *Lophelia pertusa* can acclimate to high-CO_2 conditions after some months, while undergoing strong negative effects in the short term (Form and Riebesell, 2011). On the other hand, some short-term responses to high CO_2 could require too much energy to be maintained in the long term (Lombardi *et al.*, 2011).

Most factors considered above can vary during an organism's life cycle, and larvae are more vulnerable than adults in many cases, since their regulatory system is usually less developed than that of adults (Ellis *et al.*, 2009; Melzner *et al.*, 2009). A recent meta-analysis seems to confirm that echinoderm larval

stages are more sensitive to ocean acidification than adults (Dupont *et al.*, 2010). In general, however, differences in responses between life stages are probably less pronounced than those between taxonomic groups, and the most sensitive life stage can vary between taxa (Kroeker *et al.*, 2013a). It is therefore important to consider the whole life cycle of a species before drawing conclusions regarding its sensitivity to increased seawater CO_2.

1.3.2 Changes in biological interactions

Changes in biological communities caused by elevated CO_2 will depend on the responses of single species and the subsequent changes in their interactions. Although only a few studies examine the effect of ocean acidification on biological interactions, there is evidence that competition will be influenced. For instance, elevated CO_2 levels can increase coral mortality due to enhanced competition from seaweeds (Diaz-Pulido *et al.*, 2011) or negatively influence kelp recruitment through increased turf cover (Connell and Russell, 2010). Furthermore, coralline algae with high-Mg calcite skeletons have their fitness reduced when seawater pCO_2 is high, causing them to be outcompeted by non-calcifying algae, commonly fast-growing species (Russell *et al.*, 2009; Hofmann *et al.*, 2012; Kroeker *et al.*, 2013c; Short *et al.*, 2014).

CO_2-related changes in plant-herbivore interactions are poorly known. However, it seems that grazers' consumption rates do not change only because of variations in the animal's metabolic rates, but also as a consequence of the alteration in algal palatability. Since a wide range of reactions to high CO_2 is expected in algal taxa, it is not surprising that gastropod herbivores have increased (Falkenberg *et al.*, 2013b) and decreased (Swanson and Fox, 2007; Russell *et al.*, 2013) feeding rates at high CO_2 when grazing on primary

producers. In one study, the detected decrease in feeding rates is probably caused by an increase in kelp phlorotannins, a class of substances involved with herbivore deterrence in seaweeds (Swanson and Fox, 2007). Seagrasses show an opposite trend since their phenolic protective substances concentrations decrease as CO_2 increases, with potential positive effects on grazing organisms (Arnold *et al.*, 2012). Accordingly, sea urchins have been found to increase their seagrass consumption when pCO_2 increases (Burnell *et al.*, 2013). In other cases, change in pH alone has no significant effects on algal palatability, and changes in feeding rates only occur when interaction between temperature and pH is examined (Poore *et al.*, 2013).

There are also very few studies dealing with the response of predator-prey interactions to increased CO_2 levels. An experiment on four species of reef fish larvae and one of their predators (Ferrari *et al.*, 2011) found that at high CO_2 small fish recruits of all species suffered higher predation rates compared to the control. At the same time, predator's preferences seem to switch from two of the species to the other two. As for the cause of these changes, there is evidence to suggest that high CO_2 impairs some fish sensory perceptions (Munday *et al.*, 2014), but an effect on predator behaviour could not be excluded. CO_2-driven changes in the predator-prey interaction between the intertidal snail *Littorina littorea* and the green crab *Carcinus maenas* have also been recently studied (Bibby *et al.*, 2007; Landes and Zimmer, 2012). Although crabs had reduced claw strength (Landes and Zimmer, 2012) and snails exhibited weaker shells and increased avoidance behaviour with increased CO_2 (Bibby *et al.*, 2007; Landes and Zimmer, 2012), the overall interaction strength between the two species was not affected by pCO_2 (Landes and Zimmer, 2012). Predator-prey

interactions are thus likely to show a wide range of responses to ocean acidification, which are rarely predictable from single-species studies.

1.4 Adaptation potential

Most experiments on ocean acidification effects so far have tested whether present populations of marine organisms can cope with future seawater CO_2 levels. Although this approach gives essential information on the physiological mechanisms involved in coping with ocean acidification, it excludes the possibility an organism could adapt (i.e. genetically change) to increased CO_2. Experiments to test directly for adaptation to ocean acidification have mostly been performed on unicellular phytoplankton due to their extremely rapid generation time (reviewed in Collins *et al.*, 2014). Results so far suggest that taxa negatively affected by ocean acidification, such as calcifying coccolithophores, are under strong adaptive pressure and evolve to partially restore calcification and growth rates (Lohbeck *et al.*, 2012; Benner *et al.*, 2013). On the other hand, non-calcifying taxa such as the diatom *Thalassiosira pseudonana* were able to reduce their usage of energy-expensive carbon-concentrating mechanisms (CCMs), but no genetic adaptation seemed to take place (Crawfurd *et al.*, 2011).

For organisms with a longer life cycle, experimental evolution is generally not feasible, and alternative approaches need to be used. Variation in responses to ocean acidification among genotypes can hint at a species' potential for adaptation. Variability in fitness with increased CO_2 have been found in bryozoans (Pistevos *et al.*, 2011), oysters (Parker *et al.*, 2012), amphipods (Calosi *et al.*, 2013b) and coccolithophores (Langer *et al*., 2009). It is also possible to measure within-population genetic diversity as a proxy for their

potential of undergoing rapid evolution (Kelly *et al.*, 2013). Results from these studies revealed that species with shorter generation times do not always have higher adaptation potential than species with longer generation times, but greater genetic diversity (Sunday *et al.*, 2011).

Another approach to assess adaptation or acclimation/acclimatisation potential in marine organisms (for definitions see Box 1) is using natural pCO_2 gradients, such as those found at volcanic seeps or in upwelling areas, to assess whether local populations have acclimated or adapted to elevated CO_2 levels (Reusch, 2014). Individuals from areas with different pH can be exposed to the same CO_2 conditions in the laboratory ("common garden experiments") or reciprocally transplanted between sites to assess local adaptation (Sanford and Kelly, 2011). So far, both common garden experiments and reciprocal transplants have found significant inter-population differences in responses to pCO_2 in sea urchins, barnacles and polychaetes (Moulin *et al.*, 2011; Calosi *et al.*, 2013c; Evans *et al.*, 2013; Kelly *et al.*, 2013; Pansch *et al.*, 2014). Sea urchins naturally exposed to elevated pCO_2 have offspring that show increased resistance to ocean acidification (Moulin *et al.*, 2011; Evans *et al.*, 2013; Kelly *et al.*, 2013), while tolerant polychaete species transplanted between CO_2 levels can either adapt or acclimatise to high and variable CO_2 (Calosi *et al.*, 2013c). Short-term acclimation or acclimatisation to high pCO_2 can buffer populations against negative impacts of ocean acidification, giving them a chance to survive until adaptation takes place (Sunday *et al.*, 2014). This process, however, can be energetically expensive: barnacles populations not adapted to high and variable pCO_2 could cope with moderate carbonate dioxide levels, but only if food was abundant, whereas the adapted population was unaffected by food levels (Pansch *et al.*, 2014). The adaptation potential to ocean acidification of most

marine organisms is still unknown, and more evidence is urgently needed to fully determine which species will be able to adapt to the rapid environmental changes predicted for the next decades (Kelly and Hofmann, 2012).

Box 1: Acclimation, acclimatisation and adaptation (Angilletta, 2009)

Acclimatisation: the process by which an individual organism adjusts to a gradual change in its environment (such as a change in temperature or pH), allowing it to maintain performance across a range of environmental conditions.

Acclimation: similar to acclimatisation, but refers to changes occurring in response to an artificial or controlled situation.

Adaptation: a process involving the selection on genetic variation that shifts the average phenotype toward the fitness peak.

1.5 Interaction with other anthropogenic stressors

As well as ocean acidification, anthropogenic CO_2 emissions are causing an increase in seawater temperature (IPCC, 2014). Studying how these two factors will interact is essential to understand the future of marine ecosystems. Nonetheless, our knowledge of the combined effect of high pCO_2 and higher temperatures is currently lower than that of the effects of each factor alone. As with responses to changes in carbonate chemistry, interactions with temperature appear to have very variable effects on an organism's physiology, depending on which taxa it belongs to and which physiological responses are measured (e.g. Lischka *et al*., 2010; Noisette *et al.*, 2013a), although there is a trend towards an increase in negative effects of ocean acidification when organisms are concurrently exposed to elevated temperature (Kroeker *et al.*, 2013a). One possible explanation for this pattern is that the energetic costs of coping with ocean acidification (e.g. maintaining intracellular pH or calcification rates) narrow an organism's aerobic scope (Kelly and Hofmann, 2012).

Hypoxic zones are also expanding in the world oceans, both in coastal areas and in the subsurface open ocean waters (Diaz and Rosenberg, 2008). As hypoxic zones are the result of microbial respiration, decreased oxygen levels are paired with increased pCO_2. Carbon dioxide could then reach levels much higher than those predicted for the world oceans at the end of this century in hypoxic zones, threatening the survival of species otherwise resistant to ocean acidification (Melzner *et al.*, 2013). However, the effects of hypoxia and ocean acidification have mostly been studied in isolation, even though pteropods from hypoxic areas show increased resistance to increased pCO_2, suggesting that carbon dioxide is an important stressor in hypoxic areas (Maas *et al.*, 2012). To date, the only study assessing the combined effect of hypoxia and ocean acidification on marine organisms found that the two stressors interact to affect organisms in ways not predictable from single-stressor experiments (Gobler *et al.*, 2014).

Climate change is also expected to increase the intensity of ultra-violet (UV) radiation in marine systems following depletion of the ozone layer (Austin *et al.*, 1992). Marine organisms utilise many mechanisms for photoprotection against excessive radiation, most of which are energetically expensive and could decrease their resistance to other stressors, including ocean acidification (Häder *et al.*, 2007). The combination of increased CO_2 and UV radiation seems in fact to promote production of protective compounds (phlorotannins) in some brown algae (Swanson and Fox, 2007), even though not all taxa show an enhanced sensitivity to the combination of those stressors (Beardall *et al.*, 2009). For calcifying algae, the synergistic effect of CO_2 and UV radiations could be due to the reduction of the calcified layer as CO_2 increases, which impairs its photoprotective function (Gao *et al.*, 2009; Gao and Zheng, 2010),

even though not all coralline algae are negatively affected by the interaction of elevated carbon dioxide and UV radiations (Yildiz *et al.*, 2013).

Local stressors such as eutrophication and heavy metal pollution can also worsen community responses to ocean acidification, and managing them is essential to improve the resilience of marine ecosystems (Ghedini *et al.*, 2013). While at the single species level increased nutrient levels can offset the negative impacts of ocean acidification (Chauvin *et al.*, 2011; Thomsen *et al.*, 2013; Pansch *et al.*, 2014), elevated energy input often alters the outcome of inter-specific interactions, with more opportunistic species becoming more competitive (Connell and Russell, 2010; Falkenberg *et al.*, 2013a). The interactive effects of ocean acidification and heavy metals have not been studied at the community levels so far, but evidence from single-species experiments suggests that copper will enhance the negative effects of ocean acidification in some marine organisms, such as amphipods and polychaetes (Lewis *et al.*, 2012; Roberts *et al.*, 2013).

1.6 Thesis aims and objectives

Ocean acidification is a relatively new research field and studies on its community effects at temperate rocky reefs are in their infancy. Volcanic seeps are proving useful to study community responses of ocean acidification, but more sites are needed to build confidence in predictions developed using these systems. In addition, there is evidence that indirect effects of carbon dioxide could play a crucial role in the detected community changes, but our knowledge on the relative importance of direct or indirect effects of carbon dioxide is extremely limited. There is also little knowledge on the adaptation potential of

macroalgae and on possible interactions of ocean acidification with other stressors, such as copper pollution.

The overall thesis structure is illustrated in Figure 1.4: this project aimed to determine how benthic communities and their epifauna change along natural CO_2 gradients in the oligotrophic Mediterranean Sea, and investigate whether community changes were caused by direct or indirect effects; the interactive effects of CO_2 and a short-term copper pulse on macroalgae and their epifauna was also assessed. The specific objectives were to:

- Determine whether volcanic seeps off Methana (Greece) are suitable to study the effects of increased pCO_2 on benthic communities by monitoring carbonate chemistry, temperature, salinity, total alkalinity and measuring inorganic nutrients, hydrogen sulphide, as well as total and bioavailable heavy metals (Chapter 2).
- Determine how benthic communities and epifauna of main canopy-forming species change along Mediterranean pCO_2 gradients by assessing community structure and composition (Chapters 3 and 4).
- Determine whether changes in herbivores abundance contribute to the detected changes in benthic communities along pCO_2 gradients by excluding intertidal and subtidal herbivores (Chapter 5).
- Determine whether two abundant macroalgal species, one articulated coralline (*Jania rubens*) and one fucoid (*Cystoseira corniculata*), have acclimatised to high pCO_2 by transplanting them within and between high CO_2 and reference sites off Methana (Chapter 6).
- Determine whether two abundant macroalgal species, one articulated coralline and one fucoid, respond differently to copper exposure at

different pCO_2 levels and how this affects the fucoid epifauna by exposing macroalgae to copper *in situ* (Chapter 7).

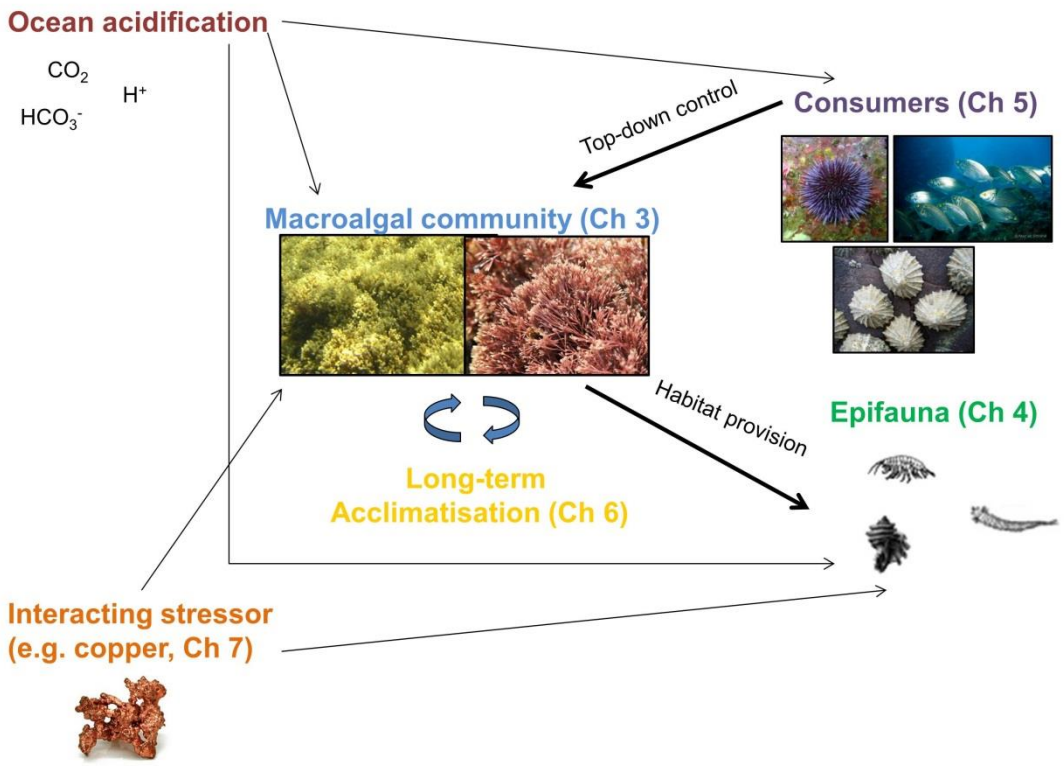

Figure 1.4. Visual abstract of thesis aims; using CO_2 seeps as natural analogues for ocean acidification, I assessed how macroalgal communities (Chapter 3) and their epifauna (Chapter 4) change with increasing pCO_2 levels, and whether long-term acclimatisation to elevated pCO_2 increases adaptation potential of dominant macroalgal species (Chapter 6). I also examined how changes in herbivores densities affect the strength of top-down control on macroalgal communities (Chapter 5), and how interaction of ocean acidification with another stressor (short-term copper pollution) may influence dominant macroalgal species and their epifauna (Chapter 7).

Table 1.1. Summary of this thesis' surveys and experiments, with measured parameters and sample sizes. (A) Summary of sampling for Chapter 2, with sampling date, site, measured parameters and sample sizes: pH, temperature and salinity (pH/T/S), water samples for total alkalinity (TA), water samples for inorganic nutrients (nitrites, nitrates, ammonium, phosphates, silicates), water samples for free sulphides, sediment samples for heavy metals content, macroalgal samples for heavy metals content. (B) Summary of sampling for Chapter 3, with sampling date, sites and number of 20 x 20 cm visual quadrats (Methana) or 20 x 20 cm quadrats scraped from rocky substratum (Vulcano). (C) Summary of sampling for Chapter 4, with sampling dates, sites and species (only Vulcano) and number of 20 x 20 cm quadrats of *Cystoseira corniculata* scraped from the substratum (Methana) or number of collected thalli (Vulcano). (D) Summary of sampling for the two experiments described in Chapter 5. For the limpet exclusion experiment at Vulcano, the table shows sampling dates and number of pH, temperature and salinity measurements (pH/T/S), number of limpet abundance and length measurements, number of experimental plots per treatment where macroalgal cover or biomass were measured (C=controls, P=procedural controls, E=exclusions) and number of wax discs used to quantify limpet grazing. For the herbivore exclusion experiment at Methana, the table shows sampling dates and number of pH, temperature and salinity measurements (pH/T/S), number of transects for sea urchins (*Paracentrotus lividus* and *Arbacia lixula*) abundance and herbivore fish (*Sarpa salpa*, *Siganus luridus* and *Sparisoma cretense*) biomass and number of experimental plots per treatment where macroalgal cover or biomass were measured (C=controls, P=procedural controls, E=exclusions). (E) Summary of sampling for *Cystoseira corniculata* (01-05/10/2012 to 22-25/06/2013) and *Jania rubens* (22-25/06/2013 to 04-09/09/2013) transplants described in Chapter 6. The table shows macroalgal species, treatment (expressed as "Site of origin"."Site of transplant", for a detailed description of the experimental design see Chapter 6), number of thalli used to measure growth and epiphyte cover (*=only epiphytes measured), photosynthetic parameters, pigments content, carbon, nitrogen and phosphorous (C,N,P) content (**P not measured) and total phenols content. N.u.=not used because samplesize was too small; lost=all thalli lost; N/A=not applicable. (F) Summary of sampling for the copper exposure experiments described in Chapter 7. For the

environmental monitoring, the table shows experiment dates, sites and number of pH, salinity and temperature measurements (pH/S/T) and number of water samples collected for total alkalinity measurements (TA). For the copper pulse experiments, the table shows macroalgal species (*Cystoseira corniculata* on 18-25/06/2013 and *Jania rubens* on 04-09/09/2013), treatment (expressed as "Site of origin"."Site of transplant"."Copper exposure", for a detailed description of the experimental design see Chapter 7), number of plaster blocks used, number of thalli used to measure copper content, maximum quantum yield, pigments content and epifaunal communities. N.u. treatment not used because sample size was too small; N/A=not applicable.

(A) Chapter 2: Assessing the suitability of a volcanic seep area off Methana (Greece) for ocean acidification studies.							
Date	Site	pH/T/S	TA	Inorganic nutrients	Sulphides	Metals - sediment	Metals - macroalgae
01/09/2011	SEEP	1					
01/09/2011	200 W	1					
01/09/2011	200 E	1					
11-12/02/2012	SEEP	2	3				
11-12/02/2012	200 W	2	3				
11-12/02/2012	200 E	2	4				
22/05/2012 to 06/06/2012	SEEP	11	5			3	5
22/05/2012 to 06/06/2012	200 W	11	6			3	5
22/05/2012 to 06/06/2012	200 E	11	3			3	5
22/05/2012 to 06/06/2012	REF A	1	3			3	5
22/05/2012 to 06/06/2012	REF B	4	3			3	5
27/09/2012 to 05/10/2012	SEEP	11	6				
27/09/2012 to 05/10/2012	200 W	3	6				
27/09/2012 to 05/10/2012	200 E	3	6				
27/09/2012 to 05/10/2012	REF A	8	6				
27/09/2012 to 05/10/2012	REF B	3	3				
18-25/06/2013	SEEP	13	6	3	7		
18-25/06/2013	200 W	7	6	3	3		
18-25/06/2013	200 E	7	6	3	3		
18-25/06/2013	REF A	9	6	3	3		
18-25/06/2013	REF B	8	6	3	3		
04-09/09/2013	SEEP	3	3				
04-09/09/2013	200 W	3	3				
04-09/09/2013	200 E	3	3				
04-09/09/2013	REF A	3	3				

04-09/09/2013	REF B	4	3				

(B) Chapter 3: Changes in subtidal macroalgal communities along pCO_2 gradients at Mediterranean volcanic seeps

Methana - visual quadrats of benthic communities

Date	SEEP	200 W	200 E	REF A	REF B
23-29/05/2012	7	7	7	7	7
30/09/2012 to 05/10/2012	6	6	6	6	6

Vulcano - destructively sampled quadrats

Date	REF A	Mid CO_2	High CO_2
15/05/2010	4	4	4

(C) Chapter 4: Canopy algal epifauna changes at elevated pCO_2 at two Mediterranean volcanic seeps

Methana - quadrats of *Cystoseira corniculata* scraped

Date	SEEP	200 W	200 E	REF A	REF B
26/05/2012 to 06/06/2012	3	3	3	3	3

Vulcano - macroalgal thalli collected

Date	Species	600 ppm	1200 ppm
04-08/06/2013	*Cystoseira* spp.	15	14
04-08/06/2013	*Sargassum vulgare*	9	10

(D) Chapter 5: Effect of herbivores on benthic communities at different pCO_2 levels

Vulcano - limpets exclusion experiment

Date	Measured parameter	Treatment	600	1200
08/05/2012	pH/T/S	N/A	1	1
18-19/07/2012	pH/T/S	N/A	2	2
22-23/09/2012	pH/T/S	N/A	2	2
27/10/2012	pH/T/S	N/A	1	1
08/05/2012	Limpets abundance/length	N/A	7	9
18-19/07/2012	Limpets abundance/length	N/A	18	18
22-23/09/2012	Limpets abundance/length	N/A	9	9
27/10/2012	Limpets abundance/length	N/A	9	9
08/05/2012	Macroalgal cover	C	3	3
08/05/2012	Macroalgal cover	P	3	3
08/05/2012	Macroalgal cover	E	6	6
18-19/07/2012	Macroalgal cover	C	3	3
18-19/07/2012	Macroalgal cover	P	3	3
18-19/07/2012	Macroalgal cover	E	6	6
22-23/09/2012	Macroalgal cover	C	3	3
22-23/09/2012	Macroalgal cover	P	3	3
22-23/09/2012	Macroalgal cover	E	6	4
27/10/2012	Macroalgal cover	C	3	3
27/10/2012	Macroalgal cover	P	3	0
27/10/2012	Macroalgal cover	E	6	4
20/11/2012	Macroalgal biomass	C	3	3
20/11/2012	Macroalgal biomass	P	3	0
20/11/2012	Macroalgal biomass	E	6	4
20/11/2012	Limpets grazing rates	N/A	41	34

Methana - herbivore exclusion experiment

Date	Measured parameter	Treatment	REF A	SEEP
30/09/2012 to 05/10/2012 and 20-25/06/2013	Sea urchins abundance	N/A	6 per species	6 per species
08/09/2013	Fish biomass	N/A	3	3
20/06/2013	Macroalgal cover/biomass	C	4	4
20/06/2013	Macroalgal cover/biomass	P	3	3
20/06/2013	Macroalgal cover/biomass	E	4	3

(E) Chapter 6: Seaweed acclimatisation to high pCO_2 at volcanic seeps						
Species	Treatment	Growth/ epiphytes	Photosynthetic parameters	Pigments content	C, N, P content	Phenol content
C. corniculata	SEEP.SEEP	5	5	5	5	5
C. corniculata	REFB.SEEP	8	6	8	7	7
C. corniculata	REFA.SEEP	3	3	3	3	3
C. corniculata	REFA.REFA	5	4	5	4	4
C. corniculata	SEEP.REFA	10	9	10	9	10
C. corniculata	REFB.REFB	8	7	8	4	4
C. corniculata	SEEP.REFB	4	3	4	4	3
C. corniculata	SEEP	7*	6	7	7	6
C. corniculata	REFA	7*	7	6	7	7
C. corniculata	REFB	7*	4	7	7	7
J. rubens	SEEP.SEEP	4	4	4	4**	N/A
J. rubens	REFB.SEEP	4	5	4	3**	N/A
J. rubens	REFA.SEEP	n.u.	n.u.	n.u.	n.u.	N/A
J. rubens	REFA.REFA	lost	lost	lost	lost	N/A
J. rubens	SEEP.REFA	lost	lost	lost	lost	N/A
J. rubens	REFB.REFB	5	5	5	9**	N/A
J. rubens	SEEP.REFB	6	5	6	4**	N/A
J. rubens	SEEP	N/A	7	7	5**	N/A
J. rubens	REFA	N/A	7	7	5**	N/A
J. rubens	REFB	N/A	7	7	5**	N/A

(F) Chapter 7: A short-term copper pulse affects macroalgal copper accumulation and indirectly alters epifaunal colonisation at elevated pCO_2

Environmental monitoring

Date	Site	pH/T/S	TA
18-25/06/2013	SEEP	13	6
18-25/06/2013	REF A	9	6
18-25/06/2013	REF B	8	6
04-09/09/2013	SEEP	3	3
04-09/09/2013	REF A	3	3
04-09/09/2013	REF B	4	3

Copper pulse experiments

Species	Treatment	Plaster	Copper content	Maximum quantum yield	Pigments content	Epi fauna
C. corniculata	REFA.REFA.Cu-	4	5	5	5	4
C. corniculata	REFA.REFA.Cu+		5	5	5	5
C. corniculata	SEEP.REFA.Cu-		5	5	5	N/A
C. corniculata	SEEP.REFA.Cu+		5	5	4	N/A
C. corniculata	REFB.REFA.Cu-		n.u.	3	n.u.	N/A
C. corniculata	REFB.REFA.Cu+		n.u.	3	n.u.	N/A
C. corniculata	REFA.SEEP.Cu-	4	5	5	4	N/A
C. corniculata	REFA.SEEP.Cu+		5	5	5	N/A
C. corniculata	SEEP.SEEP.Cu-		4	4	4	5
C. corniculata	SEEP.SEEP.Cu+		5	5	5	5
C. corniculata	REFB.SEEP.Cu-		n.u.	4	n.u.	N/A
C. corniculata	REFB.SEEP.Cu+		n.u.	5	n.u.	N/A
J. rubens	REFA.REFA.Cu-	4	4	4	5	N/A
J. rubens	REFA.REFA.Cu+		5	4	5	N/A
J. rubens	SEEP.REFA.Cu-		5	5	4	N/A
J. rubens	SEEP.REFA.Cu+		5	5	4	N/A
J. rubens	REFB.REFA.Cu-		4	3	n.u.	N/A
J. rubens	REFB.REFA.Cu+		4	4	n.u.	N/A
J. rubens	REFA.SEEP.Cu-	4	5	4	4	N/A
J. rubens	REFA.SEEP.Cu+		5	5	3	N/A

J. rubens	SEEP.SEEP.Cu-		5	5	4	N/A
J. rubens	SEEP.SEEP.Cu+		5	5	5	N/A
J. rubens	REFB.SEEP.Cu-		5	5	n.u.	N/A
J. rubens	REFB.SEEP.Cu+		5	3	n.u.	N/A

Chapter 2

Assessing the suitability of a volcanic seep area off Methana (Greece) for ocean acidification studies

Aspects of this chapter have been published as:

C. Baggini, M. Salomidi, E. Voutsinas, L. Bray, E. Krasakopoulou, J.M. Hall-Spencer (2014). Seasonality affects macroalgal community response to increases in pCO_2. *PLoS ONE*, 9: e106520.

Abstract

Ocean acidification poses a threat to a wide range of marine systems, but little work has been carried out at the ecosystem level due to logistical constraints. Work in areas with naturally high CO_2 is starting to show community effects of ocean acidification. Replication of these observations across a range of settings is needed to build confidence in predictions developed using these systems as ocean acidification analogues. The aim of this study was therefore to assess whether seeps off Methana, in the oligotrophic Aegean Sea, are appropriate for studying the community effects of ocean acidification. Monitoring of the gradient from 2011 to 2013 showed that median seawater pH decreased from present day values at reference sites (median pH = 8.12) to levels predicted for the end of this century at the seep sites (median pH = 7.69) with no confounding gradients in total alkalinity, salinity, temperature or wave exposure. Most nutrient levels were similar along the pH gradient; silicate lelves increased significantly with decreasing pH, but they were high enough at all sites not to limit algal growth. Metal concentrations in sediment and seaweed tissues varied between study sites but did not consistently increase with increasing pCO_2. Methana seeps have the same limitations as other seeps used for ocean acidification studies, i.e. variable pCO_2 and relatively small area influenced. Seeps off Methana, however, influence a relatively large area (~10 km of shore) compared to other seeps used for ocean acidification studies, which may limit the amount of mobile organisms and larvae coming from reference areas. It is therefore concluded that seeps off Methana are suitable for studies into the effects of ocean acidification, provided the limitations of using seep systems in ocean acidification studies are taken into account.

2.1 Introduction

Early work on the effects of ocean acidification involved experiments that focused on single species in laboratory conditions, where pH variability was minimised, for periods of up to 18 months (Kroeker *et al.*, 2013a). This body of work has rapidly advanced our knowledge of the relative sensitivity of different species, which can be used to formulate hypotheses about community responses. Nevertheless, surprising and unpredicted community responses to increased levels of pCO_2 can occur because of interactions between species. For instance, Hale *et al*. (2011) reports that most invertebrate taxa in a community mesocosm experiments responded to increased pCO_2 as expected from single species experiments. Nematodes, however, unexpectedly increased in abundance, probably because of the decreased competition with, and predation by, taxa sensitive to ocean acidification.

Community responses to ocean acidification will also depend on indirect effects of carbon dioxide, such as those which alter animal behaviour (Briffa *et al.*, 2012) and affect their neuroreceptors (Munday *et al.*, 2014). Thus, physiology and ecological niche cannot fully predict a species' susceptibility to environmental changes (Spicer, 2014). Moreover, laboratory and mesocosm experiments are usually too brief to ascertain the effect of increased carbon dioxide on climax communities comprising long-lived organisms (Kroeker *et al.*, 2013a). Hypotheses formulated using data from short-term single-species laboratory experiments thus need to be tested in complex communities, ideally in real marine ecosystems (Garrard *et al.*, 2013).

Areas chronically exposed to high pCO_2 can be used to assess long-term community responses to ocean acidification (Hall-Spencer *et al.*, 2008;

Fabricius *et al.*, 2011; Boatta *et al.*, 2013; Inoue *et al.*, 2013). Although in their infancy, there are widespread opportunities for such studies since hydrothermal seeps characterised by low pH and high pCO_2 levels occur worldwide (Tarasov *et al.*, 2005). However, many of these areas also have gradients in temperature, salinity, total alkalinity, inorganic nutrients, toxic gases and metals (Dando *et al.*, 1999; Karlen *et al.*, 2010), which could confound the ecological effects of carbon dioxide. As a consequence, geochemical baseline surveys are needed to check the extent to which seep systems can be used as natural ocean acidification laboratories (Kerrison *et al.*, 2011; Boatta *et al.*, 2013).

Only a few CO_2 seeps have so far been located that are suitable for use as ocean acidification analogues, namely seeps off Italy (Hall-Spencer *et al.*, 2008; Kerrison *et al.*, 2011; Boatta *et al.*, 2013), Papua-New Guinea (Fabricius *et al.*, 2011) and Japan (Inoue *et al.*, 2013). These studies have shown that increasing levels of seawater pCO_2 reduce benthic biodiversity, especially that of calcifying organisms (Martin *et al.*, 2008; Dias *et al.*, 2010; Fabricius *et al.*, 2014). Replication of such studies in a wider range of settings would strengthen the evidence for the ecosystem effects of increasing pCO_2 at the landscape scale. Data from a natural ocean acidification analogue in the Eastern Mediterranean would be useful due to its extremely low nutrient levels, which could exacerbate the effects of high pCO_2 due to the increased metabolic costs of coping with ocean acidification (Holcomb *et al.*, 2010; Melzner *et al.*, 2011; Kletou and Hall-Spencer, 2012).

The aim of this chapter is to assess the suitability of volcanic seeps off Methana (Saronikos Gulf, Aegean Sea, Greece) for ocean acidification studies. Temperature, pH, salinity, total alkalinity and the concentrations of heavy metals, hydrogen sulphide and major nutrients (nitrite, nitrate, ammonium, phosphate

and silicate) were monitored. In addition, wave exposure was determined using effective fetch (see section 2.2.8) as it affects the distribution of Mediterranean fucoid algae (Spatharis *et al.*, 2011).

2.2 Methods

2.2.1 Study area

The Methana peninsula is the westernmost volcanic system of the northern Aegean Volcanic Arc, derived from the subduction of the African tectonic plate beneath the Eurasian plate. The last volcanic eruption dates back to 230 BC, but the system is still hydrothermally active (Dando *et al.*, 1999). The seeps are shallow (0-5 m depth) and situated on the NE part of the peninsula (Figure 2.1). They appeared shortly after the last volcanic eruption, and the Pausania thermal baths nearby have been used since late Roman times (Bowden and Gill, 1997).

Geothermal fluids rise very slowly from the geological reservoir below Methana (2-3 km underground), where temperatures could be as high as 210 °C; they mix with shallow fluids in the process (D'Alessandro *et al.*, 2008). The released gases are dominated by CO_2, as in most Mediterranean hydrothermal systems (Dando *et al.*, 1999), and are mainly derived from limestone. The estimated CO_2 flux from the whole peninsula is about 0.03 kg s^{-1}, well below the range generally measured worldwide in volcanic/hydrothermal areas (0.2-450 kg s^{-1}; Pecoraino *et al.*, 2005) and lower than those of the rest of the Aegean Volcanic Arc (0.2 kg s^{-1} at Nea Kameni, Chiodini *et al.*, 1998; 0.6 kg s^{-1} at Sousaki, D'Alessandro *et al.*, 2006; and 1.0 kg s^{-1} at Nisyros, Cardellini *et al.*, 2003).

Gas concentrations have been recently measured in Pausanias baths, which are extremely close (<20 meters) to the seeps studied here. Gas emissions

were measured on two occasions, and gas composition was relatively stable over time (D'Alessandro *et al.*, 2008). Gas bubbles in the baths are mostly carbon dioxide, with small amounts of nitrogen, carbon monoxide and methane (Table 2.1). Methane concentrations (17-26 ppm) are much lower than those detected at ocean acidification analogues in Ischia (200 - 800 ppm; Hall-Spencer *et al.*, 2008), Vulcano (1700 ppm; Boatta *et al.*, 2013) and Papua New Guinea (87 - 4360 ppm; Fabricius *et al.*, 2011).

Table 2.1. Composition of gases bubbling at Pausanias baths in ppm (D'Alessandro *et al.*, 2008). These baths are adjacent to the submarine seeps. Carbon dioxide (CO_2) accounts for over 90% of the emitted gases, with smaller percentages of nitrogen (N_2), oxygen (O_2), methane (CH_4), carbon monoxide (CO), helium (He) and hydrogen (H_2). Methane levels are much lower than in other seeps used as ocean acidification proxies.

Date	**CO_2**	**N_2**	**O_2**	**CH_4**	**CO**	**He**	**H_2**
04/06/2006	991000	10700	<400	26	1.6	<5	<5
23/06/2006	970000	30900	5600	17	1.7	<5	<5

The Pausanias bath water composition is moderately enriched in calcium and silicates due to the interaction of thermal waters and limestone and silicate rocks, respectively. Rock-water interactions were responsible for the detected enrichment in K, B and Li as well (D'Alessandro *et al.*, 2008).

2.2.2 Site descriptions

Two preliminary surveys were carried out in September 2011 and February 2012 to characterise carbonate chemistry and find areas with elevated pCO_2 as well as reference sites. These surveys showed that a relatively small area (approximately 20 m of shoreline) near a seep had a pH_{NBS} constantly below 8.0 (Figure 2.1), whereas a much larger area was characterised by variable pH.

This area (shown in light grey in Figure 2.1) had a pH_{NBS} varying from 6.6 to 8.1, with lower values in autumn and higher in winter. Sediment Eh and dissolved oxygen analyses at the sediment-water interface confirmed that volcanic activity did not produce an anoxic layer in the sediment (Krasakopoulou *et al.*, unpublished data).

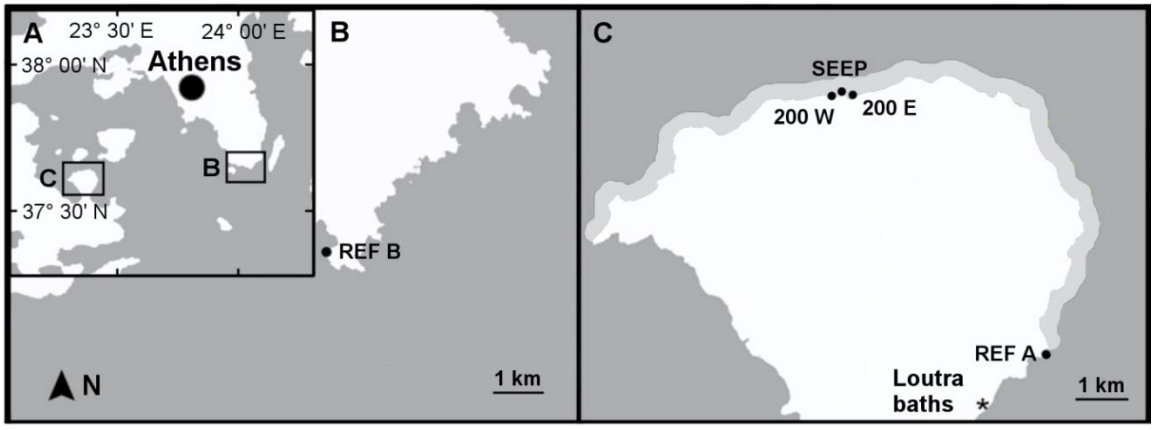

Figure 2.1. (A) Saronikos Gulf, Greece, with study areas marked by rectangles B and C. (B) Study site REF B (black point). (C) Study sites 200 W, SEEP, 200 E and REF A (black points), Loutra baths (*) and area where pH was more variable than at reference sites (light grey).

Five sites with comparable habitats but different pH levels were selected: a site with pH<8.0 near the main seeps (SEEP), two sites with variable pH located approximately 200 m eastwards and westwards of the seep area (200 E and 200 W) and two reference sites, one just outside the variable pH area (REF A) and one at a more distant site unaffected by volcanic activity (REF B). Pictures of the typical benthic communities at SEEP and 200 E are shown in Figure 2.2. All sites had the same type of coastal morphology (large sparse boulders) and similar degrees of urbanisation, as only small villages and hotels were found in their vicinities. The dominant canopy-forming macroalgal species at all sites was *Cystoseira corniculata*, a fucoid alga characteristic of the Eastern

Mediterranean Sea (Taskin *et al.*, 2012). The genus *Cystoseira* indicates good environmental conditions (Ballesteros *et al.*, 2007) and *C. corniculata* is characteristic of sites with high wave exposure (Spatharis *et al.*, 2011).

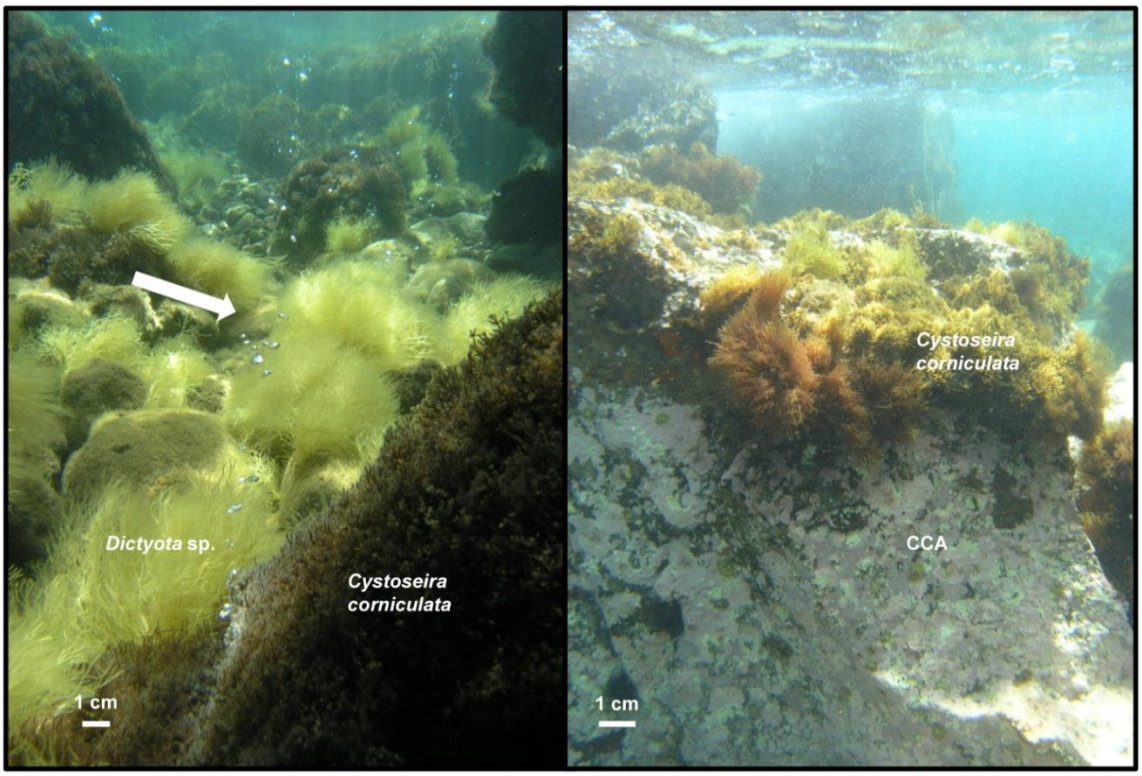

Figure 2.2. Typical appearance of benthic communities at SEEP (left) and 200 E (right) sites at 0.5 m depth in May 2012 with CO_2 bubbles seeping from the sea floor (arrow). Brown algae (e.g. *Dictyota* sp.) were dominant near the seeps; crustose coralline algae (CCA) became dominant as CO_2 levels decreased. Photos by Laura Bray (May 2012).

2.2.3 Seawater physicochemical parameters

The seeps were monitored from 2011 to 2013 (September 2011, January, February, May and September 2012, June and September 2013 - detailed sampling dates and sample sizes are reported in Table 1.1A); seawater physicochemical parameters were measured at different times of the day and in different meteorological conditions during each trip. Seawater pH, temperature and salinity were measured using a multiprobe (YSI 63) from shore. The probe was calibrated before use with pH 4.01, 7.01 and 10.01 NBS standards. Since

variations of up to 1 pH unit were detected over a few hours at the low pH site, the lack of precision in using the NBS scale for seawater measurements (approximately 0.05 pH, Riebesell *et al.*, 2010) was considered acceptable for this study. For pH, medians and interquartile ranges (IQ) were calculated from hydrogen ion concentrations before re-converting back to pH values following seep monitoring methods provided by Kerrison *et al.* (2011).

Seawater samples for total alkalinity determination were collected in 125 ml borosilicate glass bottles with Teflon caps. Three independent samples per site were collected at each visit, immediately poisoned with $HgCl_2$ and stored in the dark until analysis. Samples were analysed by Gran titration (AS-ALK 2, Apollo SciTech) and the reliability of the measurements was checked against standard seawater samples provided by A. Dickson (batches 112 and 121). The average total alkalinity value per site and individual pH measurements were used to calculate pCO_2, HCO_3^-, CO_3^{2-}, Ω_{Ar} and Ω_{Ca} using the CO2SYS software (Lewis and Wallace, 1998).

2.2.4 Seawater nutrient concentration

In June 2013 three water samples per site were collected for nutrient analysis; the analyses were performed by the nutrient laboratory staff at the Hellenic Centre for Marine Research. Samples were stored frozen (-20°C), then analysed using a BRAN+LUEBBE II autoanalyser. Inorganic phosphate determination followed the colorimetric method of Murphy and Riley (1962) and nitrite ions (NO_2^-) were measured colorimetrically according to Bendscheider and Robinson (1952). Determination of nitrate (NO_3^-) was performed after its reduction to nitrite, which was then determined colorimetrically as above. Silicate was determined by adding a molybdate solution to the sample. The

silicomolybdic acid that formed was then reduced to an intensely blue-coloured complex by adding ascorbic acid as a reducing agent (Mullin & Riley, 1955). The determination of ammonium was performed according to Koroleff (1970) using a Perkin Elmer 25 Lambda spectrophotometer.

2.2.5 Free sulphides in seawater

Free sulphides were determined using a method modified from Cline (1989). Three seawater samples per site were collected using plastic syringes to measure within- and between- site variability in sulphides contents; 2 ml of seawater were injected into a nitrogen-filled septum vial containing a small crystal of cadmium chloride. As the area near the seeps had the highest probability of having high sulphide concentrations, four additional samples were taken on two separate dates (22 and 25 May 2012). In order to validate the method, one sample was taken at the sulphide-rich Loutra thermal baths (location shown in Figure 2.1). For laboratory analysis, most of the water was removed by syringe after allowing the precipitate to settle. The samples were thus reduced to 0.8 ml volume, agitated to suspend all the precipitate and drawn up in a 1 ml disposable syringe which had been flushed with Ar.

Subsequently, 0.2 ml of a solution prepared using 400 mg of N,N-dimethyl-p-phenylene-diamine-dihydrochloride and 600 mg $FeCl_3.6H_2O$ dissolved in 100 ml 50% HCl were drawn into the same syringe. The argon bubble in the syringe was used to mix by inverting it a few times. The sample was left to stand for 20 minutes and then injected into a 1 ml semi-microcuvette and read in a Perkin Elmer Lambda 35 UV-VIS spectrometer at 670 nm. Standards were made using a 10 mM sodium sulphide stock solution (249 mg $Na_2S.9\ H_2O$ in 100 ml

degassed Milli-Q water). The stock solution was diluted immediately before use in degassed seawater to give a range of 0.1 to 100 µM.

2.2.6 Heavy metals in sediment

Sediments were examined for metals that can exhibit increased concentrations in volcanic areas (Al, As, Ca, Cd, Co, Cr, Cu, Fe, Li, Mg, Ni, Pb, Zn; Hübner *et al.*, 2004); S was also analysed to verify wheter the area was contaminated by hydrogen sulphide emitted by the seeps, and Cr was analysed to determine sediment quality (see below). In May 2012, sediments were sampled for heavy metal analysis at the three sites where contamination from volcanic activity was likely (SEEP, 200 W and 200 E). Sediment was collected using plastic pots immediately closed with a lid. Three stations were selected for each site to assess within-site variability, and one sample per station was collected. Immediately after sampling, sediment was transferred to polypropylene bags and kept frozen until analysis.

Samples were oven-dried at 30°C until constant mass was reached. They were subsequently reduced to a fine powder and passed through a 180 µm plastic sieve. Triplicate replicates for each station were prepared for analysis by digesting them with aqua regia. First, approximately 0.5 grams of sample were carefully weighed on an analytical balance (precision ± 0.1 mg) and transferred into a pre-cleaned and dry digestion tube (Tecator type). Subsequently, 7.5 ml of hydrochloric acid and 2.5 ml of nitric acid were added. One hour of pre-digestion allowed easily oxidised materials to be destroyed at low temperature. Temperature was then gradually increased in several steps: firstly samples were kept at 60 °C for 30 minutes, then at 85 °C for one hour, then at 105 °C for another hour, then at 120 °C for an hour and finally at 140 °C for a further hour.

After cooling, the digested material was transferred quantitatively to a 50 ml volumetric flask and diluted to volume with distilled water. The blank was prepared following the same steps as above, but without adding sediment. Three replicates of reference material (Harbour Sediment, LGC6156) were prepared following the same procedure.

Digested samples were then analysed for Al, Ca, Cr, Cu, Fe, Mg, Mn, Pb, S and Zn using inductively coupled plasma optical emission spectrometry (ICP-OES, Varian 725-ES; Melbourne, Australia) using a v-groove nebuliser and a Sturman-Masters spray chamber. The analysis parameters were as follows: forward power 1.4 kW, plasma gas flow 15 L min^{-1}, auxiliary gas flow 1.5 L min^{-1}, nebuliser gas flow 0.68 L min^{-1}. Each sample was read three times, with four seconds of replicate read time and a viewing height of 8 mm. Every ten samples analysed, one of the standards was measured again in order to detect any deviation from the initial calibration.

As, Cd, Co, Li and Ni were present in very small quantities, so their concentrations were determined using an inductively coupled plasma mass spectrometry (ICP-MS, Thermo Scientific X series 2, Hemel Hampstead, UK) with a concentric glass nebuliser and a conical spray chamber with an impact bead. The analysis parameters were as follows: forward power 1.4 kW, plasma gas flow 13 L min^{-1}, auxiliary gas flow 0.7 L min^{-1}, nebuliser gas flow 0.8 L min^{-1}. Each sample was read 50 times, with 10 ms read time. Every eleven samples, one of the standards was measured again to detect any deviation from the initial calibration. In addition, an internal reference (iridium) was used to correct for the density difference between standards and digested samples.

Biological effects of heavy metal enrichment of the sediments were examined using an index of ecological risk, the mean Sediment Quality Guidelines-quotient (SQG-Q). This index is an indicator of adverse biological effects caused by different concentrations of heavy metals. This type of numerical SQG can be used to obtain a fist approximation of sediment toxicity (Long and MacDonald, 1998; Chapman and Wang, 2001). Mean SQG-Q using two sediment quality guidelines, ERM (effect range-median) and PEL (probable effect levels) was calculated for each site using the following equations (Long and MacDonald, 1998):

$$SQG - Q\alpha\_PEL = \frac{\sum_{i=1}^{n}(PEL - Qi)\alpha}{n} \quad (1)$$

and

$$SQG - Q\alpha\_ERM = \frac{\sum_{i=1}^{n}(ERM - Qi)\alpha}{n} \quad (2)$$

where

$$PEL - Qa = \frac{C}{PEL} \quad (3)$$

and

$$ERM - Qa = \frac{C}{ERM} \quad (4)$$

PEL-Q = Probable effect level quotient

ERM-Q = Effect range-median quotient

C- Heavy metal concentration in each station

PEL - Probable effect level of each heavy metal

ERM - Effect range-median of each heavy metal

n – Number of contaminants used.

PEL and ERM are the concentrations above which adverse effects frequently occur and although they have been calculated with slightly different methods, they both are reliable methods to predict sediment toxicity (Long *et al.*, 1998). PEL and ERM values for the analysed elements are reported in Table 2.2.

Table 2.2. PEL and ERM threshold values used to calculate the potential biological effect of contaminants (Long *et al.*, 1998). They are concentration expressed as mg/g of dry sediment, and have been calculated from a database of toxicity tests.

	Cd	Cr	Cu	Pb	Ni	Zn
PEL	4.21	160	108	112	42.8	271
ERM	9.6	370	270	218	51.6	410

Each site can be assigned to one of the following impact level categories:

Category 1: *SQG-Q* < 0.1 unimpacted - lowest potential for observing adverse biological effects;

Category 2: 0.1 < *SQG-Q* < 1 impacted - moderate potential for observing adverse biological effects;

Category 3: *SQG-Q* > 1 highly impacted - potential for observing adverse biological effects.

2.2.7 Heavy metals in macroalgae

A common phaeophyte, *Dictyota* sp., was analysed for heavy metal concentrations at all five sites. This macroalga was chosen as it was present at all sites and had low epiphyte load. Five individuals per species per site were

collected by snorkelers in May 2012, rinsed with fresh water to eliminate salt, gently brushed to remove epiphytes, kept frozen until transported to the laboratory and then freeze-dried. Freeze-dried macroalgae were ground with pestle and mortar and approximately 0.1 g of each sample was weighed in acid-washed Teflon tubes with a high precision digital scale (0.1 mg accuracy). Two ml of concentrated nitric acid were then added, and the tube containing the digestant was placed in a high-Throughput Microwave Reaction System Run (MARSXpress, CEM Corporation, Matthews, USA) and gently heated to boiling for at least 1 h to ensure full digestion. Samples were allowed to cool and then quantitatively transferred into pre-cleaned 10 ml volumetric flasks and diluted to volume with Milli-Q water. Blanks were prepared following the same procedure, but omitting the sample; a certified reference material (NIES Standard Reference Material No. 3, Chlorella) was simultaneously digested and analysed. Samples were then analysed for content of toxic metals (Al, As, Cd, Cr, Co, Cu, Pb, Ni, Zn; Baumann *et al.*, 2009; Mendes *et al.*, 2013; Khan *et al.*, 2015) and Fe, which had values higher than reference ones and showed between-site variability in the sediment samples. Analyses were performed using ICP-OES and ICP-MS following the procedure outlined in the previous section.

2.2.8 Wave exposure

Wave exposure was estimated using a method from Howes *et al.* (1994), which uses modified effective fetch and maximum fetch to calculate a site-specific index of wave exposure, which is a first approximation of wave exposure. Other factors such as the associated local wind climate and wave refraction are ignored for simplifying the estimate. Modified effective fetch involves the measurement of three fetch distances: the normal to shoreline direction and the

two fetches at 45° to the left and to the right of the normal fetch. The effective fetch is then calculated with the formula:

$$Fe = \frac{\sum_{i=0}^{n} cos\alpha i * Fi}{\sum_{i=0}^{n} cos\alpha i} \quad (5)$$

Where Fe is the effective fetch measure in kilometres, αi is the angle between the shore normal and the direction i and Fi is the fetch distance in kilometres along direction i. The wave climate of a particular point cannot be characterized by effective fetch alone because waves may be generated in an area remote from the site and propagate into the area. These waves, normally referred to as swell, can be approximated using maximum fetch, which is the maximum fetch distance in kilometres that can be measured from the site. The two indexes are then combined in a matrix (Table 2.3) to determine the wave exposure category for each site. The wave exposure was only calculated for the sites SEEP, REF A and REF B, as the sites 200 W and 200 E are very close to SEEP and have a very similar shore orientation.

Table 2.3. Classification of a shore point wave exposure based on the combination of maximum fetch and modified effective fetch (both in km). Depending on the combination of these two factors, a point on the shore can be classified as very protected, protected, semi-protected, semi-exposed, exposed and very exposed (Howes *et al.*, 1994).

Maximum Fetch (km)	Modified Effective Fetch (km)				
	<1	1-10	10-50	50-500	>500
<1	very protected	n/a	n/a	n/a	n/a
<10	protected	protected	n/a	n/a	n/a
10-50	n/a	semi-protected	semi-protected	n/a	n/a
50-500	n/a	semi-exposed	semi-exposed	semi-exposed	n/a
500-1000	n/a	n/a	semi-exposed	exposed	exposed
<1000	n/a	n/a	n/a	very exposed	very exposed

2.2.9 Statistical analyses

Analysis of nutrient and metal concentration data was performed using separate multivariate analyses of variance (MANOVA) with one factor (site). Normality and homogeneity of variances were tested by visually examining boxplots and residual error plots and using Levene's test, and transformed when necessary. When the data did not meet Mauchly's test of sphericity, the degrees of freedom were corrected using Greenhouse-Geisser estimates of sphericity. Tukey HSD tests were used for multiple comparisons. Analysis of pH data was performed using a non-parametric analysis (Kruskal-Wallis ANOVA) followed by pairwise

multiple comparisons. All of the analyses above were performed using SPSS v. 19 (IBM, USA)

2.3 Results

2.3.1 Seawater physicochemical parameters

The seeps had the lowest median pH_{NBS} (7.69, IQ range 7.57 - 7.85, n=40) and were significantly different from the intermediate sites (200 W and 200 E), which had higher median values (7.87, n=26 and 7.96, n=26 for 200 E and 200 W, respectively) and comparable variability (IQ ranges 7.75 - 8.04 and 7.73 - 8.03 for 200 E and 200 W, respectively). At intermediate sites pH sometimes exceeded 8.0, whereas at SEEP the measured pH never reached 8.0. The reference sites had significantly higher pH values (median values of 8.11, n=21 and 8.12, n=19 for REF A and REF B, respectively) and lower variability (Figure 2.3).

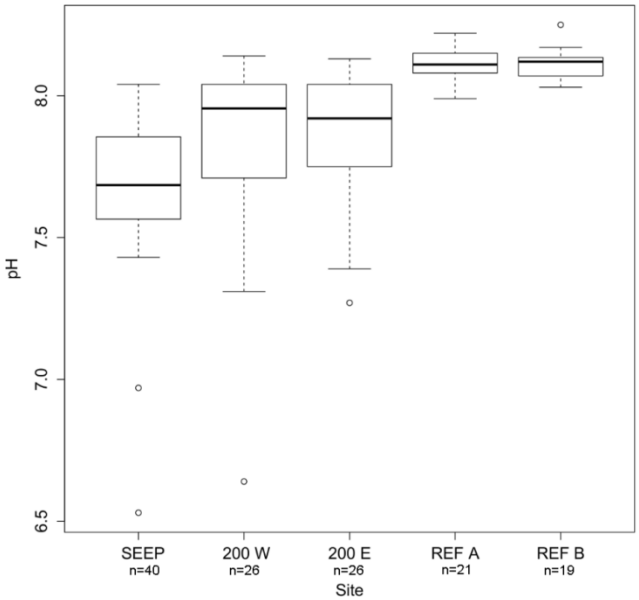

Figure 2.3. Variability in pH at the five study sites off Methana between September 2011 and September 2013. Horizontal line = median, vertical boxes = 25th and 75th percentiles, whiskers = min/max values if smaller than 1.5 times the inter-quartile range and dots = outliers.

Temperature and salinity varied seasonally and were uniform across sites. The minimum temperature was 14.2˚C in February, whereas in summer the temperature could reach 26.8˚C; salinity varied from 37.5 to 40.0 ppt. Total alkalinity varied from 2.615 to 2.944 mmol kg^{-1} with no seasonal trend (Table 2.4), with slightly lower values and less variability than CO_2 seeps off Vulcano, where total alkalinity varies between 2.78 to 3.17 mmol kg^{-1} (Boatta *et al.*, 2013). Seawater pCO_2 had a median value of over 1300 µatm at the SEEP site, almost three times the values calculated for the reference sites. The median saturation state of calcite and aragonite was always > 1, although sites with high and intermediate pCO_2 levels were occasionally under-saturated with respect to both calcite and aragonite (Table 2.4).

Table 2.4. Values of measured (pH and total alkalinity (TA)) and calculated (bicarbonate (HCO_3^-) and carbonate ions (CO_3^{2-}) concentrations, pCO_2, saturation state of calcite (Ω_{Ca}) and aragonite (Ω_{Ar})) carbonate system parameters at the five sites using data from six surveys from September 2011 to September 2013. Sample sizes for pH and total alkalinity are shown below site name.

Site		**pH** (NBS)	**TA** (mmol kg^{-1})	***p*CO$_2$** (µatm)	**HCO$_3^-$** (mmol kg^{-1})	**CO$_3^{2-}$** (mmol kg^{-1})	**Ω_{Ar}**	**Ω_{Ca}**
SEEP	Min	6.53	2.639	24092	2.771	0.006	0.09	0.13
(n_{pH}=40, n_{TA}=23)	Median	7.69	2.794	1754	2.538	0.104	1.16	2.45
	Max	7.99	2.944	691	2.243	0.225	3.45	5.20
200 W	Min	6.64	2.696	18652	2.773	0.007	0.11	0.17
(n_{pH}=26, n_{TA}=24)	Median	7.96	2.771	872	2.366	0.177	2.70	4.12
	Max	8.14	2.941	526	2.138	0.271	4.18	6.29
200 E	Min	7.27	2.693	4505	2.658	0.038	0.57	0.88
(n_{pH}=26, n_{TA}=22)	Median	7.88	2.739	1042	2.403	0.152	2.30	3.50
	Max	8.13	2.836	532	2.114	0.263	4.05	6.10
REF A	Min	7.99	2.640	773	2.261	0.183	2.84	4.30
(n_{pH}=21, n_{TA}=18)	Median	8.11	2.708	550	2.106	0.246	3.78	5.70
	Max	8.22	2.769	393	2.049	0.269	4.04	6.18
REF B	Min	8.03	2.615	674	2.254	0.185	2.81	4.30
(n_{pH}=19, n_{TA}=15)	Median	8.12	2.697	539	2.145	0.231	3.54	5.33
	Max	8.25	2.858	362	2.024	0.280	4.23	6.46

2.3.2 Seawater nutrient concentrations

Nutrient concentrations were similar to background levels in the Saronikos Gulf (Friligos, 1991) except for silicate, which was mostly higher than the background value of 1.22 μM even at one of the reference sites (Table 2.5). When values were < LOQ. (Limit Of Quantification) they were substituted with LOQ/2; LOQ. = 0.126 μM for NO_2 + NO_3 and 0.102 μM for NH_4. Statistically significant differences between sites were only detected for nitrite and silicate. Nitrite, however, had a very small range, varying from 0.040 ± 0.005 μM in REF B to 0.054 ± 0.002 μM in 200 E, and these were the only two sites that were significantly different. Silicate had a wider range (from 1.180 ± 0.269 μM in REF B to 6.371 ± 1.841 μM in 200 W); only site 200 W was significantly different from the reference sites according to pairwise comparisons. No significant differences and relatively uniform values were measured for phosphate, whereas nitrate and ammonium showed higher values at 200 E, although these differences were not significant, possibly due to high within-site variability.

Table 2.5. Average seawater nutrient concentrations (± SD, n=3) at Methana in June 2013. For the five sites, nitrite (NO_2^-), nitrate (NO_3^-), ammonium (NH_4^+), phosphate (PO_4^{3-}) and silicate (SiO_4^{4-}) concentrations are shown. Background values (Bgd) for the Aegean Sea from Friligos (1991). Different letters indicate significant differences according to post-hoc pairwise comparisons; n.d. = not determined.

	SEEP	**200 W**	**200 E**	**REF A**	**REF B**	**Bgd**
NO_3^- (μM)	0.070 ± 0.062	0.094 ± 0.069	0.559 ± 0.297	0.054 ± 0.054	0.085 ± 0.045	0.42
NO_2^- (μM)	0.054 ± 0.003^{a,b}	0.044 ± 0.005^{a,b}	0.059 ± 0.004^{b}	0.042 ± 0.004^{a,b}	0.040 ± 0.009^{a}	n.d.
NH_4^+ (μM)	0.232 ± 0.172	0.265 ± 0.189	1.075 ± 0.318	0.203 ± 0.189	0.298 ± 0.091	0.36
PO_4^{3-} (μM)	0.025 ± 0.008	0.031 ± 0.011	0.038 ± 0.009	0.024 ± 0.006	0.044 ± 0	0.12
SiO_4^{4-} (μM)	4.018 ± 0.671^{a,b}	6.371 ± 3.189^{a}	1.607 ± 0.288^{c}	1.883 ± 0.221^{b,c}	1.180 ± 0.466^{c}	1.22

2.3.3 Free sulphides in seawater

Free sulphides concentrations were below the measurable limit for this method (1 μM) at all five sites. In contrast, the sample from Loutra thermal baths had a concentration of free sulphides of 35 μM.

2.3.4 Heavy metals in sediment

Results in mg kg^{-1} of dry sediment (normalised to dry mass) are reported in Table 2.6 for each site and compared to the minimum values reported in a survey of heavy metal concentrations in sediments from the Aegean Sea (Karageorgis *et al*., 2005). As and Mn results were not considered reliable, as the concentrations determined in the reference material exceeded the confidence interval of the certified values, and are therefore not reported.

Table 2.6. Concentration of analysed elements in mg kg^{-1} of dry sediment from three sites with low (SEEP) and intermediate (200 W, 200 E) pH compared to reference values for the Aegean Sea (minimum values reported by Karageorgis *et al*., 2005; n.m. = not measured); for SEEP, 200 W and 200 E values are expressed as average ± standard deviation, n=3.

Element	SEEP	200 W	200 E	Reference values
Al	43916 ± 545	41804 ± 775	43166 ± 739	27000
Ca	25056 ± 428	23119 ± 282	24463 ± 380	46900
Cd	0.07 ± 0.04	0.06 ± 0.01	0.05 ± 0.01	n.m.
Co	2.85 ± 0.35	3.53 ± 0.35	2.24 ± 0.16	10
Cr	11.71 ± 0.57	15.46 ± 1.00	9.37 ± 0.87	39
Cu	3.67 ± 0.32	4.41 ± 0.37	3.95 ± 0.95	4
Fe	9436 ± 266	17802 ± 1084	8443 ± 257	13700
Li	7.39 ± 1.02	7.28 ± 0.70	7.11 ± 0.43	n.m.
Mg	2444 ± 153	2943 ± 123	2271 ± 29	17900
Ni	5.32 ± 0.81	5.89 ± 0.59	3.72 ± 0.31	35
Pb	14.99 ± 3.94	16.30 ± 2.56	10.76 ± 5.08	17
S	796.45 ± 100.16	561.06 ± 49.52	1746.45 ± 247.45	n.m.
Zn	13.31 ± 0.52	20.43 ± 0.78	12.43 ± 0.87	33

Average values of the two ecological risk indicators (SQG-Q_PEL and SQG-Q_ERM) are shown in Figure 2.4; all three sites are unimpacted according to

both indexes, except for the site 200 W, which is classified as impacted according to the SQG-Q_PEL index.

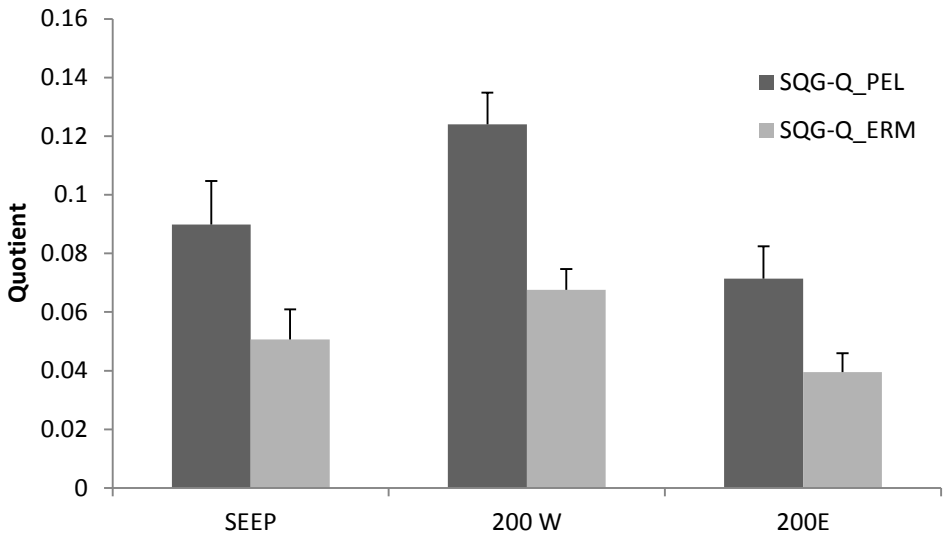

Figure 2.4. Mean (± SD) Sediment Quality Guidelines-quotient (SQG-Q) calculated with PEL and ERM for each site. If the index value is below 0.1, biological effects of heavy metals are unlikely. This is the case of the average value for most samples analysed here, except for 200 W, which is considered impacted according to the SQG-Q_PEL index. N=9 for all sites except SEEP, where n=6.

2.3.5 Heavy metals in macroalgae

Log-transformed metal concentrations were significantly different between sites for all elements analysed. Average concentration of elements in *Dictyota* sp. tissues and results of pairwise comparisons test are shown in Table 2.7. There was large spatial variability in metal content, but no specific metal concentration consistently increased with decreasing pH. Elevated concentrations were recorded at station 200 W for aluminium, arsenic and iron, and at REF A for aluminium and zinc.

Table 2.7. *Dictyota* sp. metal content at the five sites. Means (± SD; mg kg^{-1} dry mass; n=5) are shown for each metal and site; different letters indicate significant differences according to Tukey HSD test.

Element	SEEP	200 W	200 E	REF A	REF B
Al	66.58 ± 66.58^{a}	391.84 ± 497.99^{b}	75.01 ± 31.78^{a,b}	314.62 ± 243.57^{a,b}	89.77 ± 39.92^{a,b}
As	15.90 ± 2.30^{a}	39.02 ± 5.06^{d}	25.79 ± 6.00^{c}	18.41 ± 2.91^{a,b}	22.52 ± 0.83^{b,c}
Cd	0.014 ± 0.004^{a}	0.018 ± 0.006^{a,b}	0.034 ± 0.013^{b,c}	0.573 ± 0.228^{c}	0.067 ± 0.035^{d}
Co	0.059 ± 0.051^{a}	0.107 ± 0.044^{a}	0.096 ± 0.029^{a}	1.613 ± 0.706^{b}	0.119 ± 0.036^{a}
Cr	0.857 ± 0.156^{a,b}	2.526 ± 1.179^{c}	0.579 ± 0.112^{a}	1.204 ± 0.544^{b}	1.093 ± 0.489^{a,b}
Cu	2.069 ± 0.510^{a}	3.160 ± 0.602^{a,b}	3.435 ± 1.273^{a,b}	7.726 ± 3.337^{c}	4.771 ± 0.678^{b,c}
Fe	587.1 ± 95.7^{b}	5659.8 ± 1350.3^{a}	485.5 ± 104.6^{b,c}	316.3 ± 197.9^{c,d}	146.3 ± 72.8^{d}
Ni	0.916 ± 0.223^{a}	1.325 ± 0.281^{a}	1.338 ± 0.231^{a}	4.181 ± 1.292^{b}	2.554 ± 0.596^{b}
Pb	2.704 ± 0.480^{a}	17.605 ± 21.164^{b}	2.378 ± 0.616^{a}	25.979 ± 26.174^{b}	10.820 ± 12.842^{b}
Zn	10.95 ± 11.73^{a}	11.70 ± 1.19^{a}	8.22 ± 1.85^{a}	42.02 ± 20.75^{b}	14.68 ± 1.33^{a,b}

Values higher than ranges reported in the literature for seaweed tissues from unpolluted sites (Table 2.8) were found for aluminium, arsenic and iron at 200W and for aluminium and zinc in REF A.

Table 2.8. Comparison of metal concentration (mg kg^{-1} dry mass) in *Dictyota* spp. measured in this study with values found in the literature for unpolluted sites (n.d. = not determined; b.d.l. = below detection limit).

Element	This study (means range)	Abdallah *et al.*, 2005 (mean ± SD, n= 3)	McDermid and Stuercke, 2003 (range)	Raman *et al.*, 2013 (mean ± S.D., n=3)	Maher and Clarke, 1984
Al	66 – 391	n.d.	n.d.	n.d.	n.d.
As	15 – 39	n.d.	n.d.	n.d.	26.3
Cd	0.014 – 0.573	0.98 ± 0.3	n.d.	3.9 ± 0.3	n.d.
Co	0.059 – 1.613	4.3 ± 1.2	n.d.	5.5 ± 0.2	n.d.
Cr	0.579 – 2.526	1.1 ± 0.3	n.d.	b.d.l.	n.d.
Cu	2 – 8	1.3 ± 0.4	5	6.4 ± 0.3	n.d.
Fe	316 – 5659	n.d.	438 - 608	504 ± 12.4	n.d.
Ni	0.916 – 4.181	2.2 ± 0.6	n.d.	27 ± 0.4	n.d.
Pb	2 – 25	19.2 ± 5.5	n.d.	28.5 ± 3.5	n.d.
Zn	8 – 42	4.9 ± 1.2	13 - 16	11.7 ± 0.3	n.d.

2.3.6 Wave exposure

Values of modified effective fetch and maximum fetch for the three sites examined are shown in Table 2.9. All sites are classified as semi-exposed with regards to wave exposure.

Table 2.9. Table showing modified effective fetch (in km) and maximum fetch (in km) for the three sites examined. Fetch values were not calculates for the sites 200 W and 200 E because they were extremely close and with a very similar orientation to SEEP. All sites are considered semi-exposed according to the classification in table 2.3.

Site	Modified effective fetch (km)	Maximum fetch (km)
SEEP	11.17	51.37
REF A	18.91	130.42
REF B	15.81	53.12

2.4 Discussion

Seeps off northern Methana had a median pH value (7.69) similar to that predicted for 2100 according to the IPCC “business as usual” scenario (Caldeira and Wickett, 2005), whereas the reference sites had median values above 8. The seeps had no confounding gradients in temperature, salinity, total alkalinity, hydrogen sulphide or wave exposure. The low pH area off Methana had pCO_2 levels comparable to those reported at other ocean acidification analogues (Hall-Spencer *et al*., 2008; Kroeker *et al.*, 2011; Fabricius *et al.*, 2011; Kerrison *et al.*, 2011; Boatta *et al.*, 2013), making it suitable to assess community responses to increased pCO_2.

Enrichment in silicate, which was significantly different from reference values in one of the intermediate sites, is likely due to water-rock interactions common in

hydrothermal environments (D'Alessandro *et al.*, 2008). However, it is unlikely that silicate is limiting in the Aegean Sea; for instance, Si becomes limiting to diatoms when the N:Si ratio in seawater is higher than two (Gilpin *et al.*, 2004), whereas the background ratio for the Aegean Sea is 0.64 (Friligos, 1991). Significant differences in nitrite concentrations among sites are unlikely to explain the community changes either, as their range is very small (0.040 – 0.059 μM). Mediterranean organisms are normally not limited by silicate or inorganic nitrogen, but by phosphate (Zohary and Robarts, 1998), for which no confounding gradient was found.

No free sulphides were detected near the seeps, although they were present at the Loutra thermal baths, over 10 km from the study site. Hydrogen sulphide is toxic for cellular respiration, and it is often emitted from Mediterranean volcanic vents (Dando *et al.*, 1999; Caramanna *et al.*, 2011). However, sulphides are extremely reactive and oxidise quickly to sulphates in oxygenated waters. It is therefore common to find very low or undetectable sulphide concentrations just a few meters away from volcanic seeps. For instance, at Vulcano sulphides become undetectable at 30 m from the main vents, even though hydrogen sulphide gas has a concentration of 400 ppm at the main bubbling site (Boatta *et al.*, 2013).

No enrichment in sediment heavy metal in the low and intermediate pH sites was detected, even though sediment enriched in various elements have been reported from a nearby area (Hübner *et al.*, 2004). In addition, analysis of *Dictyota* sp. shows that no metal consistently increased in concentration as pCO_2 increased. Brown algae are considered a good indicator of bioavailable metals since they greatly bioaccumulate metals, often proportionally to metals concentration in surrounding seawater (Phillips, 1990). Values higher than

ranges reported in the literature were found for aluminium, arsenic and iron at 200 W and for aluminium and zinc in REF A (Table 2.8). Aluminium variability is likely to be related to local mineralogy (Karageorgis *et al.*, 2005), while enrichment in the other elements has previously been linked to hydrothermal activity (Hübner *et al.*, 2004). Metal bioaccumulation is a common occurrence at shallow and deep hydrothermal vents (Tarasov *et al.*, 2005; Couto *et al.*, 2010), but at Methana metal enrichment did not seem to have major effects at the community and species level. The intermediate and reference sites enriched in some elements (200 W and REF A) were not significantly different from the other intermediate and reference sites (200 E and REF B) with regards to key species percent cover and overall community structure (see Chapter 3).

As with other carbon dioxide seeps used as natural analogues for ocean acidification, Methana has some limitations. Motile taxa such as fish are able to move in and out of high CO_2 areas (Riebesell, 2008) and pelagic larvae can come from unaffected populations (Cigliano *et al.*, 2010). Moreover, carbonate chemistry is much more variable near the seeps than in reference conditions, as changes in current direction and intensity influence the dispersal of the dissolved gas emissions. Compared to other volcanic seeps, at Methana seawater pCO_2 is high and variable on a greater scale (>15 vs <0.3 km of shoreline; Hall-Spencer *et al*., 2008; Fabricius *et al.*, 2011; Boatta *et al.*, 2013). Thus, Methana might offer an opportunity to study ecological processes such as recruitment in a high CO_2 area probably less influenced by unaffected populations than smaller sites.

The need to translate results from laboratory experiments to more realistic systems has led to several areas with naturally high pCO_2 to be used to infer biological community responses to ocean acidification. Examples include

estuaries acidified by acid sulphate soils (Amaral *et al.*, 2011), groundwater submarine springs (Crook *et al*., 2012), upwelling regions (Manzello, 2010; Thomsen *et al.*, 2010; Mayol *et al.*, 2012) and rockpools with different carbonate chemistry (Moulin *et al.*, 2011; Evans *et al.*, 2013). None of the above are perfect ocean acidification analogues, as they can have confounding gradients in salinity and alkalinity (groundwater springs) or in temperature and nutrients (upwelling areas). In addition, low pH recorded in groundwater springs and acidified estuaries is not always caused by increased carbon dioxide concentrations, so only the effects of low pH on biological communities can be tested. However, studies from low pH/high CO_2 sites mostly report decreased abundance and diversity of calcifying organisms, in accord with findings from CO_2 seeps and laboratory experiments (Hall-Spencer *et al.*, 2008; Kroeker *et al.*, 2013a; Fabricius *et al.*, 2014). General patterns of community responses to ocean acidification can then be detected using areas with naturally low pH, even though confounding factors should always be taken into account.

Overall, our data show that the examined seeps off Methana offer an opportunity to study the effects of high pCO_2 levels on natural benthic communities in an oligotrophic environment. The general limitations of using CO_2 seeps should, however, be taken into account. These seeps could also be used to study how ecological processes are influenced by carbon dioxide on a scale of kilometres, not tens of meters as the other seeps currently used as ocean acidification analogues.

Chapter 3

Changes in subtidal macroalgal communities along pCO_2 gradients at Mediterranean volcanic seeps

Aspects of this chapter have been published as:

C. Baggini, M. Salomidi, E. Voutsinas, L. Bray, E. Krasakopoulou, J.M. Hall-Spencer (2014). Seasonality affects macroalgal community response to increases in pCO_2. *PLoS ONE*, 9: e106520.

Abstract

Shifts in macroalgal communities have been detected along pCO_2 gradients at volcanic seeps in a few temperate (Italy) and tropical (Papua New Guinea) settings. However, replication of these observations is needed to expand our ability to predict how marine ecosystems will change due to ocean acidification. The present study determined macroalgal diversity and abundance along pCO_2 gradients caused by volcanic seeps off Methana (Greece) and Vulcano (Italy) using visual census and destructive sampling methods, respectively. At Methana, *Cystoseira corniculata* was dominant in autumn and *Sargassum vulgare* C.Agardh was dominant in spring near the seeps. The articulated coralline alga *Jania rubens* had significantly higher cover at reference sites, but only in autumn. Diversity decreased with increasing CO_2 regardless of sampling season. At Vulcano, the main habitat-forming algal species changed as CO_2 level increased: at the reference site *Cystoseira* spp. and *Dictyopteris polypodioides* (A.P.De Candolle) J.V.Lamouroux were dominant, at elevated pCO_2 levels *Sargassum vulgare* greatly increased in abundance replacing *D. polypodioides*. These data are consistent with results from laboratory experiments and observations at other Mediterranean CO_2 seep sites in that benthic communities decreased in calcifying algal cover with increasing pCO_2. This chapter demonstrates that natural pCO_2 gradients can help us envisage how benthic communities will be affected by ocean acidification in a range of environmental conditions, and that benthic community responses to ocean acidification can be strongly affected by season.

3.1 Introduction

Studies on single species can be very useful for formulating hypotheses about how biological communities may respond to ocean acidification. However, work on global warming demonstrates that most temperature-associated causes of severe population decline originate not from direct physiological responses to heat, but result from modified species interactions (Cahill *et al.*, 2013). Similar trends arise in lake acidification (Locke and Sprules, 2000) and it is anticipated that consequences of ocean acidification will be similar (Gaylord *et al.*, 2014). Responses of seaweed species to increased carbon dioxide are poorly known (Harley *et al.*, 2012; Koch *et al.*, 2013), with laboratory experiments to date concentrated on calcifying red and green algae (Gao *et al.*, 1993; Büdenbender *et al.*, 2011; Price *et al.*, 2011). So far, evidence indicates that calcifying algae will be negatively affected by ocean acidification while some fleshy algae may thrive (Kroeker *et al.*, 2013a; Brodie *et al.*, 2014). There is very little information on brown seaweed responses to elevated pCO_2 despite the fact that they are key species in temperate rocky habitats worldwide (Steneck *et al.*, 2002). In addition, a species can respond differently to ocean acidification in single species experiments and in natural communities because of inter-specific interaction; for instance, crustose coralline algae may cope with elevated CO_2, but be outcompeted by fleshy algae (Kroeker *et al.*, 2013c).

Our limited ability to predict community responses of macroalgal communities to ocean acidification worldwide and the few experiments performed on Mediterranean species add value to studies examining community responses using CO_2 seeps in the Mediterranean Sea. Results from surveys at seeps off Ischia and Vulcano (both in Italy) show how increased carbon dioxide is likely to cause shifts in macroalgal communities. As CO_2 increases at these sites,

coralline algae are replaced by canopy-forming brown algae such as *Sargassum vulgare* in the shallow subtidal off Ischia (Porzio *et al.*, 2011) or brown foliose algae such as *Dictyota* spp. and non-calcified *Padina* sp. off Vulcano (Johnson *et al.*, 2012; Graziano *et al*., unpublished data). This response to increased CO_2 differs from shifts towards opportunistic green macroalgal species such as *Ulva* spp. or mat-forming algae reported in stressed marine benthic ecosystems, such as those exposed to eutrophication (Airoldi and Beck, 2007; Connell *et al.*, 2008), where decreased floral complexity can have detrimental effects on local biodiversity (Scherner *et al*., 2013) and indirectly affect the abundance of many commercial species (Harley *et al.*, 2012). On the other hand, increased abundance of brown perennial algae near volcanic CO_2 seeps suggests that carbon dioxide may be a useful resource that can benefit perennial habitat-forming algae (Porzio *et al.*, 2011; Connell *et al.*, 2013).

This study aims to assess changes in macroalgal communities along pCO_2 gradients off Greece and Italy. I characterised benthic communities at a shallow subtidal site in the Eastern Mediterranean Sea (Methana, Greece) in spring and autumn as well as those off Vulcano (Italy) at a depth of 3-5 metres in spring. I was mindful of the fact that responses to increased carbon dioxide in these two environments could be substantially different from those previously recorded, since the Aegean Sea has lower average nutrient concentrations than those in the Thyrrenian Sea (Moutin and Raimbault, 2002). Food limitation has been shown to exacerbate the negative influence of ocean acidification on benthic invertebrates (Melzner *et al.*, 2011; Rodolfo-Metalpa et al., 2011), so nutrient limitation may act in combination with ocean acidification to negatively affect seaweed communities. At ambient levels of CO_2 around Methana and Vulcano,

subtidal brown algae such as *Cystoseira* spp. and *Dictyopteris polypodioides* have the highest biomass (Pérès and Picard, 1964). These subtidal species are expected to be less sensitive to ocean acidification than calcifying algae (Kroeker *et al.*, 2013a), but they could be more sensitive to ocean acidification than intertidal brown algae. As subtidal habitats are more stable than intertidal ones, subtidal organisms are generally thought to be more vulnerable to environmental changes (Lobban and Harrison, 1994).

In addition, there are very few studies dealing with the seasonal patterns of benthic community changes along pCO_2 gradients, even though temperate coastal waters vary greatly among seasons (Coma *et al.*, 2000). These ecosystems undergo large yearly changes in light and temperature regimes, which indirectly influence other factors important for biological communities, such as nutrient levels (Pingree *et al.*, 1976). In the Mediterranean Sea, these three factors strongly influence macroalgal communities: macroalgal biomass peaks in late spring, and community composition changes among seasons (Sala and Boudouresque, 1997). Specifically, many mat-forming algae disappear and most erect algae decrease in cover during the cold season (Piazzi *et al.*, 2004).

3.2 Methods

3.2.1 Methana experimental design and data analysis

The first part of the work for this thesis chapter was conducted along a pCO_2 gradient off Methana (Greece). Five sites at three pCO_2 levels were used: SEEP (high CO_2 level), 200 W and 200 E (intermediate CO_2 level), REF A and REF B (reference CO_2 level); for a detailed description of study sites, see Chapter 2. Benthic community composition was assessed in May and

September 2012 using visual census (detailed sampling dates and sample sizes are reported in Table 1.1B): samples were collected between 0.7 and 1.0 m below mean sea level using 20×20 cm quadrats on horizontal and sub-horizontal rocky substrata (Fraschetti *et al.*, 2005). A frame with 25 4×4 cm squares was used to assess percentage cover (C%) and number of taxa (S). Percentage cover of algae and sessile invertebrates was determined by assigning each taxon a score ranging from 0 to 4 within each square and summing the 25 estimates (Dethier *et al.*, 1993). Final values were expressed as percentages. Taxa were identified to the lowest possible level, usually species, except for turf algae; this functional group was defined as sparse to thick mats of small and juvenile algae less than 2 cm high (Steneck and Dethier, 1994). Seven replicate quadrats randomly chosen but placed at least 4-5 m from each other were assessed for every site in May 2012 and six replicates were collected in September 2012. The selected sample size represented the maximum number of samples that could be randomly collected from sub-horizontal surfaces at the smallest site (SEEP, ~20 m of shoreline) at the selected depth (0.7-1.0 m below sea level). Samples were collected in May, when Mediterranean seaweeds reach their biomass peak (Ballesteros, 1984) and September, when Greek shallow benthic communities have been exposed for over three months to temperatures > 25°C (Maria Salomidi, personal communication).

Differences in community structure and composition were assessed using Permutational Multivariate Analysis of Variance (PERMANOVA, (Anderson *et al.*, 2003); PRIMER 6 and PERMANOVA + package (Clarke and Gorley, 2006)). The analysis had two fixed factors: season (two levels) and site (five levels). The analyses were performed on Bray-Curtis measures of square root

transformed data, using 9999 permutations of residuals under a reduced model. Pair-wise comparisons were then performed for significant factors with more than two levels. Since site was a significant factor in the PERMANOVA, its levels were compared using a SIMPER analysis to identify the taxa driving dissimilarities.

Macroalgal cover data were used to calculate Shannon diversity (Shannon and Weaver, 1949) and Pielou's evenness (Pielou, 1966) for each sample. The two indices were analysed using an ANOVA followed by a Tukey HSD test for multiple comparisons. After testing for normality and homoscedasticity, canopy-forming and calcifying algae arcsin-transformed percent cover was analysed using a two-way ANOVA with site and functional group as fixed factors; seasons were tested separately. The site*species interaction was then decomposed to obtain multiple comparisons among sites for each season separately. The same analysis was then performed for selected single species. All univariate analyses were performed using SPSS v19 (IBM, USA).

3.2.2 Vulcano study site

The second part of the work for this thesis chapter was conducted along a pCO_2 gradient off the island of Vulcano in the Eolian archipelago (Italy). This island is an active volcano formed in the collision of the Eurasian and Asian plates. The gradient is caused by submarine volcanic seeps emitting over 97% CO_2 (Inguaggiato *et al.*, 2012; Boatta *et al.*, 2013), which lower seawater pH to 5.5-5.6 at the main bubbling site. The hydrothermal fluids also contain hydrogen sulphide (Italiano *et al.*, 1984; Capaccioni *et al.*, 2001), which is potentially toxic to cellular respiration. However, hydrogen sulphide rapidly oxidises to sulphate; sulphide concentrations are in fact very low (< 50 μMol kg^{-1}) at > 20 m from the main seeps as water is well-oxygenated all over the bay (Boatta *et al.*, 2013). I

chose an area for this study that was a ~200 m stretch of rocky shore at >30 m from the main seeps, where pH ranges from 7.55 to 8.2 (Boatta *et al.*, 2013). Along this gradient, the three sites (pH ± S.D.) shown in Figure 3.1 were selected, one with high (High CO_2; pH 7.57 ± 0.23, n = 19), one with intermediate (Mid CO_2; pH 7.94 ± 0.16, n = 18) and one with reference pCO_2 (REF A; pH 8.14 ± 0.05, n = 11); pH data are from monitoring conducted in September 2009 and April 2010 from Graziano *et al.* (unpublished data).

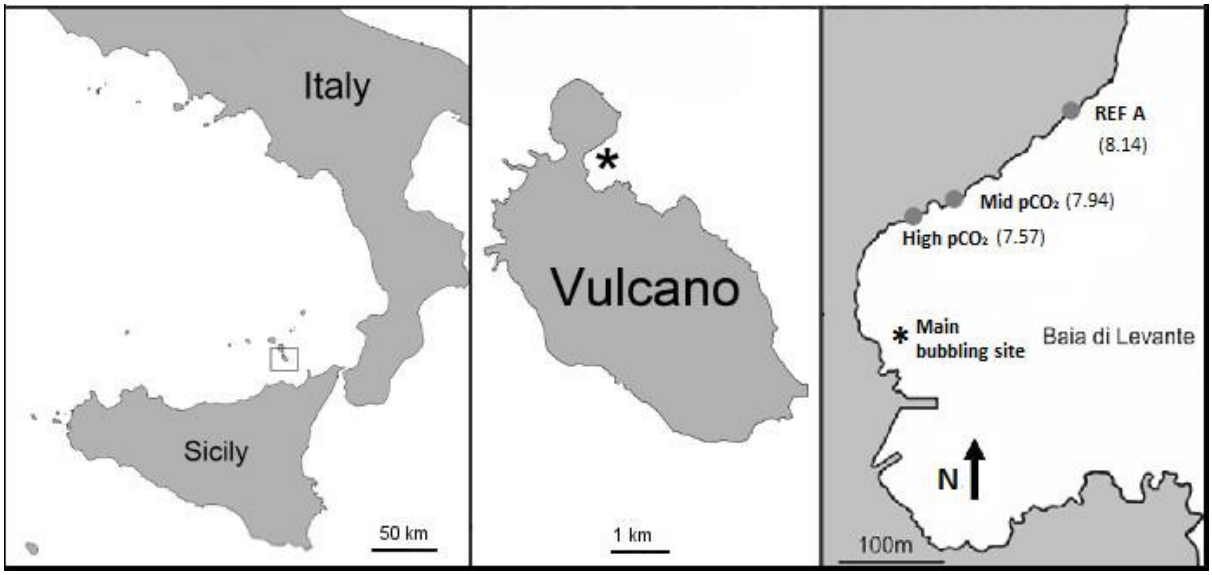

Figure 3.1. Vulcano Island (Sicily, Southern Italy) and study sites; the asterisk marks the main bubbling area, whereas grey circles indicate the three sampling sites and their average pH, with decreasing pCO_2 moving away from the bubbling area.

Geochemical surveys in Levante bay in 2011 have shown that these seeps do not influence the main seawater elements and data in Table 3.1A demonstrate that temperature, salinity and total alkalinity do not change significantly among the sites used for this chapter (Boatta *et al.*, 2013). Nutrients were also measured (Table 3.1B); nitrite and silicate concentrations were significantly different among sites, while nitrate levels were relatively stable along the CO_2 gradient and phosphate levels remained below detection limit (~10 nmol L^{-1}) at

all sites (Johnson, 2012). The increase in nitrates was very small (0.01 µM), and silicates are not believed to be limiting for marine organisms at the reference site, as phosphates are the limiting nutrient in Mediterranean waters (Zohary and Robarts, 1998).

Table 3.1. (A) Mean (±SD) seawater temperature (T), salinity (S) and total alkalinity (TA) recorded from September 2009 to July 2011 at three sites used for this chapter (data from Boatta *et al.*, 2013). (B) Mean (± SD) dissolved nutrient concentrations at three studied sites at Vulcano (n = 5-6). Phosphate was also determined but at all stations was below the detection limit of the AutoAnalyser, i.e. ~10 nmol L^{-1} (data from Johnson, 2012).

A)

Site	T (°C)	S (‰)	n	TA (µEq kg^{-1})	n
High CO_2	21.71 ± 4.93	37.49 ± 0.64	41	2524.7 ± 0.6	9
Mid CO_2	21.67 ± 4.93	37.59 ± 0.58	41	2520.5 ± 6.6	9
REF A	21.66 ± 4.22	37.45 ± 0.66	22	2532.5 ± 20.9	7

B)

Site	Nitrite (µM)	Nitrate (µM)	Silicate (µM)
High CO_2	0.02 ± 0.002	0.33 ± 0.22	19.39 ± 2.77
Mid CO_2	0.02 ± 0.007	0.16 ± 0.13	15.12 ± 5.48
REF A	0.01 ± 0.002	0.24 ± 0.11	3.43 ± 0.11

As for minor seawater elements, there was a marked increase in iron concentration, which reached values up to three orders of magnitude higher than ambient concentrations reported for the Mediterranean Sea (Sarthou and Jeandel, 2001; Figure 3.2). Iron is an essential micronutrient for marine algae and is a limiting factor for their growth in many areas in the world ocean (Geider and La Roche, 1994). In the Mediterranean Sea, however, iron is only limiting in special circumstances (Bennet and Guien, 2006) due to the very low phosphate concentrations in the region (Zohary and Robarts, 1998). The minimum iron value measured off Vulcano during a recent geochemical survey was 57 nMol/kg (Boatta *et al.*, 2013), much higher than phosphate concentrations in the area (< 10 nMol/kg; Johnson, 2012). According to the modified Redfield ratio

(Martin *et al.*, 1990), iron is limiting when its concentration is lower than 10% of that of phosphate, which is not the case in Vulcano.

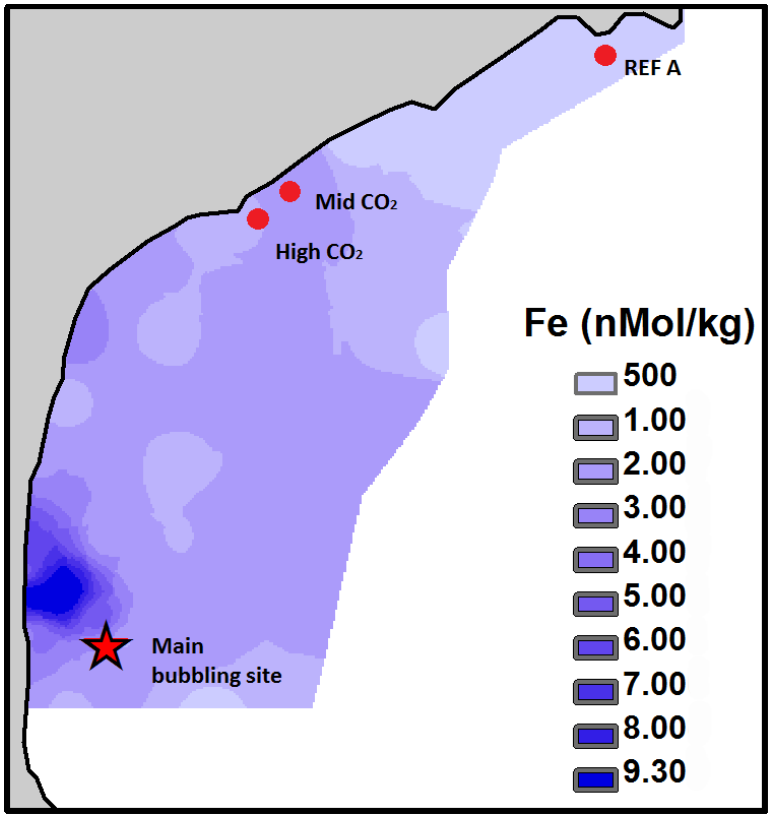

Figure 3.2. Distribution map adapted from a recent geochemical survey (Boatta *et al.*, 2013) in the Baia di Levante showing the iron concentrations measured in the area in April 2011. The sites used for this thesis have been superimposed (red dots); the red star indicates the main bubbling site. Data for these maps were collected from around 70 sampling points within the bay.

Elevated heavy metal concentrations are also a common feature of volcanic areas (Tarasov *et al.*, 2005). A recent geological survey of Baia di Levante (Figure 3.3) revealed that parts of the bay have sediment of poor or bad quality according to the Marine Sediment Pollution Index (MSPI; Shin and Lam, 2001). The sites chosen for the present study have average or good sediment condition, which only have a moderate potential for causing adverse biological effects according to the Sediment Quality Guideline Quotient (SQG-Q, for its

definition see Chapter 2; Vizzini *et al.*, 2013). The change in pCO_2 values caused by the seeps is therefore the most likely driver of any biological change observed at the study sites.

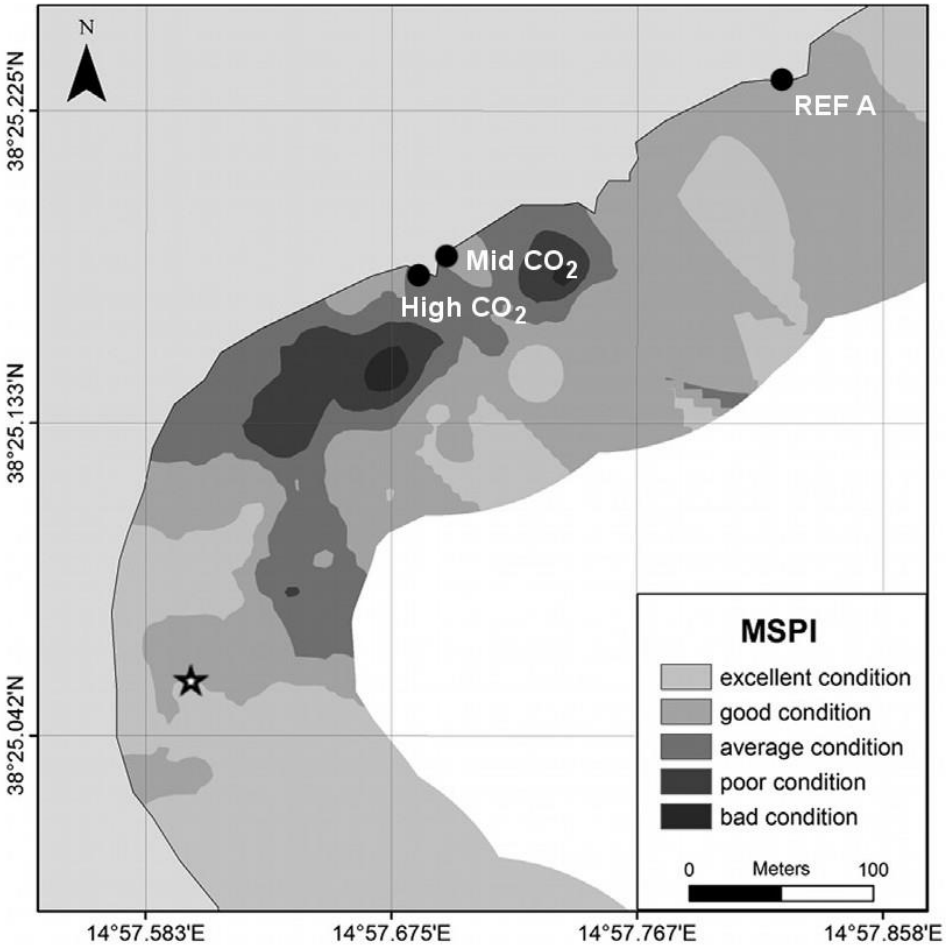

Figure 3.3. Results from a recent geochemical survey in the Baia di Levante showing the Marine Sediment Pollution Index (MSPI) from sediment collected in autumn 2011. The sites used for this thesis have been superimposed (black dots); the star indicates the main bubbling site. Data for these maps were collected from 50 sampling points within the bay (Vizzini *et al.*, 2013).

3.2.3 Vulcano experimental design and data analysis

Macroalgae were collected by scraping 20 x 20 cm squares of rock with hammer and chisel following a method developed for this type of Mediterranean shore (Ballesteros, 1986). Four replicates were collected in three sites in May

2010 by Mariagrazia Graziano and Kristy Kroeker, immediately frozen and transported to the laboratory (detailed sampling dates and sample sizes are reported in Table 1.1B). Samples were then sorted and identified to the lowest possible taxonomic level, mostly to the species level, except for turf algae; this functional group was defined as sparse to thick mats of small and juvenile algae less than 2 cm high (Steneck and Dethier, 1994). For biomass determination, dry biomass of each taxon was obtained drying the identified samples in an oven at 60ºC for 24 hours. The obtained data was analysed using the same procedure outlined above for Methana, but using an experimental design with one fixed factor with three levels ("Site") and log-transforming the biomass data for functional groups and single species analyses.

3.3 Results

3.3.1 Methana benthic community

Overall, 18 macroalgal taxa and three invertebrate taxa (two sponges and one hydrozoan) were recorded. Benthic communities significantly differed among sites and seasons (Table 3.2A), with a significant interaction between the two factors (pseudo-$F_{4,55}$=1.754, p(perm)=0.0457). In spring the high pCO_2 site was significantly different from the reference sites, while the intermediate pCO_2 sites were not significantly different from any of them. In autumn, the high pCO_2 site was significantly different from all other sites (Table 3.2B). Site had a significant effect on diversity (p = 0.049, Table 3.3) with a clear decrease as CO_2 increased (0.94 ± 0.10, n=26 to 0.55 ± 0.08, n=13; mean ± SE).

Table 3.2. (A) PERMANOVA analysis on square-root transformed percentage cover of Methana benthic communities. The first table shows main factors and their interaction and degrees of freedom (df), sum of squares (SS), pseudo-F, permutational p and unique permutations for each of them. Season, site and their interaction all have a significant effect. (B) Results from pair-wise comparisons between sites for each season (different letters represent significantly different groups).

(A)

Source	df	SS	Pseudo-F	p (perm)	Unique perms
Season	1	31069	19.234	**0.0001**	9949
Site	4	21820	3.377	**0.0001**	9918
Season x Site	4	11330	1.754	**0.0457**	9916
Residual	55	88840			
Total	64	1.5273E5			

(B)

Season	Sites				
Spring	SEEP [a]	200 W [a,b]	200 E [a,b]	REF A [b]	REF B [b]
Autumn	SEEP [a]	200 W [b]	200 E [b]	REF A [b]	REF B [b]

Shannon diversity (H') and Pielou's evenness (J') of benthic communities off Methana were pooled among seasons and sites as no significant differences were detected between seasons and between sites with the same CO_2 level (Figure 3.4). Although the factor 'site' had a significant effect on Shannon diversity (Table 3.3), no significant differences were detected by the Tukey test. However, both indices show a clear decreasing trend in the diversity of the rocky shore sessile communities from reference to high CO_2 levels, with Shannon's diversity index almost halving (0.94 ± 0.40 to 0.55 ± 0.37; mean ± SD).

Table 3.3. ANOVA results for (A) Shannon diversity (H') and (B) Pielou's evenness (J') of Methana benthic communities. The Tables show main factors and their interactions and sum of squares (SS), degrees of freedom (df), Mean Squares (MS), F-ratios (F) and p values. Significant p values (< 0.05) are highlighted. Results from pairwise comparisons among sites were never significant and are not reported.

A) Source	Type III SS	df	MS	F	p
Site	1.438	4	0.359	2.557	**0.049**
Season	0.261	1	0.261	1.859	0.178
Site x Season	0.232	4	0.058	0.413	0.798
Error	7.731	55	0.141		
Total	9.664	64			

B) Source	Type III SS	df	MS	F	p
Site	0.282	4	0.071	1.285	0.287
Season	0.166	1	0.166	3.022	0.088
Site x Season	0.119	4	0.030	0.539	0.708
Error	3.022	55	0.055		
Total	3.568	64			

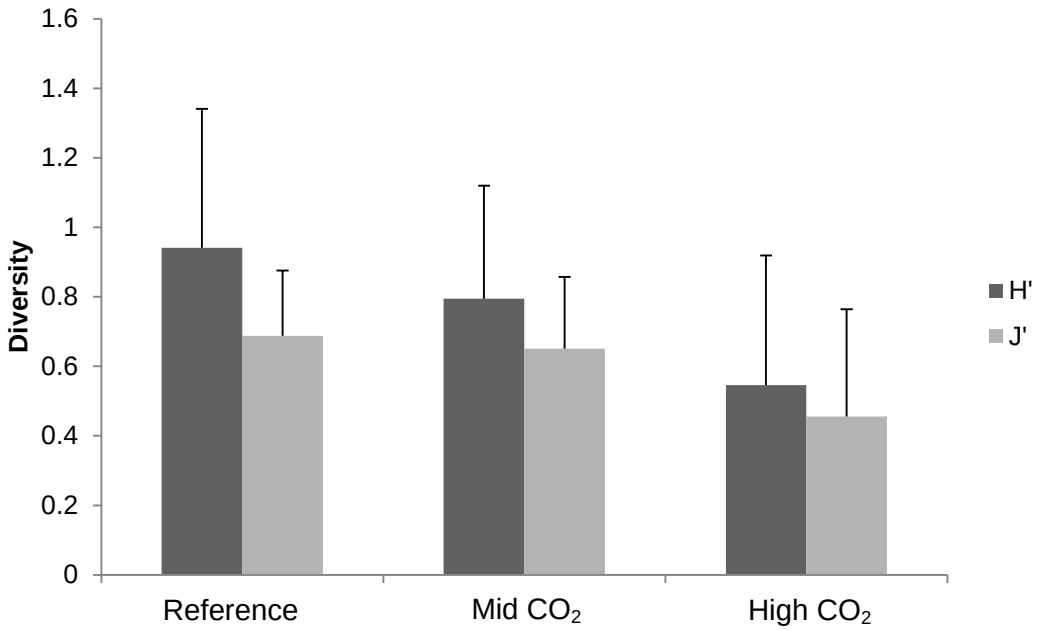

Figure 3.4. Mean (± SD) Shannon diversity (H') and Pielou's evenness (J') at high (n=13), intermediate (n=26) and reference (n=26) CO_2 at Methana rocky shores at depths between 0.7 and 1.0 m pooling sites and season.

The SIMPER analysis among sites shows which taxa contributed most to the detected differences (Table 3.4). The main drivers of differences between groups were canopy-forming algae such as *Cystoseira corniculata* and *Sargassum vulgare* and calcareous algae such as coralline crustose algae (CCA), the articulated coralline alga *Jania rubens* and the calcified brown alga *Padina pavonica*.

Table 3.4. SIMPER analysis of Methana benthic communities showing the average dissimilarities between each pair of sites and which species contributed up to 90% of the dissimilarity. For each taxon, the average abundance in the two groups that are being compared, their average dissimilarity, the dissimilarity to standard deviation ration and the taxon contribution and cumulative contribution are shown. CCA stands for coralline crustose algae.

Groups SEEP & 200 E; Average dissimilarity = 65.40						
Taxon	SEEP Av.Abund	200 E Av.Abund	Av.Diss	Diss/SD	Contrib%	Cum.%
Cystoseira corniculata	5.27	6.76	14.85	1.28	22.71	22.71
CCA	0.11	2.86	8.80	0.88	13.45	36.16
Sargassum vulgare	2.58	0.85	8.46	0.74	12.93	49.09
Jania rubens	0.00	2.63	7.70	0.78	11.77	60.85
Dictyota sp.	1.16	1.59	6.14	0.91	9.38	70.24
Sargassum sp.	1.50	0.00	4.28	0.45	6.54	76.78
Padina pavonica (not calcified)	1.12	0.27	3.93	0.51	6.02	82.79
Bare substratum	1.08	0.00	3.16	0.60	4.83	87.62
Falkenbergia sp.	0.46	0.00	1.38	0.51	2.10	89.73
Cladophora sp.	0.50	0.00	1.36	0.39	2.08	91.80
Groups SEEP & 200 W; Average dissimilarity = 63.83						
Taxon	SEEP Av.Abund	200 W Av.Abund	Av.Diss	Diss/SD	Contrib %	Cum.%
Cystoseira corniculata	5.27	6.52	14.63	1.30	22.92	22.92
Sargassum vulgare	2.58	0.59	8.96	0.70	14.04	36.96
Cladostephus spongiosus	0.36	1.95	6.54	0.85	10.24	47.20
Dictyota sp.	1.16	1.56	6.18	0.85	9.68	56.88
Jania rubens	0.00	1.90	5.46	0.65	8.56	65.44
CCA	0.11	1.57	4.81	0.63	7.53	72.97
Sargassum sp.	1.50	0.55	4.27	0.52	6.69	79.65

Padina pavonica (not calcified)	1.12	0.26	3.96	0.51	6.21	85.86
Bare substratum	1.08	0.64	2.89	0.58	4.53	90.39

Groups 200 E & 200 W; Average dissimilarity = 43.27

Taxon	200 E Av.Abund	200 W Av.Abund	Av.Diss	Diss/SD	Contrib%	Cum.%
Cystoseira corniculata	6.76	6.52	9.58	1.11	22.14	22.14
CCA	2.86	1.57	8.68	0.92	20.06	42.21
Cladostephus spongiosus	0.00	1.95	5.86	0.82	13.54	55.74
Jania rubens	2.63	1.90	3.41	0.60	7.87	63.61
Dictyota sp.	1.59	1.56	3.11	0.66	7.18	70.80
Sargassum vulgare	0.85	0.59	2.81	0.74	6.50	77.30
Bare substratum	0.00	0.64	1.62	0.40	3.75	81.05
Padina pavonica (not calcified)	0.27	0.26	1.54	0.40	3.56	84.61
Halopteris scoparia	0.15	0.42	1.54	0.39	3.56	88.17
Sargassum sp.	0.00	0.55	1.44	0.49	3.33	91.49

Groups SEEP & REF A; Average dissimilarity = 74.58

Taxon	SEEP Av.Abund	REF A Av.Abund	Av.Diss	Diss/SD	Contrib%	Cum.%
Cystoseira corniculata	5.27	5.01	15.26	1.36	20.46	20.46
Jania rubens	0.00	3.77	11.28	0.94	15.13	35.59
Sargassum vulgare	2.58	0.34	8.76	0.70	11.75	47.34
Bare substratum	1.08	1.71	6.83	1.29	9.15	56.50
Dictyota sp.	1.16	1.98	6.49	0.76	8.70	65.20
CCA	0.11	1.83	5.13	0.87	6.87	72.07
Sargassum sp.	1.50	0.00	4.28	0.45	5.74	77.81
Padina pavonica (not calcified)	1.12	0.00	3.27	0.44	4.38	82.19
Cystoseira amentacea	0.00	0.93	2.93	0.53	3.93	86.12
Padina pavonica (calcified)	0.00	0.75	2.44	0.52	3.27	89.40
Halopteris scoparia	0.00	0.66	2.03	0.40	2.73	92.12

Groups 200 E & REF A; Average dissimilarity = 46.56

Taxon	200 E Av.Abund	REF A Av.Abund	Av.Diss	Diss/SD	Contrib%	Cum.%
Cystoseira corniculata	6.76	5.01	11.28	1.21	24.22	24.22
CCA	2.86	1.83	6.48	0.78	13.93	38.15
Bare substratum	0.00	1.71	5.02	0.99	10.77	48.92
Dictyota sp.	1.59	1.98	4.84	0.84	10.39	59.31
Jania rubens	2.63	3.77	4.39	0.86	9.43	68.74
Sargassum vulgare	0.85	0.34	3.15	0.77	6.77	75.50
Cystoseira amentacea	0.00	0.93	2.81	0.53	6.04	81.55
Padina pavonica (calcified)	0.00	0.75	2.34	0.52	5.04	86.58
Halopteris scoparia	0.15	0.66	2.30	0.48	4.95	91.53

Groups 200 W & REF A; Average dissimilarity = 53.21

Taxon	200 W Av.Abund	REF A Av.Abund	Av.Diss	Diss/SD	Contrib%	Cum.%
Cystoseira corniculata	6.52	5.01	10.33	1.20	19.42	19.42
CCA	1.57	1.83	6.12	0.92	11.50	30.92
Bare substratum	0.64	1.71	5.85	1.14	10.99	41.91
Jania rubens	1.90	3.77	5.74	0.80	10.78	52.69
Cladostephus spongiosus	1.95	0.00	5.66	0.81	10.64	63.33
Dictyota sp.	1.56	1.98	4.96	0.78	9.32	72.65
Cystoseira amentacea	0.00	0.93	2.82	0.53	5.31	77.96
Halopteris scoparia	0.42	0.66	2.56	0.48	4.82	82.77
Sargassum vulgare	0.59	0.34	2.40	0.58	4.51	87.29
Padina pavonica (calcified)	0.00	0.75	2.35	0.52	4.42	91.71

Groups SEEP & REF B; Average dissimilarity = 72.33

Taxon	SEEP Av.Abund	REF B Av.Abund	Av.Diss	Diss/SD	Contrib%	Cum.%
Cystoseira corniculata	5.27	4.64	15.07	1.30	20.84	20.84
Sargassum vulgare	2.58	0.60	8.90	0.71	12.31	33.15
Sargassum sp.	1.50	1.86	7.36	0.81	10.18	43.33
CCA	0.11	2.44	6.80	1.15	9.41	52.73
Jania rubens	0.00	2.09	5.96	0.79	8.24	60.97
Dictyota sp.	1.16	1.61	5.76	0.76	7.97	68.94
Bare substratum	1.08	1.46	4.65	0.88	6.42	75.36
Padina pavonica (calcified)	0.00	1.18	3.66	0.87	5.06	80.42
Padina pavonica (not calcified)	1.12	0.00	3.26	0.44	4.51	84.92
Halopteris scoparia	0.00	0.97	2.98	0.43	4.12	89.04
Falkenbergia sp.	0.46	0.00	1.32	0.51	1.82	90.86

Groups 200 E & REF B; Average dissimilarity = 53.38

Taxon	200 E Av.Abund	REF B Av.Abund	Av.Diss	Diss/SD	Contrib%	Cum.%
Cystoseira corniculata	6.76	4.64	12.03	1.18	22.55	22.55
CCA	2.86	2.44	7.52	1.06	14.08	36.62
Sargassum sp.	0.00	1.86	5.37	0.69	10.06	46.69
Jania rubens	2.63	2.09	4.08	0.76	7.64	54.33
Bare substratum	0.00	1.46	4.00	0.70	7.49	61.81
Sargassum vulgare	0.85	0.60	3.96	0.68	7.42	69.23
Dictyota sp.	1.59	1.61	3.96	0.79	7.41	76.64
Padina pavonica (calcified)	0.00	1.18	3.50	0.87	6.56	83.20
Halopteris scoparia	0.15	0.97	3.12	0.49	5.84	89.04
Padina pavonica (not calcified)	0.27	0.00	0.83	0.30	1.55	90.59

Groups 200 W & REF B; Average dissimilarity = 57.06

Taxon	200 W Av.Abund	REF B Av.Abund	Av.Diss	Diss/SD	Contrib%	Cum.%
Cystoseira corniculata	6.52	4.64	11.48	1.23	20.13	20.13
CCA	1.57	2.44	6.89	1.09	12.07	32.20
Cladostephus spongiosus	1.95	0.00	5.55	0.82	9.73	41.93
Sargassum sp.	0.55	1.86	5.48	0.80	9.60	51.54
Bare substratum	0.64	1.46	4.21	0.78	7.38	58.92
Dictyota sp.	1.56	1.61	4.17	0.76	7.32	66.24
Jania rubens	1.90	2.09	4.04	0.75	7.09	73.32
Halopteris scoparia	0.42	0.97	3.83	0.54	6.71	80.03
Padina pavonica (calcified)	0.00	1.18	3.49	0.87	6.12	86.15
Sargassum vulgare	0.59	0.60	3.22	0.52	5.64	91.79

Groups REF A & REF B; Average dissimilarity = 54.82

Taxon	REF A Av.Abund	REF B Av.Abund	Av.Diss	Diss/SD	Contrib%	Cum.%
Cystoseira corniculata	5.01	4.64	10.88	1.19	19.84	19.84
Jania rubens	3.77	2.09	6.05	0.89	11.03	30.87
Bare substratum	1.71	1.46	6.03	1.13	10.99	41.86
Sargassum sp.	0.00	1.86	5.24	0.68	9.55	51.41
Dictyota sp.	1.98	1.61	4.95	0.75	9.03	60.44
CCA	1.83	2.44	4.91	1.23	8.95	69.39
Halopteris scoparia	0.66	0.97	4.17	0.61	7.60	76.99
Padina pavonica (calcified)	0.75	1.18	3.78	0.93	6.89	83.88
Cystoseira amentacea	0.93	0.00	2.65	0.53	4.84	88.71
Sargassum vulgare	0.34	0.60	2.58	0.40	4.70	93.42

Taxa driving community differences among sites (Table 3.4) were grouped into two categories; canopy-forming algae (*Cystoseira corniculata*, *Cystoseira amentacea* (C.Agardh) Bory de Saint-Vincent, *Sargassum vulgare* and *Cladostephus spongiosum* (Hudson) C.Agardh) and calcifying algae (CCA, *Jania rubens*, *Corallina* sp., *Amphiroa* sp. and *Padina pavonica*). The two categories are shown for May (Figure 3.5A) and September (Figure 3.5B). As no significant differences were found within intermediate and reference sites, pCO_2 levels were pooled for clarity. Both categories showed very strong seasonal patterns: no differences in canopy-forming algal cover were detected

in May, but in September the high pCO_2 site had higher canopy cover than the reference sites. Likewise, calcifying algae showed no significant difference among pCO_2 levels in spring, but in autumn the high pCO_2 site had a significantly lower cover of calcareous algae compared to intermediate and control pCO_2 levels.

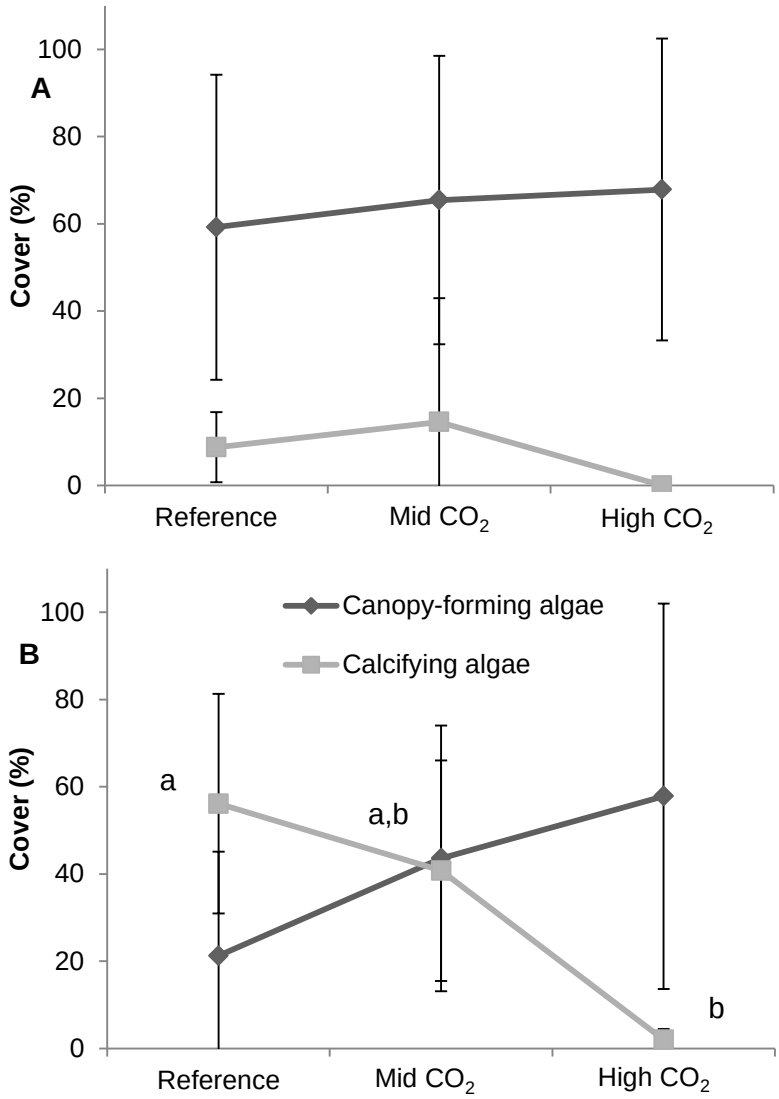

Figure 3.5. Mean percentage cover (± SD) of canopy-forming algae (black) and calcifying algae (grey) in May (a) and September (b) at high (n=6), intermediate (n=14) and reference (n=14) CO_2 conditions off Methana. Different letters indicate significant differences between groups.

The species forming these two categories changed along the pCO_2 gradient depending on the season, and the main canopy-forming and calcareous species covers are shown for May and September in Figure 3.7A and 3.7B, respectively. As no significant differences were found within intermediate and reference sites, pCO_2 levels were pooled for clarity. In spring, *S. vulgare* was more abundant at the high pCO_2 site, but it was almost absent from all sites in autumn. In contrast, *C. corniculata* cover significantly increased in the high pCO_2 site from spring to autumn, while the opposite was true for the intermediate and reference sites, where *C. corniculata* cover decreased from spring to autumn. As for the coralline algae, CCAs recruited earlier than *J. rubens* and reached their maximum cover in spring at the intermediate sites, while in the reference sites their cover increased from spring to autumn. The articulate coralline alga *J. rubens* had extremely low abundances at all sites in spring, while in autumn its percent cover decreased with increasing pCO_2 levels (Figure 3.6).

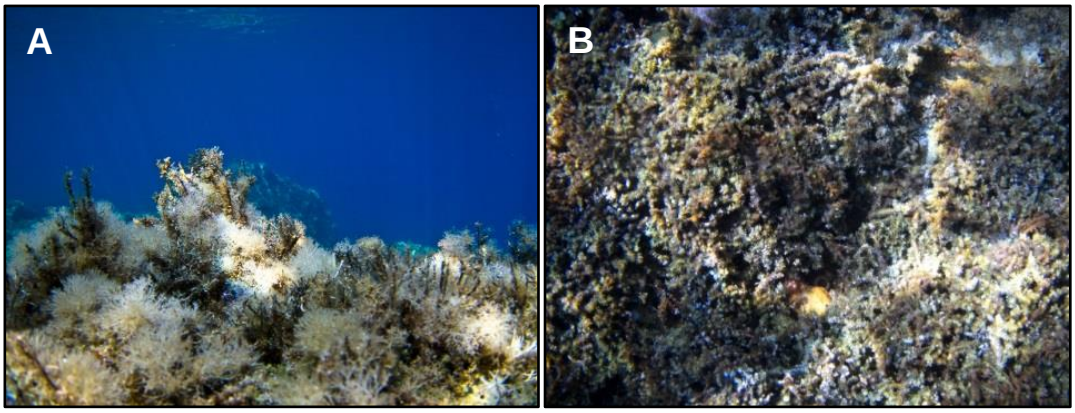

Figure 3.6. Typical appearance of macroalgal communities off Methana in autumn at (A) reference sites, with high cover of the articulated coralline alga *J. rubens*, and (B) near the CO_2 seeps, where *C. corniculata* is dominant (photos by Maria Salomidi).

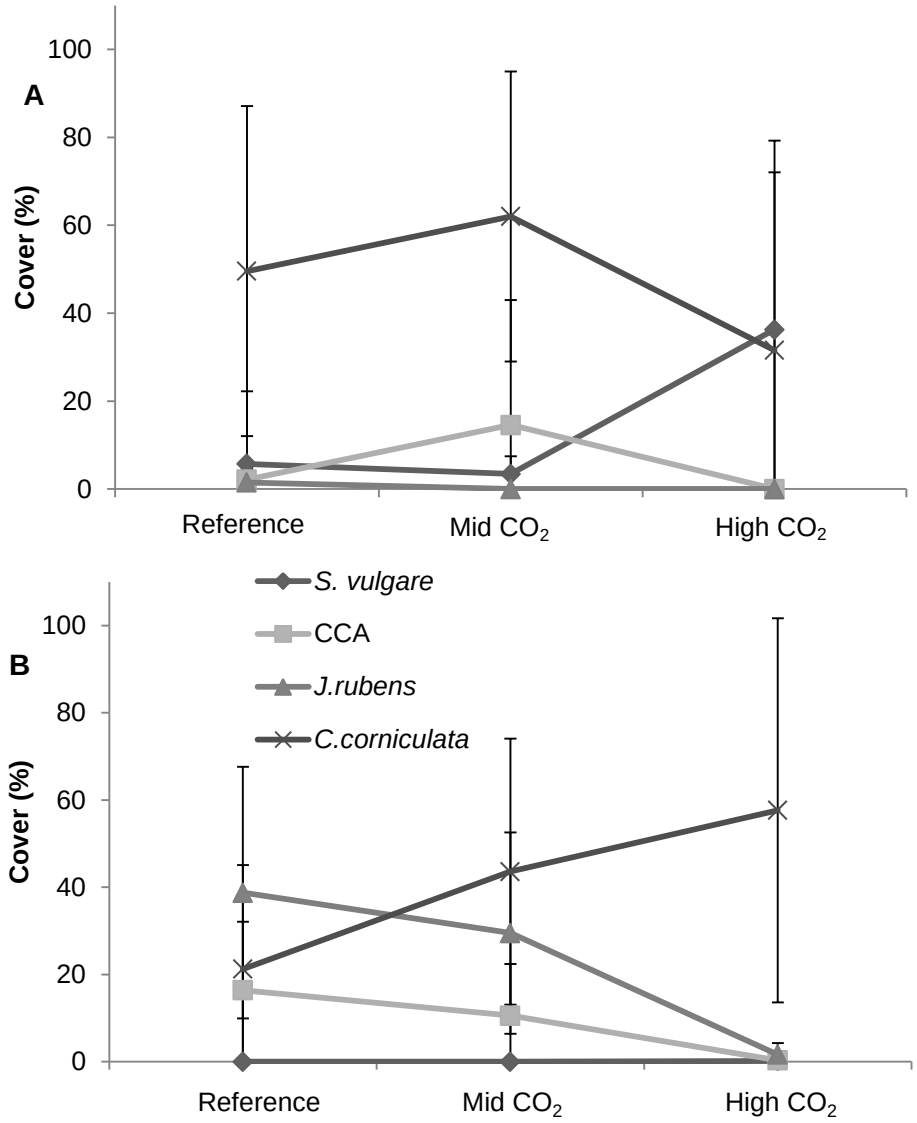

Figure 3.7. Mean percentage cover (± SD) of dominant macroalgal species in May (A) and September (B) at high (n=6), intermediate (n=14) and reference (n=14) levels of CO_2 in Methana. Different letters and numbers indicate significant differences between groups.

3.3.2 Vulcano macroalgal communities

At Vulcano, 32 macroalgal taxa were recorded, five of which were calcifying algae. Results from PERMANOVA analysis on square-root transformed data (Table 3.5a) show that macroalgal communities were significantly different among sites (pseudo-$F_{2,9}$=2.702, p(perm)=0.0005). Pair-wise comparisons (Table 3.5b) show that there was a significant difference between the

communities at the High CO_2 and reference sites ($t_{2,6}$=1.793, p(MC)=0.045), whereas the Mid CO_2 site was intermediate between the other two.

Table 3.5. (A) PERMANOVA analysis on square-root transformed biomass of Vulcano benthic communities. The Table shows degrees of freedom (df), sum of squares (SS), pseudo-F, permutational p and unique permutations for the factor "pCO_2 level". (B) Since "Site" had a significant effect (p<0.05), pair-wise comparisons between CO_2 levels were carried out and are shown in the lower part of the table. Since the number of possible permutations was low (<100), Monte Carlo p (p(MC)) was used as the most reliable p value, and shows that the t-values of High CO_2 and reference site were significantly different.

(A)

Source	df	SS	MS	Pseudo-F	p (perm)	Unique perms
Site	2	6950.7	3475.4	2.7017	**0.005**	4732
Residual	9	11577	1286.4			
Total	11	18528				

(B)

Groups	t	p (perm)	Unique perms	p (MC)
High CO_2, Mid CO_2	1.5833	0.0277	35	0.0692
High CO_2, REF A	1.7925	**0.0291**	35	**0.0450**
Mid CO_2, REF A	1.5589	0.0259	35	0.0912

Shannon diversity (H') and Pielou's evenness (J') were not significantly different among sites (Table 3.6), and Figure 3.8 shows that no specific trend was detectable.

Table 3.6. ANOVA results for (A) Shannon diversity (H') and (B) Pielou's evenness (J') of Vulcano macroalgal communities. The Tables show main factors and their interactions and sum of squares (SS), degrees of freedom (df), Mean Squares (MS), F-ratios (F) and p values.

(A)	Source	Type III SS	df	MS	F	p
	Site	0.657	2	0.328	0.911	0.436
	Error	3.245	9	0.361		
	Total	3.902	11			
(B)	**Source**	**Type III SS**	**df**	**MS**	**F**	**p**
	Site	0.087	2	0.043	0.963	0.418
	Error	0.405	9	0.045		
	Total	0.491	11			

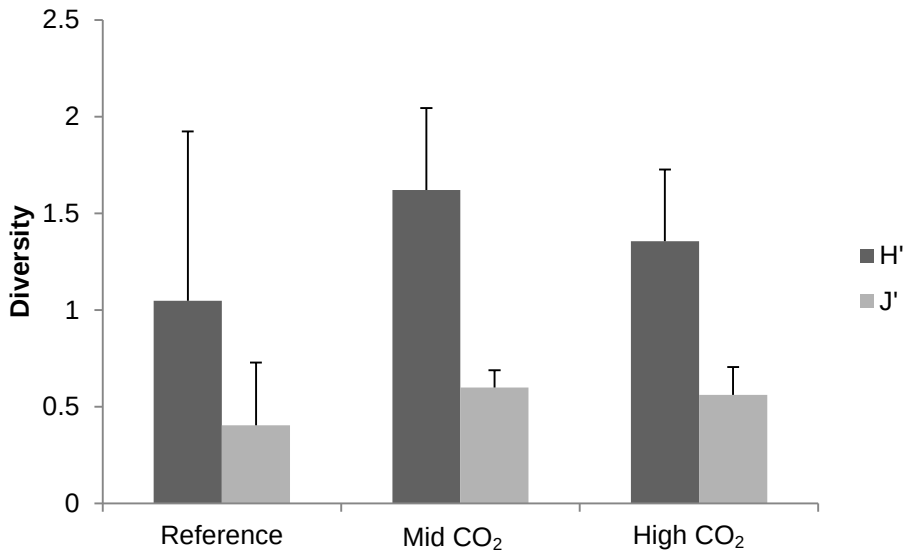

Figure 3.8. Mean (± SD, n = 4) Shannon diversity (H') and Pielou's evenness (J') at high, intermediate and reference pCO_2 at Vulcano.

SIMPER analysis shows which taxa contribute most to the detected differences among sites (Table 3.7). Dissimilarity levels are highest between the high CO_2 and reference sites (60.20), followed by the dissimilarity between reference and intermediate sites (59.77); intermediate and high pCO_2 sites were the most similar groups (average dissimilarity = 58.03). These results are consistent with

the pair-wise comparison of macroalgal communities (see Table 3.5b). The main drivers of differences between groups were canopy-forming algae such as *Cystoseira* sp., *Sargassum vulgare* and *Dictyopteris polypodioides*, calcifying algae such as crustose coralline algae (CCA) and the calcified brown alga *Padina pavonica*, green algae such as *Flabellia petiolata* (Turra) Nizamuddin, *Caulerpa prolifera* (Forsskål) J.V.Lamouroux and *Caulerpa racemosa* (Forsskål) J.Agardh and turf algae.

Table 3.7. SIMPER analysis of Vulcano benthic communities showing average dissimilarities between each pair of pCO_2 levels and which species contributed to the dissimilarity by up to 90%. For each taxon, the average abundance at the two groups that are being compared, their average dissimilarity, the dissimilarity to standard deviation ratio and the taxon contribution and cumulative contribution are shown.

Groups High CO_2 & Mid CO_2; Average dissimilarity = 58.03						
	High CO_2	**Mid CO_2**				
Taxa	**Av.Ab**	**Av.Ab**	**Av.Diss**	**Diss/SD**	**Contr%**	**Cum%**
***Cystoseira* sp.**	4.39	1.91	12.11	1.57	20.87	20.87
Flabellia petiolata	2.45	0.61	7.62	1.74	13.13	34.00
***Sargassum* sp.**	1.29	0.00	5.03	0.95	8.66	42.66
Caulerpa prolifera	1.40	0.40	4.86	1.37	8.37	51.04
CCA	0.38	1.05	4.01	1.17	6.91	57.94
***Peyssonnelia* sp.**	0.06	0.74	3.08	0.70	5.31	63.25
Turf algae	2.05	1.61	2.96	1.70	5.10	68.36
***Cystoseira* with *Peyssonnelia* epiphyte**	0.00	0.53	2.27	0.54	3.92	72.28
Dictyopteris polypodioides	0.00	0.55	2.21	1.51	3.81	76.09
***Dictyota* sp.**	0.80	0.87	2.01	1.32	3.47	79.56
Caulerpa racemosa	0.07	0.49	1.86	1.14	3.20	82.76
Taonia atomaria	0.34	0.15	1.75	0.86	3.02	85.78
Padina pavonica	0.00	0.29	1.25	2.72	2.16	87.94
Halopteris scoparia	0.00	0.31	1.25	0.54	2.15	90.08
Groups High CO_2 & REF A; Average dissimilarity = 60.20						
	High CO_2	**REF A**				
Taxa	**Av.Ab**	**Av.Ab**	**Av.Diss**	**Diss/SD**	**Contr%**	**Cum%**
***Cystoseira* sp.**	4.39	4.77	12.64	1.08	21.00	21.00
Flabellia petiolata	2.45	0.37	7.77	2.03	12.9	33.91

Caulerpa prolifera	1.40	0.00	5.97	2.24	9.92	43.83
Turf algae	2.05	0.80	5.04	1.54	8.37	52.20
***Sargassum* sp.**	1.29	0.41	4.91	1.09	8.16	60.35
Dictyopteris polypodioides	0.00	1.17	4.50	0.92	7.47	67.82
Halopteris scoparia	0.00	0.73	2.80	0.90	4.66	72.48
CCA	0.38	0.75	2.77	1.12	4.60	77.08
Articulated coralline	0.00	0.56	2.32	2.04	3.85	80.93
Taonia atomaria	0.34	0.25	1.82	0.97	3.02	83.95
***Dictyota* sp.**	0.80	0.78	1.80	1.22	2.99	86.94
Dictyota fasciola	0.00	0.36	1.33	0.75	2.21	89.15
***Cystoseira* with *Peyssonnelia* epiphyte**	0.00	0.28	1.03	0.54	1.72	90.86

Groups Mid CO_2 & REF A; Average dissimilarity = 59.77

	Mid CO_2	**REF A**				
Taxa	**Av.Ab**	**Av.Ab**	**Av.Diss**	**Diss/SD**	**Contr%**	**Cum%**
***Cystoseira* sp.**	1.91	4.77	13.93	1.19	23.31	23.31
Dictyopteris polypodioides	0.55	1.17	5.19	1.44	8.68	31.99
Turf algae	1.61	0.80	4.07	1.26	6.82	38.80
CCA	1.05	0.75	3.77	1.28	6.31	45.11
Halopteris scoparia	0.31	0.73	3.27	1.00	5.47	50.58
***Peyssonnelia* sp.**	0.74	0.00	3.24	0.70	5.43	56.01
***Cystoseira* with *Peyssonnelia* epiphyte**	0.53	0.28	3.00	0.74	5.02	61.03
***Dictyota* sp.**	0.87	0.78	2.72	1.23	4.55	65.58
Flabellia petiolata	0.61	0.37	2.67	1.25	4.47	70.05
Articulated coralline	0.00	0.56	2.62	2.28	4.38	74.42
Caulerpa racemosa	0.49	0.00	2.03	1.04	3.40	77.83
***Sargassum* sp.**	0.00	0.41	1.73	0.59	2.89	80.72
Caulerpa prolifera	0.4	0.00	1.70	0.86	2.84	83.56
Dictyota fasciola	0.00	0.36	1.49	0.76	2.49	86.05
Padina pavonica	0.29	0.02	1.25	3.17	2.09	88.14
Taonia atomaria	0.15	0.25	1.15	1.27	1.93	90.07

Taxa driving differences among sites were grouped in four categories, canopy-forming algae, calcifying algae, non-calcifying green algae and turf algae. The canopy-forming algae category consisted of the sum of the biomass of *Cystoseira* sp., *Dictyopteris polypodioides* and *Sargassum vulgare*; the calcifying algae group included CCA, articulate coralline algae, *Padina*

pavonica, *Peyssonnelia* sp. and *Acetabularia acetabulum* P.C.Silva. Non-calcifying green algae consisted of *Flabellia petiolata*, *Caulerpa prolifera* and *Caulerpa racemosa*, while turf algae were already grouped in one category. Biomass of these categories is shown below (Figure 3.9), and the pattern is consistent with that of Methana in spring. Canopy-forming algae did not show a clear pattern and calcifying algae had the highest biomass at the intermediate site, although this difference was not significant (see Figure 3.5a). Non-calcifying green algae had a significant increase as pCO_2 increased, and turf algae biomass was significantly higher in the high pCO_2 site than in the control, with the Mid CO_2 site having intermediate values between the other two sites.

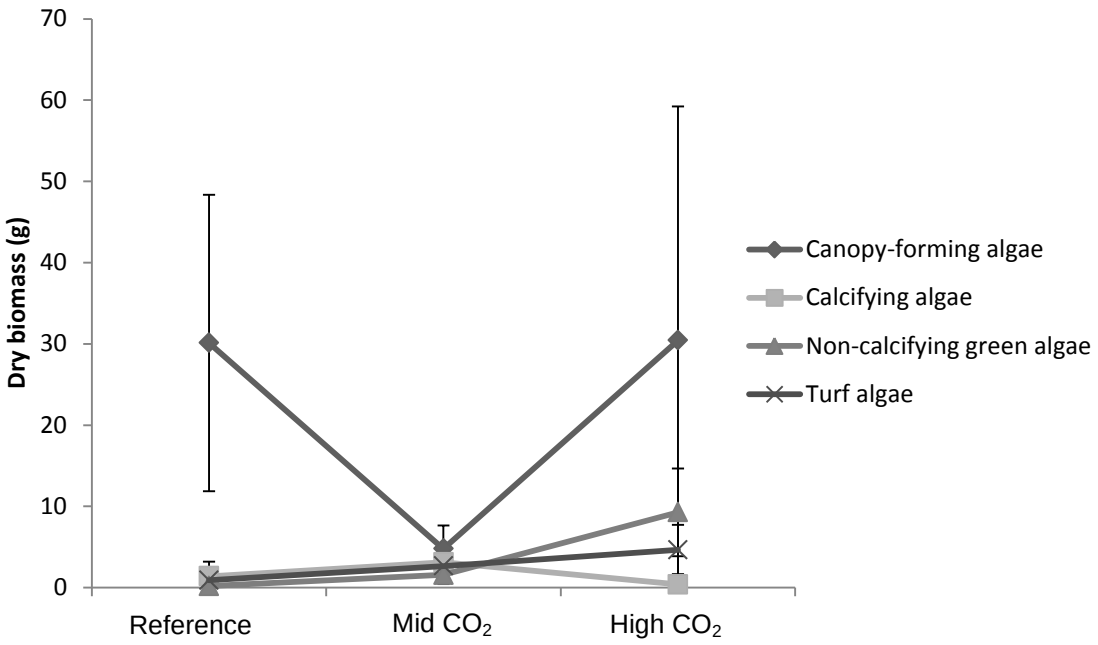

Figure 3.9. Mean (± SD, n=4) biomass of canopy-forming algae, calcifying algae, non-calcifying green algae and turf algae at sites with high, mid and reference pCO_2 at Vulcano.

The most representative canopy-forming and non-calcifying green algae biomass is shown below (Figure 3.10). The two canopy-forming algae *S. vulgare* and *D. polypodioides* showed opposite trends, with the first substituting the latter as pCO_2 increased. On the other hand, the two most abundant non-

calcifying green algae (*F. petiolata* and *C. prolifera*) had a significant increase in biomass at the high CO_2 site compared to the reference site.

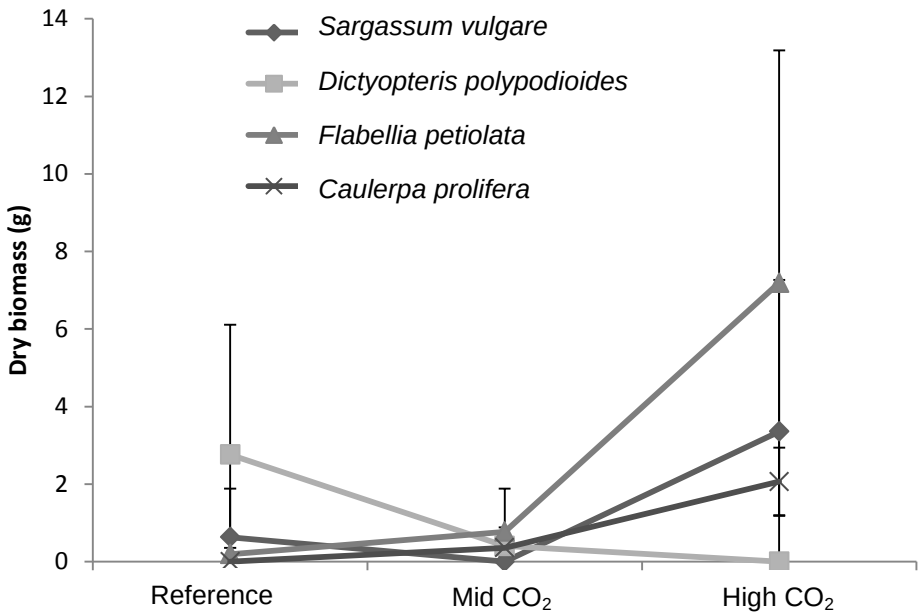

Figure 3.10. Mean (± SD, n=4) biomass of *Sargassum vulgare*, *Dictyopteris polypodioides*, *Flabellia petiolata* and *Caulerpa prolifera* at sites with high, mid and reference pCO_2 at Vulcano.

3.4 Discussion

These results show that increased seawater pCO_2 can have profound effects on macroalgal communities in oligotrophic conditions and that sampling season strongly affects the response of benthic communities to ocean acidification. At Methana, coralline algal cover decreased while canopy-forming algae became more abundant as pCO_2 increased, but the difference was only statistically significant in autumn. Macroalgal communities off Methana had year-round decreased diversity, especially of calcifying species, as carbon dioxide increased, in line with results from surveys at other CO_2 seeps (Porzio *et al.*, 2011; Fabricius *et al.*, 2011,2014) and from laboratory experiments (Hale *et al.*, 2011; Kroeker *et al.*, 2013a).

The seasonal effects of ocean acidification on macroalgal communities have not been detected until now since most field studies have been carried out in one season, while laboratory and mesocosm experiments rarely last long enough to incorporate seasonality effects. Godbold and Solan (2013) found that seasonality greatly affected invertebrate responses to both ocean acidification and increased temperature. A recent study showed that in tropical seagrass epiphyte communities fleshy algae substituted coralline algae as CO_2 increased, and that this pattern was more pronounced in winter (Campbell and Fourqurean, 2014). One of the very few long-term studies of algal physiological responses to ocean acidification showed that coralline algae respond differently to increased pCO_2 depending on season: net calcification was negatively affected by the interaction of increased pCO_2 and temperature in summer, but not in the other seasons (Martin *et al.*, 2013).

At Vulcano, where samples were only collected in spring, results are consistent with Methana; calcifying algal biomass decreased with increasing pCO_2 whereas biomass of canopy-forming algae did not show any specific trend, although the dominant canopy-forming species shifted with increasing CO_2. Here, more taxa were detected because of the different method used, revealing that less conspicuous species such as non-calcifying green algae (e.g. *Flabellia petiolata*) and turf algae increased with increasing seawater pCO_2.

Non-calcifying green algal biomass increased at elevated pCO_2; this trend was particularly evident for *Flabellia petiolata* and *Caulerpa prolifera*. Increased *F. petiolata* abundance at intermediate pCO_2 levels was also reported from Ischia, where this species becomes dominant when pH drops to about 7.8 (Porzio *et al.*, 2011); this is consistent with findings from Vulcano, where average pH at the high CO_2 site is about 7.6 (Boatta *et al.*, 2013). The reason why *F. petiolata*

benefits from increased CO_2 is not currently known, but previous studies have shown that this species is unlikely to use carbon concentrating mechanisms (CCMs; Raven *et al.*, 2002; Mercado et al., 2009). It is therefore possible that increased CO_2 levels give this species a competitive advantage as they would have more substratum available for photosynthesis (Cornwall *et al.*, 2012; Koch *et al.*, 2013).

The increase in fleshy algae with increasing pCO_2 recorded in Vulcano is consistent with previous results from volcanic seeps (Porzio *et al*., 2011; Graziano *et al.*, unpublished data). Shifts towards fleshy macroalgae in response to ocean acidification have also been reported in laboratory and mesocosm studies, where small fleshy algae increase their biomass and percent cover by outcompeting coralline crusts as CO_2 goes up (Connell and Russell, 2010). Since these algae can have a negative effect on kelp recruitment, ocean acidification has the potential to cause dramatic phase shifts in temperate habitats (Connell and Russell 2010), although nutrient and light levels will determine their significance (Russell *et al.*, 2009; Russell *et al.*, 2011). In contrast, at Methana turf-forming algae cover did not increase as CO_2 increased. Another shallow subtidal survey off Italian CO_2 seeps (Porzio *et al.*, 2011) detected a decrease in turf-forming algal biomass at pCO_2 levels of about 1000 ppm. This shows that shifts to turf-forming algae do not necessarily happen at intermediate pCO_2 levels, especially if not associated with increased nutrient levels (Connell and Russell, 2010) or other disturbances disrupting fucoid algal cover (Falkenberg *et al*., 2012).

Decreased abundance of calcifying algae at high CO_2 sites off Vulcano and Methana is consistent with previous results from volcanic seeps off Ischia, in Italy (Porzio *et al.*, 2011). Here, the articulated coralline *Jania rubens* was one

of the dominant species at reference CO_2 levels, but it was absent at elevated CO_2. At Methana, this species was not completely absent from the high CO_2 site, possibly because here the average pH was higher than in Ischia (see Chapter 2). Cover of crustose coralline algae (CCA) decreased with increasing pCO_2 as well both in Italy and in Greece, confirming that calcifying algae are likely to be threatened by ocean acidification (Gao *et al.*, 1993; Anthony *et al.*, 2008; Kuffner *et al.*, 2008; Martin *et al.*, 2008; Ries *et al.*, 2009; Martin and Gattuso, 2009; Gao and Zheng, 2010), especially those species living near their thermal limit (Koch *et al.*, 2013). CCA producing Mg-calcite appear to be extremely sensitive to ocean acidification, whereas those species containing dolomite-rich calcium carbonate seem more resistant to dissolution in high CO_2 conditions (Nash *et al.*, 2012). Intermediate pCO_2 levels seem to increase CCA abundance in spring both off Vulcano and Methana, possibly because carbon fertilisation could enhance calcification. This pattern has been observed in some laboratory studies (Ries *et al.*, 2009; Hofmann *et al.*, 2012) when pCO_2 is below 1000 µatm. However, calcifying algae appear unable to cope with the high energetic demands of calcification when pCO_2 reaches levels above 1000 µatm (Bradassi *et al.*, 2013). Recent studies found that CCA are more sensitive to rates, not magnitude, of ocean acidification (Kamenos *et al.*, 2013) and that fluctuating pH reduces growth in an articulated coralline alga (Cornwall *et al.*, 2013): high variability in pCO_2 at the seeps could therefore lead to an over-estimation of its negative effects on coralline algae.

The increase in canopy-forming algal cover at high CO_2 was mostly caused by an increased abundance of *Sargassum vulgare* in spring along both pCO_2 gradients and of *Cystoseira corniculata* in autumn at Methana. *Sargassum vulgare* was more abundant at high CO_2 also at volcanic seeps off Ischia

(Porzio *et al.*, 2011). However, this species was absent at Methana in autumn because of its pronounced seasonal cycle (Belegratis *et al.*, 1999). As for *C. corniculata*, it is likely that the higher autumnal cover at the elevated pCO_2 site was due to the absence of *S. vulgare* and *J. rubens*. In fact, the genus *Sargassum* can be advantaged over *Cystoseira* when competing for space (Engelen *et al.*, 2008), while *J. rubens* is an epiphyte that can overgrow canopy-forming algae and become dominant in autumn (Belegratis *et al.*, 1999). Physiological responses of *J. rubens* to high pCO_2 are likely to be the main determinant of its decrease in cover, but enhanced defensive compound production by *C. corniculata* cannot be excluded. It has in fact been shown that some fucoid algae are carbon limited, and elevated CO_2 can cause a sharp increase in their defensive compound contents (Swanson and Fox, 2007).

At Vulcano, *Dictyopteris polypodioides* biomass sharply decreased as pCO_2 increased. This is surprising, as *Dictyota* sp. did not seem to be affected by ocean acidification at Vulcano and actually increase its biomass with increasing CO_2 at Ischia (Porzio *et al.*, 2011).This pattern could be either explained by differences in these species' physiologies or by their different palatability to herbivores, as abundances of their main consumer, the sea urchin *Paracentrotus lividus*, decrease with increasing pCO_2 at Vulcano (Johnson *et al*., 2012; Calosi *et al.*, 2013a). Since no studies on this species' physiological responses to ocean acidification have been conducted so far, there is no information available on the underlying physiological mechanisms. This is a further proof that biological response to ocean acidification can greatly vary even within families (Miller *et al*., 2009; Kroeker *et al.*, 2011), and that some non-calcifying species can be as sensitive to increased pCO_2 as calcifiers.

Overall, this study shows that phase shifts in benthic communities as seawater pCO_2 increases are likely to be consistent between Western and Eastern Mediterranean Sea and between intertidal and shallow subtidal (2-3 metres depth) habitats. Loss of diversity and reduced abundance of ecologically important calcifying algae at elevated carbon dioxide levels found in this study add to a growing body of evidence showing that ocean acidification is likely to alter community composition (Hall-Spencer *et al.*, 2008; Fabricius *et al.*, 2011; Kroeker *et al.*, 2011; Porzio *et al.*, 2011; Hofmann *et al.*, 2012; Brodie *et al.*, 2014). Changes in benthic community structure have potential profound effects on biological processes such as food web dynamics, nutrient cycling and primary productivity (Tilman, 1999), thus affecting ecosystem functioning.

Chapter 4

Canopy algal epifauna changes at elevated pCO_2 at two Mediterranean volcanic seeps

Abstract

Only a few studies have dealt with epifaunal community responses to ocean acidification, and they have not reported consistent results. As for canopy-forming algal epifauna, there is virtually no information on their responses to elevated pCO_2. This chapter investigates how epifauna of the main canopy-forming macroalgae at volcanic seeps in Italy and Greece changed with increasing pCO_2. Rocky shores at both sites were dominated by fucoid algae; at Vulcano (Italy) there was a change from *Dictyopteris polypodioides* to *Sargassum vulgare* with increasing pCO_2, while the genus *Cystoseira* remained abundant at all sites, but there was a shift in species. In contrast, *Cystoseira corniculata* was the main canopy-forming alga at volcanic seeps off Methana (Greece) and at nearby reference sites. Canopy-forming algal samples were collected at Methana (*C. corniculata*) and Vulcano (*Cystoseira* spp. and *S. vulgare*) to examine their epifaunal communities. The hypotheses tested were: (i) abundance and diversity of calcifiers will decrease as CO_2 increases; (ii) the magnitude of change in epifaunal communities will differ depending on the macroalgal species they inhabit. At both sites fauna was collected in spring, from 20 x 20 cm quadrats off Methana and by collecting individual thalli of fucoid algae off Vulcano. Although macroalgal morphology and mobile epifauna changed significantly with increasing pCO_2, sessile epiphyte communities did not show consistent changes among pCO_2 levels. The lack of a clear CO_2 effect on epiphytes could be due to the ability of canopy-forming algae to locally raise pH due to photosynthesis; epifauna may still be affected by changes in pCO_2 because it is more mobile than epiphytes and therefore often leaves the macroalgal boundary layer. The abundance of calcifying organisms was strongly affected by increasing pCO_2, whereas non-calcified taxa such as many

polychaetes were more abundant at high CO_2, probably because of reduced competition for space and resources. However, at Vulcano the structure of epifaunal communities inhabiting *S. vulgare* did not change significantly with pCO_2, unlike epifaunal communities living on *Cystoseira* spp. at Vulcano and *C. corniculata* at Methana. Thus, canopy-forming macroalgae and their associated communities are expected to change as seawater carbon dioxide levels increase, but the magnitude of change is expected to differ depending on the macroalgal host.

4.1 Introduction

Although research on biological responses to ocean acidification is in its infancy, there is evidence that an increase in seawater pCO_2 often has strong negative effects on calcifying organisms (Kroeker *et al.*, 2013a). Evidence from volcanic CO_2 seeps used as ocean acidification analogues supports this conclusion (e.g. Hall-Spencer *et al.*, 2008; Cigliano *et al.*, 2010; Fabricius *et al.*, 2011; Kroeker *et al.*, 2011; Inoue *et al*., 2013), although abundant food supplies can help animals to cope with increased pCO_2: for example, mussels and barnacles can remain dominant in eutrophic conditions despite being exposed to high CO_2 levels in Kiel fjord (Thomsen *et al.*, 2010). Community responses do not always reflect single species responses that would be predicted from laboratory-based physiological tests because of biological interactions. For instance, in a mesocosm study of communities from artificial substrata mimicking mat-forming algae Hale *et al*. (2011) reported an unexpected increase in nematode abundance at high CO_2 because of reduced competition for space with taxa sensitive to hypercapnia, such as molluscs. In a field study of turf-associated fauna along pCO_2 gradients in the Mediterranean Sea, Kroeker *et al.* (2011) found that small crustaceans such as amphipods and

tanaids, not nematodes, increased in abundance at low pH. Crustaceans in the mesocosm study (Hale *et al.*, 2011) decreased with increasing pCO_2. There are therefore great uncertainties in predicting the responses of benthic communities to ocean acidification, although both studies report a strong decrease in calcifying organisms' abundance and diversity at increased pCO_2 (Hale *et al*. 2011; Kroeker *et al.*, 2011).

Marine macroalgae are dominant on temperate rocky reefs worldwide (Steneck *et al.*, 2002) and are considered ecosystem engineers because they add structural complexity to the substratum. Invertebrate communities associated with macroalgae have higher species richness and diversity than unvegetated substrata (Dean and Connell, 1987). Epifaunal abundance and diversity can be influenced by hydrodynamics and sedimentation rate (Sánchez-Moyano *et al.*, 2000), and is usually correlated with the complexity of their macroalgal habitat. For instance, densely branched Mediterranean macroalgae host more diverse invertebrate communities because of reduced predation risk and hydrodynamism (Chemello and Milazzo, 2002). Differences in epifaunal communities can also be determined by other seaweed characteristics, such as the presence of defensive compounds (Hay *et al.*, 1987; Jormalainen *et al.*, 2001). Macroalgae and seagrasses raise pH near their fronds through photosynthesis; this process controls calcification rates of their coralline algal epiphytes (Semesi *et al.*, 2009) and has been proven to reduce the negative effects of ocean acidification on some macroalgae, especially if water movement is slow (Cornwall *et al.*, 2014). Invertebrates living on macroalgae might be exposed to smaller changes in ambient pCO_2 compared to animals living in the water column or on bare substrata, and community changes may therefore be less dramatic.

At volcanic seeps off Vulcano (Italy), dominant macroalgae change along a pCO_2 gradient: *Cystoseira* spp. and *Dictyopteris polypodioides* are abundant at reference sites, whereas *Sargassum vulgare* becomes extremely abundant at high pCO_2 (see Chapter 3). On the other hand, no such change was recorded at volcanic seeps off Methana (Greece), where *Cystoseira corniculata* remains the dominant canopy-forming species, even though *Sargassum vulgare* cover increases with pCO_2 (see Chapter 3). Macroalgal communities associated with *Sargassum muticum* have been proven to cope better with ocean acidification than those associated with *Cystoseira tamariscifolia* (Olabarria *et al.*, 2013), but responses of canopy-forming algae epifauna to ocean acidification have not been studied yet.

Based on previous evidence, I expect that canopy-forming algae will not be negatively affected as the oceans acidify (Kroeker *et al.*, 2013a). However, diversity of biological communities can still decrease as pCO_2 increases even if their habitat resists ocean acidification (Martin *et al.*, 2008; Fabricius *et al.*, 2014). Epifaunal communities are the main constituent of diets for seagrass-associated fish, and are therefore an important link to higher trophic level organisms, such as juvenile fish (Yamada *et al.*, 2010). The aim of this study was to assess changes in epifauna of the main canopy-forming algal species along two pCO_2 gradients at volcanic seeps off Vulcano (Italy) and Methana (Greece) given their importance for coastal ecosystem functioning and fisheries. The hypotheses tested are; (i) invertebrate diversity and abundance will decrease with increasing CO_2, and (ii) the manner of these changes in diversity and abundance will depend on the host macroalgal species.

4.2 Methods

4.2.1 Methana

In May 2012, samples were collected by scraping 20 x 20 cm quadrats of *C. corniculata* (Figure 4.2A) growing on horizontal or sub-horizontal rock using a hammer and chisel while covering the area with a 200 µm mesh size nylon net to avoid loss of vagile fauna. Three samples were collected from each of the five sites described in Chapter 2 (SEEP, 200 W, 200 E, REF A and REF B); detailed sampling dates and sample sizes are reported in Table 1.1C. Samples were fixed in 4% buffered formaldehyde for approximately 48 h, transferred to 70% IMS (Industrial Methylated Spirit) and stored until analysis. Samples were then sorted, separating *C. corniculata* from its epiphytic algae, which were assigned to functional groups, and from its epifauna. *Cystoseira corniculata* and its epiphytes were then dried at 50°C for 72 h and weighed (± 1 mg accuracy) to obtain dry mass. Over 29000 individual invertebrates were sorted under a stereoscope and identified to the lowest possible taxonomic level, hereafter termed the operational taxonomic unit (OTU). Amphipods were identified using keys from Bellan-Santini *et al.* (1982, 1989, 1993, 1998), molluscs were identified using the key from Doneddu and Trainito (2005) and taxonomic expertise by Prof. Renato Chemello (University of Palermo, Italy), and all other taxa were identified using the guide from Riedl (1991). The invertebrates collected included foraminiferans, sipunculids, molluscs (bivalves and gastropods), polychaetes (including serpulid worms), crustaceans (amphipods, decapods, isopods, tanaids and copepods) and echinoderms.

4.2.2 Vulcano

In June 2013, samples were collected by placing nets (200 µm mesh size) over 15 individual thalli per site of *Cystoseira* spp. (Figure 4.2B) and on 10 thalli per site of *Sargassum vulgare* (Figure 4.2C) and delicately detaching the thallus from the rock with a chisel. Two sites shown in Figure 4.1 were used, one with high pCO_2 (1200 ppm) and one with lower pCO_2 (600 ppm); detailed sampling dates and sample sizes are reported in Table 1.1C. Samples were sieved and transferred to 70% Industrial Methylated Spirit (IMS) for storage. Over 14000 individual invertebrates were sorted under a stereoscope and identified to the lowest possible taxonomic level, hereafter termed the operational taxonomic unit (OTU). Amphipods were identified using keys from Bellan-Santini *et al.* (1982, 1989, 1993, 1998), molluscs were identified using the key from Doneddu and Trainito (2005) and taxonomic expertise by Prof. Renato Chemello (University of Palermo, Italy), and all other taxa were identified using the guide from Riedl (1991). The invertebrates collected included molluscs (bivalves and gastropods), polychaetes, crustaceans (amphipods, decapods, isopods and tanaids) and echinoderms.

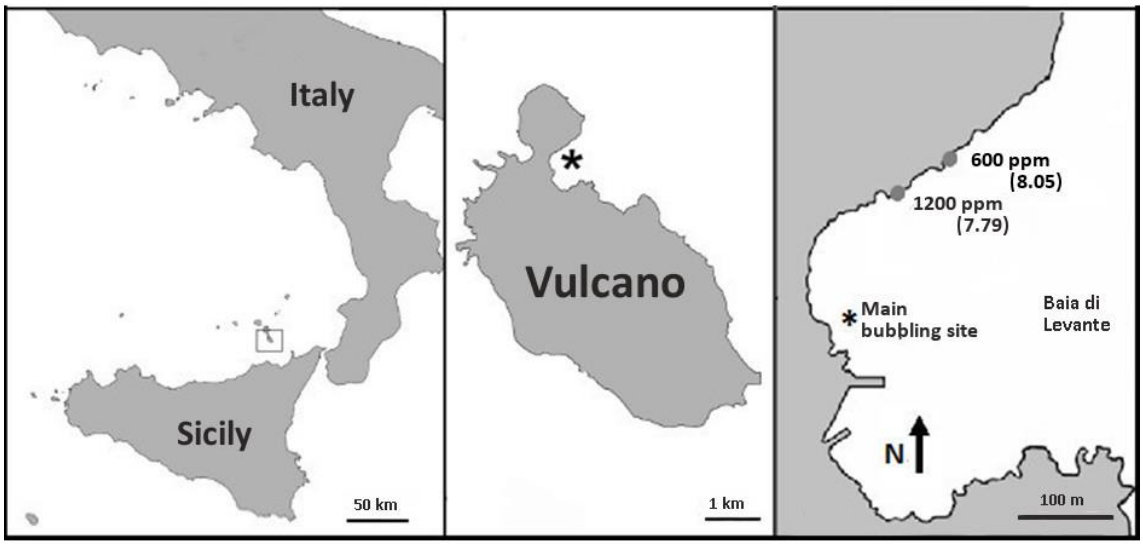

Figure 4.1. Location of Vulcano Island (Sicily, Southern Italy) and of the study area. Asterisk marks the main venting site, grey circles show two experimental sites, with decreasing pCO_2 moving away from the bubbling site. Average pH from environmental monitoring performed in 2012 (data reported in Chapter 5).

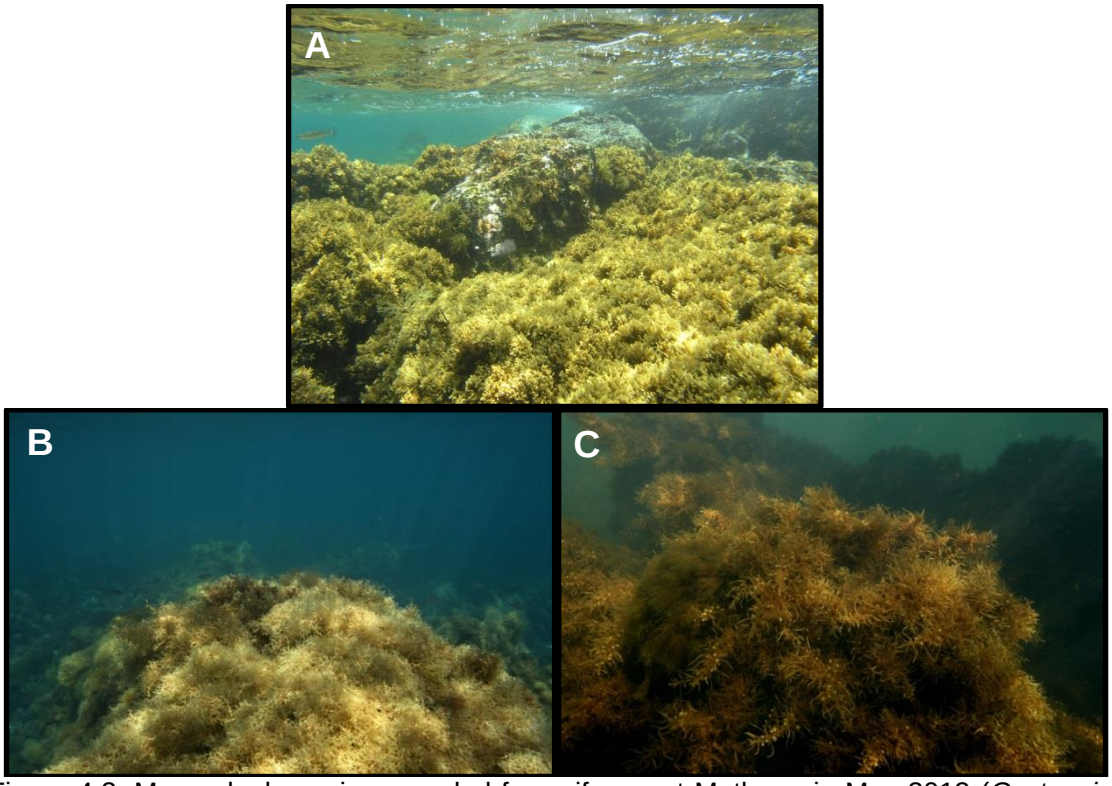

Figure 4.2. Macroalgal species sampled for epifauna at Methana in May 2012 (*Cystoseira corniculata*; A) and at Vulcano in June 2013 (*Cystoseira* spp. and *Sargassum vulgare*; B and C).

Several algal morphological parameters that could influence invertebrate density were measured for each thallus; parameters were selected based on Chemello and Milazzo (2002). Macroalgal biomass was measured with a balance (± 0.001 g accuracy) after it was blot-dried (fresh mass) and dried in an oven for 72 h at 50°C (dry mass). The other morphological parameters used were:

- Axis length: length of main axis measured in mm, measured by spreading the macroalgal thalli on graph paper;
- Frond density: number of primary branches on longest frond/axis length;
- Branching arrangement: total tip number/frond density;
- Canopy volume: maximum height (mm) x maximum length (mm) x maximum width (mm), measured by spreading the macroalgal thalli on graph paper;
- Volume: ml of water displaced, measured in a graduated cylinder;
- Interstitial volume: canopy volume - volume;
- Index of compactness: canopy volume/volume;
- Order of branching: counted from the distal branch to the stem. The final branches were classed first order, and whenever two branches of the same order joined, the order of the resultant branch was increased by one;
- Fractal dimension: calculated from black and white photos using the box counting method with the Fractalyse 2.4 software (CNRS, France).

4.2.3 Statistical analyses

ANOVA was used to analyse the biomass of *C. corniculata* samples from Methana (fixed factor: site) and morphological parameters influencing epifauna

on algal thalli from Vulcano (fixed factors: site and species) after checking they complied with the normality and variance homogeneity requirements of ANOVA. These analyses were performed using SPSS v19 (IBM, USA).

The structure and composition of epiphytic communities from Methana samples and patterns in morphological parameters in samples from Vulcano were tested using a PERMANOVA on square-root (Methana) and normalised (Vulcano) data, with the same experimental designs outlined above. Type III sums of squares with 9,999 unrestricted permutations of the raw data were used for Methana data to account for small sample sizes, whereas Vulcano morphological data were analysed using 9,999 permutations of residuals under a reduced model. Pairwise tests were performed when a factor with more than two levels was significant.

The same procedure was used to analyse epifaunal community data, but a BIO-ENV analysis (Clarke and Ainsworth, 1993) was first used to determine the best combination of variables (epiphyte community and *C. corniculata* biomass for Methana samples, morphological parameters for Vulcano samples) to use as covariates for PERMANOVA (i.e. the combination of variables that explained the most epifaunal variation); when covariates were used, type I sums of squares were used. Epifaunal diversity (Vulcano) and changes in abundance of individual broad taxonomic groups (Vulcano and Methana) were also analysed using the experimental design described above. Where appropriate and meaningful, nMDS plots were used to visually inspect similarities among samples. All analyses above were performed using PRIMER 6 with PERMANOVA+ extension (Plymouth Routines In Multivariate Ecological Research, version 6).

4.3 Results

4.3.1 Methana

Dry mass of *C. corniculata* growing in 20 x 20 cm quadrats off Methana showed significant differences among study sites (Table 4.1). Pairwise comparisons among sites then showed no consistent differences between different pH levels, although average dry mass of *C. corniculata* decreased from the seep site (mean ±SE, n=3: 78.967 ± 12.782 g) to the reference sites (mean ±SE, n=6: 44.700 ± 8.996 g), as shown in Figure 4.3.

Table 4.1. ANOVA on biomass of *C. corniculata* from 20 x 20 cm quadrats in May 2012. The Table shows the main factor, sum of squares (SS), degrees of freedom (df), Mean Squares (MS), F-ratios (F) and p values. The p values < 0.05 are highlighted. The lower part of the Table shows subsets detected by post-hoc pairwise comparisons, with different letters representing significantly different groups.

Source	**Type III SS**	**df**	**MS**	**F**	**p**
Site	5163.609	4	1290.902	5.333	**0.015**
Error	2420.427	10	242.043		
Total	7584.036	14			
Subsets	SEEP[a]	200 W[a,b]	200 E[a]	REF A[a,b]	REF B[b]

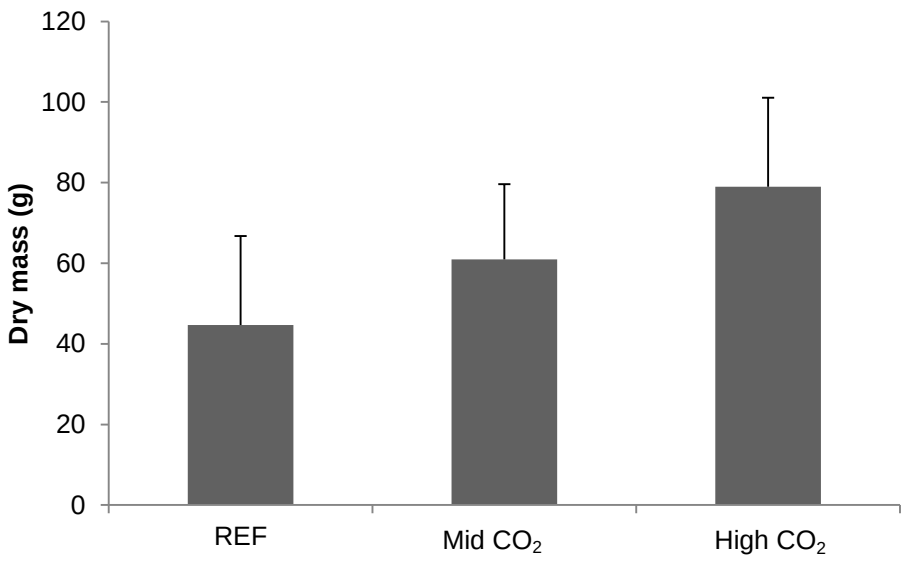

Figure 4.3. Mean (± SD) dry mass of *C. corniculata* from 20 x 20 cm quadrats scraped from rock in May 2012 at reference (REF, n=6), intermediate (n=6) and high CO_2 (n=3) off Methana.

Epiphyte communities on *C. corniculata* also showed significant differences among sites, but no consistent effect of pCO_2 was revealed by pairwise comparisons (Table 4.2).

Table 4.2. PERMANOVA on epiphyte communities of *C. corniculata* from 20 x 20 cm quadrats scraped from rocky substratum in May 2012. The table shows the main factor, degrees of freedom (df), sum of squares (SS), Mean Squares (MS), pseudo F-ratios (Pseudo-F), permutational p and number of unique permutations. Significant p values (< 0.05) are highlighted. The lower part of the table shows subsets detected by post-hoc pairwise comparisons, with different letters representing significantly different groups.

Source	**df**	**SS**	**MS**	**Pseudo-F**	**P(perm)**	**Unique perms**
Site	4	9361.90	2340.50	2.5891	**0.0095**	9903
Residual	10	9039.90	903.99			
Total	14	18402.00				
Subsets		SEEP[a]	200 W[a,b]	200 E[a,b]	REF A[b]	REF B[a,b]

BIO-ENV analysis showed that among the measured covariates, dry biomass of Porifera epiphytes (white species) explained most of the variability between samples. Spearman correlation coefficient for this analysis was 0.101, meaning that white Porifera epiphytes explained 10.1% of the variability of invertebrate abundance among samples. PERMANOVA of the invertebrate data using white Porifera epiphytes as a covariate showed a significant effect of site (Table 4.3). Pairwise comparisons showed that invertebrate communities at SEEP were significantly different from those at reference sites, while sites with intermediate pCO_2 were not significantly different from either SEEP or the closest reference site (REF A).

Table 4.3. PERMANOVA on epifaunal communities of *C. corniculata* from 20 x 20 cm quadrats scraped from rocky substratum in May 2012 using biomass of epiphytic Porifera (white) as covariate. The Table shows the main factors and their interaction, degrees of freedom (df), sum of squares (SS), Mean Squares (MS), pseudo F-ratios (Pseudo-F), permutational p and number of unique permutations. Significant p values (< 0.05) are highlighted. The lower part of the Table shows subsets detected by post-hoc pairwise comparisons, with different letters representing significantly different groups.

Source	**df**	**SS**	**MS**	**Pseudo-F**	**P(perm)**	**Unique perms**
Porifera	1	946.61	946.61	2.5386	**0.0283**	9951
Site	4	8207.80	2052.00	5.5030	**0.0001**	9930
Porifera x Site	3	726.85	242.28	0.6498	0.8743	9918
Residual	6	2237.30	372.88			
Total	14	12119.00				
Subsets		SEEP[a]	200 W[a,b]	200 E[a,b]	REF A[b,c]	REF B[c]

To further explore general patterns of changes in invertebrate communities along the Methana pCO_2 gradient, the community analysis was repeated grouping OTUs into general categories. BIO-ENV analysis of these data showed that among the measured covariates, dry biomass of Porifera epiphytes

(white species) and of Porifera epiphytes (yellow species) explained most of the variability between samples. Spearman correlation coefficient for this analysis was 0.122, meaning that white and yellow Porifera epiphytes explained 12.2% of the variability in invertebrate abundance among samples. However, PERMANOVA of the invertebrate data using the two categories above as covariates showed that they did not have a significant effect. PERMANOVA was then repeated without covariates, and a significant effect of site was detectable (Table 4.4). Pairwise comparisons showed that invertebrate communities at SEEP were significantly different from those at reference sites. Sites with intermediate pCO_2 levels were not significantly different from each other, but 200 W was also not significantly different from SEEP.

Table 4.4. PERMANOVA on invertebrate communities of *C. corniculata* from 20 x 20 cm quadrats in May 2012 grouping taxa into broad taxonomic groups. The Table shows the main factor, degrees of freedom (df), sum of squares (SS), Mean Squares (MS), pseudo F-ratios (Pseudo-F), permutational p and number of unique permutations. Significant p values (< 0.05) are highlighted. The lower part of the Table shows subsets detected by post-hoc pairwise comparisons, with different letters representing significantly different groups.

Source	**df**	**SS**	**MS**	**Pseudo-F**	**P(perm)**	**Unique perms**
Site	4	4742.7	1185.70	8.0678	**0.0001**	9918
Residual	10	1469.6	146.96			
Total	14	6212.4				
Subsets	SEEP[a]		200 W[a,b]	200 E[b]	REF A[c]	REF B[c]

A MDS plot of these data (Figure 4.4) is consistent with pairwise comparisons; it shows that reference sites were clearly different from sites with intermediate and high pCO_2 levels, while the latter were only loosely separated.

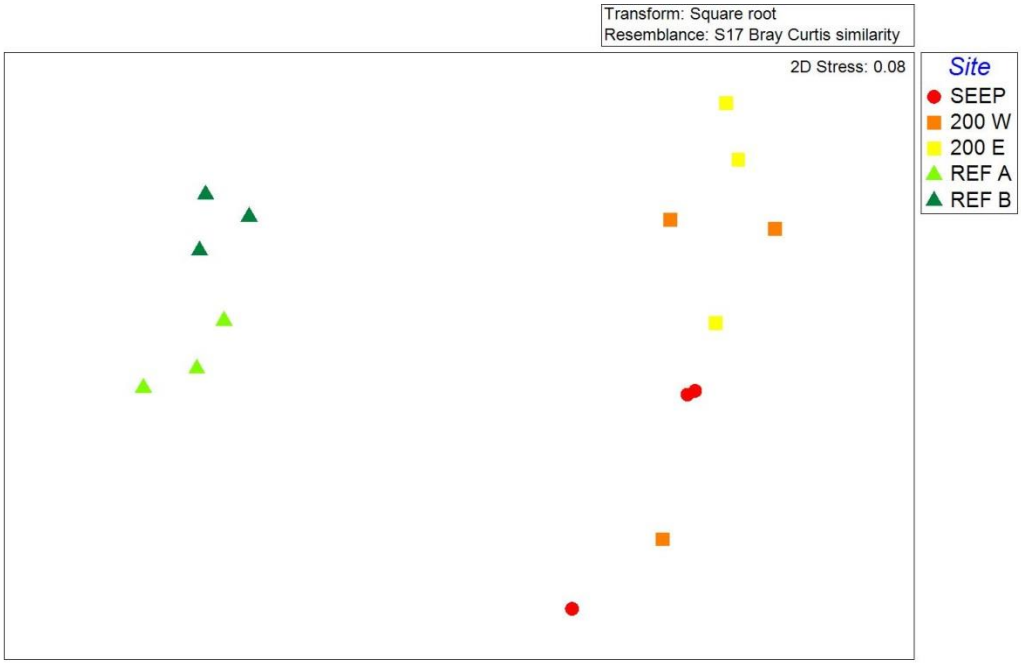

Figure 4.4: MDS plot of invertebrate assemblages on *C. corniculata* thalli collected from 20 x 20 cm quadrats at SEEPS, 200 W, 200 E, REF A and REF B at Methana in May 2012.

Abundances of invertebrate categories that showed significant responses to increased pCO_2 are reported in Figure 4.5. The most abundant invertebrates were amphipods, polychaetes and foraminifera (Figure 4.5A), while bivalves, ophiuroids, sipuncula, gastropods and serpulids were present in lower abundances (Figure 4.5B). In general, heavily calcified taxa (foraminifera, bivalves, gastropods and serpulids) showed decreased abundances with increasing pCO_2, while others (amphipods, polychetes, ophiuroids) had a parabolic pattern (with highest abundances at intermediate CO_2) whilst sipunculids showed no clear trend in relation to carbon dioxide levels.

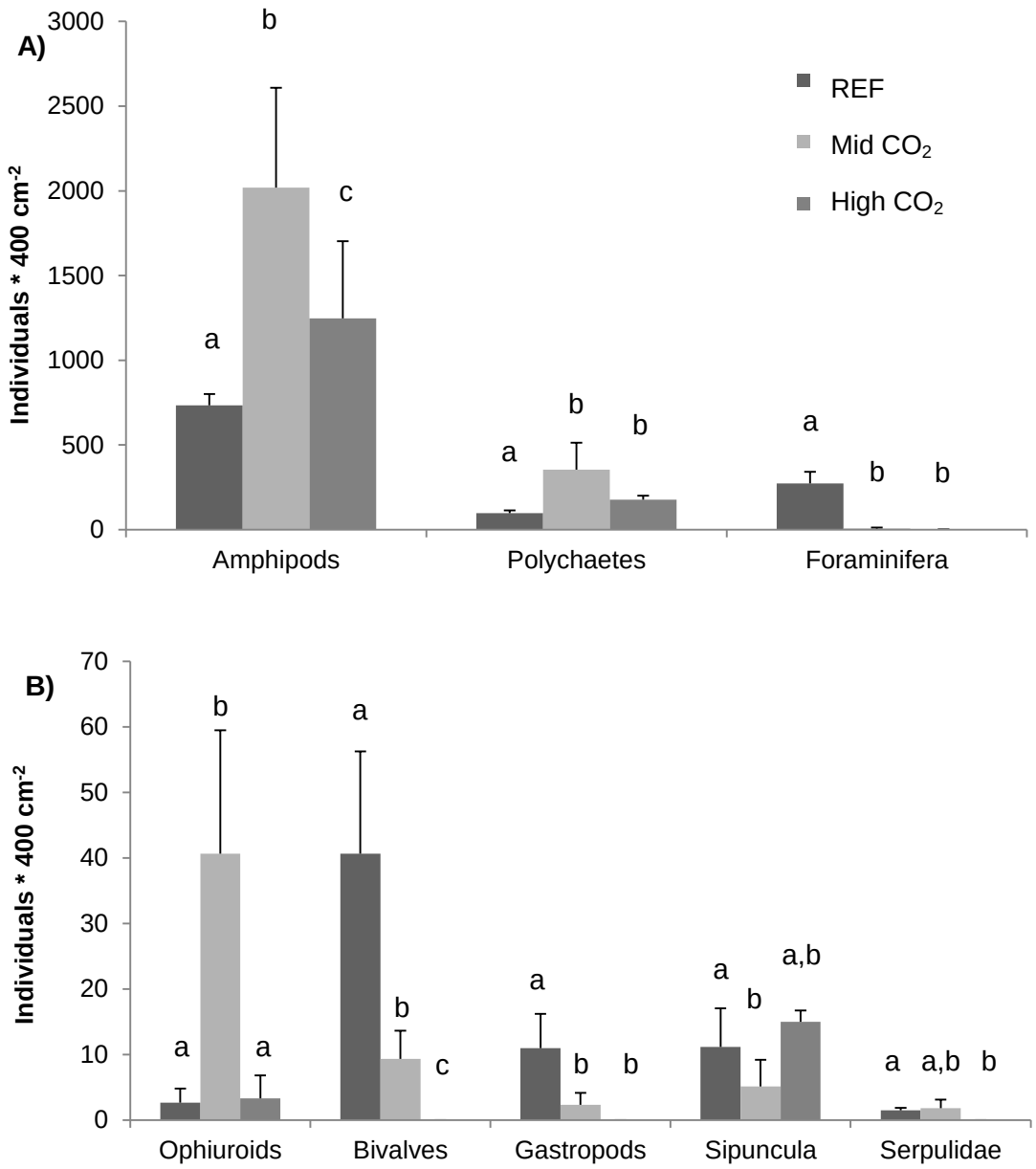

Figure 4.5. Mean (±SD, n=3) number of individuals for each of the main taxonomic groups of invertebrates found on *C. corniculata* from 20 x 20 cm quadrats in May 2012 at reference (REF, n=6), intermediate (n=6) and high CO_2 levels (n=3). The groups are divided depending whether they could have more (A) or less (B) than 100 individuals per sample. Different letters represent significantly different groups according to pairwise comparisons.

4.3.2 Vulcano

Normalised morphological parameters of macroalgae were significantly different between sites, and changed differently in *Cystoseira* spp. and *S. vulgare* (Table 4.5). All combinations of site and species were significantly different in pairwise comparisons (Table 4.5). The MDS plot clearly shows that while all combinations of site and species were different from each other, *Cystoseira* spp. samples were more tightly grouped than those of *S. vulgare*, which were separated into two very distinct groups (600 and 1200; Figure 4.6).

Table 4.5. PERMANOVA on morphology of *Cystoseira* spp. and *S. vulgare* thalli collected at Vulcano in June 2013. The table shows the main factors and their interaction, degrees of freedom (df), sum of squares (SS), Mean Squares (MS), pseudo F-ratios (Pseudo-F), permutational p and number of unique permutations. Significant p values (< 0.05) are highlighted. The lower part of the table shows subsets detected by post-hoc pairwise comparisons, with different letters representing significantly different groups.

Source	**df**	**SS**	**MS**	**Pseudo-F**	**p(perm)**	**Unique perms**
Site	1	32.662	32.662	5.9684	**0.0003**	9935
Species	1	45.812	45.812	8.3715	**0.0001**	9942
Site x Species	1	114.23	114.23	20.874	**0.0001**	9940
Residual	44	240.79	5.4724			
Total	47	415.99				
Pairwise comparisons	600 S[a]	1200 S[b]	600 C[c]	1200 C[d]		

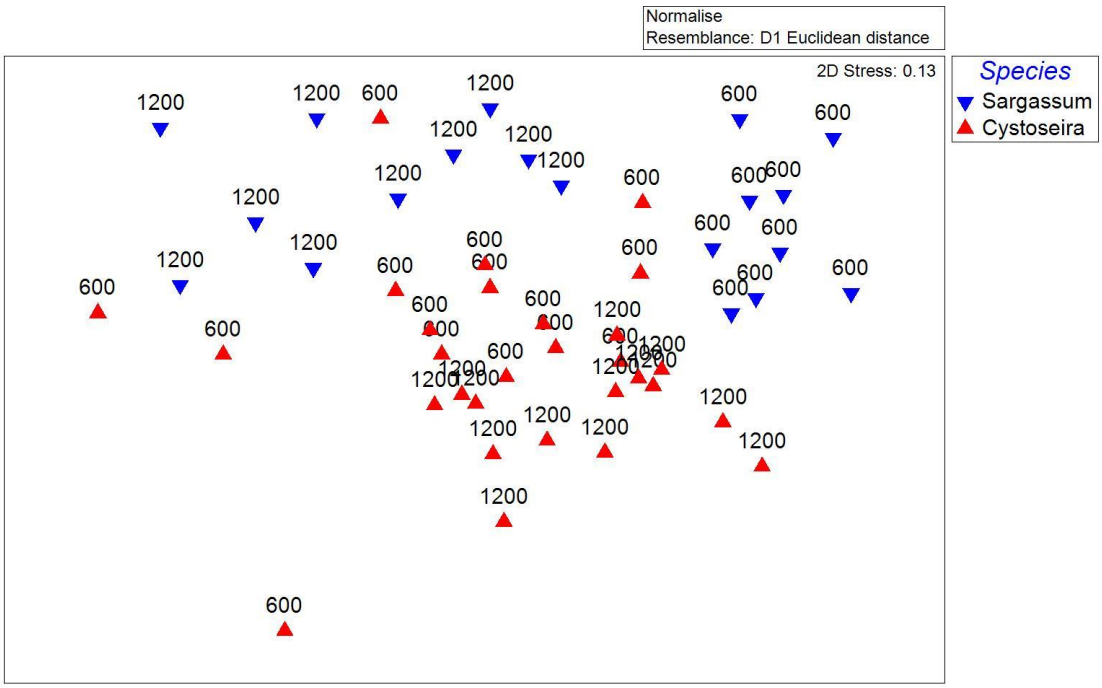

Figure 4.6: MDS plot of macroalgal morphology of *Cystoseira* spp. and *S. vulgare* thalli collected at Vulcano in June 2013 at sites with 600 and 1200 ppm average seawater pCO_2.

The morphological variables best explaining epifaunal patterns were axis length, order of branching and frond density; these three parameters explained 29.3% of the epifauna variability according to the BIO-ENV analysis. ANOVAs of the parameters above showed that axis length of *Cystoseira* spp. and *S. vulgare* exhibited opposite patterns. Main axes of *S. vulgare* were longer at elevated CO_2, increasing from under 150 mm to over 400 m, whereas those of *Cystoseira* spp. were shorter at the high CO_2 site (Figure 4.7A). Order of branching was mostly similar for all sites and species, but *S. vulgare* at the low pCO_2 site had a much simpler structure (Figure 4.7B). On the other hand, frond density was not significantly different between sites, but was significantly higher in *Cystoseira* spp. than in *S. vulgare* (Figure 4.7C).

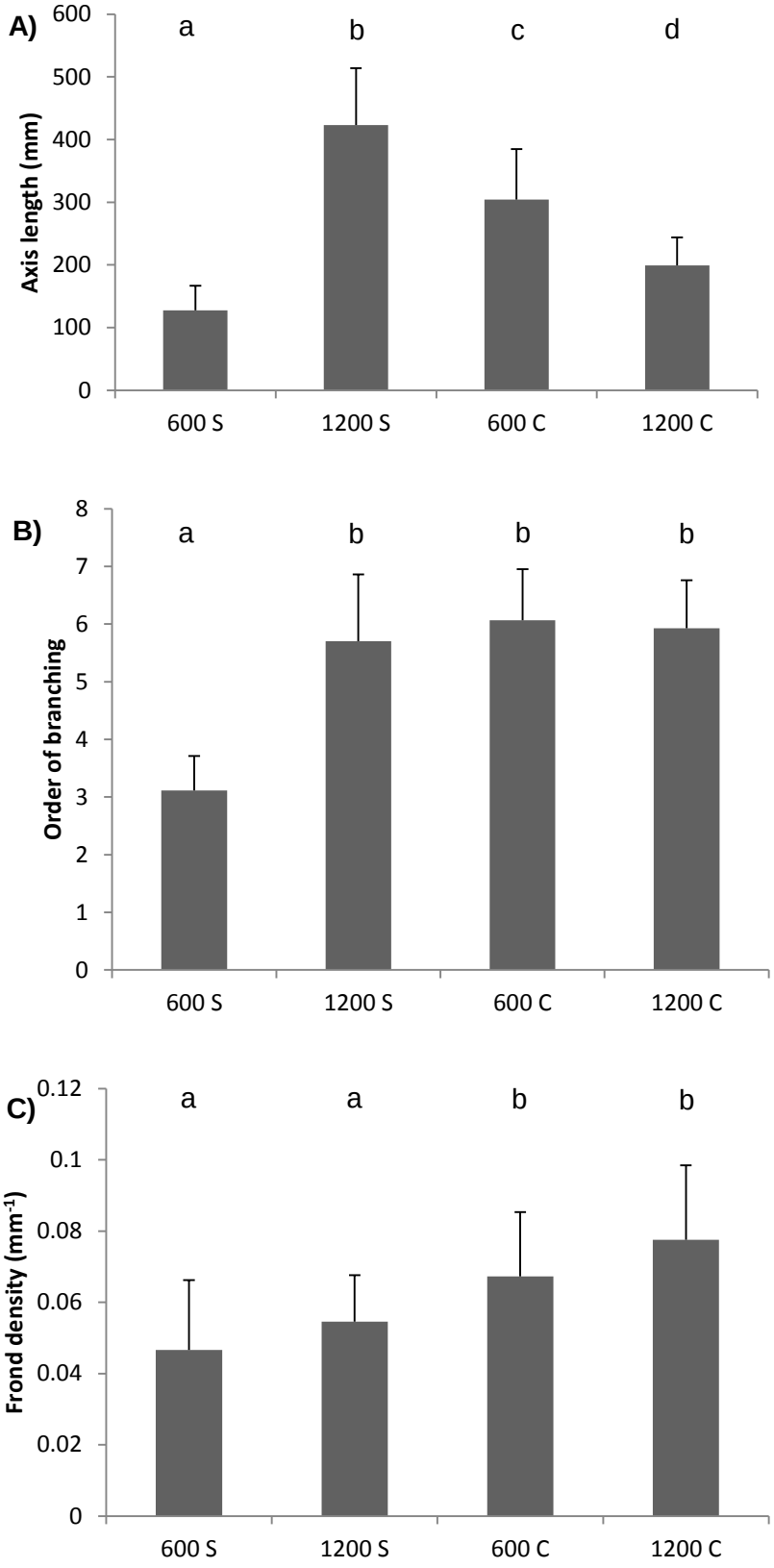

Figure 4.7: Mean (± SD, n=9-15) axis length (A), order of branching (B) and frond density (C) of *Cystoseira* spp. and *S. vulgare* thalli collected at Vulcano in June 2013 at sites with 600 and 1200 ppm average seawater pCO_2. Different letters represent significantly different groups identified by pairwise comparisons.

As for the invertebrate community analysis, no significant interactions between factors and covariates were detected; those interactions were therefore removed from the analysis. The results show that after taking into account the three covariates, invertebrate communities were significantly different between sites and between species, but the two factors did not interact (Table 4.6). Pairwise comparisons revealed that while epifauna of *Cystoseira* spp. was significantly different between sites, epifauna of *S. vulgare* did not change significantly as pCO_2 increased, and its community structure was not significantly different from that of *Cystoseira* spp. (Table 4.6). As analysis of broad taxonomic categories gave the same results, they are not reported here.

Table 4.6. PERMANOVA on invertebrate communities of *Cystoseira* spp. and *S. vulgare* thalli collected at Vulcano in June 2013 using axis length, order of branching and frond density as covariates. The table shows the main factors and their interaction, degrees of freedom (df), sum of squares (SS), Mean Squares (MS), pseudo F-ratios (Pseudo-F), permutational p and number of unique permutations. Significant p values (< 0.05) are highlighted. The lower part of the table shows subsets detected by post-hoc pairwise comparisons, with different letters representing significantly different groups.

Source	**df**	**SS**	**MS**	**Pseudo-F**	**p(perm)**	**Unique perms**
Axis length	1	5313.9	5313.9	6.1971	**0.0001**	9926
Order of branching	1	4385.8	4385.8	5.1148	**0.0001**	9925
Frond density	1	2865.6	2865.6	3.3419	**0.0003**	9935
Site	1	7833.2	7833.2	9.1352	**0.0001**	9926
Species	1	4895.1	4895.1	5.7088	**0.0002**	9934
Site x Species	1	1245.6	1245.6	1.4527	0.1366	9924
Residual	41	35156	857.47			
Total	47	61696				
Pairwise comparisons	600 $S^{a,b}$	1200 $S^{a,b}$	600 C^{a}	1200 C^{b}		

Epifaunal diversity was not significantly affected by any morphological parameters, so covariates were removed from the analysis. Similarly to the epifaunal community structure, Shannon diversity was significantly affected by site and species, but the two factors did not interact (Table 4.7). Although epifauna of both macroalgae had lower diversity at elevated CO_2, the difference was clearer in *Cystoseira* spp. (Figure 4.8).

Table 4.7. ANOVA on epifaunal diversity of *Cystoseira* spp. and *S. vulgare* thalli collected at Vulcano in June 2013. The table shows the main factors and their interaction, degrees of freedom (df), sum of squares (SS), Mean Squares (MS), pseudo F-ratios (Pseudo-F), permutational p and number of unique permutations. Significant p values (< 0.05) are highlighted. The lower part of the table shows subsets detected by post-hoc pairwise comparisons, with different letters representing significantly different groups.

Source	**df**	**SS**	**MS**	**Pseudo-F**	**p(perm)**	**Unique perms**
Site	1	0.67246	0.67246	6.9354	**0.0113**	9824
Species	1	0.39158	0.39158	4.0385	**0.0485**	9830
Site x Species	1	0.10733	0.10733	1.1069	0.3002	9835
Residual	44	4.2662	0.097			
Total	47	5.5516				
Pairwise comparisons	600 $S^{a,b}$	1200 S^{b}	600 C^{a}	1200 C^{c}		

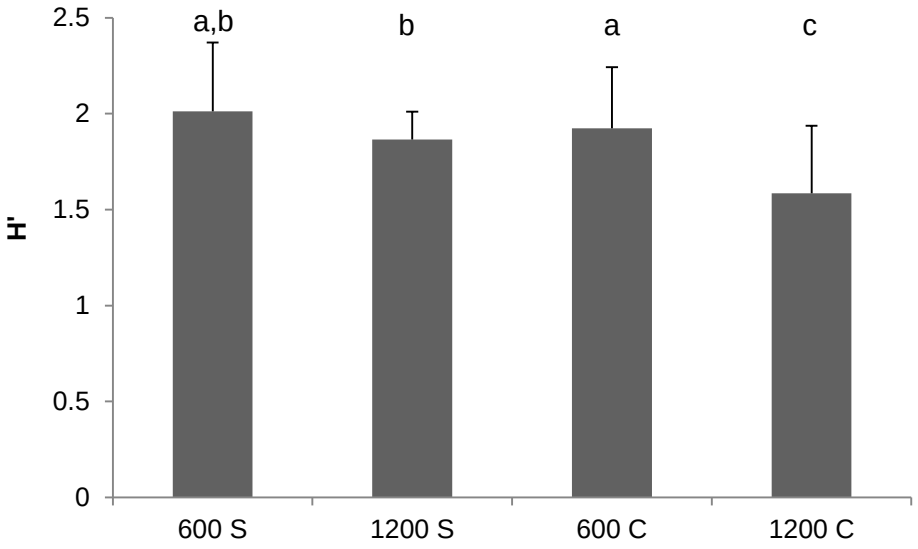

Figure 4.8: Mean (± SD, n=9-15) diversity of epifaunal communities on *Cystoseira* spp. and *S. vulgare* thalli collected at Vulcano in June 2013 at sites with 600 and 1200 ppm average seawater pCO_2. Different letters represent significantly different groups identified by pairwise comparisons.

Graphs of the number of individuals of the most abundant taxa are shown in Figure 4.9. Values are reported as individuals per ml of water displaced by the macroalga, as this was the morphological parameter that seemed to influence invertebrate abundance the most (BIO-ENV analyses on single taxa, results not shown). Amphipods and tanaids showed a clear decrease with increasing pCO_2 on *S. vulgare*, but a trend towards increasing abundance on *Cystoseira* spp.. Gastropods decreased at the high CO_2 site in both macroalgal species, whereas polychaetes and isopods became more abundant as CO_2 increased.

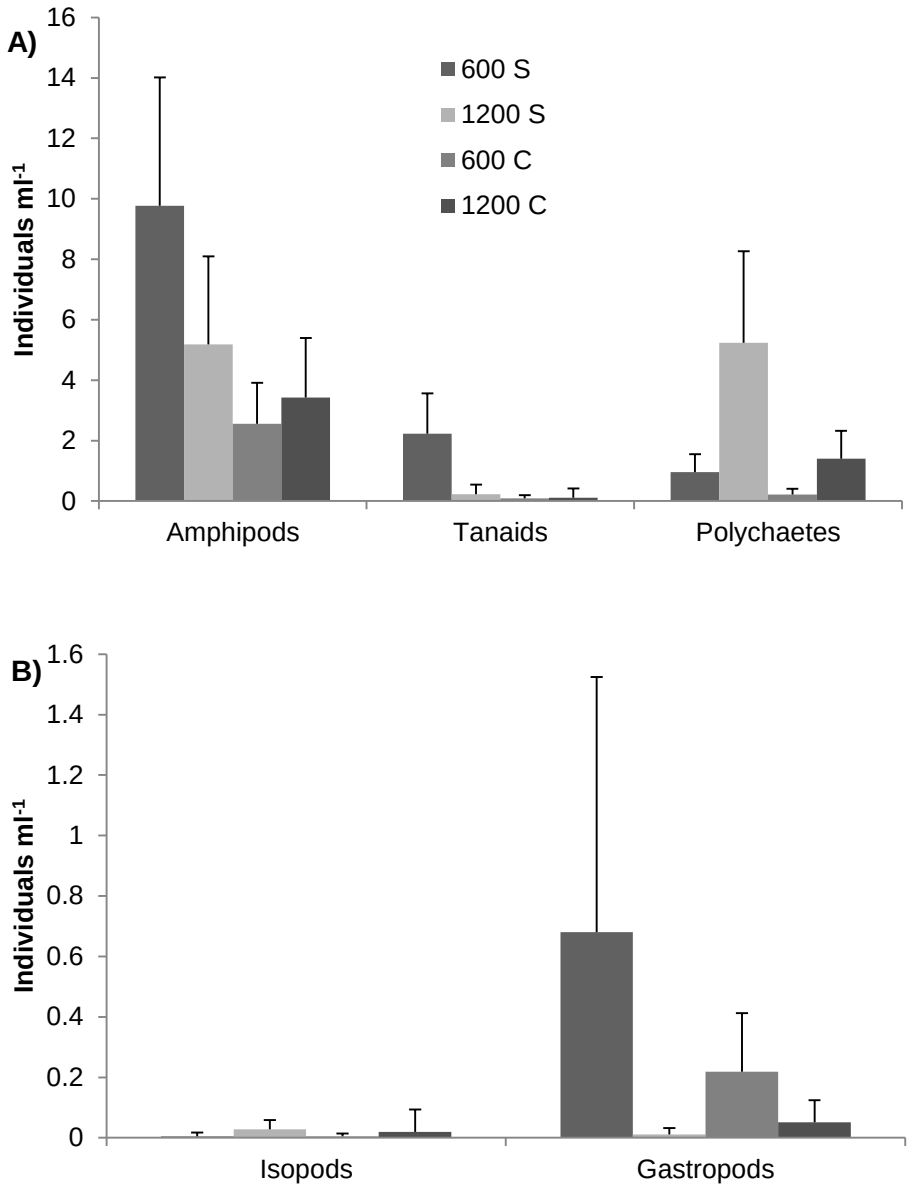

Figure 4.9. Mean (±SD, n=9-15) number of individuals for each of the main taxonomic groups of invertebrates per ml of water displaced by thalli of *Cystoseira* spp. and *S. vulgare* collected at Vulcano in June 2013 at sites with 600 and 1200 ppm average seawater pCO_2. The groups are divided depending whether they had more (A) or less (B) than 1 individual per ml of water displaced.

4.4 Discussion

This is the first study to assess how epifauna of different canopy-forming algae responds to elevated CO_2 levels. Epifauna of macroalgae and seagrasses represents the main food source for many commercial fish, especially for juvenile individuals (Yamada *et al.*, 2010); changes in their abundance and specific composition could therefore have dramatic consequences for coastal ecosystems and fisheries. Epifauna of *Cystoseira* spp. collected at two CO_2 seeps was significantly affected by elevated carbon dioxide levels, but epifauna of *Sargassum vulgare* was not affected by changes in pCO_2. This has implications for ecosystem functioning, as epifauna can contribute 70-98% of secondary productivity on temperate rocky reefs (Taylor, 1998).

Community structure of *Cystoseira* spp. epifauna significantly changed with increasing pCO_2 at both sites, but at Vulcano *S. vulgare* epifauna did not change significantly with pCO_2 levels. The changes in epifaunal communities are in accord with previous studies on epifaunal responses to ocean acidification, which reported significant changes in community structure (Hale *et al.*, 2011; Kroeker *et al.*, 2011). A pH < 7.2 can cause communities to shift from net calcification to net dissolution, although total invertebrate biomass does not change with pCO_2 (Kroeker *et al.*, 2011; Christen *et al.*, 2013). At Vulcano, epifaunal diversity significantly decreased at the high CO_2 site on *Cystoseira* spp. thalli, but epifauna of *S. vulgare* did not show significant changes in community structure and diversity between sites. Although invertebrate communities often decrease in diversity as CO_2 increases (Cigliano *et al.*, 2010; Hale *et al.*, 2011; Kroeker *et al.*, 2011), *Cystoseira*-associated macroalgal communities are more sensitive to ocean acidification compared to those associated with *Sargassum muticum* (Olabarria *et al.*, 2013). In addition, the

increase in *S. vulgare* structural complexity at the high CO_2 site might have helped maintain epifaunal diversity, as morphological complexity of macroalgal hosts has been linked with higher diversity and abundance of their associated epifauna (Chemello and Milazzo, 2002; Bates, 2009).

Heavily calcified taxa decreased in abundance with increasing pCO_2, both at Methana and Vulcano (results summarised in Table 4.8). The only taxa that increased in abundance at elevated pCO_2 were polychaetes and amphipods, although the former showed a clearer increase. Compensatory increase in abundance of CO_2-resistant taxa in ocean acidification conditions has been reported by Hale *et al.* (2011) and Kroeker *et al.* (2011) for nematodes and crustaceans, respectively. These results show that different taxa can be advantaged as CO_2 increases depending on system characteristics; specifically, different taxa can be advantaged by decreased predation rates or reduced competition for space and resources (Micheli *et al.*, 1999). Taxa producing carbonate structures are negatively affected by elevated CO_2 (Kroeker *et al.*, 2013a), whereas crustaceans experience less severe effects because their chitinous skeletons are less prone to dissolution than calcium carbonate structures (Whiteley, 2011). At both study sites, crustaceans indeed showed small or unclear changes in abundance at different CO_2 levels. At Vulcano, changes in epifaunal densities with increased CO_2 were more marked in *S. vulgare*, possibly because its increase in thallus length and complexity at the high CO_2 site increased available habitat for epifauna, therefore masking direct effects of carbon dioxide on their abundance.

Table 4.8. Response to increasing CO_2 of the main epifaunal taxa living on *Cystoseira corniculata* (Methana) or *Cystoseira* spp. and *Sargassum vulgare* (Vulcano); symbols indicate increase (↗), decrease (↘) or no change (—) with elevated CO_2; n.f. = not found.

Taxon	Methana	Vulcano	
	Cystoseira corniculata	*Cystoseira* spp.	*Sargassum vulgare*
Foraminifera	↘	n.f.	n.f.
Sipunculida	—	n.f.	n.f.
Bivalves	↘	n.f.	n.f.
Gastropods	↘	↘	↘
Polychaetes	↗	↗	↗
Serpulids	↘	n.f.	n.f.
Amphipods	↗	↗	↘
Isopods	—	↗	↗
Tanaids	↗	↘	—
Copepods	↘	n.f.	n.f.
Ophiuroids	∩	n.f.	n.f.

At Methana, biomass of *C. corniculata* and of its epiphytes did not change consistently among pCO_2 levels, even though there were clear differences among sites. *C. corniculata* biomass increased, albeit not significantly, at elevated CO_2. This is consistent with a recent meta-analysis showing that some fleshy algae exhibit faster growth rates at elevated pCO_2 levels (Kroeker *et al*., 2013a). The lack of significant effects of pCO_2 on *C. corniculata* epiphytes is surprising, as it contrasts with the clear decrease in calcifying epiphytes off Vulcano as CO_2 increased (Papworth, 2012), for macroalgal communities (Chapter 3) and epifauna (this chapter). Other factors may be influencing epiphyte communities and masking direct effects of CO_2; for instance, epiphytes are often controlled by grazers such as amphipods or gastropods (Fong *et al.*, 2000; Whalen *et al.*, 2012), whose abundances varied among sites. Another possibility is that *C. corniculata* photosynthesis raises pH near its fronds (Hendriks *et al.*, 2014; Cornwall *et al.*, 2014). This may have reduced the impacts of ocean acidification on epiphytes, but not on mobile epifauna, which often swim in and out of macroalgal fronds (Edgar, 1992).

At Vulcano, macroalgal morphology clearly changed at elevated pCO_2. *Sargassum vulgare* was competitively advantaged at high CO_2, as it increased in length and complexity (i.e. order of branching) at the 1200 ppm site. In contrast, *Cystoseira* spp. decreased in length at elevated CO_2, but their frond densities were higher than that of *S. vulgare* at both sites. While *S. vulgare* was the only species of the genus *Sargassum* present at both study sites, several *Cystoseira* species were present off Vulcano. Specifically, *C. compressa* was very abundant at the 1200 ppm site and *C. humilis* was very abundant at the 600 ppm site. Part of the morphological variability of *Cystoseira* spp. could

therefore be attributed to changes in species composition rather than direct effects of pCO_2 on one species' morphology. Other factors, chiefly wave exposure and light, have long been known to influence macroalgal morphology (Hurd, 2000; Monro and Poore, 2005), but neither changes between the two study sites (Johnson *et al.*, 2013). On the other hand, seasonal changes only have a minor influence on most macroalgal morphological parameters (Wernberg and Vanderklift, 2010), so results from this study are unlikely to be influenced by sampling season. *Sargassum vulgare* cover increased with increasing pCO_2 at other Mediterranean seeps (Porzio *et al.*, 2011; Chapter 3), but this is the first evidence that pCO_2 levels can influence fleshy algal morphology as well.

Magnitude of change in communities associated with canopy-forming algae also depends on the type of community, as macroalgal epiphytes did not change among pCO_2 levels, whereas epifaunal communities did. At Vulcano, epifauna of *Cystoseira* spp. and *S. vulgare* were not significantly different within pCO_2 levels. Epifauna of macroalgal species belonging to the same functional group are indeed not likely to be significantly different (Bates and DeWreede, 2007). However, *S. vulgare* epifauna changed between sites less than that of *Cystoseira* spp., hinting at host-specific patterns of epifaunal change with increasing CO_2. In addition, the concurrent increase in *S. vulgare* abundance at elevated pCO_2 will amplify changes in epifaunal communities, with knock-on effects on ecosystem functioning (Taylor, 1998).

Chapter 5

Effect of herbivores on benthic communities at different pCO_2 levels

Parts of this chapter are currently under review as:

C. Baggini, Y. Issaris, M. Salomidi, J.M. Hall-Spencer (2014). Herbivore diversity improves benthic community resilience to ocean acidification. *Journal of Experimental Marine Biology and Ecology* (accepted pending revisions).

Abstract

Marine volcanic seeps exhibit profound changes in benthic communities along gradients of increasing pCO_2 on intertidal and subtidal rocky shores. As grazing by fish, sea urchins and gastropods can also structure benthic communities, decreased herbivore densities due to intolerance to acidified conditions may interact with direct CO_2 effects to determine benthic community structure in a high CO_2 world. Here, two exclusion experiments were used to test effects of herbivory in benthic communities along pCO_2 gradients. Limpets were excluded on intertidal shores at volcanic seeps off Vulcano (Italy) to examine their role in changes from coralline to fleshy algal assemblages. At volcanic seeps off Methana (Greece), herbivore exclusions were used to test whether herbivores affect subtidal algal recruitment differently as carbon dioxide levels increase. Off Vulcano, spatial heterogeneity and seasonality of benthic intertidal communities at a reference site was much higher than at a high CO_2 site. Limpets had weak effects on benthic communities at ambient CO_2 levels, and no effect at the high CO_2 site. Limpet abundances significantly decreased as pCO_2 levels increased, but higher limpet grazing rates at elevated CO_2 were not sufficient to maintain top-down control on benthic communities. Conversely, sea urchins and herbivorous fish dramatically reduced macroalgal biomass at Methana. This effect was not hampered by increased pCO_2 despite lower sea urchin densities near the CO_2 seeps, probably because fish grazing increased. In summary, we found that as long as herbivore fish are present, carbon dioxide levels up to about 2000 µatm are unlikely to significantly reduce the importance of herbivory in structuring Mediterranean benthic communities, even when herbivores strongly control benthic communities. A shift from sea urchin to fish as main

grazers highlights that ocean acidification may cause complex responses at the community level.

5.1 Introduction

Ocean acidification is expected to have profound effects on marine ecosystems worldwide (Kroeker *et al.*, 2013a). Studies at volcanic seeps have shown that increased seawater pCO_2 causes changes in benthic macroalgal and invertebrate communities (Kroeker *et al.*, 2011; Porzio *et al.*, 2011). These changes could be caused by physiological effects of CO_2 on macroalgae, altered competitive interactions (Kroeker *et al.*, 2013c), changes in chemical plant defences (Arnold *et al.*, 2012), or a combination of the above. In addition, grazers may have a determining role in the observed community changes given the strong role of herbivory in marine ecosystems (Poore *et al.*, 2012). Some herbivores, such as amphipods, become more abundant as CO_2 increase at volcanic seeps (Cigliano *et al.*, 2010; Kroeker *et al.*, 2011; Suaria *et al.*, unpublished data). Conversely, key grazers such as limpets and sea urchins decrease in abundance with increased CO_2 (Hall-Spencer *et al.*, 2008; Johnson *et al.*, 2012; Calosi *et al.*, 2013a; Graziano *et al.*, unpublished data), but their contribution to community changes along pCO_2 gradients has not previously been tested experimentally.

Coastal environments have low functional redundancy, even when diversity is relatively high (Micheli *et al.*, 2014). Decrease of limpet and sea urchin densities as seawater CO_2 increases thus leave marine ecosystem vulnerable to phase shifts, especially in the absence of herbivorous fish (Hughes, 1994). Numerous dramatic changes to benthic communities due to reduction in grazing rates have

been reported; for instance, tropical coral reefs can be overgrown by macroalgae if grazing pressure is removed (Hughes *et al.*, 2007).

Limpets of the genus *Patella* are abundant grazers in intertidal Mediterranean shores. Three species are particularly common: *P. aspera*, *P. rustica* and *P. caerulea* (Figure 5.1a). They can greatly influence benthic communities, although their influence varies in space and time (Benedetti-Cecchi *et al.*, 2000) and the algal functional groups affected change depending on several factors. For instance, Benedetti-Cecchi *et al.* (1996) showed how limpets strongly affect coarsely branched and coralline algal abundance, but not filamentous algae, whereas the opposite is true for a study performed in the same area, but on artificial structures (Bulleri *et al.*, 2000).

Limpets are negatively affected by increasing CO_2 levels and the consequent decrease in seawater calcium carbonate saturation; their densities decrease with increasing pCO_2 at seeps off Ischia and Vulcano (Hall-Spencer *et al.*, 2008; Graziano *et al.*, unpublished data). They can survive elevated pCO_2 conditions and up-regulate their calcification rates to counter increased shell dissolution rates (Rodolfo-Metalpa *et al.*, 2011). Some gastropod herbivores increase their feeding rates when pCO_2 increases (Falkenberg *et al.*, 2013b), possibly to sustain the higher energetic cost of calcification. The increase in benthic microalgal chlorophyll concentration recorded at volcanic seeps as CO_2 increases (Johnson *et al.*, 2013) could therefore give limpets a significant advantage in coping with high CO_2 conditions through increased food availability. There is thus a possibility that limpets will still affect benthic communities in a high CO_2 ocean, even with decreased densities, by means of increased feeding rates.

In Mediterranean subtidal environments, high densities of the sea urchins *Paracentrotus lividus* and *Arbacia lixula* can cause a shift from photophilic algal assemblages to “barren grounds”, impoverished assemblages dominated by encrusting algae (Sala *et al*., 1998; Figure 5.1b). Sea urchin grazing can cause a shift to barren grounds in temperate rocky reefs worldwide, which are considered an alternative stable state to kelp beds (Filbee-Dexter and Scheibling, 2014). Once established, barren grounds can be maintained by relatively low sea urchin densities (Chiantore *et al.*, 2008), although these can change back to macroalgal beds if the biomass of carnivorous fish exceeds a critical threshold (Guidetti and Sala, 2007). Herbivorous fish are normally thought to exert weaker top-down control on temperate benthic communities compared to sea urchins (Floeter *et al.*, 2005). However, in the warm-temperate Mediterranean Sea herbivorous fish can limit the distribution of some macroalgal species (Vergés *et al.*, 2009). The main herbivorous fish in the Mediterranean Sea are the sparid *Sarpa salpa* (Figure 5.1c) and the scarid *Sparisoma cretense*, as well as the lessepsian migrants *Siganus luridus* and *Siganus rivulatus*, which can account for over 90% of herbivorous fish biomass in Greek coastal waters (Kalogirou *et al.*, 2012). Increased temperatures in the Mediterranean Sea are helping *Siganus* spp. to expand their range; these fish are therefore causing and maintain barren grounds in the Eastern Mediterranean (Sala *et al.*, 2011; Vergés *et al.*, 2014).

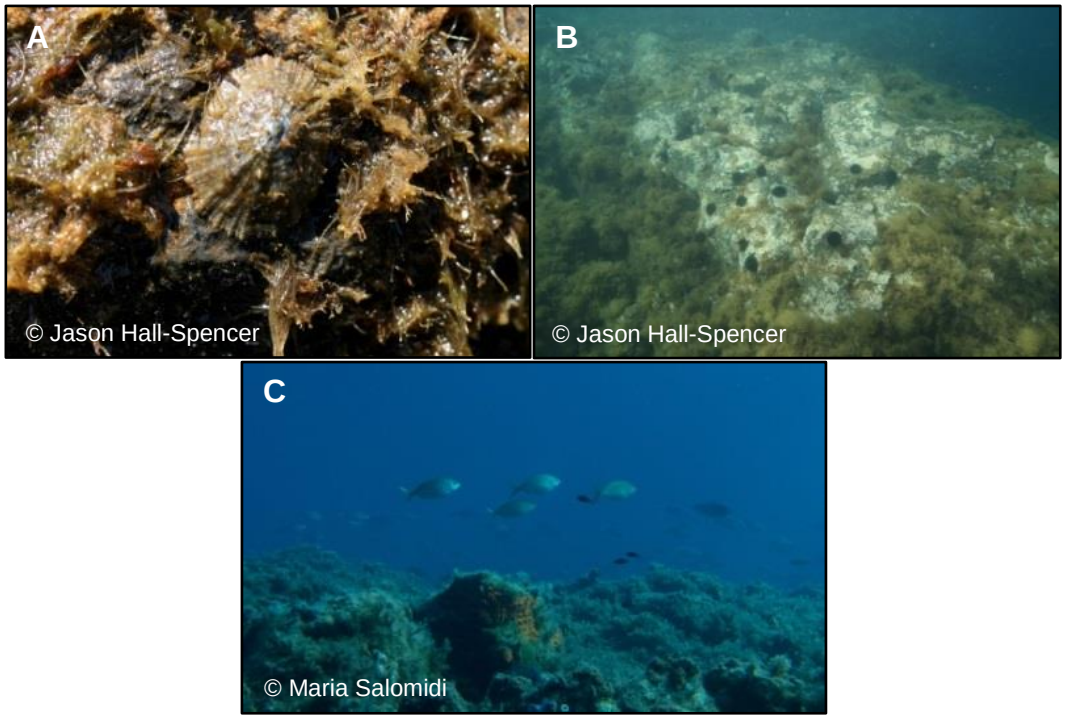

Figure 5.1. Main grazers on Mediterranean intertidal and subtidal shores: (A) Limpet on intertidal shore off Vulcano (Italy); (B) sea urchins reducing macroalgal biomass at shores off Vulcano (Italy); (C) herbivorous fish (*Sarpa salpa*) near CO_2 seeps off Methana (Greece).

Ocean acidification has a detrimental effect on the physiology of many sea urchin species (Dupont *et al.*, 2010) and their densities often decrease as seawater pCO_2 increases (Johnson *et al.*, 2012; Calosi *et al.*, 2013a). On the other hand, many adult fish seem to tolerate carbon dioxide levels predicted for the end of this century (Melzner *et al.*, 2009). Despite this, near-future levels of CO_2 can have profound effects on fish behaviour and sensory functions, particularly at larval and juvenile stages, making many fish species less alert to predators even after prolonged exposure at CO_2 seeps (McCormick *et al.*, 2013; Munday *et al.*, 2014). However, the structure of fish communities seems to be more affected by indirect effects on habitat complexity of ocean acidification than by observed direct effects of elevated pCO_2 on the behaviour of chronically exposed fish (Munday *et al.*, 2014). Being able to move in and out a pCO_2

gradient adult herbivorous fish could be advantaged by high CO_2 conditions because of increased food availability following decreased competition with sea urchins (Johnson *et al.*, 2012) and decreased plant chemical defences (Arnold *et al.*, 2012)

Our understanding of algal community change due to elevated CO_2 has evolved through a series of studies at volcanic seeps. Initial work led researchers to conclude that a shift from coralline algae dominated to fleshy algal communities was driven by dissolution effects on calcified algae (Hall-Spencer *et al.*, 2008; Martin *et al.*, 2008; Porzio *et al.*, 2011). Subsequent work investigating macroalgal succession indicated that certain coralline algae were able to withstand dissolution at CO_2 levels predicted for the end of this century, but fleshy algae were able to outcompete them at high CO_2 (Kroeker *et al.*, 2013c). In a comparison of a tropical and a temperate CO_2 seep system, Johnson *et al.* (2012) found that *Padina* spp. cover was higher at elevated CO_2 levels despite lower calcium carbonate content of thalli at the high CO_2 site. They postulated that this was possible since sea urchins, their main grazers, were unable to tolerate high CO_2 conditions (see Calosi *et al.*, 2013a; Bray *et al.*, 2014). More recent work demonstrates that most evidence of community changes does not originate from direct physiological responses of species to ocean acidification, but from indirect ocean acidification effects on habitat changes or trophic interactions (Alsterberg *et al.*, 2013; Fabricius *et al.*, 2014; Munday *et al.*, 2014; Gaylord *et al.*, 2014). Volcanic CO_2 seeps can be used to disentangle the direct and indirect effects of ocean acidification on marine benthic communities. Here we formally test these effects of ocean acidification in experiments along natural pCO_2 gradients with and without grazers present on rocky Mediterranean shores. Specifically, two separate exclusion experiments were used to test

effects of herbivory in benthic communities along pCO_2 gradients. Limpets were excluded on intertidal shores at volcanic seeps off Vulcano (Italy) to examine their role in changes from coralline to fleshy algal assemblages. At volcanic seeps off Methana (Greece), herbivore exclusions were used to test whether herbivores differently affect subtidal algal recruitment as carbon dioxide levels increase.

5.2 Methods

5.2.1 Vulcano

5.2.1.1 Study site

The aim of this experiment was to examine the role of limpet grazing in driving changes from coralline to fleshy algal assemblages as CO_2 levels increase, and it was conducted in an area off Vulcano Island described in Chapter 3. Along this gradient, the two sites shown in Figure 5.2 were selected, one with average pH_{NBS} of about 7.8 (named “1200 ppm”) and one located about 50-60 m farther away from the main seeps (named “600 ppm”), with an average pH of approximately 8.05, slightly lower and more variable than most Mediterranean coastal waters (Boatta *et al*., 2013). The sites were visited four times during the experiment (start of experiment, i.e. May 2012; July 2012; September 2012; November 2012 - detailed sampling dates and sample sizes are reported in Table 1.1D), and each time pH (NBS scale), temperature and salinity were measured at about 0.5 m depth using a calibrated YSI (556 MPS) pH meter. For pH, means were calculated from hydrogen ion concentrations and then re-converted to pH. The other carbonate chemistry parameters were calculated with CO2Sys (Lewis and Wallace, 1998) using the average total alkalinity value

resulting from monitoring at the site in 2011 (2.525 mMol kg^{-1}, Boatta *et al.*, 2013).

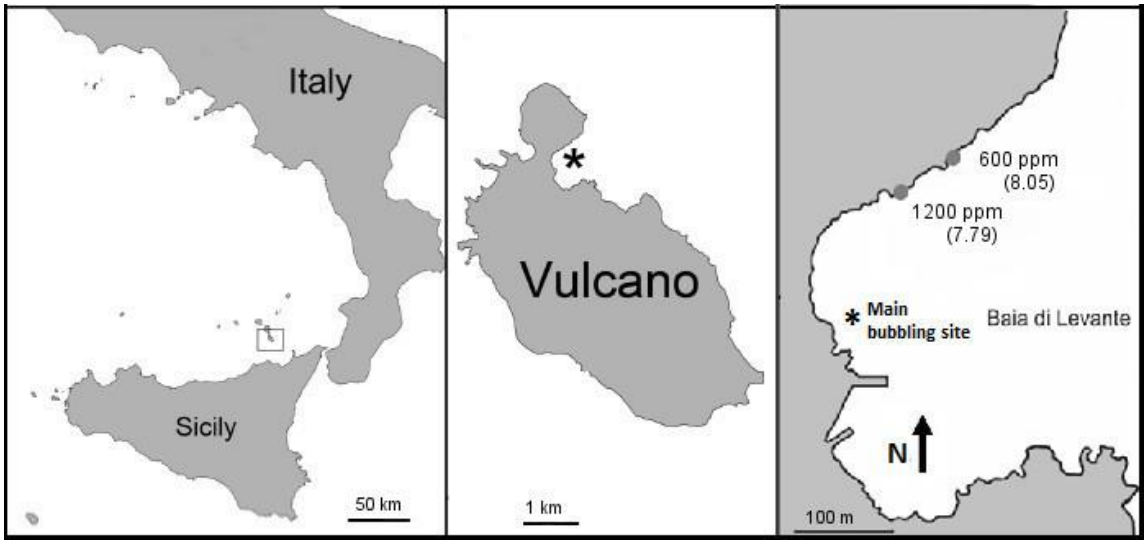

Figure 5.2. Position of Vulcano Island (Sicily, Southern Italy) and of the study area. Asterisk marks the main venting site, grey circles show the two experimental sites, with decreasing pCO_2 moving away from the bubbling site (modified from Graziano *et al.*, unpublished data). Average pH measured during the experiment shown in parentheses (n=6).

5.2.1.2 Limpet exclusion

At each site, twelve 15 cm diameter circular plots were selected in the intertidal zone (defined as the area 10 cm above the limit of the canopy-forming algae, *Cystoseira* spp.). All plots were chosen on vertical flat surfaces with similar wave exposure, as limpet grazing is more intense on vertical surfaces (Marco Milazzo, personal communication). Six of these plots were enclosed using 5 cm high copper rings, which are very rarely crossed by limpets (Harley, 2002). The rings were screwed to the substratum and any space between the ring and the rock was filled using epoxy putty. Half rings were attached in the same way to three of the remaining plots to serve as procedural controls, while the three remaining plots were marked with epoxy putty at the corners and were used as controls (Figure 5.3).

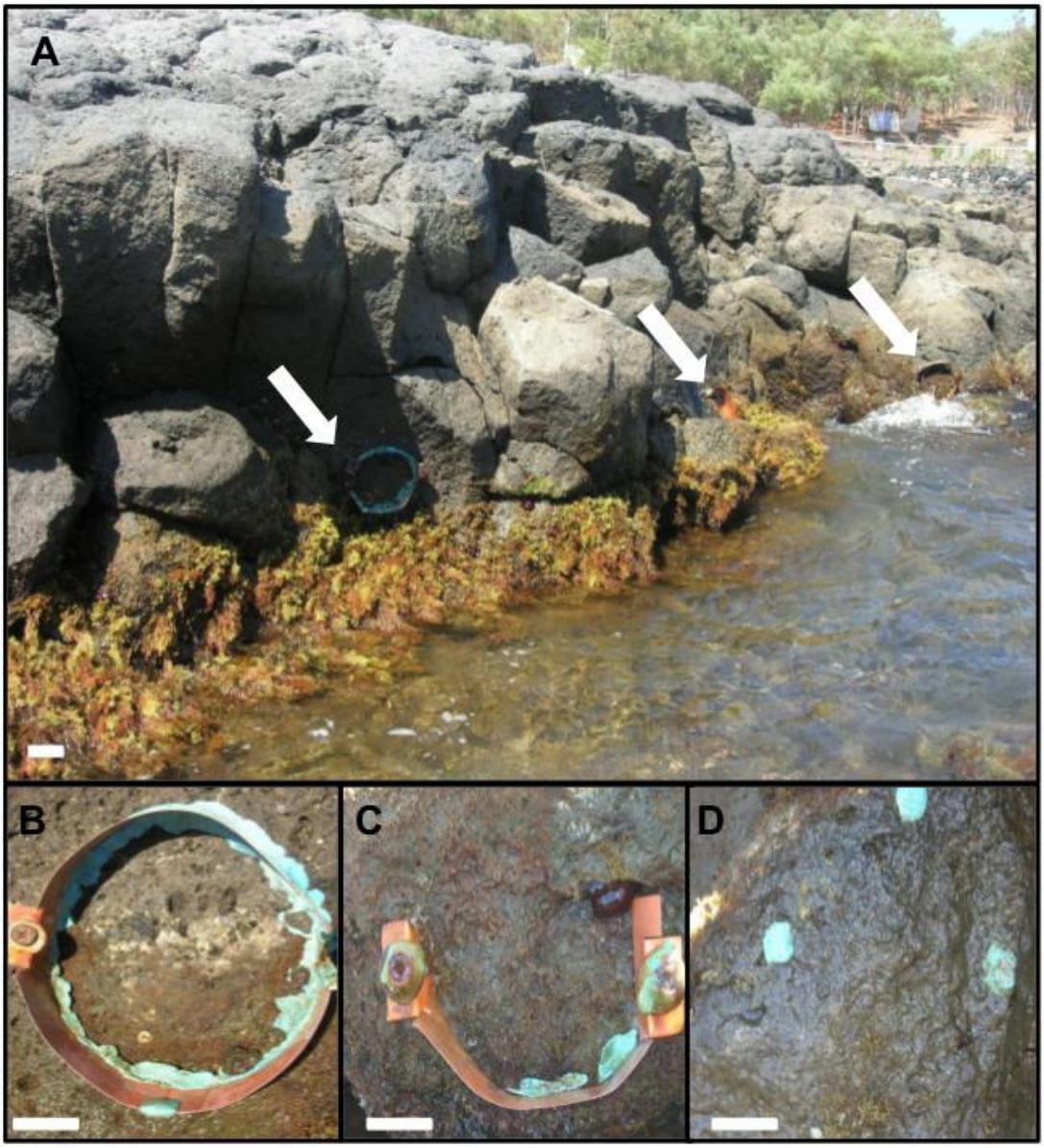

Figure 5.3. Rocky shore on Vulcano showing experimental units (arrows) at the 1200 ppm site during low tide (A). In the lower part of the figure the three treatments are shown: limpet exclosure (15 cm diameter, B), procedural control (C) and control (D); scale bars = 5 cm.

The experiment lasted six months; benthic diversity and abundance in the plots were assessed using visual census approximately every two months (start of experiment, i.e. May 2012; July 2012; September 2012; November 2012). In November 2012, a 10 x 10 cm quadrat in the centre of each plot was denuded of all macroalgae using a hammer and chisel. The samples were preserved in

70% ethanol and were identified to the lowest possible taxonomic level in the laboratory. After identification, algae from each taxon were left to dry at 60°C in the oven for 72h and weighed to obtain dry mass.

5.2.1.3 Limpet abundances and feeding rates

During each visit, limpet abundance was determined at low tide in nine haphazardly chosen replicate plots per site. The plots were the same size as the experimental plots. Limpets were counted and their shell length measured using a Vernier calliper (accuracy ± 1 mm). In July, limpet densities were also determined at high tide to determine whether there was a significant difference in limpet densities related to this parameter.

In November 2012, limpet feeding rates were also measured using wax discs (Thompson *et al.*, 1997). Individually numbered 14 mm diameter plastic holders filled with wax were placed in holes drilled in the rocky substratum. In each site, three grids of 16 holes in which wax discs could be placed were drilled, in a 4x4 configuration with 15 cm gaps between each hole. Discs were left for 14 days on the shore and then collected, and in the laboratory number of grazed discs and percentage cover of grazing marks were determined.

5.2.1.4 Statistical analyses

Benthic species composition and abundance from visual census was tested using a three-factor PERMANOVA. “Site” and “treatment” were considered fixed factors with two (600 and 1200 ppm) and three (exclusion, procedural control and control) levels, respectively, whereas “date” was a random orthogonal factor. A square-root transformation was used to reduce the influence of abundant taxa in the community, a Bray-Curtis dissimilarity matrix was built and

Type III sums of squares with 9,999 unrestricted permutations of the raw data were used to account for small sample sizes. Although the design includes repeated measures on the same plots, sphericity and normality are not necessary for PERMANOVA because the test uses a permutation procedure to generate a distribution for the pseudo-F statistic (analogous to the F statistic in ANOVA). When a limited number of permutations (<100) was available, Monte Carlo p-values were preferred over permutational p-values, which are not reliable in these cases (Anderson *et al.*, 2003). The scraping samples were analysed in the same way, but the experimental design only included the "treatment" and "site" factors. Percent changes in key groups of macroalgae were also analysed using this design.

Variance derived from significant interactions was then decomposed to determine which factor determined the significant interaction, and pairwise tests were performed when necessary. A SIMPER analysis was then used to determine the contribution of each taxon to the average Bray-Curtis dissimilarity between levels of a factor if the PERMANOVA analysis was significant. The same procedure was used to analyse scrapings data, but the design was modified to include only the "site" and "treatment" factors. All analyses above were performed using PRIMER 6 with PERMANOVA+ extension (Plymouth Routines In Multivariate Ecological Research, version 6).

Limpet abundance and length as well as percent cover of marks on wax discs and macroalgal biomass from scrapings were analysed using a two-way ANOVA with "site" and "date" as factors after checking they complied with the normality and variance homogeneity requirements of the analysis. However, no "date" factor was used for the analysis of limpet grazing rates and macroalgal biomass. All the analyses above were performed using SPSS v19.

5.2.2 Methana

To assess whether subtidal herbivores differently affect algal recruitment at different carbon dioxide levels, we conducted a second exclusion experiment at Methana CO_2 seeps.

5.2.2.1 Herbivore surveys

Off Methana, herbivore densities were determined at a site near the seeps (SEEP) and at a reference site (REF A; see Chapter 2 for sites description - detailed sampling dates and sample sizes are reported in Table 1.1D). Densities of *Paracentrotus lividus* and *Arbacia lixula* were determined separately using transects: individuals present between 1 and 2 m depth were counted by snorkelers along five transects (5 m long and 1 m wide) per site per species in September 2012 and June 2013. Fish communitiy composition and biomass were quantified in September 2013 by Maria Salomidi and Yiannis Issaris using a standard visual census technique (while SCUBA diving) within belt transects of 25 m length and 5 m width placed at 3m depth (three replicates, 125 m^2 surface each). The observer conducting the fish survey moved at constant speed identifying, counting and attributing all individuals to 5 cm size classes within 2.5 m on either side of the 25 m transect line (La Mesa and Vacchi, 1999; Giakoumi *et al.*, 2012). Length estimates of fish from the visual surveys were converted to wet biomass by using the allometric length-biomass conversion: $B = a L^b$, where B is biomass in grams and L is total length in cm. The constant parameters a and b corresponding to the closest geographical area were obtained from Morey et al. (2003).

5.2.2.2 Herbivore exclusion

Four sterile 10 x 10 cm ceramic tiles were attached to rocks using epoxy putty and deployed at the two Methana study sites at ~ 2 m depth by snorkelers as

controls; four tiles per site were enclosed in a 1 cm mesh cage to exclude herbivores, and four additional tiles per site were enclosed in a cage missing one side to act as procedural controls (Figure 5.4). The cages were painted using non-toxic antifouling paint (EP-2000, ePaint, Florida) to prevent epiphytes from growing and shading the tiles. Tiles were deployed in September 2012 and recovered in June 2013, when seaweed biomass reaches its annual peak (Ballesteros, 1984).

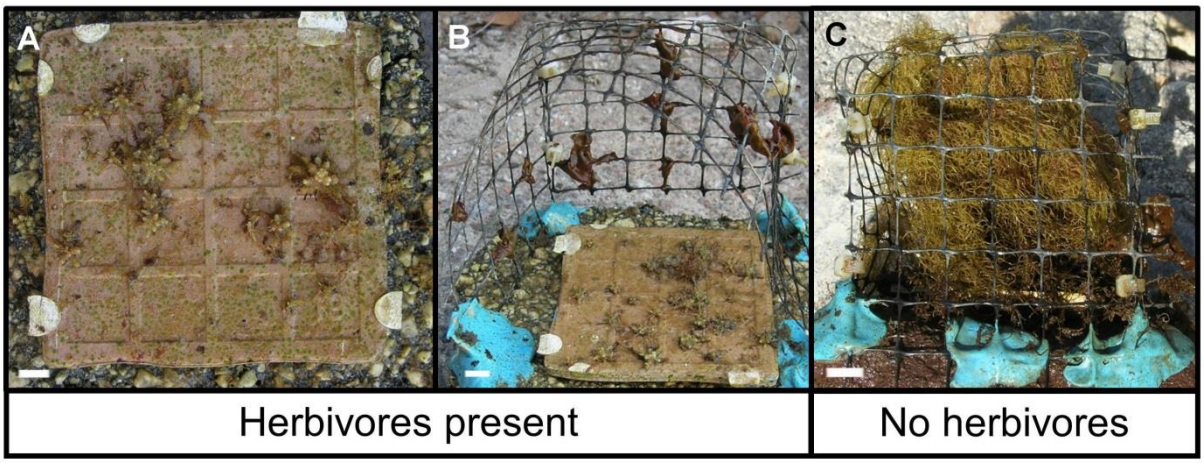

Figure 5.4. Pictures of the three treatments for the herbivore exclusion experiment at Methana taken at the end of the experiment (June 2013): control tile (10 x 10 cm; A), procedural control (B) and herbivore exclusion (C); scale bars = 1 cm.

After recovery, tiles were detached from the rock, put in individual zip-lock bags and stored frozen. In the laboratory, their cover was visually assessed and quantified as percent cover of functional groups. The functional groups used were: fucoid algae (mostly *Cystoseira* sp.), erect brown algae, fleshy brown algae (mostly *Dictyota* sp.), calcifying brown algae (mostly *Padina pavonica*), turf algae (mat-forming algae shorter than 2 cm, mostly *Halopteris scoparia* (Linnaeus) Sauvageau), encrusting black, encrusting green, filamentous green, articulated coralline algae, coralline crustose algae (CCA), serpulid worms, biofilm, bare substratum. The biomass of turf and erect algae was measured by

scraping the algae from the tiles, drying them at 60°C for 72 h and weighing them to obtain dry mass.

5.2.2.3 Statistical analyses

Sea urchin data were analysed with a three-way ANOVA after transforming them (fourth root) to comply with the normality and variance homogeneity requirements of ANOVA. The ANOVA had three fixed factors (species, date and site). Log-transformed biomass of the three recorded herbivorous fish was also analysed using an ANOVA with site and species as fixed factors. All the analyses above were performed using SPSS v19.

Tiles species composition and abundance from visual census was tested using a two-factor PERMANOVA with “site” and “treatment” as fixed factors. A square-root transformation was used to reduce the influence of abundant taxa in the community, a Bray-Curtis dissimilarity matrix was built and Type III sums of squares with 9,999 unrestricted permutations of the raw data were used to account for small sample sizes. Pairwise tests were performed when a factor with more than two levels was significant. A nMDS plot was used to visually inspect the similarities among samples. The same procedure was used to analyse biomass data.

Percent cover or biomass changes in key groups of macroalgae were analysed with a permutational ANOVA using the experimental design described above, but using dissimilarity matrices based on Euclidean distances. Percent cover was used for those functional groups that could not be reliably scraped from the tile (i.e. CCA, encrusting green, encrusting black, biofilm and bare substratum). All analyses above were performed using PRIMER 6 with PERMANOVA+ extension (Plymouth Routines In Multivariate Ecological Research, version 6).

5.3 Results

5.3.1 Vulcano

5.3.1.1 Environmental parameters

Measured and calculated carbonate chemistry parameters are shown in Table 5.1. Over the experiment duration, pH in the 1200 ppm site was approximately 7.8, more than 0.2 points lower than the 600 ppm site. In contrast, measured temperature and salinity were not significantly different between the two sites. At the elevated CO_2 site, seawater pCO_2 was double than in the reference site, even though seawater was still saturated with respect to both calcite and aragonite.

Table 5.1. Mean (± SD, n=6) pH, temperature (T) and salinity (S) measured during the experiment at Vulcano between May - October 2012 and pCO_2, bicarbonate ions (HCO_3^-), carbonate ions (CO_3^{2-}), seawater saturation with respect to calcite (Ω_{Ca}) and aragonite (Ω_{Ar}) calculated using CO2Sys.

	pH_{NBS}	**T** (˚C)	**S** (ppt)	**pCO_2** (µatm)	**HCO_3^-** (mmol kg^{-1})	**CO_3^{2-}** (mmol kg^{-1})	**Ω_{Ca}**	**Ω_{Ar}**
600 ppm	8.05 ± 0.04	25.03 ± 1.20	38.72 ± 0.15	602 ± 51	2025 ± 39	205 ± 16	4.77 ± 0.37	3.16 ± 0.25
1200 ppm	7.79 ± 0.17	25.20 ± 2.78	38.72 ± 0.39	1211 ± 192	2200 ± 53	133 ± 22	3.10 ± 0.50	2.06 ± 0.33

5.3.1.2 Limpet exclusion, abundance and feeding rates

Copper rings were highly effective at excluding limpets from experimental plots. No limpets were found in the exclosure plots during subsequent visits, except for July, when 1-2 small limpets (length < 2 mm) had recruited into three exclosure plots at the 600 ppm site, but they were removed and no limpets crossed the copper rings. The visual census data and the scraping data had

similar results, so only the visual census data analysis is reported for simplicity. Results from the PERMANOVA analysis (Table 5.2) show that the experimental treatment had a different effect at the two sites (Site*Treatment pseudo-$F_{2,68}$ = 3.997, p(perm) = 0.0086).

Table 5.2. PERMANOVA analyses of square-root transformed percentage benthic cover in the experimental plots for the experiment performed at Vulcano from May to October 2012. The first table shows main factors and their interactions and degrees of freedom (df), sum of squares (SS), pseudo-F, permutational p and unique permutations for each of them. Treatment x Date interaction and Date both have a significant effect (p<0.05). The second table shows pair-wise comparisons between treatments at both sites with no significant differences between the t-values of any of the treatments at the 1200 ppm site, while all comparisons were significant at the 600 ppm site.

Source	df	SS	Pseudo-F	p(perm)	Unique perms
Site	1	11014.0	8.3517	**0.0054**	6367
Treatment	2	3322.3	2.5128	0.0926	9950
Date	3	20601.0	5.9490	**0.0001**	9930
Site x Treatment	2	2337.8	3.9974	**0.0086**	9955
Site x Date	3	3996.6	1.1541	0.3159	9938
Treatment x Date	6	3827.9	0.5527	0.9450	9905
Site x Treatment x Date**	5	1374.9	0.2382	0.9989	9927
Res	68	78493.0			
Total	90	133570.0			

** Term has one or more empty cells

Within level '1200 ppm' of factor 'Site'			
Groups	**t**	**p(perm)**	**Unique perms**
exclosure, proc control	0.81312	0.5255	1259
exclosure, control	1.2114	0.2832	4344
proc control, control	1.0702	0.3976	420

Within level '600 ppm' of factor 'Site'			
Groups	**t**	**P(perm)**	**Unique perms**
exclosure, proc control	7.4724	**0.0016**	840
exclosure, control	2.021	**0.0444**	840
proc control, control	4.2419	**0.0019**	840

There was also a significant difference between sampling dates (pseudo-$F_{3,68}$=5.949, p(perm)=0.0001), which was consistent among sites and

treatments. Pair-wise comparisons between treatments in each site obtained by decomposing the variance in the site*treatment interaction are shown in the lower part of Table 5.2. It is evident that the 600 ppm site had a much higher heterogeneity compared to the elevated CO_2 site because all pairwise comparisons were significant in the former site. However, this means that no conclusion on the overall treatment effect can be drawn.

The SIMPER analysis between sites and among treatment levels at the 600 ppm site showed which taxa contributed the most to the detected differences (Table 5.3). The main drivers of differences between sites were bare rock and brown turf, which together account for almost 40% of the total variability. Both categories increased at the 1200 ppm site, whereas *Padina*, CCA, *Dictyotales* and *Cystoseira* showed the opposite trend. The main drivers of differences among treatments were the dominant categories such as turf algae and bare substratum. Those taxa that changed most among treatment levels such as the calcareous brown alga *Padina pavonica* and the barnacle *Chtamalus stellatus* were also important determinants of the differences between treatments.

Table 5.3. SIMPER analysis showing the average dissimilarities between sites, as well as that among treatments at the 600 ppm site at Vulcano in 2012 pooling dates and which cover group contributes to the dissimilarity up to 90%. For each species, the average abundance in the two groups that are being compared, their average dissimilarity, the dissimilarity to standard deviation ration and the taxon contribution and cumulative contribution are shown.

Groups 600 ppm and 1200 ppm; Average dissimilarity = 53.94						
Taxa	**1200 ppm Av.Abund**	**600 ppm Av.Abund**	**Av.Diss**	**Diss/SD**	**Contrib%**	**Cum.%**
Bare rock	5.22	4.14	10.81	1.30	20.04	20.04
Brown turf	6.26	5.10	9.56	1.25	17.72	37.77
Padina	0.64	2.64	7.08	1.10	13.13	50.89
CCA	0.60	2.49	6.68	1.33	12.38	63.28

Dictyotales	0.19	1.22	3.59	0.80	6.66	69.94
Cystoseira	0.51	0.68	2.89	0.62	5.36	75.30
Anadyomene	0.53	0.55	2.38	0.80	4.40	79.70
Chthamalus	0.05	0.76	2.26	0.59	4.19	83.89
Dasycladus	0.09	0.73	2.16	0.58	4.00	87.89
Green turf	0.43	0.05	1.45	0.31	2.68	90.57
Groups exclosure and control; Average dissimilarity = 42.52						
Taxa	**Exclosure Av.Abund**	**Control Av.Abund**	**Av.Diss**	**Diss/SD**	**Contrib%**	**Cum.%**
Bare rock	4.04	4.82	9.06	1.4	21.31	21.31
Brown turf	5.35	4.97	6.45	1.07	15.17	36.48
Padina	2.73	1.32	5.87	1.24	13.81	50.29
Dictyotales	1.02	1.86	4.72	0.96	11.1	61.39
CCA	2.68	3.01	3.93	1.11	9.24	70.63
Chthamalus	1.28	0.19	3.04	0.74	7.14	77.77
Cystoseira	0.9	0.26	2.85	0.64	6.71	84.47
Dasycladus	0.74	0.48	2.28	0.69	5.36	89.83
Anadyomene	0.55	0.29	1.34	0.64	3.16	92.99
Groups exclosure and proc control; Average dissimilarity = 45.14						
Taxa	**Exclosure Av.Abund**	**Proc control Av.Abund**	**Av.Diss**	**Diss/SD**	**Contrib%**	**Cum.%**
Padina	2.73	3.77	7.66	1.22	16.98	16.98
Bare rock	4.04	3.69	7.51	1.11	16.63	33.6
Brown turf	5.35	4.75	6.56	1.06	14.53	48.14
CCA	2.68	1.59	5.28	1.23	11.71	59.84
Dictyotales	1.02	0.97	3.17	0.89	7.03	66.87
Chthamalus	1.28	0.29	3.06	0.76	6.78	73.65
Cystoseira	0.9	0.66	2.99	0.8	6.62	80.27
Dasycladus	0.74	0.94	2.97	0.75	6.58	86.84
Anadyomene	0.55	0.8	1.77	0.8	3.92	90.76
Groups control and proc control; Average dissimilarity = 48.22						
Taxa	**Control Av.Abund**	**Proc control Av.Abund**	**Av.Diss**	**Diss/SD**	**Contrib%**	**Cum.%**
Bare rock	4.82	3.69	9.59	0.99	19.88	19.88
Padina	1.32	3.77	9.31	1.14	19.31	39.2
Brown turf	4.97	4.75	7.23	0.88	15	54.19
CCA	3.01	1.59	5.12	0.97	10.62	64.81
Dictyotales	1.86	0.97	4.91	0.96	10.18	74.99
Dasycladus	0.48	0.94	2.93	0.64	6.07	81.06
Cystoseira	0.26	0.66	2.24	0.71	4.65	85.71
Anadyomene	0.29	0.8	2.04	0.85	4.24	89.95
Chthamalus	0.19	0.29	0.94	0.49	1.96	91.91

Some individual species showed patterns related to the experimental treatment (Figure 5.5). The treatments had a significant effect on percent cover of *Padina pavonica* and *Dictyota* sp., but there was no pattern coherent with grazing reduction (i.e. control and procedural control had different values), meaning that these two taxa likely responded to some artefact effect such as changes in light

or water circulation. On the other hand, the barnacle *Chthamalus stellatus* and the red alga *Laurencia* sp. significantly increased their cover when limpets were excluded, the former only at the 600 ppm site and the latter showing a diminished effect at the elevated CO_2 site.

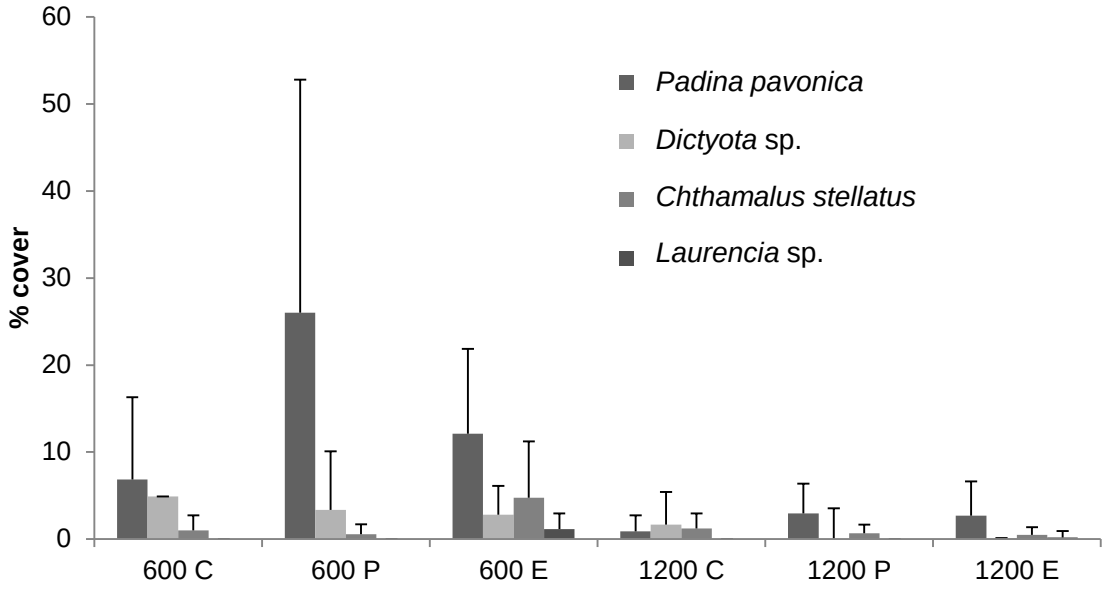

Figure 5.5. Mean percent cover (± SD, n=9-18) of species significantly affected by experimental treatments at the exclusion experiment at Vulcano in 2012 (C is control, P is procedural control, E is exclusion) pooling sampling dates at the 600 ppm and 1200 ppm sites.

Statistical analysis of limpet abundance data shows that both site (pseudo-$F_{1,4}$=18.223, p(perm)=0.006) and date (pseudo-$F_{4,78}$=3.5842, p(perm)=0.01) had a significant effect. Pairwise comparisons confirm that at the 1200 ppm site there was no significant seasonal pattern. Conversely, at the 600 ppm site limpet abundances were higher than those in the 1200 ppm site in spring and summer, but in autumn there was a sudden drop in limpet densities, bringing their values close to those of the 1200 ppm site (Figure 5.6). Limpet abundances sampled at high and low tide in July did not differ significantly.

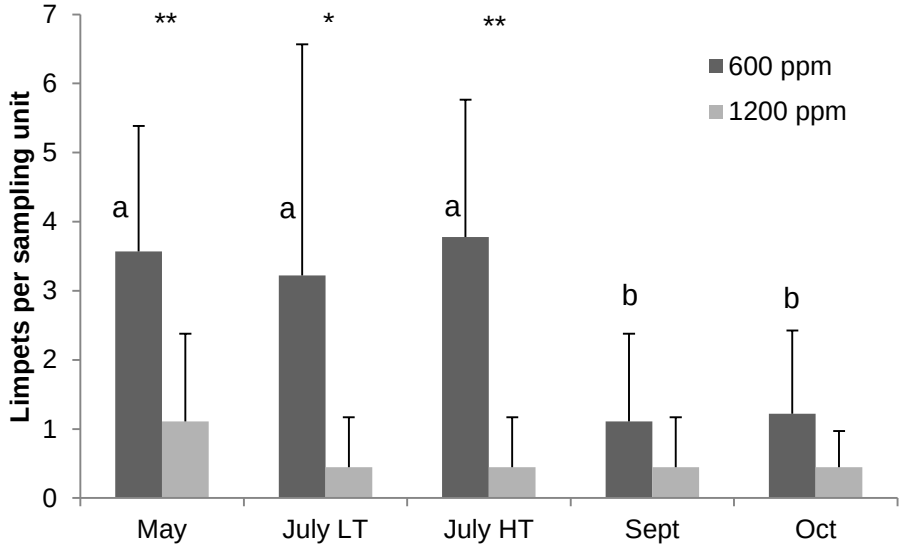

Figure 5.6. Mean (± SD, n=9) limpet abundance per sampling unit on the four sampling dates for 600 ppm and 1200 ppm sites at Vulcano during the exclusion experiment (May-October 2012). In July limpet densities were assessed twice, once at low tide (LT) and once at high tide (HT) to determine the variability of limpet abundances within a tidal cycle; all other densities were determined at low tide. Different letters mean that limpet abundances are significantly different among sampling dates. Asterisks show when the two sites are significantly different (* = $p<0.05$; ** = $p<0.01$).

As for limpet length measurements, the permutational ANOVA results report only a significant effect of site (pseudo-$F_{1,7}$=17.861, p(perm)=0.028). Limpets from the 1200 ppm site were bigger than those living in the 600 ppm site, especially in spring and summer. This difference, however, was never significant in pairwise comparisons and was strongly reduced in autumn (Figure 5.7).

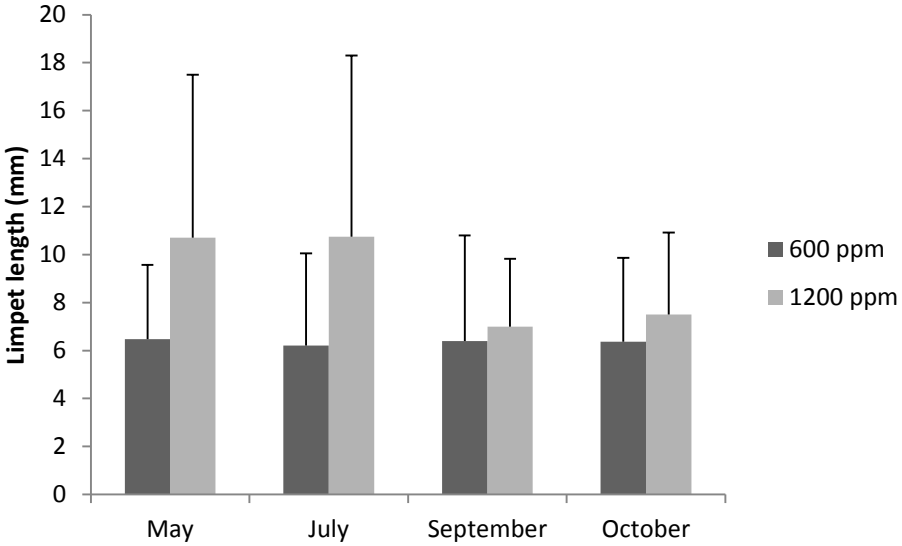

Figure 5.7. Mean (± SD) limpet length in the four sampling dates (May, July, September and October 2012) at the 600 and 1200 ppm sites off Vulcano. Limpets in the 1200 ppm site are slightly longer than those in the 600 ppm site. N=4-29.

After verifying that quadrat and position of disc in the quadrat (high or low) had no significant effect on the percentage of grazed disc, arcsin-transformed data were analysed using a one-way ANOVA. Results from the analysis show that there was no significant difference in grazing rates between sites, even though there was a clear trend for higher grazing rates at the 600 ppm site (Figure 5.8).

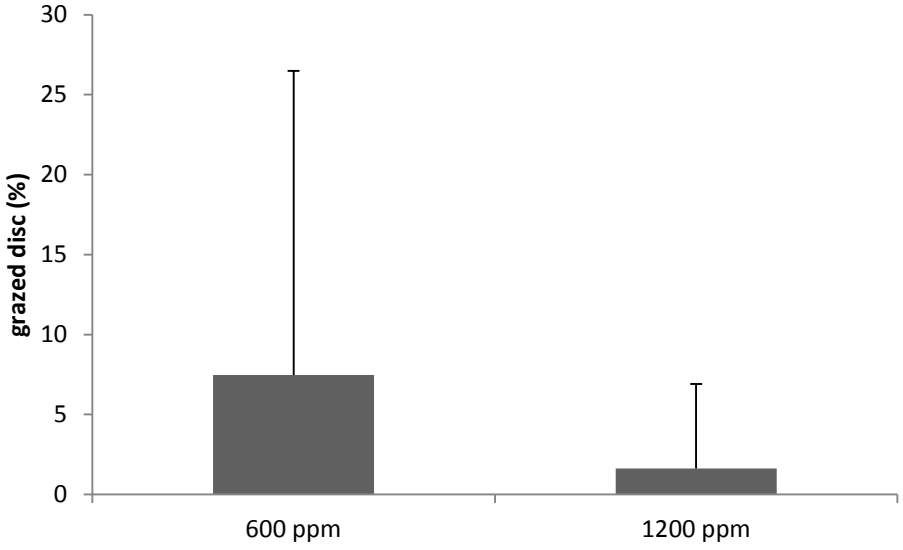

Figure 5.8: Mean (± SD) percentage of wax disc grazed by limpets in the 600 ppm site (n=41) and the 1200 ppm site (n = 34) at Vulcano in November 2012.

5.3.2 Methana

5.3.2.1 Environmental parameters

Measured and calculated carbonate chemistry parameters are shown in Table 5.4. The mean pH near the seeps was approximately 7.7, more than 0.3 points lower than the reference site. On the other hand, temperature and salinity were not significantly different between the two sites. At the high CO_2 site, seawater pCO_2 was double that of the reference site, even though on average seawater was still saturated with respect to both calcite and aragonite.

Table 5.4. Mean (± SD, n=11-24) pH, temperature (T) and salinity (S) measured at Methana in September 2012 and June 2013 as well as pCO_2, bicarbonate ions (HCO_3^-), carbonate ions (CO_3^{2-}), seawater saturation with respect to calcite (Ω_{Ca}) and aragonite (Ω_{Ar}) calculated using CO2Sys.

	pH_{NBS}	**T** (˚C)	**S** (ppt)	**pCO_2** (µatm)	**HCO_3^-** (mmol kg^{-1})	**CO_3^{2-}** (mmol kg^{-1})	**Ω_{Ca}**	**Ω_{Ar}**
SEEP	7.70 ± 0.16	25.34 ± 0.85	38.77 ± 0.93	1676.8 ± 643.5	2485.4 ± 112.4	125.0 ± 46.5	2.91 ± 1.06	1.93 ± 0.71
REF A	8.09 ± 0.06	25.01 ± 1.05	38.94 ± 0.87	586.9 ± 106.7	2140.5 ± 63.3	232.1 ± 25.9	5.40 ± 0.59	3.57 ± 0.39

5.3.2.2 Herbivore surveys

Sea urchin densities significantly differed between REF A and SEEP, and the densities of the two species were significantly different as well (Table 5.5). On the other hand, no effect of date was detected, and the lack of significant interactions indicates that both *A. lixula* and *P. lividus* densities changed consistently between sites. As no significant effect of date was detected, sea urchin densities were pooled between dates for easier representation.

Table 5.5. ANOVA on fourth-root transformed sea urchin densities measured at Methana in September 2012 and June 2013. The table shows main factors and their interactions and sum of squares (SS), degrees of freedom (df), Mean Squares (MS), F-ratios (F) and p values. Significant p values (< 0.05) are highlighted.

Source	**SS**	**df**	**MS**	**F**	**p**
Site	5.629	1	5.629	17.047	**< 0.001**
Date	0.704	1	0.704	2.131	0.153
Species	3.952	1	3.952	11.969	**0.001**
Site * Date	0.085	1	0.085	0.257	0.615
Site * Species	0.029	1	0.029	0.089	0.767
Date * Species	0.487	1	0.487	1.476	0.232
Site * Date * Species	0.068	1	0.068	0.206	0.653
Error	11.887	36	0.330		
Total	51.118	44			

Densities of *A. lixula* were consistently higher than those of *P. lividus* (Figure 5.9), with average densities of the former species ranging from 1.9 to 7.5 individuals in a five-metre transect. On the other hand, *P. lividus* densities ranged from 0.2 to 1.6 individuals. There was also a clear reduction in the densities of both species near the seeps, with *P. lividus* being almost absent at the high CO_2 site.

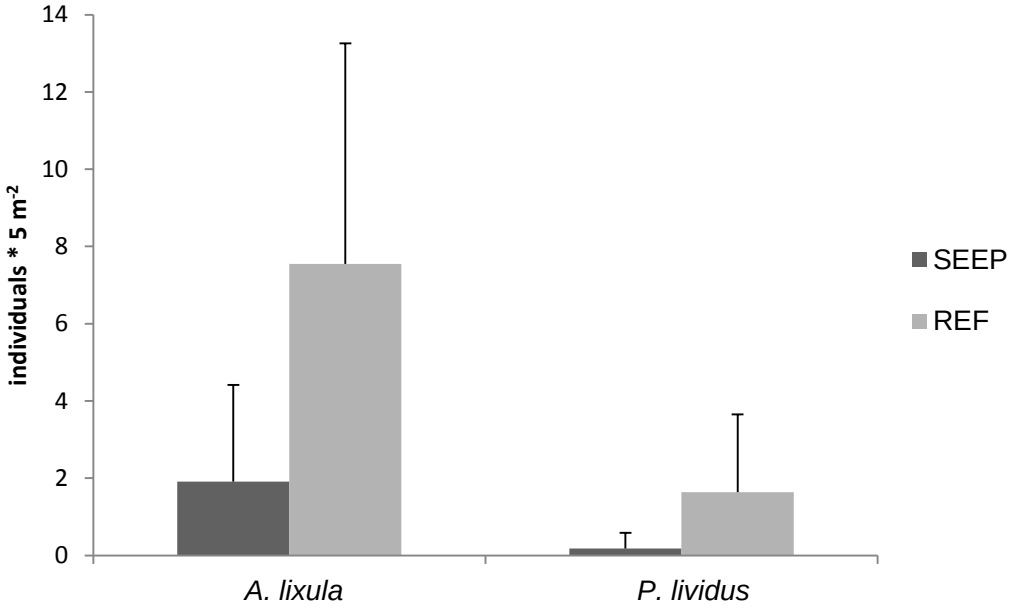

Figure 5.9. Average number (± SD, n=11) of sea urchin individuals along a 5 m transect at Methana study sites (SEEP and REF A) pooling data from September 2012 and June 2013.

Three herbivorous fish species were recorded at the study sites: *Sarpa salpa*, *Siganus luridus* and *Sparisoma cretense*. Results from ANOVA (Table 5.6) show that, just as with sea urchins, both site and species had a significant effect on fish biomass. No significant interactions were found, meaning that changes in all species' biomass between sites followed a similar pattern.

Table 5.6. ANOVA on log-transformed herbivorous fish biomass at Methana in June 2013 showing main factors and their interactions and sum of squares (SS), degrees of freedom (df), Mean Squares (MS), F-ratios (F) and p values. Significant p values (< 0.05) are highlighted.

Source	**SS**	**df**	**MS**	**F**	**p**
Species	52.403	2	26.201	4.291	**0.039**
Site	35.608	1	35.608	5.831	**0.033**
Species * Site	17.190	2	8.595	1.408	0.282
Error	73.279	12	6.107		
Total	363.430	18			

All herbivorous fish species increased in biomass (i.e. total biomass per 25 m transect) near the seeps (Figure 5.10), but the magnitude of the change was very different among species: while *S. cretense* had a low biomass that changed very little between sites, the two other species had very marked changes in biomass between sites. *S. luridus* was present at both sites and its mean biomass increased from 65 to 1565 g from REF A to SEEP. *S. salpa* was absent from REF A, while at SEEP it was the dominant species in terms of biomass (2009 ± 3145 g).

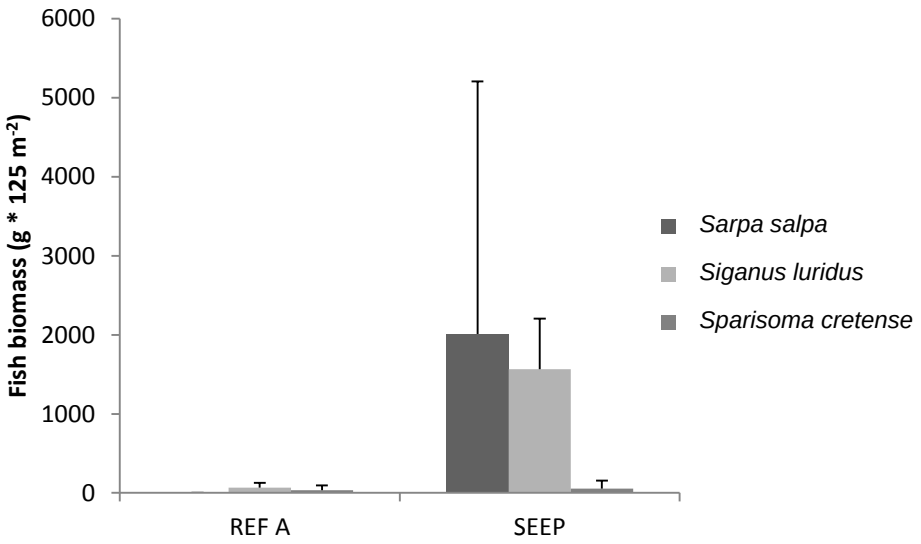

Figure 5.10. Average total biomass (± SD, n=3) of herbivorous fish (*Sarpa salpa*, *Siganus luridus* and *Sparisoma cretense*) per 25 m transect at REF A and SEEP in September 2013.

5.3.2.3 Herbivore exclusion

PERMANOVA analysis of tiles cover (Table 5.7) shows that both site and treatment had a significant effect on benthic assemblages, but there was no interaction between the two factors. Since the treatment factor was significant, pairwise comparisons were performed among treatment levels to detect which

pairs were significantly different. The results (Table 5.7, lower part) show that exclusions were significantly different from both control and procedural control, which did not differ between each other.

Table 5.7. PERMANOVA on square-root transformed percentage cover of the uncaged and caged tiles deployed at Methana from September 2012 to June 2013. The first table shows main factors and their interactions and degrees of freedom (df), sum of squares (SS), Mean Square (MS), pseudo-F, permutational p and unique permutations for each of them. The second table shows pair-wise comparisons between treatments pooling sites; for each comparison the t value, p value and number of unique permutations are shown.

Source	**df**	**SS**	**MS**	**Pseudo-F**	**P(perm)**	**Unique perms**
Site	1	5380.7	5380.7	5.3584	**0.0003**	9938
Treatment	2	11675	5837.4	5.8133	**0.0001**	9937
Site x Treatment	2	2318.5	1159.2	1.1544	0.3204	9945
Residual	15	15062	1004.2			
Total	20	34487				

Groups	**t**	**P(perm)**	**Unique perms**
Control, Exclusion	2.7397	**0.0001**	9937
Control, Proc control	1.2182	0.2271	9918
Exclusion, Proc control	2.3722	**0.0009**	9878

The MDS plot (Figure 5.11) shows that SEEP and REF A were clearly different for all treatments. Controls and procedural controls were closely grouped whereas exclusion tiles were very different. At the SEEP site, a different group of algae (erect brown algae, fleshy brown algae, calcifying brown algae) was dominant in each exclusion tile, whereas at the reference site there was mostly an increase in calcifying brown algal cover when herbivores were excluded.

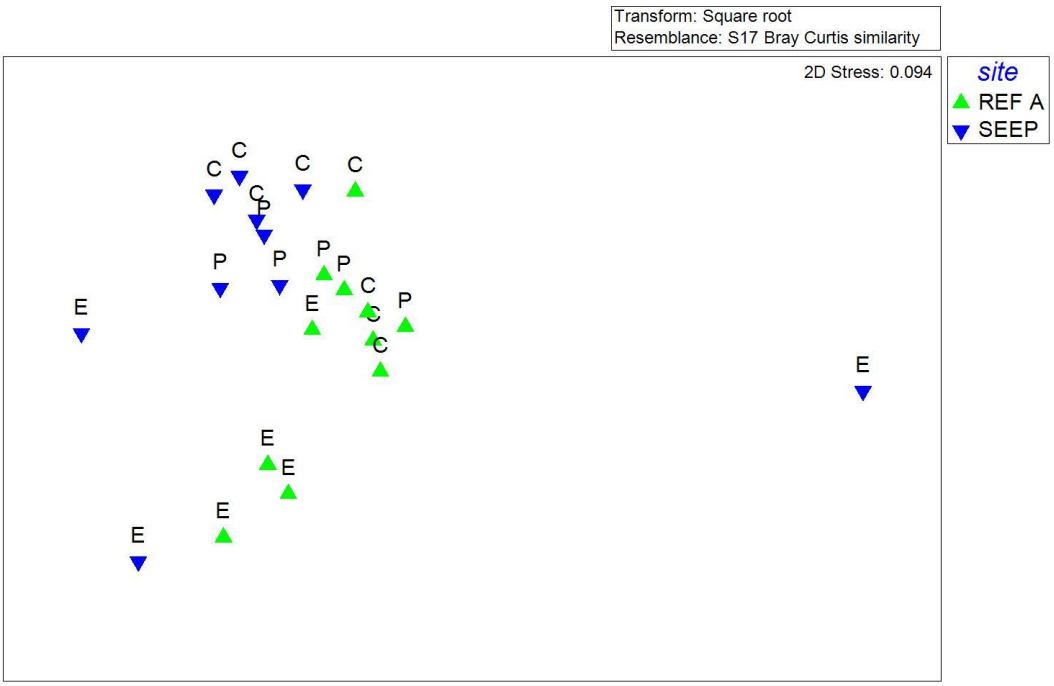

Figure 5.11: MDS plot for the herbivore exclusion experiment performed at Methana from September 2012 to June 2013; green triangles represent tiles placed in REF A, blue triangles are tiles placed in SEEP. Letters above the symbols represent the treatments: C is control, P is procedural control, E is exclusion.

Statistical analysis of the scraping data produced results analogous to the percent cover data at the community level, so only the latter are reported as they are more comprehensive (i.e. they also include encrusting forms). Total biomass significantly differed among treatments (Table 5.8), ranging from about 0.1 g in the controls to approximately 3 g in the exclusions (Figure 5.12). However, at the reference site procedural controls had values intermediate between controls and exclusions.

Table 5.8. PERMANOVA on square-root transformed biomass of macroalgae growing on uncaged and caged tiles deployed at Methana from September 2012 to June 2013. The table shows main factors and their interactions and degrees of freedom (df), sum of squares (SS), Mean Square (MS), pseudo-F, permutational p and unique permutations for each of them.

Source	df	SS	MS	Pseudo-F	p(perm)	Unique perms
Site	1	0.2548	0.2548	1.5942	0.2271	9835
Treatment	2	8.3648	4.1824	26.166	**0.0002**	9955
Site x Treatment	2	0.3737	0.1869	1.1691	0.334	9959
Residual	15	2.3976	0.1598			
Total	20	11.706				

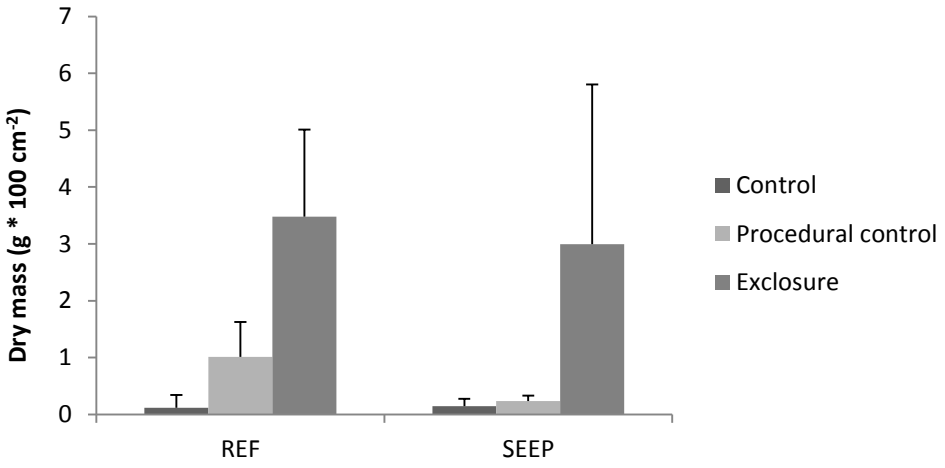

Figure 5.12. Average biomass (± SD) of fleshy and erect algae grown on tiles for all three treatments of the herbivore exclusion experiment conducted at Methana from September 2012 to June 2013; n = 3-4.

Eight functional groups were significantly different between treatments or sites, four turf or erect and four encrusting forms. Overall, turf and erect algae increased in herbivore exclusions (Figure 5.13A), whereas encrusting forms showed the opposite trend (Figure 5.13B). Biofilm percent cover did not show any clear effect of herbivore exclusion, but it significantly increased at the high CO_2 site. The effect of herbivore exclusion was always clear at SEEP, while at

REF A some functional groups (turf algae, CCA and bare substratum) had biomass or cover values similar between exclusion and procedural control. There were significant differences between sites as well, with turf algae, calcifying brown algae and CCA decreasing as CO_2 increased and fucoid algae, fleshy brown algae, biofilm and bare substratum showing the opposite trend.

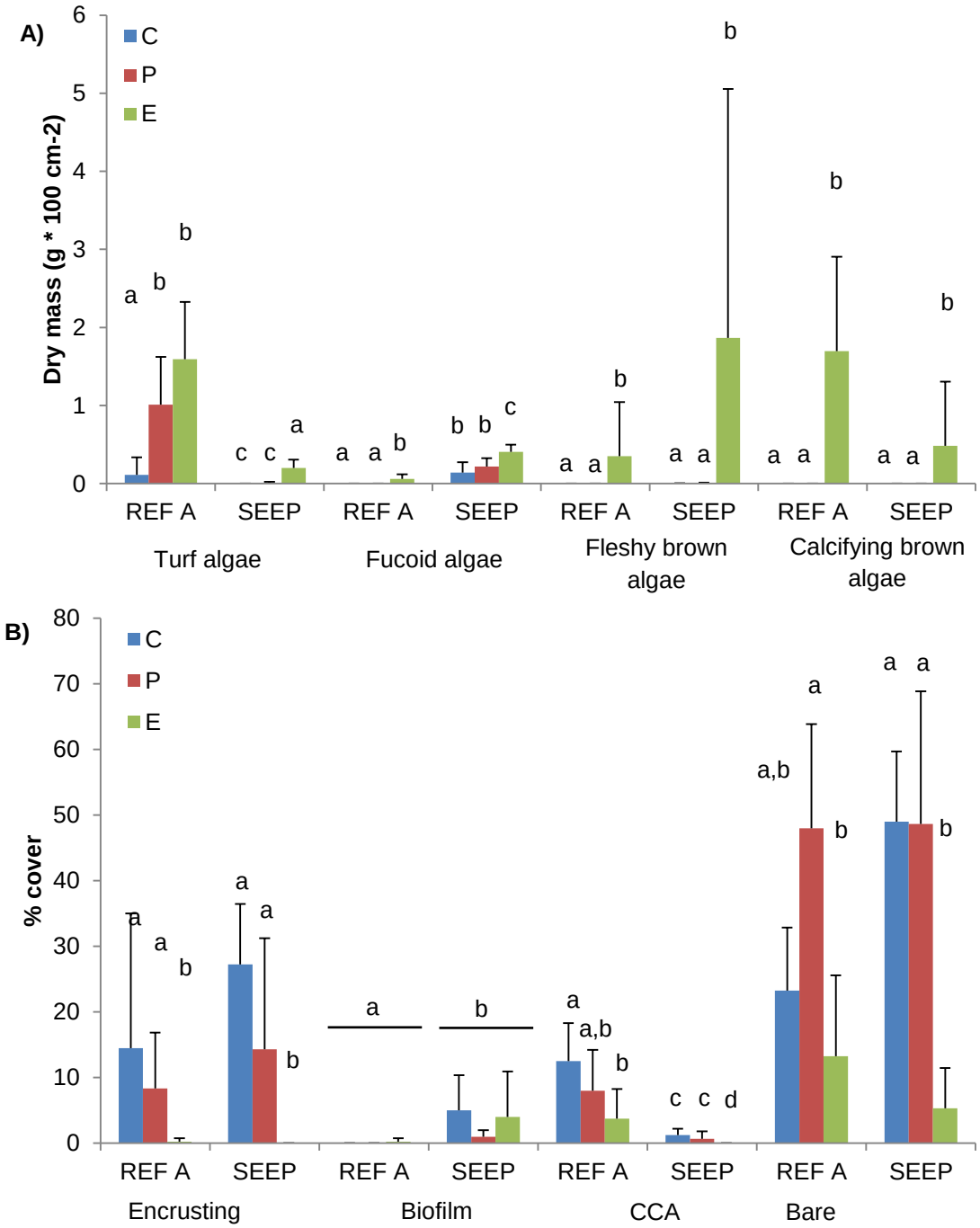

Figure 5.13. Mean (± SD, n=3-4) biomass (A) or percent cover (B) of functional groups that showed significant differences between sites (REF A and SEEP) or treatments (C=controls;

P=procedural controls; E=herbivore exclusions). Different letters indicate significantly different sub-groups within a functional group.

5.4 Discussion

The relative role of bottom-up and top-down processes in shaping marine ecosystems has long been a critical issue in marine ecology research. Previous research has shown that relative importance of these two types of processes is highly context-dependant (Burkepile and Hay, 2006). This study shows that in Mediterranean intertidal and subtidal rocky reefs increased pCO_2 (bottom-up) has a significant effect on benthic communities. On the other hand, limpet herbivory (top-down) only had a weak influence on benthic communities at an intertidal rocky shore off Vulcano (Italy), but sea urchin and fish grazing strongly controlled seaweed biomass and community structure in a subtidal habitat off Methana (Greece), even though herbivore community composition changed dramatically as CO_2 levels increased.

Direct effects of carbon dioxide were mostly consistent between Vulcano and Methana. In both areas, bare substratum increased and CCA cover decreased with increasing CO_2. Many crustose coralline algae are well known to be sensitive to ocean acidification (Kroeker *et al.*, 2010; Brodie *et al.*, 2014), and even tolerant species can be outcompeted by non-calcifying algae at elevated CO_2 levels (Kroeker *et al.*, 2013c). The “bare substratum” functional group used at Vulcano included biofilms, which are known to increase in high CO_2 environments (Johnson *et al.*, 2013; Kroeker *et al.*, 2013; Taylor *et al.*, 2014).

At Methana, fleshy brown and fucoid algae also significantly increased near the seeps, whereas *Padina pavonica* abundance decreased with increased CO_2 at both sites. Fucoid algae are commonly found in high abundances near volcanic

CO_2 seeps (Porzio *et al.*, 2011; Chapter 3), while fleshy brown algae may have increased in cover at high CO_2 after outcompeting *P. pavonica*. Recently, Johnson *et al.* (2012) reported increasing *P. pavonica* densities as CO_2 increased in shallow subtidal waters off Vulcano, possibly because of lower consumption by sea urchins. The decreased *P. pavonica* cover at elevated CO_2 found at Vulcano may be due to the different sampling depth (personal observation): *Paracentrotus lividus*, the species that mostly grazes on *P. pavonica* (Chiantore *et al.*, 2008), is easily dislodged by waves (Bulleri *et al.*, 1999). Intertidal shores off Vulcano are subject to high wave activity, so *P. pavonica* is not likely to be influenced by sea urchin grazing there. On the other hand, *P. pavonica* (the main calcifying brown alga) biomass decreased with increasing CO_2 at Methana, but only when herbivores were excluded, unlike in the study from Johnson *et al.* (2012). This probably happened because fleshy brown algae (*Dictyota* sp.) had a competitive advantage over the calcifier *P. pavonica* as CO_2 increased.

On the other hand, turf algae showed opposite responses to increased CO_2, as their cover increased at Vulcano and decreased at Methana. Turf algae are often advantaged by increased CO_2, as many turf species are extremely fast-growing and possibly carbon-limited (Connell *et al.*, 2013). However, a recent survey at seeps off Ischia reported decreased turf biomass at high CO_2 levels (Porzio *et al.*, 2011). Turf algae is a functional group that includes many species, some of which may be palatable to grazers (Falkenberg *et al.*, 2014), and therefore exhibit very different responses to ocean acidification.

Limpets exerted a weak top-down control on benthic communities off Vulcano in reference conditions, whereas carbon dioxide caused major changes in benthic community structure. Limpets have a decreasing influence on benthic

communities as latitude decreases (Coleman *et al.*, 2006), and in the Mediterranean Sea their effect is not consistent in space and time (Benedetti-Cecchi *et al.*, 2001). When consistent negative effects on filamentous algae were recorded in the Mediterranean Sea, limpet densities were much higher than in this study (Bulleri *et al.*, 2000). Moreover, when the physical environment is stressful limpet grazing has weaker effects on macroalgae (Bazterrica *et al.*, 2007); this could be the case at Vulcano, where communities are exposed to strong wave action.

At Vulcano, limpets influenced percent cover of the barnacle *Chthamalus stellatus* and of a red alga (*Laurencia* sp.). At the 600 ppm site, percent cover of both taxa decreased when limpets were present, while at elevated CO_2 limpets did not have any significant influence on the experimental plots. Limpets can reduce barnacle recruitment by dislodging young individuals (Menge *et al.*, 2010), but at elevated CO_2 levels barnacle recruitment was strongly reduced and no significant effect of limpets was detectable. This may be due to negative effects of elevated carbon dioxide on barnacles in a food-limited habitat (Pansch *et al.*, 2014), decreased limpet densities at elevated CO_2 (this study) or a combination of the above. The genus *Laurencia* is probably vulnerable to grazing, as limpets are thought to control the upper limit of the *Laurencia-Gigartina* belt found in some parts of Britain (Lewis, 1964). At the 1200 ppm site, *Laurencia* sp. percent cover was extremely low even in the control plots; consequently, lack of significant differences among experimental treatments at this site is probably due to this taxon response to elevated carbon dioxide rather than to decreased limpet grazing. So far, no experiments have been performed on this genus' response to ocean acidification, but at volcanic seeps off Ischia

Laurencia obtusa is only present at pH 8.1 and disappears even at moderate pCO_2 levels (Porzio *et al.*, 2011).

The slight increase in limpet length with high CO_2 confirms findings from seeps off Ischia (Hall-Spencer *et al.*, 2008) and could partly explain the trend towards increased grazing rates detected in this study. Increased feeding rates at elevated CO_2 levels have already been reported for some sea snails (Falkenberg *et al.*, 2013b), whereas other species decrease their food consumption at high CO_2 (Russell *et al.*, 2013). Changes in herbivore feeding rates may be due to altered food quality rather than to direct effects of CO_2 on their metabolism (Falkenberg *et al.*, 2013b; Poore *et al.*, 2013), and changes in macroalgal nutritional value at Vulcano could explain the higher feeding rates of limpets living at the 1200 ppm site. Increased calcification costs (Wood *et al.*, 2010), compensatory hyper-calcification at high CO_2 levels (Rodolfo-Metalpa *et al.*, 2011) and shifts in limpet shell mineralogy from calcite to the more energy-expensive aragonite (Langer *et al.*, 2014) could also explain increased limpet grazing rates.

Subtidal herbivore exclusion at Methana dramatically changed benthic communities grown on tiles after nine months. Previous studies show that herbivores have a greater influence on recruiting compared to established macroalgal communities (Korpinen *et al.*, 2008), and subtidal herbivores exert a stronger top-down control than limpets, whose effect is very variable (Benedetti-Cecchi *et al.*, 2001). Herbivore exclusion caused an increase in algal biomass regardless of site, but in the reference site only calcifying brown algae (*Padina pavonica*) colonised the caged tiles. On the other hand, every caged tile at the high CO_2 site was colonised by a different species (*Padina pavonica*, *Dictyota* sp. and erect brown algae). This confirms that non-calcifying algae become

more abundant as pCO_2 increases, likely because of a decreased competitiveness of calcifying species (Porzio *et al.*, 2011; Kroeker *et al.*, 2013).

Herbivory is known to alter outcomes of macroalgal competition, favouring less palatable species (Hereu *et al.*, 2008). At Methana, herbivore-resistant encrusting algae became more abundant at both CO_2 levels when herbivores were present. In addition, macroalgal communities at Methana showed smaller differences between CO_2 levels when herbivores were present (Figure 5.10). Recent evidence shows that grazers can indeed dampen the effects of environmental changes on primary producers, both in terrestrial and in marine ecosystems (Post and Pedersen, 2008; Anthony *et al.*, 2011; Falkenberg *et al.*, 2014).

At Methana, both sea urchin species had reduced densities near the seeps regardless of sampling date, which is in accord with their predicted sensitivity to high CO_2 resulting from laboratory experiments (Dupont *et al.*, 2010). There is a partial disagreement with results from Vulcano, where *P. lividus* densities decreased, but *A. lixula* densities increased with increasing CO_2 (Calosi *et al.*, 2013a). Increased sea urchin densities near volcanic seeps have previously been correlated with low structural complexity of high-CO_2 habitats (Fabricius *et al.*, 2014); *A. lixula* may therefore tolerate moderate carbon dioxide enrichment, but high habitat complexity may prevent its colonisation at seeps off Methana. Sea urchins were replaced by herbivorous fish at high CO_2 levels; functional redundancy of herbivores can maintain top-down control on macroalgal biomass and reduce the effects of multiple stressors on benthic communities (Blake and Duffy, 2010; Eriksson *et al.*, 2011). Fish, however, are highly mobile and could swim in and out of the high CO_2 area (Riebesell, 2008), masking

potential negative effects of ocean acidification such as those on many species' neuroreceptors (Shaw *et al.*, 2013).

Coastal assemblages often have low functional redundancy, and the loss of a few species can negatively affect ecosystem functioning (Micheli and Halpern, 2005). Taxonomic diversity can help marine community resilience to increased temperatures (Allison, 2004), but there is no evidence this applies to community responses to ocean acidification. Here we show that taxonomic diversity helps improving resilience to ocean acidification: herbivorous fish kept grazing pressure high at elevated CO_2, even though sea urchin densities decreased near the seeps. Overfishing of apex predators has led to higher abundances of Mediterranean sea urchins and herbivorous fish, as they are usually not targeted by commercial fisheries (Guidetti and Dulčić, 2007; Guidetti and Sala, 2007). High herbivore densities can often lead to impoverished macroalgal communities, very different from unexploited Mediterranean coastal ecosystems (Sala *et al.*, 2012). Thus, unvaried grazing pressure at different CO_2 levels may maintain suboptimal community structure. However, at a global level herbivorous fish abundance is strongly reduced by overfishing (Micheli and Halpern, 2005), and when this is combined with other herbivores disappearing (e.g. sea urchin mass mortality in Jamaica) benthic habitat can experience dramatic phase shifts (Hughes, 1994).

Bottom-up control (i.e. increase in CO_2) seemed to be the main factor influencing benthic community structure regardless of herbivore consumption levels. Recent research has shown that indirect effects can be as important as the direct effects of CO_2 in shaping community responses to ocean acidification (Kroeker *et al.*, 2013). However, herbivores have the strongest effect and when they are present other indirect effects are reduced or disappear altogether

(Alsterberg *et al.*, 2013). Here we show that carbon dioxide still affects the specific composition of benthic communities in subtidal habitats even when herbivore pressure is strong, even though grazing reduced community structure variability. The most striking finding of this study is that herbivore functional redundancy can offset indirect effects of ocean acidification; this, however, is only possible in unpolluted ecosystems, as diversity is reduced in contaminated marine systems (Johnston and Roberts, 2009). Although neither of the sites studied in this Chapter is a nature reserve, these areas are not heavily impacted by human activities (author's personal observation); it is therefore possible that impacts of ocean acidification on benthic communities will be more severe in polluted areas. Managing local stressors (e.g. eutrophication, heavy metals) is thus essential to maintain high diversity and increase ecosystem resilience to environmental change (Ghedini *et al.*, 2013).

Chapter 6

Seaweed acclimatisation to high pCO_2 at volcanic seeps

Abstract

Most experiments on organism responses to ocean acidification have been conducted for a relatively short time, so there is little evidence for most species' potential for long-term acclimatisation or adaptation, except for some species of phytoplankton. Volcanic seeps can expose benthic communities to increased CO_2 for centuries, and are starting to be used to study adaptive effects of elevated CO_2 on marine organisms. This chapter aims to determine whether dominant macroalgal species at volcanic seeps off Methana (Greece) show evidence of long-term acclimatisation. Ten thalli of the canopy-forming alga *Cystoseira corniculata* and ten thalli of the articulated coralline alga *Jania rubens* were transplanted within and between one high CO_2 and two reference sites, and their physiological performance was assessed after long-term transplants. Neither species showed signs of non-reversible acclimatisation to elevated CO_2 levels, since there were only very small differences between thalli depending on their site of origin. *C. corniculata* seemed to be favoured by increased CO_2, as it had reduced epiphyte cover and higher $rETR_{max}$ (maximum relative electron transport rate) when transplanted near the seeps. At high CO_2, this species also had increased chlorophyll *c* and antheraxanthin content, as well as increased C:N ratios. *Jania rubens* also showed an increase in some pigment concentrations (chlorophyll *a*, violaxanthin, zeaxanthin and phycocyanin) at high CO_2 levels, but in this species all other parameters were unaffected by the transplant. *Cystoseira corniculata* and *Jania rubens* appear not to permanently acclimatise to ocean acidification, but their different physiological responses may alter their competitive interactions. This would help explain the reduction in *J. rubens* cover recorded at increased CO_2 levels off Methana.

6.1 Introduction

Currently, most of the work on ocean acidification biological responses is performed using short-term experiments. As a consequence, there is limited information on the potential for marine algae to permanently acclimatise or adapt to ocean acidification, except for short-lived organisms. For example, the coccolitophore *Emiliania huxleyi* adapted after being exposed to high pCO_2 for about 500 generations. Actually, calcification rates at high CO_2 were always lower than those in reference conditions, but adapted organisms had much higher calcification rates than non-adapted ones (Lohbeck *et al.*, 2012). For longer-lived macroalgae a solution could be studying individuals from volcanic seeps, which can have high CO_2 levels for centuries (Dando *et al.*, 2000).

Genetic adaptation and non-reversible acclimatisation are thought to be rare in marine environments due to their connectivity, which increases the genetic exchange of adults, larvae or other propagules (Palumbi, 1994). However, there are only a few examples of gene flow preventing or slowing down local adaptation in marine species, whereas local adaptation, especially to temperature, is relatively common in marine environments (Sanford and Kelly, 2011). Connectivity of marine environments is therefore unlikely to be as high as previously thought, and speciation can occur over relatively short distances (e.g. Tellier *et al.*, 2011). Moreover, short dispersal distances decrease inter-population gene flow, increasing the likelihood of local adaptation (Endler, 1977). Dominant macroalgal species at seeps off Methana, *Cystoseira corniculata* and *Jania rubens*, have short dispersal distances (< 5 km; Jones and Moorjani, 1973; Susini et al., 2007). It is thus possible that these two species have acclimatised to high and variable pCO_2, as seeps off Methana influence approximately 10 km of shoreline (Baggini *et al.*, 2014).

Porzio (2010) showed that brown algae of the genus *Dictyota* had altered their morphology and had distinct genotypes when seawater pCO_2 was high. In fact, macroalgae exposed to other stressors on relatively short time scales can undergo permanent changes in their physiology or genome. For instance, exposure to low salinity in the Baltic Sea has led to the evolution of a new *Fucus* species after only a few thousand years (Bergström *et al.*, 2005). In another case, *Fucus serratus* individuals from copper-contaminated areas and their offspring are more tolerant to this heavy metal compared with individuals from more pristine areas, although it is not known whether this is transgenerational acclimation or genetic adaptation (Nielsen *et al.*, 2003).

Non-reversible acclimatisation to high pCO_2 might therefore occur in macroalgae, and studying species from volcanic seeps might give us an insight on the possible mechanisms. The aim of this chapter is to assess whether two dominant seaweed species growing near CO_2 seeps off Methana (Greece) were permanently acclimatised to high and variable pCO_2 conditions using reciprocal transplantations (Sanford and Kelly, 2011). Hypotheses tested were:

1) Growth rates and maximum quantum yield (F_v/F_m) are higher in individuals transplanted at the same CO_2 level they are acclimatised to, since acclimatised populations perform best in their origin conditions (Leimu and Fischer, 2008);
2) Pigment content is higher in coralline algae acclimatised to reference conditions and decreases at elevated CO_2 (*Jania rubens*; Gao and Zheng, 2010), whereas chlorophyll in brown algae increases as seawater pCO_2 increases (*Cystoseira corniculata*; Johnson *et al.*, 2012);

3) Total phenolic compounds, such as phlorotannins, are higher in brown algae acclimatised to high pCO_2 (Swanson and Fox, 2007);
4) Carbon:nitrogen ratio increases in seaweed exposed to elevated carbon dioxide in the long term because there is more inorganic carbon available, not as a result of acclimatisation (Koch *et al.*, 2013);
5) Inorganic carbon content in *J. rubens* decreases in individuals from reference conditions transplanted to the high CO_2 area because of skeleton dissolution, whereas individuals from high CO_2 have higher inorganic carbon content when transplanted to the reference sites because of persistent hyper-calcification (Rodolfo-Metalpa *et al.*, 2011).

Evidence from macroalgae that have acclimatised to high CO_2 conditions is essential to assess the adaptation potential of macroalgae to ocean acidification. There is relatively little information on long-term responses of macroalgae to elevated CO_2, and only a few studies have tackled the issue using field-based experiments. To date, evidence from laboratory experiments indicates that temperate macroalgal communities will change their specific composition as seawater pCO_2 increases; this has potential knock-on effects on marine food webs, nutrient cycling and carbon storage (Brodie *et al.*, 2014). However, there is very little information on macroalgal adaptation potential to increased CO_2, meaning that coastal ecosystems might not change as much as anticipated if macroalgae can acclimatise to elevated pCO_2 levels (Sunday *et al.*, 2014).

6.2 Methods

6.2.1 Experimental design and field sampling

Two common and abundant macroalgal species in Methana were examined for signs of long-term acclimatisation to high pCO_2; detailed sampling dates and sample sizes are reported in Table 1.1E. Ten thalli for each species were transplanted within and between one high CO_2 site (SEEP) and two reference sites (REF A and REF B) as shown in Figure 6.1; see Chapter 2 for site descriptions. All specimens were transplanted by detaching thalli with a small chip of rock still attached using hammer and chisel and attaching them to rocky substratum in the target site using epoxy putty (Z-Spar A-788 Splash Zone Epoxy Putty). This method has been previously used for *Cystoseira* in the Mediterranean Sea and has a good success rate (Sales *et al.*, 2011). Physiological parameters were then measured in the transplanted seaweeds and in seven unmanipulated thalli of each species per site; the number of unmanipulated thalli was selected to reflect the average number of transplanted thalli left at the end of the experiments.

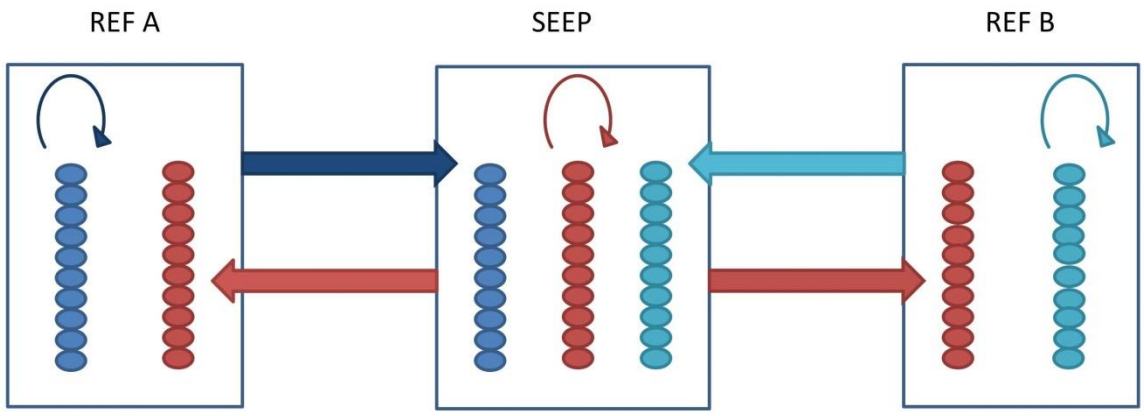

Figure 6.1. Scheme of the experimental design for reciprocal transplantations of *Cystoseira corniculata* transplanted from September 2012 to June 2013 and *Jania rubens* transplanted from June to September 2013. Ten individuals of each species from the high CO_2 site

(SEEP) and the two reference sites (REF A and REF B) were transplanted within their site of origin as procedural controls (round arrows). Ten individuals per species from both reference sited were also transplanted to the SEEP site (blue and light blue arrows). Furthermore, ten individuals per species originally from the high CO_2 site were transplanted to REF A and other ten individuals were transplanted to REF B (red arrows).

Cystoseira corniculata is a fucoid alga and this genus is the main canopy-former in the Mediterranean Sea, where it indicates relatively pristine environmental conditions (Benedetti-Cecchi *et al.*, 2001). It was the dominant macroalgal species at seeps off Methana, and has a biomass maximum between May and June in the region (Haritonidis *et al.*, 1986). This species was transplanted in September 2012 and physiological parameters were measured in June 2013 (in correspondence to its biomass peak). The articulate coralline alga *Jania rubens* is an epiphytic thermophilic species and is extremely common in the study area in spring and summer, with a bloom around August (Belegratis *et al.*, 1999). *Jania rubens* thalli were transplanted in June 2013 (when thalli are large enough to be visible) and their physiological parameters were measured in September 2013 (in correspondence to its biomass peak); thalli of this species transplanted to REF A were all lost due to stormy weather, so only samples from SEEP and REF B were analysed.

Difference in maximum thallus height between the beginning and the end of transplantation was measured placing thalli on graph paper (accuracy ± 1 mm) and used to calculate relative growth for *C. corniculata* and *J. rubens*. Tips were checked for grazer marks. While measuring growth, epiphyte cover of *C. corniculata* thalli was also evaluated using a scale from 1 (epiphyte cover < 25%) to 4 (epiphyte cover > 75%). Chlorophyll *a* fluorescence of the macroalgae was measured with a pulse amplitude modulated fluorometer

(Diving PAM, Walz, Effeltrich, Germany). The maximum photochemical quantum yield of photosystem II (F_v/F_m) was measured after 15 minutes of dark adaptation (Schreiber *et al.*, 1995), then rapid light curves (eight points at 20 s intervals, E1=16, E2=24, E3=34, E4=52, E5=77, E6=118, E7=176 and E8=250 µmol photon m^{-2} s^{-1}) were conducted and non-photochemical quenching (NPQ) was measured. The physiological parameters I_k, $rETR_{max}$ and α_{ETR} (saturation irradiance for ETR, maximum relative electron transport rate and photochemical efficiency, respectively) were calculated using a non-linear regression analysis (Eilers and Peeters, 1988).

Tissue samples for laboratory analyses were collected between 8:00 and 10:00 to avoid the confounding effect of mid-day photoinhibition on pigments (Häder *et al*., 1996) and dried with silica gel for C:N ratio analysis (for all species), total phenolic compounds and tissue P analyses (*C. corniculata* only) and inorganic carbon content (*J. rubens*). More tissue was placed in liquid nitrogen and stored at -60 ºC for pigment analysis (all species).

6.2.2 Laboratory analyses

The total carbon and nitrogen content in dried samples of *C. corniculata* and the organic carbon and nitrogen content of *J. rubens* thalli was measured using a CHN Analyzer (CE Instruments EA1110 elemental analyser). Approximately 1-3 mg of tissue were ground to a powder and packed into aluminum capsules for analysis of total carbon and nitrogen. For organic carbon and nitrogen content of *J. rubens*, approximately 10 mg of sample was ground to powder, placed in silver capsules, acidified with 20 µl of 2M HCl 12 times at 6-12 hours intervals and dried in an oven at 60°C. Separate tissue samples from *J. rubens* were dried for 72 h at 60°C, weighed to obtain dry mass and then put for 24h in a

muffle furnace at 400°C to burn all organic matter and obtain the mass of inorganic carbon. For total phenolic compounds analysis, ~100 mg of freeze-dried tissue was ground and extracted in methanol at 4°C for 24 h. Total phenolic compounds of *C. corniculata* were then analysed using a method modified from Kamal (2011). Seaweed extracts were diluted in distilled water (10% methanol extract, 90% distilled water) and absorbance at 765 nm was measured using a 96 well plate and a FLUOstar Omega microplate reader (BMG Labtech). Each well contained 20 µl 50% Folin-Ciocalteu reagent (Folin and Ciocalteu, 1927), 10 µl Na_2CO_3 (1.5 M) and 10 µl sample solution. Phloroglucinol (1,3,5-tryhydroxybenzene) was used as a standard. Plates were refrigerated overnight before measurement, and eight replicate measurements per sample were made.

Samples of *C. corniculata* and *J. rubens* for pigment analysis were freeze-dried in the dark for 24h, after which they were ground in pure acetone using a mortar and pestle. Extraction occurred at 4ºC for 24 h in the dark. After extraction, samples were centrifuged at 4000 rpm for 15 min at 4ºC. Pigment content was then analysed using the Gauss-Peak Spectra method (Küpper *et al.*, 2007). Samples were scanned in a dual-beam spectrophotometer from 350 nm to 750 nm at 1 nm steps. The absorbance spectra were introduced in the GPS fitting library, using SigmaPlot. The employment of this library allowed to identify and quantify Chlorophyll *a*, Chlorophyll c_1 and c_2, Pheophytin *a*, Fucoxanthin, Antheraxanthin, β-carotene, Violaxanthin and Zeaxanthin for *C. corniculata* (Küpper *et al.*, 2007) and Chlorophyll *a*, Pheophytin *a*, β-cryptoxanthin, Antheraxanthin, β-carotene, Violaxanthin and Zeaxanthin for *J. rubens*. *J. rubens* carotenoids were selected based on Schübert *et al.* (2006). For phycobiliproteins in *J. rubens* samples approximately 0.5 g of tissue was

homogenised in 10 mL 0.1 M phosphate buffer (pH 6.8). After being left at 4ºC in the dark overnight, extracts were centrifuged for 10 minutes at 1000g and then read in the spectrophotometer at the wavelengths determined by Beer and Eshel (1985).

6.2.3 Statistical analyses

All data were checked for compliance with ANOVA assumptions (normality by visually inspecting data and homogeneity of variance using Levene's test) and transformed when necessary. Growth was analysed using a two way ANOVA with 'site of origin' and 'site of destination' as fixed factors. When a factor had a significant effect, a Tukey HSD pair-wise test was performed. Epiphyte cover of *C. corniculata* was analysed using a Kruskal-Wallis analysis with 'treatment' as a fixed factor. Separate MANOVAs were used to analyse treatment effects on C:N and N:P ratios (*C. corniculata*), C and N content (*J. rubens*), photochemical parameters (both species), pigments content (both species) and phycobilins (*J. rubens*). When the data did not meet Mauchly's test of sphericity, the degrees of freedom were corrected using Greenhouse-Geisser estimates of sphericity. $CaCO_3$ content (*J. rubens*) and total phenolic compounds (*C. corniculata*) were analysed using one-way ANOVAs with 'treatment' as a fixed factor.

6.3 Results

6.3.1 Growth and epiphyte cover

Relative growth of *C. corniculata* thalli was significantly different among transplantation sites (Table 6.1). Pairwise comparisons showed that thalli transplanted to the high CO_2 site (SEEP) and one reference site (REF A) grew more than those transplanted to the other reference site (REF B; Figure 6.2).

Different pCO_2 did not seem to have significant effects on linear growth of this macroalgal species.

Table 6.1. ANOVA results for transplanted *C. corniculata* thalli growth. The table shows main factors and their interactions and sum of squares (SS), degrees of freedom (df), Mean Squares (MS), F-ratios (F) and p values. Significant p values (< 0.05) are highlighted. The last row shows results from pairwise comparisons between sites of destination, different letters represent significantly different groups.

Source	**Type III SS**	**df**	**MS**	**F- ratio**	**p**
Origin	0.065	2	0.032	1.028	0.368
Destination	0.614	2	0.307	9.766	**<0.001**
Origin * Destination	0.114	2	0.057	1.822	0.176
Error	1.131	36	0.031		
Total	1.826	42			
Post-hoc subsets	REF B[a]	REF A[b]	SEEP[b]		

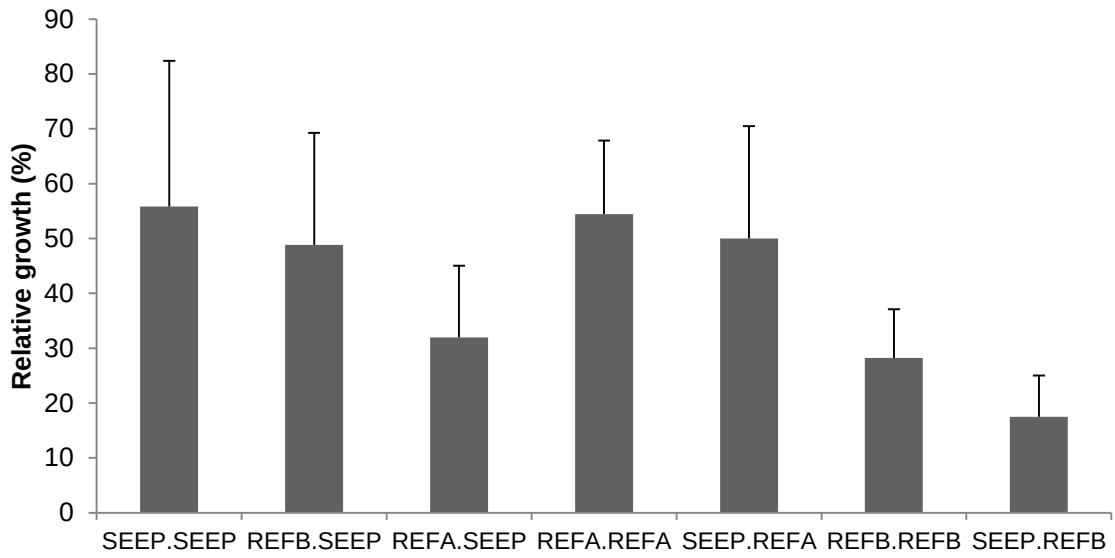

Figure 6.2. Mean relative growth (± SD, n=3-10) of *C. corniculata* thalli transplanted at Methana from September 2012 to June 2013 within and between two reference sites (REF A and REF B) and one high CO_2 site (SEEP). Treatments are shown as "Site of origin.Site of transplant".

Transplanted *J. rubens* thalli did not exhibit any significant difference in relative growth (Table 6.2). Even though thalli transplanted from SEEP had higher

average growth than those transplanted from the reference site (REF A), the two groups did not show any significant difference as variability was very high (Figure 6.3).

Table 6.2. ANOVA results for transplanted *J. rubens* thalli growth. The table shows main factors and their interactions and sum of squares (SS), degrees of freedom (df), Mean Squares (MS), F-ratios (F) and p values.

Source	Type III SS	df	MS	F-ratio	p
Origin	1869.486	1	1869.486	2.312	0.149
Destination	5.400	1	5.400	0.007	0.936
Origin * Destination	75.479	1	75.479	0.093	0.764
Error	12130.052	15	808.670		
Total	14019.002	18			

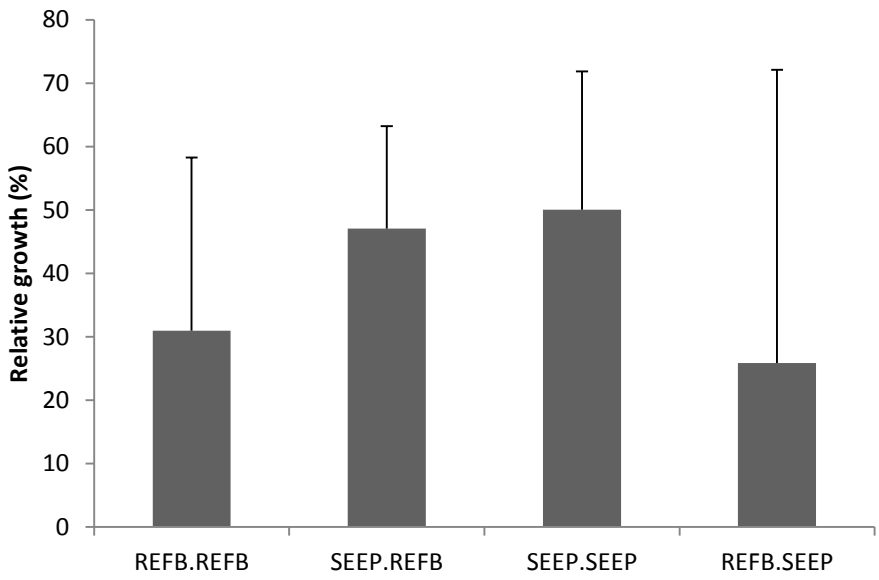

Figure 6.3. Mean relative growth (± SD, n=4-6) of *J. rubens* thalli transplanted at Methana from June 2013 to September 2013 within and between one reference site (REF B) and one high CO_2 site (SEEP). Treatments are shown as “Site of origin.Site of transplant”.

Epiphytes cover of *C. corniculata* thalli was significantly different among treatments according to a Kruskal-Wallis test. In general, thalli collected from or transplanted to the high CO_2 site (SEEP) had lower epiphytes cover compared

to those collected from or transplanted to the two reference sites (REF A and REF B). Macroalgae transplanted from high CO_2 levels to the reference sites (i.e. SEEP.REFA and SEEP. REFB) have lower epiphytes cover than those transplanted within the same reference site (i.e. REFA.REFA and REFB.REFB; Figure 6.4).

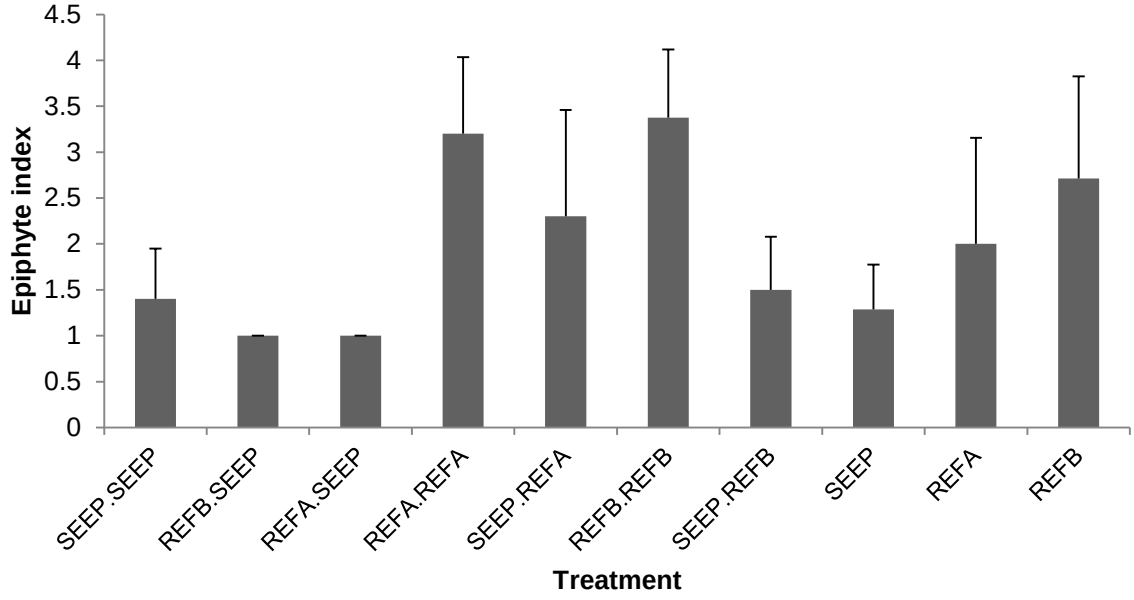

Figure 6.4. Mean epiphyte cover (± SD, n=3-10) of *C. corniculata* thalli transplanted at Methana from September 2012 to June 2013 within and between two reference sites (REF A and REF B) and one high CO_2 site (SEEP). Treatments are shown as "Site of origin.Site of transplant"; the last three treatments (SEEP, REF A and REF B) are unmanipulated thalli collected in June 2013.

6.3.2 Photosynthetic parameters

Maximum relative electronic transport rate ($rETR_{max}$) and saturation irradiance for ETR (I_k) were significantly different among treatments for *C. corniculata* transplanted at Methana from September 2012 to June 2013 (Table 6.3). The main differences in relative electron transport rates were connected with site of transplant, with thalli transplanted to SEEP generally having higher values of

$rETR_{max}$ than those transplanted to the reference sites (Table 6.4). On the other hand, I_k did not show any consistent trend related to the experimental treatments.

Table 6.3. MANOVA on photosynthetic parameters in *C. corniculata* thalli transplanted at Methana from September 2012 to June 2013 within and between two reference sites (REF A and REF B) and one high CO_2 site (SEEP). F-ratios (F) and p values are reported when significant ($p<0.05$).

Response variable	Treatment
$rETR_{max}$	F(9,44)=4.01; p=0.001
I_k	F(9,44)=2.46; p=0.023
α	-
NPQ	-
F_v/F_m	-

Table 6.4. Mean photosynthetic parameters (± SD, n=3-9) of *C. corniculata* thalli transplanted at Methana from September 2012 to June 2013 within and between two reference sites (REF A and REF B) and one high CO_2 site (SEEP). Treatments are shown as "Site of origin.Site of transplant"; the last three treatments (SEEP, REF A and REF B) are unmanipulated thalli collected in June 2013.

Origin.Destination	$rETR_{max}$ (µmol e m^{-2} s^{-1})	I_k (µmol photons m^{-2} s^{-1})	α_{ETR}	NPQ	F_v/F_m
SEEP.SEEP	21.7 ± 12.2	87.4 ± 44.1	0.247 ± 0.052	0.065 ± 0.104	0.644 ± 0.053
REFB.SEEP	19.3 ± 11.4	66.0 ± 37.2	0.305 ± 0.059	0.104 ± 0.109	0.665 ± 0.053
REFA.SEEP	15.5 ± 3.4	62.2 ± 5.2	0.247 ± 0.036	0.231 ± 0.041	0.664 ± 0.022
REFA.REFA	9.6 ± 3.6	53.5 ± 22.1	0.185 ± 0.033	0.379 ± 0.240	0.594 ± 0.035
SEEP.REFA	17.0 ± 13.5	100.7 ± 94.3	0.194 ± 0.078	0.280 ± 0.292	0.587 ± 0.083
REFB.REFB	13.3 ± 25.7	108.0 ± 248.3	0.369 ± 0.417	0.313 ± 0.192	0.672 ± 0.069
SEEP.REFB	7.3 ± 3.7	67.6 ± 37.8	0.132 ± 0.072	0.219 ± 0.240	0.590 ± 0.123
SEEP	30.5 ± 16.7	133.3 ± 62.5	0.225 ± 0.055	0.293 ± 0.193	0.628 ± 0.064
REFA	13.3 ± 5.3	60.4 ± 33.0	0.364 ± 0.374	0.311 ± 0.206	0.610 ± 0.098
REFB	3.8 ± 0.7	17.2 ± 7.0	0.242 ± 0.075	0.176 ± 0.097	0.588 ± 0.041

No significant differences among treatments were detected using a MANOVA for *J. rubens* transplanted from June to September 2013 (Table 6.5). The

measured (NPQ, F_v/F_m) and calculated ($rETR_{max}$, I_k, α_{ETR}) parameters for *J. rubens* are reported in Table 6.6, and all parameters are generally lower in *J. rubens* than in *C. corniculata* (Table 6.4).

Table 6.5. MANOVA on photosynthetic parameters in *J. rubens* thalli transplanted at Methana from June 2013 to September 2013 within and between one reference site (REF B) and one high CO_2 site (SEEP). F-ratios (F) and p values are reported when significant ($p<0.05$).

Response variable	Treatment
$rETR_{max}$	-
I_k	-
α	-
NPQ	-
F_v/F_m	-

Table 6.6. Mean photosynthetic parameters (± SD, n=3-4) of *J. rubens* thalli transplanted at Methana from June 2013 to September 2013 within and between one reference site (REF B) and one high CO_2 site (SEEP). Treatments are shown as "Site of origin.Site of transplant"; the last three treatments (SEEP, REF A and REF B) are unmanipulated thalli collected in September 2013.

Origin.Destination	$rETR_{max}$ (µmol e m^{-2} s^{-1})	I_k (µmol photons m^{-2} s^{-1})	α_{ETR}	NPQ	F_v/F_m
SEEP.SEEP	5.2 ± 5.2	39.9 ± 44.7	0.136 ± 0.031	0.095 ± 0.083	0.485 ± 0.018
REFB.SEEP	5.4 ± 4.1	57.7 ± 47.0	0.163 ± 0.126	0.147 ± 0.140	0.441 ± 0.078
REFB.REFB	10.1 ± 13.5	76.4 ± 83.7	0.110 ± 0.038	0.094 ± 0.162	0.454 ± 0.054
SEEP.REFB	6.9 ± 4.8	128.7 ± 155.2	0.489 ± 0.826	0	0.394 ± 0.119
SEEP	3.5 ± 3.2	48.4 ± 21.4	0.069 ± 0.041	0.110 ± 0.056	0.383 ± 0.080
REFA	2.4 ± 0.5	35.4 ± 16.1	0.077 ± 0.032	0.158 ± 0.106	0.397 ± 0.042
REFB	3.1 ± 0.4	30.7 ± 18.4	0.136 ± 0.089	0.253 ± 0.116	0.458 ± 0.046

6.3.3 Pigment contents

Chlorophyll *c* and antheraxanthin content of *C. corniculata* transplanted from September 2012 to June 2013 significantly differed among treatments, while all other pigments were not significantly affected (Table 6.7). Thalli transplanted to

reference sites had lower chlorophyll *c* and anteraxanthin content than those transplanted to the high CO_2 site (Figure 6.5). Unmanipulated thalli, however, did not show a similar pattern, with very small differences among sites.

Table 6.7. MANOVA on pigments content in *C. corniculata* thalli transplanted at Methana from September 2012 to June 2013 within and between two reference sites (REF A and REF B) and one high CO_2 site (SEEP). F-ratios (F) and p values are reported when significant ($p<0.05$).

Response variable	Treatment
Chl *a*	-
Chl *c*	F(9,53)=3.552 p=0.002
Pheophytin *a*	-
β-carotene	-
Fucoxanthin	-
Violaxanthin	-
Antheraxanthin	F(9,53)=4.117 p<0.001
Zeaxanthin	-

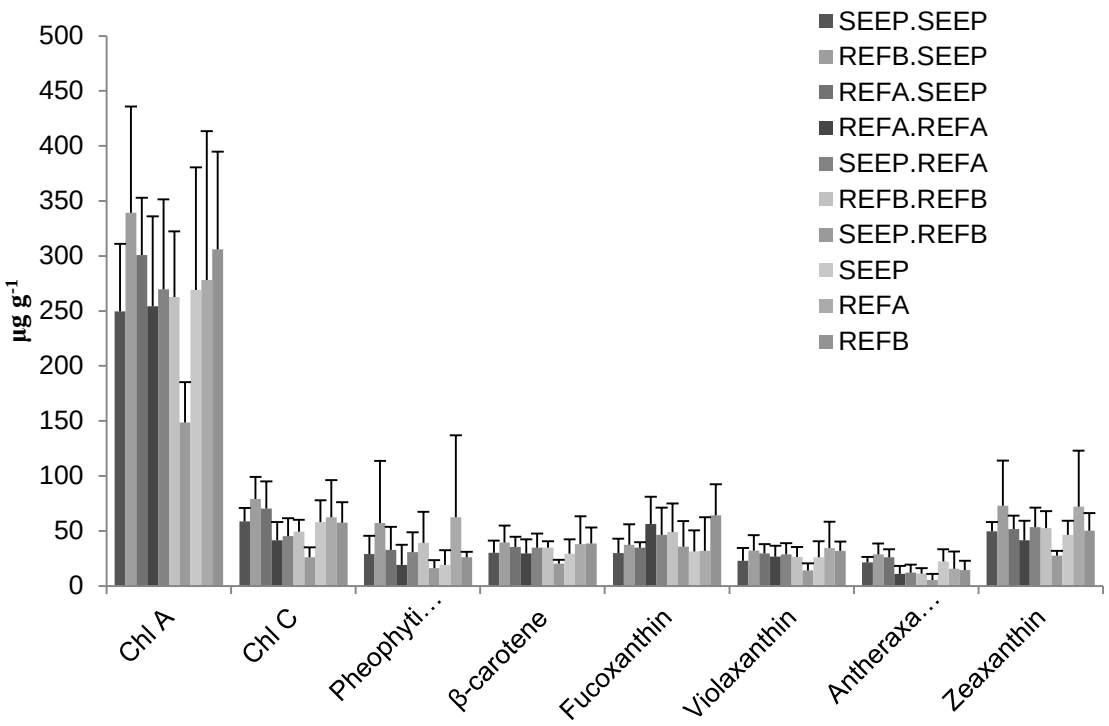

Figure 6.5. Mean pigments content (± SD, n=3-10) of *C. corniculata* thalli transplanted at Methana from September 2012 to June 2013 within and between two reference sites (REF

A and REF B) and one high CO_2 site (SEEP). Treatments are shown as “Site of origin.Site of transplant”; the last three treatments (SEEP, REF A and REF B) are unmanipulated thalli collected in June 2013.

MANOVA on log-transformed pigments content for *J. rubens* transplanted at Methana from June to September 2013 showed that treatment had a significant effect on all pigments analysed except for β-cryptoxanthin and antheraxanthin (Table 6.8). Chlorophyll *a*, violaxanthin and zeaxanthin content was higher in thalli transplanted to the high CO_2 site (SEEP), especially in those which also came from the high CO_2 site (SEEP.SEEP) and the unmanipulated thalli collected from that site (Figure 6.6). Pheophytin *a* and β-carotene were mostly present in higher quantities in unmanipulated thalli or in those transplanted to their site of origin (e.g. SEEP.SEEP) compared to those transplanted to a different site.

Table 6.8. MANOVA on pigments content in *J. rubens* thalli transplanted at Methana from June 2013 to September 2013 within and between one reference site (REF B) and one high CO_2 site (SEEP). F-ratios (F) and p values are reported when significant ($p<0.05$).

Response variable	Treatment
Chl *a*	$F(6,33)=8.874$ $p<0.001$
Pheophytin *a*	$F(6,33)=14.414$ $p<0.001$
β-cryptoxanthin	-
β-carotene	$F(6,33)=3.925$ $p=0.005$
Violaxanthin	$F(6,33)=7.151$ $p<0.001$
Antheraxanthin	-
Zeaxanthin	$F(6,33)=10.702$ $p<0.001$

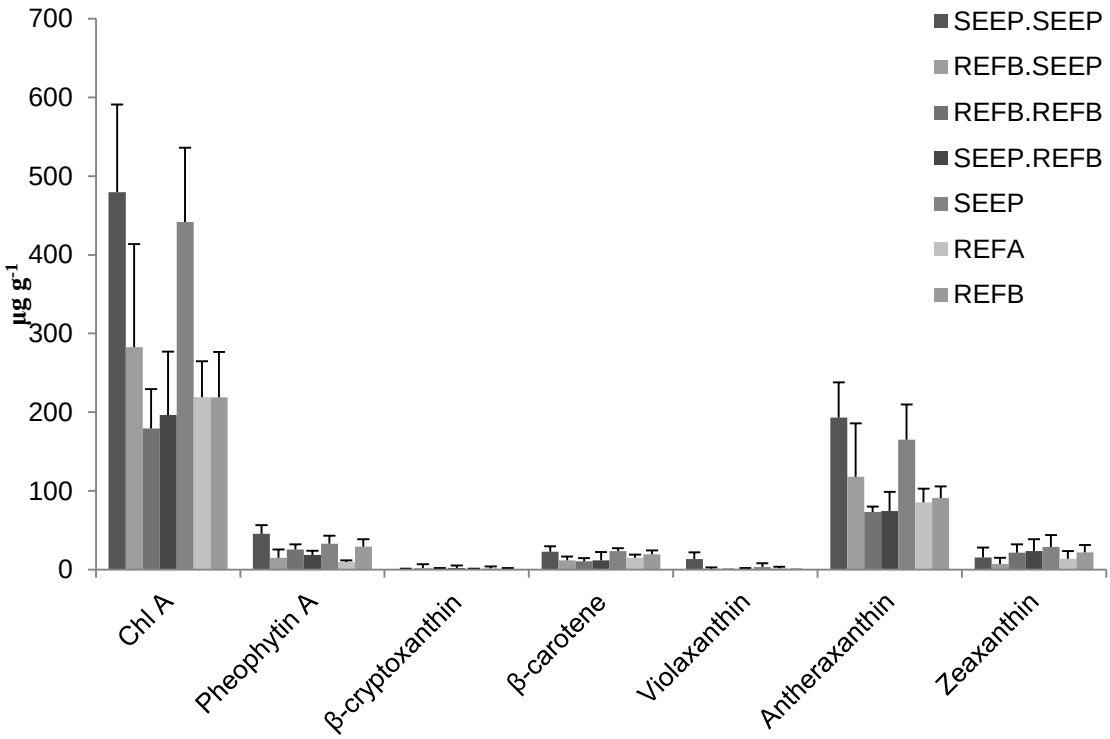

Figure 6.6. Mean pigments content (± SD, n=4-7) of *J. rubens* thalli transplanted at Methana from June 2013 to September 2013 within and between one reference site (REF B) and one high CO_2 site (SEEP). Treatments are shown as "Site of origin.Site of transplant"; the last three treatments (SEEP, REF A and REF B) are unmanipulated thalli collected in September 2013.

MANOVA on log-transformed phycobilins content for *J. rubens* transplanted at Methana from June to September 2013 showed that treatment had a significant effect on phycocyanin (Table 6.9). Similarly to some pigments, phycocyanin content was higher in thalli transplanted to the high CO_2 site or unmanipulated thalli collected from SEEP (Figure 6.7).

Table 6.9. MANOVA on phycobilins content in *J. rubens* thalli transplanted at Methana from June 2013 to September 2013 within and between one reference site (REF B) and one high CO_2 site (SEEP). F-ratios (F) and p values are reported when significant ($p<0.05$).

Response variable	Treatment
Phycoerythrin	-
Phycocyanin	$F(6,32)=5.542$ $p<0.001$

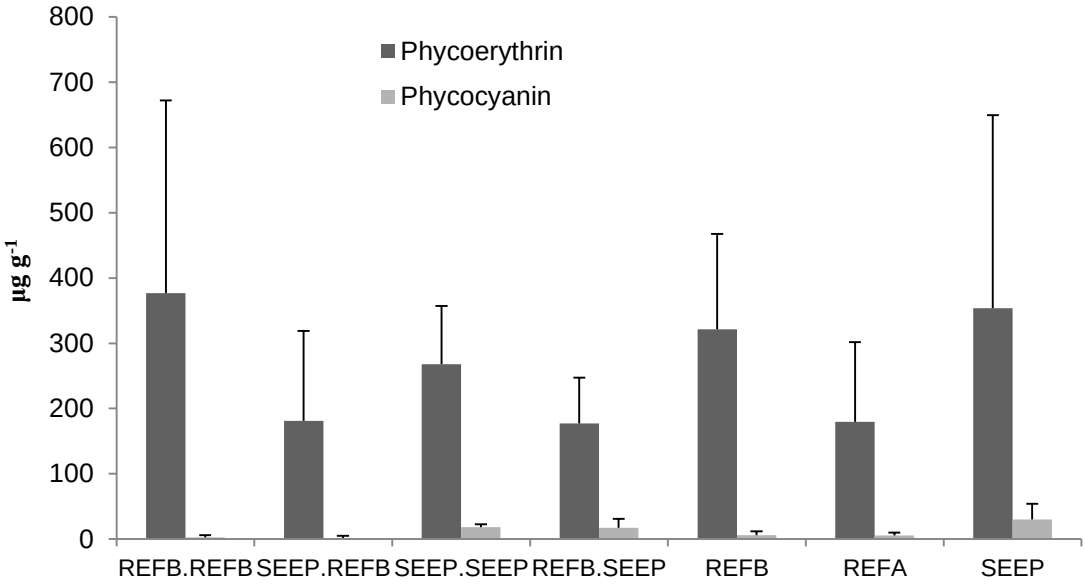

Figure 6.7. Mean phycobilins content (± SD, n=3-7) of *J. rubens* thalli transplanted at Methana from June 2013 to September 2013 within and between one reference site (REF B) and one high CO_2 site (SEEP). Treatments are shown as "Site of origin.Site of transplant"; the last three treatments (SEEP, REF A and REF B) are unmanipulated thalli collected in September 2013.

6.3.4 Carbon, nitrogen and phosphorus content

There was a significant difference among treatments for C:N ratio of *C. corniculata* thalli transplanted at Methana from September 2012 to June 2013, but not for N:P ratio (Table 6.10). C:N ratio was in fact higher in unmanipulated thalli collected at SEEP compared to those collected at reference sites (Figure

6.8). Similarly, thalli transplanted to the high CO_2 site had higher C:N ratio than those transplanted to the reference sites.

Table 6.10. MANOVA on C:N and N:P ratios in *C. corniculata* thalli transplanted at Methana from September 2012 to June 2013 within and between two reference sites (REF A and REF B) and one high CO_2 site (SEEP). F-ratios (F) and p values are reported when significant ($p<0.05$).

Response variable	Treatment
C:N	$F(9,44)=5.404$ $p<0.001$
N:P	-

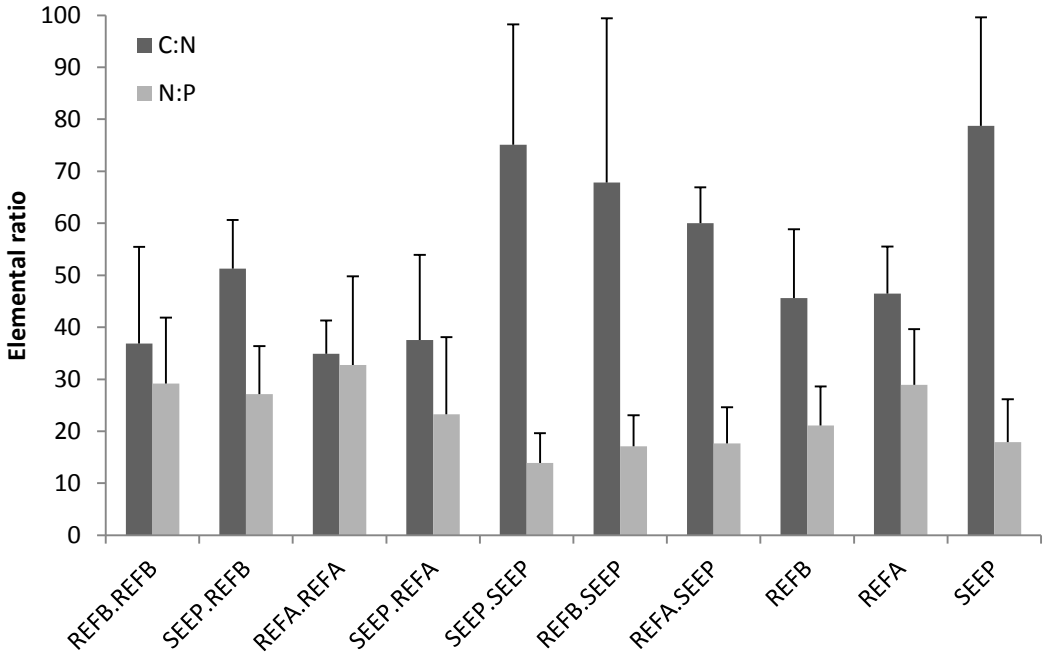

Figure 6.8. Mean C:N and N:P ratios (± SD, n=3-9) of *C. corniculata* thalli transplanted at Methana from September 2012 to June 2013 within and between two reference sites (REF A and REF B) and one high CO_2 site (SEEP). Treatments are shown as "Site of origin.Site of transplant"; the last three treatments (SEEP, REF A and REF B) are unmanipulated thalli collected in June 2013.

Calculating C:N ratios was not possible for many *J. rubens* samples because the nitrogen content was below detection limit; C and N were therefore analysed separately using a MANOVA, and results are reported in Table 6.11. Nitrogen content was significantly different among treatments, and it was higher in thalli

transplanted within the high CO_2 site and in unmanipulated thalli collected at SEEP (Figure 6.9).

Table 6.11. MANOVA on C and N content in *J. rubens* thalli transplanted at Methana from June 2013 to September 2013 within and between one reference site (REF B) and one high CO_2 site (SEEP). F-ratios (F) and p values are reported when significant ($p<0.05$).

Response variable	Treatment
C	-
N	F(6,22)=3.021; p=0.026

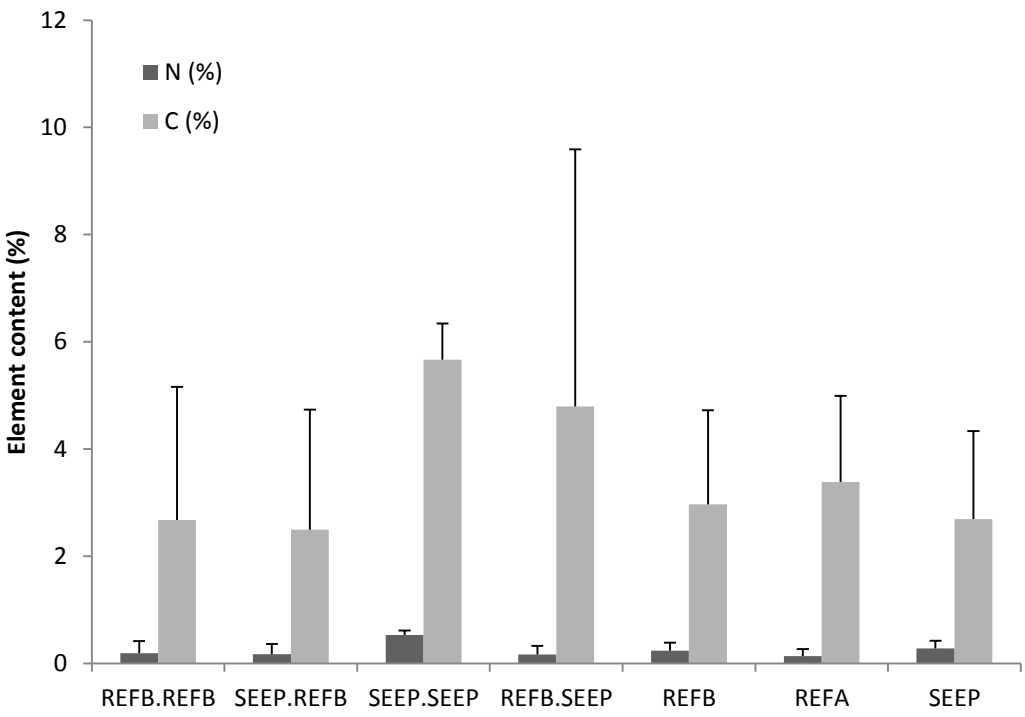

Figure 6.9. Mean C and N percent content (± SD, n=3-5) of *J. rubens* thalli transplanted at Methana from June 2013 to September 2013 within and between one reference site (REF B) and one high CO_2 site (SEEP). Treatments are shown as "Site of origin.Site of transplant"; the last three treatments (SEEP, REF A and REF B) are unmanipulated thalli collected in September 2013.

On the other hand, no significant differences among treatments were detected for inorganic carbon content of *J. rubens* transplants (Table 6.12). Percent

inorganic carbon content varies little among treatment, as it is around 80% for all of them (Figure 6.10).

Table 6.12. ANOVA results for transplanted *J. rubens* thalli inorganic carbon content. The table shows the source of variation and sum of squares (SS), degrees of freedom (df), Mean Squares (MS), F-ratios (F) and p values.

Source	Type III SS	df	MS	F	p
Treatment	124.378	8	15.547	1.756	0.129
Error	247.854	28	8.852		
Total	372.232	36			

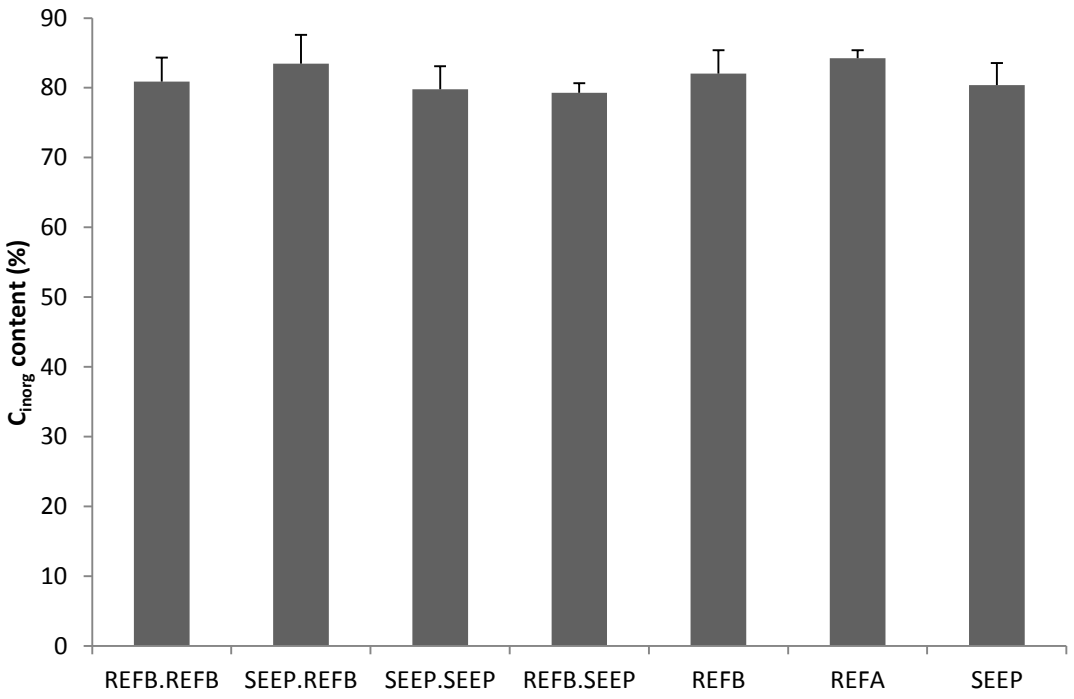

Figure 6.10. Mean inorganic carbon percent content (± SD, n=3-7) of *J. rubens* thalli transplanted at Methana from June 2013 to September 2013 within and between one reference site (REF B) and one high CO_2 site (SEEP). Treatments are shown as "Site of origin.Site of transplant"; the last three treatments (SEEP, REF A and REF B) are unmanipulated thalli collected in September 2013.

6.3.5 Total phenolic compounds

Total phenolic compounds of *C. corniculata* thalli were significantly different among treatments (Table 6.13). In general, thalli transplanted to the high CO_2 site (SEEP) had higher phenols content compared to those transplanted to the two reference sites (REF A and REF B). However, macroalgae transplanted from high CO_2 levels to the reference sites (i.e. SEEP.REFA and SEEP. REFB) had higher phenols content than those transplanted within the same reference site (i.e. REFA.REFA and REFB.REFB), whereas unmanipulated thalli did not show clear patterns, possibly because of high within-site variability (Figure 6.11).

Table 6.13. ANOVA on phenols content of *C. corniculata* thalli transplanted at Methana from September 2012 to June 2013 within and between two reference sites (REF A and REF B) and one high CO_2 site (SEEP). The table shows the source of variation and sum of squares (SS), degrees of freedom (df), Mean Squares (MS), F-ratios (F) and p values.

Source	Type III SS	df	MS	F	p
Treatment	10.922	9	1.214	3.202	**0.004**
Error	18.189	48	0.379		
Total	29.111	57			

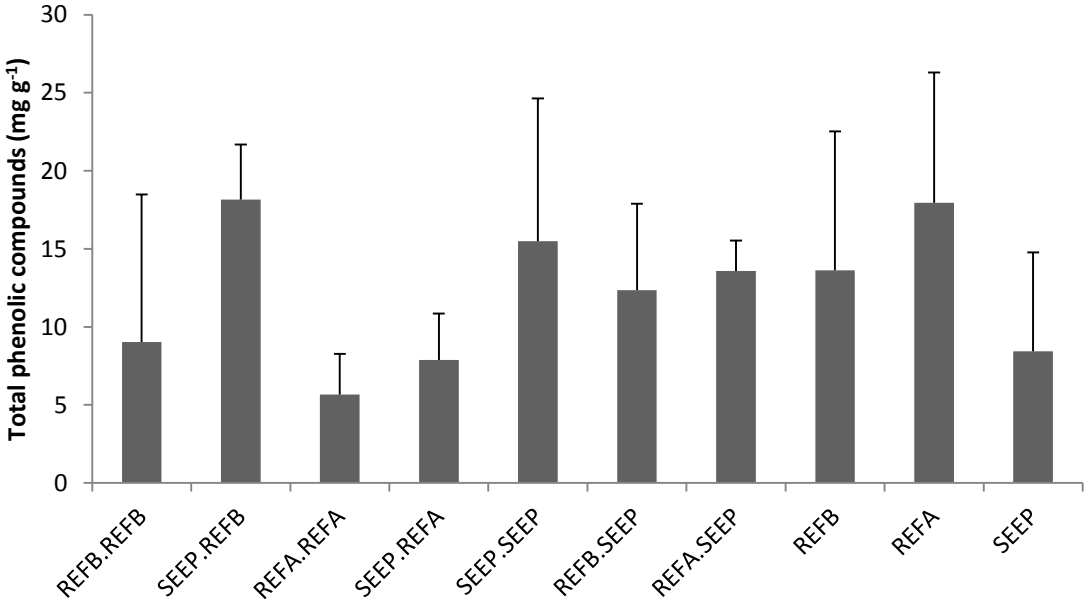

Figure 6.11. Mean phenols concentration (± SD, n=3-10) of *C. corniculata* thalli transplanted at Methana from September 2012 to June 2013 within and between two reference sites (REF A and REF B) and one high CO_2 site (SEEP). Treatments are shown as "Site of origin.Site of transplant"; the last three treatments (SEEP, REF A and REF B) are unmanipulated thalli collected in June 2013.

6.4 Discussion

For the first time, long-term acclimatisation of macroalgae to ocean acidification has been assessed using reciprocal transplantations within and between areas with reference and elevated CO_2 levels. Results from these experiments suggest that phenotypic plasticity allowed *C. corniculata* and *J. rubens* to alter their physiological performance depending on the carbonate chemistry at the site of transplant. Although both species could survive pCO_2 levels up to 1700 µatm, *C. corniculata* seemed to be favoured at elevated CO_2; this might lead to reduced abundances of *J. rubens* and increased abundances of *C. corniculata* at elevated pCO_2 as a consequence of altered inter-specific competition.

In contrast with the initial hypothesis, linear growth and photosynthetic performance of both species were not higher in thalli transplanted within pCO_2 levels. No effects of site were detected for *J. rubens* growth, while *C. corniculata* growth was significantly lower at one of the reference sites (REF B). These findings are in contrast with recent studies reporting decreased growth of articulated coralline algae (Gao and Zheng, 2010; Hofmann *et al.*, 2011; Hofmann *et al.*, 2012; Cornwall *et al.*, 2014; Johnson *et al.*, 2014) and fucoid algae (Gutow *et al.*, 2014) at elevated CO_2 levels. However, responses to ocean acidification in macroalgae present high inter-specific variability (Kroeker *et al*., 2013a), and fucoid algae can show no change or increase in growth rates as CO_2 increases (Swanson and Fox, 2007; Chen and Zou, 2014). In addition, experiments have mostly been conducted in laboratories for relatively short periods of time, whereas this field experiment lasted three and nine months for *J. rubens* and *C. corniculata*, respectively. In the field, many macroalgae do not reach their maximum potential frond size as their linear growth is limited by external factors, such as wave motion or nutrient limitation (Fisher and Martone, 2014). As *C. corniculata* dry biomass showed an increasing trend with increasing seawater pCO_2 at Methana (see Chapter 4), biomass of transplanted seaweeds might have shown a response to pCO_2 levels. However, measuring biomass change was not possible in this study, as the seaweeds were permanently attached to the substratum using epoxy putty, which remained on the transplanted thalli after they were collected at the end of the experiment.

Photosynthetic performance of *J. rubens* was unaffected by the transplant, whereas *C. corniculata* had higher $rETR_{max}$ when transplanted to elevated CO_2. This is in accord with recent findings by Johnson *et al.* (2014), who did not find strong and consistent effects of ocean acidification on algal photophysiology.

Previous studies on articulated coralline algae have shown that although photosynthetic parameters are often not affected by increased CO_2 (Hofmann *et al.*, 2012), oxygen production can be negatively affected by ocean acidification (Hofmann *et al.*, 2011). However, oxygen production in articulated coralline algae is less affected by increased CO_2 compared to crustose forms (Noisette *et al.*, 2013b), and algae acclimatised to elevated CO_2 in tidal pools do not show changes in their productivity as carbon dioxide increases (Egilsdottir *et al.*, 2013). As for brown algae, maximum quantum yield (F_v/F_m) is normally not affected by elevated CO_2, although it can decrease in combination with elevated temperature (Johnson *et al.*, 2012; Olabarria *et al.*, 2013). Similarly to *C. corniculata*, increased photosynthetic capacity ($rETR_{max}$) at high CO_2 has been reported for *Padina pavonica* at seeps off Vulcano (Johnson *et al.*, 2012).

Both macroalgal species showed an increase in some pigment contents when transplanted to elevated CO_2 levels. This is in accord with the initial hypothesis for *C. corniculata*, but not for *J. rubens*, possibly because most information about coralline algal responses to ocean acidification comes from laboratory studies, while there are a few field studies on brown algae. *Cystoseira corniculata* thalli transplanted to the seeps had increased chlorophyll *c* and antheraxanthin, although unmanipulated thalli did not show any CO_2-dependent pattern. Antheraxanthin is an intermediate and volatile compound in the xanthophyll cycle (Goss and Jakob, 2010); its increase is thus unlikely to have physiological significance, especially since de-epoxidation state did not change significantly among treatments (data not shown). *J. rubens* thalli transplanted to SEEP had higher chlorophyll *a*, violaxanthin, zeaxanthin and phycocyanin content. Some pigments of *J. rubens* were affected by the transplant: thalli transplanted to their site of origin had higher pheophytin *a* and β-carotene

content than those transplanted to another site. Few studies have examined changes in macroalgal pigment content with increased CO_2; laboratory experiments performed so far have not found significant effects of ocean acidification on pigments in brown and red algae (Egilsdottir *et al.*, 2013; Noisette *et al.*, 2013a; Noisette *et al.*, 2013b; Yildiz *et al.*, 2013; Bender *et al.*, 2014). However, the only study examining macroalgal pigment content at volcanic seeps found increased chlorophyll *a* and *c* content in *Padina pavonica* grown at elevated CO_2 (Johson *et al.*, 2012). Most laboratory experiments were conducted over a relatively short time (up to three months); it is then possible that macroalgae increase some species' pigment production at increased CO_2 levels, but only in the long term. However, the crustose coralline alga *Lithophyllum cabiochae* did not show significant changes in chlorophyll *a* concentration after being exposed to elevated CO_2 for one year (Martin *et al.*, 2013); more studies are therefore needed to test this phenomenon.

Epiphyte cover of *C. corniculata* was lower in thalli transplanted near the seeps, and was slightly lower in thalli transplanted from the SEEP site than in thalli from reference sites. This could be partly explained by the increase in total phenolic compounds in thalli transplanted to SEEP and the smaller phenols increase in those transplanted from SEEP; increased total phenolic compounds with elevated CO_2 have already been found in other brown algae, although not all species exhibit this pattern (Swanson and Fox, 2007; Poore *et al.*, 2013). Although phenolic compounds, mostly phlorotannins, have been proven to inhibit grazers and protect brown seaweeds from UV radiation (Halm *et al.*, 2010), their effect on seaweed epiphyte load is not clear (Jennings and Steinberg, 1997; Brock *et al.*, 2008). In fact, epiphyte settlement on macroalgae

is likely controlled by other factors, including macroalgal morphology and polar secondary metabolites such as terpenoids (Jennings and Steinberg, 1997).

Phenols are carbon-dense compounds, and their increase could explain the increased C:N ratio in *C. corniculata* thalli transplanted to SEEP. The increase in C:N ratio was caused by increased carbon and decreased nitrogen content in thalli transplanted to SEEP. This is in contrast with other studies reporting decreased C:N ratio in macroalgae exposed to high CO_2; in one case this was caused by decreased in nitrogen content with increased CO_2 (Falkenberg *et al.*, 2013b; Gutow *et al.*, 2014). Decreased nitrogen content with increased CO_2 is also reported by Kübler *et al.* (1999) for the red alga *Lomentaria articulata*, but coupled with decreased carbon content. However, increased CO_2 did not change carbon and nitrogen content in many brown and red macroagae (Olabarria *et al.*, 2013; Poore *et al.*, 2013). The strong grazing pressure at Methana could have driven an enhanced carbon-dense chemical defences production at SEEP thanks to increased CO_2 availability (Connell *et al.*, 2013); chemical defences of brown algae and seagrasses may therefore be differently affected by ocean acidification, as the latter had lower defensive compound contents at elevated pCO_2 levels (Arnold *et al*., 2012).

Unaltered inorganic carbon content of *J. rubens* among treatments suggests that this species is not locally adapted to elevated pCO_2 and can maintain calcification rates at high CO_2 and counter increased dissolution rates at volcanic seeps. Work to date has shown that articulated coralline algal calcification is less affected by increased CO_2 that that of crustose forms; although net calcification rates of articulated coralline algae can decrease at elevated CO_2, crustose coralline algae often start dissolving at pCO_2 levels above 1000 µatm (Hofmann *et al.*, 2011; Noisette *et al.*, 2013b; Johnson *et al.*,

2014). However, maintaining calcification rates at decreased calcium carbonate saturation is energetically expensive (Bradassi *et al.*, 2013), and *J. rubens* thalli grown at reference sites might not be able to maintain them when exposed to elevated CO_2 for longer periods. Some coralline algae exposed to high CO_2 for two months or more have lower proportions of very soluble high-Mg calcite in their skeletons (Egilsdottir *et al.*, 2013; Diaz-Pulido *et al*., 2014). *Jania rubens* transplanted near seeps at Methana could therefore have modified mineralogy or increased the production of calcification-inducing compounds to improve survival at elevated CO_2 levels (Koch *et al.*, 2013). However, articulated coralline algae appear to increase their Mg content with increasing seawater temperatures (Williamson *et al.*, 2014). The concurrent increase in seawater pCO_2 levels and temperatures predicted for 2100 may therefore impair the ability of articulated coralline algae to modify their mineralogy to better resist to ocean acidification.

To summarise, the two seaweeds examined changed their physiology depending on the environmental conditions at the site of transplant. The possibility of genotypic differentiation among populations of these macroalgal species depending on their acclimatisation to elevated CO_2 cannot be excluded until genetic studies are performed. Species with high phenotypic plasticity could in fact have genetically adapted to elevated CO_2 levels, but show similar physiological performances, a phenomenon named “phenotypic buffering” (Sunday *et al.*, 2014). Changes in the physiological performance of dominant macroalgal species are likely to alter the outcome of competition between them; this is reflected by the macroalgal community composition near seeps off Methana. Here, *J. rubens* cover decreased, whereas *C. corniculata* cover increased with increasing pCO_2 (Chapter 3; Figure 6.12). This study therefore

shows that even after centuries of exposure to high CO_2 levels, two dominant macroalgal species did not appear to have permanently acclimatised to elevated carbon dioxide levels. This is likely to heavily influence temperate coastal ecosystems, as the observed changes in benthic community structure are likely to indirectly influence upper trophic levels and ecosystem processes such as nutrient cycling or carbon sequestration.

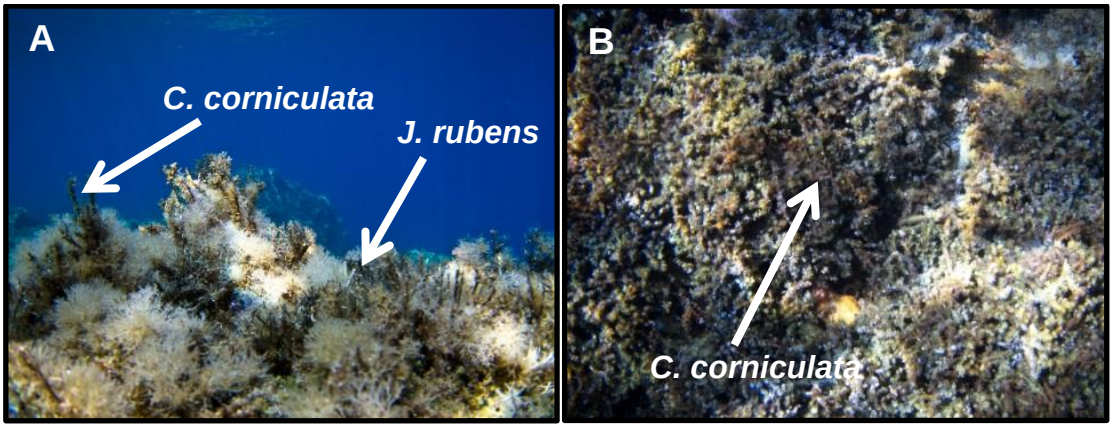

Figure 6.12. Typical macroalgal assemblage off Methana in September 2013 at reference sites (A) with abundant *J. rubens* overgrowing *C. corniculata*, and near the seeps (B), where *C. corniculata* could grow undisturbed; photos by Maria Salomidi.

Chapter 7

A short-term copper pulse affects macroalgal copper accumulation and indirectly alters epifaunal colonisation at elevated pCO_2.

Abstract

Ocean acidification is expected to interact with other anthropogenic stressors to modify marine ecosystems. Copper is toxic to marine organisms, and copper pulses are a common source of pollution in coastal areas. In this study, calcifying and non-calcifying seaweeds acclimatised to high CO_2 at volcanic seeps or from reference sites were exposed to elevated CO_2 and a 36-hour copper pulse in two field experiments. Invertebrate re-colonisation of a fucoid alga exposed to copper at different pCO_2 levels was also assessed. *Cystoseira corniculata* and *Jania rubens* accumulated more copper in high CO_2 conditions. *Jania rubens* grown near the seeps accumulated more copper than those transplanted from reference sites. These changes had no effect on maximum quantum yield of both species. *Cystoseira corniculata* pigment contents changed little, but total carotenoids decreased in *J. rubens* thalli exposed to copper at both sites. Phycoerythrin content in *J. rubens* slightly increased in thalli exposed to copper at the reference site, whereas it decreased following copper exposure at elevated CO_2 levels. Previous acclimatisation to high CO_2 did not influence seaweed responses to copper. However, copper accumulation at high CO_2 altered epifaunal community structure near the seeps, but not in reference conditions. Thus, multiple stressors can interact and increase the magnitude of changes in benthic communities.

7.1 Introduction

Macroalgal responses to increased CO_2 differ in calcifying and non-calcifying species (Porzio *et al.*, 2011). Carbon concentrating mechanisms (CCMs) are used by most macroalgae to convert bicarbonate ions into carbon dioxide; these are energy expensive, so increased dissolved CO_2 decreases the energy needed to obtain the substratum for photosynthesis (Cornwall *et al.*, 2012). On the other hand, calcifying algae face increased energetic costs of calcification as calcium carbonate saturation levels fall due to ocean acidification (Bradassi *et al.*, 2013; Koch *et al.*, 2013). The combination of increased carbon availability and higher energetic cost of calcification may cause shifts from coralline-dominated to fleshy seaweed communities as atmospheric CO_2 increases (Connell *et al.*, 2013), not only because of reduced coralline algae growth (Küffner *et al.*, 2008; Martin *et al.*, 2008; Kroeker *et al.*, 2010), but also because of altered competitive interactions between calcified and non-calcified algae (Kroeker *et al.*, 2013c; Short *et al.*, 2014).

Acclimatisation or adaptation to high pCO_2 could improve the ecological performance of calcifying algae as oceans become acidified (Hofmann *et al.*, 2010). Algae living in high-CO_2 environments could therefore be helpful in determining the potential for acclimatisation in these organisms. So far, very few studies have tackled this issue. For instance, the green microalga *Chlamydomonas reinhardtii* changes its physiology when exposed to elevated carbon dioxide over multiple generations, showing reduced CO_2 uptake using carbon-concentrating mechanisms (Collins *et al.*, 2006) and a marine coccolithophore has the potential to adapt to future CO_2 concentrations (Lohbeck *et al.*, 2012). Unpublished work at volcanic seeps off Ischia (Italy)

indicates that the genome of the brown macroalga *Dictyota* sp. changes at high pCO_2, resulting in the dominance of a stress-resistant form (Porzio, 2010).

Although there is scant information regarding macroalgal acclimatisation to elevated CO_2, their response to other changing abiotic conditions is widely studied. For example, there are species-specific differences in the tolerance of macroalgae to changes in salinity (Ryan *et al.*, 2004), temperature (Collén and Davison, 2001) and light (Bischof *et al.*, 2006) depending on the natural variability of their habitat. In some cases, intraspecific differences in responses to environmental stressors have been detected (Pearson *et al.*, 2009). These differences can have a hereditary component (Nielsen *et al.*, 2003) and environmental isolation can lead to rapid speciation, such as for *Fucus* spp. in the Baltic Sea (Bergström *et al.*, 2005).

Epifaunal communities are affected by increased CO_2 as well, with decreased abundance of molluscs and an increase of some crustacean taxa (Kroeker *et al.*, 2011). The above responses mostly conform to predictions based on laboratory experiments (Kroeker *et al.*, 2013a), but communities studies have also found unexpected community changes due to altered inter-specific interactions (Hale *et al.*, 2011). Invertebrates can also exhibit enhanced sensitivity to ocean acidification if they are concurrently exposed to another stressor, such as increased temperature or low food availability (Rodolfo-Metalpa *et al.*, 2011; Kroeker *et al.*, 2013a; Thomsen *et al.*, 2013).

Since ocean acidification is only one of the changes humans are causing in the marine realm, we have to consider that several abiotic factors are acting interdependently, with interactive and sometimes unexpected results (Shears and Ross, 2010; Gaylord *et al.*, 2014). Even if calcifying macroalgae have the

potential to acclimatise or adapt to high CO_2, they could be more sensitive to any additional stressors due to the increased energetic cost of calcification (Bradassi *et al*., 2013). On the other hand, non-calcifying algae could be more resistant to additional stressors as they have more energy available after reducing their use of carbon concentrating mechanisms (CCMs; Cornwall *et al.*, 2012), leading to more drastic community changes compared to the effects of CO_2 alone.

In coastal waters, copper is a common pollutant as it is mined in many regions (Figure 7.1); however, copper can also derive from urban runoff (Pitt, 1995), industrial waste (Apte and Day, 1998) or antifouling paints (Paulson *et al.*, 1989). Copper is extremely toxic at high concentrations, especially before binding to organic material (Hall *et al.*, 1998). As a consequence, copper pulses are common in coastal waters near human settlements and industries. Copper accumulates in macroalgal tissues and can strongly inhibit photosynthesis by damaging photosystem II (Schröder *et al.*, 1994). Many invertebrate taxa are negatively affected by copper as well (Johnston *et al.*, 2002), and seaweed epifauna is more strongly affected because they are exposed to copper through the macroalgae they live in and feed upon (Roberts *et al.*, 2006). Other effects of elevated copper concentrations on marine flora and fauna include reduced growth and calcification, altered osmoregulatory processes and oxidative damage (Thurberg *et al.*, 1973; Kangwe *et al.*, 2001; Collén *et al.*, 2003), although there is large among-taxa variability in copper sensitivity (Mayer-Pinto *et al.*, 2010). In addition, some organisms can be more sensitive to copper exposure at elevated CO_2 levels because of the higher energetic cost of maintaining physiological processes (Roberts *et al.*, 2013).

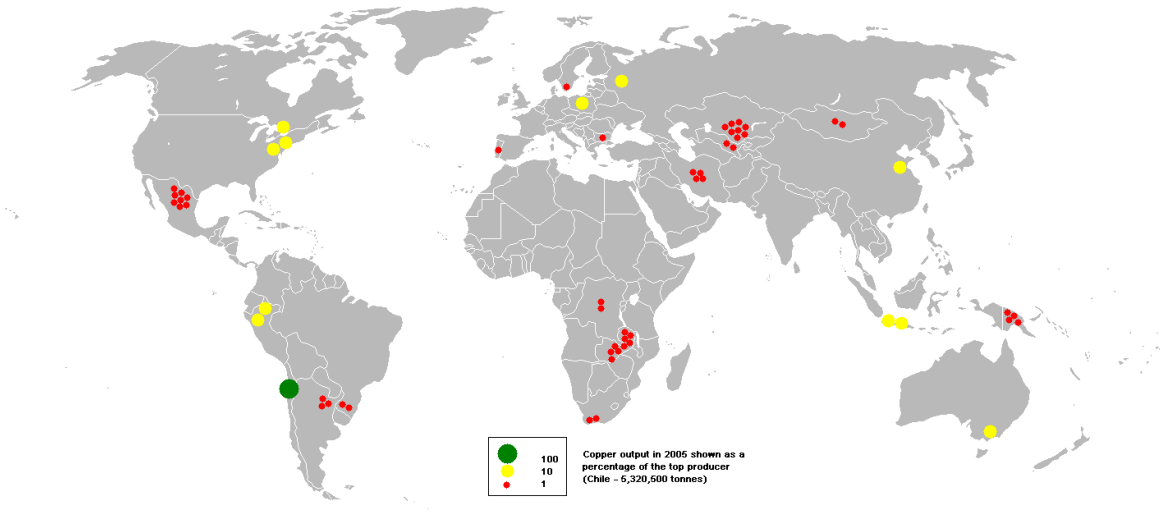

Figure 7.1. Copper production in 2005 shown as a percentage of the top producer (Chile, 5320500 tonnes). Data from British Geological Survey.

This study investigated how populations of a calcifying and a non-calcifying alga from high or reference pCO_2 areas responded to a short-term copper pulse *in situ*, and assesses how re-colonisation by seaweed epifauna was affected by copper exposure at different pCO_2 levels. The hypotheses tested were:

1) A non-calcifying alga (*Cystoseira corniculata*) is more resistant to short-term copper stress in high CO_2 conditions;
2) A calcifying alga (*Jania rubens*) is less resistant to short-term copper stress in high pCO_2 conditions, but this effect is reduced for algae acclimatised to high CO_2;
3) *Cystoseira corniculata* epifaunal colonisation is negatively affected by copper exposure, and the effect of copper is stronger at high CO_2.

7.2 Methods

7.2.1 Study area

Experiments were carried out in June and September 2013 at two sites (see Chapter 2, Figure 2.1), one characterised by high pCO_2 due to hydrothermal activity (SEEP) and a reference site (REF A); detailed sampling dates and sample sizes are reported in Table 1.1F. Macroalgae were also collected from another reference site (REF B). A geochemical survey of the area revealed that none of the study sites was contaminated with respect to copper, making the area suitable for testing the effects of copper pollution on non-adapted organisms (Chapter 2).

7.2.2 Experimental design

Two common macroalgal species were chosen to test the combined effects of elevated carbon dioxide and copper, the brown alga *Cystoseira corniculata* in June 2013 and the articulated coralline *Jania rubens* in September 2013. Similarly sized thalli were collected from three sites, one characterised by high pCO_2 (SEEP) and two reference sites (REF A and REF B). The algae were kept in coolers and transported from their site of origin to the sites REF A and SEEP, and attached with cable ties on plastic attached to concrete blocks and deployed at the same depth the thalli were collected from (<0.5 m). Individuals from REF A and SEEP were transplanted both in their site of origin and in the other site, while individuals from REF B were transplanted to REF A and SEEP. Ten individuals per species per treatment were attached to nets, left 48 h to acclimatise to the new conditions and then half of them were exposed for three days to increased copper levels via plaster blocks containing copper attached to

their nets. A scheme of the experimental design is shown in Figure 7.2, and transplanted *J. rubens* is shown in Figure 7.3.

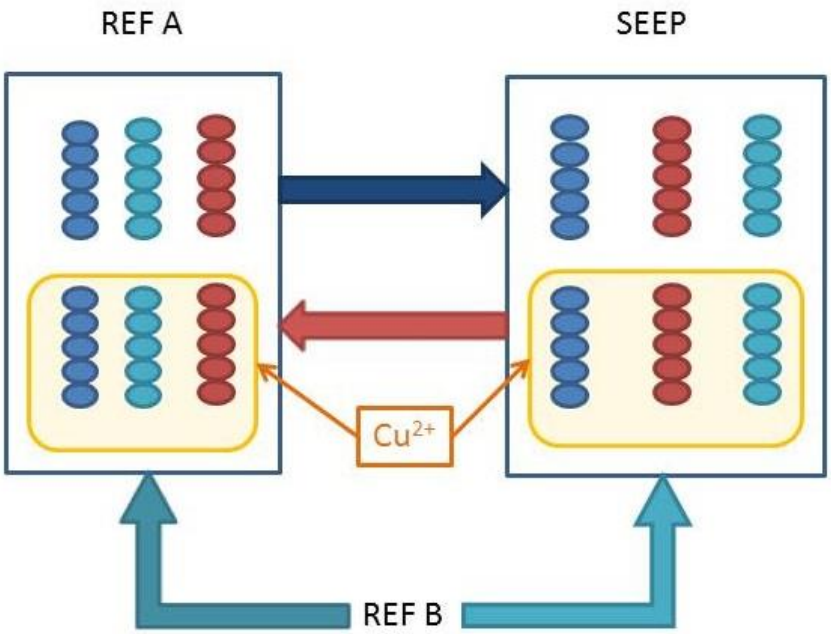

Figure 7.2. Off Methana (Greece), ten individuals from SEEP (red circles), REF A (blue circles) and REF B (light blue circles) were transplanted to SEEP and REF A (blue rectangles) in June (*C. corniculata*) and September 2013 (*J. rubens*). After 48 h, half were exposed to 36 h copper pulses (shaded).

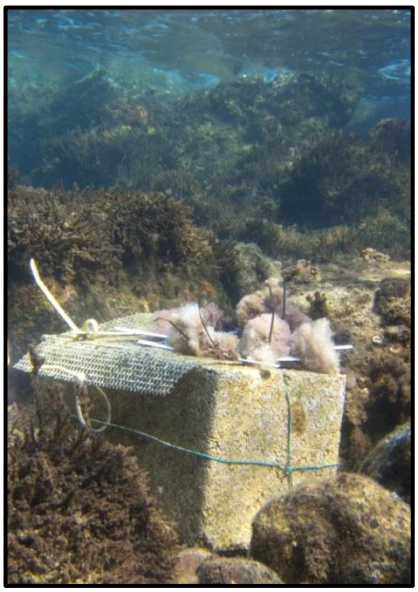

Figure 7.3. *Jania rubens* transplanted near seeps off Methana (Greece) in September 2013 before being exposed to copper; the individual thalli were attached to plastic nets using

cable ties, and the net was attached to a concrete block deployed on the rocky shore at depth < 0.5 m.

For these experiments, $CuSO_4$ (copper II sulfate anhydrous) was used as a reference toxicant following methods described by Johnston and Webb (2000). 3.2 g of $CuSO_4$ were dissolved in 13 g of deionized water and refrigerated at 4°C for 60 min. Fifteen grams of dental plaster were refrigerated for 60 min, then mixed with the cool copper solution. The plaster was poured into 4 cm diameter plastic cups and left to dry for seven days. The same process was used to make control blocks except for the $CuSO_4$ addition. Plaster was changed daily and the removed blocks were air dried and weighed to check that all macroalgae were exposed to a comparable amount of copper.

In June 2013, an additional experiment was performed to test how *C. corniculata* re-colonisation by invertebrates was influenced by copper at different pCO_2 levels. Ten similarly sized *C. corniculata* thalli per site were detached from the rocky substratum using hammer and chisel, briefly rinsed with fresh water to remove all mobile invertebrates and attached to the nets used for the macroalgal physiology experiment, resulting in five copper-exposed and five control thalli per site.

7.2.3 Environmental parameters monitoring

Environmental parameters were measured daily for the duration of the experiments. Temperature, salinity and pH were monitored in both sites with a multiprobe (YSI Professional Series, Professional Plus) and total alkalinity was sampled twice per site on the first and the last day of the experiment using borosilicate bottles. Total alkalinity samples were treated and analysed according to the procedures detailed in Chapter 2. The other carbonate

chemistry parameters were calculated from pH and total alkalinity using CO2Sys software (Lewis and Wallace, 1998).

7.2.4 Sampling and laboratory analyses

Physiological responses of transplanted thalli of both species were assessed by measuring *in vivo* chlorophyll *a* fluorescence associated with Photosystem II by using a portable pulse amplitude modulated fluorometer Diving-PAM (Diving PAM, Walz, Effeltrich, Germany). The maximum quantum yield (F_v/F_m) of apical shoots was measured after 10 minutes of dark acclimation before transplanting the seaweeds, after the acclimation period and after copper exposure. Appropriate duration of dark acclimation was determined by measuring F_v/F_m of ten thalli per species after 5, 10, 15 and 20 minutes in the dark. Maximum quantum yield (F_v/F_m) relates the capacity for photochemical quenching ($F_v = F_m - F_0$, where F_0 is the basal fluorescence of dark-adapted thalli and F_m is the maximal fluorescence after a saturation light pulse of > 4000 µmol m^{-2} s^{-1}) to the total fluorescence emission of closed PSII reaction centres (F_m). F_v/F_m is then directly proportional to the quantum efficiency of PSII photochemistry (Butler 1978), and its reduction from maximal values is an indicator of stress responses, and specifically of metal stress (Mallick and Mohn, 2003).

After 36 h of copper exposure, *C. corniculata* thalli were collected and transported to the field laboratory in coolers. There their apical parts were gently scrubbed of epiphytes, rinsed with distilled water and immediately frozen in liquid nitrogen. The samples were subsequently stored at -80°C until they were analysed for copper content and pigment composition. In June 2013, *C. corniculata* thalli for the invertebrate re-colonisation experiment were covered with plastic zip-lock bags, taken from the site and transported to the field

laboratory, where they were sieved (200 µm mesh) and stored in 70% Industrial Methylated Spirit (IMS). Samples were later sorted and mobile invertebrates identified to the lowest possible taxonomic level. Macroalgal thalli were dried in an oven at 50 ºC for 72h and weighed (± 1 mg accuracy) to determine dry mass (DW).

Samples for copper concentration were freeze-dried for 24h and ground with pestle and mortar; approximately 0.1 g of each sample was weighed in acid-washed Teflon tubes with a high precision digital scale (0.1 mg accuracy). Two ml of concentrated nitric acid were then added; the tube containing the digestant was then placed in a high-Throughput Microwave Reaction System Run (MARSXpress, CEM Corporation, Matthews, USA) and gently heated to boiling for at least 1 h to ensure full digestion. Samples were allowed to cool, quantitatively transferred into pre-cleaned 10 ml volumetric flasks and diluted to volume with Milli-Q water. Blanks were prepared following the same procedure, but omitting the sample; the digested samples were then analysed using inductively coupled plasma optical emission spectrometry (ICP-OES).

Samples for pigment analysis were freeze-dried in the dark for 24h, after which they were grinded in pure acetone using mortar and pestle. Extraction occurred at 4ºC for 24 h in the dark. After extraction samples were centrifuged at 4000 rpm for 15 min at 4ºC. Pigment content was then analysed using the Gauss-Peak Spectra method (Küpper *et al.*, 2007). Samples were scanned in a dual-beam spectrophotometer from 350 nm to 750 nm at 1 nm steps. The absorbance spectra were introduced in the GPS fitting library using SigmaPlot. The employment of this library allowed to identify and quantify Chlorophyll a, Chlorophyll c1 and c2, Pheophytin a, Fucoxanthin, Antheraxanthin, β-carotene, Violaxanthin and Zeaxanthin for *C. corniculata* and Chlorophyll a, Pheophytin a,

β-cryptoxanthin, Antheraxanthin, β-carotene, Violaxanthin and Zeaxanthin for *J. rubens*. For phycobiliproteins approximately 0.5 g of tissue was homogenised in 10 mL 0.1 M phosphate buffer (pH 6.8). After being left at 4ºC in the dark overnight, extracts were centrifuged for 10 minutes at 1000g and read in the spectrophotometer at the wavelengths determined by Beer and Eshel (1985).

7.2.5 Statistical analyses

All data were tested for normality and homogeneity of variances by visual evaluation of boxplots and residuals and using Levene's test, respectively. Analysis of pH data was performed using a non-parametric analysis (Kruskal-Wallis ANOVA); the two study periods were analysed separately. Mass loss of plaster blocks containing copper was performed using a one-way ANOVA with site as fixed factor. Copper content in seaweed tissues and changes in F_v/F_m following transplant and copper exposure were analysed using three-way ANOVAs with three fixed factors (site of origin, site of transplant, copper exposure). The analysis of hydrophilic pigments and phycobilins (only for September 2013) was performed through three-way MANOVAs with the same factors of previous analyses. When the data did not meet Mauchly's test of sphericity, the degrees of freedom were corrected using Greenhouse-Geisser estimates of sphericity. All of the analyses above were performed using SPSS v. 19 (IBM, USA).

Mobile invertebrates community composition and abundance was tested using a two-factor PERMANOVA with "site" and "copper" as fixed factors and "biomass" as a covariate. A square-root transformation was used to reduce the influence of abundant taxa in the community, and Type I sums of squares with 9,999 permutation of residuals under a reduced model was used. Variance

derived from significant interactions was then decomposed to determine which factor determined the significant interaction, and pairwise tests were performed when necessary. A nMDS plot was also used to visually inspect the similarities among samples. A SIMPER analysis was then used to determine the contribution of each taxon to the average Bray-Curtis dissimilarity between levels of a factor if the PERMANOVA analysis was significant. The SIMPER analysis was performed on broad taxonomic categories for ease of interpretation. All analyses above were performed using PRIMER 6 with PERMANOVA+ extension (Plymouth Routines In Multivariate Ecological Research, version 6).

7.3 Results

7.3.1 Environmental parameters

Data for environmental parameters monitored during the experiments are shown in Table 7.1. Statistical analyses of pH data revealed significant differences among sites in both seasons, and pH was lower at the SEEP site compared to the controls. On the other hand, average total alkalinity was similar among all sites and seasons. Temperature and salinity varied seasonally, but only showed small variability among sites.

Table 7.1. Mean (± SD) pH, total alkalinity (TA), temperature (T) and salinity (S) measured during the experiments, as well as parameters calculated with CO2SYS (pCO_2, bicarbonate (HCO_3^-) and carbonate (CO_3^{2-}) ions concentrations and saturation state of aragonite (Ω_{Ar}) and calcite (Ω_{Ca})); n=3-13.

June 2013									
	pH_{NBS}	**TA** (mmol kg^{-1})	**T** (ºC)	**S** (ppt)	**pCO_2** (µatm)	**HCO_3^-** (mmol kg^{-1})	**CO_3^{2-}** (mmol kg^{-1})	**Ω_{Ar}**	**Ω_{Ca}**
SEEP	7.59 ± 0.06	2.785	24.77 ± 0.69	37.93 ± 0.11	2205.9 ± 312.4	2578.2 ± 25.6	86.6 ± 10.7	2.03 ± 0.25	1.34 ± 0.17
REF A	8.10 ± 0.08	2.701	24.12 ± 0.43	38.20 ± 0.42	575.1 ± 134.0	2148.9 ± 78.5	229.0 ± 32.1	5.36 ± 0.73	3.53 ± 0.48
REF B	8.11 ± 0.04	2.703	22.96 ± 0.45	38.16 ± 0.45	543.4 ± 54.9	2156.9 ± 24.8	226.5 ± 10.3	5.30 ± 0.25	3.48 ± 0.16
September 2013									
	pH_{NBS}	**TA** (mmol kg^{-1})	**T** (ºC)	**S** (ppt)	**pCO_2** (µatm)	**HCO_3^-** (mmol kg^{-1})	**CO_3^{2-}** (mmol kg^{-1})	**Ω_{Ar}**	**Ω_{Ca}**
SEEP	7.65 ± 0.03	2.785	26.50 ± 0.17	39.60 ± 0.10	1913.9 ± 121.1	2532.2 ± 14.2	105.5 ± 3.2	2.44 ± 0.13	1.62± 0.09
REF A	8.12 ± 0.02	2.701	25.87 ± 0.06	39.07 ± 0.35	534.2 ± 33.4	2097.6 ± 16.5	249.8 ± 0.9	5.81 ± 0.23	3.86± 0.15
REF B	8.10 ± 0.04	2.703	25.60 ± 0.36	38.90 ± 0.08	572.8 ± 68.6	2129.3 ± 39.1	237.8 ± 1.8	5.54 ± 0.38	3.67± 0.24

7.3.2 Copper exposure and accumulation

In June 2013, plaster blocks containing copper in the sites REF A and SEEP did not show significant differences in mass loss as they were deployed in the field ($F_{1,7}$=0.016, p=0.903); at both sites, plaster blocks lost approximately 68% of their initial mass, releasing comparable amounts of copper in seawater. Tissue copper content in *C. corniculata*, however, was significantly different between transplant sites, and copper had a significant effect as well (Table 7.2). Samples originating from REF B had to be removed from analysis due to high sample loss. Figure 7.4 shows that *C. corniculata* exposed to copper had much higher tissue copper concentration than control thalli, and that site of transplant had a major effect on copper accumulation, with individuals transplanted to SEEP accumulating 3-4 times more copper than those transplanted to REF A.

Table 7.2. ANOVA on log-transformed copper concentration in *C. corniculata* thalli measured at the end of the experiment of June 2013. The table shows main factors and their interactions and sum of squares (SS), degrees of freedom (df), Mean Squares (MS), F-ratios (F) and p values. Significant p values (< 0.05) are highlighted.

Source	**Type III SS**	**df**	**MS**	**F ratio**	**p**
Copper	89.456	1	89.456	209.475	**< 0.001**
Origin	0.836	1	0.836	1.958	0.172
Transplant	22.459	1	22.459	52.591	**< 0.001**
Copper * Transplant	0.434	1	0.434	1.017	0.321
Origin * Transplant	0.568	1	0.568	1.330	0.258
Origin * Copper	1.087	1	1.087	2.545	0.121
Origin * Transplant * Copper	0.124	1	0.124	0.290	0.594
Error	13.239	31	0.427		
Total	130.769	38			

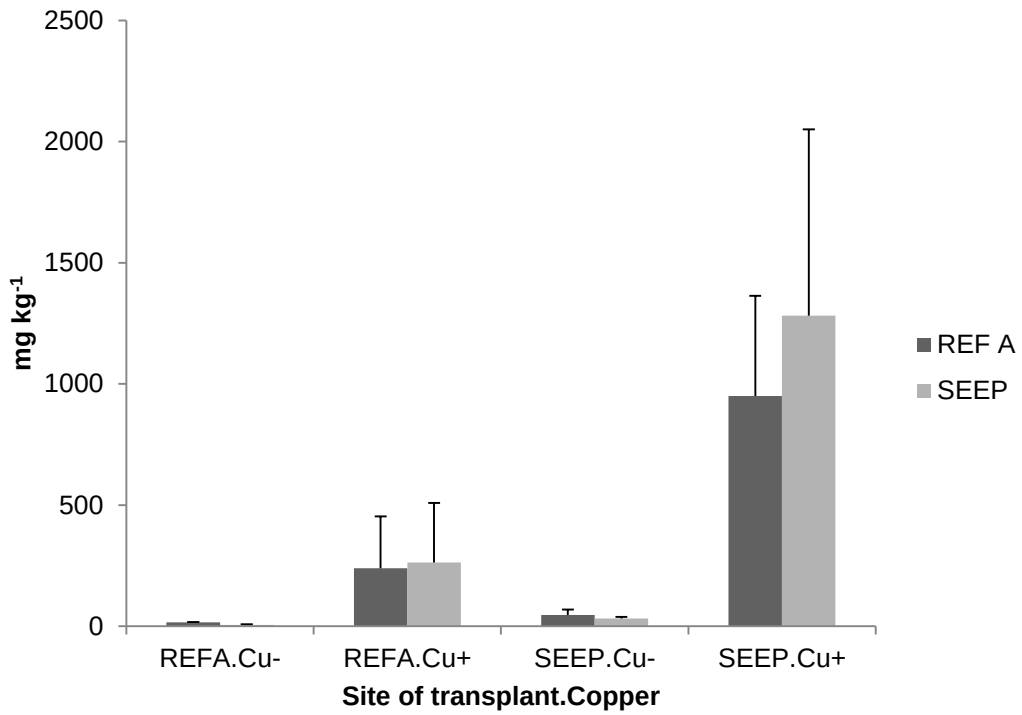

Figure 7.4. Mean (± SD, n=4-5) copper concentration (mg kg^{-1}) of *C. corniculata* thalli transplanted from REF A or SEEP not exposed (Cu-) or exposed (Cu+) to copper at REF A and SEEP in June 2013.

In September 2013, percent mass loss of plaster blocks containing copper significantly differed between the sites REF A and SEEP ($F_{1,7}$=14.926, p=0.008); plaster blocks deployed at REF A lost approximately 78% of their initial mass, releasing more copper in seawater compared to the SEEP site, where plaster blocks only decreased in mass by 55%. Statistical analysis of tissue copper content in *J. rubens* showed that copper exposure caused different effects in the two sites (site of transplant * copper interaction significant) and that copper concentration depended on the macroalgae origin as well (Table 7.3). Figure 7.5 shows that *J. rubens* exposed to copper had higher tissue copper concentration than control thalli, but this difference was much more evident at the SEEP site than at REF A. Furthermore, thalli originally from SEEP accumulated more copper than those originating from the reference sites.

Table 7.3. ANOVA on log-transformed copper concentration in *J. rubens* thalli measured at the end of the experiment of September 2013. The table shows main factors and their interactions and sum of squares (SS), degrees of freedom (df), Mean Squares (MS), F-ratios (F) and p values. Significant p values (< 0.05) are highlighted.

Source	**Type III SS**	**df**	**MS**	**F ratio**	**p**
Origin	1.896	2	0.948	6.652	**0.003**
Transplant	1.243	1	1.243	8.719	**0.005**
Copper	21.126	1	21.126	148.212	**< 0.001**
Origin * Transplant	0.209	2	0.105	0.734	0.485
Origin * Copper	0.458	2	0.229	1.607	0.212
Transplant * Copper	0.593	1	0.593	4.161	**0.047**
Origin * Transplant * Copper	0.172	2	0.086	0.604	0.551
Error	6.557	46	0.143		
Total	32.106	57			

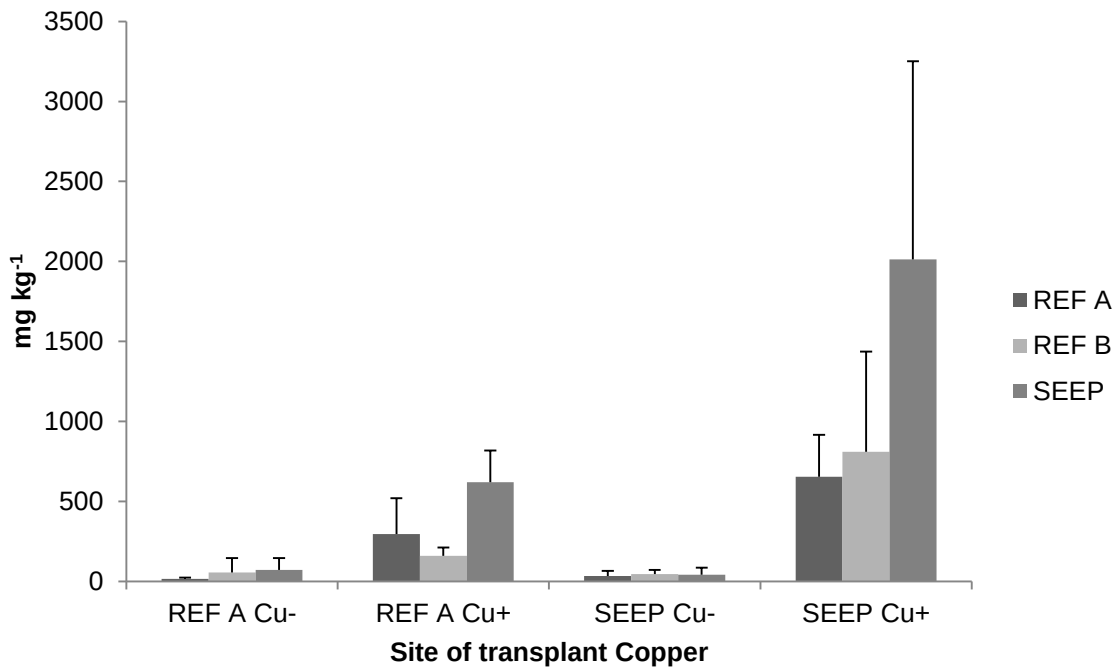

Figure 7.5. Mean (± SD, n=3-5) copper concentration (mg kg^{-1}) of *J.rubens* thalli transplanted from REF A, REF B or SEEP not exposed (Cu-) or exposed (Cu+) to copper at REF A and SEEP in September 2013.

7.3.3 Maximum quantum yield (F_v/F_m)

Change in maximum quantum yield in *C. corniculata* exposed to copper in June 2013 showed a significant interaction of origin and copper both after transplant and after copper exposure (Table 7.4). This was due to a sharp decrease in maximum quantum yield of the thalli from REF B that were to be exposed to copper; the same thalli recovered from the transplant later than the other groups, leading to a median increase in maximum quantum yield of about 0.2 after copper exposure, whereas all other groups showed no significant effects of copper (Figure 7.6).

Table 7.4. ANOVA on change in maximum quantum yield (F_v/F_m) after transplant (upper part) and after copper exposure (lower part) for *C. corniculata* thalli in June 2013. The table shows main factors and their interactions and sum of squares (SS), degrees of freedom (df), Mean Squares (MS), F-ratios (F) and p values. Significant p values (< 0.05) are highlighted.

Effect of transplant:

Source	**Type III SS**	**df**	**MS**	**F ratio**	**p**
Origin	0.194	2	0.097	7.054	**0.002**
Transplant	0.065	1	0.065	4.731	**0.035**
Copper	0.048	1	0.048	3.488	0.069
Origin * Transplant	0.051	2	0.025	1.842	0.171
Origin * Copper	0.163	2	0.082	5.941	**0.005**
Transplant * Copper	<0.001	1	<0.001	0.022	0.882
Origin * Transplant * Copper	0.002	2	0.001	0.072	0.931
Error	0.578	42	0.014		
Total	1.046	53			

Effect of copper:

Source	**Type III SS**	**df**	**MS**	**F ratio**	**p**
Origin	0.126	2	0.063	8.867	**0.001**
Transplant	0.005	1	0.005	0.658	0.422
Copper	0.020	1	0.020	2.782	0.103
Origin * Transplant	0.016	2	0.008	1.091	0.345
Origin * Copper	0.061	2	0.030	4.254	**0.021**
Transplant * Copper	0.002	1	0.002	0.323	0.573
Origin * Transplant * Copper	0.002	2	0.001	0.158	0.854
Error	0.299	42	0.007		
Total	0.519	53			

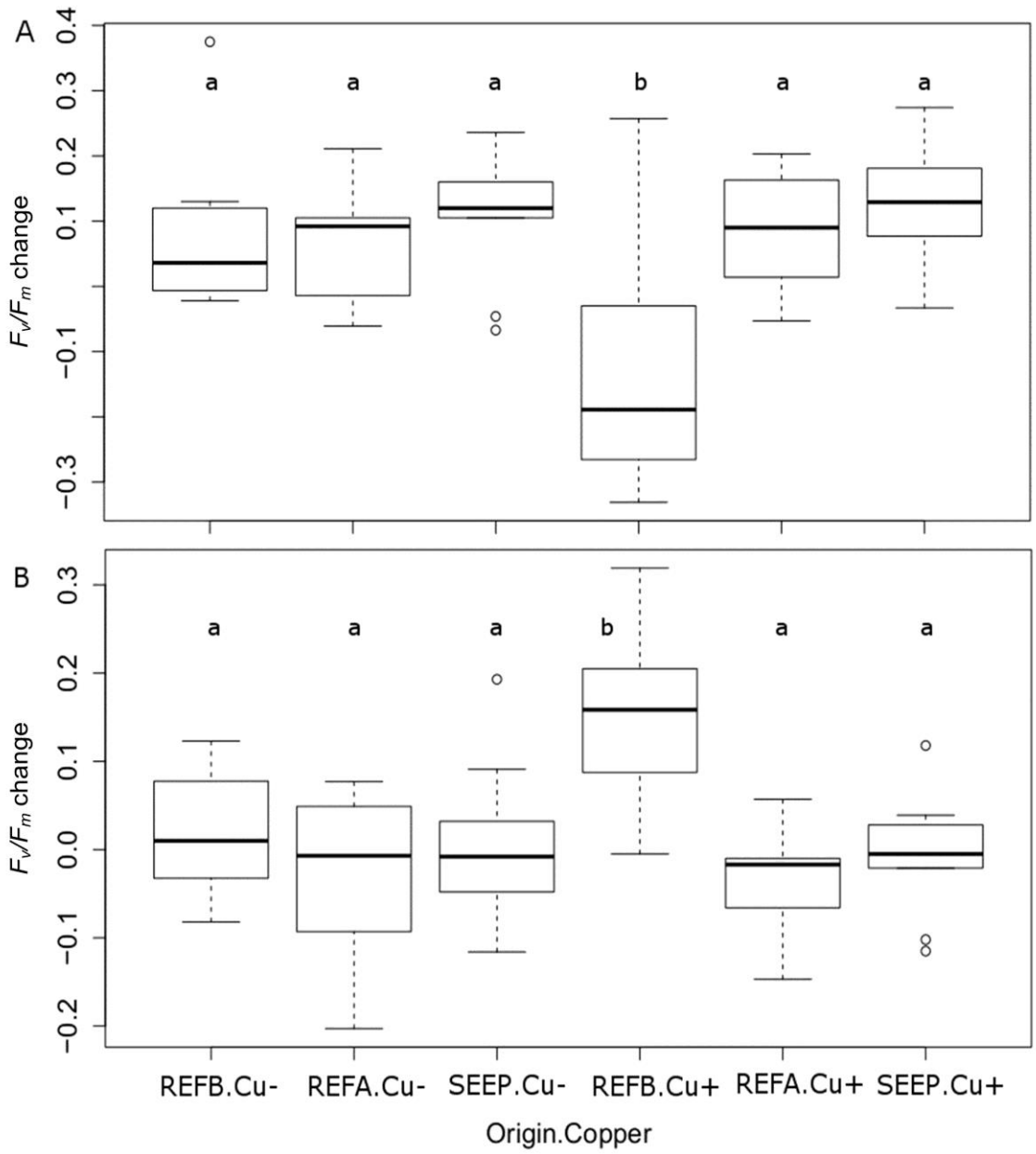

Figure 7.6. Changes in maximum quantum yield (F_v/F_m) following *C. corniculata* thalli transplant (A) and copper exposure (B) in June 2013 depending on their site of origin (REF A, REF B or SEEP) and their exposure to copper (Cu- = no; Cu+ = yes); n = 7-10. Horizontal line = median, vertical boxes = 25th and 75th percentiles, whiskers = min/max values if smaller than 1.5 times the inter-quartile range and dots = outliers.

Change in maximum quantum yield in *J. rubens* exposed to copper in September 2013 showed a significant interaction of site of origin and site of transplant before copper exposure, but no significant effects of copper exposure (Table 7.5). This was due to a decrease in maximum quantum yield of the thalli

from REF A transplanted at SEEP and a concurrent increase in maximum quantum yield of thalli from the other reference site transplanted at SEEP (Figure 7.7).

Table 7.5. ANOVA on change in maximum quantum yield (F_v/F_m) after transplant (upper part) and after copper exposure (lower part) for *J. rubens* thalli in September 2013. The table shows main factors and their interactions and sum of squares (SS), degrees of freedom (df), Mean Squares (MS), F-ratios (F) and p values. Significant p values (< 0.05) are highlighted.

Effect of transplant					
Source	**Type III SS**	**df**	**MS**	**F ratio**	**p**
Origin	0.036	2	0.018	1.162	0.323
Transplant	0.012	1	0.012	0.779	0.383
Copper	0.001	1	0.001	0.048	0.827
Origin * Transplant	0.138	2	0.069	4.417	**0.018**
Origin * Copper	0.010	2	0.005	0.326	0.724
Transplant * Copper	0.015	1	0.015	0.962	0.333
Origin * Transplant * Copper	0.053	2	0.026	1.681	0.199
Error	0.627	40	0.016		
Total	0.920	51			
Effect of copper					
Source	**Type III SS**	**df**	**MS**	**F ratio**	**p**
Origin	0.003	2	0.002	0.069	0.934
Transplant	0.004	1	0.004	0.171	0.681
Copper	0.032	1	0.032	1.275	0.266
Origin * Transplant	0.093	2	0.046	1.871	0.167
Origin * Copper	0.014	2	0.007	0.274	0.762
Transplant * Copper	0.049	1	0.049	1.997	0.165
Origin * Transplant * Copper	0.014	2	0.007	0.275	0.761
Error	0.989	40	0.025		
Total	1.208	51			

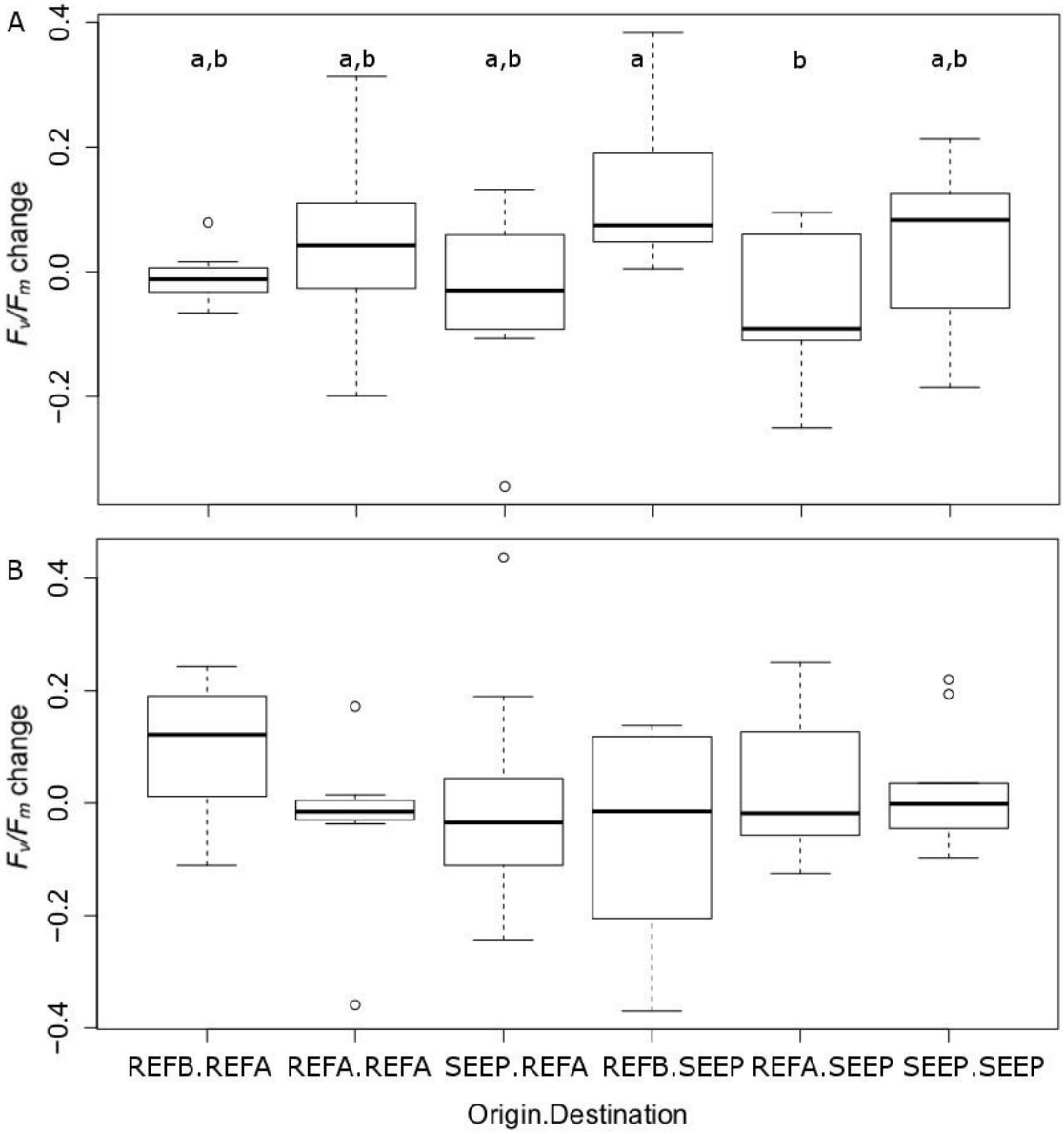

Figure 7.7. Changes in maximum quantum yield (F_v/F_m) following *J.rubens* thalli transplant (A) and copper exposure (B) in September 2013 depending on their site of origin (REF A, REF B or SEEP) and their site of transplant (REF A or SEEP); n = 7-10. Horizontal line = median, vertical boxes = 25th and 75th percentiles, whiskers = min/max values if smaller than 1.5 times the inter-quartile range and dots = outliers.

7.3.4 Pigment contents

In the experiment performed in June 2013 on *C. corniculata*, copper had a significant effect on pheophytin *a* and antheraxanthin, while chlorophyll *c*, pheophytin *a* and fucoxanthin were significantly affected by the site of origin (Table 7.6). Figure 7.8 shows that thalli exposed to copper had higher antheraxanthin concentration, but lower pheophytin *a*. On the other hand, thalli originally from SEEP had higher chlorophyll *c* and lower pheophytin *a* and fucoxanthin compared with samples originally from REF A. Samples originating from REF B had to be removed from analysis due to high sample loss.

Table 7.6. MANOVA on pigment concentrations in *C. corniculata* thalli measured after the end of the experiment of June 2013. The table shows main factors and their interactions and dependent variables. F-ratios (F) and p values are reported when significant ($p<0.05$).

Response variable	Origin	Transplant	Copper	Origin * Transplant	Origin* Copper	Transplant * Copper	Origin * Transplant * Copper
Chl *a*	-	-	-	-	-	-	-
Chl *c*	F(1,29)= 5.1 p=0.032	-	-	-	-	-	-
Pheophytin *a*	F(1,29)= 25.8 p<0.001	-	F(1,29)= 6.0 p=0.021	-	-	-	-
β-carotene	-	-	-	-	-	-	-
Fucoxanthin	F(1,29)= 5.6 p=0.025	-	-	-	-	-	-
Violaxanthin	-	-	-	-	-	-	-
Antheraxanthin	-	-	F(1,29)= 7.8 p=0.009	-	-	-	-
Zeaxanthin	-	-	-	-	-	-	-

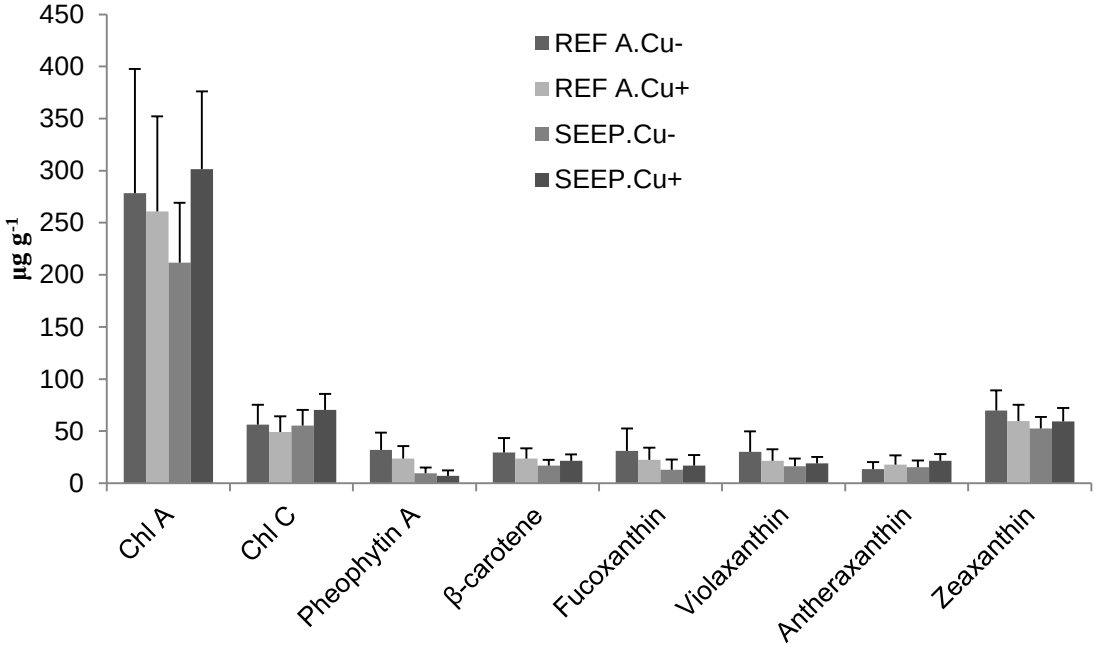

Figure 7.8. Mean (± SD, n=9-10) pigment concentrations (µg g^{-1} dry mass) of *C. corniculata* thalli transplanted from REF A or SEEP not exposed (Cu-) or exposed (Cu+) to copper in June 2013.

In the experiment performed in September 2013 on *J. rubens*, copper had a significant effect on β-cryptoxanthin, β-carotene and zeaxanthin, while pheophytin A was significantly affected by the site of transplant and zeaxanthin was significantly affected by the interaction of site of origin and site of transplant (Table 7.7). Figure 7.9 shows that thalli exposed to copper had lower β-carotene and zeaxanthin concentration, but higher β-cryptoxanthin. On the other hand, thalli transplanted to SEEP had higher pheophytin A than those transplanted to REF A. Zeaxanthin concentration was higher in thalli transplanted from their site of origin to a different site (i.e. REF A to SEEP and vice versa) compared to concentrations in thalli that remained in their site of origin.

Table 7.7. MANOVA on pigment concentrations in *J. rubens* thalli measured after the end of the experiment of September 2013. The table shows main factors and their interactions and dependent variables. F-ratios (F) and p values are reported when significant ($p<0.05$).

Response variable	Origin	Transplant	Copper	Origin * Transplant	Origin * Copper	Transplant * Copper	Origin * Transplant * Copper
Chl *a*	-	-	-	-	-	-	-
Pheophytin *a*	-	F(1,26)= 15.3 p=0.001	-	-	-	-	-
βcryptoxanthin	-	-	F(1,26)= 13.5 p=0.001	-	-	-	-
Antheraxanthin	-	-	-	-	-	-	-
β-carotene	-	-	F(1,26)= 7.9 p=0.009	-	-	-	-
Violaxanthin	-	-	-	-	-	-	-
Zeaxanthin	-	-	F(1,26)= 9.2 p=0.005	F(1,26)=5.0 p=0.033	-	-	-

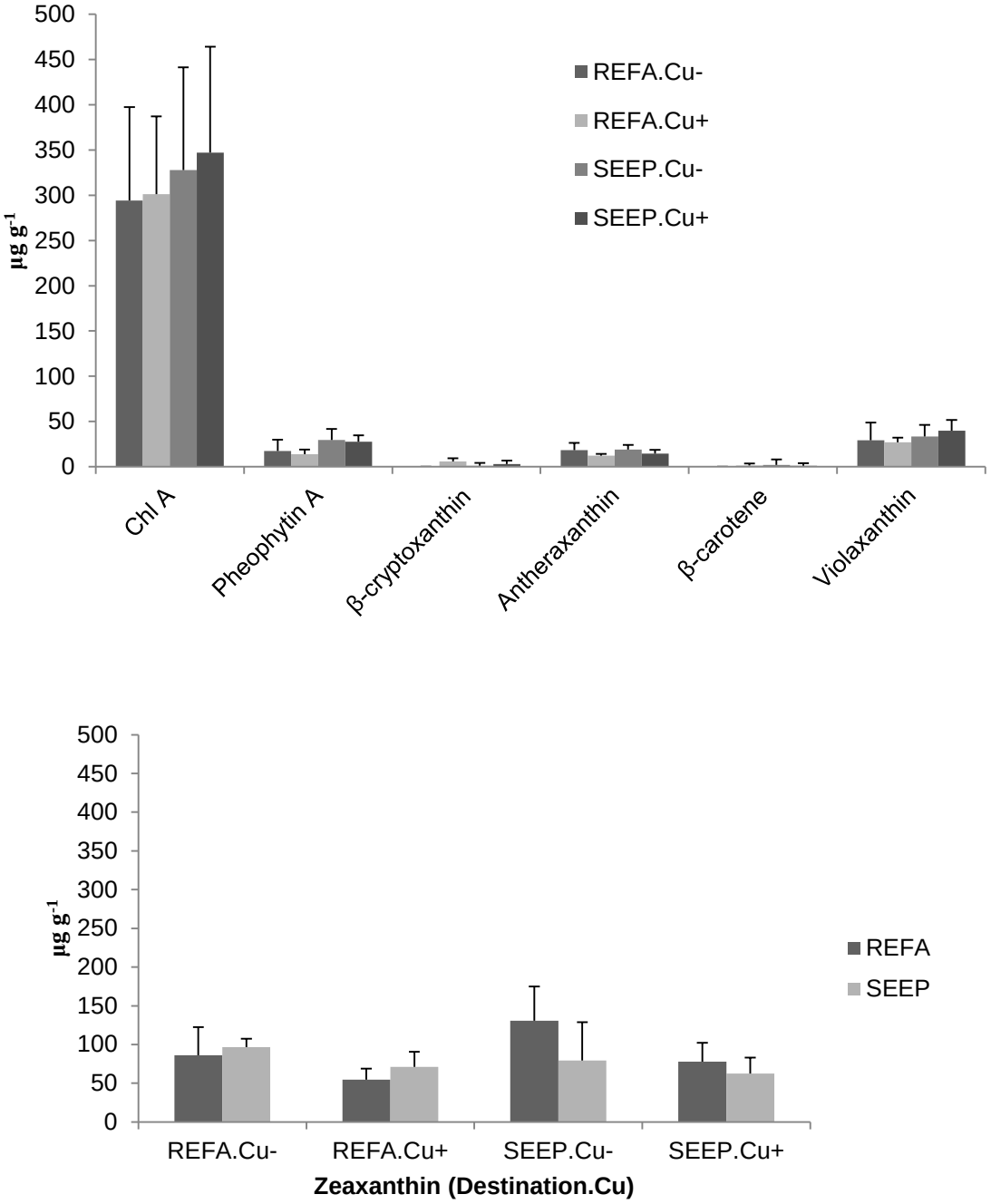

Figure 7.9. Upper part: mean (± SD, n=8-9) pigment concentrations (µg g^{-1} dry mass) of *J. rubens* thalli transplanted to REF A or SEEP not exposed (Cu-) or exposed (Cu+) to copper in September 2013. Lower part: mean (± SD, n=3-5) zeaxanthin concentration (µg g^{-1} dry mass) of *J. rubens* thalli transplanted to REF A or SEEP from REF A and SEEP not exposed (Cu-) or exposed (Cu+) to copper in September 2013.

With regards to phycobilins, only phycoerythrin (PE) showed any significant difference among treatments, with a significant site of transplant * copper interaction, whereas phycocyanin (PC) seemed unaffected by the experiment (Table 7.8). At REF A, phycoerythrin concentration increased in thalli exposed to copper, while the opposite was true from *J. rubens* individuals at SEEP, where thalli exposed to copper had lower phycoerythrin concentration compared with controls (Figure 7.10).

Table 7.8. MANOVA on phycoerythrin (PE) and phycocyanin (PC) concentrations in *J. rubens* thalli measured after the end of the experiment of September 2013. The table shows main factors and their interactions and dependent variable, sum of squares (SS), degrees of freedom (df), Mean Squares (MS), F-ratios (F) and p values. Significant p values (< 0.05) are highlighted.

Source	**Dependent Variable**	**Type III SS**	**df**	**MS**	**F-ratio**	**p**
Origin	PE	0.118	1	0.118	0.262	0.614
	PC	0.001	1	0.001	0.001	0.977
Transplant	PE	1.623	1	1.623	3.591	0.071
	PC	1.227	1	1.227	1.506	0.232
Copper	PE	0.005	1	0.005	0.011	0.919
	PC	1.627	1	1.627	1.997	0.171
Origin * Transplant	PE	1.361	1	1.361	3.012	0.096
	PC	0.644	1	0.644	0.790	0.383
Origin * Copper	PE	0.002	1	0.002	0.004	0.947
	PC	2.402	1	2.402	2.947	0.099
Transplant * Copper	PE	2.572	1	2.572	5.692	**0.026**
	PC	1.409	1	1.409	1.729	0.202
Origin * Transplant * Copper	PE	0.016	1	0.016	0.035	0.853
	PC	0.989	1	0.989	1.213	0.282
Error	PE	10.394	23	0.452		
	PC	18.742	23	0.815		
Total	PE	15.965	30			
	PC	26.690	30			

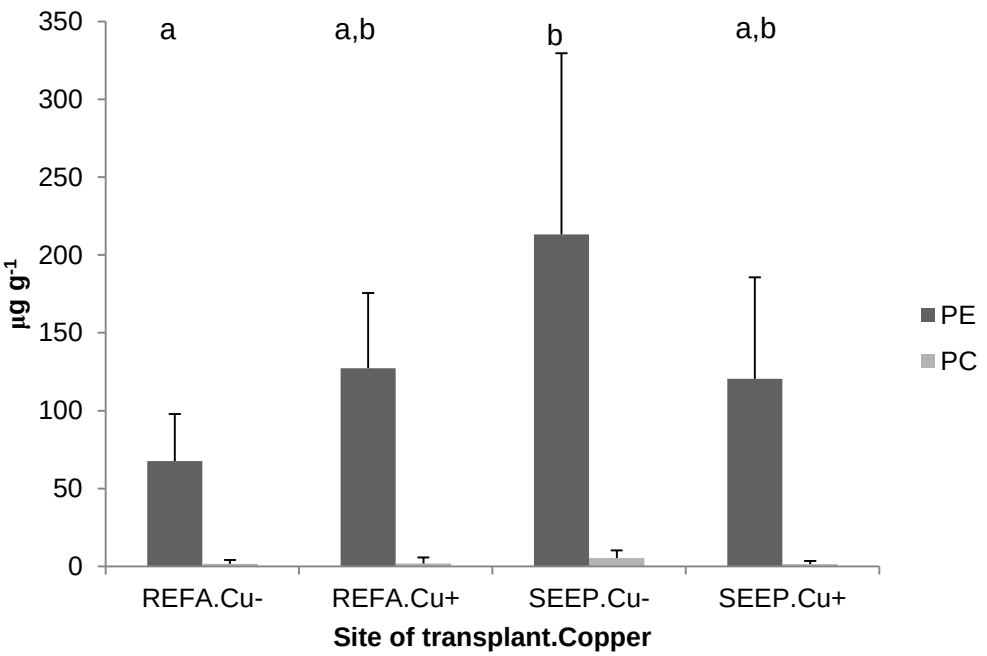

Figure 7.10. Mean (± SD, n=6-9) phycoerythrin (PE) and phycocyanin (PC) concentrations (µg/g) of *J.rubens* thalli transplanted to REF A or SEEP not exposed (Cu-) or exposed (Cu+) to copper in REF A and SEEP in September 2013.

7.3.5 Invertebrate re-colonisation

Invertebrate communities inhabiting *C. corniculata* thalli were significantly affected by copper, but this effect was not consistent between sites (Site x Copper interaction significant), even after considering the effect of individual thalli biomass on invertebrate community structure (Table 7.9a). Pairwise comparisons showed that copper only had a significant effect near the seeps, but not in the reference site (Table 7.9b). This was also evident from the nMDS plot, where samples from REF A exposed and not exposed to copper are all grouped together, whereas samples from SEEP are separated from REF A samples, but also clearly grouped depending on their copper exposure (Figure 7.11).

Table 7.9. PERMANOVA analyses of square-root transformed invertebrate abundances in *C. corniculata* thalli from copper exposure experiment in June 2013. The first table shows main factors and their interactions and degrees of freedom (df), sum of squares (SS), pseudo-F, permutational p and unique permutations for each of them. The second table shows pair-wise comparisons between copper treatments at both sites. Significant p values (< 0.05) are highlighted.

A)

Source	df	SS	MS	Pseudo-F	P(perm)	Unique perms
Biomass	1	2193.4	2193.4	3.2403	**0.0029**	9937
Site	1	5429.8	5429.8	8.0213	**0.0001**	9916
Copper	1	1510.2	1510.2	2.2310	**0.0116**	9920
Biomass x Site	1	1036.5	1036.5	1.5312	0.1236	9930
Biomass x Copper	1	441.99	441.99	0.6529	0.7933	9926
Site x Copper	1	1373.5	1373.5	2.0291	**0.0244**	9933
Biomass x Site x Copper	1	554.56	554.56	0.8192	0.6289	9938
Residual	11	7446.1	676.92			
Total	18	19986				

B)

Within level 'REF A' of factor 'Site'			
Groups	**t**	**P**(perm)	**Unique perms**
Cu+, Cu-	1.2129	0.1598	9805
Within level 'SEEP' of factor 'Site'			
Groups	**t**	**P(perm)**	**Unique perms**
Cu+, Cu-	1.6212	**0.0102**	9917

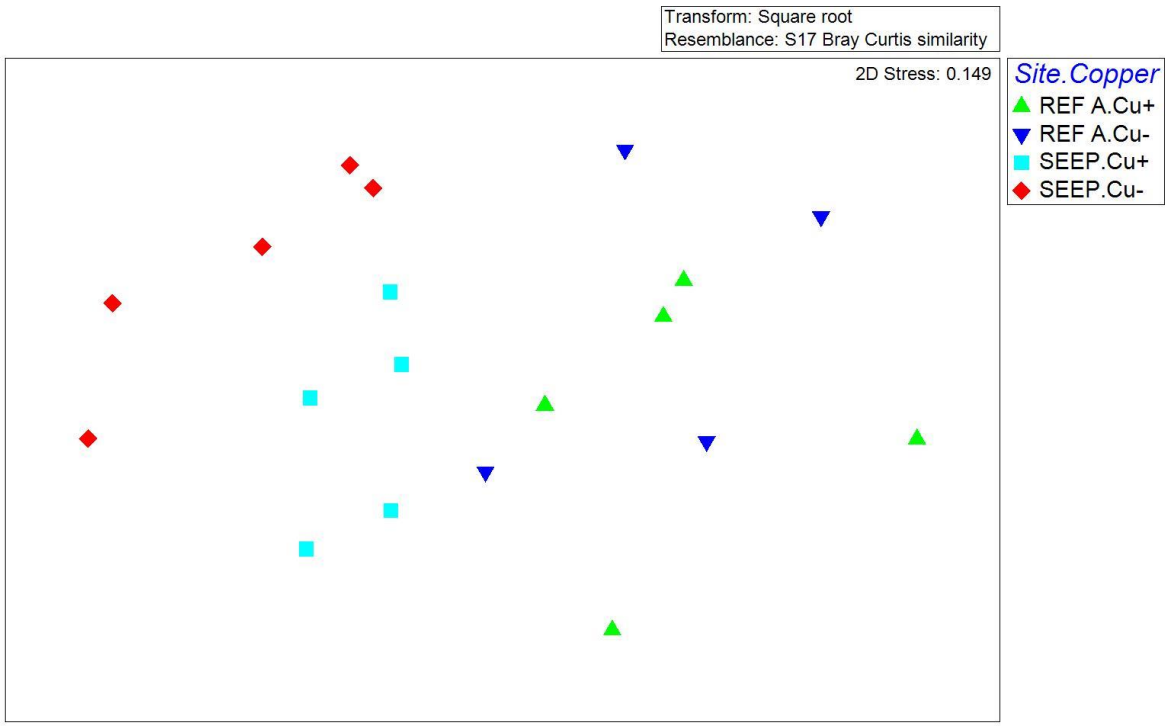

Figure 7.11: MDS plot of invertebrate assemblages on *C. corniculata* thalli placed at REF A or SEEP, and not exposed (Cu-) or exposed (Cu+) to copper in June 2013.

SIMPER analysis showed that crustaceans, molluscs and polychaetes were the main taxa driving differences between sites and copper treatments (Table 7.10). Mean abundance of these taxa is shown in Figure 7.12, showing that all crustacean groups and ophiuroids consistently increased near the seeps when seaweed thalli were not exposed to copper; copper exposure had a negligible effect on their abundance in the reference site and a dramatic negative effect at SEEP. On the other hand, polychaetes were largely unaffected by changes in pCO_2, but their abundance greatly increased in the thalli exposed to copper near the seeps. Gastropods exhibited another type of response, with their abundance decreasing near the seeps and further decreasing when exposed to copper at elevated CO_2. Bivalve and oligochaete abundances were very low and no clear pattern was detectable.

Table 7.10. SIMPER analysis showing the average dissimilarities between sites and copper treatments and which taxonomic groups contributes to the dissimilarity up to 90%. For each taxon, the average abundance in the two groups, their average dissimilarity, the dissimilarity to standard deviation ration and the taxon contribution and cumulative contribution are shown.

Groups REF A & SEEP; Average dissimilarity = 32.05

Species	REF A Av.Abund	SEEP Av.Abund	Av.Diss	Diss/SD	Contrib%	Cum.%
Copepods	5.46	8.52	6.53	1.28	20.36	20.36
Gastropods	2.15	0.10	3.94	2.18	12.28	32.65
Amphipods	3.49	5.34	3.86	1.23	12.04	44.68
Polychaetes	3.72	4.06	3.57	1.12	11.13	55.81
Tanaids	3.19	4.55	2.93	1.32	9.14	64.95
Ostracods	1.72	2.37	2.29	1.25	7.16	72.10
Isopods	1.98	2.56	2.11	0.90	6.59	78.69
Bivalves	0.92	0.34	1.43	1.35	4.45	83.14
Ophiuroids	0.16	0.72	1.34	0.79	4.19	87.33
Oligochaetes	0.73	0.20	1.28	0.96	4.00	91.34

Groups Cu+ & Cu-; Average dissimilarity = 27.61

Species	Cu+ Av.Abund	Cu- Av.Abund	Av.Diss	Diss/SD	Contrib%	Cum.%
Copepods	6.19	8.05	5.42	1.26	19.64	19.64
Polychaetes	4.50	3.24	3.85	1.08	13.94	33.58
Amphipods	4.10	4.87	3.14	1.38	11.38	44.97
Isopods	1.70	2.93	3.10	1.78	11.21	56.18
Ostracods	2.34	1.75	2.54	1.28	9.21	65.39
Decapods	3.61	4.24	1.98	1.31	7.18	72.57
Gastropods	1.11	1.03	1.39	0.70	5.02	77.59
Ophiuroids	0.24	0.69	1.35	0.80	4.89	82.47
Oligochaetes	0.31	0.60	1.16	0.86	4.21	86.68
Bivalves	0.54	0.69	1.00	0.92	3.63	90.31

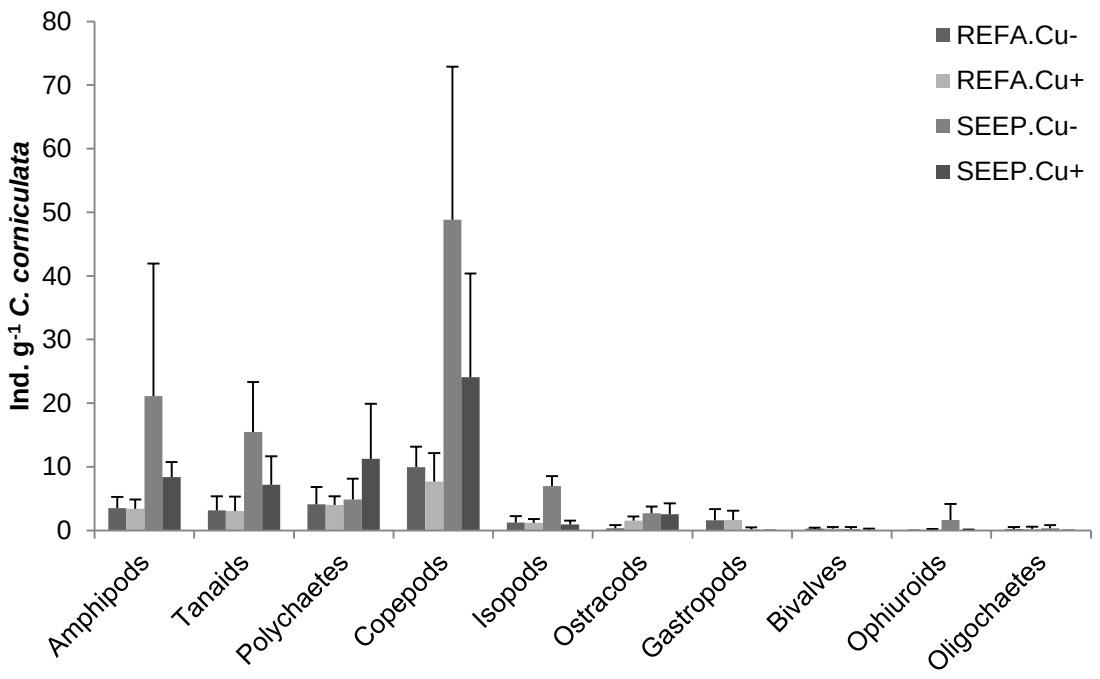

Figure 7.12. Mean (±SD, n=4-5) number of individuals for each of the main taxonomic groups. Abundances were normalised by *C. corniculata* dry mass; *C. corniculata* thalli were placed in REF A or SEEP and exposed (Cu+) or not exposed (Cu-) to copper for 36h in June 2013.

7.4 Discussion

This is the first investigation of the combined effect of elevated carbon dioxide and metal toxicity on macroalgal physiology and invertebrate communities. Copper accumulation in both *C. corniculata* and *J. rubens* increased at elevated pCO_2 levels, even though copper released from plaster blocks was the same (June 2013) or less (September 2013) near the seeps than at the reference site. Long-term acclimatisation effects on copper accumulation were evident for the coralline alga *J. rubens*, as thalli grown near the seeps accumulated significantly more copper than those transplanted from reference sites.

Copper bioavailability is expected to increase with decreased seawater pH (Richards *et al.*, 2011) and might explain increased copper accumulation at high

CO_2. However, seaweeds accumulate copper for over 24 h after its addition to seawater (Connan and Stengel, 2011a). As Cu^{2+} ions were not complexed immediately while plaster block continuously released them, copper was equally bioavailable at both sites. Copper uptake, however, is regulated by metabolic activity (Connan and Stengel, 2011a), so it is possible that macroalgae had more energy available after down-regulating carbon concentrating mechanisms (CCMs). Reduced use of CCMs following increased CO_2 availability has already been proven for some macroalgae (Olischläger and Wiencke, 2013), and this might explain the copper accumulation pattern observed in *C. corniculata*.

As elevated CO_2 increases the energetic cost of calcification (Bradassi *et al.*, 2013), *J. rubens* thalli just transplanted from reference sites probably used most of the surplus energy derived from increased CO_2 levels to maintain calcification rates. They thus showed a relatively small increase in copper accumulation. On the other hand, thalli grown at high CO_2 may have mechanisms in place to make calcification at high pCO_2 energetically sustainable in the long term. They are therefore likely to have higher metabolic activity and accumulate more copper than thalli not acclimatised to elevated CO_2 levels. Coralline algal calcification is controlled by alginic acid and sulfated polysaccharides (Koch *et al.*, 2013), which are also known to have a high affinity for metals (Raize *et al.*, 2004). Increased production of calcification-inducing compounds in *J. rubens* acclimatised to high CO_2 could enhance copper accumulation, potentially increasing its vulnerability to metal toxicity.

Physiological responses to copper examined in both macroalgal species were not influenced by acclimatisation to increased carbon dioxide (i.e. no significant site of origin * copper interactions). In fact, maximum quantum yield (F_v/F_m) was only affected by transplant, while some pigments showed effects of site of origin

and copper in *C. corniculata* and of site of transplant, copper and site of origin in *J. rubens*. Copper is known to decrease F_v/F_m in some species of red algae (Küpper *et al.*, 2002; Brown and Newman, 2003; Baumann *et al.*, 2009), whereas maximum quantum yield of brown algae is mostly unaffected at moderate copper levels (Nielsen *et al.*, 2003; Nielsen and Nielsen, 2005; Baumann *et al.*, 2009; Nielsen and Nielsen, 2010).

Copper exposure only caused a small decrease of pheophytin A and a small increase of antheraxanthin in *C. corniculata*. Since the latter was not associated with an increase in the xanthophyll cycle pool size, these pigments are unlikely to play a role in copper defence for this species. This is in accord with previous studies on *Fucus serratus*, where no change in xanthophyll pool size was found in light-adapted thalli after copper exposure (Nielsen *et al.*, 2003; Nielsen and Nielsen, 2010). On the other hand, *J. rubens* thalli exposed to copper showed a small increase in β-cryptoxanthin, but a bigger decrease in β-carotene and zeaxanthin, resulting in a decrease in total carotenoids. Decreased carotenoids concentrations were previously found in a red alga exposed to high copper concentrations (5-10 ppm; Gouveia *et al.*, 2013), whereas red algae exposed to Cu^{2+} concentrations of 0.2-0.5 ppm often increase their carotenoids content to counter copper toxicity (Brown and Newman, 2003; Collén *et al.*, 2003; Pinto *et al.*, 2011). *J. rubens*, however, did not show the reduction in chlorophyll *a* found in another red alga at high Cu^{2+} concentrations (Gouveia *et al.*, 2013). This suggests the experimental copper pulse exposed *J. rubens* to relatively high Cu^{2+} concentrations. There was a reduction in phycoerithrin content when *J. rubens* was exposed to copper at SEEP, but not at REF A. Decreased phycobilins concentration is considered a sensitive indicator of copper stress (Küpper *et al.*, 2002; Brown and Newman, 2003; Xia *et al.*, 2004). *J. rubens*

transplanted near the seeps might be more sensitive to copper exposure because of the increased energetic cost of maintaining calcification rates at elevated CO_2 (Bradassi *et al.*, 2013) or because of increased copper accumulation.

Macroalgae counter negative effects of copper exposure by synthetizing metal-binding compounds such as metallothioneins and phytochelatins (Lobban and Harrison, 1994) and by increasing the activity of antioxidant enzymes (Collén *et al.*, 2003). Synthesis of complex molecules is energy expensive, so growth is reduced in many macroalgal species even at low copper levels (Collén *et al.*, 2003; Brown and Newman, 2003; Nielsen *et al.*, 2003; Xia *et al*., 2004). Fucoid and articulate coralline algae, however, are relatively slow-growing species whose growth rates are unlikely to be measurable after 36 hours. In brown algae, phlorotannins movement to the cell wall and exudation in the surrounding seawater provides additional defence against copper damage (Connan and Stengel, 2011b). Phlorotannins are polyphenols characteristic of phaeophytes that bind metal ions reducing their toxicity; their increased proportion in the cell walls of algae exposed to copper and increased release in the environment could have contributed to the lack of observed effects of copper in *C. corniculata*. However, it is possible that some effects of copper exposure have not been detected in this study. Lipid peroxidation, antioxidant enzymes activity and antioxidant compounds all increase following copper exposure of 48 to 96 hours (Collén *et al.*, 2003; Contreras *et al.*, 2005). In red algae, mycosporine-like amino-acids (MAAs) are important antioxidant compounds that are up-regulated after short exposure to oxidative stress (Karsten *et al.*, 1998). Further research is therefore needed before concluding that *C. corniculata* is not negatively affected by copper pulses at high CO_2 levels.

Although acclimatisation to elevated CO_2 had no effects on macroalgal responses to copper, *C. corniculata* thalli collected at SEEP had higher chlorophyll *c* content and slightly lower phaeophytin A and fucoxanthin contents compared to those collected at reference sites. On the other hand, pheophytin a content increased in *J. rubens* transplanted near the seeps, possibly a short-term response to increased CO_2. *J. rubens* pigments also showed some transplant effect, with zeaxanthin content being higher in thalli transplanted to a different site (i.e. SEEP. REFA and REFA.SEEP) compared to those transplanted to their site of origin (i.e. SEEP.SEEP and REFA.REFA). Short-term and long-term effects of CO_2 on macroalgal physiology will be compared in the next Chapter.

Invertebrate colonisation was significantly affected by copper exposure, but only at the high CO_2 site. This is probably due to very high copper accumulation by *C. corniculata* at elevated CO_2, as copper release rates in seawater were similar between sites in June 2013. Some crustaceans are more sensitive to copper at elevated CO_2 levels (Roberts *et al.*, 2013), which could contribute to their observed decrease when exposed to copper near the seeps. The specific responses of invertebrate taxa are consistent with previous studies: many crustaceans increase in abundance with increased CO_2 (Kroeker *et al.*, 2011), but are negatively affected by copper (Roberts *et al.*, 2006). Gastropods abundance is negatively affected by both carbon dioxide (Hale *et al.*, 2011; Kroeker *et al.*, 2011) and copper (Roberts *et al.*, 2006), while many polychaete species are largely unaffected by both factors (Roberts *et al.*, 2006; Cigliano *et al.*, 2010). The increase in polychaete abundances in *C. corniculata* thalli exposed to copper at the high CO_2 site was therefore unexpected, but it is possible they had more space and resources available following the marked

decrease in crustaceans. A similar pattern has already been detected by Hale *et al.* (2011), who found increased nematode abundance following a decrease in the abundance of sensitive taxa as CO_2 increased. Copper exposure combined with ocean acidification could however affect polychete larval stages (Lewis *et al.*, 2012; Campbell *et al.*, 2014).

Overall, *J. rubens* appeared more sensitive to copper than *C. corniculata*, especially at elevated CO_2, as well as showing changes in copper accumulation patterns following long-term exposure to high CO_2. These species are currently the two main space occupiers on shallow rocky shores off Methana, but *J. rubens* is at competitive disadvantage with *C. corniculata* when CO_2 levels are high (see Chapter 3). This study shows that *J. rubens* is likely to be negatively affected by the interaction of ocean acidification and copper pollution, and therefore at risk of local extinction. Since only two species (a calcifying red alga and a non-calcifying brown alga) were examined in the present study, the results are not applicable to all competitive interaction between calcifying and non-calcifying algae, as red and brown algae have very different physiologies, which could also influence *J. rubens* and *C. corniculata* interactions (Lobban and Harrison, 1994).

Ocean acidification increased seaweed copper bioaccumulation, and had significant effects on their epifauna. This adds to a growing body of research showing that indirect effects of ocean acidification are at least as important as its direct effects (Kroeker *et al.*, 2013c). Decreased growth rates of coralline algae with increased CO_2 can make them less competitive and cause communities to become dominated by fleshy algae (Kroeker *et al.*, 2013c), or cause changes in herbivore performance through decreased food quality (Rossoll *et al.*, 2012; Poore *et al.*, 2013). Interactive negative effects of ocean

acidification and copper pollution on competitive ability of *J. rubens* and abundance of many epifaunal taxa, especially heavily calcified ones, suggest that benthic communities will dramatically change in copper-polluted areas. These areas are relatively common worldwide and include the copper mining regions illustrated in Figure 7.2; here, it is essential that local managers reduce copper pollution to reduce the negative effects of ocean acidification on macroalgal communities and the services they provide.

Chapter 8

General discussion

8.1 Main findings and implications for marine systems

Macroalgal beds are an extremely important habitat in temperate coastal environments, as they provide vital ecosystem services such as oxygen production, nutrient cycling, water depuration, fisheries production and shore protection from waves (Rönnbäck *et al.*, 2007). Information on macroalgal beds responses to ocean acidification at the community level that take into account biological interactions and adaptation potential are therefore needed to reliably forecast future ecosystem state and take appropriate measures to adapt to or mitigate the possible reduction of ecosystem services provided by those habitats. This thesis contributes to achieving this objective, and its main findings are illustrated in Figure 8.1. All this thesis' objectives were achieved; specifically:

- Geochemical surveys at seeps off Methana showed that this site is suitable to study the effects of high CO_2 on benthic communities, as no confounding gradients in temperature, salinity, total alkalinity, nutrients, hysrogen sulphide or heavy metals were found (Chapter 2).
- At Mediterranean CO_2 seeps off Italy and Greece, macroalgal communities greatly changed, with fucoid algal abundance increasing and coralline algal abundance decreasing as pCO_2 increased (Chapter 3). Epifaunal communities changed as well: at high CO_2 sites, abundance of heavily calcified taxa (e.g. gastropods, bivalves) decreased, while more resistant taxa (mainly polychaetes) abundances increased at high CO_2 (Chapter 4).
- Strength of herbivore top-down control did not appear to change at different pCO_2 levels, even though densities of calcifying intertidal and

subtidal herbivores (i.e. limpets and sea urchins) decreased at elevated pCO_2 (Chapter 5).

- Non-reversible acclimatisation did not seem to play a role in benthic community changes with increased pCO_2, as the responses of transplanted calcified and non-calcified macroalgae to elevated CO_2 did not depend on their history of pCO_2 exposure (Chapter 6).
- Exposure to an additional stressor (i.e. copper pollution) had no additional negative effects on the physiology of a calcifying alga, but there were strong interactive effects on seaweed epifauna, reducing abundances of some taxa that were weakly affected or advantaged by exposure to elevated pCO_2 alone (e.g. amphipods; Chapter 7).

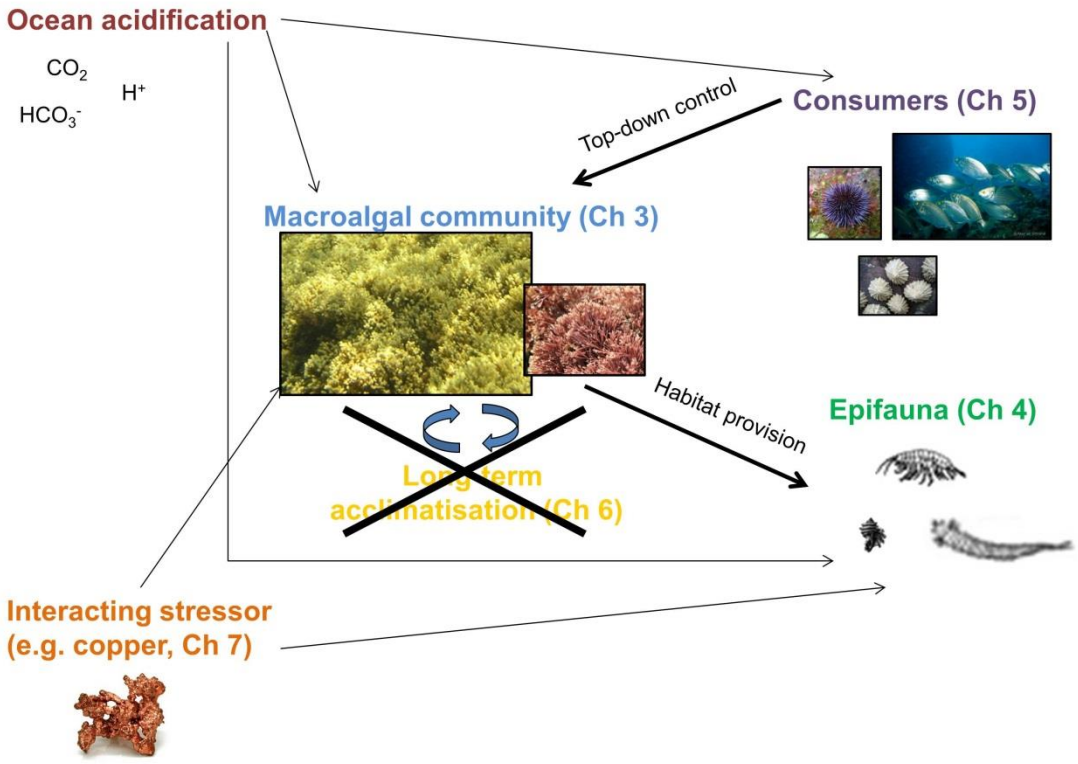

Figure 8.1. Visual abstract of thesis results; macroalgal communities (Chapter 3) and their epifauna (Chapter 4) change with increasing pCO_2 levels, with heavily calcified macroalgae and invertebrates decreasing in abundance at elevated CO_2. Long-term acclimatisation to

elevated pCO_2 did not seem to have permanent effects on dominant macroalgal species, as no significant effects of origin site on macroalgal physiology were found (Chapter 6). I also found that decreased calcifying herbivores densities do not significantly affect the strength of top-down control on macroalgal communities (Chapter 5), and that ocean acidification and short-term copper pollution interact and produce larger negative effect on a dominant calcifying macroalga, but especially on seaweed epifauna (Chapter 7).

8.1.1 Benthic community responses to ocean acidification

General patterns of benthic community changes with increasing pCO_2 levels at volcanic seeps off Italy and Greece were consistent with results from laboratory experiments and other ocean acidification analogues in that diversity and abundance of calcifying organisms decreased as CO_2 levels increased (Kroeker *et al.*, 2013a). Macroalgal communities responded in very similar ways at all Mediterranean seep sites studied so far, with a decrease in calcifying macroalgae and an increase in *Sargassum vulgare* abundance (Porzio *et al.*, 2011; Chapter 3). Epifaunal communities showed different patterns depending on the study area and the habitat studied (Chapter 4). While epifaunal communities of fucoid algae show a decrease of most invertebrate taxa at elevated pCO_2 at Methana, polychaete abundance increased at high CO_2 at Vulcano (Chapter 4). On the other hand, turf epifauna at seeps off Ischia showed an increase in crustaceans at elevated CO_2 (Kroeker *et al.*, 2011), seagrass-dwelling amphipods and polychaetes increase in abundance at elevated CO_2 levels off Ischia (Garrard *et al.*, 2014), and nematode abundance increased in Atlantic turf epifaunal communities exposed to ocean acidification conditions (Hale *et al.*, 2011). In addition, epiphyte communities of *Cystoseira corniculata* at Methana did not change significantly with CO_2 (Chapter 4), possibly because *C. corniculata* photosynthesis raised local pH and protected

epiphytes from the negative effects of increased CO_2 (Cornwall *et al.*, 2014). This clearly shows that site- and habitat-specific interactions among species result in different communities at high CO_2.

Studies in nutrient-rich areas have shown that calcifiers can remain abundant in areas with naturally high pCO_2 if food is not limiting. For instance, barnacles and mussels are dominant in upwelling water off Kiel fjord, where pCO_2 reaches concentrations over 1000 µatm but nutrient levels are high (Thomsen *et al.*, 2010), while spirorbid worms from an upwelling area in the Baltic Sea are negatively affected by CO_2 only at levels over 3000 µatm (Saderne and Wahl, 2013). However, climate change is expected to reduce nutrient availability in surface waters due to increased water stratification (Sarmiento *et al.*, 2004), meaning that results from upwelling areas might underestimate the negative impacts of ocean acidification. Seeps off Methana and Vulcano are oligotrophic, and have similar nutrient concentrations (Chapter 2; Johnson, 2012). Although the Eastern Mediterranean is usually more oligotrophic than the Western basin (Siokou-Frangou *et al.*, 2010), the Saronikos Gulf has relatively high nutrient concentrations due to riverine inputs and urbanisation (Tsiamis *et al.*, 2013). In contrast, south-eastern Mediterranean coastal waters are ultra-oligotrophic ([Chl a] < 0.06 $mg*m^{-3}$; Shushkina *et al.*, 1997) during the warmest part of the year (Siokou-Frangou *et al.*, 2010); comparable chlorophyll concentrations are only found in the Northern Red Sea (Labiosa *et al.*, 2003) and in subtropical gyres (Kletou and Hall-Spencer, 2012). As low food availability impairs organisms' ability to cope with increased CO_2 (Thomsen *et al.*, 2013), these nutrient-poor ecosystems are probably highly vulnerable to ocean acidification. However, community responses to elevated CO_2 in ultra-oligotrophic coastal areas are virtually unstudied.

This thesis contributes to revealing general patterns of community responses to high CO_2. However, general limitations of using volcanic seeps as ocean acidification laboratories, described in detail in Chapter 2, should be taken into account. In addition, more controlled studies (e.g. using mesocosms or field pCO_2 manipulations) would determine the exact CO_2 concentrations that trigger the observed community changes (Gattuso *et al.*, 2014). Insights could also be gained from the study of a wider range of habitats (e.g. soft substrata).

8.1.2 Changes in biological interactions at elevated pCO_2

Changes in biological interactions with increasing CO_2 are poorly known, although there is evidence that calcifying macroalgae become less competitive at elevated CO_2 (Kroeker *et al.*, 2013c; Short *et al.*, 2014) and reduced sea urchin grazing appears to favour increased macroalgal biomass (Johnson *et al.*, 2012). In this thesis, experiments on intertidal and subtidal rocky shores demonstrated that reduced abundances of calcifying herbivores at elevated CO_2 do not necessarily have a significant effect on sessile community composition (Chapter 5). At Vulcano, limpets had little effect on macroalgal communities in reference conditions, and their reduced densities with increasing CO_2 did not affect macroalgal communities, whereas carbon dioxide changed the specific composition and structure of intertidal communities. On the other hand, sea urchins strongly controlled macroalgal biomass on subtidal rocky reefs off Methana, but grazing control on macroalgal biomass was maintained at high CO_2 thanks to a marked increase in the abundance of herbivorous fish.

These results show that while ocean acidification can profoundly affect marine ecosystems, functional redundancy within trophic groups such as herbivores can reduce its effect. Since coastal environments have low functional redundancy, even when diversity is relatively high (Micheli *et al.*, 2014),

preserving diversity in marine ecosystems is essential for maintaining ecosystem function in the face of future environmental changes. In the Mediterranean Sea, overfishing of apex predators has led to higher abundances of sea urchins and herbivorous fish, as they are usually not targeted by commercial fisheries (Guidetti and Dulčić, 2007; Guidetti and Sala, 2007). High herbivore densities can often lead to impoverished macroalgal communities with much lower diversity biomass than unexploited Mediterranean coastal ecosystems (Sala *et al.*, 2012).

Thus, unvaried grazing pressure at different CO_2 levels may maintain suboptimal community structure. Figure 8.2A shows typical subtidal communities found at Methana at elevated pCO_2, with high fish biomass and a *Cystoseira* belt reaching depths of up to 12 meters (author's personal observation). This suggests that in the long term, non-calcifying macroalgae benefit from increased CO_2 levels and overall primary productivity is likely higher near the seeps than at reference sites, where the biomass of macroalgae and fish is lower (Figure 8.2B).

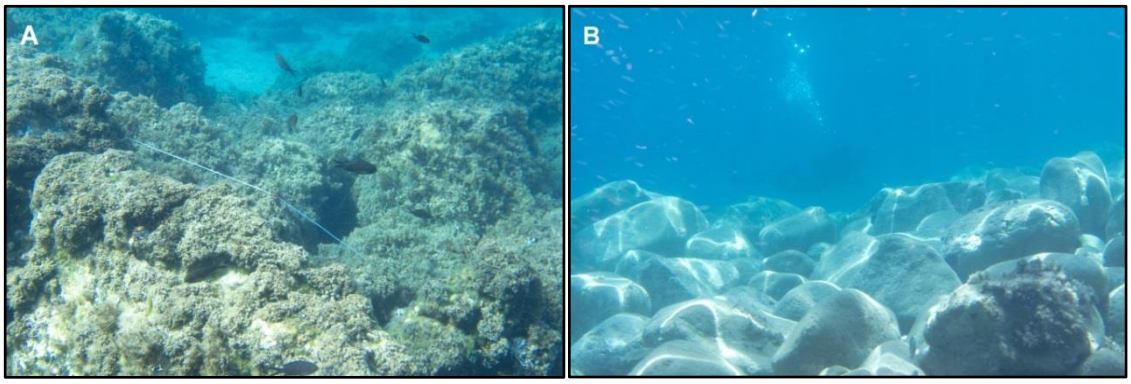

Figure 8.2. Typical seascape near seeps off Methana (A) and at reference sites (B) at ~ 3 m depth; areas near the seeps had higher macroalgal cover and higher fish biomass than reference sites, which were dominated by crustose coralline algae and sea urchins (photos by Maria Salomidi, September 2013).

Findings of this thesis have improved our knowledge on how herbivory will be affected by elevated CO_2. There is still very little research on how other biological interactions, especially predator-prey interactions, will be influenced by ocean acidification in temperate systems, but Amaral *et al.* (2012) found that mussels grown at low pH are more vulnerable to crab predation. In tropical environments, recent studies show that changes in vulnerability to predators are size- and species-specific for fish, as some predators will be negatively affected by elevated pCO_2 as well (Ferrari *et al.*, 2011; Allan *et al.*, 2013). In addition, this thesis shows that changes in herbivory due to ocean acidification vary depending on the habitat studied, meaning that more research would be needed to predict responses of marine communities in a variety of habitats.

Both herbivore exclusion experiments reported in this thesis were performed at one reference and one high CO_2 site only. At Vulcano and Methana, pCO_2 is considered the main driver of change, with other environmental factors (e.g. temperature, salinity, heavy metals, hydrogen sulphide, wave exposure) not varying significantly between study sites (Boatta *et al.*, 2013; Chapter 2). Between-sites differences reported in Chapter 5 are therefore likely to be caused by changes in pCO_2 levels, but repeating these experiments in more than one reference site would improve their power and give more reliable results.

8.1.3 Adaptation potential to ocean acidification

In this thesis, two dominant macroalgal species (the fucoid alga *Cystoseira corniculata* and the coralline alga *Jania rubens*) were transplanted between reference and high CO_2 sites for several months in order to assess whether they had permanently acclimatised to elevated pCO_2, which might give an indication of their adaptation potential (Chapter 6). In addition, short-term effects

of elevated CO_2 were assessed on some physiological parameters in the same two species (Chapter 7). Comparison of short- and long-term effects of carbon dioxide on *C. corniculata* and *J. rubens* (Table 8.1) shows that there were very small effects on *C. corniculata* physiology in the short term, while in the long term it was evident that some pigments (chlorophyll *c* and antheraxanthin) concentration increase in thalli exposed to elevated CO_2 for several months. In addition, in the long term elevated carbon dioxide increased *C. corniculata* maximum electron transport rates ($rETR_{max}$), C:N ratio and phlorotannin content, as well as decreasing epiphyte cover. *J. rubens* showed increases in some pigments concentration when transplanted to elevated CO_2; in the short term, pheophytin a and phycoerithryin increased in thalli exposed to high CO_2, whereas in the long term there was an increase in chlorophyll a, violaxanthin, zeaxanthin and phycocyanin. On the other hand, all other parameters measured in *J. rubens* did not change significantly after the thalli were transplanted near the seeps.

Table 8.1. Summary of the effect of elevated CO_2 on physiological parameters measured in thalli of *Cystoseira corniculata* and *Jania rubens* transplanted for 3 days (short term; Chapter 7) or 4-9 months (long term; Chapter 6). +: increase in parameter value; -: decrease in parameter value; n.s.: no significant effect; n.m.: parameter not measured.

Response variable	*Cystoseira corniculata*		*Jania rubens*	
	Short-term	Long-term	Short-term	Long-term
Photochemistry				
F_v/F_m	n.s.	n.s.	n.s.	n.s.
$rETR_{max}$	n.m.	+	n.m.	n.s.
I_k	n.m.	n.s.	n.m.	n.s.
α_{ETR}	n.m.	n.s.	n.m.	n.s.
NPQ	n.m.	n.s.	n.m.	n.s.
Pigments				
Chlorophyll *a*	n.s.	n.s.	n.s.	+
Chlorophyll *c*	n.s.	+	n.m.	n.m.
Pheophytin *a*	n.s.	n.s.	+	n.s.
β-carotene	n.s.	n.s.	n.s.	n.s.
Fucoxanthin	n.s.	n.s.	n.m.	n.m.
Violaxanthin	n.s.	n.s.	n.s.	+
Antheraxanthin	n.s.	+	n.s.	n.s.
Zeaxanthin	n.s.	n.s.	n.s.	+
β-cryptoxanthin	n.m.	n.m.	n.s.	n.s.
Phycoerithryin	n.m.	n.m.	+	n.s.
Phycocyanin	n.m.	n.m.	n.s.	+
Growth	n.m	n.s.	n.m	n.s.
Epiphyte cover	n.m	-	n.m	n.m
C:N	n.m	+	n.m	n.s.
C_{inorg}	n.m	n.m	n.m	n.s.
Phenol content	n.m.	+	n.m.	n.m.

Overall, both species seemed to change their physiology relatively quickly (more than three days, but less than four or nine months for *J. rubens* and *C. corniculata*, respectively), as the site of origin had very little effect on the physiology of long-term transplants. Macroalgae commonly show high phenotypic plasticity (Demes *et al.*, 2009), which could help calcifying species such as *J. rubens* to physiologically buffer negative effects of ocean acidification. However, phenotypic plasticity is known to slow down genetic adaptation by reducing selection gradients (Sunday *et al.*, 2014), meaning that if CO_2 will increase over *J. rubens*' current tolerance, this species may disappear.

Some physiological parameters were significantly different depending on the site of transplant in both species. While *C. corniculata* seemed to be favoured at high CO_2 levels (decreased epiphyte cover, higher phlorotannin content and maximum electron transport rates), *J. rubens* only showed increased concentration of some pigments. This probably leads to increased competitiveness of *C. corniculata*, as proven by the increase in its cover and the concurrent decrease of *J. rubens* cover as CO_2 increases (Chapter 3).

This highlights the importance of studying ocean acidification responses at the community level, as even calcifying algae that seem to cope relatively well with increased carbon dioxide, such as *J. rubens*, can be outcompeted by non-calcifying macroalgae that benefit from increased CO_2 levels, such as *C. corniculata*. This is in accord with a previous study showing that that some calcifying algae can survive a moderate increase in pCO_2 levels, but their slower growth rates at high CO_2 reduce their competitive abilities (James *et al.*, 2014). Reduced growth rates at increased CO_2 have commonly been reported for coralline algae (Kroeker *et al.*, 2013a), although articulated coralline algae are less sensitive to ocean acidification than crustose forms (Johnson *et al.*, 2014).

J. rubens did not show significant differences in linear growth rates between sites, but it is possible that other life stages of this species are negatively affected by elevated CO_2. Increased chemical defences or altered morphology of *C. corniculata* could have deterred *J. rubens* settlement at elevated CO_2 levels. Changes in macroalgal morphology or chemical defences influence the cover of their epiphytes, such as *J. rubens* (Jennings and Steinberg, 1997; Jones and Thornber, 2010). It is also possible that an episode of extremely high CO_2 drastically decreased *J. rubens* abundance. Recovery of *J. rubens*

population might be extremely difficult at elevated CO_2, especially considering the limited distance its gametes travel (Jones and Moorjani, 1973). This hypothesis is supported by the fact that thalli of *J. rubens* transplanted to the seeps created areas of high *J. rubens* cover (Figure 8.3), suggesting that recruitment of this species is not impaired by moderate CO_2 enrichment, but recovery after extreme events is difficult because of the small distance its gametes travel.

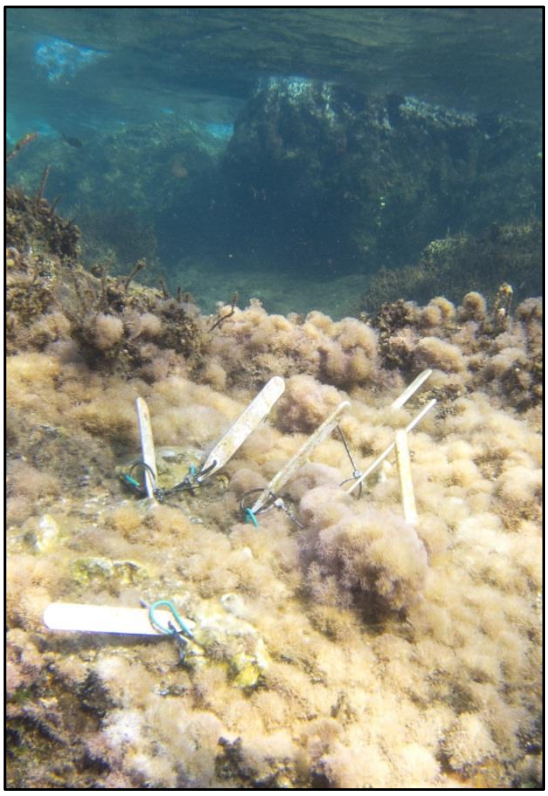

Figure 8.3. *J. rubens* thalli transplanted near seeps off Methana are indicated by white plastic labels, and the high cover of *J. rubens* around them suggests this species' recruitment is not impaired by moderate pCO_2 enrichment.

Not all the physiological responses of these two macroalgal species may have been detected: many replicates were lost due to high wave action, leaving one treatment of *C. corniculata* with only three replicates and leaving only one usable reference site for *J. rubens* transplants. Low sample sizes reduce our

ability to detect small differences among treatments (Quinn and Keough, 2002), and reciprocal transplants to test for local adaptation should be performed using multiple reference sites (Sanford and Kelly, 2011). The species studied in this thesis should ideally be repeated in laboratory conditions (i.e. common garden experiment) to better assess the mechanisms of macroalgal responses to elevated CO_2.

8.1.4 Interaction with other stressors

Studying the interaction of ocean acidification with other anthropogenic stressors is essential to reliably predict future conditions of marine ecosystems, as multiple stressors often interact synergistically; it is therefore very difficult to understand their combined effect from single-stressor experiments (Crain *et al.*, 2008). In this thesis, copper levels were manipulated *in situ* at different pCO_2 levels near volcanic seeps (Chapter 7). Results from these copper manipulation experiments showed that the combined effects of ocean acidification and copper pollution interact to increase copper accumulation in two macroalgal species (*Cystoseira corniculata* and *Jania rubens*), and this amplified the effects of ocean acidification on epifaunal communities. Interactive effects of ocean acidification and copper pollution have been largely overlooked by researchers so far, although it has been proven that these factors have synergistic negative effect on amphipods and polychaetes (Lewis *et al.*, 2012; Roberts *et al.*, 2013; Campbell *et al.*, 2014). The experiments in this thesis showed for the first time that tackling a local stressor such as copper pollution can help managing the impacts of a global stressor such as ocean acidification, similarly to what has already been demonstrated for other local stressors (e.g. eutrophication, sediment runoff; Ghedini *et al.*, 2013).

Many others anthropogenic stressors interact with ocean acidification to influence marine ecosystems. For instance, climate change is also causing an increase of temperature and UV radiation as well as decreased oxygen in marine systems (IPCC, 2014); further pressures on marine ecosystems include eutrophication, overfishing, invasive species and metal pollution (Halpern *et al.*, 2007). While ocean acidification and increased temperature are increasingly studied together (Kroeker *et al.*, 2013a), combinations of more than two stressors are rarely studied because of logistical constraints (Crain *et al.*, 2008). This thesis concentrated on one stressor only (ocean acidification) due to the difficulties in manipulating the environment *in situ*, but its only experiment concurrently investigating two factors highlighted that synergistic effects of anthropogenic stressors are likely and that future research needs to address the cumulative impacts of multiple variables.

8.2 Summary and direction for future research

Ocean acidification has the potential to influence a wide range of physical, chemical and biological processes in the marine environment (Doney *et al.*, 2009). This thesis contributes to a growing body of research assessing the effects of ocean acidification on marine temperate rocky reefs. It is clear from these findings that temperate macroalgal communities and their epifauna change significantly with increasing CO_2, and subtidal herbivore communities drastically shift from sea urchins to fish with increasing CO_2. Experiments performed as part of this thesis have also shown that dominant macroalgal species at Methana have very high phenotypic plasticity, and change their physiology in a few months to acclimatise to pCO_2 levels up to 1700 µatm. Interactive effects of ocean acidification and copper pollution have also been proven to increase copper accumulation in macroalgae and indirectly affect their

epifauna. These findings have implications for the modelling of impacts of elevated CO_2 on marine ecosystems.

The findings from this thesis have highlighted that some marine taxa can tolerate, and sometimes thrive at, CO_2 levels up to 1700 µatm. Fucoid algae were the main group to benefit from increased carbon dioxide, and at Methana *Cystoseira corniculata* could be found much deeper near the seeps than at the reference sites (~ 12 m vs ~ 2 m; author's personal observation). Since overall macroalgal biomass was higher at elevated CO_2, it is very likely that primary productivity increases when CO_2 levels are high at Mediterranean rocky reefs. On the other hand, decreased diversity at elevated CO_2 has implications for ecosystem functioning of communities exposed to ocean acidification, especially if key species are lost. For instance, decreased coralline algal abundance and diversity near the studied seeps has the potential to influence carbon cycling in temperate systems. Coralline algae are one of the most important taxa for long-term carbon storage in the marine environment (Andersson *et al.*, 2008). Their decreasing abundance could therefore reduce the ability of temperate macroalgal beds to act as carbon sinks, even though an increase in fucoid algal biomass might counter that effect (Chung *et al.*, 2011).

Our knowledge of ecosystem effects of ocean acidification is, however, still in its infancy. Using volcanic CO_2 seeps is a powerful approach to test hypotheses formulated following laboratory and mesocosm experiments, and can produce hypotheses to be verified in controlled conditions. Results from this thesis have revealed how temperate communities may change and how some organisms may change their physiology when exposed to ocean acidification. Patterns of rocky reef community changes are becoming clear after consistent results from mesocosm and field observations (Kroeker *et al.*, 2011; Porzio *et al.*, 2011;

Kroeker *et al.*, 2013a). Changes in ecosystem functions with increasing CO_2, however, have rarely been tested in complex marine ecosystems. Ocean acidification is known to increase seagrass productivity at seeps off Vulcano (Apostolaki *et al.*, 2014), but macroalgal productivity responses are not as clear and have not been measured *in situ* so far (Hofmann *et al.*, 2011; Noisette *et al.*, 2013b; Olabarria *et al.*, 2013). Macroalgal communities not only contribute to coastal primary productivity, but offer other valuable ecosystem services, such as nutrient cycling, water depuration, fisheries production and shore protection from waves (Rönnbäck *et al.*, 2007). Responses of these processes to ocean acidification have scarcely been studied, and are a priority for future research.

Populations of *Cystoseira corniculata* and *Jania rubens* exposed for centuries to high and variable pCO_2 do not seem to have permanently acclimatised to ocean acidification, as their physiology was not influenced by their site of origin after a few months of acclimatisation to different pCO_2 levels. Very high phenotypical plasticity may slow down genetic adaptation, meaning that pCO_2 values above those physiological mechanisms can buffer could be detrimental to the two species studied in this thesis (Sunday *et al.*, 2014). However, it is possible that these species have in fact adapted to elevated pCO_2, but their high phenotypic plasticity might have masked inter-population differences. Genetic studies are therefore needed to confirm that only phenotypical plasticity is at play in this instance. Furthermore, adaptation potential to ocean acidification is known for very few species and more studies are urgently needed to understand how marine organisms may adapt to ocean acidification (Reusch, 2014).

Predictions of community responses to ocean acidification are extremely important, but anthropogenic CO_2 emissions are causing other environmental changes, such as increased temperatures (IPCC, 2014). Moreover, human

pressures such as pollution and overfishing are contributing to degradation of marine ecosystems, and managing them is essential to improve the resilience of marine ecosystems to climate change (Ghedini *et al.*, 2013). Although laboratory experiments have been conducted to examine interactions between anthropogenic stressors, chiefly temperature (Kroeker *et al.*, 2013a), *in situ* studies are extremely rare because of the logistical difficulties in manipulating stressors in the field. Although complex, field experiments involving more than one stressor will be essential to understand how marine ecosystems will respond to future environmental changes, as interactive effects of stressors are often not predictable from single-stressor experiments (Gobler *et al.*, 2014).

References:

Abdallah A.M.A., Abdallah M.A. and Beltagy A.I. (2005). Contents of heavy metals in marine seaweeds from the Egyptian coast of the Red Sea. *Chemistry and Ecology*, 21: 399-411.

Airoldi L. and Beck M. (2007). Loss, status and trends for coastal marine habitats of Europe. *Oceanography and Marine Biology: An Annual Review*, 45: 347-407.

Al-Horani F.A., Al-Moghrabi S.M. and de Beer D. (2003). Microsensor study of photosynthesis and calcification in the scleractinian coral, *Galaxea fascicularis*: active internal carbon cycle. *Journal of Experimental Marine Biology and Ecology*, 288: 1-15.

Allan B.J.M., Domenici P., McCormick M.I., Watson S.-A. and Munday P.L. (2013). Elevated CO_2 affects predator-prey interactions through altered performance. *PLoS ONE*, 8: e58520.

Allison G. (2004). The influence of species diversity and stress intensity on community resistance and resilience. *Ecological Monographs*, 74: 117-134.

Alsterberg C., Eklöf J.S., Gamfeldt L., Havenhand J.N. and Sundbäck K. (2013). Consumers mediate the effects of experimental ocean acidification and warming on primary producers. *Proceedings of the National Academy of Sciences*, 110: doi: 10.1073/pnas.1303797110.

Amaral V., Cabral H.N. and Bishop M.J. (2011). Resistance among wild invertebrate populations to recurrent estuarine acidification. *Estuarine, Coastal and Shelf Science*, 93: 460-467.

Amaral V., Cabral H.N. and Bishop M.J. (2012). Effects of estuarine acidification on predator-prey interactions. *Marine Ecology Progress Series*, 445: 117-127.

Anderson M.J. and Ter Braak C.J.F. (2003). Permutation tests for multi-factorial analysis of variance. *Journal of Statistical Computational Simulation*, 73: 85-113.

Andersson A.J., Mackenzie F.T. and Lerman A. (2005). Coastal ocean and carbonate systems in the high CO_2 world of the Anthropocene. *American Journal of Science*, 305: 875-918.

Andersson A.J., Mackenzie F.T. and Bates N.R. (2008). Life on the margin: implications of ocean acidification on Mg-calcite, high latitude and cold-water marine calcifiers. *Marine Ecology Progress Series*, 373: 265-273.

Andersson A.J., Kuffner I.B., Mackenzie F.T., Jokiel P.L., Rodgers K.S. and Tan A. (2009). Net loss of $CaCO_3$ from a subtropical calcifying community due to seawater acidification: mesocosm-scale experimental evidence. *Biogeosciences*, 6: 1811-1823.

Angilletta M.J. (2009) Thermal adaptation: a theoretical and empirical synthesis. Oxford University Press, 289 pp.

Anthony K.R.N., Kline D.I., Diaz-Pulido G., Dove S. and Hoegh-Guldberg O. (2008). Ocean acidification causes bleaching and productivity loss in coral reef builders. *Proceedings of the National Academy of Sciences*, 105: 17442-17446.

Anthony K.R.N., Kleypas J.A. and Gattuso J.-P. (2011a). Coral reefs modify their seawater carbon chemistry - implications for impacts of ocean acidification. *Global Change Biology*, 17: 3655-3666.

Anthony K.R.N., Maynard J.A., Diaz-Pulido G., Mumby P.J., Marshall P.A., Cao L. and Hoegh-Guldberg O.V.E. (2011b). Ocean acidification and warming will lower coral reef resilience. *Global Change Biology*, 17: 1798-1808.

Apostolaki E.T., Vizzini S., Hendriks I.E. and Olsen Y.S. (2014). Seagrass ecosystem response to long-term high CO_2 in a Mediterranean volcanic vent. *Marine Environmental Research*, 99: 9-15.

Apte S.C. and Day G.M. (1998). Dissolved metal concentrations in the Torres Strait and Gulf of Papua. *Marine Pollution Bulletin*, 36:298-304.

Arnold T., Mealey C., Leahey H., Miller A.W., Hall-Spencer J.M., Milazzo M. and Maers K. (2012). Ocean acidification and the loss of phenolic substances in marine plants. *PLoS ONE*, 7: e35107.

Austin J., Butchart N. and Shine K.P. (1992). Possibility of an Arctic ozone hole in a doubled-CO_2 climate. *Nature*, 360: 221-225.

Baggini C., Salomidi M., Voutsinas E., Bray L., Krasakopoulou E. and Hall-Spencer J.M. (2014). Seasonality affects macroalgal community response to increases in pCO_2. *PLoS ONE*, 9: e106520.

Ballesteros, E. (1984). Els vegetals i la zonació litoral: espècies, comunitats i factors que influenixen en la seva distribució. PhD thesis, Universitat de Barcelona, Spain.

Ballesteros E. (1986). Métodos de análisis estructural en comunidades naturales, en particular del fitobentos. *Oecologia Aquatica*, 8: 117-131.

Ballesteros E., Torras X., Pinedo S., García M., Mangialajo L. and de Torres M. (2007). A new methodology based on littoral community cartography dominated by macroalgae for the implementation of the European Water Framework Directive. *Marine Pollution Bulletin*, 55: 172-180.

Barton A., Hales B., Waldbusser G.G., Langdon C. and Feely R.A. (2012). The Pacific oyster, *Crassostrea gigas*, shows negative correlation to naturally

elevated carbon dioxide levels: implications for near-term ocean acidification effects. *Limnology Oceanography*, 57: 698 - 710.

Bates C.R. and DeWreede R.E. (2007). Do changes in seaweed biodiversity influence associated invertebrate epifauna? *Journal of Experimental Marine Biology and Ecology*, 344: 206-214.

Bates C.R. (2009). Host taxonomic relatedness and functional-group affiliation as predictors of seaweed-invertebrate epifaunal associations. *Marine Ecology Progress Series*, 387: 125-136.

Baumann H.A., Morrison L. and Stengel D.B. (2009). Metal accumulation and toxicity measured by PAM-Chlorophyll fluorescence in seven species of marine macroalgae. *Ecotoxicology and Environmental Safety*, 72: 1063-1075.

Bazterrica M.C., Silliman B.R., Hidalgo F.J., Crain C.M. and Bertness M.D. (2007). Limpet grazing on a physically stressful Patagonian rocky shore. *Journal of Experimental Marine Biology and Ecology*, 353: 22-34.

Beardall J., Stojkovic S. and Larsen S. (2009). Living in a high CO_2 world: Impacts of global climate change on marine phytoplankton. *Plant Ecology and Diversity*, 2: 191-205.

Beer S. and Eshel A. (1985). Determining phycoerithrin and phycocyanin concentrations in aqueous crude extract of red algae. *Australian Journal of Marine and Freshwater Research*, 36: 785-792.

Belegratis M.R., Bitis I., Economou-Amilli A. and Ott J.A. (1999). Epiphytic patterns of macroalgal assemblages on *Cystoseira* species (Fucales, Phaeophyta) in the east coast of Attica (Aegean Sea, Greece). *Hydrobiologia*, 412: 67-80.

Bellan-Santini D., Karaman G., Krapp-Schickel G., Ledoyer M., Myers A., Ruffo S. and Schiecke U. (1982). The Amphipoda of the Mediterranean. Part 1: Gammaridae (Acanthonotozomatidae to Gammaridae). *Mémoires de l'Institut océanographique, Monaco*, 13. Institut Océanographique: Monaco. ISBN 2-7260-0133-5. 364 pp.

Bellan-Santini D., Diviacco G., Krapp-Schickel G. and Ruffo S. (1989). The Amphipoda of the Mediterranean. Part 2. Gammaridea (Haustoriidae to Lysianassidae). *Mémoires de l'Institut océanographique, Monaco*, 13. Institut Océanographique: Monaco. ISBN 2-7260-0140-8. 576 pp.

Bellan-Santini D., Karaman G., Krapp-Schickel G., Ledoyer M. and Ruffo S. (1993). The Amphipoda of the Mediterranean. Part 3: Gammaridea (Melphidippidae to Talitridae), Ingolfiellidea, Caprellidea. *Mémoires de l'Institut océanographique, Monaco*, 13. Institut Océanographique: Monaco. ISBN 2-7260-0160-2. 813 pp.

Bellan-Santini D., Karaman G., Ledoyer M., Myers A., Ruffo S. and Vader W. (1998). The Amphipoda of the Mediterranean. Part 4: Localities and Map, Addenda to Parts 1-3, Key to Families, Ecology, Faunistics and Zoogeography, Bibliography, Index. *Mémoires de l'Institut océanographique, Monaco*, 13. Institut Océanographique: Monaco. ISBN 2-7260-0201-3. 959 pp.

Bender D., Diaz-Pulido G. and Dove S. (2014). The impact of CO_2 emission scenarios and nutrient enrichment on a common coral reef macroalga is modified by temporal effects. *Journal of Phycology*, 50: 203-215.

Bendscheider K. and Robinson R.J. (1952). A new spectrometric method for the determination of nitrite in seawater. *Journal of Marine Research*, 11: 87-96.

Benedetti-Cecchi L., Nuti S. and Cinelli F. (1996). Analysis of spatial and temporal variability in interactions among algae, limpets and mussels in low-shore habitats on the west coast of Italy. *Marine Ecology Progress Series*, 144:87-96.

Benedetti-Cecchi L., Bulleri F. And Cinelli F. (2000). The interplay of physical and biological factors in maintaining mid-shore and low-shore assemblages on rocky coasts in the north-west Mediterranean. *Oecologia*, 123: 406-417.

Benedetti-Cecchi L., Bulleri F., Acunto S. and Cinelli F. (2001). Scales of variation in the effects of limpets on rocky shores in the northwest Mediterranean. *Marine Ecology Progress Series*, 209: 131-141.

Benner I., Diner R.E., Lefebvre S.C., Li D., Komada T., Carpenter E.J. and Stillman J.H. (2013). *Emiliania huxleyi* increases calcification but not expression of calcification-related genes in long-term exposure to elevated temperature and pCO_2. *Philosophical Transactions of the Royal Society B: Biological Sciences*, 368: 20130049.

Bergström L., Tatarenkov A., Johannesson K., Jönsson R.B. and Kautsky L. (2005). Genetic and morphological identification of *Fucus radicans* sp. nov. (Fucales, Phaeophyceae) in the brackish Baltic Sea. *Journal of Phycology*, 41:1025-1038.

Bianchi C.N., Dando P.R. and Morri C. (2011). Increased diversity of sessile epibenthos at subtidal hydrothermal vents: seven hypotheses based on observations at Milos Island, Aegean Sea. *Advances in Oceanography and Limnology*, 2: 1-31.

Bibby R., Cleall-Harding P., Rundle S., Widdicombe S. and Spicer J. (2007). Ocean acidification disrupts induced defences in the intertidal gastropod *Littorina littorea*. *Biology Letters*, 3: 699-701.

Bischof K., Gómez I., Molis M., Hanelt D., Karsten U., Lüder U., Roleda M.Y., Zacher K., Wiencke C., Amils R., Ellis-Evans C. and Hinghofer-Szalkay H. (2006). Ultraviolet radiation shapes seaweed communities. *Review of Environmental Sciences and Biotechnology*, 5:141–166.

Blackford J.C. (2010). Predicting the impacts of ocean acidification: challenges from an ecosystem perspective. *Journal of Marine Systems*, 81: 12-18.

Blake R.E. and Duffy J.E. (2010). Grazer diversity affects resistance to multiple stressors in an experimental seagrass ecosystem. *Oikos*, 119: 1625-1635.

Boatta F., D'Alessandro W., Gagliano A.L., Liotta M., Milazzo M., Rodolfo-Metalpa R., Hall-Spencer J.M. and Parello F. (2013). Geochemical survey of Levante Bay, Vulcano Island (Italy), a natural laboratory for the study of ocean acidification. *Marine Pollution Bulletin*, 73: 485-494.

Borowitzka M.A. (1987). Calcification in algae - mechanisms and the role of metabolism. *Critical Reviews in Plant Sciences,* 6: 1-45.

Bradassi F., Cumani F., Bressan G. and Dupont S. (2013). Early reproductive stages in the crustose coralline alga *Phymatolithon lenormandii* are strongly affected by mild ocean acidification. *Marine Biology*, 160: 2261-2269.

Bray L., Pancucci-Papadopulou M.A. and Hall-Spencer J.M. (2014). Sea urchin response to rising pCO_2 shows ocean acidification may fundamentally alter the chemistry of marine skeletons. *Mediterranean Marine Science*. DOI: 10.12681/mms.579.

Breitbarth E., Bellerby, R.J., Neill, C.C., Ardelan M.V., Meyerhöfer M., Zöllner E., Croot P.L. and Riebesell U. (2010). Ocean acidification affects iron speciation during a coastal seawater mesocosm experiment. *Biogeosciences*, 7: 1065-1073.

Brewer P.O., Goyet C. and Friederich G. (1997). Direct observation of the oceanic CO_2 increase revisited. *Proceedings of the National Academy of Sciences USA*, 94: 8308-8313.

Brewer P. G. and Hester K. C. (2009). Ocean acidification and the increasing transparency of the ocean to low-frequency sound. *Oceanography*, 22: 86-93.

Briffa M., de la Haye K. and Munday P.L. (2012). High CO_2 and marine animal behaviour: Potential mechanisms and ecological consequences. *Marine Pollution Bulletin*, 64: 1519-1528.

Brock E., Åberg P. and Pavia H. (2008). Phlorotannins as chemical defense against macroalgal epiphytes on *Ascophyllum nodosum*. *Journal of Phycology*, 37: 8.

Brodie J., Williamson C.J., Smale D.A., Kamenos N.A., Mieszkowska N., Santos R., Cunliffe M., Steinke M., Yesson C., Anderson K.M., Asnaghi V., Brownlee C., Burdett H.L., Burrows M.T., Collins S., Donohue P.J., Harvey B., Foggo A., Noisette F., Nunes J., Ragazzola F., Raven J.A., Schmidt D.N., Suggett D., Teichberg M. and Hall-Spencer J.M. (2014). The future of the northeast Atlantic benthic flora in a high CO_2 world. *Ecology and Evolution*, 4: 2787-2798.

Brown M.T. and Newman J.E. (2003). Physiological responses of *Gracilariopsis longissima* (S.G. Gmelin) Steentoft, L.M. Irvine and Farnham (Rhodophyceae) to sub-lethal copper concentrations. *Aquatic Toxicology*, 64: 201-213.

Bubel A. (1975). An ultrastructural study of the mantle of the barnacle, *Elminius modestus* (Darwin) in relation to shell formation. *Journal of Experimental Marine Biology and Ecology*, 20: 287-324.

Büdenbender J., Riebesell U. and Form A. (2011). Calcification of the Arctic coralline red alga *Lithothamnion glaciale* in response to elevated CO_2. *Marine Ecology Progress Series*, 441: 79-87.

Bulleri F., Benedetti-Cecchi L. and Cinelli F. (1999). Grazing by the sea urchins *Arbacia lixula* L. and *Paracentrotus lividus* Lam. in the Northwest Mediterranean. *Journal of Experimental Marine Biology and Ecology*, 241: 81-95.

Bulleri F., Menconi M., Cinelli F. and Benedetti-Cecchi L. (2000). Grazing by two species of limpets on artificial reefs in the northwest Mediterranean. *Journal of Experimental Marine Biology and Ecology*, 255: 1-19.

Burkepile D.E. and Hay M.E. (2006). Herbivore vs nutrient control of marine primary producers: context-dependent effects. *Ecology*, 87: 3128-3139.

Burnell O.W., Russell B.D., Irving A.D. and Connell S.D. (2013). Eutrophication offsets increased sea urchin grazing on seagrass caused by ocean warming and acidification. *Marine Ecology Progress Series*, 485: 37-46.

Butler W.L. (1978). Energy distribution in the photochemical apparatus of photosynthesis. *Annual Review of Plant Physiology*, 29: 345-378.

Cahill A.E., Aiello-Lammens M.E., Fisher-Reid M.C., Hua X., Karanewsky C.J., Ryu H.Y., Sbeglia G.C., Spagnolo F., Waldron J.B., Warsi O. and Wiens J.J. (2013). How does climate change cause extinction? *Proceedings of the Royal Society B: Biological Sciences*, 280: 20121890.

Caldeira K. and Wickett M.E. (2003). Oceanography: Anthropogenic carbon and ocean pH. *Nature*, 425: 365-365.

Caldeira K. and Wickett M.E. (2005). Ocean model predictions of chemistry changes from carbon dioxide emissions to the atmosphere and ocean. *Journal of Geophysical Research*, 110: C09S04.

Calosi P., Rastrick S.P.S., Graziano M., Thomas S.C., Baggini C., Carter H.A., Hall-Spencer J.M., Milazzo M. and Spicer J.I. (2013a). Distribution of sea urchins living near shallow water CO_2 vents is dependent upon species acid-base and ion-regulatory abilities. *Marine Pollution Bulletin*, 73: 470-484.

Calosi P., Turner L.M., Hawkins M., Bertolini C., Nightingale G., Truebano M. and Spicer J.I. (2013b). Multiple physiological responses to multiple environmental challenges: an individual approach. *Integrative and Comparative Biology*, 53: 660-670.

Calosi P., Rastrick S.P.S., Lombardi C., de Guzman H.J., Davidson L., Jahnke M., Giangrande A., Hardege J.D., Schulze A., Spicer J.I. and Gambi M.-C. (2013c). Adaptation and acclimatization to ocean acidification in marine ectotherms: an *in situ* transplant experiment with polychaetes at a shallow CO_2 vent system. *Philosophical Transactions of the Royal Society B: Biological Sciences*, 368: 20120444.

Cameron J.N. (1985). Post-moult calcification in the blue crab (*Callinectus sapidus*): relationship between apparent net H^+ excretion, calcium and bicarbonate. *Journal of Experimental Biology*, 119: 275-285.

Campbell J.E. and Fourqurean J.W. (2011). Novel methodology for *in situ* carbon dioxide enrichment of benthic ecosystems. *Limnology and Oceanography Methods*, 9: 97-109.

Campbell J.E. and Fourqurean J.W. (2013). Effects of in situ CO_2 enrichment on the structural and chemical characteristics of the seagrass *Thalassia testudinum*. *Marine Biology*, 160: 1465-1475.

Campbell J.E. and Fourqurean J.W. (2014). Ocean acidification outweighs nutrient effects in structuring seagrass epiphyte communities. *Journal of Ecology*, 102: 730-737.

Campbell A.L., Mangan S., Ellis R.P. and Lewis C. (2014). Ocean acidification increases copper toxicity to the early life-history stages of the polychaete *Arenicola marina* in artificial seawater. *Environmental Science & Technology*, DOI 10.1021/es502739m.

Capaccioni B.,Tassi F. and Vaselli O. (2001). Organic and inorganic geochemistry of low temperature gas discharges at the Baia di Levante beach, Vulcano Island, Italy. *Journal of Volcanological and Geothermal Research*, 108: 173-185.

Caramanna G., Voltattorni N. and Maroto-Valer M.M. (2011). Is Panarea Island (Italy) a valid and cost-effective natural laboratory for the development of detection and monitoring techniques for submarine CO_2 seepage? *Greenhouse Gases: Science and Technology*, 1: 200-210.

Cardellini C., Chiodini G. and Frondini F., 2003. Application of stochastic simulation to CO_2 flux from soil: mapping and quantification of gas release. *Journal of Geophysical Research*, 108 (B9): 2425.

Chauvin A., Denis V. and Cuet P. (2011). Is the response of coral calcification to seawater acidification related to nutrient loading? *Coral Reefs*, 30: 1-13.

Chapman P. M. and Wang F. (2001). Assessing sediment contamination in estuaries*. Environmental Toxicology and Chemistry,* 20: 3-22.

Chemello R. and Milazzo M. (2002). Effect of algal architecture on associated fauna: some evidence from phytal molluscs. *Marine Biology*, 140: 981-990.

Chiantore M., Vielmini I., Privitera D., Mangialajo L. and Cattaneo-Vietti R. (2008). Habitat effects on the population structure of *Paracentrotus lividus* and *Arbacia lixula. Chemistry and Ecology,* 24: 145–157.

Chiodini G., Cioni R., Guidi M., Raco B. and Marini L. (1998). Soil CO_2 flux measurements in volcanic and geothermal areas. *Applied Geochemistry*, 13: 543-552.

Christen N., Calosi P., McNeill C.L. and Widdicombe S. (2013). Structural and functional vulnerability to elevated pCO_2 in marine benthic communities. *Marine Biology*, 160: 2113-2128.

Christie H., Norderhaug K.M. and Fredriksen S. (2009). Macrophytes as habitat for fauna. *Marine Ecology Progress Series*, 396: 221-233.

Chung I., Beardall J., Mehta S., Sahoo D. and Stojkovic S. (2011). Using marine macroalgae for carbon sequestration: a critical appraisal. *Journal of Applied Phycology*, 23: 877-886.

Cigliano M., Gambi M.C., Rodolfo-Metalpa R., Patti F.P. and Hall-Spencer J.M. (2010). Effects of ocean acidification on invertebrate settlement at volcanic CO_2 vents. *Marine Biology*, 157: 2489-2502.

Clarke K.R. and Ainsworth M. (1993). A method of linking multivariate community structure to environmental variables *Marine Ecology Progress Series*, 92: 205-219.

Clarke K.R. and Gorley R.N. (2006). PRIMER v6: User Manual/Tutorial. PRIMER-E, Plymouth.

Cline J.D. (1989). Spectrophotometric determination of hydrogen sulphide in natural waters. *Limnology and Oceanography*, 14: 454-458.

Cohen A.L. and Holcomb M. (2009). Why corals care about ocean acidification: Uncovering the mechanism. *Oceanography*, 22: 118-127.

Coleman R., Underwood A., Benedetti-Cecchi L., Åberg P., Arenas F., Arrontes J., Castro J., Hartnoll R., Jenkins S., Paula J., Santina P. and Hawkins S. (2006). A continental scale evaluation of the role of limpet grazing on rocky shores. *Oecologia*, 147: 556-564.

Collén J. and Davison I.R. (2001). Seasonality and thermal acclimation of reactive oxygen metabolism in *Fucus vesiculosus* (Phaeophycaeae). *Journal of Phycology*, 37: 474-481.

Collén J., Pinto E., Pedersen M. and Colepicolo P. (2003). Induction of oxidative stress in the red macroalga *Gracilaria tenuistipitata* by pollutant metals. *Archives of Environmental Contamination and Toxicology*, 45:337-342.

Collins S., Rost B. and Rynearson T.A. (2014). Evolutionary potential of marine phytoplankton under ocean acidification. *Evolutionary Applications*, 7: 140-155.

Coma R., Ribes M., Gili J.-M. and Zabala M. (2000). Seasonality in coastal benthic ecosystems. *Trends in Ecology & Evolution*, 15: 448-453.

Connan S. and Stengel D.B. (2011a). Impacts of ambient salinity and copper on brown algae: 1. Interactive effects on photosynthesis, growth, and copper accumulation. *Aquatic Toxicology*, 104: 94-107.

Connan S. and Stengel D.B. (2011b). Impacts of ambient salinity and copper on brown algae: 2. Interactive effects on phenolic pool and assessment of metal binding capacity of phlorotannin. *Aquatic Toxicology*, 104: 1-13.

Connell S.D., Russell B.C., Turner D.J., Shepherd S.A., Kildae T., Miller D.J., Airoldi L. and Cheshire, A. (2008). Recovering a lost baseline: Missing kelp forests from a metropolitan coast. *Marine Ecology Progress Series*, 360: 63-72.

Connell S.D. and Russell B.D. (2010). The direct effects of increasing CO_2 and temperature on non-calcifying organisms: Increasing the potential for phase shifts in kelp forests. *Proceedings of the Royal Society B: Biological Sciences*, 277: 1409-1415.

Connell S.D., Kroeker K.J., Fabricius K.E., Kline D.I. and Russell B.D. (2013). The other ocean acidification problem: CO_2 as a resource among competitors for ecosystem dominance. *Philosophical Transactions of the Royal Society B: Biological Sciences*, 368: 20120442.

Contreras L., Moenne A. and Correa J.A. (2005). Antioxidant responses in *Scytosiphon lomentaria* (Phaeophyceae) inhabiting copper-enriched coastal environments. *Journal of Phycology*, 41: 1184-1195.

Cornwall C.E., Hepburn C.D., Pritchard D., Currie K.I., McGraw C.M., Hunter K.A. and Hurd C.L. (2012). Carbon-use strategies in macroalgae: Differential responses to lowered pH and implications for ocean acidification. *Journal of Phycology*, 48:137-144.

Cornwall C.E., Hepburn C.D., McGraw C.M., Currie K.I., Pilditch C.A., Hunter K.A., Boyd P.W. and Hurd C.L. (2013). Diurnal fluctuations in seawater pH influence the response of a calcifying macroalga to ocean acidification. *Proceedings of the Royal Society B: Biological Sciences*, 280: 20132201.

Cornwall C.E., Boyd P.W., McGraw C.M., Hepburn C.D., Pilditch C.A., Morris J.N., Smith A.M. and Hurd C.L. (2014). Diffusion boundary layers ameliorate the

negative effects of ocean acidification on the temperate coralline macroalga *Arthrocardia corymbosa*. *PLoS ONE*, 9: e97235.

Couto R.P., Neto A.I. and Rodrigues A.S. (2010). Metal concentration and structural changes in *Corallina elongata* (Corallinales, Rhodophyta) from hydrothermal vents. *Marine Pollution Bulletin*, 60: 509-514.

Crain C.M., Kroeker K. and Halpern B.S. (2008). Interactive and cumulative effects of multiple human stressors in marine systems. *Ecology Letters*, 11: 1304-1315.

Crawfurd K.J., Raven J.A., Wheeler G.L., Baxter E.J. and Joint I. (2011). The Response of *Thalassiosira pseudonana* to Long-Term Exposure to Increased CO_2 and Decreased pH. *PLoS ONE*, 6: e26695.

Crook E., Potts D., Rebolledo-Vieyra M., Hernandez L. and Paytan A. (2012). Calcifying coral abundance near low-pH springs: implications for future ocean acidification. *Coral Reefs*, 31: 239-245.

D'Alessandro W., Brusca L., Kyriakopoulos K., Rotolo S., Michas G., Minio M. and Papadakis G. (2006). Diffuse and focused carbon dioxide and methane emissions from the Sousaki geothermal system, Greece. *Geophysical Research Letters*, 33: L05307.

D'Alessandro W., Brusca L., Kyriakopouios K., Michas G. and Papadakis G. (2008). Methana, the westernmost active volcanic system of the South Aegean Arc (Greece): Insight from fluids geochemistry. *Journal of Volcanology and Geothermal Research*, 178: 818-828.

Dando P.R., Stüben D. and Varnavas S.P. (1999). Hydrothermalism in the Mediterranean Sea. *Progress In Oceanography*, 44: 333-367.

Dando P.R., Aliani S., Arab H., Bianchi C.N., Brehmer M., Cocito S., Fowlers S.W., Gundersen J., Hooper L.E., Kölbh R., Kuevere J., Linke P., Makropoulosr K.C., Meloni R., Miquel J.C., Morri C., Müller S., Robinson C., Schlesner H., Sieverts S., Störr R., Stüben D., Thormm M., Varnavas S.P. and Ziebiss W. (2000). Hydrothermal studies in the Aegean Sea. *Physics and Chemistry of the Earth, Part B: Hydrology, Oceans and Atmosphere*, 25: 1-8.

De Biasi A.M. and Aliani S. (2003). Shallow-water hydrothermal vents in the Mediterranean Sea: Stepping stones for Lessepsian migration? *Hydrobiologia*, 503: 37-44.

De Bodt C., Van Oostende N., Harlay J., Sabbe K. and Chou L. (2010). Individual and interacting effects of pCO_2 and temperature on *Emiliania huxleyi* calcification: Study of the calcite production, the coccolith morphology and the coccosphere size. *Biogeosciences*, 7: 1401-1412.

Dean R.L. and Connell J.H., 1987. Marine invertebrates in an algal succession. III. Mechanisms linking habitat complexity with diversity. *Journal of Experimental Marine Biology and Ecology*, 109: 249-273.

Decker G.L. and Lennarz W.J. (1988). Skeletogenesis in the sea urchin embryo. *Development*, 103: 231-247.

Demes K.W., Graham M.H. and Suskiewicz T.S. (2009). Phenotypic plasticity reconciles incongruous molecular and morphological taxonomies: the giant kelp, *Macrocystis* (Laminariales, Phaeophyceae), is a monospecific genus. *Journal of Phycology*, 45: 1266-1269.

Dethier M.N., Graham E.S., Cohen S. and Tear L.M. (1993). Visual versus random-point percent cover estimation: ‘objective’ is not always better. *Marine Ecology Progress Series*, 96: 93-100.

Dias B.B., Hart M.B., Smart C.W. and Hall-Spencer J.M. (2010). Modern seawater acidification: The response of foraminifera to high-CO_2 conditions in the Mediterranean Sea. *Journal of the Geological Society*, 167: 843-846.

Diaz-Pulido G., Gouezo M., Tilbrook B., Dove S. and Anthony K.R.N. (2011). High CO_2 enhances the competitive strength of seaweeds over corals. *Ecology Letters*, 14: 156-162.

Diaz R.J. and Rosenberg R. (2008). Spreading dead zones and consequences for marine ecosystems. *Science*, 321: 926-929.

Doneddu M. and Trainito E. (2005). Conchiglie del Mediterraneo. Guida al riconoscimento dei molluschi conchigliati, 2nd edition. Il Castello Editore; 256 pp.

Doney S.C., Fabry V.J., Feely R.A. and Kleypas J.A. (2009). Ocean acidification: the Other CO_2 problem. *Annual Review of Marine Science*, 1: 169-192.

Dupont S., Dorey N. and Thorndyke M. (2010). What meta-analysis can tell us about vulnerability of marine biodiversity to ocean acidification? *Estuarine Coastal and Shelf Science*, 89: 182-185.

Edgar G.J. (1992). Patterns of colonization of mobile epifauna in a Western Australian seagrass bed. *Journal of Experimental Marine Biology and Ecology*, 157: 225-246.

Egilsdottir H., Noisette F., Noël L.L.J., Olafsson J. and Martin S. (2013). Effects of pCO_2 on physiology and skeletal mineralogy in a tidal pool coralline alga *Corallina elongata*. *Marine Biology*, 160: 2103-2112.

Eilers P.H.C. and Peeters J.C.H. (1988). A model for the relationship between light intensity and the rate of photosynthesis in phytoplankton. *Ecological Modelling*, 42: 199-215.

Ellis R.P., Bersey J., Rundle S.D., Hall-Spencer J.M. and Spicer J.I. (2009). Subtle but significant effects of CO_2 acidified seawater on embryos of the intertidal snail, *Littorina obtusata*. *Aquatic Biology*, 5: 41-48.

Endler J.A. (1977). Geographic variation, speciation, and clines. Princeton University Press, Princeton, NJ. 262 pp.

Engelen A.H., Espirito-Santo C., Simões T., Monteiro C., Serrão E.A., Pearson G.A. and Santos R.O.P. (2008). Periodicity of propagule expulsion and settlement in the competing native and invasive brown seaweeds, *Cystoseira humilis* and *Sargassum muticum* (Phaeophyta). *European Journal of Phycology*, 43: 275-282.

Eriksson B.K., van Sluis C., Sieben K., Kautsky L. and Raberg S. (2011). Omnivory and grazer functional composition moderate cascading trophic effects in experimental Fucus vesiculosus habitats. *Marine Biology*, 158: 747-756.

Evans T.G., Chan F., Menge B.A. and Hofmann G.E. (2013). Transcriptomic responses to ocean acidification in larval sea urchins from a naturally variable pH environment. *Molecular Ecology*, 22: 1609-25.

Fabricius K.E., Langdon C., Uthicke S., Humphrey C., Noonan S., De'ath G., Okazaki R., Muehllehner N., Glas M.S. and Lough J.M. (2011). Losers and winners in coral reefs acclimatized to elevated carbon dioxide concentrations. *Nature Climate Change*, 1: 165-169.

Fabricius K.E., De'ath G., Noonan S. and Uthicke S. (2014). Ecological effects of ocean acidification and habitat complexity on reef-associated macroinvertebrate communities. *Proceedings of the Royal Society B: Biological Sciences*, 281: 20132479.

Fabry V.J., Seibel B.A., Feely R.A. and Orr J.C. (2008). Impacts of ocean acidification on marine fauna and ecosystem processes. *Ices Journal of Marine Science*, 65: 414-432.

Falkenberg L.J., Russell B.D. and Connell S.D. (2012). Stability of strong species interactions resist the synergistic effects of local and global pollution in kelp forests. *PLoS ONE*, 7: e33841.

Falkenberg L., Russell B. and Connell S. (2013a). Contrasting resource limitations of marine primary producers: implications for competitive interactions under enriched CO_2 and nutrient regimes. *Oecologia*, 172: 575-583.

Falkenberg L.J., Russell B.D. and Connell S.D. (2013b). Future herbivory: the indirect effects of enriched CO_2 may rival its direct effects. *Marine Ecology Progress Series*, 492: 85-95.

Falkenberg L.J., Connell S.D. and Russell B.D. (2014). Herbivory mediates the expansion of an algal habitat under nutrient and CO_2 enrichment. *Marine Ecology Progress Series*, 497: 87-92.

Feely R.A., Sabine C.L., Hernandez-Ayon J.M., Ianson D. and Hales B. (2008). Evidence for upwelling of corrosive "acidified" water onto the continental shelf. *Science*, 320: 1490-1492.

Feely R.A., Alin S.R., Newton J., Sabine C.L., Warner M., Devol A., Krembs C. and Maloy C. (2010). The combined effects of ocean acidification, mixing, and respiration on pH and carbonate saturation in an urbanized estuary. *Estuarine Coastal and Shelf Science*, 88: 442-449.

Ferrari M.C.O., McCormick M.I., Munday P.L., Meekan M.G., Dixson D.L., Lonnstedt Ö. and Chivers D.P. (2011). Putting prey and predator into the CO_2

equation - qualitative and quantitative effects of ocean acidification on predator–prey interactions. *Ecology Letters*, 14: 1143-1148.

Filbee-Dexter K. and Scheibling R.E. (2014). Sea urchin barrens as alternative stable states of collapsed kelp ecosystems. *Marine Ecology Progress Series*, 495, 1-25.

Findlay H.S., Kendall M.A., Spicer J.I. and Widdicombe S. (2010). Relative influences of ocean acidification and temperature on intertidal barnacle post-larvae at the northern edge of their geographic distribution. *Estuarine Coastal and Shelf Science*, 86: 675-682.

Findlay H.S., Wood H.L., Kendall M.A., Spicer J.I., Twitchett R.J. and Widdicombe S. (2011). Comparing the impact of high CO_2 on calcium carbonate structures in different marine organisms. *Marine Biology Research*, 7: 565-575.

Fisher K. and Martone P.T. (2014). Field study of growth and calcification rates of three species of articulated coralline algae in British Columbia, Canada. *The Biological Bulletin*, 226: 121-130.

Floeter S.R., Behrens M.D., Ferreira C.E.L., Paddack M.J. and Horn M.H. (2005). Geographical gradients of marine herbivorous fishes: patterns and processes. *Marine Biology*, 147: 1435-1447.

Folin O. and Ciocalteu V. (1927). On tyrosine and tryptophane determinations in proteins. *Journal of Biological Chemistry*, 73, 627-650.

Fong C.W., Lee S.Y. and Wu R.S.S. (2000). The effects of epiphytic algae and their grazers on the intertidal seagrass *Zostera japonica*. *Aquatic Botany*, 67: 251-261.

Form A.U. and Riebesell U. (2011). Acclimation to ocean acidification during long-term CO_2 exposure in the cold-water coral *Lophelia pertusa*. *Global Change Biology*. DOI: 10.1111/j.1365-2486.2011.02583.x

Fraschetti S., Terlizzi A. and Benedetti-Cecchi L. (2005). Patterns of distribution of marine assemblages from rocky shores: evidence of relevant scales of variation. *Marine Ecology Progress Series*, 296: 13-29.

Friligos N. (1991). Eutrophication assessment in Greek coastal waters. *Water and the Environment*, edited by J. Rose. Gordon and Breach Science Publishers.

Frommel A.Y., Maneja R., Lowe D., Malzahn A.M., Geffen A.J., Folkvord A., Piatkowski U., Reusch T.B.H. and Clemmesen C. (2012). Severe tissue damage in Atlantic cod larvae under increasing ocean acidification. *Nature Climate Change*, 2: 42-46.

Gao K., Aruga Y., Asada K., Ishihara T., Akano T. and Kiyohara M. (1993). Calcification in the articulated coralline alga *Corallina pilulifera*, with special reference to the effect of elevated CO_2 concentration. *Marine Biology*, 117: 129-132.

Gao K.S., Ruan Z.X., Villafane V.E., Gattuso J.P. and Helbling E.W. (2009). Ocean acidification exacerbates the effect of UV radiation on the calcifying phytoplankter Emiliania huxleyi. *Limnology and Oceanography*, 54: 1855-1862.

Gao K.S. and Zheng Y.Q. (2010). Combined effects of ocean acidification and solar UV radiation on photosynthesis, growth, pigmentation and calcification of the coralline alga *Corallina sessilis* (Rhodophyta). *Global Change Biology*, 16: 2388-2398.

Garrard S., Hunter R.C., Frommel A.Y., Lane A.C., Phillips J.C., Cooper R., Dineshram R., Cardini U., McCoy S.J., Arnberg M., Rodrigues Alves B.G., Annane S., Orte M.R., Kumar A., Aguirre-Martínez G.V., Maneja R.H., Basallote M.D., Ape F., Torstensson A. and Bjoerk M.M. (2013). Biological impacts of ocean acidification: a postgraduate perspective on research priorities. *Marine Biology*, 160: 1789-1805.

Garrard S.L., Gambi M.C., Scipione M.B., Patti F.P., Lorenti M., Zupo V., Paterson D.M. and Buia M.C. (2014). Indirect effects may buffer negative responses of seagrass invertebrate communities to ocean acidification. *Journal of Experimental Marine Biology and Ecology*, 461: 31-38.

Gattuso J.-P., Bijma J., Gehlen M., Riebesell U. and Turley C. (2011). Ocean acidification: knowns, unknowns, and perspectives. In Gattuso J.-P. and Hansson L. (eds.) *Ocean Acidification.* 352 pp. Oxford University Press, UK.

Gattuso J.P., Kirkwood W., Barry J.P., Cox E., Gazeau F., Hansson L., Hendriks I., Kline D.I., Mahacek P., Martin S., McElhany P., Peltzer E.T., Reeve J., Roberts D., Saderne V., Tait K., Widdicombe S. and Brewer P.G. (2014). Free Ocean CO_2 Enrichment (FOCE) systems: present status and future developments. *Biogeosciences Discussion*, 11: 4001-4046.

Gaylord B., Kroeker K.J., Sunday J.M., Anderson K.M., Barry J.P., Brown N.E., Connell S.D., Dupont S., Fabricius K.E., Hall-Spencer J.M., Klinger T., Milazzo M., Munday P.L., Russell B.D., Sanford E., Schreiber S.J., Thiyagarajan V., Vaughan M.L.H., Widdicombe S. and Harley C.D.G. (2014). Ocean acidification through the lens of ecological theory. *Ecology*, 140902120430003.

Geider R. and La Roche J. (1994). The role of iron in phytoplankton photosynthesis, and the potential for iron-limitation of primary productivity in the sea. *Photosynthesis Research*, 39: 275-301.

Ghedini G., Russell B. and Connell S. (2013). Managing local coastal stressors to reduce the ecological effects of ocean acidification and warming. *Water*, 5: 1653-1661.

Giakoumi S., Cebrian E., Kokkoris G.D., Ballesteros E. and Sala E. (2012). Relationships between fish, sea urchins and macroalgae: The structure of shallow sublittoral communities in the Cyclades, Eastern Mediterranean. *Estuarine, Coastal and Shelf Science*, 109: 1-10.

Gibbs S.J., Bown P.R., Sessa J.A., Bralower T., and Wilson P. (2006). Nannoplankton extinction and origination across the Paleocene – Eocene Thermal Maximum. *Science*, 314: 1770-1773.

Gilpin L.C., Davidson K. and Roberts E. (2004). The influence of changes in nitrogen: silicon ratios on diatom growth dynamics. *Journal of Sea Research*, 51:21-35.

Gobler C.J., DePasquale E.L., Griffith A.W. and Baumann H. (2014). Hypoxia and acidification have additive and synergistic negative effects on the growth, survival, and metamorphosis of early life stage bivalves. *PLoS ONE*, 9: e83648.

Godbold J.A. and Solan M. (2013). Long-term effects of warming and ocean acidification are modified by seasonal variation in species responses and environmental conditions. *Philosophical Transactions of the Royal Society of London. Series B, Biological sciences*, 368: 20130186.

Gooding R.A., Harley C.D.G. and Tang E. (2009). Elevated water temperature and carbon dioxide concentration increase the growth of a keystone

echinoderm. *Proceedings of the National Academy of Sciences of the United States of America*, 106: 9316-9321.

Goss R. and Jakob T. (2010). Regulation and function of xanthophyll cycle-dependent photoprotection in algae. *Photosynthesis Research*, 106: 103-122.

Gouveia C., Kreusch M., Schmidt É.C., Felix M.R.d.L., Osorio L.K.P., Pereira D.T., dos Santos R., Ouriques L.C., Martins R.d.P., Latini A., Ramlov F., Carvalho T.J.G., Chow F., Maraschin M. and Bouzon Z.L. (2013). The Effects of Lead and Copper on the Cellular Architecture and Metabolism of the Red Alga *Gracilaria domingensis*. *Microscopy and Microanalysis*, 19: 513-524.

Graham M.H. (2004). Effects of local deforestation on the diversity and structure of Southern California giant kelp forest food webs. *Ecosystems*, 7: 341-357.

Griffith G.P., Fulton E.A. and Richardson A.J. (2011). Effects of fishing and acidification-related benthic mortality on the southeast Australian marine ecosystem. *Global Change Biology*, 17: 3058-3074.

Guidetti P. and Dulčić J. (2007). Relationships among predatory fish, sea urchins and barrrens in Mediterranean rocky reefs across a latitudinal gradient. *Marine Environmental Research*, 63: 168-184.

Guidetti P. and Sala E. (2007). Community-wide effects of marine reserves in the Mediterranean Sea. *Marine Ecology Progress Series*, 335: 43-56.

Gutow L., Rahman M.M., Bartl K., Saborowski R., Bartsch I. and Wiencke C. (2014). Ocean acidification affects growth but not nutritional quality of the seaweed *Fucus vesiculosus* (Phaeophyceae, Fucales). *Journal of Experimental Marine Biology and Ecology*, 453: 84-90.

Gutowska M.A., Melzner F., Portner H.O. and Meier S. (2010). Cuttlebone calcification increases during exposure to elevated seawater pCO_2 in the cephalopod *Sepia officinalis*. *Marine Biology*, 157: 1653-1663.

Häder D.-P., Lebert M., Mercado J., Aguilera J., Salles S., Flores-Moya A., Jiménez C. and Figueroa F.L. (1996). Photosynthetic oxygen production and PAM fluorescence in the brown alga *Padina pavonica* measured in the field under solar radiation. *Marine Biology*, 127: 61-66.

Hale R., Calosi P., McNeill L., Mieszkowska N. and Widdicombe S. (2011). Predicted levels of future ocean acidification and temperature rise could alter community structure and biodiversity in marine benthic communities. *Oikos*, 120: 661-674.

Hall L.W.J., Scott M.C. and Killen W.D. (1998). Ecological risk assessment of copper and cadmium in surface waters of Chesapeake Bay Watershed. *Environmental Toxicology and Chemistry*, 17:1172-1189.

Hall-Spencer J.M., Rodolfo-Metalpa R., Martin S., Ransome E., Fine M., Turner S.M., Rowley S.J., Tedesco D. and Buia M.-C. (2008). Volcanic carbon dioxide vents show ecosystem effects of ocean acidification. *Nature*, 454: 96-99.

Halm H., Lüder U.H. and Wiencke C. (2010). Induction of phlorotannins through mechanical wounding and radiation conditions in the brown macroalga *Laminaria hyperborea*. *European Journal of Phycology*, 46: 16-26.

Halpern B.S., Selkoe K.A., Micheli F. and Kappel C.V. (2007). Evaluating and ranking the vulnerability of global marine ecosystems to anthropogenic threats. *Conservation Biology*, 21: 1301-1315.

Haritonidis S., Nikolaidis G.and Tsekos I. (1986). Seasonal variation in the biomass of marine macrophyta from Greek coasts. *Marine Ecology*, 7: 359-370.

Harley C.D.G. (2002). Light availability indirectly limits herbivore growth and abundance in a high rocky intertidal community during the winter. *Limnology and Oceanography*, 47: 1217–1222.

Harley C.D.G., Anderson K.M., Demes K.W., Jorve J.P., Kordas R.L., Coyle T.A. and Graham M.H. (2012). Effect of climate change on global seaweeds communities. *Journal of Phycology*, 48: 1064-1078.

Hay M.E., Duffy J.E., Pfister C.A. and Fenical W. (1987). Chemical defense against different marine herbivores: are amphipods insect equivalents? *Ecology,* 68: 1567-1580.

Hendriks I.E., Olsen Y.S., Ramajo L., Basso L., Steckbauer A., Moore T.S., Howard J. AND Duarte C.M. (2014). Photosynthetic activity buffers ocean acidification in seagrass meadows. *Biogeosciences*, 11: 333-346.

Hereu B., Zabala M. and Sala E. (2008). Multiple controls of community structure and dynamics in a sublittoral marine environment. *Ecology*, 89: 3423-3435.

Hester K.C., Peltzer E.T., Kirkwood W.J. and Brewer, P.G. (2008). Unanticipated consequences of ocean acidification: A noisier ocean at lower pH. *Geophysical Research Letters*, 35: doi: 10.1029/2008GL034913.

Hilmi N., Allemand D., Dupont S., Safa A., Haraldsson G., Nunes P.L.D., Moore C., Hattam C., Reynaud S., Hall-Spencer J., Fine M., Turley C., Jeffree R., Orr J., Munday P. and Cooley S. (2012). Towards improved socio-economic assessments of ocean acidification's impacts. *Marine Biology*, doi: 10.1007/s00227-012-2031-5.

Hofmann G.E., Barry J.P., Edmunds P.J., Gates R.D., Hutchins D.A., Klinger T. and Sewell M.A. (2010). The effect of ocean acidification on calcifying

organisms in marine ecosystems: an organism-to-ecosystem perspective. *Annual Review of Ecology, Evolution and Systematics*, 41:127-147.

Hofmann G.E., Smith J.E., Johnson K.S., Send U., Levin L.A., Micheli F., Paytan A., Price N.N., Peterson B., Takeshita Y., Matson P.G., Crook E.D., Kroeker K.J., Gambi M.C., Rivest E.B., Frieder C.A., Yu P.C. and Martz T.R. (2011). High-frequency dynamics of ocean pH: a multi-ecosystem comparison. *PLoS ONE*, 6: e28983.

Hofmann L.C., Yildiz G., Hanelt D. and Bischof K. (2011). Physiological responses of the calcifying rhodophyte, *Corallina officinalis* (L.), to future CO_2 levels. *Marine Biology*, 159: 783-792.

Hofmann L.C., Straub S. and Bischof K. (2012). Competition between calcifying and noncalcifying temperate marine macroalgae under elevated CO_2 levels. *Marine Ecology Progress Series*, 464: 89-105.

Holcomb M., McCorkle D.C. and Cohen A.L. (2010). Long-term effects of nutrient and CO_2 enrichment on the temperate coral *Astrangia poculata* (Ellis and Solander, 1786). *Journal of Experimental Marine Biology and Ecology*, 386: 27-33.

Holcomb M., Cohen A.L. and McCorkle D.C. (2011). A gender bias in the calcification response to ocean acidification. *Biogeosciences Discussion*, 8: 8485-8513.

Hönisch B., Hemming N.G., Archer D., Siddall M., and McManus J.F. (2009). Atmospheric carbon dioxide concentration across the mid-Pleistocene transition. *Science*, 324: 1551-4.

Hoppe C.J.M., Langer G. and Rost B. (2011). *Emiliania huxleyi* shows identical responses to elevated pCO_2 in TA and DIC manipulations. *Journal of Experimental Marine Biology and Ecology*, 406: 54-62.

Howes D.E., Harper J.R. and Owens E.H. (1994). British Columbia physical shore-zone mapping system. Resources Inventory Committee (RIC) report by the Coastal Task Force, RIC Secretariat, Victoria, B.C., 71 pp.

Hübner A., Rahders E., Rahner S., Halbach P. and Varnavas S.P. (2004). Geochemistry of hydrothermally influenced sediments off Methana (Western Hellenic Volcanic Arc). *Chemie der Erde - Geochemistry*, 64: 75-94.

Hughes T.P. (1994). Catastrophes, phase shifts, and large-scale degradation of a Caribbean coral reef. *Science*, 265: 1547-1551.

Hughes T.P., Rodrigues M.J., Bellwood D.R., Ceccarelli D., Hoegh-Guldberg O., McCook L., Moltschaniwskyj N., Pratchett M.S., Steneck R.S. and Willis B. (2007). Phase shifts, herbivory, and the resilience of coral reefs to climate change. *Current Biology*, 17: 360-365.

Hurd C.L. (2000). Water motion, marine macroalgal physiology, and production. *Journal of Phycology*, 36: 453-472.

Hutchins D.A., Mulholland M.R. and Fu F.X. (2009). Nutrient cycles and marine microbes in a CO_2-enriched ocean. *Oceanography*, 22: 128-145.

Iglesias-Rodriguez M.D., Halloran P.R., Rickaby R.E.M., Hall I.R., Colmenero-Hidalgo E., Gittins J.R., Green D.R.H., Tyrrell T., Gibbs S.J., von Dassow P., Rehm E., Armbrust E.V. and Boessenkool K.P. (2008). Phytoplankton calcification in a high-CO_2 world. *Science*, 320: 336-340.

Inguaggiato S., Mazot A., Diliberto I.S., Inguaggiato C., Madonia P., Rouwet D. and Vita F. (2012). Total CO_2 output from Vulcano island (Aeolian Islands, Italy).

Geochemistry Geophysics Geosystems, 13: Q02012, doi:10.1029/2011GC003920.

Inoue S., Kayanne H., Yamamoto S. and Kurihara H. (2013). Spatial community shift from hard to soft corals in acidified water. *Nature Climate Change*, 3: 683-687.

Intergovernmental Panel on Climate Change (2014). Climate change 2014: the physical science basis. Contribution of working group I to the fourth assessment report of the Intergovernmental Panel on Climate Change. Cambridge University Press, Cambridge, UK.

Italiano F., Nuccio P.M. and Sommaruga C. (1984). Gas/steam and thermal energy release measured at the gaseous emissions of the Baia di Levante of Vulcano Island, Italy. *Acta Vulcanologica*, 5: 89-94.

James R.K., Hepburn C.D., Cornwall C.E., McGraw C.M. and Hurd C.L. (2014). Growth response of an early successional assemblage of coralline algae and benthic diatoms to ocean acidification. *Marine Biology*, 161: 1687-1696.

Jennings J.G. and Steinberg P.D. (1997). Phlorotannins versus other factors affecting epiphyte abundance on the kelp *Ecklonia radiata*. *Oecologia*, 109: 461-473.

Johnson V.R. (2012). A study of marine benthic algae along a natural carbon dioxide gradient. PhD thesis, Plymouth University, UK, 274 pp.

Johnson V.R., Russell B.D., Fabricius K.E., Brownlee C. and Hall-Spencer J.M. (2012). Temperate and tropical brown macroalgae thrive, despite decalcification, along natural CO_2 gradients. *Global Change Biology*, 18: 2792-2803.

Johnson V., Brownlee C., Rickaby R., Graziano M., Milazzo M. and Hall-Spencer J. (2013). Responses of marine benthic microalgae to elevated CO_2. *Marine Biology*, 160: 1813-1824.

Johnson M.D., Price N.N. and Smith J.E. (2014). Contrasting effects of ocean acidification on tropical fleshy and calcareous algae. *PeerJ*, 2: e411.

Johnston E.L. and Webb J.A. (2000). Novel techniques for field assessment of copper toxicity on fouling assemblages. *Biofouling* 15:165-173.

Johnston E.L. and Keough M.J. (2002). Direct and indirect effects of repeated pollution events on marine hard-substrate assemblages. *Ecological Applications*, 12:1212-1228.

Johnston E.L. and Roberts D.A. (2009). Contaminants reduce the richness and evenness of marine communities: A review and meta-analysis. *Environmental Pollution*, 157: 1745-1752.

Jokiel P.L., Rodgers K.S., Kuffner I.B., Andersson A.J., Cox E.F. and Mackenzie F.T. (2008). Ocean acidification and calcifying reef organisms: A mesocosm investigation. *Coral Reefs*, 27: 473-483.

Jones W.E. and Moorjani S.A. (1973). The attachment and early development of the tetraspores of some coralline red algae. *Special Publications of the Marine Biological Associations of India*, 1973: 293-304.

Jones E. and Thornber C.S. (2010). Effects of habitat-modifying invasive macroalgae on epiphytic algal communities. *Marine Ecology Progress Series*, 400: 87-100.

Jormalainen V., Honkanen T. and Heikkila N. (2001). Feeding preferences and performance of a marine isopod on seaweed hosts: cost of habitat specialization. *Marine Ecology Progress Series,* 220: 219-230.

Kalogirou S., Wennhage H. and Pihl L. (2012). Non-indigenous species in Mediterranean fish assemblages: Contrasting feeding guilds of *Posidonia oceanica* meadows and sandy habitats. *Estuarine, Coastal and Shelf Science*, 96: 209-218.

Kamal J. (2011). Quantification of alkaloids, phenols and flavonoids in sunflower (*Helianthus annuus* L.). *African Journal of Biotechnology*, 10: 3149-3151.

Kamenos N.A., Burdett H.L., Aloisio E., Findlay H.S., Martin S., Longbone C., Dunn J., Widdicombe S. and Calosi P. (2013). Coralline algal structure is more sensitive to rate, rather than the magnitude, of ocean acidification. *Global Change Biology*, 19: 3621-3628.

Kangwe J.W., Hellblom F., Semesi A.K., Mtolera M.S.P. and Bjork M. (2001). Heavy metal inhibition of calcification and photosynthetic rates of the geniculate calcareous alga *Amphiroa tribulus*. *Marine Science Development in Tanzania and Eastern Africa*, 1:147-157.

Karageorgis A.P., Anagnostou C.L. and Kaberi H. (2005). Geochemistry and mineralogy of the NW Aegean Sea surface sediments: implications for river runoff and anthropogenic impact. Applied Geochemistry, 20:69-88.

Karlen D.J., Price R.E., Pichler T. and Garey J.R. (2010). Changes in benthic macrofauna associated with a shallow-water hydrothermal vent gradient in Papua New Guinea. *Pacific Science*, 64: 391-404.

Karsten U., Franklin L.A., Lüning K. and Wiencke C. (1998). Natural ultraviolet radiation and photosynthetically active radiation induce formation of mycosporine-like amino acids in the marine macroalga *Chondrus crispus* (Rhodophyta). *Planta*, 205: 257-262.

Kelly M.W. and Hofmann G.E. (2012). Adaptation and the physiology of ocean acidification. *Functional Ecology*, 27: 980-990.

Kelly M.W., Padilla-Gamiño J.L. and Hofmann G.E. (2013). Natural variation and the capacity to adapt to ocean acidification in the keystone sea urchin *Strongylocentrotus purpuratus*. *Global Change Biology*, 19: 2536-2546.

Kerrison P., Hall-Spencer J.M., Suggett D.J., Hepburn L.J. and Steinke M. (2011). Assessment of pH variability at a coastal CO_2 vent for ocean acidification studies. *Estuarine, Coastal and Shelf Science*, 94: 129-137.

Key R.M., Kozyr A., Sabine C.L., Lee K., Wanninkhof R., Bullister J.L., Feely R.A., Millero F.J., Mordy C. and Peng T.H. (2004). A global ocean carbon climatology: Results from Global Data Analysis Project (GLODAP). *Global Biogeochemical Cycles*, 18: GB4031.

Khan N., Ryu K.Y., Choi J.Y., Nho E.Y., Habte G., Choi H., Kim M.H., Park K.S. and Kim K.S. (2015). Determination of toxic heavy metals and speciation of arsenic in seaweeds from South Korea. *Food Chemistry*, 169: 464-470.

Kletou D. and Hall-Spencer J.M. (2012) Threats to ultraoligotrophic marine ecosystems. In Cruzado A. (ed.) *Marine Ecosystems.* InTech - Open Access Publisher. ISBN 979-953-307-4305.

Kline D.I., Teneva L., Schneider K., Miard T., Chai A., Marker M., Headley K., Opdyke B., Nash M., Valetich M., Caves J.K., Russell B.D., Connell S.D., Kirkwood B.J., Brewer P., Peltzer E., Silverman J., Caldeira K., Dunbar R.B., Koseff J.R., Monismith S.G., Mitchell B.G., Dove S. and Hoegh-Guldberg O. (2012). A short-term *in situ* CO_2 enrichment experiment on Heron Island (GBR). *Scientific Reports*, 2: doi:10.1038/srep00413.

Koch M., Bowes G., Ross C. and Zhang X.-H. (2013). Climate change and ocean acidification effects on seagrasses and marine macroalgae. *Global Change Biology*, 19: 103-132.

Koroleff, F. (1970). Direct determination of ammonia in natural waters as indophenol blue. In*: Information on Techniques and Methods for Seawater Analysis*. Charlottenlund, International Council for the Exploration of the Sea. Interlab. Report, 3: 19-22.

Korpinen S., Jormalainen V. and Ikonen J. (2008). Selective consumption and facilitation by mesograzers in adult and colonizing macroalgal assemblages. *Marine Biology*, 154: 787-794.

Kroeker K.J., Kordas R.L., Crim R.N. and Singh G.G. (2010). Meta-analysis reveals negative yet variable effects of ocean acidification on marine organisms. *Ecology Letters*, 13: 1419-1434.

Kroeker K.J., Micheli F., Gambi M.C. and Martz T.R. (2011). Divergent ecosystem responses within a benthic marine community to ocean acidification. *Proceedings of the National Academy of Sciences*, 108: 14515-14520.

Kroeker K.J., Kordas R.L., Crim R., Hendriks I.E., Ramajo L., Singh G.S., Duarte C.M. and Gattuso J.-P. (2013a). Impacts of ocean acidification on marine organisms: quantifying sensitivities and interaction with warming. *Global Change Biology*, 19: 1884-1896.

Kroeker K.J., Gambi M.C. and Micheli F. (2013b). Community dynamics and ecosystem simplification in a high-CO_2 ocean. *Proceedings of the National Academy of Sciences USA*, 110: 12721-6.

Kroeker K.J., Micheli F. and Gambi M.C. (2013c). Ocean acidification causes ecosystem shifts via altered competitive interactions. *Nature Climate Change*, 3: 156-159.

Kübler J.E., Johnston A.M. and Raven J.A. (1999). The effects of reduced and elevated CO_2 and O_2 on the seaweed *Lomentaria articulata*. *Plant, Cell & Environment*, 22: 1303-1310.

Küffner I.B., Andersson A.J., Jokiel P.L., Rodgers K.S. and Mackenzie F.T. (2008). Decreased abundance of crustose coralline algae due to ocean acidification. *Nature Geoscience*, 1: 114-117.

Küpper H., Šetlík I., Spiller M., Küpper F.C. and Prášil O. (2002). Heavy metal-induced inhibition of photosynthesis: targets of in vivo heavy metal chlorophyll formation. *Journal of Phycology*, 38: 429-441.

Küpper H., Seibert S. and Aravind P. (2007). A fast, sensitive and inexpensive alternative to analytical pigment HPLC: quantification of chlorophylls and carotenoids in crude extracts by fitting with Gauss-peak-spectra. *Analytical Chemistry*, 79: 7611-7627.

La Mesa G. and Vacchi M. (1999). An analysis of the coastal fish assemblage of the Ustica island marine reserve (Mediterranean Sea). *Marine Ecology*, 20: 147-165.

Labiosa R.G., Arrigo K.R., Genin A., Monismith S.G. and van Dijken G. (2003). The interplay between upwelling and deep convective mixing in determining the seasonal phytoplankton dynamics in the Gulf of Aqaba: Evidence from SeaWiFS and MODIS. *Limnology and Oceanography*, 48: 2355-2368.

Landes A. and Zimmer M. (2012). Acidification and warming affect both a calcifying predator and prey, but not their interaction. *Marine Ecology Progress Series*, 450: 1-10.

Langer G., Nehrke G., Probert I., Ly J. and Ziveri P. (2009). Strain-specific responses of *Emiliania huxleyi* to changing seawater carbonate chemistry, *Biogeosciences*, 6: 2637-2646.

Langer G., Nehrke G., Baggini C., Rodolfo-Metalpa R., Hall-Spencer J. and Bijma J. (2014). Limpets counteract ocean acidification induced shell corrosion by thickening of aragonitic shell layers. *Biogeosciences Discussion*, 11: 12571-12590.

Lawrence J.M. (2013). Edible sea urchins: biology and ecology. 3rd edition. Elsevier, Boston, 380 pp.

Le Quéré C., Raupach M.R., Canadell J.G., Marland G. *et al.* (2009). Trends in the sources and sinks of carbon dioxide. *Nature Geoscience*, 2: 831-836.

Leimu R. and Fischer M. (2008). A meta-analysis of local adaptation in plants. *PLoS ONE*, 3: e4010.

Lewis J.R. (1964). The ecology of rocky shores. English University Press, London, 323 pp.

Lewis E. and Wallace W.R. (1998) Program developed for CO_2 system calculations. Carbon dioxide information analysis center, Oak Ridge National Laboratory. US Department of Energy, Oak Ridge.

Lewis C., Clemow K. and Holt W. (2012). Metal contamination increases the sensitivity of larvae but not gametes to ocean acidification in the polychaete *Pomatoceros lamarckii* (Quatrefages). *Marine Biology*, 160: 2089-2101.

Lischka S., Büdenbender J., Boxhammer T. and Riebesell U. (2010). Impact of ocean acidification and elevated temperatures on early juveniles of the polar shelled pteropod *Limacina helicina*: Mortality, shell degradation, and shell growth. *Biogeosciences Discussion*, 7: 8177-8214.

Lobban C.S. and Harrison P.J. (1994). Seaweed ecology and physiology. Cambridge University Press.

Locke A. and Sprules W.G. (2000). Effects of acidic pH and phytoplankton on survival and condition of *Bosmina longirostris* and *Daphnia pulex*. *Hydrobiologia*, 437: 187-196.

Lohbeck K.T., Riebesell U. and Reusch T.B.H. (2012). Adaptive evolution of a key phytoplankton species to ocean acidification. *Nature Geosciences*, 5: 346-351.

Lombardi C., Cocito S., Gambi M., Cisterna B., Flach F., Taylor P., Keltie K., Freer A. and Cusack M. (2011). Effects of ocean acidification on growth, organic tissue and protein profile of the Mediterranean bryozoan *Myriapora truncata*. *Aquatic Biology*, 13: 251-262.

Long E. R. and MacDonald D. D. (1998). Recommended uses of empirically derived, sediment quality guidelines for marine and estuarine ecosystems. *Human and Ecological Risk Assessment.* 4: 1019-1039.

Lüthi D., Le Floch M., Bereiter B., Blunier T., Barnola J.M., Siegenthaler U., Raynaud D., Jouzel J., Fischer H., Kawamura K. and Stocker T.F. (2008). High-resolution carbon dioxide concentration record 650,000-800,000 years before present. *Nature*, 453: 379-382.

Maas A.E., Wishner K.F. and Seibel B.A. (2012). The metabolic response of pteropods to acidification reflects natural CO_2-exposure in oxygen minimum zones. *Biogeosciences*, 9: 747-757.

Maher W.A. and Clarke S.M. (1984). The occurrence of arsenic in selected marine macroalgae from two coastal areas of South Australia. *Marine Pollution Bulletin*, 15: 111-112.

Mallick N. and Mohn F.H. (2003). Use of chlorophyll fluorescence in metal-stress research: a case study with the green microalga *Scenedesmus*. *Ecotoxicology and Environmental Safety*, 55: 64-69.

Manzello D.P. (2010). Coral growth with thermal stress and ocean acidification: lessons from the eastern tropical Pacific. *Coral Reefs*, 29: 749-758.

Manzello D.P., Enochs I.C., Melo N., Gledhill D.K. and Johns E.M. (2012). Ocean Acidification Refugia of the Florida Reef Tract. *PLoS ONE*, 7: e41715.

Marshall D.J., Santos J.H., Leung K.M.Y. and Chak W.H. (2008). Correlations between gastropod shell dissolution and water chemical properties in a tropical estuary. *Marine Environmental Research*, 66: 422-429.

Martin J.H., Gordon R.M. and Fitzwater S.E. (1990). Iron in Antarctic waters. *Nature*, 345: 156-158.

Martin S., Rodolfo-Metalpa R., Ransome E., Rowley S., Buia M.C., Gattuso J.P. and Hall-Spencer J. (2008). Effects of naturally acidified seawater on seagrass calcareous epibionts. *Biology Letters*, 4: 689-692.

Martin S. and Gattuso J.P. (2009). Response of Mediterranean coralline algae to ocean acidification and elevated temperature. *Global Change Biology*, 15: 2089-2100.

Martin S., Cohu S., Vignot C., Zimmerman G. and Gattuso J.-P. (2013). One-year experiment on the physiological response of the Mediterranean crustose coralline alga, *Lithophyllum cabiochae*, to elevated pCO_2 and temperature. *Ecology and Evolution*, 3: 676-693.

Mayol E., Ruiz-Halpern S., Duarte C.M., Castilla J.C. and Pelegrí J.L. (2012). Coupled CO_2 and O_2-driven compromises to marine life in summer along the Chilean sector of the Humboldt Current System. *Biogeosciences*, 9: 1183-1194.

McConnaughey T.A. and Whelan J.F. (1997). Calcification generates protons for nutrient and bicarbonate uptake. *Earth Science Reviews,* 42: 95-117.

McCormick M.I., Watson S.-A. and Munday P.L. (2013). Ocean acidification reverses competition for space as habitats degrade. *Scientific Reports*, 3, doi:10.1038/srep03280.

McDermid K. and Stuercke B. (2003). Nutritional composition of edible Hawaiian seaweeds. *Journal of Applied Phycology*, 15: 513-524.

McDonald M.R., McClintock J.B., Amsler C.D., Rittschof D., Angus R.A., Orihuela B. and Lutostanski K. (2009). Effects of ocean acidification over the life history of the barnacle *Amphibalanus amphitrite*. *Marine Ecology Progress Series*, 385: 179-187.

Melwani A.R. and Kim S.L. (2008). Benthic infaunal distributions in shallow hydrothermal vent sediments. *Acta Oecologica*, 33: 162-175.

Melzner F., Gutowska M.A., Langenbuch M., Dupont S., Lucassen M., Thorndyke M.C., Bleich M. and Portner H.O. (2009). Physiological basis for high CO_2 tolerance in marine ectothermic animals: Pre-adaptation through lifestyle and ontogeny? *Biogeosciences*, 6: 2313-2331.

Melzner F., Stange P., Trübenbach K., Thomsen J., Casties I., Panknin U., Gorb S.N. and Gutowska M.A. (2011). Food supply and seawater pCO_2 impact calcification and internal shell dissolution in the blue mussel *Mytilus edulis*. *PLoS ONE*, 6: e24223.

Melzner F., Thomsen J., Koeve W., Oschlies A., Gutowska M., Bange H., Hansen H. and Körtzinger A. (2013). Future ocean acidification will be amplified by hypoxia in coastal habitats. *Marine Biology*, 160: 1875-1888.

Mendes L., Zambotti-Villela L., Colepicolo P., Marinho-Soriano E., Stevani C. and Yokoya N. (2013). Metal cation toxicity in the alga *Gracilaria domingensis* as evaluated by the daily growth rates in synthetic seawater. *Journal of Applied Phycology*, 25: 1939-1947.

Menge B.A., Foley M.M., Pamplin J., Murphy G. and Pennington C. (2010). Supply-side ecology, barnacle recruitment, and rocky intertidal community dynamics: Do settlement surface and limpet disturbance matter? *Journal of Experimental Marine Biology and Ecology*, 392: 160-175.

Mercado J.M., Santos C.B., Perez-Llorens J.L. and Vergara J.J. (2009). Carbon isotopic fractionation in macroalgae from Cadiz Bay (Southern Spain): Comparison with other bio-geographic regions. *Estuarine Coastal and Shelf Science*, 85: 449-458.

Mayer-Pinto M., Underwood A.J., Tolhurst T. and Coleman R.A. (2010). Effects of metals on aquatic assemblages: What do we really know? *Journal of Experimental Marine Biology and Ecology*, 391: 1-9.

Micheli, F., Cottingham K.L., Bascompte J., Bjørnstad O.N., Eckert G.L., Fischer J.M., Keitt T.H., Kendall B.E., Klug J.L. and Rusak J.A. (1999). The dual nature of community variability. *Oikos*, 85: 161-169.

Micheli F. and Halpern B.S. (2005). Low functional redundancy in coastal marine assemblages. *Ecology Letters*, 8: 391-400.

Micheli F., Mumby P.J., Brumbaugh D.R., Broad K., Dahlgren C.P., Harborne A.R., Holmes K.E., Kappel C.V., Litvin S.Y. and Sanchirico J.N. (2014). High vulnerability of ecosystem function and services to diversity loss in Caribbean coral reefs. *Biological Conservation*, 171: 186-194.

Miller A.W., Reynolds A.C., Sobrino C. and Riedel G.F. (2009). Shellfish face uncertain future in high CO_2 world: Influence of acidification on oyster larvae calcification and growth in estuaries. *PLoS ONE*, 4(5): e5661.

Millero F.J., Woosley R., Ditrolio B. and Waters J. (2009). Effect of ocean acidification on the speciation of metals in seawater. *Oceanography*, 22: 72-85.

Monro K. and Poore A.G.B. (2005). Light quantity and quality induce shade-avoiding plasticity in a marine macroalga. *Journal of Evolutionary Biology*, 18: 426-435.

Morey G., Moranta J., Massutí E., Grau A., Linde M., Riera F. and Morales-Nin B. (2003). Weight-length relationships of littoral to lower slope fishes from the Western Mediterranean. *Fisheries Research*, 62: 89-96.

Morri C., Bianchi C.N., Cocito S., Peirano A., Biase A.M.D., Aliani S., Pansini M., Boyer M., Ferdeghini F., Pestarino M. and Dando P. (1999). Biodiversity of marine sessile epifauna at an Aegean island subject to hydrothermal activity: Milos, eastern Mediterranean Sea. *Marine Biology*, 135: 729-739.

Moulin L., Catarino A.I., Claessens T. and Dubois P. (2011). Effects of seawater acidification on early development of the intertidal sea urchin *Paracentrotus lividus* (Lamarck 1816). *Marine Pollution Bulletin*, 62: 48-54.

Moutin T. and Raimbault P. (2002). Primary production, carbon export and nutrients availability in western and eastern Mediterranean Sea in early summer 1996 (MINOS cruise). *Journal of Marine Systems*, 33: 273-288.

Mucci A., Starr M., Gilbert D. and Sundby B. (2011). Acidification of Lower St. Lawrence estuary bottom waters. *Atmosphere-Ocean*, 49: 206-218.

Mullin J.B. and Riley J.P. (1955). The colorimetric determination of silicate with special reference to sea and natural waters. *Analytica Chimica Acta*, 12: 162-176.

Munday P.L., Cheal A.J., Dixson D.L., Rummer J.L. and Fabricius K.E. (2014). Behavioural impairment in reef fishes caused by ocean acidification at CO_2 seeps. *Nature Climate Change*, doi:10.1038/nclimate2195.

Murphy J. and Riley J.P. (1962). A modified solution method for determination of phosphate in natural waters. *Analytica Chimica Acta*, 27: 31-36.

Nash M.C., Opdyke B.N., Troitzsch U., Russell B.D., Adey W.H., Kato A., Diaz-Pulido G., Brent C., Gardner M., Prichard J. and Kline D.I. (2012). Dolomite-rich coralline algae in reefs resist dissolution in acidified conditions. *Nature Climate Change*, doi:10.1038/nclimate1760.

Nielsen H.D., Brownlee C., Coelho S.M. and Brown M.T. (2003). Inter-population differences in inherited copper tolerance involve photosynthetic adaptation and exclusion mechanisms in *Fucus serratus*. *New Phytologist*, 160:157-165.

Nielsen H.D. and Nielsen S.L. (2005). Photosynthetic responses to Cu^{2+} exposure are independent of light acclimation and uncoupled from growth inhibition in *Fucus serratus* (Phaeophyceae). *Marine Pollution Bulletin*, 51: 715-721.

Nielsen H.D. and Nielsen S.L. (2010). Adaptation to high light irradiances enhances the photosynthetic Cu^{2+} resistance in Cu^{2+} tolerant and non-tolerant populations of the brown macroalgae *Fucus serratus*. *Marine Pollution Bulletin*, 60: 710-717.

Nienhuis S., Palmer A.R. and Harley C.D.G. (2010). Elevated CO_2 affects shell dissolution rate but not calcification rate in a marine snail. *Proceedings of the Royal Society B-Biological Sciences*, 277: 2553-2558.

Noisette F., Duong G., Six C., Davoult D. and Martin S. (2013a). Effects of elevated pCO_2 on the metabolism of a temperate rhodolith *Lithothamnion corallioides* grown under different temperatures. *Journal of Phycology*, 49: 746-757.

Noisette F., Egilsdottir H., Davoult D. and Martin S. (2013b). Physiological responses of three temperate coralline algae from contrasting habitats to near-future ocean acidification. *Journal of Experimental Marine Biology and Ecology*, 448: 179-187.

Norderhaug K.N., Christie H., Fossa J.H. and Fredriksen S. (2005). Fish-macrofauna interactions in a kelp (*Laminaria hyperborea*) forest. *Journal of the Marine Biological Association of the U.K.*, 85: 1279-1286.

Ockendon N., Baker D.J., Carr J.A., White E.C., Almond R.E.A., Amano T., Bertram E., Bradbury R.B., Bradley C., Butchart S.H.M., Doswald N., Foden W., Gill D.J.C., Green R.E., Sutherland W.J., Tanner E.V.J. and Pearce-Higgins J.W. (2014). Mechanisms underpinning climatic impacts on natural populations: altered species interactions are more important than direct effects. *Global Change Biology*, 20: 2221-2229.

Olabarria C., Arenas F., Viejo R.M., Gestoso I., Vaz-Pinto F., Incera M., Rubal M., Cacabelos E., Veiga P. and Sobrino C. (2013). Response of macroalgal assemblages from rockpools to climate change: effects of persistent increase in temperature and CO_2. *Oikos*, 122: 1065-1079.

Olischläger M. and Wiencke C. (2013). Ocean acidification alleviates low-temperature effects on growth and photosynthesis of the red alga *Neosiphonia harveyi* (Rhodophyta). *Journal of Experimental Botany*, 64: 5587-5597.

Orr J.C., Fabry V.J., Aumont O., Bopp L., Doney S.C., Feely R.A., Gnanadesikan A., Gruber N., Ishida A., Joos F., Key R.M., Lindsay K., Maier-Reimer E., Matear R., Monfray P., Mouchet A., Najjar R.G., Plattner G.-K., Rodgers K.B., Sabine C.L., Sarmiento J.L., Schlitzer R., Slater R.D., Totterdell I.J., Weirig M.-F., Yamanaka Y. and Yool A. (2005). Anthropogenic ocean acidification over the twenty-first century and its impact on calcifying organisms. *Nature*, 437: 681-686.

Orr J.C. (2011). Recent and future changes in ocean carbonate chemistry. In Gattuso J.-P. and Hansson L. (eds.) *Ocean Acidification.* 352 pp. Oxford University Press, UK.

Palumbi S.R. (1994). Genetic divergence, reproductive isolation, and marine speciation. *Annual Review of Ecology and Systematics*, 25: 547-572.

Pansch C., Schaub I., Havenhand J. and Wahl M. (2014). Habitat traits and food availability determine the response of marine invertebrates to ocean acidification. *Global Change Biology*, 20: 765-777.

Pansini M., Morri C. and Bianchi C.N. (2000). The sponge community of a subtidal area with hydrothermal vents: Milos island, Aegean Sea. *Estuarine, Coastal and Shelf Science*, 51: 627-635.

Papworth D. (2012). Relationship between high pCO_2 levels and calcareous epibiota of the seaweed Sargassum vulgare. Undergraduate dissertation, Plymouth University, 12 pp.

Parker L.M., Ross P.M., O'Connor W.A., Borysko L., Raftos D.A. and Pörtner H.-O. (2012). Adult exposure influences offspring response to ocean acidification in oysters. *Global Change Biology*, 18: 82-92.

Paulson A.J., Curl H.C.J. and Feely R.A. (1989). Estimates of trace metal inputs from non-point sources discharged into estuaries. *Marine Pollution Bulletin*, 20:549-555.

Pearson G.A., Lago-Leston A. and Mota C. (2009). Frayed at the edges: selective pressure and adaptive response to abiotic stressors are mismatched in low diversity edge populations. *Journal of Ecology*, 97:450-462.

Pecoraino G., Brusca L., D'Alessandro W., Giammanco S., Inguaggiato S. and Longo M. (2005). Total CO_2 output from Ischia Island volcano (Italy). *Geochemistry Journal*, 39: 451-458.

Pérès J.M. and Picard J. (1964). Nouveau manuel de bionomie benthique de la Méditerranée. *Rec. Trav. Stat. mar. Endoume*, 31: 1-37.

Phillips D.J.H. (1990). Use of macroalgae and invertebrates as monitors of metal levels in estuarine and coastal waters. In R. W. Furness & P. S. Rainbow (Eds.), *Heavy metals in the marine environment* (pp. 81-100). CRC, Boca Raton, Florida.

Piazzi L., Balata D., Pertusati M. and Cinelli F. (2004). Spatial and temporal variability of Mediterranean macroalgal coralligenous assemblages in relation to habitat and substratum inclination. *Botanica Marina*, 47: 105-115.

Pielou E.C. (1966). The measurement of diversity in different types of biological collections. *Journal of Theoretical Biology*, 13: 131-144.

Pingree R.D., Holligan P.M., Mardell G.T. and Head R.N. (1976). The influence of physical stability on spring, summer and autumn phytoplankton blooms in the Celtic Sea. *Journal of the Marine Biological Association of the United Kingdom*, 56: 845-873.

Pinto E., Carvalho A.P., Cardozo K.H.M., Malcata F.X., Anjos F.M.d. and Colepicolo P. (2011). Effects of heavy metals and light levels on the biosynthesis of carotenoids and fatty acids in the macroalgae *Gracilaria tenuistipitata* (var. liui Zhang & Xia). *Revista Brasileira de Farmacognosia*, 21: 349-354.

Pistevos J.C.A., Calosi P., Widdicombe S. and Bishop J.D.D. (2011). Will variation among genetic individuals influence species responses to global climate change? *Oikos*, 120: 675-689.

Pitt R.E. (1995). Effects of urban runoff on aquatic biota. In Hoffman D.J., Rattner B.A., Burton G.A.J. and Cairns J.J., Eds. *Handbook of ecotoxicology*. Lewis Publishers, Boca Raton, Florida, USA, pp. 609-630.

Poore A.G.B., Campbell A.H. and Steinberg P.D. (2009). Natural densities of mesograzers fail to limit growth of macroalgae or their epiphytes in a temperate algal bed. *Journal of Ecology*: 97, 164-175.

Poore A.G.B., Campbell A.H., Coleman R.A., Edgar G.J., Jormalainen V., Reynolds P.L., Sotka E.E., Stachowicz J.J., Taylor R.B., Vanderklift M.A. and Emmett Duffy J. (2012). Global patterns in the impact of marine herbivores on benthic primary producers. *Ecology Letters*, 15: 912-922.

Poore A.B., Graba-Landry A., Favret M., Sheppard Brennand H., Byrne M. and Dworjanyn S. (2013). Direct and indirect effects of ocean acidification and warming on a marine plant-herbivore interaction. *Oecologia*, 173: 1113-1124.

Pörtner H.O., Langenbuch M. and Reipschlager A. (2004). Biological impact of elevated ocean CO_2 concentrations: Lessons from animal physiology and earth history. *Journal of Oceanography*, 60: 705-718.

Porzio, L. (2010). Water acidification: effects on the macroalgal community. PhD Thesis, University of Naples Federico II (Italy), 214 pp.

Porzio L., Buia M.C. and Hall-Spencer J.M. (2011). Effects of ocean acidification on macroalgal communities. *Journal of Experimental Marine Biology and Ecology*, 400: 278-287.

Porzio L., Garrard S.L. and Buia M.C. (2013). The effect of ocean acidification on early algal colonization stages at natural CO_2 vents. *Marine Biology*, 160: 2247-2259.

Post E. and Pedersen C. (2008). Opposing plant community responses to warming with and without herbivores. *Proceedings of the National Academy of Sciences*, 105: 12353-12358.

Price N.N., Hamilton S.L., Tootell J.S. and Smith J.E. (2011). Species-specific consequences of ocean acidification for the calcareous tropical green algae *Halimeda*. *Marine Ecology Progress Series*, 440: 67-78.

Privitera D., Chiantore M., Mangialajo L., Glavic N., Kozul W. and Cattaneo-Vietti R. (2008). Inter- and intra-specific competition between *Paracentrotus lividus* and *Arbacia lixula* in resource-limited barren areas. *Journal of Sea Research*, 60: 184-192.

Quinn G.P. and Keough M.J. (2002). Experimental design and data analysis for biologists. *Cambridge University Press*, Cambridge, UK.

Raize O., Argaman Y. and Yannai S. (2004). Mechanisms of biosorption of different heavy metals by brown marine macroalgae. *Biotechnology and Bioengineering*, 87: 451-458.

Raman D., Venkateshwarlu Reddy P., Vijay Kumar B. and Murthy U.S.N. (2013). Atomic Absorption Spectroscopic determination and comparison of trace elements in the seaweeds. *International Journal of Modern Chemistry and Applied Science*, 1: 12-24.

Raven J.A., Johnston A.M., Kübler J.E., Korb R.E., McInroy S.G., Handley L.L., Scrimgeour C.M., Walker D.I., Beardall J., Vanderklift M., Fredriksen S. and Dunton K.M. (2002). Mechanistic interpretation of carbon isotope discrimination by marine macroalgae and seagrasses. *Functional Plant Biology*, 29: 355-78.

Raven J., Caldeira K., Elderfield H., Hoegh-Guldberg O., Liss P., Riebesell U., Shepherd J., Turley C. and Watson A. (2005). Ocean acidification due to increasing atmospheric carbon dioxide. *Royal Society Special Report*. Policy document 12/05. London.

Raven J.A., Giordano M., Beardall J. and Maberly S.C. (2012). Algal and aquatic plant carbon concentrating mechanisms in relation to environmental change. *Photosynthesis Research*, 109: 281-96.

Reusch T.B.H. (2014). Climate change in the oceans: evolutionary versus phenotypically plastic responses of marine animals and plants. *Evolutionary Applications*, 7: 104-122.

Richards R., Chaloupka M., Sanò M. and Tomlinson R. (2011). Modelling the effects of "coastal" acidification on copper speciation. *Ecological Modelling*, 222: 3559-3567.

Ridgwell A. and Schmidt D. (2010). Past constraints on the vulnerability of marine calcifiers to massive carbon dioxide release. *Nature Geoscience*, 3: 196-200.

Riebesell U., Zondervan I., Rost B., Tortell P.D., Zeebe R.E. and Morel F.M.M. (2000). Reduced calcification of marine plankton in response to increased atmospheric CO_2. *Nature*, 407: 364-367.

Riebesell U. (2008). Climate change: Acid test for marine biodiversity. *Nature*, 454: 46-47.

Riebesell U., Fabry V.J., Hansson L. and Gattuso J.-P. (Eds.) (2010). Guide to best practices for ocean acidification research and data reporting: Luxembourg: Publications Office of the European Union.

Riedl R. (1991). Fauna e flora del Mediterraneo; dalle alghe ai mammiferi una guida sistematica alle specie che vivono nel Mar Mediterraneo. Franco Muzzio Editore, Roma. 777 pp.

Ries J.B., Cohen A.L. and McCorkle D.C. (2009). Marine calcifiers exhibit mixed responses to CO_2-induced ocean acidification. *Geology*, 37: 1131-1134.

Rink S., Kuhl M., Bijima J. and Spero H.J. (1998). Microsensor studies of photosynthesis and respiration in the symbiotic foraminifer, *Orbulina universa*. *Marine Biology,* 131: 583-595.

Roberts D.A., Poore A.G.B. and Johnston E.L. (2006). Ecological consequences of copper contamination in macroalgae: Effects on epifauna and

associated herbivores. *Environmental Toxicology and Chemistry*, 25: 2470-2479.

Roberts D.A., Johnston E.L. and Poore A.G.B. (2008). Contamination of marine biogenic habitats and effects upon associated epifauna. *Marine Pollution Bulletin*, 56:1057-1065.

Roberts D.A., Birchenough S.N.R., Lewis C., Sanders M.B., Bolam T. and Sheahan D. (2013). Ocean acidification increases the toxicity of contaminated sediments. *Global Change Biology*, 19: 340-351.

Rodolfo-Metalpa R., Houlbreque F., Tambutte E., Boisson F., Baggini C., Patti F.P., Jeffree R., Fine M., Foggo A., Gattuso J.P. and Hall-Spencer J.M. (2011). Coral and mollusc resistance to ocean acidification adversely affected by warming. *Nature Climate Change*, 1: 308-312.

Rodriguez-Tovar F.J., Uchman A., Alegret L. and Molina E. (2011). Impact of the Paleocene-Eocene Thermal Maximum on the macrobenthic community: Ichnological record from the Zumaia section, northern Spain. *Marine Geology*, 282: 178-187.

Rönnbäck P., Kautsky N., Pihl L., Troell M., Söderqvist T. and Wennhage H. (2007). Ecosystem goods and services from Swedish coastal habitats: Identification, valuation, and implications of ecosystem shifts. *Ambio*, 36: 534-544.

Rosa R. and Seibel B.A. (2008). Synergistic effects of climate-related variables suggest future physiological impairment in a top oceanic predator. *Proceedings of the National Academy of Sciences of the United States of America*, 105: 20776-20780.

Rossoll D., Bermúdez R., Hauss H., Schulz K.G., Riebesell U., Sommer U. and Winder M. (2012). Ocean acidification-induced food quality deterioration constrains trophic transfer. *PLoS ONE*, 7: e34737.

Russell B.D., Thompson J.A.I., Falkenberg L.J. and Connell S.D. (2009). Synergistic effects of climate change and local stressors: CO_2 and nutrient-driven change in subtidal rocky habitats. *Global Change Biology*, 15: 2153-2162.

Russell B.D., Passarelli C.A. and Connell S.D. (2011). Forecasted CO_2 modifies the influence of light in shaping subtidal habitat. *Journal of Phycology*, 47: 744-752.

Russell B.D., Connell S.D., Findlay H.S., Tait K., Widdicombe S. and Mieszkowska N. (2013). Ocean acidification and rising temperatures may increase biofilm primary productivity but decrease grazer consumption. *Philosophical Transactions of the Royal Society B: Biological Sciences*, 368: 20120438.

Ryan K.G., Ralph P. and McMinn A. (2004). Acclimation of Antarctic bottom-ice algal communities to lowered salinities during melting. *Polar Biology*, 27:679-686.

Saderne V. and Wahl M. (2013). Differential responses of calcifying and non-calcifying epibionts of a brown macroalga to present-day and future upwelling pCO_2. *PLoS ONE*, 8: e70455.

Sala E. and Boudouresque C.F. (1997). The role of fishes in the organization of a Mediterranean sublittoral community.: I: Algal communities. *Journal of Experimental Marine Biology and Ecology*, 212: 25-44.

Sala E., Boudouresque C.F. and Harmelin-Vivien M.L. (1998). Fishing, trophic cascades, and the structure of algal assemblages: evaluation of an old but untested paradigm. *Oikos*, 82: 425-439.

Sala E., Kizilkaya Z., Yildirim D. and Ballesteros E. (2011). Alien marine fishes deplete algal biomass in the Eastern Mediterranean. *PLoS ONE*, 6: e17356.

Sala E., Ballesteros E., Dendrinos P., Di Franco A., Ferretti F., Foley D., Fraschetti S., Friedlander A., Garrabou J., Güçlüsoy H., Guidetti P., Halpern B.S., Hereu B., Karamanlidis A.A., Kizilkaya Z., Macpherson E., Mangialajo L., Mariani S., Micheli F., Pais A., Riser K., Rosenberg A.A., Sales M., Selkoe K.A., Starr R., Tomas F. and Zabala M. (2012). The structure of Mediterranean rocky reef ecosystems across environmental and human gradients, and conservation implications. *PLoS ONE*, 7: e32742.

Sales M., Cebrian E., Tomas F. and Ballesteros E. (2011). Pollution impacts and recovery potential in three species of the genus *Cystoseira* (Fucales, Heterokontophyta). *Estuarine, Coastal and Shelf Science*, 92: 347-357.

Sánchez-Moyano J.E., García-Adiego E.M., Estacio F.J. and García-Gómez J.C. (2000). Effect of environmental factors on the spatial distribution of the epifauna of the alga *Stypocaulon scoparia* in Algeciras Bay, Southern Spain. *Aquatic Ecology*, 34:355-367.

Sanford E. and Kelly M.W. (2011). Local adaptation in marine invertebrates. *Annual Review of Marine Science*, 3, 509-535.

Sarmiento J.L., Slater R., Barber R., Bopp L., Doney S.C., Hirst A.C., Kleypas J., Matear R., Mikolajewicz U., Monfray P., Soldatov V., Spall S.A. and Stouffer R. (2004). Response of ocean ecosystems to climate warming. *Global Biogeochemical Cycles*, 18: GB3003.

Sarthou G. and Jeandel C. (2001). Seasonal variations of iron concentrations in the Ligurian Sea and iron budget in the Western Mediterranean Sea. *Marine Chemistry*, 74: 115-129.

Schreiber U., Endo T., Mi H. and Asada K. (1995). Quenching analysis of chlorophyll fluorescence by the saturation pulse method: particular aspects relating to the study of eukaryotic algae and cyanobacteria. *Plant and Cell Physiology*, 36: 873-882.

Schröder W.P., Arellano J.B., Bitter T., Barón M., Eckert H.J. and Regner G. (1994). Flash-induced absorption spectroscopy studies of copper interaction with photosystem II in higher plants. *Journal of Biological Chemistry*, 269:32865-32870.

Schubert N., García-Mendoza E. and Pacheco-Ruiz I. (2006). Carotenoid composition of marine red algae. *Journal of Phycology*, 42: 1208-1216.

Schulz K.G., Ramos J.B.E., Zeebe R.E. and Riebesell U. (2009). CO_2 perturbation experiments: Similarities and differences between dissolved inorganic carbon and total alkalinity manipulations. *Biogeosciences*, 6: 2145-2153.

Seely G.R., Duncan M.J. and Vidaver W.E. (1972). Preparative and analytical extraction of pigments from brown algae with dimethyl sulfoxide. *Marine Biology*, 12:184-188.

Semesi I.S., Beer S. and Bjork M. (2009). Seagrass photosynthesis controls rates of calcification and photosynthesis of calcareous macroalgae in a tropical seagrass meadow. *Marine Ecology Progress Series*, 382: 41-47.

Shannon C.E. and Weaver W. (1949). A mathematical theory of communication. University of Illinois Press. ISBN 0-252-72548-4.

Shaw E.C., Munday P.L. and McNeil B.I. (2013). The role of CO_2 variability and exposure time for biological impacts of ocean acidification. *Geophysical Research Letters*, 40: 4685-4688.

Shears N.T. and Ross P.M. (2010). Toxic cascades: multiple anthropogenic stressors have complex and unanticipated interactive effects on temperate reefs. *Ecology Letters*, 13:1149-1159.

Shi D.L., Xu Y., Hopkinson B.M. and Morel F.M.M. (2010). Effect of ocean acidification on iron availability to marine phytoplankton. *Science*, 327: 676-679.

Shin P.K.S. and Lam W.K.C. (2001). Development of a marine sediment pollution index. *Environmental Pollution*, 113: 281-291.

Short J., Kendrick G.A., Falter J. and McCulloch M.T. (2014). Interactions between filamentous turf algae and coralline algae are modified under ocean acidification. *Journal of Experimental Marine Biology and Ecology*, 456, 70-77.

Shushkina E.A., Vinogradov M.E., Lebedeva L.P., and Anokhina L.L. (1997). Productivity characteristics of epipelagic communities of the world's oceans. *Oceanology*, 37: 346-353.

Siokou-Frangou I., Christaki U., Mazzocchi M.G., Montresor M., Ribera d'Alcalá M., Vaqué D. and Zingone A. (2010). Plankton in the open Mediterranean Sea: a review. *Biogeosciences*, 7: 1543-1586.

Small D., Calosi P., White D., Spicer J.I. and Widdicombe S. (2010). Impact of medium-term exposure to CO_2 enriched seawater on the physiological functions of the velvet swimming crab *Necora puber*. *Aquatic Biology*, 10: 11-21.

Spatharis S., Orfanidis S., Panayotidis P. and Tsirtsis G. (2011). Assembly processes in upper subtidal macroalgae: the effect of wave exposure. *Estuarine, Coastal and Shelf Science*, 91: 298-305.

Spicer J.I. (2014). What can an ecophysiological approach tell us about the physiological responses of marine invertebrates to hypoxia? *The Journal of Experimental Biology*, 217: 46-56.

Steinacher M., Joos F., Frolicher T.L., Plattner G.-K. and Doney S.C. (2009). Imminent ocean acidification projected with the NCAR global coupled carbon cycle-climate model. *Biogeosciences*, 6: 515-33.

Steneck R.S. and Dethier M.N. (1994). A functional group approach to the structure of algal-dominated communities. *Oikos*, 69: 476-498.

Steneck R.S., Graham M.H., Bourque B.J., Corbett D., Erlandson J.M., Estes J.A. and Tegner M.J. (2002). Kelp forest ecosystems: biodiversity, stability, resilience and future. *Environmental Conservation*, 29: 436-459.

Sunday J.M., Crim R.N., Harley C.D.G. and Hart M.W. (2011). Quantifying rates of evolutionary adaptation in response to ocean acidification. *PLoS ONE*, 6: e22881.

Sunday J.M., Calosi P., Dupont S., Munday P.L., Stillman J.H. and Reusch T.B.H. (2014). Evolution in an acidifying ocean. *Trends in Ecology & Evolution*, 29: 117-125.

Susini M.-L., Thibaut T., Meinesz A. and Forcioli D. (2007). A preliminary study of genetic diversity in *Cystoseira amentacea* (C. Agardh) Bory var. *stricta* Montagne (Fucales, Phaeophyceae) using random amplified polymorphic DNA. *Phycologia*, 46: 605-611.

Swanson A.K. and Fox C.H. (2007). Altered kelp (Laminariales) phlorotannins and growth under elevated carbon dioxide and ultraviolet-B treatments can influence associated intertidal food webs. *Global Change Biology*, 13: 1696-1709.

Tarasov V.G., Gebruk A.V., Mironov A.N. and Moskalev L.I. (2005). Deep-sea and shallow-water hydrothermal vent communities: Two different phenomena? *Chemical Geology*, 224: 5-39.

Taskin E., Jahn R., Öztürk M., Furnari G. and Cormaci M. (2012). The Mediterranean *Cystoseira* (with photographs). Manisa, Turkey: Celar Bayar University, pp. 1-75.

Taylor R.B. (1998). Density, biomass and productivity of animals in four subtidal rocky reef habitats: the importance of small mobile invertebrates. *Marine Ecology Progress Series*, 172: 37-51.

Taylor J.D., Ellis R., Milazzo M., Hall-Spencer J.M. and Cunliffe M. (2014). Intertidal epilithic bacteria diversity changes along a naturally occurring carbon dioxide and pH gradient. *FEMS Microbiology Ecology*, 89: 670-678.

Tellier F., Tapia J., Faugeron S., Destombe C. and Valero M. (2011). The *Lessonia nigrescens* species complex (Laminariales, Phaeophyceae) shows strict parapatry and complete reproductive isolation in a secondary contact zone. *Journal of Phycology*, 47: 894-903.

Thiermann F., Akoumianaki I., Hughes J.A. and Giere O. (1997). Benthic fauna of a shallow-water gaseohydrothermal vent area in the Aegean Sea (Milos, Greece). *Marine Biology*, 128: 149-159.

Thomas E. (2007). Cenozoic mass extinctions in the deep sea: what disturbs the largest habitat on Earth? *Geological Society of America Special Papers*, 424: 1-23.

Thomsen J., Gutowska M.A., Saphorster J., Heinemann A., Trubenbach K., Fietzke J., Hiebenthal C., Eisenhauer A., Kortzinger A., Wahl M. and Melzner F. (2010). Calcifying invertebrates succeed in a naturally CO_2-rich coastal habitat

but are threatened by high levels of future acidification. *Biogeosciences*, 7: 3879-3891.

Thomsen J. and Melzner F. (2010). Moderate seawater acidification does not elicit long-term metabolic depression in the blue mussel *Mytilus edulis*. *Marine Biology*, 157: 2667-2676.

Thomsen J., Casties I., Pansch C., Körtzinger A. and Melzner F. (2013). Food availability outweighs ocean acidification effects in juvenile *Mytilus edulis*: laboratory and field experiments. *Global Change Biology*, 19: 1017-1027.

Thurberg F.P., Dawson M.A. and Collier R.S. (1973). Effects of copper and cadmium on osmoregulation and oxygen consumption in two species of estuarine crabs. *Marine Biology*, 23: 171-175.

Tilman D. (1999). The ecological consequences of changes in biodiversity: a search for general principles. *Ecology*, 80: 1455-1474.

Tittensor D.P., Baco A.R., Hall-Spencer J.M., Orr J.C. and Rogers A.D. (2010). Seamounts as refugia from ocean acidification for cold-water stony corals. *Marine Ecology - Evolutionary Perspective*, 31: 212-225.

Tsiamis K., Panayotidis P., Salomidi M., Pavlidou A., Kleinteich J., Balanika K. and Küpper F.C. (2013). Macroalgal community response to re-oligotrophication in Saronikos Gulf. *Marine Ecology Progress Series*, 472: 73-85.

Tyrrell T. (2008). Calcium carbonate cycling in future oceans and its influence on future climates. *Journal of Plankton Research*, 30: 141-156.

Venn A., Tambutté E., Holcomb M., Allemand D. and Tambutté S. (2011). Live tissue imaging shows reef corals elevate pH under their calcifying tissue relative to seawater. *PLoS ONE*, 6: e20013.

Vergés A., Alcoverro T. and Ballesteros E. (2009). Role of fish herbivory in structuring the vertical distribution of canopy algae *Cystoseira* spp. in the Mediterranean Sea. *Marine Ecology Progress Series*, 375: 1-11.

Verges A., Steinberg P.D., Hay M.E., Poore A.G., Campbell A.H., Ballesteros E., Heck K.L., Jr., Booth D.J., Coleman M.A., Feary D.A., Figueira W., Langlois T., Marzinelli E.M., Mizerek T., Mumby P.J., Nakamura Y., Roughan M., van Sebille E., Gupta A.S., Smale D.A., Tomas F., Wernberg T. and Wilson S.K. (2014). The tropicalization of temperate marine ecosystems: climate-mediated changes in herbivory and community phase shifts. *Proceedings of the Royal Society B: Biological Sciences*, 281: 20140846.

Vizzini S., Di Leonardo R., Costa V., Tramati C.D., Luzzu F. and Mazzola A. (2013). Trace element bias in the use of CO_2-vents as analogues for low-pH environments: Implications for contamination levels in acidified oceans. *Estuarine, Coastal and Shelf Science*, 134: 19-30.

Waz P.M., Kirkwood W.J., Peltzer E.T., Hester K.C. and Brewer P.G. (2008). Creating controlled CO_2 perturbation experiments on the seafloor - development of FOCE techniques. In: *Oceans 2008 - Mts/Ieee Kobe techno-ocean, vols 1-3*, pp. 750-753.

Whalen M.A., Duffy J.E. and Grace J.B. (2012). Temporal shifts in top-down vs. bottom-up control of epiphytic algae in a seagrass ecosystem. *Ecology*, 94: 510-520.

Whiteley N.M. (2011). Physiological and ecological responses of crustaceans to ocean acidification. *Marine Ecology Progress Series*, 430: 257-271.

Wernberg T. and Vanderklift M.A. (2010). Contribution of temporal and spatial components to morphological variation in the kelp *Ecklonia* (Laminariales). *Journal of Phycology*, 46: 153-161.

Widdicombe, S., Dupont, S. and Thorndyke, M. (2010). Laboratory experiments and benthic mesocosm studies. In *Guide to best practices for ocean acidification research and data reporting*, edited by Riebesell U., Fabry V.J., Hansson L. and Gattuso J.-P. Luxembourg: Publications Office of the European Union. p. 53-66.

Wilbur K.M. (1964). Shell formation and regeneration, in: *Physiology of the Mollusca 1*, edited by: Wilbur K.M. and Yonge C.M., Academic Press, New York, 243-282.

Williamson C.J., Najorka J., Perkins R., Yallop M.L. and Brodie J. (2014). Skeletal mineralogy of geniculate corallines: providing context for climate change and ocean acidification research. *Marine Ecology Progress Series*, 513: 71-84.

Wood H.L., Spicer J.I. and Widdicombe S. (2008). Ocean acidification may increase calcification rates, but at a cost. *Proceedings of the Royal Society B-Biological Sciences*, 275: 1767-1773.

Wood H.L., Spicer J.I., Lowe D.M. and Widdicombe S. (2010). Interaction of ocean acidification and temperature; the high cost of survival in the brittlestar *Ophiura ophiura*. *Marine Biology*: 157, 2001-2013.

Wootton J.T., Pfister C.A. and Forester J.D. (2008). Dynamic patterns and ecological impacts of declining ocean pH in a high-resolution multi-year dataset. *Proceedings of the National Academy of Sciences*, 105: 18848-18853.

Xia J.R., Li Y.J., Lu J. and Chen B. (2004). Effects of copper and cadmium on growth, photosynthesis, and pigment content in *Gracilaria lemaneiformis*. *Bulletin of Environmental Contamination and Toxicology*, 73: 979-986.

Yamada K., Hori M., Tanaka Y., Hasegawa N. and Nakaoka M. (2010). Contribution of different functional groups to the diet of major predatory fishes at a seagrass meadow in northeastern Japan. *Estuarine, Coastal and Shelf Science*, 86: 71-82.

Yildiz G., Hofmann Laurie C., Bischof K. and Dere Ş. (2013). Ultraviolet radiation modulates the physiological responses of the calcified rhodophyte *Corallina officinalis* to elevated CO_2. *Botanica Marina*, 56: 161-168.

Zachos J.C., Rähl U., Schellenberg S.A., Sluijs A., Hodell D.A., Kelly D.C., Thomas E., Nicolo M., Raffi I., Lourens L.J., McCarren H. and Kroon D. (2005). Rapid acidification of the ocean during the Paleocene-Eocene Thermal Maximum. *Science*, 308: 1611-1615.

Zeebe R.E. and Westbroek P. (2003). A simple model for the $CaCO_3$ saturation state of the ocean: the 'Strangelove', the 'Neritan', and the 'Cretan' Ocean. G*eochemistry Geophysics Geosystems,* 4: 1104, doi:10.1029/2003GC000538.

Zeebe R.E. and Ridgwell A. (2011). Past Changes of Ocean Carbonate Chemistry. In *Ocean acidification* edited by Gattuso J.-P. and Hansson L. Oxford University Press, UK.

Zohary T. and Robarts R.D. (1998). Experimental study of microbial P limitation in the eastern Mediterranean. *Limnology and Oceanography*, 43(3): 387-395.

Appendix A:

Benthic percent cover at Methana and biomass at Vulcano (Chapter 3)

Appendix A1: mean (± SE, n=3) percent cover of benthic organisms at Methana in May and September 2012.

May 2012	Site				
Taxon	REF A	REF B	200 E	200 W	SEEP
Cystoseira corniculata	51.43 ± 14.00	47.71 ± 15.47	62.57 ± 13.36	61.43 ± 12.57	31.57 ± 15.29
Cystoseira amentacea	7.86 ± 4.98	0	0	0	0
Dictyota sp.	21.14 ± 8.78	14.29 ± 5.71	10.71 ± 4.94	11.43 ± 4.59	14.43 ± 9.44
Cladostephus spongiosus	0	0	0	7.71 ± 3.96	3.14 ± 3.14
Padina pavonica (non-calcified)	0	0	1.71 ± 1.71	1.57 ± 1.57	15.29 ± 10.18
Padina pavonica (calcified)	5.29 ± 3.21	5.00 ± 1.89	0	0	0
Sargassum vulgare	2.86 ± 2.86	8.57 ± 8.57	4.00 ± 1.65	2.86 ± 1.49	36.29 ± 16.25
Cladophora sp.	0	0	0	0	0.57 ± 0.57
Halimeda tuna	0	0.14 ± 0.14	0	0.14 ± 0.14	0.14 ± 0.14
Halopteris scoparia	1.43 ± 1.43	11.43 ± 7.69	0.57 ± 0.57	0	0
CCA	0.86 ± 0.70	3.43 ± 1.41	19.29 ± 12.56	9.86 ± 9.21	0
Porifera (black)	0	0	1.14 ± 1.14	0	0
Bare substratum	7.71 ± 3.27	2.14 ± 1.49	0	0	0
Jania rubens	2.14 ± 1.49	0.86 ± 0.70	0	0	0
Sargassum sp.	0	5.71 ± 4.14	0	0	0
Caulerpa racemosa	0	0.71 ± 0.71	0	0	0
Falkenbergia sp.	0	0	0	0	0
Porifera (orange)	0	0	0	0	0
Amphiroa sp.	0	0	0	0	0
Corallina caespitosa	0	0	0	0	0
Turf algae	0	0	0	0	0
Hydrozoa	0	0	0	0	0

September 2012	Site				
Taxon	REF A	REF B	200 E	200 W	SEEP
Cystoseira corniculata	18.33 ± 7.15	24.17 ± 12.41	47.50 ± 11.74	39.67 ± 14.02	57.67 ± 17.98
Cystoseira amentacea	0	0	0	0	0
Dictyota sp.	0	0	0	0	0
Cladostephus spongiosus	0	0	0	10.83 ± 7.24	0
Padina pavonica (non-calcified)	0	0	0	0	0
Padina pavonica (calcified)	0	1.17 ± 0.83	0	0	0
Sargassum vulgare	0	0	0	0	0.17 ± 0.17
Cladophora sp.	0	0	0	0	3.33 ± 3.33
Halimeda tuna	0	0	0.17 ± 0.17	0	0.33 ± 0.33
Halopteris scoparia	5.00 ± 5.00	0	0	5.00 ± 5.00	0
CCA	15.00 ± 4.83	17.83 ± 8.11	13.67 ± 4.01	7.50 ± 5.59	0.33 ± 0.33
Porifera (black)	0	0	0	0	0
Bare substratum	4.17 ± 3.27	11.67 ± 6.67	0	5.83 ± 3.75	8.67 ± 3.38
Jania rubens	55.83 ± 10.83	21.67 ± 8.43	35.67 ± 10.02	23.33 ± 8.91	1.67 ± 1.05
Sargassum sp.	0	16.17 ± 12.99	0	3.00 ± 1.63	25.83 ± 15.78
Caulerpa racemosa	0	0	0	0	0
Falkenbergia sp.	0	0	0	0	2.00 ± 0.93
Porifera (orange)	0.83 ± 0.83	0	1.67 ± 1.67	0	1.67 ± 1.67
Amphiroa sp.	0	0.67 ± 0.49	0.50 ± 0.50	0	0
Corallina caespitosa	0	0	0.83 ± 0.83	0	0
Turf algae	0	3.00 ± 3.00	0	5.00 ± 5.00	0
Hydrozoa	0.83 ± 0.83	0.83 ± 0.83	0	0	0

Appendix A2: mean (± SE, n=4) macroalgal biomass (grams of dry weight) at Vulcano in May 2010.

	Site		
Taxon	REF A	Mid pCO_2	High pCO_2
Cystoseira sp.	26.724 ± 10.946	4.373 ± 1.460	27.083 ± 29.746
Flabellia petiolata	0.192 ± 0.083	0.770 ± 0.557	7.192 ± 5.994
Caulerpa prolifera	0	0.358 ± 0.265	2.061 ± 0.880
Turf algae	0.912 ± 0.415	2.648 ± 0.391	4.651 ± 3.093
Sargassum sp.	0.629 ± 0.627	0	3.353 ± 3.915
Caulerpa racemosa	0	0.454 ± 0.343	0.022 ± 0.045
Nitophyllum punctatum	0	0	0.005 ± 0.010
Chylocladia pelagosae	0	0	0
CCA	0.919 ± 0.634	1.531 ± 0.633	0.372 ± 0.665
Rytiphloea tinctoria	0.016 ± 0.016	0.028 ± 0.028	0.008 ± 0.015
Peyssonnelia sp.	0	1.491 ± 1.385	0.015 ± 0.030
Halopteris scoparia	1.121 ± 0.753	0.374 ± 0.374	0
Gigartinales	0	0.010 ± 0.010	0
Cladophorales	0	0.006 ± 0.006	0
Dictyopteris membranacea	2.760 ± 1.676	0.403 ± 0.140	0
Ulothrix sp.	0	0.002 ± 0.002	0
Ceramium sp.	0	0.002 ± 0.002	0
Acetabularia acetabulum	0.110 ± 0.110	0	0
Dictyota sp.	0.821 ± 0.300	1.032 ± 0.541	0.669 ± 0.309
Articulated coralline	0.363 ± 0.166	0	0
Cladophora sp.	0	0.044 ± 0.041	0.043 ± 0.055
Ceramiales	0.002 ± 0.002	0	0.044 ± 0.088
Rhodymenia ligulata	0	0	0.042 ± 0.024
Stilophora tenella	0	0.031 ± 0.031	0.005 ± 0.009
Halopteris sp.	0.006 ± 0.005	0.056 ± 0.032	0
Anadyomene stellata	0	0.005 ± 0.005	0.026 ± 0.052
Pterocladia sp.	0	0.033 ± 0.021	0
Taonia atomaria	0.133 ± 0.082	0.054 ± 0.043	0.463 ± 0.926
Osmundea truncata	0	0.002 ± 0.001	0
Padina pavonica	0.001 ± 0.001	0.087 ± 0.025	0
Dictyota fasciola	0.332 ± 0.295	0	0

Appendix B:

Epifaunal abundance at Methana and Vulcano (Chapter 4)

Appendix B1: mean (± SE, n=3) abundance of epifaunal invertebrates at Methana in May 2012.

OTU	REF A	REF B	200 E	200 W	SEEP
Foraminifera					
Amphistegina lobifera	220.00 ± 95.55	173.33 ± 25.18	5.67 ± 3.28	7.33 ± 5.04	0.67 ± 0.21
Agglutinated	119.00 ± 83.92	28.33 ± 10.73	0	0	0
Calcified sp. 1	2.67 ± 0.33	3.33 ± 1.76	0	0	0
Calcified sp. 2	0	0	2.00 ± 1.00	0	0
Sipuncula	7.00 ± 1.53	15.33 ± 6.17	1.67 ± 0.67	8.67 ± 3.84	15.00 ± 0.32
Platyhelminthes	0	0	2.00 ± 1.53	1.33 ± 0.88	2.00 ± 0.37
Bryozoa	0.01 ± 0.01	0.02 ± 0.01	0.16 ± 0.08	0.01 ± 0.01	0
Mollusca					
Bivalvia					
Arca noeae	0.67 ± 0.67	0	0	0.67 ± 0.67	0
Arcidae sp. 1	1.33 ± 0.33	0.33 ± 0.33	0	0.33 ± 0.33	0
Arcidae sp. 2	0.33 ± 0.33	0	0	0	0
Arcidae sp. 3	0.33 ± 0.33	0	0	0	0
Bivalvia sp. 1	35.33 ± 15.34	41.67 ± 12.55	11.67 ± 4.33	5.00 ± 1.53	0
Bivalvia sp. 2	0	0.67 ± 0.67	0.33 ± 0.33	0.33 ± 0.33	0
Cardita sp.	0	0.67 ± 0.33	0	0	0
Ostreoidea sp.	0	0	0.33 ± 0.33	0	0
Gastropoda					
Alvania cimex	0	0.33 ± 0.33	0	0	0
Alvania geryonia	0.33 ± 0.33	0	0	0	0
Alvania lactea	0	0.33 ± 0.33	0	0	0

Cerithiopsis sp. 1	0.33 ± 0.33	0.67 ± 0.33	0	0	0
Cerithiopsis sp. 2	0	1.00 ± 1.00	0	0	0
Cerithiopsis tubercularis	0	0.33 ± 0.33	0	0	0
Cerithium vulgatum	0	0.33 ± 0.33	0	0	0
Columbella rustica var. 1	0.33 ± 0.33	1.00 ± 0.58	1.67 ± 0.88	0.33 ± 0.33	0
Columbella rustica var. 2	0	0.33 ± 0.33	0	0	0
Columbella rustica var. 3	0	0	0	0.33 ± 0.33	0
Columbella rustica var. 4	0	0	1.00 ± 1.00	0	0
Columbella sp.	0	0.33 ± 0.33	0	0.33 ± 0.33	0
Diodora graeca	0.33 ± 0.33	0	0	0	0
Gasteropoda sp. 1	0.33 ± 0.33	1.33 ± 0.88	0	0	0
Gasteropoda sp. 2	0	0.33 ± 0.33	0	0	0
Gasteropoda sp. 3	0	0.33 ± 0.33	0	0	0
Gasteropoda sp. 4	0.67 ± 0.33	0	0	0	0
Gasteropoda sp. 5	0.67 ± 0.67	0	0	0	0
Gasteropoda sp. 6	0.33 ± 0.33	0	0	0	0
Gasteropoda sp. 7	0	0.33 ± 0.33	0	0	0
Hinia costulata	1.00 ± 0.58	0	0	0.67 ± 0.67	0
Jujubinus sp.	0	0.33 ± 0.33	0	0	0
Jujubinus striatus	0	0.33 ± 0.33	0	0	0
Muricidae sp.	0	0	0.33 ± 0.33	0	0
Omalogyridae sp.	0.33 ± 0.33	4.33 ± 2.19	0	0	0
Patella sp.	0.33 ± 0.33	0.33 ± 0.33	0	0	0
Pusillina sp.	1.00 ± 1.00	1.00 ± 0.58	0	0	0
Rissoina sp.	0	0.33 ± 0.33	0	0	0

Setia maculata	0	2.00 ± 1.53	0	0	0
Triphora perversa	0	0.33 ± 0.33	0	0	0
Polychaeta					
Polychaeta	107.67 ± 1.67	85.00 ± 19.52	217.00 ± 37.27	490.00 ± 149.29	176.33 ± 4.49
Serpulidae	1.33 ± 0.33	1.67 ± 0.33	3.00 ± 1.00	0.67 ± 0.67	0
Crustacea					
Amphipoda					
Amphilocus sp.	1.67 ± 0.33	2.00 ± 0.58	2.00 ± 1.53	1.67 ± 1.20	2.00 ± 0.37
Ampithoe sp.	22.33 ± 2.19	9.33 ± 4.37	351.00 ± 28.02	159.00 ± 59.18	150.67 ± 14.63
Aoridae sp.	16.67 ± 11.20	41.33 ± 17.25	32.00 ± 20.13	14.00 ± 2.52	22.33 ± 5.15
Apherusa sp.	10.67 ± 4.10	10.33 ± 6.84	0	0.67 ± 0.67	0.67 ± 0.21
Peltocoxa sp.	0	1.00 ± 0.58	0	0	0
Dexamine spiniventris	0	1.00 ± 1.00	0	0.33 ± 0.33	0
Hyale sp.	204.00 ± 55.77	68.33 ± 26.57	681.33 ± 357.19	837.33 ± 211.58	367.67 ± 13.45
Gammaropsis sp.	80.00 ± 20.53	34.33 ± 8.29	574.00 ± 158.35	70.00 ± 35.34	245.33 ± 12.72
Microprotopus sp.	0	0.33 ± 0.33	0	0	0
Ericthonius sp.	8.33 ± 2.67	1.67 ± 1.20	325.67 ± 77.62	323.33 ± 170.95	180.00 ± 22.10
Ischyrocerus sp.	0.67 ± 0.67	1.67 ± 1.20	13.00 ± 8.14	1.33 ± 0.88	10.00 ± 2.21
Jassa sp.	74.00 ± 18.03	9.00 ± 5.51	145.00 ± 93.74	29.00 ± 14.01	39.00 ± 5.48
Leucothoe sp.	1.00 ± 1.00	0	9.67 ± 5.93	0	1.00 ± 0.18
Elasmopus sp.	39.00 ± 11.68	38.67 ± 0.67	54.33 ± 9.84	37.00 ± 3.61	73.33 ± 10.88
Maera sp.	21.33 ± 16.34	36.00 ± 5.86	17.00 ± 9.29	5.67 ± 4.18	31.33 ± 5.56
Pereionotus sp.	0	20.33 ± 5.24	4.33 ± 1.20	62.3 3 ± 48.84	33.33 ± 4.42
Podocerus sp.	57.00 ± 8.50	124.33 ± 27.94	180.33 ± 12.84	7.33 ± 3.18	84.33 ± 4.96
Stenothoe spp.	142.67 ± 83.79	340.33 ± 61.50	80.00 ± 26.95	4.33 ± 1.86	6.00 ± 0.63

Caprella sp.	11.33 ± 5.24	35.33 ± 2.96	12.33 ± 4.91	2.33 ± 1.33	0
Ostracoda	1.00 ± 0.58	19.00 ± 13.05	2.67 ± 1.45	4.33 ± 2.33	0.33 ± 0.11
Copepoda					
Harpacticoida	4.00 ± 2.52	93.67 ± 51.27	14.00 ± 6.11	17.00 ± 7.77	6.33 ± 1.19
Cirripedia	0.67 ± 0.67	0	4.00 ± 2.08	0	0
Tanaidacea					
Leptochelia savignyi	30.67 ± 3.84	14.33 ± 4.98	175.33 ± 38.89	215.00 ± 52.74	126.00 ± 7.77
Tanais dulongii	2.33 ± 0.33	72.00 ± 8.02	5.00 ± 1.15	5.33 ± 4.33	0
Araphura brevimanus	0	1.33 ± 0.33	0	0	0
Isopoda					
Asellota	61.00 ± 32.73	81.00 ± 60.18	160.67 ± 35.93	25.67 ± 2.31	84.67 ± 7.98
Sphaeromatidea	5.33 ± 3.38	12.00 ± 5.29	1.67 ± 0.88	0.67± 0.67	4.00 ± 0.63
Decapoda	2.66 ± 1.33	8.00 ± 2.60	0.66 ±	0	0
Pycnogonida	1.67 ± 0.88	0.67 ± 0.33	10.00 ± 5.20	1.33 ± 0.33	1.33 ± 0.28
Echinodermata					
Asterina gibbosa	0	0	0	0	0.33 ± 0.11
Ophiuroidea	2.67 ± 2.19	2.67 ± 1.76	37.00 ± 17.58	44.33 ± 16.29	3.33 ± 0.64

Appendix B2: mean (± SE) abundance of epifaunal invertebrates at Vulcano in June 2013.

Macroalgal host	*Sargassum vulgare*		*Cystoseira* spp.	
pCO_2	600 ppm (n=9)	1200 ppm (n=10)	600 ppm (n=15)	1200 ppm (n=14)
Polychaeta				
Filter feeder	4.56 ± 2.43	159.00 ± 36.96	1.07 ± 0.27	4.64 ± 1.28
Non filter feeder	13.33 ± 3.15	145.30 ± 25.53	7.13 ± 1.55	43.71 ± 8.07
Mollusca				
Polyplacophora				
Acanthochitona fascicularis	0	0	0.07 ± 0.07	0
Bivalvia				
Cardita calyculata	0	0	0.07 ± 0.07	0

Musculus discors	0	0.10 ± 0.10	0.40 ± 0.19	0
Musculus sp. juv.	0	0	0	0.07 ± 0.07
Mytilaster minimus	0	0	0.53 ± 0.47	0
Gasteropoda				
Alvania cfr hirta	0	0	0	0.07 ± 0.07
Ammonicera fischeriana	0	0	0.40 ± 0.29	0.43 ± 0.20
Barleeia rubra	0	0	0.13 ± 0.13	0
Barleeia rubra juv.	0	0	0.07 ± 0.07	0
Cerithium lividulum	0.22 ± 0.15	0	0.07 ± 0.07	0
Cerithium cfr scabridum	0	0	0.07 ± 0.07	0
Columbella rustica juv	0	0.10 ± 0.10	1.07 ± 1.07	0.14 ± 0.14
Columbella rustica	0.11 ± 0.11	0	0.20 ± 0.14	0
Eatonina cossurae	2.00 ± 0.88	0	3.07 ± 0.88	0.07 ± 0.07
Eatonina cossurae juv	1.33 ± 0.90	0	0.13 ± 0.13	0
Gastropoda indet. juv.	0.22 ± 0.22	0	0.07 ± 0.07	0.43 ± 0.29
Gibbula racketti	0	0	0.07 ± 0.07	0
Gibbula varia	0	0	0.07 ± 0.07	0
Gibbula sp. juv.	0	0	0.60 ± 0.40	0.07 ± 0.07
Jujubinus sp. juv	0.11 ± 0.11	0	0.07 ± 0.07	0
Omalogyra simplex	0.11 ± 0.11	0	0.20 ± 0.11	0
Pollia cfr dorbignyi juv	0	0.10 ± 0.10	0	0
Rissoa auriscalpium	0	0	0	0.07 ± 0.07
Rissoa guerinii	0.11 ± 0.11	0	0	0
Rissoa variabilis juv.	0	0	1.13 ± 0.61	0.14 ± 0.10
Rissoa sp juv	0.11 ± 0.11	0.10 ± 0.10	0.13 ± 0.09	0.29 ± 0.22
Rissoidae indet.	0	0	0	0.07 ± 0.07
Setia cfr maculata	0.22 ± 0.22	0	0	0
Setia cfr amabilis	1.11 ± 0.75	0	0.07 ± 0.07	0
Setia sp. juv.	1.00 ± 0.78	0	0.07 ± 0.07	0.07 ± 0.07
Crustacea				
Copepoda (Harpacticoida)	0	0	0	0.21 ± 0.15
Amphipoda				
Amphilochus neapolitanus	0.33 ± 0.17	0	0.07 ± 0.07	0
Ampithoe sp.	0	0	0	0.07 ± 0.07
Ampithoe ferox	0.11 ± 0.11	0.20 ± 0.20	0.13 ± 0.09	0
Ampithoe helleri	0	0	0.07 ± 0.07	0.21 ± 0.11
Ampithoe ramondi	1.89 ± 0.59	33.20 ± 8.53	2.40 ± 0.58	5.57 ± 3.03
Ampithoe riedli	0	0	0	0.07 ± 0.07
Ampithoe spuria	8.89 ± 2.47	49.80 ± 5.44	49.73 ± 8.30	73.36 ± 19.57
Cymadusa crassicornis	3.89 ± 0.90	0	5.07 ± 1.02	1.14 ± 0.54
Aoridae sp.	0.33 ± 0.24	6.40 ± 2.48	0	0.14 ± 0.14
Apherusa sp.	7.78 ± 1.79	0.50 ± 0.27	0.67 ± 0.35	0.29 ± 0.22

Dexamine spiniventris	0.33 ± 0.24	0	0.40 ± 0.24	0.07 ± 0.07
Dexamine spinosa	0.11 ± 0.11	0	0	0
Hyale sp.	5.89 ± 1.88	35.00 ± 18.63	8.40 ± 3.85	1.86 ± 0.61
Hyale camptonyx	0.11 ± 0.11	1.90 ± 1.28	1.00 ± 0.59	1.43 ± 0.54
Hyale crassipes	0	0	0	0.36 ± 0.25
Hyale perieri	0	0.10 ± 0.10	0.20 ± 0.14	0
Hyale schmidti	4.33 ± 1.35	12.30 ± 3.33	4.33 ± 1.94	4.86 ± 1.73
Ericthonius sp.	102.00 ± 31.51	98.10 ± 17.22	16.07 ± 5.89	20.21 ± 3.17
Ischyrocerus sp.	0	0	0	0.07 ± 0.07
Jassa marmorata	0	0.10 ± 0.10	0.13 ± 0.13	0
Lysianassa costae	0.11 ± 0.11	0.20 ± 0.13	0	0.07 ± 0.07
Elasmopus sp.	0	0	0.07 ± 0.07	0
Maera inaequipes	0	0	0.07 ± 0.07	0
Pereionotus testudo	1.89 ± 0.98	0.20 ± 0.13	0.60 ± 0.35	0.21 ± 0.11
Podocerus variegatus	0.89 ± 0.39	0	0.47 ± 0.27	0
Stenothoe sp.	15.44 ± 5.86	0.50 ± 0.22	7.20 ± 4.62	0.29 ± 0.16
Urothoe elegans	0.11 ± 0.11	0	0	0
Caprella sp.	6.56 ± 2.75	15.00 ± 5.70	1.93 ± 0.96	0.36 ± 0.17
Amphipod asp.	10.00 ± 2.19	35.20 ± 6.11	14.87 ± 2.82	15.29 ± 3.37
Tanaidacea				
Araphura brevimanus	2.22 ± 0.85	0.10 ± 0.10	0	0.07 ± 0.07
Leptochelia savignyi	41.22 ± 12.59	14.20 ± 6.36	2.47 ± 0.56	2.29 ± 1.33
Tanais dulongii	0.11 ± 0.11	0.30 ± 0.15	0.80 ± 0.38	0.14 ± 0.14
Isopoda				
Sphaeromatidea	0.11 ± 0.11	1.70 ± 0.67	0.27 ± 0.15	0.36 ± 0.36
Asellota	0	0	0.13 ± 0.13	0
Decapoda	0	0	0.07± 0.07	0
Pagurus sp.	0.11 ± 0.11	0	0	0
Pycnogonida	0.11 ± 0.11	0	0	0
Acarina	0.22 ± 0.15	0	0	0
Echinodermata (Ophiuroidea)	0	0	0.13 ± 0.13	0

Appendix C:

Benthic functional groups cover at Vulcano and Methana (Chapter 5)

Appendix C1: mean (± SE, n=3-6) percent cover of benthic functional groups at Vulcano in 2012; C=control, P=procedural control, E=exclusion.

	May 2012					
Taxon	600 C	600 P	600 E	1200 C	1200 P	1200 E
Padina pavonica	4.17 ± 3.00	25.00 ± 12.58	8.33 ± 2.71	1.67 ± 1.67	4.17 ± 3.00	1.67 ± 0.83
Brown turf algae	25.00 ± 21.26	23.33 ± 23.33	20.42 ± 7.08	28.33 ± 8.33	36.67 ± 6.67	42.08 ± 10.42
Bare substratum	57.50 ± 28.98	39.17 ± 22.38	53.33 ± 6.31	73.33 ± 4.41	43.33 ± 21.86	40.83 ± 11.65
Filamentous brown algae	0	0	0	0	0	3.33 ± 3.33
Dictyotales	8.33 ± 6.01	5.00 ± 2.89	4.58 ± 1.87	1.67 ± 1.67	0	0
Chtamalus stellatus	0	0	1.25 ± 0.85	1.67 ± 1.67	0	0
Green turf algae	0	1.67 ± 1.67	0.42 ± 0.42	0	15.83 ± 15.83	9.58 ± 7.76
Filamentous green algae	0	0	0	0	0	1.67 ± 1.67
Acetabularia acetabulum	0	1.67 ± 0.83	0.42 ± 0.42	0	0	0.42 ± 0.42
CCA	0.83 ± 0.83	0.83 ± 0.83	3.33 ± 1.67	0	0	0
Laurencia sp.	0	0	0.42 ± 0.42	0	0	0
Anadyomene stellata	0	0	0.42 ± 0.42	0	0	0
Encrusting brown algae	0.83 ± 0.83	0.83 ± 0.83	0	0	0	0
Dasycladus sp.	0	0.83 ± 0.83	0.42 ± 0.42	0	0	0
Cystoseira sp.	3.33 ± 3.33	1.67 ± 1.67	1.67 ± 1.67	0	0	0
Serpulidae	0	0	0.83 ± 0.83	0	0	0
Cladophora sp.	0	0	0	0	0	0
Valonia utricularis	0	0	0	0	0	0
Actinia equina	0	0	0	0	0	0
Anemonia viridis	0	0	0	0	0	0
Articulated coralline algae	0	0	0	0	0	0

Verrucaria sp.	0	0	0	0	0	0
Peyssonnelia sp.	0	0	0	0	0	0
Ralfsia verrucosa	0	0	0	0	0	0
Caulerpa racemosa	0	0	0	0	0	0

	July 2012					
Taxon	600 C	600 P	600 E	1200 C	1200 P	1200 E
Padina pavonica	15.67 ± 6.98	34.67 ± 25.33	16.00 ± 4.68	1.00 ± 1.00	3.00 ± 2.08	4.50 ± 2.43
Brown turf algae	18.67 ± 15.30	11.00 ± 9.54	17.17 ± 8.83	45.00 ± 17.79	22.00 ± 4.36	39.33 ± 13.79
Bare substratum	36.67 ± 18.66	35.67 ± 19.06	36.50 ± 6.15	42.33 ± 15.59	65.67 ± 4.33	51.33 ± 12.66
Filamentous brown algae	1.00 ± 1.00	0	0	1.00 ± 1.00	2.33 ± 2.33	0
Dictyotales	0.67 ± 0.67	1.00 ± 1.00	1.67 ± 1.67	3.33 ± 3.33	0	0.33 ± 0.33
Chtamalus stellatus	0.67 ± 0.67	0.67± 0.67	6.17 ± 3.29	0.67 ± 0.67	1.33 ± 0.67	0.67 ± 0.42
Green turf algae	0	0	0	0	0	0
Filamentous green algae	0	0	0	0	0	0
Acetabularia acetabulum	0.67 ± 0.67	0.67 ± 0.67	1.67 ± 0.33	0	0	0.50 ± 0.50
CCA	18.33 ± 6.01	6.00 ± 4.58	11.00 ± 2.21	0.67 ± 0.67	1.67 ± 0.88	0.33 ± 0.33
Laurencia sp.	0	0	2.17 ± 0.79	0	0	0.50 ± 0.50
Anadyomene stellata	1.67 ± 0.88	1.00 ± 1.00	0.83 ± 0.54	4.00 ± 2.08	0.67 ± 0.67	1.17 ± 0.83
Encrusting brown algae	0	0	0	0	0	0
Dasycladus sp.	2.33 ± 2.33	3.33 ± 3.33	3.17 ± 1.30	0	0	0
Cystoseira sp.	0.67 ± 0.67	1.67 ± 0.88	1.50 ± 0.50	0	0	0
Serpulidae	1.67 ± 0.88	0	1.50 ± 1.15	0.67 ± 0.67	0	0.67 ± 0.42
Cladophora sp.	0	0	0.33 ± 0.33	0	1.67 ± 1.67	0
Valonia utricularis	0	0	0	0	0	0.67 ± 0.67
Actinia equina	0	0	0	0	1.00 ± 1.00	0
Anemonia viridis	0	1.00 ± 1.00	0	0	0	0
Articulated coralline algae	0	0.67 ± 0.67	0	0	0	0
Verrucaria sp.	0	0.67 ± 0.67	0	0	0	0

Peyssonnelia sp.	0	1.00 ± 1.00	0.33 ± 0.33	0	0	0
Ralfsia verrucosa	0	0	0	0	0	0
Caulerpa racemosa	0	0	0	0	0	0

September 2012

Taxon	600 C	600 P	600 E	1200 C	1200 P	1200 E
Padina pavonica	0.67 ± 0.67	18.33 ± 9.53	12.00 ± 4.31	0	1.67 ± 0.88	2.00 ± 0.77
Brown turf algae	48.33 ± 13.64	49.00 ± 11.79	52.00 ± 3.60	40.67 ± 21.30	80.33 ± 5.24	71.83 ± 14.50
Bare substratum	20.67 ± 11.10	8.33 ± 4.41	8.67 ± 5.24	25.00 ± 9.07	8.33 ± 4.41	10.50 ± 9.91
Filamentous brown algae	0	0	0	0	0	0
Dictyotales	5.67 ± 2.96	4.00 ± 1.00	2.17 ± 0.79	0	0	0.33 ± 0.33
Chtamalus stellatus	2.33 ± 1.45	1.00 ± 1.00	6.83 ± 2.93	1.33 ± 0.67	0.67 ± 0.67	4.17 ± 3.39
Green turf algae	0	0	0	0	1.00 ± 1.00	0.33 ± 0.33
Filamentous green algae	0	0	0	0	0	0
Acetabularia acetabulum	0	0.67 ± 0.67	0.33 ± 0.33	0.67 ± 0.67	0	0.33 ± 0.33
CCA	15.00 ± 5.00	8.33 ± 7.36	11.33 ± 4.14	3.33 ± 0.88	3.33 ± 0.88	1.83 ± 0.87
Laurencia sp.	0	0	0.83 ± 0.83	0	0	0.83 ± 0.83
Anadyomene stellata	1.67 ± 0.88	3.00 ± 1.73	2.83 ± 0.65	3.33 ± 2.03	1.00 ± 1.00	1.67 ± 1.17
Encrusting brown algae	0	0	0	0	0.67 ± 0.67	0
Dasycladus sp.	3.33 ± 3.33	3.33 ± 3.33	1.33 ± 0.88	0	0.67 ± 0.67	0.50 ± 0.50
Cystoseira sp.	0	1.00 ± 1.00	1.00 ± 0.63	8.00 ± 8.00	1.33 ± 0.67	1.17 ± 0.54
Serpulidae	0	1.00 ± 1.00	0.67 ± 0.42	0	0	0.33 ± 0.33
Cladophora sp.	0	0	0	10.67 ± 10.67	0	0.50 ± 0.50
Valonia utricularis	0	0	0	1.00 ± 1.00	0	0.33 ± 0.33
Actinia equina	0	0	0	0	1.00 ± 1.00	0
Anemonia viridis	0	0.67 ± 0.67	0	0	0	0
Articulated coralline algae	0	0.67 ± 0.67	0	0	0	0
Verrucaria sp.	0	0	0	0	0	0

Peyssonnelia sp.	0	0	0	0	0	0
Ralfsia verrucosa	2.33 ± 2.33	0	0	5.33 ± 1.67	0	3.33 ± 3.33
Caulerpa racemosa	0	0	0	0	0	0
			October 2012			
Taxon	600 C	600 P	600 E	1200 C	1200 P	1200 E
Padina pavonica	1.67 ± 0.88	12.33 ± 11.35	7.33 ± 3.24	0	lost	1.80 ± 1.36
Brown turf algae	41.33 ± 7.69	49.67 ± 14.10	46.67 ± 6.64	45.67 ± 13.86	lost	46.80 ± 15.56
Bare substratum	20.00 ± 1.00	10.33 ± 6.06	4.17 ± 3.60	23.00 ± 5.57	lost	28.80 ± 12.76
Filamentous brown algae	0	0	0	0	lost	0
Dictyotales	17.33 ± 11.85	0	4.17 ± 2.71	0.67 ± 0.67	lost	2.00 ± 1.55
Chtamalus stellatus	0	1.00 ± 1.00	4.33 ± 3.37	1.33 ± 0.67	lost	1.20 ± 0.49
Green turf algae	0	0	0	0	lost	0
Filamentous green algae	0	0	0	0	lost	0
Acetabularia acetabulum	0	0.67 ± 0.67	0	0	lost	0.40 ± 0.40
CCA	17.67 ± 3.71	13.33 ± 8.82	14.50 ± 4.75	5.00 ± 1.15	lost	3.80 ± 2.46
Laurencia sp.	0	0	0.83 ± 0.83	0	lost	0
Anadyomene stellata	0.67 ± 0.67	3.00 ± 0.58	1.83 ± 0.75	2.67 ± 1.45	lost	2.00 ± 2.00
Encrusting brown algae	0	0	0	0	lost	0
Dasycladus sp.	0	8.33 ± 8.33	4.33 ± 2.76	0	lost	1.00 ± 1.00
Cystoseira sp.	0	1.67 ± 1.67	10.33 ± 5.58	15.33 ± 15.33	lost	7.80 ± 4.07
Serpulidae	0.67 ± 0.67	0.67 ± 0.67	0.50 ± 0.50	0	lost	0.60 ± 0.60
Cladophora sp.	0	0	0	2.33 ± 2.33	lost	0.40 ± 0.40
Valonia utricularis	0	0.67 ± 0.67	0.33 ± 0.33	0	lost	0
Actinia equina	0	0	0	0	lost	0
Anemonia viridis	0	1.00 ± 1.00	0	0	lost	0
Articulated coralline algae	0	0	0	0	lost	0
Verrucaria sp.	0	0	0	3.33 ± 3.33	lost	3.40 ± 3.40
Peyssonnelia sp.	0	0	0	0	lost	0

Ralfsia verrucosa	0	0	0	0	lost	0
Caulerpa racemosa	0	0	0.67 ± 0.42	0	lost	0

Appendix C2: mean (± SE, n=3-4) percent cover of benthic functional groups at Methana in June 2013; C=control, P=procedural control, E=exclusion.

Functional group	REF A_C	REF A_P	REF A_E	SEEP_C	SEEP_P	SEEP_E
Turf algae	49.50 ± 16.59	33.00 ± 6.51	29.25 ± 7.98	4.00 ± 1.83	25.33 ± 9.40	1.67 ± 1.67
Fucoid algae	0	0.33 ± 0.33	0.50 ± 0.50	9.25± 4.11	9.67 ± 1.45	1.33 ± 1.33
Fleshy brown algae	0	1.67 ± 1.67	0	0	0	33.33 ± 33.33
Calcifying brown algae	0	0	50.75 ± 17.72	0	0	30.00 ± 28.02
Encrusting black sponge	0.25 ± 0.25	0	0	2.00 ± 2.00	0.33 ± 0.33	0
Encrusting green algae	14.50 ± 10.27	8.33 ± 4.91	0.25 ± 0.25	27.25 ± 4.61	14.33 ± 9.77	0
Erect brown algae	0	0.33 ± 0.33	2.00 ± 2.00	2.25 ± 2.25	0	24.33 ± 19.55
Biofilm	0	0	0.25 ± 0.25	5.00 ± 2.68	1.00 ± 0.58	4.00 ± 4.00
Serpulids	0	0.33 ± 0.33	0	0	0	0
CCA	12.50 ± 2.90	8.00 ± 3.61	3.75 ± 2.25	1.25 ± 0.48	0.67 ± 0.67	0
Bare substratum	23.25 ± 4.80	48.00 ± 9.17	13.25 ± 6.17	49.00 ± 5.35	48.67 ± 11.67	5.33 ± 3.53

Appendix D:

Epifaunal abundance at Methana (Chapter 7)

Appendix D1: mean (± SE) abundance of epifaunal invertebrates exposed or not exposed to copper at Methana in June 2013.

Site	REF		SEEP	
Copper	no (n=4)	yes (n=5)	no (n=5)	yes (n=5)
Polychaeta				
non calcifying	14.75± 3.97	14.40 ± 3.01	10.60 ± 5.56	31.40 ± 11.45
Serpulidae	0.25 ± 0.25	0.40 ± 0.40	0	0
Oligochaeta	1.50 ± 0.96	1.00 ± 0.63	0.40 ± 0.24	0
Sipuncula	0.75 ± 0.48	0.20 ± 0.20	0	0
Mollusca				
Gasteropoda				
Bittium reticulatum	0.50 ± 0.29	0.40 ± 0.24	0	0
Columbella rustica	0.50 ± 0.29	0	0	0
Gasteropoda sp. 1	0	0.20 ± 0.20	0	0
Gasteropoda sp. 2	0.25 ± 0.25	0.20 ± 0.20	0	0
Gasteropoda sp. 3	0.25 ± 0.25	0	0	0
Gasteropoda sp. 4	0.25 ± 0.25	0	0	0
Muricidae sp 1	0.25 ± 0.25	0	0	0
Odostomia acuta	3.00 ± 1.78	4.60 ± 2.04	0	0
Rissoa sp.	0	0	0.20 ± 0.20	0
Rissoidae sp. 1	0.75 ± 0.75	0	0	0
Bivalvia				
Arca noeae	0.50 ± 0.50	0	0.20 ± 0.20	0
Bivalvia sp. 1	0.25 ± 0.25	0.80 ± 0.37	0.20 ± 0.20	0.20 ± 0.20
Bivalvia sp. 2	0.25 ± 0.25	0	0.20 ± 0.20	0
Ostrea sp.	0.25 ± 0.25	0	0	0
Striarca lactea	0	0.20 ± 0.20	0	0
Crustacea				
Ostracoda	2.25 ± 1.65	5.80 ± 1.56	6.80 ± 3.40	6.20 ± 1.56
Copepoda	41.00 ± 12.21	25.40 ± 6.36	110.40 ± 56.21	64.20 ± 20.12
Amphipoda				
Elasmopus sp.	2.25 ± 1.03	1.60 ± 0.68	3.60 ± 1.83	4.00 ± 1.14
Hyale perieri	0	0	0	0.20 ± 0.20
Hyale schmidtii	0	0	8.00 ± 3.79	1.20 ± 0.49
Hyale camptonyx	0	0	1.40 ± 0.75	0
Hyale crassipes	0.25 ± 0.25	0.20 ± 0.20	0.40 ± 0.24	0
Apherusa chierieghinii	0.50 ± 0.29	0.40 ± 0.24	0	0
Dexamine spiniventris	0	0.20 ± 0.20	0	0

Erichtonius sp.	0	0.20 ± 0.20	1.40 ± 0.98	0.80 ± 0.37
Pereionotus testudo	0	0.20 ± 0.20	1.40 ± 0.98	1.00 ± 0.45
Peltocoxa gibbosa	0	0	0.20 ± 0.20	0
Podocerus variegatus	1.50 ± 1.19	0.60 ± 0.40	0.60 ± 0.24	0.80 ± 0.37
Stenothoe sp.	5.75 ± 1.89	2.80 ± 0.80	0.80 ± 0.58	1.40 ± 0.93
Gammaropsis sp.	0	0	0.20 ± 0.20	2.60 ± 1.66
Maera grossimana	0	0	0.40 ± 0.24	0
Maera inaequipes	0	0.80 ± 0.80	0.20 ± 0.20	1.60 ± 1.12
Maera sp.	2.25 ± 0.95	3.60 ± 1.60	3.00 ± 1.58	4.60 ± 1.60
Ampithoe riedlii	0	0	7.40 ± 1.89	1.60 ± 0.51
Ampithoe ramondi	0	0	4.20 ± 2.18	1.20 ± 0.73
Aoridae sp.	1.00 ± 0.01	0	5.00 ± 2.59	2.40 ± 0.51
Tanaidacea				
Caprella acanthifera	0.50 ± 0.50	0.40 ± 0.24	0	0.40 ± 0.24
Leptocheira savignyi	11.00 ± 2.38	9.80 ± 3.40	25.00 ± 3.91	17.60 ± 2.64
Tanais cavolinii	0.25 ± 0.25	0.80 ± 0.37	0	0
Leptognathia brevimanu	0.50 ± 0.50	0	0	0
Isopoda				
Asellopoda	3.75 ± 2.39	1.00 ± 0.45	13.40 ± 4.87	2.40 ± 0.40
Flabellifera	2.50 ± 0.96	2.80 ± 0.92	0.80 ± 0.37	0
Cumacea	0.50 ± 0.29	0	0	0
Decapoda	0.50 ± 0.29	0	0	0
Pycnogonida	0.25 ± 0.25	0.20 ± 0.20	0	0.40 ± 0.24
Echinodermata				
Amphiura sp.	0	0.40 ± 0.40	2.80 ± 1.50	0.20 ± 0.20

Appendix E:

Publications

Appendix E1:

C. Baggini, M. Salomidi, E. Voutsinas, L. Bray, E. Krasakopoulou, J.M. Hall-Spencer (2014). Seasonality affects macroalgal community response to increases in pCO_2. *PLoS ONE*, 9: e106520.

OPEN ACCESS Freely available online

PLOS | ONE

Seasonality Affects Macroalgal Community Response to Increases in pCO_2

Cecilia Baggini[1]*, Maria Salomidi[2], Emanuela Voutsinas[2], Laura Bray[1,2], Eva Krasakopoulou[2,3], Jason M. Hall-Spencer[1]

1 Marine Biology and Ecology Research Centre, Plymouth University, Plymouth, United Kingdom, **2** Institute of Oceanography, Hellenic Centre for Marine Research, Anavissos, Attica, Greece, **3** Department of Marine Sciences, University of the Aegean, Lesvos, Greece

Abstract

Ocean acidification is expected to alter marine systems, but there is uncertainty about its effects due to the logistical difficulties of testing its large-scale and long-term effects. Responses of biological communities to increases in carbon dioxide can be assessed at CO_2 seeps that cause chronic exposure to lower seawater pH over localised areas of seabed. Shifts in macroalgal communities have been described at temperate and tropical pCO_2 seeps, but temporal and spatial replication of these observations is needed to strengthen confidence our predictions, especially because very few studies have been replicated between seasons. Here we describe the seawater chemistry and seasonal variability of macroalgal communities at CO_2 seeps off Methana (Aegean Sea). Monitoring from 2011 to 2013 showed that seawater pH decreased to levels predicted for the end of this century at the seep site with no confounding gradients in Total Alkalinity, salinity, temperature or wave exposure. Most nutrient levels were similar along the pH gradient; silicate increased significantly with decreasing pH, but it was not limiting for algal growth at all sites. Metal concentrations in seaweed tissues varied between sites but did not consistently increase with pCO_2. Our data on the flora are consistent with results from laboratory experiments and observations at Mediterranean CO_2 seep sites in that benthic communities decreased in calcifying algal cover and increased in brown algal cover with increasing pCO_2. This differs from the typical macroalgal community response to stress, which is a decrease in perennial brown algae and proliferation of opportunistic green algae. *Cystoseira corniculata* was more abundant in autumn and *Sargassum vulgare* in spring, whereas the articulated coralline alga *Jania rubens* was more abundant at reference sites in autumn. Diversity decreased with increasing CO_2 regardless of season. Our results show that benthic community responses to ocean acidification are strongly affected by season.

Citation: Baggini C, Salomidi M, Voutsinas E, Bray L, Krasakopoulou E, et al. (2014) Seasonality Affects Macroalgal Community Response to Increases in pCO_2. PLoS ONE 9(9): e106520. doi:10.1371/journal.pone.0106520

Editor: Erik V. Thuesen, The Evergreen State College, United States of America

Received May 15, 2014; **Accepted** August 2, 2014; **Published** September 3, 2014

Data Availability: The authors confirm that all data underlying the findings are fully available without restriction. All relevant data are within the paper and its Supporting Information files.

Funding: This work was funded through a MARES Grant to CB. MARES is a Joint Doctorate programme selected under Erasmus Mundus coordinated by Ghent University (FPA 2011-0016). Check www.mares-eu.org for extra information. Part of the sampling was funded by the EU FP7 project 'Mediterranean Sea Acidification under a changing climate' (grant agreement no. 265103). The funders had no role in study design, data collection and analysis, decision to publish, or preparation of the manuscript.

Competing Interests: The authors have declared that no competing interests exist.

* Email: cecilia.baggini@plymouth.ac.uk

Introduction

Increasing anthropogenic atmospheric CO_2 is altering the chemistry of surface seawater worldwide, resulting in ocean acidification. Mean surface ocean pH has already decreased by 0.1 units (a 30% increase in H^+ concentration) compared to pre-industrial times, and is rapidly decreasing [1]. Studies on the effects of ocean acidification indicate that it will impact a wide array of fundamental biogeochemical and biological processes. Early work on the effects of ocean acidification involved experiments that focused on single species in laboratory conditions, where pH variability was minimised, for periods of up to 18 months [2]. This body of work has rapidly advanced our knowledge of the relative sensitivity of different species, which can be used to formulate hypotheses on responses at the community level, although there is a growing realisation of the need to incorporate natural pH variability and species interactions into ocean acidification research [3,4].

Interactions between species can cause unpredicted responses to increased levels of pCO_2. For instance, Hale *et al*. [5] report that most invertebrate taxa in a mesocosm experiment responded to increased pCO_2 as expected from single species experiments. Nematodes, however, unexpectedly increased in abundance, probably because of altered species interactions. Community responses to ocean acidification will also depend on indirect effects of carbon dioxide, such as altered animal behaviour [6]. Thus, physiology and ecological niche cannot fully predict a species'susceptibility to environmental changes [7]. Moreover, laboratory and mesocosm experiments are usually too brief to ascertain the effect of increased carbon dioxide on climax communities comprising long-lived organisms [2]. Hypotheses formulated using data from short-term single-species laboratory experiments thus need to be tested in complex communities, ideally in real marine ecosystems [8].

Areas chronically exposed to high pCO_2 can be used to assess long-term community responses to ocean acidification [9,10].

Hydrothermal seeps with high pCO_2 levels occur worldwide [11], but many CO_2 seeps also have steep gradients in temperature, salinity, total alkalinity, toxic gases and metals, which could confound the ecological effects of carbon dioxide [12]. In addition, volcanic fluids are often enriched in ammonia, silicate and phosphate [13]. Baseline surveys are therefore needed to check the extent to which vent systems can be used as natural ocean acidification laboratories [14,15].

Only a few CO_2 seeps have so far been located that are suitable for use as ocean acidification analogues, namely seeps off Italy [9], Papua-New Guinea [16] and Japan [18]. Studies of these sites have shown that benthic biodiversity decreases as seawater pCO_2 levels increase [10,19–22]. Replication of such studies in a wider range of settings would strengthen the evidence for the ecosystem effects of increasing pCO_2 at the landscape scale. Previous studies found that well-fed individuals are more resilient to ocean acidification [23]; a natural ocean acidification analogue in the Eastern Mediterranean could reveal how marine organisms respond to increased CO_2 levels in oligotrophic areas. This is of global relevance since nutrient-poor regions are thought to be expanding worldwide due to increased thermal stratification of ocean waters caused by ongoing climate change [24].

Most laboratory experiments into the effects of ocean acidification on macroalgae have focused on calcifying species such as coralline algae and *Halimeda* spp.; responses of brown seaweeds to increased carbon dioxide are poorly known [25,26], even though they are keystone habitat-forming species in temperate regions worldwide[27]. In addition, many experiments on temperate seaweeds have been performed under constant temperature and light regimes, which are not representative of the daily and seasonal fluctuation these organisms experience in nature [28]. Even when macroalgae are exposed to natural temperature and light fluctuation (e.g. using outdoor mesocosms with continuous seawater pumping), experiments are rarely replicated to encapsulate seasonal responses. Seasonal surveys can easily be made at shallow coastal ocean acidification analogues [22], but have rarely been performed. We therefore have scarce knowledge of how seaweeds may respond to ocean acidification over yearly cycles, even though seasonality heavily influences biological responses to ocean acidification [29].

Temperate marine ecosystems undergo large yearly changes in light and temperature regimes, which indirectly influence other factors important for biological communities such as nutrient levels [30]. In the Mediterranean Sea, these three factors strongly influence macroalgal communities: macroalgal biomass peaks in late spring, and community composition changes among seasons [31]. Specifically, many turf algae disappear and most erect algae decrease in cover during the cold season [32].

Our limited ability to predict community responses of macroalgal communities to ocean acidification, and an overall paucity of research performed on Mediterranean species, add value to studies examining community responses to ocean acidification using CO_2 vents in the Mediterranean Sea. Results from surveys off Ischia and Vulcano (both in Italy) show how increased carbon dioxide is likely to cause changes in macroalgal communities: as CO_2 increases coralline algae are replaced by fleshy brown algae such as *Dictyota* spp., *Cystoseira* spp. and *Sargassum vulgare* [22] together with decalcified *Padina pavonica* [33]. This response to increased CO_2 differs from shifts towards opportunistic macroalgal species such as *Ulva* spp. or mat-forming algae reported in stressed marine benthic ecosystems [34–38]; there decreased floral complexity can have detrimental effects on local biodiversity [39] and indirectly affect the abundance of many fish species of commercial importance, such as labrids [25,40]. Carbon dioxide can be a resource that benefits carbon-limited fleshy algae [22,36].

The aim of this study was first to determine whether CO_2 seeps off Methana (Aegean Sea, Greece) were suitable for ocean acidification studies, so we monitored temperature, salinity, pH, Total Alkalinity and the concentrations of heavy metals, hydrogen sulphide and inorganic nutrients (nitrite, nitrate, ammonium, phosphate and silicate). As identifying changes in benthic community composition and abundance in a wide range of environmental conditions is crucial to improve predictions of future ecosystem function, we assessed whether benthic communities changed near the CO_2 seeps in a manner that could be predicted from previous studies. Since timing can influence biological responses to increased carbon dioxide, from mollusc and coral calcification [41] to change in crops yield [42], we assessed whether responses to ocean acidification were modulated by seasonality.

Methods

Study area

Methana is a peninsula on the NE coast of Peloponnese in Greece, located at the western end of the Southern Aegean Volcanic Arc, formed by subduction of the African tectonic plate beneath the Eurasian plate. The last eruption on Methana was in 230 BC, but the area is still hydrothermally active [13]. The CO_2 seeps studied here are located on the northern part of the peninsula. They appeared shortly after the last volcanic eruption, and thermal baths adjacent to the marine seeps have been used since at least the 1st century AD [43]. Gas emissions at our Methana study site are mainly carbon dioxide, with smaller amounts of nitrogen, carbon monoxide and methane (Table 1). Methane concentrations (17–26 ppm) are much lower than those detected at ocean acidification analogues off Ischia (200–800 ppm [9]), Vulcano (1700 ppm [15]) and Papua New Guinea (87–4360 ppm [16]).

The study area is part of the Saronikos Gulf (Central Aegean Sea); this part of Greece is characterised by a Mediterranean climate with strong seasonal differences in temperature, precipitation and day length (Figure 1). The Saronikos Gulf is generally oligotrophic except for its NE part, where wastewater treatment and other anthropogenic pressures along the wider Athens metropolitan coastal front result in increased nutrient loads [44]. Average air temperature varies from 10°C in winter to over 28°C in summer, with sea temperature ranging from 14°C in winter to 25°C in summer. Day length peaks at 14 hours and 43 minutes in June, and is shortest in December (9 hours and 51 minutes).

Site descriptions

Preliminary surveys revealed that a small area (~20 m of shoreline) near the main CO_2 seeps had a pH_{NBS} constantly below 8.0 (Figure 2), while a much more extensive area had pH variability that exceeded the background conditions of the reference sites.

Five sites were selected that had comparable geomorphology and wave exposure, but different pH regimes: a site with pH<8.0 near the main seeps (SEEP), two sites with variable pH located approximately 200 m eastwards and westwards of the seep area (200 E and 200 W) and two reference sites, one just outside the variable pH area (REF A) and one at a more distant site unaffected by volcanic activity (REF B). Wave exposure was estimated using methods in Howes *et al.* [45]. All sites had large boulders and a low degree of urbanisation. Photographs of the typical benthic communities at SEEP and 200 E are shown in Figure 3. The

Table 1. Composition of gases at Methana seep site.

Date	CO_2 (ppm)	N_2 (ppm)	O_2 (ppm)	CH_4 (ppm)	CO (ppm)	He (ppm)	H_2 (ppm)
04/06/2006	991000	10700	<400	26	1.6	<5	<5
23/06/2006	970000	30900	5600	17	1.7	<5	<5

Carbon dioxide accounts for over 90% of the emitted gases, with smaller percentages of nitrogen, oxygen, methane, carbon monoxide, helium and hydrogen (data from [17]).
doi:10.1371/journal.pone.0106520.t001

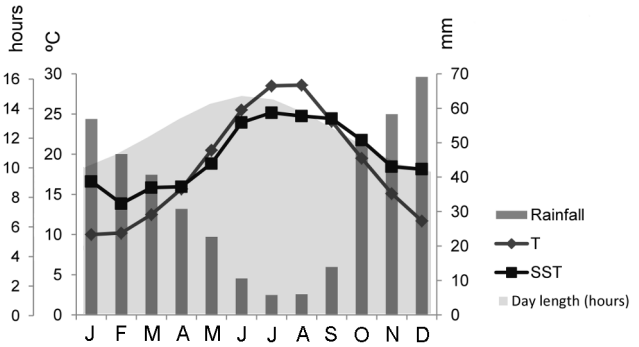

Figure 1. Long-term monthly average day length (hours), rainfall (mm), air temperature (T, °C) and Sea Surface Temperature (°C) for the Saronikos Gulf. SST data are from the World Ocean Atlas 2013 (NOAA), all other data from the World Meteorological Organisation.
doi:10.1371/journal.pone.0106520.g001

dominant canopy-forming macroalgal species in all sites at < 1.5 m depth was *Cystoseira corniculata*, a fucoid alga characteristic of the Eastern Mediterranean Sea [46]. *Cystoseira* spp. are considered indicators of good environmental conditions [47,48] and *C. corniculata* is common on relatively exposed Eastern Mediterranean rocky shores [49]. No specific permits were required for collecting samples in the present location, as none of the sampling sites are subject to particular protection restrictions, privately-owned or protected in any way; no protected species were sampled in this study.

Seawater physico-chemical parameters

The seeps were monitored from 2011 to 2013 (September 2011, January, February, May and September 2012, June and September 2013); seawater physicochemical parameters were measured at different times of the day and in different meteorological conditions during each trip. Surface seawater pH, temperature and salinity were measured using a multiprobe (YSI 63). The probe was calibrated before use with pH 4.01, 7.01 and 10.01 NBS standards. Since variations of up to 1 pH unit were detected over a few hours at the high CO_2 site, the uncertainty in using the NBS scale for seawater pH measurements (approximately 0.05 pH [50]) was considered acceptable for this study. For pH, medians and interquartile ranges (IQ) were calculated from hydrogen ion concentrations before re-converting back to pH values following seep monitoring methods advised by Kerrison *et al.* [14].

Seawater samples for Total Alkalinity (A_T) determination were collected in 125 ml borosilicate glass bottles with Teflon caps. Three samples per site were collected during each visit, immediately poisoned with $HgCl_2$ and stored in the dark until analysis. Samples were analysed by Gran titration (AS-ALK 2, Apollo SciTech) and the reliability of the measurements was checked against standard seawater samples provided by A. Dickson (batch 121). The average A_T value per site and individual pH measurements were used to calculate pCO_2, HCO_3^-, CO_3^{2-}, Ω_{Ar} and Ω_{Ca} using the CO2SYS software [51].

Seawater nutrient concentrations

In June 2013 three water samples per site were collected for nutrient analysis. Samples were stored frozen (−20°C), then analysed using a BRAN+LUEBBE II autoanalyser. Inorganic phosphate determination followed the colorimetric method of Murphy and Riley [52] and nitrite ions (NO_2^-) were measured colorimetrically according to Bendscheider and Robinson [53].

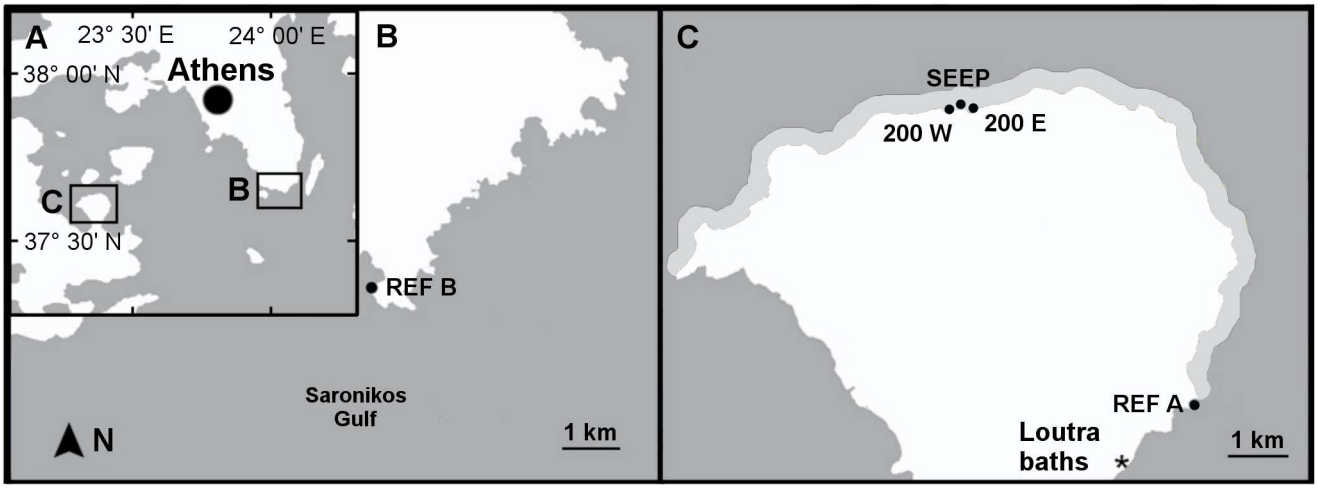

Figure 2. Study sites (points), Loutra baths (*) and area where pH was more variable than at reference sites (light grey). Geographical data downloaded from OpenStreetMap and modified using GNU Image Manipulation Program 2.8.
doi:10.1371/journal.pone.0106520.g002

Determination of nitrate (NO_3^-) was performed after its reduction to nitrite, which was then determined colorimetrically as above. Silicate was determined by adding a molybdate solution to the sample. The silicomolybdic acid that formed was then reduced to an intensely blue-coloured complex by adding ascorbic acid as a reducing agent [54]. The determination of ammonium was performed according to Koroleff [55] using a Perkin Elmer 25 Lambda spectrophotometer.

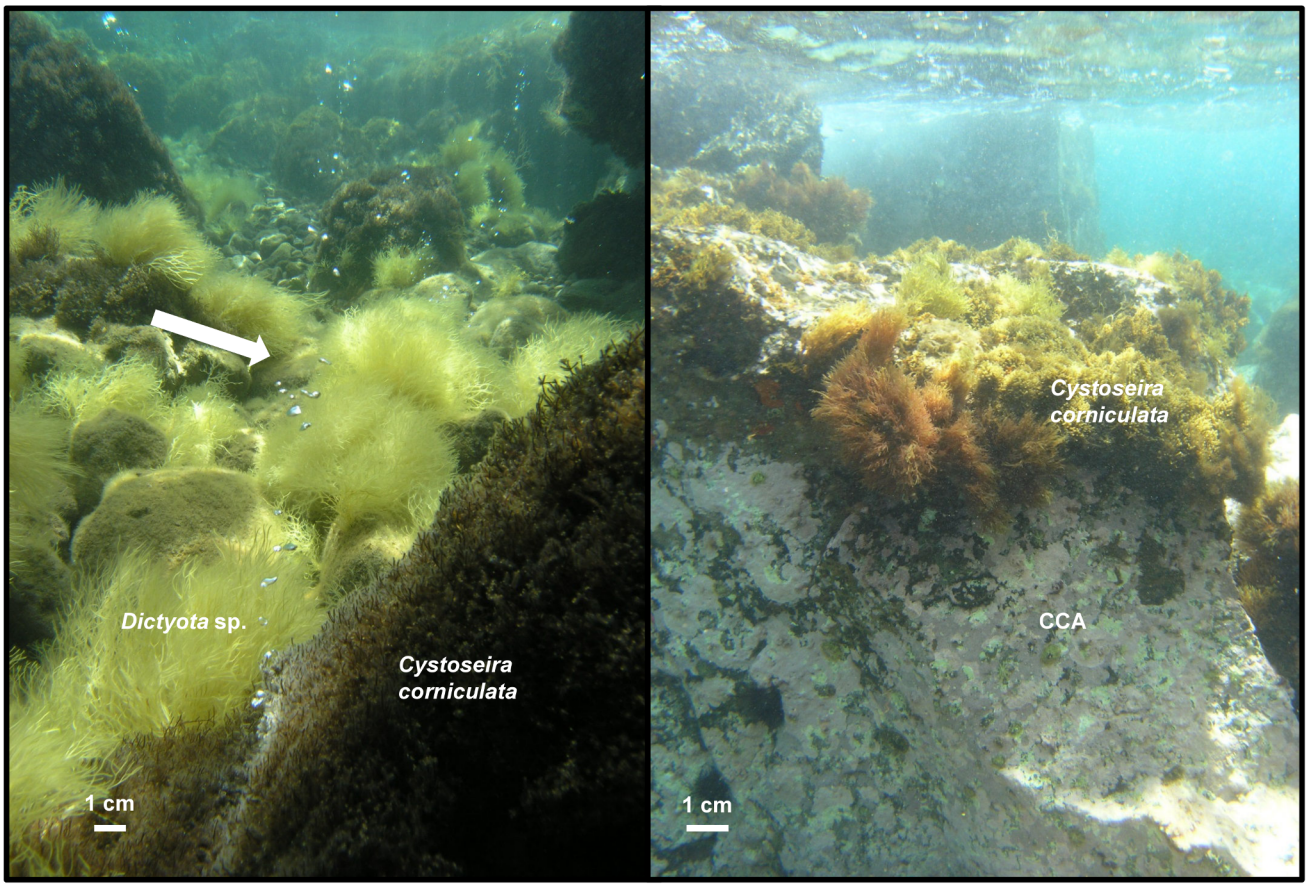

Figure 3. Typical appearance of benthic communities at SEEP (left) and 200 E (right) sites at 0.5 m depth in May 2012 with CO_2 bubbles seeping from the sea floor (arrow). Brown algae (e.g. *Dictyota* sp.) are dominant near the seeps; crustose coralline algae (CCA) become dominant as CO_2 levels decrease.
doi:10.1371/journal.pone.0106520.g003

Table 2. Seawater carbonate chemistry at Methana.

Site		pH (NBS)	TA (mmol/kg)	pCO_2 (μatm)	HCO_3^- (mmol/kg)	CO_3^{2-} (mmol/kg)	Ω_{Ar}	Ω_{Ca}
SEEP	Min	6.53	2.639	24092	2.771	0.006	0.09	0.13
($n_{pH} = 40$, $n_{TA} = 23$)	Median	7.69	2.794	1754	2.538	0.104	1.16	2.45
	Max	7.99	2.944	691	2.243	0.225	3.45	5.20
200 W	Min	6.64	2.696	18652	2.773	0.007	0.11	0.17
($n_{pH} = 26$, $n_{TA} = 24$)	Median	7.96	2.771	872	2.366	0.177	2.70	4.12
	Max	8.14	2.941	526	2.138	0.271	4.18	6.29
200 E	Min	7.27	2.693	4505	2.658	0.038	0.57	0.88
($n_{pH} = 26$, $n_{TA} = 22$)	Median	7.88	2.739	1042	2.403	0.152	2.30	3.50
	Max	8.13	2.836	532	2.114	0.263	4.05	6.10
REF A	Min	7.99	2.640	773	2.261	0.183	2.84	4.30
($n_{pH} = 21$, $n_{TA} = 18$)	Median	8.11	2.708	550	2.106	0.246	3.78	5.70
	Max	8.22	2.769	393	2.049	0.269	4.04	6.18
REF B	Min	8.03	2.615	674	2.254	0.185	2.81	4.30
($n_{pH} = 19$, $n_{TA} = 15$)	Median	8.12	2.697	539	2.145	0.231	3.54	5.33
	Max	8.25	2.858	362	2.024	0.280	4.23	6.46

Measured (pH and total alkalinity) and corresponding calculated carbonate system parameters (pCO_2, bicarbonate and carbonate ions concentrations, saturation state of calcite and aragonite) at five sites using data from six surveys from September 2011 to September 2013. Sample sizes for pH and total alkalinity are shown below site name.

doi:10.1371/journal.pone.0106520.t002

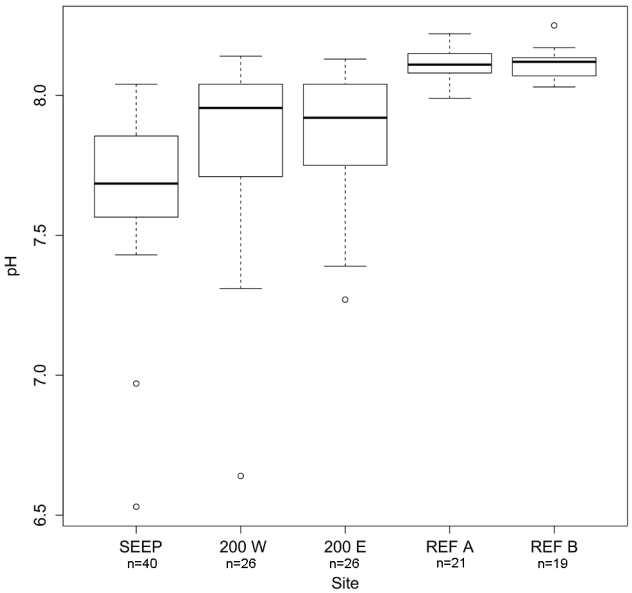

Figure 4. Variability in pH at the five study sites off Methana between September 2011 and September 2013. Horizontal line = median, vertical boxes = 25th and 75th percentiles, whiskers = min/max values if smaller than 1.5 times the inter-quartile range and dots = outliers.
doi:10.1371/journal.pone.0106520.g004

Free sulphides in seawater

Free sulphides were determined using a method modified from Cline [56]. Three seawater samples per site were collected in May 2012 using plastic syringes, and 2 ml of seawater were injected into a nitrogen-filled septum vial containing a small crystal of cadmium chloride. In order to validate the method, one sample was taken at the sulphide-rich Loutra thermal baths (location shown in Figure 2). For laboratory analysis, most of the water was removed by syringe after allowing the precipitate to settle. The samples were thus reduced to 0.8 ml volume, agitated to suspend all the precipitate and drawn up in a 1 ml disposable syringe which had been flushed with Ar.

Subsequently, 0.2 ml of a solution prepared using 400 mg of N,N-dimethyl-p-phenylene-diamine-dihydrochloride and 600 mg $FeCl_3.6H_2O$ dissolved in 100 ml 50% HCl were drawn into the same syringe. The argon bubble in the syringe was used to mix by inverting it a few times. The sample was left to stand for 20 minutes and then injected into a 1 ml semi-microcuvette and read in a Perkin Elmer Lambda 35 UV-VIS spectrometer at 670 nm. Standards were made using a 10 mM sodium sulphide stock solution (249 mg $Na_2S.9\ H_2O$ in 100 ml degassed Milli-Q water). The stock solution was diluted immediately before use in degassed seawater to give a range of 0.1 to 100 μM.

Heavy metals in macroalgae

Five individuals of *Dictyota* sp. (Phaeophyta) per site were collected at <2 m depth in May 2012, rinsed with fresh water to eliminate salt, gently brushed to remove epiphytes, kept frozen until transported to the laboratory and then freeze-dried. Freeze-dried macroalgae were ground with pestle and mortar and approximately 0.1 g of each sample was weighed in acid-washed Teflon tubes with a high precision digital scale (0.1 mg accuracy). Two ml of concentrated nitric acid were then added, and the tube containing the digestant was placed in a high-Throughput Microwave Reaction System Run (MARSXpress, CEM Corporation, Matthews, USA) and gently heated to boiling for at least 1 h to ensure full digestion. Samples were allowed to cool and then quantitatively transferred into pre-cleaned 10 ml volumetric flasks and diluted to volume with Milli-Q water. Blanks were prepared following the same procedure, but omitting the sample; a certified reference material (NIES Certified Reference Material No. 3, Chlorella) was simultaneously digested and analysed. Samples were then analysed for heavy metal content (Al, Cd, Cr, Co, Cu, Fe, Pb, Ni, Zn) using inductively coupled plasma optical emission spectrometry ICP-OES) and inductively coupled plasma mass spectrometry (ICP-MS) when concentrations were below the confidence interval of the ICP-OES.

Benthic communities

Benthic community composition was assessed in May and September 2012: samples were collected from 0.7–1.0 m below mean sea level using 20×20 cm quadrats on sub-horizontal rocky substratum following methods described by Fraschetti *et al*. [57]. A frame with 25 4×4 cm squares was used to assess percentage cover (C%) and number of taxa (S). Percentage cover of algae and sessile invertebrates was determined by assigning each taxon a score ranging from 0 to 4 within each square and summing the 25 estimates following methods described by Dethier *et al*. [58]. Taxa were identified to the lowest possible taxonomic level, usually species. Seven replicate quadrats, randomly chosen but placed at least 4–5 m from each other were assessed for every site in May 2012 and six replicates were collected in September 2012.

Statistical analyses

Analysis of nutrient and metal concentration data was performed using separate multivariate analyses of variance (MANOVA) with one factor (site). Normality and homogeneity of variances were tested by visually examining boxplots and residual error plots and using Levene's test, and transformed when necessary. When significant differences among sites were detected, a Tukey HSD test for multiple comparisons was performed. Analysis of pH data was performed using a non-parametric analysis (Kruskal-Wallis ANOVA) followed by pairwise multiple comparisons.

Differences in macroalgal community structure and composition were assessed by analysing macroalgal species percent cover with a Permutational Multivariate Analysis of Variance (PRIMER 6 and PERMANOVA + package [59]). The analysis had two fixed factors, season and site. The analysis was performed on Bray-Curtis measures of square-root transformed data, using 9999 permutations of residuals under a reduced model. Pair-wise comparisons were then performed for significant factors with more than two levels. The SIMPER analysis was then used to identify the taxa primarily responsible for the dissimilarity between sites.

Macroalgal cover data were used to calculate Shannon diversity [60] for each sample. The index was analysed using an ANOVA followed by a Tukey HSD test for multiple comparisons. Taxa driving community differences among sites (Table S6 in File S1) were grouped in two categories, canopy-forming algae (*Cystoseira corniculata*, *Cystoseira amentacea*, *Sargassum vulgare* and *Cladostephus spongiosum*) and calcifying algae (CCA, *Jania rubens*, *Corallina* sp., *Amphiroa* sp. and *Padina pavonica*). After testing for normality and homoscedasticity, canopy-forming and calcifying algae arcsin-transformed percent cover was analysed using a two-way ANOVA with site and functional group as fixed factors; seasons were tested separately. The site*functional group interaction was then decomposed to obtain multiple comparisons among sites for each season separately. The same analysis was then

Table 3. Average seawater nutrient concentrations (±SE, n = 3) at Methana in June 2013.

	SEEP	200 W	200 E	REF A	REF B	Bgd
NO_3 (μM)	0.070±0.036	0.094±0.040	0.559±0.297	0.054±0.032	0.085±0.026	0.42
NO_2 (μM)	0.054±0.002[a,b]	0.044±0.003[a,b]	0.059±0.004[b]	0.042±0.002[a,b]	0.040±0.005[a]	n.d.
NH_4 (μM)	0.232±0.099	0.265±0.109	1.075±0.318	0.203±0.109	0.298±0.053	0.36
PO_4 (μM)	0.025±0.005	0.031±0.007	0.038±0.009	0.024±0.004	0.044±0	0.12
SiO_4 (μM)	4.018±0.387[a,b]	6.371±1.841[a]	1.607±0.288[c]	1.883±0.127[b,c]	1.180±0.269[c]	1.22

For the five sites, nitrite, nitrate, ammonium, phosphate and silicate are shown. Background values (Bgd) for the Aegean Sea from Friligos [61]. Different letters indicate significantly different values according to post-hoc pairwise comparisons; n.d. = not determined.
doi:10.1371/journal.pone.0106520.t003

performed for selected single species. All univariate analyses were performed using SPSS v19.

Results

Seawater physico-chemical parameters

All sites were classified as semi-exposed according to the classification suggested by Howes *et al*. [45]. Table 2 shows that the seeps had the lowest median pH_{NBS} (7.69, IQ range 7.57–7.85, n = 40) and were significantly different from the intermediate sites, which had higher median values (7.87, n = 26 and 7.96, n = 26 for 200 E and 200 W, respectively; results of statistical analysis shown in Table S1 in File S1) and comparable variability (IQ ranges 7.75–8.04 and 7.73–8.03 for 200 E and 200 W, respectively). At intermediate sites pH sometimes exceeded 8.0. The reference sites had significantly higher pH values (median values of 8.11, n = 21 and 8.12, n = 19 for REF A and REF B, respectively) and lower variability (Figure 4).

Temperature and salinity varied seasonally and were uniform across sites. The minimum temperature was 14.2°C in February, whereas in summer the temperature could reach 26.8°C; salinity varied from 37.5 to 40.0 ppt. Total Alkalinity varied from 2.615 to 2.944 mmol*kg^{-1} with no seasonal trend (Table 2), with slightly lower values and less variability than CO_2 vents off Vulcano, where A_T varies between 2.78 to 3.17 mmol*kg^{-1} [15]. Seawater pCO_2 had a median value of over 1300 μatm at the SEEP site, almost three times the values calculated for the reference sites. The median saturation state of calcite and aragonite is always >1, although sites with high and intermediate pCO_2 levels were occasionally under-saturated with respect to both calcite and aragonite (Table 2).

Free sulphide concentrations were below the measurable limit (1 μM) for the method used at all five sites. In contrast, our sample from Loutra thermal baths had a concentration of free sulphides of 35 μM. Nutrient concentrations were similar to background levels in the Saronikos Gulf [61] except for silicate, which was mostly higher than the background value of 1.22 μM even at one of the reference sites (Table 3). When values were <LOQ. (Limit Of Quantification) they were substituted with LOQ/2; LOQ. = 0.126 μM for NO_2+NO_3 and 0.102 μM for NH_4. Statistically significant differences between sites were only detected for nitrite and silicate (Table S2 in File S1). Nitrite, however, had a very small range, varying from 0.040±0.005 μM in REF B to 0.054±0.002 μM in 200 E, and these were the only two sites that were significantly different. Silicate had a wider range (from 1.180±0.269 μM in REF B to 6.371±1.841 μM in 200 W); only site 200 W was significantly different from the reference sites according to pairwise comparisons. No significant differences and relatively uniform values were measured for phosphate, whereas nitrate and ammonium showed higher values at 200 E, although these differences were not significant, possibly due to high within-site variability.

Heavy metals in macroalgae

Measured concentrations of elements in the reference materials were used to assess the quality of the sample measurements; if measured values in the reference material were within 20% of certified values, the quantification of that element was considered

Table 4. *Dictyota* sp. metal content at the five sites.

Element	SEEP	200 W	200 E	REF A	REF B
Al	66.58±29.78[a]	391.84±222.71[b]	75.01±14.21[a,b]	314.62±108.93[a,b]	89.77±17.85[a,b]
As	15.90±1.03[a]	39.02±2.26[d]	25.79±2.68[c]	18.41±1.30[a,b]	22.52±0.37[b,c]
Cd	0.014±0.002[a]	0.018±0.003[a,b]	0.034±0.006[b,c]	0.573±0.102[c]	0.067±0.016[d]
Co	0.059±0.023[a]	0.107±0.020[a]	0.096±0.013[a]	1.613±0.316[b]	0.119±0.016[a]
Cr	0.857±0.070[a,b]	2.526±0.527[c]	0.579±0.050[a]	1.204±0.243[b]	1.093±0.218[a,b]
Cu	2.069±0.228[a]	3.160±0.269[a,b]	3.435±0.569[a,b]	7.726±1.492[c]	4.771±0.303[b,c]
Fe	587.1±42.8[b]	5659.8±603.9[a]	485.5±46.8[b,c]	316.3±88.5[c,d]	146.3±32.5[d]
Ni	0.916±0.100[a]	1.325±0.126[a]	1.338±0.578[a]	4.181±0.267[b]	2.554±0.103[b]
Pb	2.704±0.215[a]	17.605±9.465[b]	2.378±0.276[a]	25.979±11.705[b]	10.820±5.743[b]
Zn	10.95±5.25[a]	11.70±0.53[a]	8.22±0.83[a]	42.02±9.28[b]	14.68±0.60[a,b]

Means (±SE; mg/kg dry weight; n = 5) are shown for each metal and site; different letters indicate significant differences according to Tukey HSD test.
doi:10.1371/journal.pone.0106520.t004

Table 5. Comparison of metal concentration (mg/kg dry weight) in *Dictyota* spp. measured in this study with values found in the literature for unpolluted sites (n.d. = not determined; b.d.l. = below detection limit).

	This study	Abdallah *et al.*, 2005 [62]	McDermid and Stuercke, 2003 [63]	Raman *et al.*, 2013 [64]	
Element	**(means range)**	**(mean±SD, n = 3)**	**(range)**	**(mean±S.D., n = 3)**	**Maher and Clarke, 1984 [65]**
Al	66–391	n.d.	n.d.	n.d.	n.d.
As	15–39	n.d.	n.d.	n.d.	26.3
Cd	0.014–0.573	0.98±0.3	n.d.	3.9±0.3	n.d.
Co	0.059–1.613	4.3±1.2	n.d.	5.5±0.2	n.d.
Cr	0.579–2.526	1.1±0.3	n.d.	b.d.l.	n.d.
Cu	2–8	1.3±0.4	5	6.4±0.3	n.d.
Fe	316–5659	n.d.	438–608	504±12.4	n.d.
Ni	0.916–4.181	2.2±0.6	n.d.	27±0.4	n.d.
Pb	2–25	19.2±5.5	n.d.	28.5±3.5	n.d.
Zn	8–42	4.9±1.2	13–16	11.7±0.3	n.d.

doi:10.1371/journal.pone.0106520.t005

reliable. In the reference material analysed, all elements except Pb were within 20% of the certified values, where reported (i.e. excluding Al, Cr, Ni, As). Log-transformed metal concentrations were significantly different between sites for all elements analysed (Table S3 in File S1). Average concentration of elements in *Dictyota* sp. tissues and results of the Tukey HSD test are shown in Table 4. There was a great spatial variability in metal content, but no specific metal concentration consistently increased with decreasing pH. Particularly high concentrations were recorded at station 200 W for aluminium, arsenic and iron, and at REF A for aluminium and zinc.

Values higher than ranges reported in the literature for seaweed tissues from unpolluted sites (Table 5) were found for aluminium, arsenic and iron at 200W and for aluminium and zinc in REF A.

Benthic communities

Overall, 18 macroalgal taxa and three invertebrate taxa (two sponges and one hydrozoan) were recorded. Benthic communities significantly differed among sites and seasons (Table 6), with a significant interaction between the two factors (pseudo-$F_{4,55} = 1.754$, p(perm) = 0.0457). In spring the high pCO_2 site was significantly different from the reference sites, while the intermediate pCO_2 sites were not significantly different from any of them. In autumn, the high pCO_2 site was significantly different from all other sites (Table 7; results of pairwise comparisons shown in Table S4 in File S1). Site had a significant effect on diversity (p = 0.049, Table S5 in File S1) with a clear decreasing trend as CO_2 increased, as shown in Figure 5 (0.94±0.10, n = 26 to 0.55±0.08, n = 13; mean ±SE).

Percent cover of canopy-forming algae and calcifying algae are shown for May (Figure 6a) and September (Figure 6b). As no significant differences were found within intermediate and reference sites, pCO_2 levels were pooled for clarity. Both categories showed very strong seasonal patterns: no differences in canopy-forming algal cover were detected in May, but in September the high pCO_2 site had a trend towards higher canopy cover compared to the control sites. Likewise, calcifying algae showed no significant difference among pCO_2 levels in spring, but in autumn the high pCO_2 site had a significantly lower cover of calcareous algae compared to intermediate and control pCO_2 levels.

The species forming these two categories changed along the pCO_2 gradient depending on the season, and the main canopy-forming and calcareous species covers are shown for May and September in Figure 7a and 7b, respectively. As no significant differences were found within intermediate and reference sites, pCO_2 levels were pooled for clarity. In spring, *S. vulgare* was more abundant at the high pCO_2 site, but it was almost absent from all sites in autumn. In contrast, *C. corniculata* was more constant over time; its cover significantly increased in the high pCO_2 site from spring to autumn, while the opposite was true for the intermediate and reference sites, where *C. corniculata* cover

Table 6. PERMANOVA analyses on square-root transformed percentage cover of Methana benthic communities.

Source	df	SS	Pseudo-F	p (perm)	Unique perms
season	1	31069	19.234	**0.0001**	9949
site	4	21820	3.377	**0.0001**	9918
Season × site	4	11330	1.754	**0.0457**	9916
Residual	55	88840			
Total	64	1.5273E5			

The table shows main factors and their interaction and degrees of freedom (df), sum of squares (SS), pseudo-F, permutational p and unique permutations for each of them.

doi:10.1371/journal.pone.0106520.t006

Table 7. Pair-wise comparisons of macroalgal community structure and composition between sites for each season (different letters represent significantly different groups).

Season	Sites				
Spring	SEEP [a]	200 W [a,b]	200 E [a,b]	REF A [b]	REF B [b]
Autumn	SEEP [a]	200 W [b]	200 E [b]	REF A [b]	REF B [b]

doi:10.1371/journal.pone.0106520.t007

decreased from spring to autumn. As for the coralline algae, CCAs recruited earlier than *J. rubens* and reached their maximum cover in spring at the intermediate sites, while in the reference sites their cover increased from spring to autumn. The articulate coralline alga *J. rubens* had extremely low abundances at all sites in spring, while in autumn its percent cover decreased with increasing pCO_2 levels.

Discussion

Our results suggest that increased seawater pCO_2 has profound effects on macroalgal communities in oligotrophic conditions, but that sampling season strongly affects the response of benthic communities to ocean acidification. Below we firstly examine the suitability of CO_2 seeps off Methana for ocean acidification studies, and then discuss the effects of increased carbon dioxide on macroalgal communities.

Site suitability for ocean acidification studies

Seeps off northern Methana had a median pH value (7.69) similar to that predicted for 2100 according to the IPCC "business as usual" scenario [66], whereas the reference sites had median values above 8. The seeps had no confounding gradients in temperature, salinity, total alkalinity, hydrogen sulphide or wave exposure. The low pH area in Methana had pCO_2 levels comparable to those reported at other ocean acidification analogues [14–16], making it suitable to assess community responses to increased pCO_2. Macroalgal community data indicated that elevated carbon dioxide had a profound influence on community composition and structure in an oligotrophic environment, although patterns varied seasonally.

Enrichment in silicate, which was significantly different from reference values in one of the intermediate sites, is likely due to water-rock interactions common in hydrothermal environments [17]. However, it is unlikely that silicate is limiting in the Aegean Sea; for instance, Si becomes limiting to diatoms when the N:Si ratio in seawater is higher than two [67], whereas the background ratio for the Aegean Sea is 0.64 [61]. Significant differences in nitrite concentrations among sites are unlikely to explain the community changes either, as their range is very small (0.040–0.059 μM). Mediterranean organisms are normally not limited by silicate or inorganic nitrogen, but by phosphate [68], for which no confounding gradient was found.

No free sulphides were detected near the seeps, although they were present at the Loutra thermal baths, over 10 km from the study site. Hydrogen sulphide is toxic for cellular respiration, and it is often emitted from Mediterranean volcanic vents [13]. However, sulphides are extremely reactive and oxidise quickly to sulphates in oxygenated waters. It is therefore common to find very low or undetectable sulphide concentrations just a few meters away from volcanic seeps. For instance, at Vulcano sulphides become undetectable at 30 m from the main vents, even though hydrogen sulphide gas has a concentration of 400 ppm at the main bubbling site [15].

Brown algae are a good indicator of bioavailable metal since they are not able to regulate metal uptake [69]. Values higher than ranges reported in the literature were found for aluminium, arsenic and iron at 200 W and for aluminium and zinc in REF A (Table 6). Aluminium variability is likely to be related to local mineralogy [70], while enrichment in the other elements has previously been linked to hydrothermal activity [71]. Metal bioaccumulation is a common occurrence at shallow and deep hydrothermal vents [11], but at Methana metal enrichment did not seem to have major effects at the community and species level. The intermediate and reference sites enriched in some elements (200 W and REF A) were not significantly different from the other intermediate and reference sites (200 E and REF B) with regards to key species percent cover and overall community structure.

The need to translate results from laboratory experiments to more realistic systems has led to several areas with naturally high pCO_2 to be used to infer biological community responses to ocean acidification. Examples include estuaries acidified by acid sulphate soils [72], groundwater submarine springs [73] and upwelling regions [74]. None of the above are perfect ocean acidification analogues, as they can have confounding gradients in salinity and alkalinity (groundwater springs) or in temperature and nutrients (upwelling areas). In addition, low pH recorded in groundwater springs and acidified estuaries is not always caused by increased carbon dioxide concentrations, so only the effects of low pH on biological communities can be tested. However, studies from low pH/high CO_2 sites mostly report decreased abundance and diversity of calcifying organisms, in accord with findings from CO_2 seeps and laboratory experiments [2,9,10]. General patterns of community responses to ocean acidification can then be detected using areas with naturally low pH, even though confounding factors should always be taken into account.

As with other carbon dioxide seeps used as natural analogues for ocean acidification, Methana has some limitations. Mobile taxa

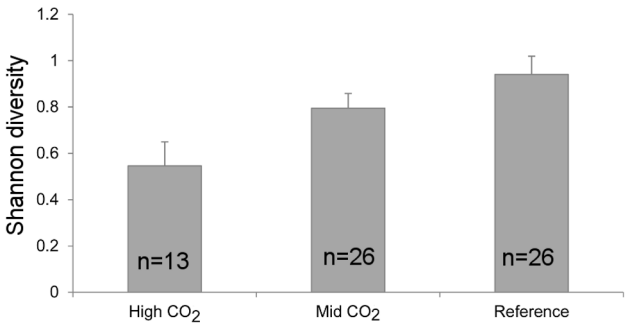

Figure 5. Shannon diversity (mean H' SE) of macroalgal communities at high, intermediate and reference CO_2 in Methana in May and September 2012.
doi:10.1371/journal.pone.0106520.g005

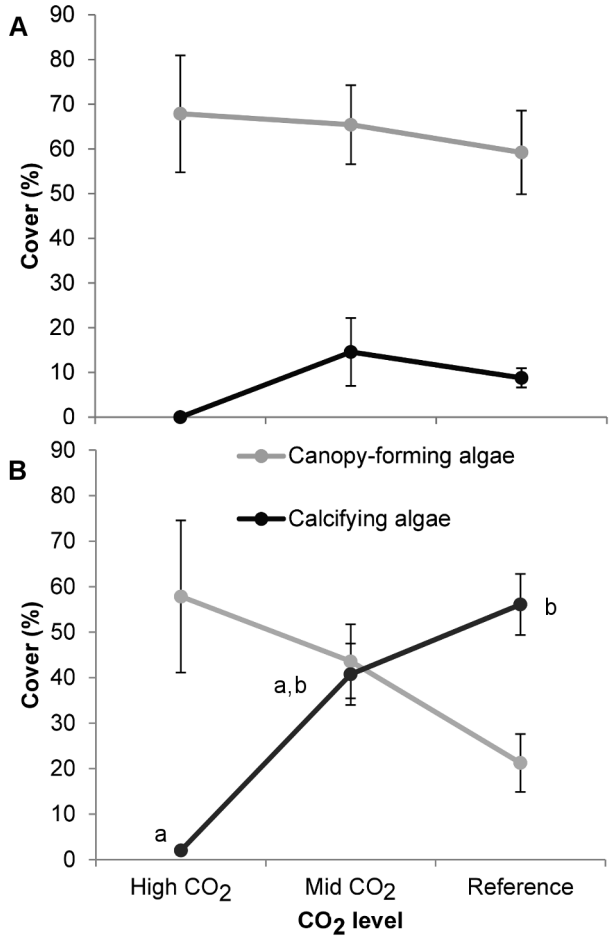

Figure 6. Mean percentage cover (±SE) of canopy-forming algae (grey) and calcifying algae (black) in May (a) and September (b) at high (n = 6), intermediate (n = 14) and reference (n = 14) CO_2 conditions off Methana. Different letters indicate significant differences between groups.
doi:10.1371/journal.pone.0106520.g006

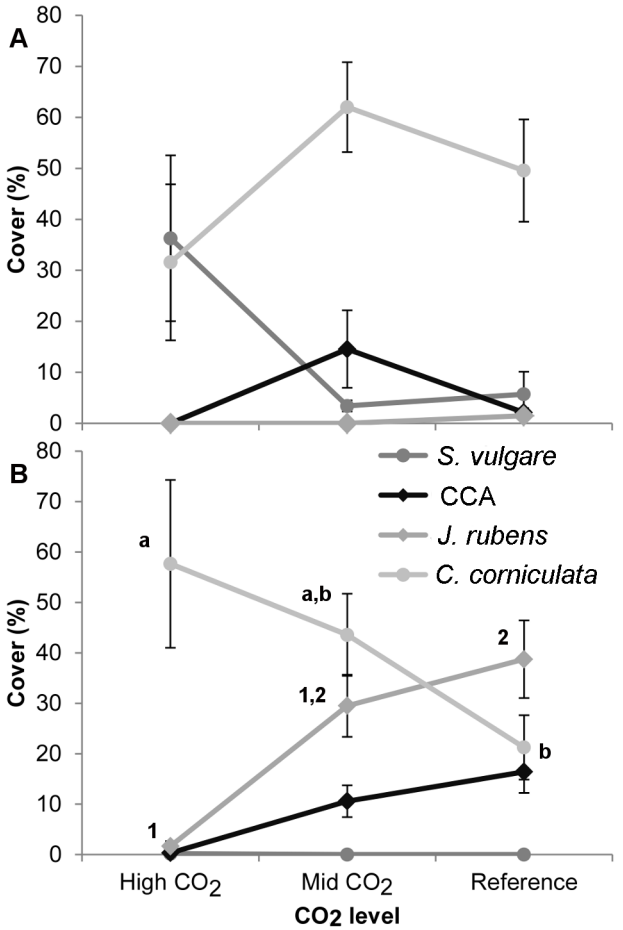

Figure 7. Mean percentage cover (±SE) of dominant macroalgal species in May (a) and September (b) at high (n = 6), intermediate (n = 14) and reference (n = 14) levels of CO_2 in Methana. Round points represent canopy-forming species (*S. vulgare* dark grey, *C. corniculata* light grey), rhomboids represent calcifying species (CCA black, *J. rubens* grey). Different letters and numbers indicate significant differences between groups.
doi:10.1371/journal.pone.0106520.g007

such as fish or some large invertebrates (e.g. cephalopods) are able to move in and out of high CO_2 areas [75] and pelagic larvae can come from unaffected populations [20]. Moreover, carbonate chemistry is much more variable near the seeps than in reference conditions, as changes in current direction and intensity influence the dispersal of the dissolved gas emissions. Compared to other volcanic seeps, at Methana seawater pCO_2 is high and variable on a greater scale (>15 vs <0.3 km of shoreline [9,15,16]). Thus, Methana might offer an opportunity to study ecological processes such as recruitment in a high CO_2 area probably less influenced by unaffected populations than smaller sites.

Macroalgal community responses to increased pCO_2

The present study shows that biological responses to elevated carbon dioxide are modulated by season. Macroalgal communities off Methana had year-round decreased diversity, especially of calcifying species, as carbon dioxide increased, in line with results from surveys at other CO_2 seeps [10,16,22] and from laboratory experiments [2,5]. Seasonality strongly affected community responses to increased pCO_2: coralline algal cover decreased while canopy-forming algae were more abundant as pCO_2 increased, but our sampling design only revealed a significant difference in autumn. This pattern has not been detected so far in macroalgal communities since most field studies have been carried out in one season, while laboratory and mesocosm experiments rarely last long enough to incorporate the effect of seasonality. Godbold and Solan [29] found that seasonality greatly affected invertebrate responses to both ocean acidification and increased temperature.

Our study did not detect an increase in mat-forming algae as CO_2 increased, in contrast with previous laboratory experiments [36]. However, another shallow subtidal survey off Italian CO_2 seeps [22] detected a decrease in mat-forming algal biomass at pCO_2 levels of about 1000 ppm. This shows that shifts to mat-forming algae do not necessarily happen at intermediate pCO_2 levels, especially if not associated with increased nutrient levels [36] or other disturbances disrupting kelp cover [76]. In this case, canopy-forming algae appear to increase their growth rates (authors' personal observation), suggesting that macroalgae can use intermediate carbon dioxide levels as a resource [77].

Decreased abundance of calcifying algae is consistent with previous results from volcanic seeps off Ischia, in Italy [22]. However, this pattern was only detected in autumn because of the marked annual cycle of the dominant coralline alga, *Jania rubens*. This species grows best at temperatures above 20°C and reaches

its biomass peak later than most other Mediterranean seaweed species [78]. Cover of crustose coralline algae (CCA) decreased as pCO_2 increased, confirming that calcifying algae are likely to be threatened by ocean acidification, especially those species living near their thermal limit [26]. Intermediate pCO_2 levels appeared to increase CCA abundance in spring, possibly because the energy surplus caused by carbon fertilisation is used to enhance calcification when pCO_2 is below 1000 µatm [79,80]. Recent studies found that CCA are more sensitive to rates, not magnitude, of ocean acidification [81] and that fluctuating pH reduces growth in an articulated coralline alga [4]: high variability in pCO_2 at the seeps could therefore lead to an over-estimation of its negative effects on coralline algae.

The increase in canopy-forming algal cover at high CO_2 was mostly caused by an increased abundance of *Sargassum vulgare* in spring and of *Cystoseira corniculata* in autumn. *Sargassum vulgare* was more abundant at high CO_2 also at volcanic seeps off Ischia [22] and Vulcano (authors' personal observation). However, this species was not seen in Methana in autumn because of its pronounced seasonal cycle. As for *C. corniculata*, it is likely that the higher autumnal cover in the elevated pCO_2 site was due to the absence of *S. vulgare* and *J. rubens*. In fact, the genus *Sargassum* can be advantaged over *Cystoseira* when competing for space [82], while *J. rubens* is an epiphyte that can overgrow canopy-forming algae and become dominant in autumn [77]. Physiological responses of *J. rubens* to high pCO_2 are likely to be the main determinant of its decrease in cover, but enhanced chemical defences of *C. corniculata* cannot be excluded, as some fucoid algae are carbon limited, and elevated CO_2 can cause a sharp increase in their defensive compounds [83].

Conclusions

Marine volcanic seeps off Methana (Aegean Sea) proved to be suitable for investigations into the response of rocky shore communities to high pCO_2 levels. We found that benthic community changes along pCO_2 gradients in the oligotrophic Mediterranean Sea are consistent across different nutrient regimes. Responses in temperate regions will probably be strongly influenced by seasonality and this alters species interactions during the year. The seeps at Methana revealed loss of diversity and reduced abundance of ecologically important calcifying algae at elevated carbon dioxide levels, adding to a growing body of evidence that ocean acidification is likely to alter coastal community composition [9,10,22].

Changes in benthic community structure may have profound effects on biological processes such as food web dynamics, nutrient cycling and primary productivity [84], thus affecting ecosystem functioning. Furthermore, ocean acidification is only one of the many changes marine ecosystems are facing. Additional stressors such as increased temperature or eutrophication are likely to exacerbate the negative effects of increased carbon dioxide [2,36]. Oligotrophic regions such as the Eastern Mediterranean are therefore extremely vulnerable to future environmental changes, since many organisms already live close to their upper thermal limits, as shown by several mass mortalities following heat waves in recent years [85]. Further research is needed to predict how benthic communities will respond to future environmental conditions, but we provide the first test of subtidal community responses to increased pCO_2 over different seasons and show that seasonal patterns can alter community responses to ocean acidification in warm-temperate coastal ecosystems.

Supporting Information

File S1 Supporting tables. Table S1. Results of the Kruskal-Wallis ANOVA and pairwise comparisons for pH data. Table S2. Effect of site on seawater nutrients as determined by MANOVA. Table S3. Effect of site on seaweed metal concentration as determined by MANOVA. Table S4. PERMANOVA pairwise comparisons of the benthic community structure and composition between sites for each season. Table S5. Effect of site and season on Shannon diversity as determined by ANOVA. Table S6. SIMPER table showing taxa driving difference between sites.
(DOCX)

Data S1 Carbonate chemistry, nutrient, heavy metal and biological community raw data.
(XLSX)

Acknowledgments

We thank A. Deidda for his invaluable help during sampling, A. Pavlidou and E. Rouselaki for analysing nutrient samples, P. Dando for help with the free sulphides analytical method, L. Pettit for reviewing the manuscript and K. Milonakis for providing us with the coordinates of the main bubbling site.

Author Contributions

Conceived and designed the experiments: CB JMHS. Performed the experiments: CB MS EV LB EK. Analyzed the data: CB. Contributed reagents/materials/analysis tools: EK. Contributed to the writing of the manuscript: CB JMHS.

References

1. Doney SC, Fabry VJ, Feely RA, Kleypas JA (2009) Ocean acidification: the other CO_2 problem. Annual Review of Marine Science 1: 169–192.
2. Kroeker KJ, Kordas RL, Crim R, Hendriks IE, Ramajo L, et al. (2013) Impacts of ocean acidification on marine organisms: quantifying sensitivities and interaction with warming. Global Change Biology 19: 1884–1896.
3. Kroeker KJ, Micheli F, Gambi MC (2013) Ocean acidification causes ecosystem shifts via altered competitive interactions. Nature Clim Change 3: 156–159.
4. Cornwall CE, Hepburn CD, McGraw CM, Currie KI, Pilditch CA, et al. (2013) Diurnal fluctuations in seawater pH influence the response of a calcifying macroalga to ocean acidification. Proceedings of the Royal Society B: Biological Sciences 280: 20132201.
5. Hale R, Calosi P, McNeill L, Mieszkowska N, Widdicombe S (2011) Predicted levels of future ocean acidification and temperature rise could alter community structure and biodiversity in marine benthic communities. Oikos 120: 661–674.
6. Briffa M, de la Haye K, Munday PL (2012) High CO_2 and marine animal behaviour: Potential mechanisms and ecological consequences. Marine Pollution Bulletin 64: 1519–1528.
7. Spicer JI (2014) What can an ecophysiological approach tell us about the physiological responses of marine invertebrates to hypoxia? The Journal of Experimental Biology 217: 46–56.
8. Garrard S, Hunter RC, Frommel AY, Lane AC, Phillips JC, et al. (2013) Biological impacts of ocean acidification: a postgraduate perspective on research priorities. Marine Biology 160: 1789–1805.
9. Hall-Spencer JM, Rodolfo-Metalpa R, Martin S, Ransome E, Fine M, et al. (2008) Volcanic carbon dioxide vents show ecosystem effects of ocean acidification. Nature 454: 96–99.
10. Fabricius KE, De'ath G, Noonan S, Uthicke S (2014) Ecological effects of ocean acidification and habitat complexity on reef-associated macroinvertebrate communities. Proceedings of the Royal Society B: Biological Sciences 281: 20132479.
11. Tarasov VG, Gebruk AV, Mironov AN, Moskalev LI (2005) Deep-sea and shallow-water hydrothermal vent communities: Two different phenomena? Chemical Geology 224: 5–39.
12. Vizzini S, Di Leonardo R, Costa V, Tramati CD, Luzzu F, et al. (2013) Trace element bias in the use of CO_2-vents as analogues for low-pH environments:

Implications for contamination levels in acidified oceans. Estuarine, Coastal and Shelf Science 134: 19–30.
13. Dando PR, Aliani S, Arab H, Bianchi CN, Brehmer M, et al. (2000) Hydrothermal studies in the Aegean Sea. Physics and Chemistry of the Earth, Part B: Hydrology, Oceans and Atmosphere 25: 1–8.
14. Kerrison P, Hall-Spencer JM, Suggett DJ, Hepburn LJ, Steinke M (2011) Assessment of pH variability at a coastal CO_2 vent for ocean acidification studies. Estuarine, Coastal and Shelf Science 94: 129–137.
15. Boatta F, D'Alessandro W, Gagliano AL, Liotta M, Milazzo M, et al. (2013) Geochemical survey of Levante Bay, Vulcano Island (Italy), a natural laboratory for the study of ocean acidification. Marine Pollution Bulletin 73: 485–494.
16. Fabricius KE, Langdon C, Uthicke S, Humphrey C, Noonan S, et al. (2011) Losers and winners in coral reefs acclimatized to elevated carbon dioxide concentrations. Nature Clim Change 1: 165–169.
17. D'Alessandro W, Brusca L, Kyriakopouios K, Michas G, Papadakis G (2008) Methana, the westernmost active volcanic system of the south Aegean arc (Greece): Insight from fluids geochemistry. Journal of Volcanology and Geothermal Research 178: 818–828.
18. Inoue S, Kayanne H, Yamamoto S, Kurihara H (2013) Spatial community shift from hard to soft corals in acidified water. Nature Climate Change 3: 683–687.
19. Martin S, Rodolfo-Metalpa R, Ransome E, Rowley S, Buia MC, et al. (2008) Effects of naturally acidified seawater on seagrass calcareous epibionts. Biology Letters 4: 689–692.
20. Cigliano M, Gambi MC, Rodolfo-Metalpa R, Patti FP, Hall-Spencer JM (2010) Effects of ocean acidification on invertebrate settlement at volcanic CO_2 vents. Marine Biology 157: 2489–2502.
21. Dias BB, Hart MB, Smart CW, Hall-Spencer JM (2010) Modern seawater acidification: the response of foraminifera to high-CO_2 conditions in the Mediterranean Sea. Journal of the Geological Society 167: 843–846.
22. Porzio L, Buia MC, Hall-Spencer JM (2011) Effects of ocean acidification on macroalgal communities. Journal of Experimental Marine Biology and Ecology 400: 278–287.
23. Thomsen J, Casties I, Pansch C, Körtzinger A, Melzner F (2013) Food availability outweighs ocean acidification effects in juvenile *Mytilus edulis*: laboratory and field experiments. Global Change Biology 19: 1017–1027.
24. Kletou D, Hall-Spencer JM (2012) Threats to Ultraoligotrophic Marine Ecosystems, In: Dr. Antonio Cruzado (Ed.) Marine Ecosystems, InTech, ISBN: 978-953-51-0176-5.
25. Harley CDG, Anderson KM, Demes KW, Jorve JP, Kordas RL, et al. (2012) Effects of climate change on global seaweed communities. Journal of Phycology 48: 1064–1078.
26. Koch M, Bowes G, Ross C, Zhang X-H (2013) Climate change and ocean acidification effects on seagrasses and marine macroalgae. Global Change Biology 19: 103–132.
27. Schiel DR, Hickford MJH (2001) Biological structure of nearshore rocky subtidal habitats in southern New Zealand. Science for Conservation, 182; 54 pp.
28. Hofmann GE, Smith JE, Johnson KS, Send U, Levin LA, et al. (2011) High-frequency dynamics of ocean pH: a multi-ecosystem comparison. PLoS ONE 6: e28983.
29. Godbold JA, Solan M (2013) Long-term effects of warming and ocean acidification are modified by seasonal variation in species responses and environmental conditions. Philosophical Transactions of the Royal Society B: Biological Sciences 368.
30. Pingree RD, Holligan PM, Mardell GT, Head RN (1976) The influence of physical stability on spring, summer and autumn phytoplankton blooms in the Celtic Sea. Journal of the Marine Biological Association of the United Kingdom 56: 845–873.
31. Sala E, Boudouresque CF (1997) The role of fishes in the organization of a Mediterranean sublittoral community.: I: Algal communities. Journal of Experimental Marine Biology and Ecology 212: 25–44.
32. Piazzi L, Balata D, Pertusati M, Cinelli F (2004) Spatial and temporal variability of Mediterranean macroalgal coralligenous assemblages in relation to habitat and substratum inclination. Botanica Marina 47: 105–115.
33. Johnson VR, Russell BD, Fabricius KE, Brownlee C, Hall-Spencer JM (2012) Temperate and tropical brown macroalgae thrive, despite decalcification, along natural CO_2 gradients. Global Change Biology 18: 2792–2803.
34. Airoldi L, Beck M (2007) Loss, status and trends for coastal marine habitats of Europe. Oceanography and Marine Biology: An Annual Review 45: 345–405.
35. Connell SD, Russell BD, Turner DJ, Shepherd SA, Kildea T, et al. (2008) Recovering a lost baseline: missing kelp forests from a metropolitan coast. Marine Ecology Progress Series 360: 63–72.
36. Connell SD, Russell BD (2010) The direct effects of increasing CO_2 and temperature on non-calcifying organisms: increasing the potential for phase shifts in kelp forests. Proceedings of the Royal Society B: Biological Sciences 277: 1409–1415.
37. Mangialajo L, Ruggieri N, Asnaghi V, Chiantore M, Povero P, et al. (2007) Ecological status in the Ligurian Sea: The effect of coastline urbanisation and the importance of proper reference sites. Marine Pollution Bulletin 55: 30–41.
38. Ballesteros E, Torras X, Pinedo S, García M, Mangialajo L, et al. (2007) A new methodology based on littoral community cartography dominated by macroalgae for the implementation of the European Water Framework Directive. Marine Pollution Bulletin 55: 172–180.
39. Scherner F, Horta PA, de Oliveira EC, Simonassi JC, Hall-Spencer JM, et al. (2013) Coastal urbanization leads to remarkable seaweed species loss and community shifts along the SW Atlantic. Marine Pollution Bulletin 76: 106–115.
40. Cheminée A, Sala E, Pastor J, Bodilis P, Thiriet P, et al. (2013) Nursery value of *Cystoseira* forests for Mediterranean rocky reef fishes. Journal of Experimental Marine Biology and Ecology 442: 70–79.
41. Rodolfo-Metalpa R, Houlbreque F, Tambutte E, Boisson F, Baggini C, et al. (2011) Coral and mollusc resistance to ocean acidification adversely affected by warming. Nature Clim Change 1: 308–312.
42. Ainsworth EA, Long SP (2005) What have we learned from 15 years of free-air CO_2 enrichment (FACE)? A meta-analytic review of the responses of photosynthesis, canopy properties and plant production to rising CO_2. New Phytologist 165: 351–372.
43. Bowden H, Gill D (1997) Roman Methana. In: Mee C, Forbes H (eds); A rough and rocky place. Liverpool University Press, pp. 77–83.
44. Tsiamis K, Panayotidis P, Salomidi M, Pavlidou A, Kleinteich J, et al. (2013) Macroalgal community response to re-oligotrophication in Saronikos Gulf. Marine Ecology Progress Series 472: 73–85.
45. Howes DE, Harper JR, Owens EH (1994) British Columbia physical shore-zone mapping system. Resources Inventory Committee (RIC) report by the Coastal Task Force, RIC Secretariat, Victoria, B.C., pp. 1–71.
46. Taskin E, Jahn R, Öztürk M, Furnari G, Cormaci M (2012) The Mediterranean Cystoseira (with photographs). Manisa, Turkey: Celar Bayar University, pp. 1–75.
47. Pinedo S, García M, Satta MP, Torres MD, Ballesteros E (2007) Rocky-shore communities as indicators of water quality: A case study in the Northwestern Mediterranean. Marine Pollution Bulletin 55: 126–135.
48. Orfanidis S, Panayotidis P, Ugland KI (2011) Ecological Evaluation Index continuous formula (EEI-c) application: a step forward for functional groups, the formula and reference condition values. Mediterranean Marine Science 12: 199–231.
49. Spatharis S, Orfanidis S, Panayotidis P, Tsirtsis G (2011) Assembly processes in upper subtidal macroalgae: The effect of wave exposure. Estuarine, Coastal and Shelf Science 91: 298–305.
50. Riebesell U, Fabry VJ, Hansson L, Gattuso J-P (Eds.) (2010) Guide to best practices for ocean acidification research and data reporting: Luxembourg: Publications Office of the European Union.
51. Lewis E, Wallace WR (1998) Program developed for CO_2 system calculations. Carbon dioxide information analysis center, Oak Ridge National Laboratory. US Department of Energy, Oak Ridge.
52. Murphy J, Riley JP (1962) A modified single solution method for the determination of phosphate in natural waters. Analytica Chimica Acta 27: 31–36.
53. Bendscheider K, Robinson RJ (1952) A new spectrometric method for the determination of nitrite in seawater. Journal of Marine Research 11: 87–96.
54. Mullin JB, Riley JP (1955) The colorimetric determination of silicate with special reference to sea and natural waters. Analytica Chimica Acta 12: 162–176.
55. Koroleff F (1970) Direct determination of ammonia in natural waters as indophenol blue. In: Information on Techniques and Methods for Seawater Analysis. Charlottenlund, International Council for the Exploration of the Sea. Interlab. Report 3: 19–22.
56. Cline JD (1989) Spectrophotometric determination of hydrogen sulphide in natural waters. Limnology and Oceanography 14: 454–458.
57. Fraschetti S, Terlizzi A, Benedetti-Cecchi L (2005) Patterns of distribution of marine assemblages from rocky shores: evidence of relevant scales of variation. Marine Ecology Progress Series 296: 13–29.
58. Dethier MN, Graham ES, Cohen S, Tear LM (1993) Visual versus random-point percent cover estimation: 'objective' is not always better. Marine Ecology Progress Series 96: 93–100.
59. Clarke KR, Gorley RN (2006) PRIMER v6: User Manual/Tutorial. PRIMER-E, Plymouth.
60. Shannon CE, Weaver W (1949) A mathematical theory of communication. University of Illinois Press. ISBN 0-252-72548-4
61. Friligos N (1991) Eutrophication assessment in Greek coastal waters. In: Rose J (Ed.), Water and the Environment. Gordon and Breach Science Publishers.
62. Abdallah AMA, Abdallah MA, Beltagy AI (2005) Contents of heavy metals in marine seaweeds from the Egyptian coast of the Red Sea. Chemistry and Ecology 21: 399–411.
63. McDermid K, Stuercke B (2003) Nutritional composition of edible Hawaiian seaweeds. Journal of Applied Phycology 15: 513–524.
64. Raman D, Venkateshwarlu Reddy P, Vijay Kumar B, Murthy USN (2013) Atomic Absorption Spectroscopic determination and comparison of trace elements in the seaweeds. International Journal of Modern Chemistry and Applied Science 1: 12–24.
65. Maher WA, Clarke SM (1984) The occurrence of arsenic in selected marine macroalgae from two coastal areas of South Australia. Marine Pollution Bulletin 15: 111–112.
66. Caldeira K, Wickett ME (2005) Ocean model predictions of chemistry changes from carbon dioxide emissions to the atmosphere and ocean. Journal of Geophysics Research 110: C09S04.
67. Gilpin LC, Davidson K, Roberts E (2004) The influence of changes in nitrogen: silicon ratios on diatom growth dynamics. Journal of Sea Research 51: 21–35.

68. Zohary T, Robarts RD (1998) Experimental study of microbial P limitation in the eastern Mediterranean. Limnology and Oceanography 43: 387–395.
69. Bryan GW, Hummerstone LG (1973) Brown seaweed as an indicator of heavy metals in estuaries in south-west England. Journal of the Marine Biological Association of the United Kingdom 53: 705–720.
70. Karageorgis AP, Anagnostou CL, Kaberi H (2005) Geochemistry and mineralogy of the NW Aegean Sea surface sediments: implications for river runoff and anthropogenic impact. Applied Geochemistry 20: 69–88.
71. Hübner A, Rahders E, Rahner S, Halbach P, Varnavas SP (2004) Geochemistry of hydrothermally influenced sediments off Methana (western Hellenic volcanic arc). Chemie der Erde - Geochemistry 64: 75–94.
72. Amaral V, Cabral HN, Bishop MJ (2011) Resistance among wild invertebrate populations to recurrent estuarine acidification. Estuarine, Coastal and Shelf Science 93: 460–467.
73. Crook E, Potts D, Rebolledo-Vieyra M, Hernandez L, Paytan A (2011) Calcifying coral abundance near low-pH springs: implications for future ocean acidification. Coral Reefs 31: 239–245.
74. Thomsen J, Gutowska MA, Saphorster J, Heinemann A, Trubenbach K, et al. (2010) Calcifying invertebrates succeed in a naturally CO_2-rich coastal habitat but are threatened by high levels of future acidification. Biogeosciences 7: 3879–3891.
75. Riebesell U (2008) Climate change: Acid test for marine biodiversity. Nature 454: 46–47.
76. Falkenberg LJ, Russell BD, Connell SD (2012) Stability of strong species interactions resist the synergistic effects of local and global pollution in kelp forests. PLoS ONE 7: e33841.
77. Connell SD, Kroeker KJ, Fabricius KE, Kline DI, Russell BD (2013) The other ocean acidification problem: CO_2 as a resource among competitors for ecosystem dominance. Philosophical Transactions of the Royal Society B: Biological Sciences 368: 20120442.
78. Belegratis MR, Bitis I, Economou-Amilli A, Ott JA (1999) Epiphytic patterns of macroalgal assemblages on *Cystoseira* species (Fucales, Phaeophyta) in the east coast of Attica (Aegean Sea, Greece). Hydrobiologia 412: 67–80.
79. Ries JB, Cohen AL, McCorkle DC (2009) Marine calcifiers exhibit mixed responses to CO_2-induced ocean acidification. Geology 37: 1131–1134.
80. Hofmann LC, Straub S, Bischof K (2012) Competition between calcifying and noncalcifying temperate marine macroalgae under elevated CO_2 levels. Marine Ecology Progress Series 464: 89–105.
81. Kamenos NA, Burdett HL, Aloisio E, Findlay HS, Martin S, et al. (2013) Coralline algal structure is more sensitive to rate, rather than the magnitude, of ocean acidification. Global Change Biology 19: 3621–3628.
82. Engelen AH, Espirito-Santo C, Simões T, Monteiro C, Serrão EA, et al. (2008) Periodicity of propagule expulsion and settlement in the competing native and invasive brown seaweeds, *Cystoseira humilis* and *Sargassum muticum* (Phaeophyta). European Journal of Phycology 43: 275–282.
83. Swanson AK, Fox CH (2007) Altered kelp (Laminariales) phlorotannins and growth under elevated carbon dioxide and ultraviolet-B treatments can influence associated intertidal food webs. Global Change Biology 13: 1696–1709.
84. Tilman D (1999) The ecological consequences of changes in biodiversity: a search for general principles. Ecology 80: 1455–1474.
85. Lejeusne C, Chevaldonné P, Pergent-Martini C, Boudouresque CF, Pérez T (2010) Climate change effects on a miniature ocean: the highly diverse, highly impacted Mediterranean Sea. Trends in Ecology & Evolution 25: 250–260.

Appendix E2:

L.C. Hofmann, K. Bischof, **C. Baggini**, A. Johnson, K. Koop-Jakobsen, M. Teichberg (2014). CO_2 and inorganic nutrient enrichment affect the performance and competitive strength of a calcifying green alga and its non-calcifying epiphyte. *Oecologia* (accepted pending revisions).

CO_2 and inorganic nutrient enrichment affect the performance and competitive strength of a calcifying green alga and its noncalcifying epiphyte

Laurie C. Hofmann[1], Kai Bischof[1], Cecilia Baggini[2], Andrew Johnson[3], Ketil Koop-Jakobsen[4] and Mirta Teichberg[5]

[1]Marine Botany, Bremen Marine Ecology Centre for Research and Education, University of Bremen, Leobener Str. NW2, 28359 Bremen, Germany

[2]Marine Biology and Ecology Research Center, Plymouth University, Plymouth, Devon PL4 8AA, United Kingdom

[3]Department of Biological Sciences, Virginia Institute of Marine Science, College of William and Mary, 1375 Greate Road, Gloucester Point, VA 23062, USA

[4]Center for Marine Environmental Sciences, Leobener Str., 28359 Bremen, Germany

[5]Leibniz Center for Tropical Marine Ecology, Fahrenheitstr. 6, 28359 Bremen, Germany

Corresponding author: Laurie C. Hofmann, l.hofmann@uni-bremen.de, t: +49 421 21863048, f: +49, 421 218 63055

Author Contributions: LCH, MT, and KB developed and designed the experiment. LCH, CB, AJ, and MT performed the experiment. KK-J measured and analyzed oxygen production and consumption data with a multi-probe optode system. LCH wrote the manuscript and analyzed the data, and MT and KB provided editorial advice.

Abstract

Ocean acidification studies in the past decade have greatly improved our knowledge of how calcifying organisms respond to increased surface ocean CO_2 levels, and it has become evident that for many organisms, nutrient availability is an important factor that influences their physiological responses and competitive interactions with other species. Therefore, we simulated ocean acidification and eutrophication (nitrate and phosphate enrichment) to investigate the physiological responses of and interactions between a calcifying chlorophyte macroalga (*Halimeda opuntia* (L.) J.V. Lamouroux) and its common noncalcifying epiphyte (*Dictyota* sp.). Inorganic nutrient enrichment (+NP) had a strong influence on all responses measured with the exception of net calcification. Elevated CO_2 alone significantly decreased electron transport rates and resulted in phosphorus limitation in both species, but had no effect on oxygen production or respiration. The combination of CO_2 and +NP significantly increased electron transport rates in both species. While +NP alone stimulated *H. opuntia* growth rates, *Dictyota* growth was significantly stimulated by nutrient enrichment only at elevated CO_2, indicating a shift in dominance between the two species when CO_2 and inorganic nutrient enrichment were combined. This shift was further supported by the highest biomass ratios of *Dictyota* to *Halimeda* occurring under elevated CO_2 +NP. Our results suggest that inorganic nutrient enrichment may alleviate the negative impacts of elevated CO_2 on *H. opuntia* physiology, but without top-down grazer control, nutrient enrichment at an elevated CO_2 concentration likely to occur by the end of this century enables *Dictyota* sp. to have a competitive advantage over *H. opuntia*.

Keywords: *Halimeda opuntia*, *Dictyota*, calcification, ocean acidification, eutrophication

Introduction

In recent decades, the increasing CO_2 concentrations in surface ocean waters (ocean acidification) as a result of anthropogenic CO_2 input into the atmosphere has been widely studied, and therefore the amount of information on the physiological responses of calcifying organisms to ocean acidification has greatly increased. Although calcifying marine organisms show a variety of responses to increasing CO_2 concentrations (Langer et al. 2006; Ries 2009; Fabricius et al. 2011; Hurd et al. 2011), a general trend is emerging that benthic marine communities with a mixture of calcifiers and noncalcifiers will become dominated by the latter under future CO_2 conditions (Jokiel et al. 2008; Kuffner et al. 2008; Porzio et al. 2011; Hofmann et al. 2012a). Furthermore, a clear trend observed in many studies is that the food or nutrient availability of an organism is an important factor influencing its response to increasing CO_2 (Renegar and Riegl 2005; Russell et al. 2009; Holcomb et al. 2010; Chauvin et al. 2011; Findlay et al. 2011; Matthiessen et al. 2012). Furthermore, as already demonstrated in subtidal rocky habitats by Russell et al. (2009), the global impact of increasing surface ocean CO_2 concentrations will differ at regional levels, depending on other abiotic factors such as temperature. In tropical environments, excess nutrient availability, or eutrophication, amplifies phase shifts on coral reefs that occur due to overfishing by increasing the competitiveness of fleshy macroalgae at the expense of corals (Done 1992; Hughes 1994; Miller and Hay 1996; Lapointe 1997; McCook 1999; McCook et al. 2001; Jompa and McCook 2002; Burkepile and Haye 2006). Such a phase shift can result in lower coral recruitment due to decreased light availability, lack of available substrate and/or chemical inhibition of settlement (Birkeland 1997; Edmunds and Carpenter 2001; McCook et al 2001 and references therein; Kuffner et al. 2006; Hughes et al. 2007; Diaz-Pulido et al. 2010). Crustose coralline algae can also be outcompeted by turf algae under such conditions (Belliveau and Paul 2002; Littler et al. 2006). However, it is unclear how the combination of

higher CO_2 and inorganic nutrient availability affect calcifiying macroalgae, their noncalcifying counterparts, and interactions between them.

McConnaughey and Whelan (1997) reported that the process of calcification serves as a proton source for nutrient and HCO_3^- uptake in calcifying marine primary producers. As such, the authors proposed that a calcified skeleton is an adaptive advantage over noncalcifiers under oligotrophic conditions. However, under eutrophied conditions, this advantage seems to be negligible when herbivory does not control the fleshy algae population, because noncalcifying macroalgae are often more stimulated by nutrient enrichment than calcifying species (Zabala and Ballesteros 1989; Delgado and Lapointe 1994; Lapointe et al. 1997). It is therefore important to investigate how calcifying and noncalcifying macroalgae will compete under future CO_2 conditions in combination with local factors such as nutrient regimes.

The calcifying chlorophyte macroalgae in the genus *Halimeda* are important coral reef sediment producing organisms whose dead skeletons produce bank-like mounds (bioherms) containing high amounts of carbonate sediment (Littler et al. 1988; Rees et al. 2007). *Halimeda* spp. are therefore important contributors to carbonate sediments (Hillis-Colinvaux 1980; Drew 1983; Marshall and Davies 1988; Drew and Abel 1988; Diaz-Pulido et al. 2007; Rees at al. 2007). Estimates suggest modern *Halimeda* bioherms accumulate globally 0.15 to 0.4 Gt $CaCO_3$ year^{-1}, which is a major part of the annual coral reef carbonate production (Milliman 1993; Hillis 1997; Rees et al. 2007). While some *Halimeda* spp., have shown sensitivity to ocean acidification (Robbins et al. 2009; Price et al. 2011; Sinutok et al. 2011), some can maintain and even increase calcification rates under moderate CO_2 levels (Ries 2009).

The calcification mechanism of *Halimeda* spp. has been well documented (Borowitzka and Larkum 1976a; 1976b; 1976c; 1977; 1987). Despite the isolated site of calcification within the intracellular (utricular) spaces of these algae with respect to the outer seawater, several species have been shown to be sensitive to low pH (Robbins et al. 2009; Price et al. 2011; Sinutok et al. 2011). While these studies did not report the nutrient levels at which their experiments were conducted, their reported sensitivity to ocean acidification could be amplified by eutrophication in natural conditions due to competition from noncalcifying opportunistic macroalgae.

The noncalcifying phaeophyte algae in the genus *Dictyota* are common competitors with *Halimeda* spp. and are stimulated by inorganic nutrient enrichment (Lapointe et al 1987; Delgado and Lapointe 1994; Lapointe et al. 1997). *Dictyota* spp. also produce phlorotannins that are protective agents against herbivores, making them strongly competitive under eutrophic conditions, even when herbivory is high (Targett et al. 1992; Stachowicz and Hay 1999). Furthermore, many noncalcifying macroalgae show stimulated photosynthesis and growth under elevated CO_2 conditions (Gao et al. 1991; 1993; Kübler et al. 1999; Gordillo et al. 2001; Zou 2005; Suárez-Álvarez et al. 2011). Therefore, we expected that combined CO_2 and inorganic nutrient enrichment would have beneficial effects for *Dictyota* sp. at the expense of the calcifying competitor *Halimeda opuntia*. We therefore tested how these two abiotic factors affect the photosynthesis, growth, calcification (for *H. opuntia*) and competitive interactions of these two important coral reef dwelling macroalgae to determine how they will respond under future CO_2 conditions depending on local nutrient regimes.

Materials and Methods

Experimental design

The macroalgae used in this experiment were collected in Willemstad, Curaçao (former Netherlands Antilles) at 5 m depth in January 2012 and maintained in a recirculating artificial seawater system at the Leibniz Center for Tropical Marine Ecology in Bremen, Germany. The algae were maintained at 25°C, salinity 33, and 150 µmol photons m^{-2} s^{-1} light intensity on a 12:12 light:dark cycle until the beginning of the experiment in March 2012.

Some coral reefs in Curaçao are exposed to eutrophication due to high sewage discharge, industrial waste, rain runoff, and groundwater seepage (Gast 1998). Healthy reef conditions in Curaçao have a dissolved inorganic nitrate (DIN) concentration of approximately 0.5 µM, while eutrophied reefs have ten times that amount (up to 5 µM) and harbor water DIN concentrations reach up to 40 µM. Phosphate concentrations on healthy reefs in Curaçao are usually below 0.05 µM, while eutrophied reefs experience up to 0.3 µM (Gast 1998). Such low concentrations of inorganic nutrients on healthy reefs are due to rapid recycling of the nutrients, but it is generally thought that higher concentrations of inorganic nutrients are available from the sediment, particulate organic matter and nitrogen-fixing bacteria, as the high productivity rates on coral reefs could not be supported by such low nutrient concentrations (Webb et al. 1975; Wiebe et al. 1975; Froelich 1983; Mwashote and Jumba 2002; Rasheed et al. 2002). Therefore, we chose relatively high concentrations of nitrate and phosphate for our enriched treatment in order to ensure that the algae used in our experiment were nutrient replete. The concentration of inorganic nutrients in our unenriched seawater were as low as we could reach using milli-Q treated distilled water with added Red Sea Reef salt.

Our experiment consisted of two CO_2 levels (400, and 890 µatm CO_2) and two inorganic nutrient levels (nitrate and phosphate enriched: 50 µM NO_3^{2-}, 5 µM PO_4^{3-} or unenriched: 1.4 µM NO_3^{2-}, 0.09, µM PO_4^{3-}). A combination of the two independent factors (CO_2 and inorganic nutrients) resulted in 4 treatments, and we had five replicate algal thalli in five separate flasks for each treatment, making a total of 20 treatment flasks. The experimental units were one liter glass round bottom flasks that were continuously bubbled with pre-mixed air containing the CO_2 concentration of interest using a computerized 3-channel gas mixing system (HTK Hamburg GmbH, Hamburg, Germany). Inorganic nutrients were added separately to each flask (1 ml of stock solution), and distilled water was added to the flasks that did not receive nutrient enrichment. Reservoir tanks for each CO_2 treatment were continuously bubbled with the pre-mixed gas, and this water was used to change the water in each flask three times per week. The experiment lasted four weeks, during which time growth, calcification and chlorophyll fluorescence were measured weekly. Photographs were taken at the beginning and end to assess changes in community composition.

Prior to the experiment, fragments of *H. opuntia* (3-4 g FW) were cleaned of epiphytes except for *Dictyota* and given three days to acclimate to the experimental set-up in artificial seawater bubbled with ambient air before the experimental treatments were applied. The initial *Dictyota* cover was standardized to approximately 10% of the *H. opuntia* thalli by analyzing images of the initial communities (see below “Community composition”).

Seawater chemistry was monitored regularly throughout the experiment. The pH, salinity and temperature in every flask were measured daily using a TetraCon 325 conductivity probe and a SenTix 81 pH electrode connected to a Multiline P4 multi-measuring device (WTW, Weilheim, Germany). The pH meter was calibrated weekly using pH buffer solutions in ampules (SI Analytics GmbH, Mainz, Germany) and any offset of the electrode was corrected

based on a tris buffer. Water samples (50 ml) were taken weekly from the reservoir tanks for alkalinity measurements. Total alkalinity was determined by the Gran titration method using a TitroLine alpha 05 plus titrator with an automated sample changer and IoLine IL-Micro pH electrode (SI Analytics). The remaining parameters (pCO_2, HCO_3^-, CO_3^{2-}) were calculated using CO2calc (Robbins et al. 2010), using the dissociation constants for CO_2 and $KHSO_4$ from Mehrbach et al. (1973) refit by Dickson and Millero (1987) and Dickson (1990), respectively.

Photosynthesis

Variable chlorophyll *a* fluorescence of macroalgal communities was measured using an Imaging Pulse Amplitude Modulated Chlorophyll Fluorometer (MAXI version Imaging-PAM *M*-Series, Heinz Walz GmbH, Effeltrich, Germany). The maximum photochemical quantum yield of photosystem II (F_v/F_m) was measured after 5 minutes of dark adaptation. Light curves were conducted in order to calculate electron transport rates (*ETR*). The time it took for *H. opuntia* and *Dictyota* sp. to recover to steady state (F_0) after a saturation pulse was measured to determine the appropriate time interval for each light step of the light curve. We determined that one minute light intervals were enough for complete recovery of the ground state chlorophyll fluorescence and therefore used one-minute light steps ranging from 0-500 µmol photons m^{-2} s^{-1}. The light intensities at each step were calibrated with a US-SQS spherical micro quantum sensor (Heinz Walz GmbH, Effeltrich, Germany). Electron transport rates were calculated according to the equation $ETR = A \times 0.5 \times \phi_{PSII} \times E$ for *Halimeda opuntia* and $ETR = A \times 0.8 \times \phi_{PSII} \times E$ for *Dictyota* sp. where 0.5 and 0.8 were the fraction of absorbed light directed to PSII for green and brown algae, respectively (Grzymski et al. 1997; Figueroa et al. 2003; Rothäusler et al. 2011), A was the mean absorbed quanta calculated as the integrated spectral absorptance from 400-700 nm, ϕ_{PSII} was the quantum yield of photosystem II (PSII) charge separations, and E was the irradiance (µmol photons m^{-2} s^{-1}) at each light

step. Absorptance was measured using an integrating sphere connected to a Shimadzu UV 2401 PC UV-Vis recording spectrophotometer and calculated according to the formula $A = 1 - T - R$, where T and R were transmittance and reflectance of the algal thallus, respectively. Five samples from different thalli were taken at the beginning of the experiment to estimate the mean absorptance for *H. opuntia*. The *ETR* of *Dictyota* was estimated using the absorptance values of *Dictyota dichotoma* as determined by Frost-Christensen and Sand-Jensen (1992). The actual absorptance values for each individual thallus could not be measured because we did not destructively sample during the experiment. Therefore the *ETR* values are still an estimation, but more accurate than r*ETR*.

The chlorophyll fluorescence parameters ETR_{max} (maximum relative electron transport rate), E_k (light saturation point) and *alpha* (electron transport efficiency) were calculated by nonlinear curve fit analysis of the *ETR* versus irradiance curves based on the model by Eilers and Peeters (1988).

Net photosynthesis and respiration rates of the communities and *H. opuntia* alone (after manual removal of *Dictyota*) were measured after four weeks of exposure to the experimental treatments using fiber optodes. Oxygen measurements were conducted directly in the treatment flasks using a custom-made multi fiber optode system (MuFO) simultaneously operating 100 independent fiber optode oxygen sensors. Construction and measuring principle of the MuFO is described in detail in Fischer and Koop-Jakobsen (2012). Each oxygen sensor was calibrated individually prior to the experimental measurements with a 3-point calibration at 0, 50 and 100% O_2 atm saturation in seawater with salinity and temperature identical to the experimental set-up.

Calcification and growth

Calcification of *H. opuntia* was measured using the buoyant weight technique (Davies 1989). During measurements, the algal communities (*H. opuntia* + *Dictyota*) were placed in a basket suspended in seawater below a balance and the buoyant weight was determined. Calcification (mg $CaCO_3$ day^{-1}) was calculated as the change in buoyant weight over time standardized to the initial buoyant weight. The buoyant weight of any shed segments was also measured and subtracted from the initial weight in the calculation of calcification rates.

The fresh weight of the communities was weighed at the beginning of the experiment and the fresh weight of *H. opuntia* was measured four weeks later after all *Dictyota* was removed. The initial fresh weight of *Dictyota* was assumed to be neglible relative to *H. opuntia*. We calculated relative growth rates (RGR) of *H. opuntia* according to the equation $RGR = \left(\ln\left(FW_t \div FW_i\right)/t\right) \times 100$, where FW_i was the initial fresh weight of *H. opuntia* containing very few *Dictyota* sp. thalli and FW_t was the fresh weight of *Halimeda* after t = 4 weeks once the *Dictyota* sp. was removed. The fresh weight of any shed segments was also weighed each week and subtracted from the initial weight in the calculation of *RGR*. The relative growth rate for *Dictyota* was calculated using the same formula and assuming the initial weight was zero, as 10% initial cover was negligible in weight compared to the *H. opuntia* thalli. The final biomass of *Dictyota* sp. was weighed after all algal material was removed from the *H. opuntia* thalli after four weeks. We also calculated growth rates (mg day^{-1}) by the same methods. The segment shedding rate was calculated as % FW_i day^{-1}, where $\%FW_i$ was the fresh weight of the total segments lost after four weeks as a percentage of the initial fresh weight.

Tissue carbon, nitrogen and phosphorus

The total carbon and nitrogen content in *H. opuntia* and *Dictyota* sp. thalli was measured using a EuroEA 3000 Elemental Analyzer (Eurovector, Milan, Italy). Algal tissue was dried at

60°C for 48 hours and ground to a powder in a FastPrep-24 Automated Homogenizer (MPI Biomedicals, Eschwege, Germany) using stainless steel beads. Approximately 1-3 mg of tissue was packed into aluminum capsules for analysis. Separate tissue samples from *H. opuntia* were weighed and packed into tin capsules for analysis of organic carbon by acidification of the inorganic fraction with 1 N HCl (100 µl per 3 mg tissue).

Total phosphorus was measured in the same ground tissue as above using the colorimetric molybdenum blue method (Koroleff, 1983). Approximately 20 mg of dried algal tissue was conbusted in a muffle furnace at 500°C for 5 hours and dissolved in 5 ml of 0.2 N HCl. Following a 30 minute heating period in a drying oven at 80°C, 10 ml of distilled water was added to each sample. The samples were shaken and allowed to settle overnight. The following day, 2 ml of supernatant was added to clean test tubes, followed by 8 ml of distilled water and 1 ml of reagent solution. After a 30 minute reaction period, determination of phosphomolybdenum blue was determined colorimetrically on a UV-vis spectrophotometer (UV-2401 PC, Shimadzu, Kyoto, Japan) at 885 nm.

Community composition

Photographs of the macroalgal communities were taken at the beginning and end of the experiment for analysis of percent cover of each species. The images were analyzed using the Coral Point Count with excel extensions (CPCE) software program (Kohler and Gill 2006). A 10 x 10 point grid was placed over each community and the species present at each point was recorded. The percent cover of each species was calculated based on the total number of points containing algae. The change in percent cover was calculated as $\left(\left(PC_t - PC_i\right)/PC_i\right)\times 100$, where PC_i was initial percent cover and PC_t was the percent cover after four weeks. Biomass ratios were calculated by dividing the percentage composition of total community weight of *Dictyota* by that of *Halimeda*.

Statistical analysis

Statistical analysis of the response variables was conducted using factorial analysis of variance (ANOVA) tests with CO_2, nutrients, and when appropriate, species as independent factors. When a response variable was measured over time, a repeated measures mixed factorial ANOVA was conducted, with time treated as a repeated measures factor. The chlorophyll fluorescence parameters calculated from nonlinear curve fitting of the *ETR* versus irradiance curves were analyzed using a multivariate analysis of variance (MANOVA), and relative growth rates and growth rates were analyzed using a separate MANOVA. The remaining response variables (C_{org}:N and biomass ratios) were measured using separate 3-way ANOVA tests with CO_2, DIN and Species as independent factors. When the data did not meet the assumption of normality, they were log or cube root transformed. When transformation did not satisfy the assumption of normality, a nonparametric test (Kruskal-Wallis) was used.

Results

Seawater chemistry

The mean seawater chemistry parameters of the reservoir tanks without nutrient enrichment are shown in Table 1. The saturation state for aragonite and calcite remained above one in all treatments. The pH ranged from 7.79 to 8.00, and pCO_2 ranged from 403-890 µatm.

Photosynthesis

The chlorophyll *a* fluorescence parameters ETR_{max}, E_k and *alpha* were all significantly stimulated by inorganic nutrients in both species (Tables 2 and 3, Fig. 1a and b). ETR_{max} was significantly lowered by CO_2 alone, but the combination of CO_2 and +NP produced the highest ETR_{max} values in both species. There was also a significant interactive effect of

species and +NP on ETR_{max} and E_k, as the ETR_{max} and E_k values in *Dictyota* were more dramatically stimulated by +NP than in *H. opuntia* (Table 3, Fig. 1a and b).

Net photosynthesis and respiration of both the communities and *H. opuntia* alone were significantly higher with inorganic nutrient enrichment compared to algae grown without inorganic nutrient enrichment (Table 2, Fig. 1c). There was no significant effect of CO_2 on net photosynthesis or respiration rates.

Calcification and growth

Net calcification rates of *H. opuntia* measured by buoyant weight were highly variable. There was a significant interaction between time of exposure and CO_2 (Table 2, Fig. 2). The data did not fulfill the sphericity test during statistical analysis, and therefore the reported degrees of freedom and p-values are based on the Huynh-Feldt Measure (Epsilon = 0.705). Overall net calcification rates of algae grown under normal CO_2 conditions increased over time, while those grown under high CO_2 decreased over time, regardless of nutrient treatment. Due to the high variability in the data, there was no nutrient effect, but a visible increasing trend over time can be seen in algae grown under normal CO_2 with nutrient enrichment.

The absolute growth rates of *H. opuntia* and *Dictyota* did not significantly differ, while the relative growth rates of *Dictyota* were significantly higher than those of *H. opuntia* (Table 2, Fig. 3a and b). Nutrient enrichment stimulated both the absolute and relative growth rates in both species. There was also a significant interactive effect of species and CO_2 on relative growth rates. Under nutrient enriched conditions, the two species showed opposite responses to elevated CO_2: *Dictyota* relative growth rates increased, while *H. opuntia* relative growth rates decreased under elevated CO_2 compared to normal CO_2 conditions.

Tissue carbon, nitrogen and phosphorus

The C_{org}:N ratios of *Dictyota* and *H. opuntia* were significantly lowered by nutrient enrichment and were affected by an interactive effect of species, CO_2 and nutrients (Table 2, Fig. 3c). Under CO_2 enrichment alone, *Dictyota* had a lower mean C_{org}:N ratio (14.3 ± 0.98) compared to normal conditions (17.0 ± 1.2), while *H. opuntia* showed the opposite trend (15.6 ± 0.94; 13.7 ± 0.63, respectively). Under nutrient enriched conditions, there was no difference in the C_{org}:N ratios of either species between CO_2 treatments. Nitrogen to phosphorus ratios in the tissue of *H. opuntia* differed among experimental treatments (Kruskal-Wallis test, X^2 = 8.43, p = 0.038, Fig. 3d). Generally, nutrient enriched algae had low N:P ratios, and the highest mean N:P ratio (153 ± 100) was in the 890-NP treatment. Variability was high in this treatment due to the high number of replicates with undetectable tissue phosphorus levels, making it impossible to calculate N:P ratios. This was also true for *Dictyota*, particularly in the 400-NP treatment, making statistical analysis impossible. However, the measurable tissue N:P ratios in *Dictyota* followed a similar pattern to that of *H. opuntia.*

Biomass Ratio

The ratio of the percentage of the community biomass of *Dictyota* sp. to *H. opuntia* was significantly affected by an interaction between CO_2 and inorganic nutrient enrichment (Table 2, Fig. 4). Under normal CO_2 conditions, there was no effect of nutrient enrichment on the biomass ratio of *Dictyota* to *H. opuntia*, but under 890 µatm CO_2, the biomass ratio of *Dictyota* to *H. opuntia* was an order of magnitude greater under nutrient enrichment (0.208 ± 0.042) compared to unenriched conditions (0.022 ± 0.005).

Discussion

We have shown that the physiology and competitive interactions between a calcifier (*H. opuntia*) and noncalcifier (*Dictyota* sp.) are affected by both CO_2 and nutrient enrichment.

The physiological responses of these macroalgae to elevated CO_2 is strongly affected by nutrient availability, and the interactive effect of increasing CO_2 and inorganic nutrients will therefore be an important factor determining competitive interactions among tropical macroalgal communities under future ocean conditions. In general, our results suggest that under nutrient replete conditions, moderate CO_2 enrichment is not a strong stress factor for *H. opuntia* physiology, but the combined factors allowed *Dictyota* to have a competitive edge over the calcifier. Growth rates of both species increased and tissue N:P ratios decreased under nutrient enrichment, but high CO_2 concentrations tipped the scale in favor of *Dictyota*, which was stimulated the most by the combination of high CO_2 and nutrient enrichment as shown by the biomass ratios. *Dictyota* sp. had the highest growth rates, ETR_{max}, and increase in percent cover when CO_2 and nutrient concentrations were high. However, at ambient CO_2, *H. opuntia* growth increased drastically with nutrient enrichment, while *Dictyota* sp. did not. These results indicate that under ambient CO_2, *H. opuntia* was competitive with *Dictyota* under both nutrient conditions, but the combination of elevated CO_2 and nutrients made *Dictyota* sp. more competitive than *H. opuntia*. The lower growth rates of *H. opuntia* at elevated CO_2 were only observed under nutrient enriched conditions when *Dictyota* sp. growth rates were highest. Therefore, our results suggest that reduced *H. opuntia* growth was not a direct result of elevated CO_2, but rather an indirect effect due to the higher growth rate of and shading by *Dictyota*. Beach et al. (2003) found that *H. tuna* heavily epiphytized with *Dictyota* sp. had slower growth rates than unepiphytized algae. The authors attributed this effect to shading, but also found that *Dictyota* chemically affected *H. tuna*, as the alga had higher respiration rates when grown without epiphytes in *Dictyota*-conditioned water. Therefore, the higher competitive success of *Dictyota* at high CO_2 and inorganic nutrient concentrations could be due to a combination of shading and chemical inhibition of its competitor, *H. opuntia*.

The high growth rates of *Dictyota* sp. under elevated CO_2 and nutrient replete conditions were accompanied by lower tissue nitrogen content. This decrease in nitrogen could decrease the nutritional values of *Dictyota* spp. for grazers under future CO_2 conditions in areas where nutrients are replete. Furthermore, *Dictyota* spp. also produce phlorotannins, which are strongly carbon-based compounds that have been shown to deter herbivory (Hay et al. 1994; Steinberg 1984; 1986; 1988; Targett et al. 1986; Targett and Arnold, 1998; Stachowicz and Hay 1999) and could be stimulated by the excess availability of CO_2 (Mattson et al. 2005). Because grazers exert strong top-down control on noncalcifying macroalgae in areas with high inorganic nutrient loads (i.e. Littler and Litter 1984; Carpenter 1986; Steneck 1988; Lapointe et al. 1997; Thacker 2001; Belliveau and Paul 2002), future studies investigating macroalgae-grazer interactions and production of anti-herbivore metabolites by macroalgae under elevated CO_2 and inorganic nutrient conditions are necessary for obtaining a more complete understanding of how external stress factors and grazing combined will control tropical macroalgal communities, particularly competition between calcifiers and noncalcifiers.

In contrast to previous studies (Price et al. 2001; Sinutok et al. 2011), we observed an increase in maximum *ETR* in *H. opuntia* after short-term exposure to moderately elevated CO_2 levels. Furthermore, we saw no CO_2 effect on photosynthesis or respiration rates. We did observe changes in calcification rates over time, but when nutrients were replete, calcification rates did not decrease below initial levels. After one week, calcification rates were actually highest in the high CO_2 treatment with nutrient enrichment, which is complementary to the results found by Ries (2009) who showed that calcification rates in *Halimeda* sp. increase slightly with moderate CO_2 enrichment. Differences between our study and other previous work on *Halimeda* (Price et al. 2001; Sinutok et al. 2011) could be due to differences in population responses or nutrient, light and temperature differences between experiments. Based on our

study and calcification rates reported by Ries (2009) and Price et al. (2001), an $\Omega_{aragonite}$ around 2.5 seems to produce the highest calcification rates in *H. opuntia* and *H. incrassata*.

The effect of elevated CO_2 on calcification rates in *H. opuntia* observed in our study is not surprising, because the chemical environment between the utricles where calcification occurs is semi-separated from the external seawater, and therefore the algae have biological control over this internal environment via photosynthetic and respiratory processes (Borowitzka and Larkum 1977). The combination of having an aragonite skeleton and a semi-isolated calcification locus suggests that *Halimeda* spp. might be less susceptible to ocean acidification than the coralline algae, which deposit the highly soluble high-Mg calcite crystals directly on their cell walls and have shown high susceptibility to ocean acidification (Gao et al. 1993; Martin and Gattuso 2009; Gao and Zheng 2010; Porzio et al. 2011; Hofmann et al. 2012a; 2012b).

The strong influence of inorganic nutrients on the relationship between *Dictyota* sp. and *H. opuntia* under different CO_2 conditions observed in this study is consistent with field observations of these two taxa (Delgado and Lapointe 1994: Lapointe 1997). Delgado and Lapointe (1994) reported that nutrient enrichment enhanced the productivity of fleshy macroalgae more than calcareous algae, and predicted that eutrophication could decrease carbonate accretion on tropical coasts. Such changes in competitive interactions between corals and fleshy algae are also well documented under low herbivory conditions (Done 1992; Hughes 1994; Miller and Hay 1996; Lapointe 1997; McCook 1999; McCook et al. 2001; Jompa and McCook 2002; Burkepile and Haye 2006). Under CO_2 enrichment alone, however, both species in our experiment became phosphate limited based on their tissue N:P ratios. Lapointe et al. 1987) reported that productivity of calcareous algae is often nitrogen limited, while productivity of fleshy, opportunistic species is phosphorus limited. This is due to the

fact that phosphate precipitates with calcium carbonate and binds to carbonate particles (Berner and Morse 1974). Teichberg et al. (2013) also showed that *H. opuntia* is stimulated by nitrogen enrichment. Because calcified green algae are well adapted to phosphate limited conditions, elevated CO_2 alone did not strongly shift the relationship between *H. opuntia* and *Dictyota* compared to the combination of CO_2 and inorganic nutrient enrichment. Our results suggest that the addition of CO_2 may exacerbate the effect of eutrophication on competitive relationships between calcifiers and noncalcifiers. However, further studies will be needed to pinpoint the direct causes, for example to determine if CO_2 stimulates macroalgal release of organic carbon, which has been shown to negatively impact coral health (Kline et al. 2006; Smith et al. 2006).

In conclusion, our results suggest that *H. opuntia* will show mild changes under ocean acidification conditions in areas where inorganic nutrients are low. In eutrophied environments, both species benefit from nutrient enrichment. However, without top-down grazer control, *Dictyota* sp. has a competitive advantage over *H. opuntia*, and this effect is amplified at an elevated CO_2 concentration that is likely to occur by the end of this century.

Acknowledgements

The authors would like to extend their gratitude to Dr. Achim Meyer for his technical assistance in experimental set-up and trouble-shooting, and Philipp Laeseke for his participation in experimental maintenance. We also thank Matthias Birkicht and Dorothea Dasbach for analysis of dissolved inorganic nutrients and tissue carbon and nitrogen, respectively. Funding for this project was provided by the German Federal Ministry of Education and Research (BMBF) through the cooperative research project Biological Impacts of Ocean Acidification (BIOACID), as well as by the Doctoral Programme on Marine

Ecosystem Helath and Conservation (MARES) and the European Project on Ocean Acidification (EPOCA).

References

Belliveau SA, Paul VJ (2002) Effects of herbivory and nutrients on the early colonization of crustose coralline and fleshy algae. Mar Ecol Prog Ser 232:105-114

Berner RA, Morse JW (1974) Dissolution kinetics of calcium carbonate in sea water IV. Theory of calcite dissolution. Am J Sci 274:108 134

Birkeland C (1977) The importance of rate of biomass accumulation in early successional stages of benthic communities to the survival of coral recruits. Proceedings of the 3rd International Coral Reef Symposium 15-21

Borowitzka MA, Larkum AWD (1976a) Calcification in the Green Alga *Halimeda* II. The exchange of Ca^{2+} and the occurence of age gradients in calcification and photosynthesis. J Exp Bot 27:864-878

Borowitzka MA, Larkum AWD (1976b) Calcification in the Green Alga *Halimeda* III. The sorces of inorganic carbon for photosynthesis and calcification and a model of the mechanism of calcification. J Exp Bot 27:879-893

Borowitzka MA, Larkum AWD (1976c) Calcification in the Green Alga *Halimeda* IV. The action of metabolis inhibitiors on photosynthesis and calcification. J Exp Bot 27:894-907

Borowitzka MA, Larkum AWD (1977) Calcification in the green alga *Halimeda*. I. An ultrastructure study of thallus development. J Phycol 13:6-16

Borowitzka MA, Larkum AWD (1987) Calcification in algae: mechanisms and the role of metabolism. Crit Rev Plant Sci 6:1-45

Burkepile DE, Hay ME (2006) Herbivore vs. nutrient control of marine primary producers: context-dependent effects. Ecology 87:3128-3139

Carpenter RC (1986) Partitioning herbivory and its effects on coral reef algal communities. Ecol Monogr 345-363

Chauvin A, Denis V, Cuet P (2011) Is the response of coral calcification to seawater acidification related to nutrient loading*?* Coral Reefs 30:911-923

Davies PS (1989) Short-term growth measurements of corals using an accurate buoyant weighing technique. Mar Biol 101:389-395

Delgado O, Lapointe BE (1994) Nutrient-limited productivity of calcareous versus fleshy macroalgae in a eutrophic, carbonate-rich tropical marine environment. Coral Reefs 13:151-159

Diaz-Pulido G, Harii S, McCook LJ, *et al.* (2010) The impact of benthic algae on the settlement of a reef-building coral. Coral reefs 29:203-208

Diaz-Pulido G, McCook LJ, Larkum AWD, Hoegh-Guldberg O (2007) Vulnerability of macroalgae of the Great Barrier Reef to climate change. In: Johnson JE, Marshall PA (eds) Climate Change and the Great Barrier Reef: A Vulnerability Assessment pp 153-192

Done TJ (1992) Phase shifts in coral reef communities and their ecological significance. Hydrobiologia 247:121-132

Drew EA (1983) *Halimeda* biomass, growth rates and sediment generation on reefs in the central Great Barrier Reef province. Coral Reefs 2:101-110

Edmunds PJ, Carpenter RC (2001) Recovery of *Diadema antillarum* reduces macroalgal cover and increases abundance of juvenile corals on a Caribbean reef. Proc Nat Acad Sci USA 98:5067-5071

Eilers PHC, Peeters JCH (1988) A model for the relationship between light intensity and the rate of photosynthesis in phytoplankton. Ecol Model 42:199-215

Fabricius KE, Langdon C, Uthicke S, Humphrey C, Noonan S, Death G, Okazaki R, Muehllehner N, Glas MS, Lough JM (2011) Losers and winners in coral reefs acclimatized to elevated carbon dioxide concentrations. Nat Clim Chang, 1:165-169

Figueroa FL, Escassi L, Pérez-Rodríguez E, Korbee N, Delia Giles A, Johnsen G (2003) Effects of short-term irradiation on photoinhibition and accumulation of mycosporine-like amino acids in sun and shade species of the red algal genus *Porphyra*. J Photochem Photobiol B: Biol 69:21-30

Findlay HS, Wood HL, Kendall MA, Spicer JI, Twitchett RJ, Widdicombe S (2011) Comparing the impact of high CO_2 on calcium carbonate structures in different marine organisms. Mar Biol Res 7:565-575

Fischer JP, Koop-Jakobsen K (2012) The multi fiber optode (MuFO): A novel system for simultaneous analysis of multiple fiber optic oxygen sensors. Sens Actuators B: Chem 168:354-359.

Frost-Christensen H, Sand-Jensen K (1992) The quantum efficiency of photosynthesis in macroalgae and submerged angiosperms. Oecologia 91:377-384

Gao K, Aruga Y, Asada K, Ishihara T, Akano T, Kiyohara M (1991) Enhanced growth of the red alga *Porphyra yezoensis* Ueda in high CO_2 concentrations. J Appl Phycol 3:355-362

Gao K, Aruga Y, Asada K, Kiyohara M (1993) Influence of enhanced CO_2 on growth and photosynthesis of the red algae *Gracilaria* sp. and *G. chilensis*. J Appl Phycol 5:563-571

Gao K, Zheng Y (2010) Combined effects of ocean acidification and solar UV radiation on photosynthesis, growth, pigmentation and calcification of the coralline alga *Corallina sessilis* (Rhodophyta). Glob Chang Biol 16:2388-2398

Gast, GJ (1998) Nutrient pollution in coral reef waters. Reef Care Curaçao Contribution no. 5. Accessed 8 Aug 2007 http://www.nacri.org/greylit/GastNutrPollWorkshop.html

Gordillo FJ, Niell FX, Figueroa FL (2001) Non-photosynthetic enhancement of growth by high CO_2 level in the nitrophilic seaweed *Ulva rigida* C. Agardh (Chlorophyta). Planta 213:64-70

Hay ME, Kappel QE, Fenical W (1994) Synergisms in plant defenses against herbivores: interactions of chemistry, calcification, and plant quality. Ecology 75:1714-1726

Hillis L (1997) Coralgal reefs from a calcareous green alga perspective, and a first carbonate budget. Proceedings of the 8th International Coral Reef Symposium, Panama, pp 761-766

Hillis-Colinvaux L (1980) Ecology and Taxonomy of *Halimeda*: Primary Producer of Coral Reefs. Adv Mar Biol 17:1-327

Hofmann LC, Straub S, Bischof K (2012a) Competition between calcifying and noncalcifying temperate marine macroalgae under elevated CO_2 levels. Mar Ecol Prog Ser 464:89-105

Hofmann LC, Yildiz G, Hanelt D, Bischof K (2012b) Physiological responses of the calcifying rhodophyte *Corallina officinalis* (L.) to future CO_2 levels. Mar Biol 159:783-792

Holcomb M, McCorkle DC, Cohen AL (2010) Long-term effects of nutrient and CO_2 enrichment on the temperate coral *Astrangia poculata* (Ellis and Solander, 1786). J Exp Mar Biol Ecol 386:27-33

Hughes TP (1994) Catastrophes, phase shifts, and large-scale degradation of a Caribbean coral reef. Science 265:1547-1551

Hughes TP, Rodrigues MJ, Bellwood DR, *et al.* (2007) Phase shifts, herbivory, and the resilience of coral reefs to climate change. Curr Biol 17:360-365

Hurd CL, Cornwall CE, Currie K, Hepburn CD, McGraw CM, Hunter KA, Boyd PW (2011) Metabolically-induced pH fluctuations by some coastal calcifiers exceed projected 22nd century ocean acidification: a mechanism for differential susceptibility*?* Glob Chang Biol 17:3254-3262

Jokiel PL, Rodgers KS, Kuffner IB, Andersson AJ, Cox EF, Mackenzie FT (2008) Ocean acidification and calcifying reef organisms: a mesocosm investigation. Coral Reefs 27:473-483

Jompa J, McCook LJ (2002) The effects of nutrients and herbivory on competition between a hard coral (*Porites cylindrica*) and a brown alga (*Lobophora variegata*). Limnol Oceanogr 527-534

Kline DI, Kuntz NM, Breitbart M, Knowlton N, Rohwer F (2006) Role of elevated organic carbon levels and microbial activity in coral mortality. Mar Ecol Prog Ser 314:119-125

Kohler KE, Gill SM (2006) Coral Point Count with Excel extensions (CPCe): A Visual Basic program for the determination of coral and substrate coverage using random point count methodology. Comput Geosci 32:1259-1269

Koroleff F (1983) Determination of phosphorus. In: Grasshoff K, Ehrhardt M, Kremling F (eds). Methods of seawater analysis. Verlag Chemie, Weinheim, pp 125-139

Kübler JE, Johnston AM, Raven JA (1999) The effects of reduced and elevated CO_2 and O_2 on the seaweed *Lomentaria articulata*. Plant Cell Environ 22:1303-1310

Kuffner IB, Walters LJ, Becerro MA, Paul VJ, Ritson-Williams R, Beach KS (2006) Inhibition of coral recruitment by macroalgae and cyanobacteria. Mar Ecol Prog Ser 323:107-117

Kuffner IB, Andersson AJ, Jokiel PL, Rodgers KS, Mackenzie FT (2008) Decreased abundance of crustose coralline algae due to ocean acidification. Nat Geosci 1:114-117

Langdon C, Broecker WS, Hammond DE, *et al.* (2003) Effect of elevated CO_2 on the community metabolism of an Exp coral reef. Glob Biogeochem Cycles 17:1-14

Langer G, Geisen M, Baumann KH, Kläs J, Riebesell U, Thoms S, Young JR (2006) Species-specific responses of calcifying algae to changing seawater carbonate chemistry. Geochem Geophys Geosystems 7:1-12

Lapointe BE, Littler MM, Littler DS (1987) A comparison of nutrient-limited productivity in macroalgae from a Caribbean barrier reef and from a mangrove ecosystem. Aquat Bot 28:243-255

Lapointe BE, Littler MM, Littler DS (1997) Macroalgal overgrowth of fringing coral reefs at Discovery Bay, Jamaica: bottom-up versus top-down control. Proceedings of the 8th International Coral Reef Symosium 1:927-923

Littler MM, Littler DS, Brooks BL (2006) Harmful algae on tropical coral reefs: Bottom-up eutrophication and top-down herbivory. Harmful Algae 5:565-585

Littler MM, Littler DS, Lapointe BE (1988) A comparison of nutrient-and light-limited photosynthesis in psammophytic versus epilithic forms of *Halimeda* (Caulerpales, *Halimeda*ceae) from the Bahamas. Coral Reefs 6:219-225

Marshall JF, Davies PJ (1988) *Halimeda* bioherms of the northern Great Barrier Reef. Coral Reefs 6:139-148

Martin S, Gattuso JP (2009) Response of Mediterranean coralline algae to ocean acidification and elevated temperature. Glob Chang Biol 15:2089-2100

Matthiessen B, Eggers SL, Krug S (2012) High nitrate to phosphorus regime attenuates negative effects of rising pCO_2 on total population carbon accumulation. Biogeosciences 9:1195-1203

Mattson WJ, Julkunen-Tiitto R, Herms DA (2005) CO_2 enrichment and carbon partitioning to phenolics: do plant responses accord better with the protein competition or the growth differentiation balance models? Oikos 111:337-347

McConnaughey TA, Whelan JF (1997) Calcification generates protons for nutrient and bicarbonate uptake. Earth Sci Rev 42:95-117

McCook LJ (1999) Macroalgae, nutrients and phase shifts on coral reefs: scientific issues and management consequences for the Great Barrier Reef. Coral Reefs 18:357-367

McCook L, Jompa J, Diaz-Pulido G (2001) Competition between corals and algae on coral reefs: a review of evidence and mechanisms. Coral Reefs 19:400-417

Miller MW, Hay ME (1996) Coral-seaweed-grazer-nutrient interactions on temperate reefs. Ecol Monogr 66:323-344

Milliman JD (1993) Production and accumulation of calcium carbonate in the ocean: Budget of a nonsteady state. Glob Biogeochem Cycles 7:927-957

Mwashote BM, Jumba IO (2002) Quantitative aspects of inorganic nutrient fluxes in the Gazi Bay (Kenya): implications for coastal ecosystems. Mar Pollut Bull 44:1194-1205

Porzio L, Buia MC, Hall-Spencer JM (2011) Effects of ocean acidification on macroalgal communities. J Exp Mar Biol Ecol 400:278-287

Price NN, Hamilton SL, Smith JE (2011) Species-specific consequences of ocean acidification for the calcareous tropical green algae *Halimeda*. Mar Ecol Prog Ser 440:67-78

Rasheed M, Badran MI, Richter C, Huettel M (2002) Effect of reef framework and bottom sediment on nutrient enrichment in a coral reef of the Gulf of Aqaba, Red Sea. Mar Ecol Prog Ser 239:277-285

Rees SA, Opdyke BN, Wilson PA, Henstock TJ (2007) Significance of *Halimeda* bioherms to the global carbonate budget based on a geological sediment budget for the Northern Great Barrier Reef, Australia. Coral Reefs 26:177-188

Renegar DA, Riegl BM (2005) Effect of nutrient enrichment and elevated CO_2 partial pressure on growth rate of Atlantic scleractinian coral Acropora cervicornis. Mar Ecol Prog Ser 293:69-76

Ries JB (2009) Effects of secular variation in seawater Mg/Ca ratio (calcite-aragonite seas) on $CaCO_3$ sediment production by the calcareous algae *Halimeda*, Penicillus and *Udotea*-evidence from recent experiments and the geological record. Terra Nova 21:323-339

Ries JB, Cohen AL, McCorkle DC (2009) Marine calcifiers exhibit mixed responses to CO_2-induced ocean acidification. Geology 37:1131

Robbins LL, Knorr PO, Hallock P (2009) Response of *Halimeda* to ocean acidification: field and laboratory evidence. Biogeosci Discuss 6:4895-4918

Rothäusler E, Gómez I, Karsten U, Tala F, Thiel M (2011) UV-radiation versus grazing pressure: long-term floating of kelp rafts (*Macrocystis pyrifera*) is facilitated by efficient photoacclimation but undermined by grazing losses. Mar Biol 158:127-141

Russell BD, Thompson J-A, Falkenberg LJ, Connell SD (2009) Synergistic effects of climate change and local stressors: CO_2 and nutrient-driven change in subtidal rocky habitats. Glob Chang Biol 15:2153-2162

Sinutok S, Hill R, Doblin MA, Wuhrer R, Ralph PJ (2011) Warmer more acidic conditions cause decreased productivity and calcification in subtropical coral reef sediment-dwelling calcifiers. Limnol Oceanogr 56:1200-1212

Smith JE, Shaw M, Edwards RA, *et al.* (2006) Indirect effects of algae on coral: algae-mediated, microbe-induced coral mortality. Ecol Lett 9:835-845

Stachowicz JJ, Hay ME (1999) Reducing predation through chemically mediated camouflage: indirect effects of plant defenses on herbivores. Ecology 80:495-509

Steinberg PD (1984) Algal chemical defense against herbivores: allocation of phenolic compounds in the kelp *Alaria marginata.* Science 223:405-407

Steinberg PD (1986) Chemical defenses and the susceptibility of tropical marine brown algae to herbivores. Oecologia 69:628-630

Steneck RS, Dethier MN (1994) A functional group approach to the structure of algal-dominated communities. Oikos 69:476-498

Suárez-Álvarez S, Gómez-Pinchetti JL, García-Reina G (2012) Effects of increased CO_2 levels on growth, photosynthesis, ammonium uptake and cell composition in the macroalga *Hypnea spinella* (Gigartinales, Rhodophyta). J Appl Phycol 24:815-823

Targett NM, Arnold TM (1998) Minireview—predicting the effects of brown algal phlorotannins on marine herbivores in tropical and temperate oceans. J Phycol 34:195-205

Targett NM, Coen LD, Boettcher AA, Tanner CE (1992) Biogeographic comparisons of marine algal polyphenolics: evidence against a latitudinal trend. Oecologia 89:464-470

Targett NM, Targett TE, Vrolijk NH, Ogden JC (1986) Effect of macrophyte secondary metabolites on feeding preferences of the herbivorous parrotfish *Sparisoma radians*. Mar Biol 92:141-148

Teichberg M, Fricke A, Bischof K (2013) Increased physiological performance of the calcifying green macroalga *Halimeda opuntia* in response to experimental nutrient enrichment on a Caribbean coral reef. Aquat Bot 104:25-33

Thacker R, Ginsburg D, Paul V (2001) Effects of herbivore exclusion and nutrient enrichment on coral reef macroalgae and cyanobacteria. Coral Reefs 19:318-329

Webb KL, DuPaul WD, Wiebe W, Sottile W, Johannes RE (1975) Enewetak (Eniwetok) Atoll: Aspects of the nitrogen cycle on a coral reef. Limnol Oceanogr 20:198-210

Wiebe WJ, Johannes RE, Webb KL (1975) Nitrogen fixation in a coral reef community. Science 188:257-259

Zabala M, Ballesteros E (1989) Surface-dependent strategies and energy flux in benthic marine communities or, why corals do not exist in the Mediterranean. Sci Mar 53:3-17

Zou D (2005) Effects of elevated atmospheric CO_2 on growth, photosynthesis and nitrogen metabolism in the economic brown seaweed, *Hizikia fusiforme* (Sargassaceae, Phaeophyta). Aquaculture 250:726-735

Table 1. Mean (± SE, n = 12) seawater chemistry parameters of the reservoir tanks treated with CO_2 only (no inorganic nutrients added).

CO_2 Treatment	Temperature (°C)	pH_{total}	A_T^* (µmol kg SW^{-1})	pCO_2 (µatm)	HCO_3^- (µmol kg SW^{-1})	CO_3^{2-} (µmol kg SW^{-1})	CO_2 (µmol kg SW^{-1})	Ω_{Ca}^*	Ω_{Ar}^*
400	24.96 ± 0.1	8.00 ± 0.02	2376 ± 140	403 ± 7	1623 ± 52	172 ± 10	11.5 ± 0.20	4.18 ± 0.23	2.74± 0.15
890	24.86 ± 0.1	7.79 ± 0.03	2619 ± 160	890 ± 13	2336 ± 129	164 ± 17	25.6 ± 0.40	4.01 ± 0.41	2.63 ± 0.26

*Abbreviations: A_T = total alkalinity, Ω = saturation state of calcite (Ca) and aragonite (Ar).

Table 2. ANOVA and MANOVA results, showing F-values and degrees of freedom in parantheses, followed by p values significant at the 95% confidence level. Only significant p-values are shown. All nonsignificant effects are shown by the symbol "-". ETR_{max}, E_k, and *alpha* were analyzed using a three-way MANOVA, and a separate MANOVA was conducted for growth rates and relative growth rates. Net calcification rates were analyzed using a 3-way repeated-measures ANOVA, with time treated as the within subject factor. The remaining response variables were analyzed using 3-way ANOVAs with CO_2, NP, and species as independent factors, except for biomass ratio, which was analyzed with just two independent factors, CO_2 and NP. When an independent factor was not used in a statistics test, n.a. (not applicable) is shown. The lines separate response variables that were used in separate tests.

Response variable	CO_2	NP	CO_2 x NP	Species	Species x NP	Species x CO_2	Species x NP x CO_2	Time x CO_2	Time x NP
ETR_{max}	F(1, 28) = 5.9 p = 0.022	F(1, 28) = 21.6 p = 7.3 E-5	-	F(1, 28) = 16.2 p = 0.015	F(1, 28) = 6.7 p = 0.015	-	-	n.a.	n.a.
E_k	-	F(1, 28) = 8.2 p = 0.008	-	F(1, 28) = 6.3 p = 0.018	F(1, 28) = 5.6 p = 0.0004	-	-	n.a.	n.a.
alpha	-	F(1, 28) = 4.8 p = 0.037	-	-	-	-	-	n.a.	n.a.
Net Photosynthesis	-	F(1, 31) = 15.6 p = 4.1 E -4	-	-	-	-	-	n.a.	n.a
Respiration	-	F(1, 31) = 31.4 p = 4.0 E -6	-	-	-	-	-	n.a.	n.a.
Net Calcification	-	-	-	-	-	-	-	F(2.1, 31.7) =3.2 p = 0.05	-
Growth Rate	-	F(1, 32) = 4.5 p = 0.042	-	-	-	-	-	n.a.	n.a.
Relative Growth Rate	-	F(1, 32) = 13.6 p = 0.001	-	F(1, 32) = 78.2 p < 1E-6	-	F(1, 32) = 5.0 p = 0.032	-	n.a.	n.a.
C_{org}:N	-	F(1, 30) = 36.4 p = 1 E-6	-	-	-	-	F(1, 30) = 4.9 p = 0.035	n.a.	n.a.
Biomass Ratio	-	F(1, 15) = 6.5 p = 0.022	F(1, 15) = 8.4 p = 0.011	n.a.	n.a.	n.a.	n.a.	n.a.	n.a.

Table 3. Mean (± SE, N = 5) curve fit paramters parameters ETR_{max}, E_k, and *alpha* calculated from the nonlinear curve fit analysis of the *ETR* vs. irradiance curves for each species and each CO_2 and nutrient treatment.

	H. opuntia			*Dictyota* sp.		
Treatment	ETR_{max}	E_k	*alpha*	ETR_{max}	E_k	*alpha*
400-	11.0 ± 1.5	74.5 ± 13.4	0.16 ± 0.02	15.3 ± 3.2	87.5 ± 14.4	0.19 ± 0.05
400+	13.1 ± 1.1	76.3 ± 15.0	0.19 ± 0.02	26.1 ± 3.7	147.6 ± 13.8	0.18 ± 0.03
890-	8.1 ± 0.9	69.9 ± 2.9	0.12 ± 0.02	8.9 ± 2.5	61.1 ± 9.3	0.14 ± 0.03
890+	11.2 ± 1.8	76.5 ± 5.7	0.14 ± 0.02	25.7 ± 3.7	111.2 ± 19.6	0.24 ± 0.01

Figure Legends

Fig. 1 Mean (± SE, N = 5) electron transport rates of a) *H. opuntia* and b) *Dictyota* sp. after four weeks of exposure to 400 (circles) and 890 (squares) µatm CO_2 under nutrient unenriched (open symbols) and enriched (closed symbols) conditions c) mean (± SE, N = 5) net photosynthetic (left panel) and respiration (right panel) rates of the communities (top panels) and *Halimeda opuntia* alone after *Dictyota* removal (bottom panels). Note the different scales on the y-axes

Fig. 2 Mean (± SE, N = 5) net calcification rates of *H. opuntia* over time at 400 (circles) and 890 (squares) µatm CO_2 without (open symbols) and with (closed symbols) nitrate and phosphate enrichment. Calcification rates are based on buoyant weight measurements standardized by initial buoyant weight

Fig. 3 a) Mean (±SE, N = 5) growth rates b) relative growth rates c) organic carbon to nitrogen ratios and d) nitrogen to phosphorus ratios of *H. opuntia* (left panels) and *Dictyota* sp. (right panels) at each CO_2 concentration under nitrate and phosphate unenriched (white bars) and enriched (grey bars) conditions. Note the different scales on the y-axes

Fig. 4 Mean (± SE, N = 5) ratios of the percent of community biomass made up by *Dictyota* sp. to *H. opuntia* at each CO_2 treatment with (grey bars) and without (white bars) nutrient enrichment after four weeks. Images of chosen communities after 4 weeks of exposure at the respective treatments are shown above each bar

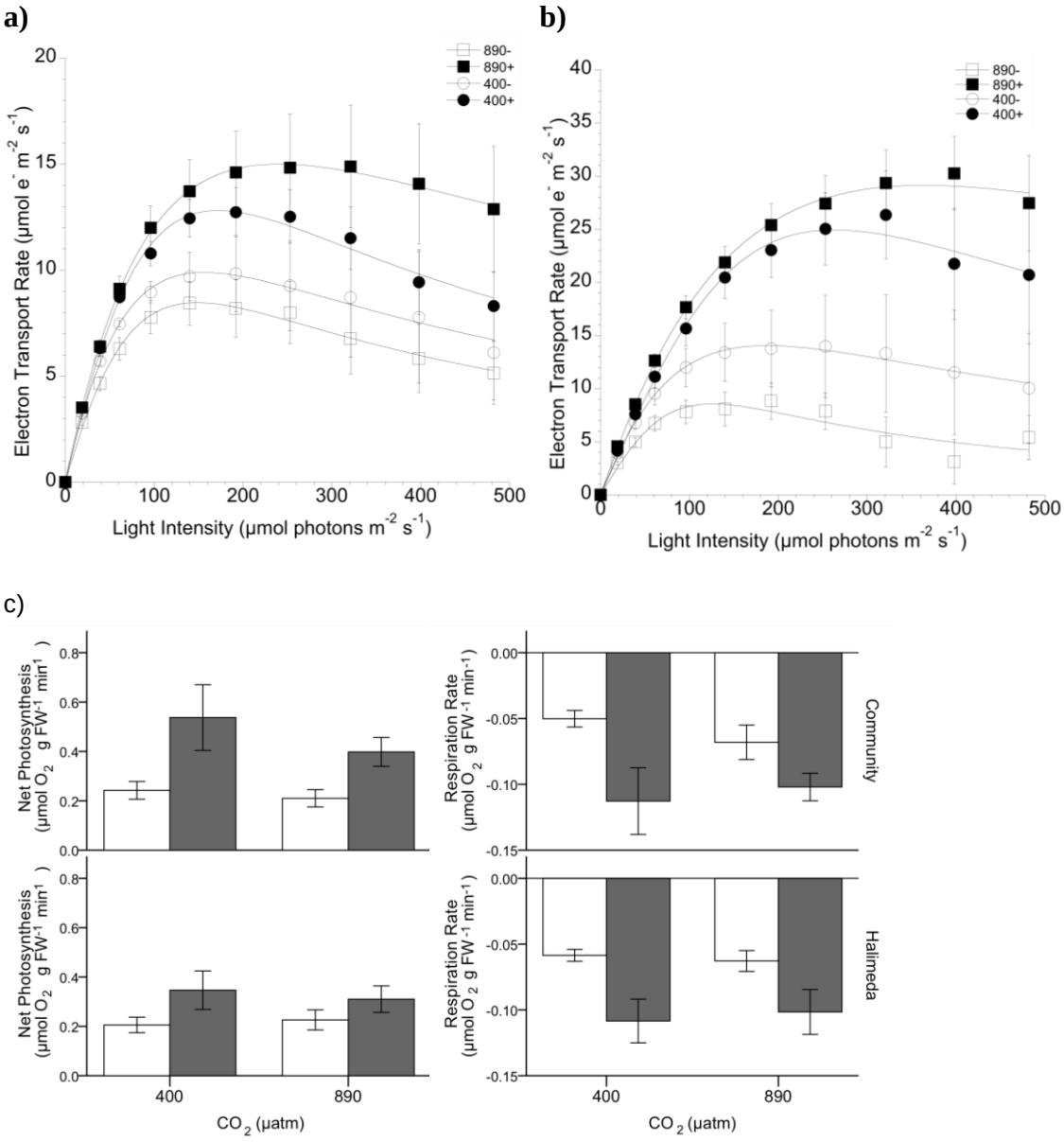
a)
b)
890-
890+
400-
400+
Electron Transport Rate (µmol e⁻ m⁻² s⁻¹)
Light Intensity (µmol photons m⁻² s⁻¹)
c)
Net Photosynthesis (µmol O2 g FW-1 min-1)
Respiration Rate (µmol O2 g FW-1 min-1)
Community
Halimeda
CO2 (µatm)
400
890

Figure 1

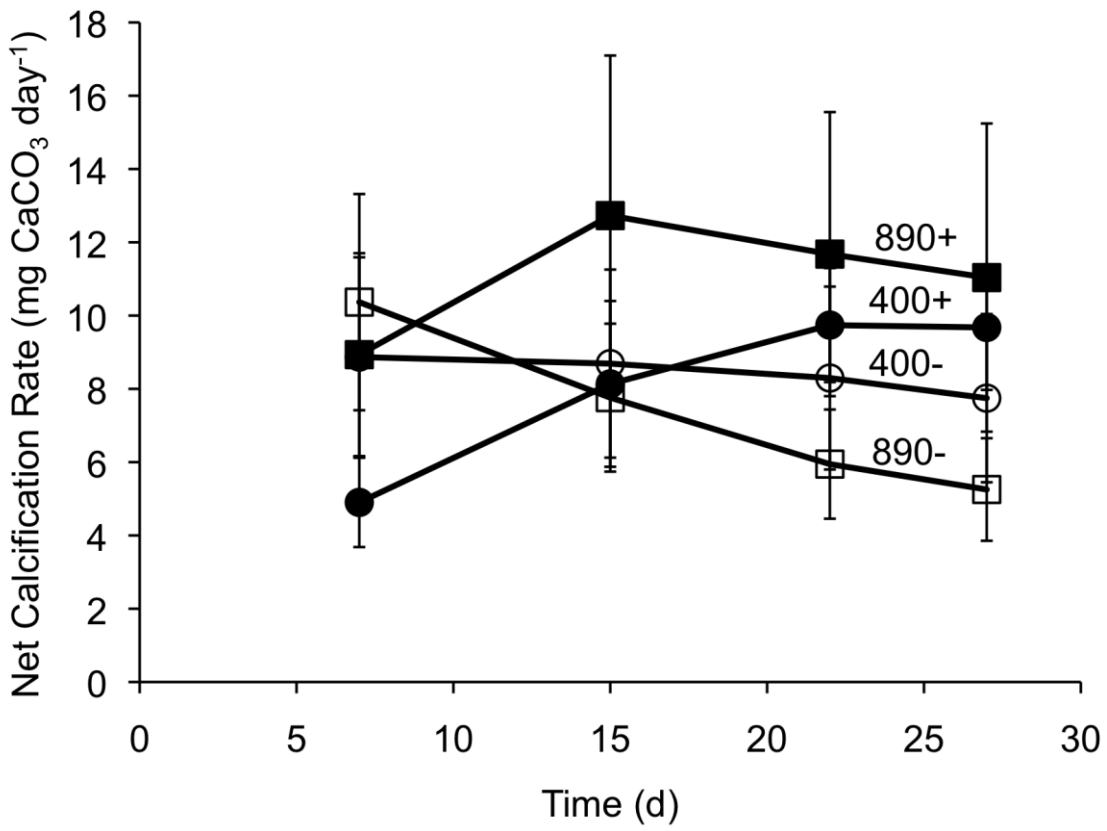
Net Calcification Rate (mg CaCO3 day-1)
18
16
14
12
10
8
6
4
2
0
0
5
10
15
20
25
30
Time (d)
890+
400+
400-
890-

Figure 2

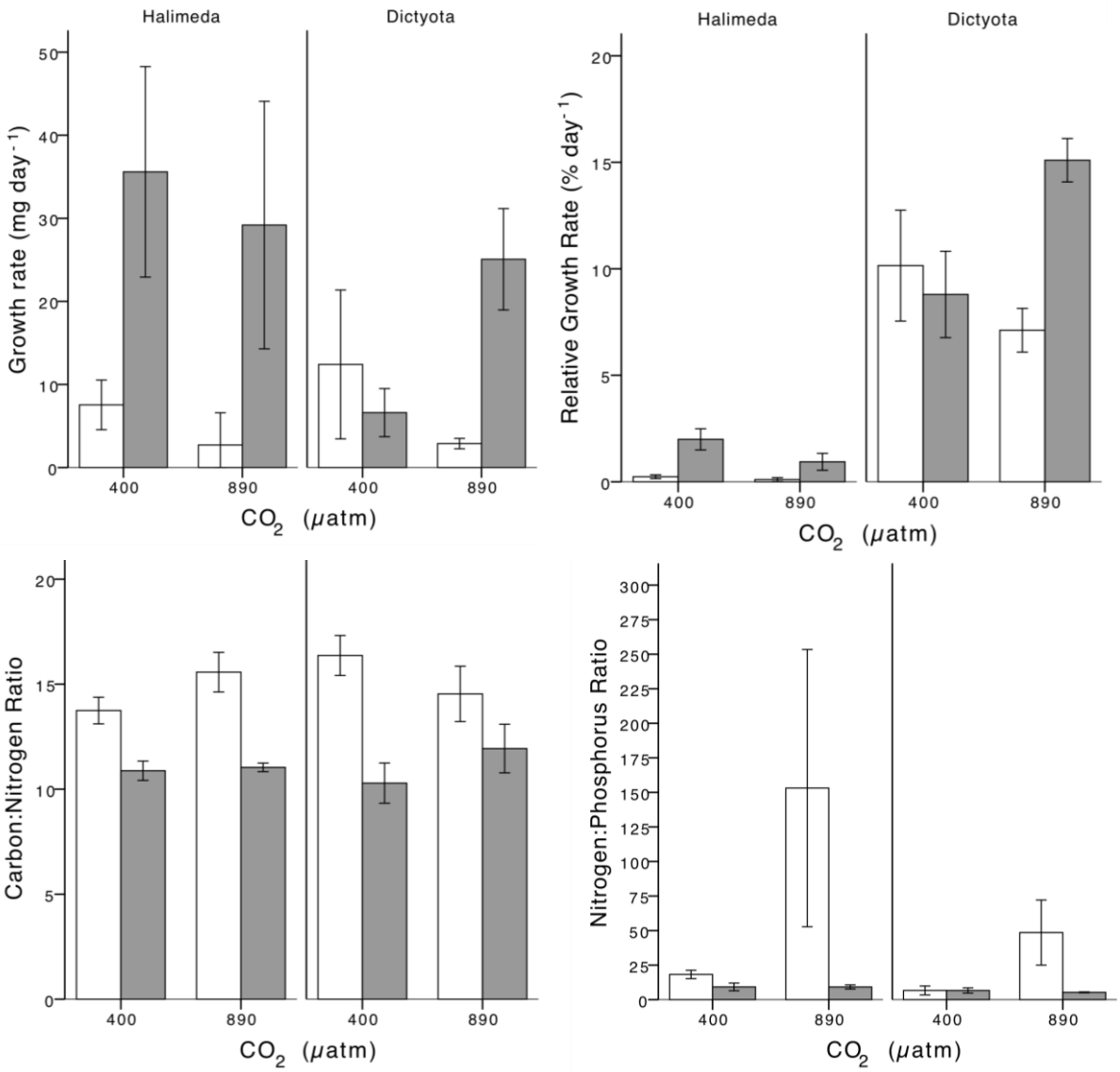
Halimeda
Dictyota
Growth rate (mg day-1)
Relative Growth Rate (% day-1)
Carbon:Nitrogen Ratio
Nitrogen:Phosphorus Ratio
400
890
CO2 (μatm)

Figure 3

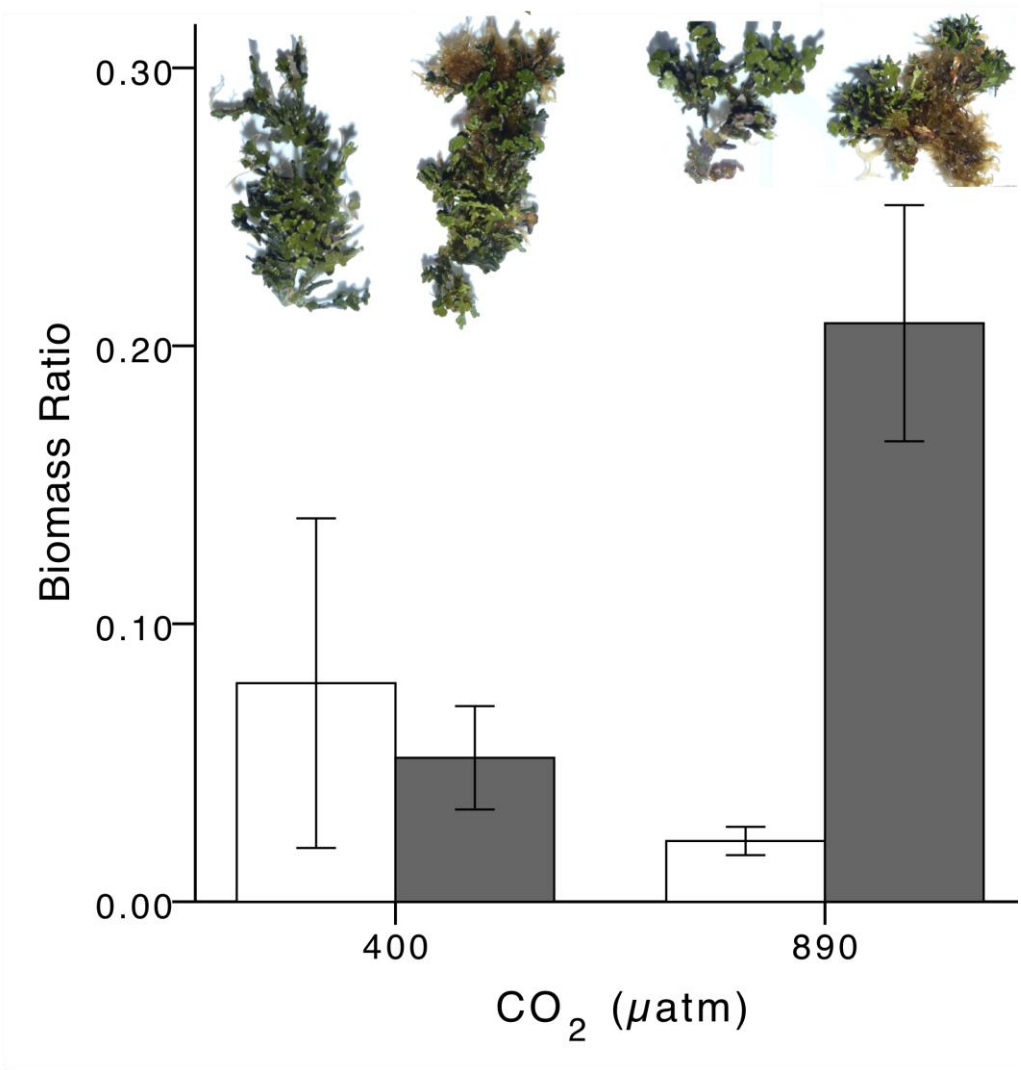

Figure 4

Appendix E3:

G. Langer., G. Nehrke, **C. Baggini**, R. Rodolfo-Metalpa, J.M. Hall-Spencer, J. Bijma (2014). Limpets counteract ocean acidification induced shell corrosion by thickening of aragonitic shell layers. *Biogeosciences Discussions*, 11: 12571-12590.

Biogeosciences Discuss., 11, 12571–12590, 2014
www.biogeosciences-discuss.net/11/12571/2014/
doi:10.5194/bgd-11-12571-2014

Biogeosciences
Discussions
Open Access

Limpets counteract ocean acidification induced shell corrosion by thickening of aragonitic shell layers

G. Langer[1], G. Nehrke[2], C. Baggini[3], R. Rodolfo-Metalpa[4], J. Hall-Spencer[3], and J. Bijma[2]

[1]Department of Earth Sciences, Cambridge University, Cambridge, UK
[2]Biogeosciences, Alfred Wegener Institute, Bremerhaven, Germany
[3]School of Marine Science and Engineering, University of Plymouth, Plymouth, UK
[4]CoRéUs, Institut de Recherche pour le Développement, Centre IRD de Noumea, Noumea, New Caledonia

Received: 1 August 2014 – Accepted: 6 August 2014 – Published: 25 August 2014

Correspondence to: G. Langer (gl345@cam.ac.uk)

Published by Copernicus Publications on behalf of the European Geosciences Union.

Abstract

Specimens of the patellogastropod limpet *Patella caerulea* were collected within (pH_{low}-shells) and outside (pH_n-shells) a CO_2 vent site at Ischia, Italy. Four pH_{low}-shells and four pH_n-shells were sectioned transversally and scanned for polymorph distribution by means of confocal Raman microscopy. The pH_{low}-shells displayed a twofold increase in aragonite area fraction and size normalised aragonite area. Size normalised calcite area was halved in pH_{low}-shells. Taken together with the increased apical and the decreased flank size normalised thickness of the pH_{low}-shells, these data led us to conclude that low pH exposed *P. caerulea* specimens counteract shell dissolution by enhanced shell production. The latter is different from normal elongation growth and proceeds through addition of aragonitic layers only, while the production of calcitic layers is confined to elongation growth. Therefore aragonite cannot be regarded as a per se disadvantageous polymorph under ocean acidification conditions.

1 Introduction

There is general consensus that anthropogenic CO_2 emissions lead to decreasing surface ocean pH and carbonate ion concentration, a process termed ocean acidification (e.g. Royal Society, 2005). The latter entails a decrease in seawater saturation state with respect to calcium carbonate. Calcium carbonates occur in the form of different polymorphs, the most resistant to dissolution being calcite, followed by aragonite. It was proposed that by the year 2100 the subarctic Pacific Ocean and the entire Southern Ocean will be under-saturated with respect to aragonite (Orr et al., 2005). Wintertime aragonite under-saturation in the Southern Ocean may even occur as early as 2030 (McNeil and Matear, 2008). Since many marine organisms use aragonite or calcite to build their shells, there have been concerns regarding the vulnerability of these organisms to ocean acidification. The fact that aragonite is more soluble than calcite has led to the widely held notion that aragonite producers are more vulnerable to ocean

BGD
11, 12571–12590, 2014

acidification than calcite producers (Field et al., 2011; Gattuso and Hansson, 2011; Royal Society, 2005). The extreme sensitivity of aragonitic pteropods to dissolution (Bednarsek et al., 2012) seems to support this view. Some molluscs, e.g. patellogastropod limpets and the Littorinidae (Hedegaard et al., 1997; Taylor and Reid, 1990), have, in addition to aragonitic shell layers, evolved outer calcitic shell layers. It was argued that calcitic shell layers are an adaptation to resist dissolution (Taylor and Reid, 1990). The latter hypothesis was questioned on the basis of a comparative dissolution study using aragonitic and calcitic bivalve microstructures (Harper, 2000). Comparing the post-mortem dissolution rates of four (two aragonitic and two calcitic) Antarctic benthic species, McClintock et al. (2009) supported the conclusion of Harper (2000). The latter two studies imply the notion that dissolution of calcium carbonate biominerals is not primarily a question of the polymorph, but depends largely on composition and microstructure of the biomineral. As regards the vulnerability to ocean acidification, shell dissolution is merely one aspect, which focuses entirely on the product, i.e. the shell. The production of the latter is another aspect, and under ocean acidification some organisms might be able to compensate for shell dissolution by increasing shell production (Rodolfo-Metalpa et al., 2011). This compensatory shell production might favour the more dissolution resistant polymorph in species producing both aragonite and calcite (see also Taylor and Reid, 1990). Specimens of the limpet *Patella caerulea*, collected at a highly acidified volcanic CO_2 vent site at Ischia, displayed higher gross calcification rates than their fellow specimens, collected outside the vent site (normal pH, Rodolfo-Metalpa et al., 2011). It was also shown that *P. caerulea* specimens collected within the vent site are considerably corroded (Hall-Spencer et al., 2008; Rodolfo-Metalpa et al., 2011). Taken together the latter two observations suggest that *P. caerulea* might be able to compensate, to a certain extent (compare Hall-Spencer et al., 2008; Rodolfo-Metalpa et al., 2011), shell dissolution by excess shell production. Since limpets produce aragonitic as well as calcitic shell layers (see above), an interesting question is whether compensatory shell production shows a bias towards a particular polymorph. Here we present the polymorph distribution of complete cross

BGD
11, 12571–12590, 2014

sections of *P.caerulea* shells collected from within and outside the Ischia CO_2 vent site (Hall-Spencer et al., 2008; Rodolfo-Metalpa et al., 2011).

2 Material and methods

2.1 Study site and sampling

The study site is an area located off the east coast of Ischia (40°43.81′ N, 13°57.98′ E), in shallow waters of 2–6 m and within 1–15 m of the shore line. Emissions from the vents in this area are composed of 90–95 % CO_2, 3–6 % N_2, 0.6–0.8 % O_2, 0.2–0.8 % CH_4 and 0.08–0.1 % Ar, without toxic sulphur compounds (Hall-Spencer et al., 2008). Since the vent gases do not contain toxic substances and are at ambient seawater temperature, this area can be used as a natural laboratory to understand ecosystem effects of ocean acidification. Gas fluxes were measured during 2006–2007, and no seasonal, tidal or diurnal variation in gas flow rates was detected, while pH and saturation states of aragonite and calcite varied with sea state, being lowest on calm days, and showed large decreases as pCO_2 amounts increased proceeding towards the vent sites (Hall-Spencer et al., 2008). *Patella caerulea* specimens were collected from two low pH sites (PL1 and PL2), and from a control site (C) in December 2009 (Fig. 1). Temperature, pH and TA were measured from September to December 2009, and the other carbonate chemistry parameters were calculated from them. PL1 and PL2 had a mean pH of 6.46 ± 0.35 (mean ± S.D.) and 6.51 ± 0.38 respectively, while the control site had a mean pH of 8.03 ± 0.05 (Table 1).

2.2 Sample preparation and Raman spectroscopy

Raman imaging was done using a WITec alpha 300 R (WITec GmbH, Germany) confocal Raman microscope. Imaging was done using a motorized scan table having a maximum scan range of up to 2.5 cm × 2.5 cm and a minimum step size of 100 nm. Scans are performed using a 532 nm diode laser and an ultra-high throughput spectrometer

BGD
11, 12571–12590, 2014

with a grating, 600 mm, and 500 mm blaze (UHTS 300, WITec, Germany). The used objective was a 20× Zeiss with a NA of 0.4.

For the imaging every 10 µm a Raman spectra was acquired with a integration time of 0.05 s per spectra. The size of the sample and its irregular shape as well as the extremely high resolution of 10 µm (resulting in huge spectral files) did not allow imaging the whole sample in one run. Therefore the sample had to be repositioned several times. Therefore the sample processing had to be done for each scan separately (using the WITec Project software, version 2.10). This resulted in slightly different colour scales for each image, since it was not possible to synchronize the latter during the data processing. However, this does only alter the optical appearance of the images after they have been stitched together using the software Gimp 2.8 and does not affect the interpretation of the images. For details on the Raman imaging of this type of samples the interested reader is referred to several other publications performed using the described setup (e.g. Nehrke and Nouet, 2011; Nehrke et al., 2012; Wall and Nehrke, 2012; Stemmer and Nehrke 2014).

2.3 Size measurements and data analysis

Transversally sectioned and resin-embedded shells were imaged using a Nikon SMZ1500 stereo microscope. Shell length and shell thickness were measured using Nikon NIS Elements 4.0 software. All bar-plots show the mean ± standard deviation of four shells (four pH_{low}-shells and four pH_n-shells were analysed). Since shells of *P. caerulea* are not symmetric we always measured the shorter of the two shell flanks. Size normalised thickness of a shell's shorter flank (SNTF) was determined by averaging ca. 35 evenly spaced thickness measurements and dividing the resulting value by the shell's length. Size normalised thickness of a shell's apex (SNTA) was determined by averaging ca. 10 evenly spaced thickness measurements and dividing the resulting value by the shell's length. The apex of a shell was arbitrarily defined as a certain distance (ca. 1.5 mm) left and right to the highest point of the shell (see Fig. 2). The latter measure was taken to avoid a one-point measurement of the highest point of a shell.

BGD
11, 12571–12590, 2014

Such a one-point measurement is prone to being not representative. The fraction of aragonite area (FA) was determined as pixels representing aragonite (measured by means of Nikon NIS Elements 4.0 software) divided by the sum of pixels representing aragonite and pixels representing calcite (Fig. 3). The size normalised aragonite area (SNAA) equals pixels representing aragonite divided by the shell length. The size normalised calcite area (SNCA) equals pixels representing calcite divided by the shell length.

3 Results

All shells selected for analysis were of similar size. The length of the pH_n-shells was 31 ± 2 mm (mean ± standard deviation of four shells), while the length of the pH_{low}-shells was 36 ± 3 mm (mean ± standard deviation of four shells). Polymorph distribution imaging revealed marked differences between pH_{low}-shells and pH_n-shells (Fig. 4). Size normalised thickness of the flank (SNTF) was 26 % lower in pH_{low}-shells (Fig. 5), while size normalised thickness of the apex (SNTA) was 26 % higher in pH_{low}-shells (Fig. 6). The fraction of aragonite area (FA) was by a factor of 2.3 higher in pH_{low}-shells (Fig. 7). Size normalised aragonite area (SNAA) was by a factor of 2.2 higher in pH_{low}-shells (Fig. 8), and size normalised calcite area (SNCA) was by a factor of 2.4 lower in pH_{low}-shells (Fig. 9).

4 Discussion

Polymorph distribution analyses of complete cross sections of Patella caerulea shells from a CO_2 vent site at Ischia revealed that this species counteracts shell dissolution in corrosive waters by enhanced production of aragonitic shell layers. The latter are even thicker in corrosion-exposed specimens than in specimens from the control site. We conclude that aragonite cannot be regarded as a per se disadvantageous polymorph under ocean acidification conditions.

BGD
11, 12571–12590, 2014

The low pH site at Ischia, from which the analysed pH_{low}-shells were taken, features seawater that is under-saturated with respect to both aragonite and calcite (Table 1). Hence shells of calcareous organisms residing in these under-saturated waters are prone to dissolution. Indeed, shells of *P. caerulea* clearly show signs of dissolution (Hall-Spencer et al., 2008; Rodolfo-Metalpa et al., 2011). Therefore, *P. caerulea* pH_{low}-shells are the product of both shell formation and dissolution, as opposed to N-shells (originating from the normal pH site), which are merely the product of shell formation. Provided they grow normally, pH_{low}-shells should, because of dissolution, display a reduced size normalized thickness (SNT). This is, for the flank area of the shell, indeed the case (Fig. 5). On the contrary, in the apex area, the SNT is higher in pH_{low}-shells (Fig. 6). The latter can only stem from enhanced shell production. From the above it can be concluded that net shell production in pH_{low}-shells is region-specific, i.e. enhanced at the apex area, and reduced along the flank area. A comparison of the mineralogical composition of the shells from the two different sites shows that the fraction of aragonite area (FA) for pH_{low}-shells is twice as big as for pH_n-shells (Fig. 7). This observation could exclusively be due to a higher SNT of the apex area, which is predominantly aragonitic. If the increased FA is related to normal shell production and dissolution, the size normalised aragonite area (SNAA) should be unaltered or decreased. We observed, contrariwise, an increased SNAA (Fig. 8), which is in line with the increased SNT of the apex area, both pointing to enhanced shell production. Along the flank area, however, the SNT is decreased in pH_{low}-shells (Fig. 5), and so is the overall size normalised calcite area (SNCA, Fig. 9). To conclude, there is ample evidence suggesting that low pH exposed *P. caerulea* specimens counteract dissolution by enhanced shell production. Hence the mineralogical analyses of the shell sections support our conclusion drawn on the basis of the thickness measurements, i.e. that enhancement of shell production is region-specific, and, by entailment, polymorph-specific. The latter conclusion is plausible when considering simultaneous shell growth and dissolution as will be detailed in the following.

BGD
11, 12571–12590, 2014

Under normal pH conditions *P. caerulea* produces shells characterized by a predominately aragonitic apex area and a flank area which is aragonitic and calcitic in the upper part but solely calcitic in the lower part. This is different for shells formed under low pH conditions. The apex area is still predominantly aragonitic but large parts of the flank area are now aragonitic as well (compare Fig. 4). This observation is related to the fact that shell growth and dissolution take place simultaneously during the complete lifespan of *P. caerulea*. Under normal pH conditions the shell is growing by the addition of calcitic material at the edges of the shell flank in form of a cross foliated structure (MacClintock, 1967). With time this material is dissolved which results in a thinning of the shell. Our observations suggest that *P. caerulea* counteracts this thinning by depositing additional layers on the inside of the shell. Since the deposition of layers at the inside of the shell is related to a mechanism producing aragonite the amount of aragonite increases while calcitic parts at the outside are dissolved. New formation of calcitic areas is only possible during elongation of the shell (increase in size) but not to counteract dissolution. The scenario described above results in the relative (as expressed by FA, Fig. 7) increase in aragonite in the pH_{low}-shells. Taken together with the absolute (as expressed by SNAA, Fig. 8) increase in aragonite and the increased SNT of the apex area (Fig. 6) in the pH_{low}-shells, this suggests a high efficacy of the compensatory shell production. Our results demonstrate that the ability of limpets to cope, to a certain extent (compare also Hall-Spencer et al., 2008; Rodolfo-Metalpa et al., 2011), with corrosive waters is not related to the preferential usage of the more dissolution resistant polymorph, but is solely governed by the mechanism of shell formation. This mechanism allows for compensatory shell thickening through the deposition of additional layers on the inside of the shell. These additional layers are aragonitic, but this is genetically determined and does not represent a response to ocean acidification. The shift towards aragonite seen in pH_{low}-shells is simply a by-product of the way limpets use calcium carbonate polymorphs in shell formation. The fact that the additional, aragonitic, layers of the pH_{low}-shells lead to an increased SNT of the apex

BGD
11, 12571–12590, 2014

(Fig. 6) also shows that aragonite cannot be regarded as a per se disadvantageous polymorph under corrosive ocean acidification.

5 Conclusions

Polymorph distribution analyses of complete cross sections of Patella caerulea shells from a CO_2 vent site at Ischia revealed that this species counteracts shell dissolution in corrosive waters by enhanced production of aragonitic shell layers. The latter are even thicker in corrosion-exposed specimens than in specimens from the control site. We conclude that aragonite cannot be regarded as a per se disadvantageous polymorph under ocean acidification conditions.

References

Bednarsek, N., Tarling, G. A., Bakker, D. C. E., Fielding, S., Jones, E. M., Venables, H. J., Ward, P., Kuzirian, A., Leze, B., Feely, R. A., and Murphy, E. J.: Extensive dissolution of live pteropods in the Southern Ocean, 5, 881–885, 2012.

Field, C. B., Barros, V., Stocker, T. F., Dahe, Q., Mach, K. J., Plattner, G., Mastrandrea, M. D., Tignor, M., and Ebi, K. L.: IPCC Workshop on Impacts of Ocean Acidification on Marine Biology and Ecosystems, 164 pp., 2011.

Gattuso, J.-P. and Hansson, L.: Ocean Acidification, Oxford University Press, 2011.

Hall-Spencer, J. M., Rodolfo-Metalpa, R., Martin, S., Ransome, E., Fine, M., Turner, S. M., Rowley, S. J., Tedesco, D., and Buia, M.-C.: Volcanic carbon dioxide vents show ecosystem effects of ocean acidification, Nature, 454, 96–99, 2008.

Harper, E. M.: Are calcitic layers an effective adaptation against shell dissolution in the Bivalvia?, J. Zool., 251, 179–186, 2000.

Hedegaard, C., Lindberg, D. R., and Bandel, K.: Shell microstructure of a Triassic patellogastropod limpet, Lethaia, 30, 331–335, 1997.

MacClintock, C.: Shell Structure of Patelloid and Bellerophontoid Gastropods (Mollusca), Peabody Museum of Natural History Yale University Bulletin, 22, New Haven, Connecticut, 1967.

BGD
11, 12571–12590, 2014

McClintock, J. B., Angus, R. A., Mcdonald, M. R., Amsler, C. D., Catledge, S. A., and Vohra, Y. K.: Rapid dissolution of shells of weakly calcified Antarctic benthic macroorganisms indicates high vulnerability to ocean acidification, Antarct. Sci., 21, 449–456, 2009.

McNeil, B. I. and Matear, R. J.: Southern Ocean acidification: a tipping point at 450-ppm atmospheric CO_2, P. Natl. Acad. Sci. USA, 105, 18860–18864, 2008.

Nehrke, G. and Nouet, J.: Confocal Raman microscope mapping as a tool to describe different mineral and organic phases at high spatial resolution within marine biogenic carbonates: case study on *Nerita undata* (Gastropoda, Neritopsina), Biogeosciences, 8, 3761–3769, doi:10.5194/bg-8-3761-2011, 2011.

Nehrke, G., Poigner, H., Wilhelms-Dick, D., Brey, T., and Abele, D.: Coexistence of three calcium carbonate polymorphs in the shell of the Antarctic clam Laternula elliptica, Geochem. Geophy. Geosy., 13, Q05014, doi:10.1029/2011GC003996, 2012.

Orr, J. C., Fabry, V. J., Aumont, O., Bopp, L., Doney, S. C., Feely, R. A., Gnanadesikan, A., Gruber, N., Ishida, A., Joos, F., Key, R. M., Lindsay, K., Maier-Reimer, E., Matear, R., Monfray, P., Mouchet, A., Najjar, R. G., Plattner, G.-K., Rodgers, K. B., Sabine, C. L., Sarmiento, J. L., Schlitzer, R., Slater, R. D., Totterdell, I. J., Weirig, M.-F., Yamanaka, Y., and Yool, A.: Anthropogenic ocean acidification over the twenty-first century and its impact on calcifying organisms, Nature, 437, 681–686, 2005.

Rodolfo-Metalpa, R., Houlbreque, F., Tambutte, E., Boisson, F., Baggini, C., Patti, F. P., Jeffree, R., Fine, M., Foggo, A., Gattuso, J.-P., and Hall-Spencer, J. M.: Coral and mollusc resistance to ocean acidification adversely affected by warming, Nature Climate Change, 1, 308–312, 2011.

Royal Society: Ocean Acidification due to Increasing Atmospheric Carbon Dioxide, Policy Document 12/05, The Royal Society, London, 60 pp., 2005.

Stemmer, K. and Nehrke, G.: The distribution of polyenes in the shell of Arctica Islandica from North Atlantic localities: a confocal Raman microscopy study, J. Mollus. Stud., 2014.

Taylor, J. D. and Reid, D. G.: Shell microstructure and mineralogy of the Littorinidae: ecological and evolutionary significance, Hydrobiologia, 193, 199–215, 1990.

Wall, M. and Nehrke, G.: Reconstructing skeletal fiber arrangement and growth mode in the coral *Porites lutea* (Cnidaria, Scleractinia): a confocal Raman microscopy study, Biogeosciences, 9, 4885–4895, doi:10.5194/bg-9-4885-2012, 2012.

BGD
11, 12571–12590, 2014

Table 1. Mean value (±S.D.) of temperature (T), pH (total scale), pCO_2, concentration of HCO_3^- and CO_3^{2-} ions, CO_2 concentration in sea water, dissolved inorganic carbon (DIC), saturation state (Ω) of aragonite and calcite for the study sites.

Site	T (°C)	pH_T	pCO_2 (µatm)	HCO_3^- (µmol kg^{-1})	CO_3^{2-} (µmol kg^{-1})	CO_2 (µmol kg^{-1})	DIC (µmol kg^{-1})	Ω_{Ca}	Ω_{Ar}
C	19.7 (±2.0)	8.03 (±0.05)	474 (±74)	2043 (±46)	220 (±19)	15 (±2)	2279 (±29)	5.15 (±0.45)	3.36 (±0.30)
PL1	20.1 (±2.2)	6.46 (±0.35)	22 047 (±13 264)	2542 (±50)	14 (±21)	758 (±510)	3315 (±526)	0.33 (±0.48)	0.22 (±0.32)
PL2	20.1 (±2.2)	6.51 (±0.38)	19 504 (±12 338)	2509 (±96)	17 (±18)	618 (±392)	3143 (±426)	0.39 (±0.43)	0.26 (±0.28)

BGD
11, 12571–12590, 2014

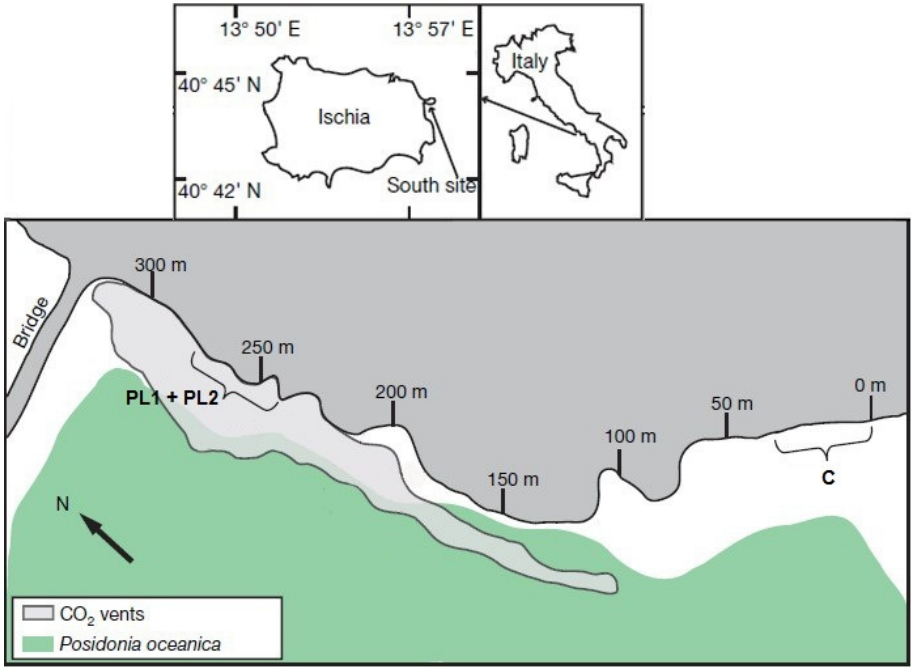

Figure 1. Map of the study area, showing the low pH sites (PL1 and PL2) and the control site (C).

BGD
11, 12571–12590, 2014

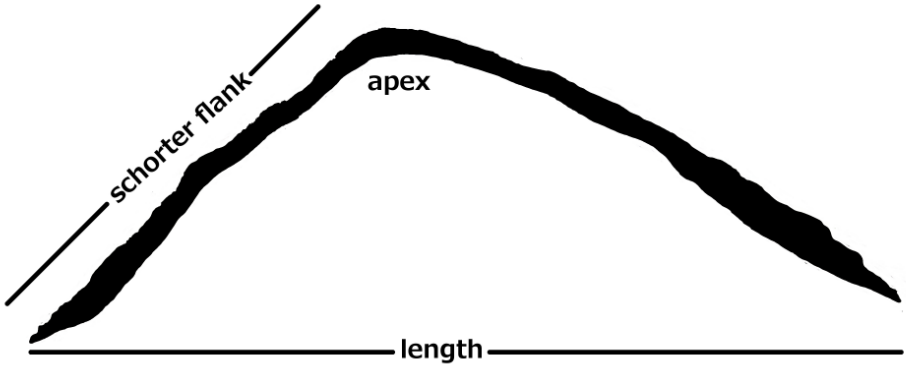

Figure 2. Sketch of a shell indicating length, apex, and shortest flank.

BGD
11, 12571–12590, 2014

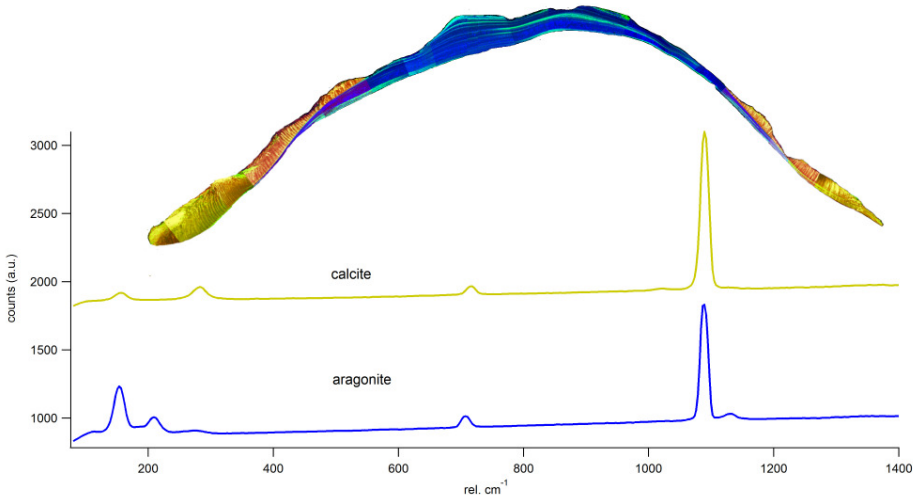

Figure 3. Example of a Raman image across the cross section of the Shell. Blue represents aragonite and yellow calcite, as identified by the corresponding Raman spectra shown.

BGD
11, 12571–12590, 2014

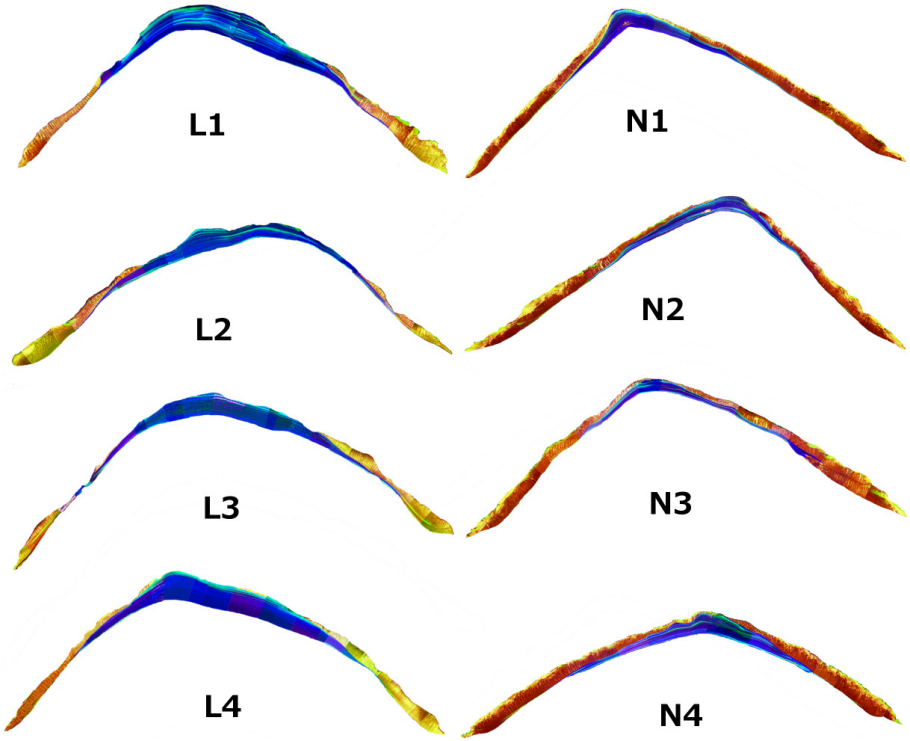

Figure 4. Polymorph distribution of transversally sectioned shells. Blue = aragonite, yellow = calcite. Normal = pH_n-shells, Low = pH_{low}-shells.

BGD
11, 12571–12590, 2014

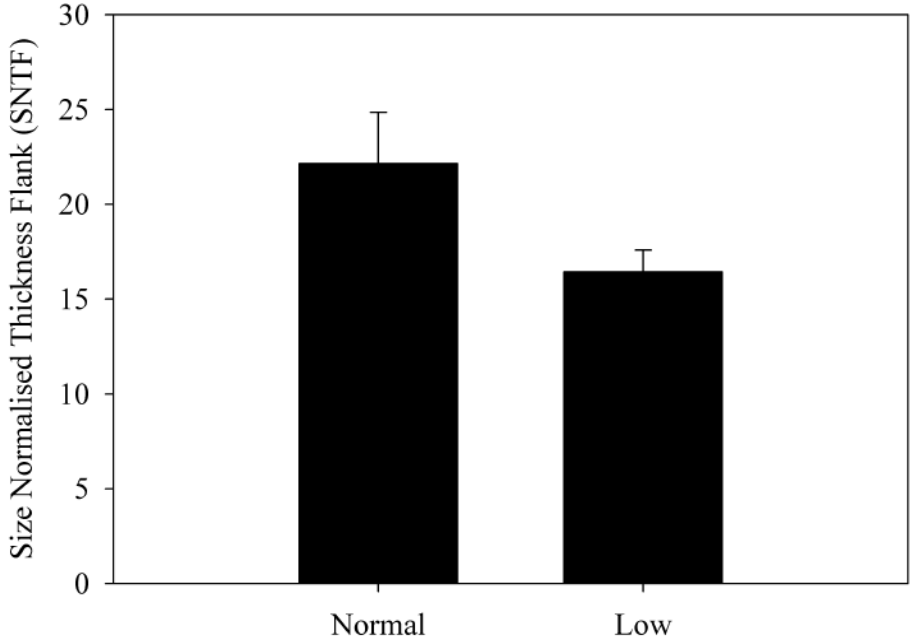

Figure 5. Size normalised thickness of the flank (SNTF). Normal = pH_n-shells, Low = pH_{low}-shells.

BGD
11, 12571–12590, 2014

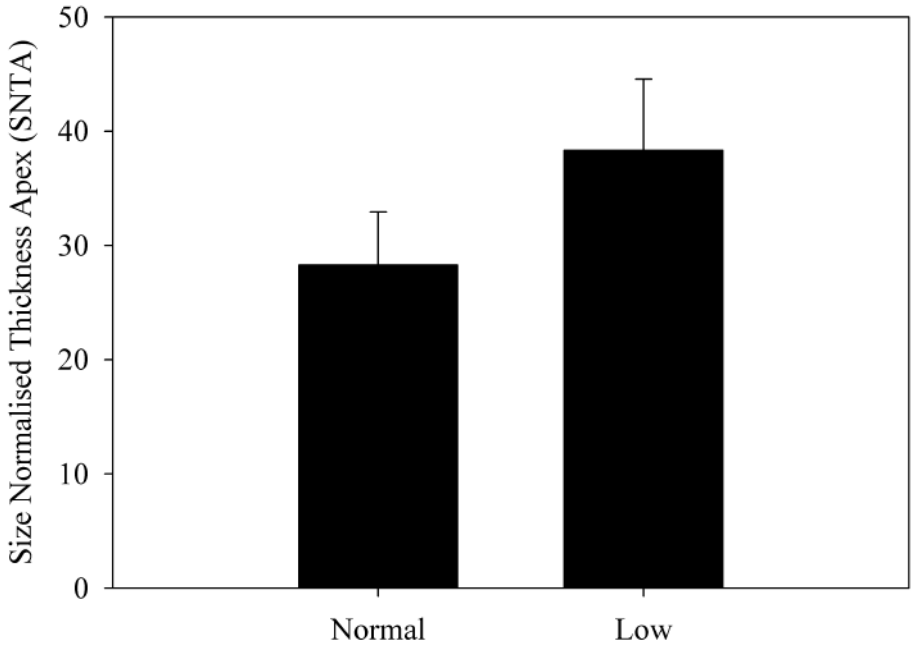

Figure 6. Size normalised thickness of the apex (SNTA). Normal = pH_n-shells, Low = pH_{low}-shells.

BGD
11, 12571–12590, 2014

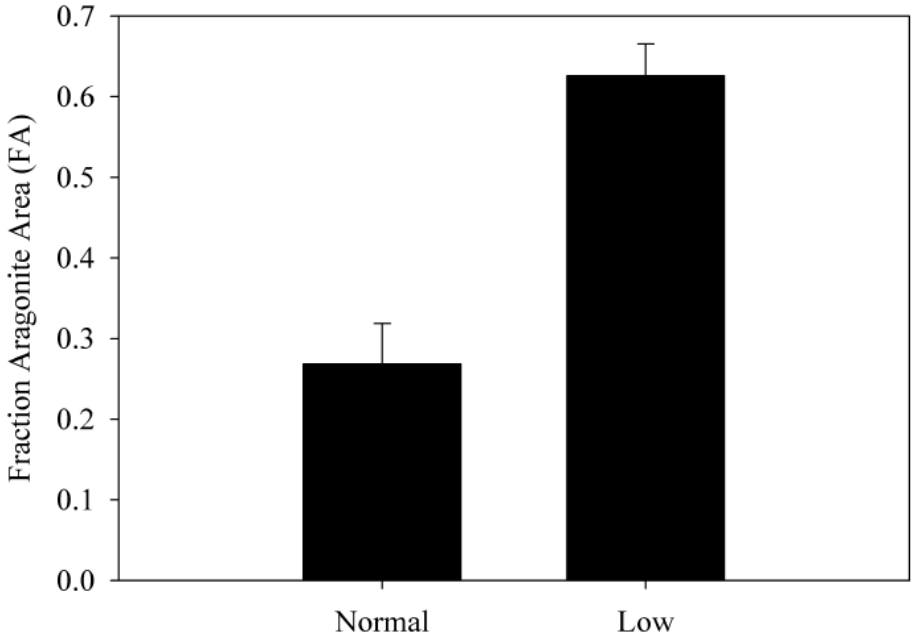

Figure 7. Fraction of aragonite area (FA). Normal = pH_n-shells, Low = pH_{low}-shells.

BGD
11, 12571–12590, 2014

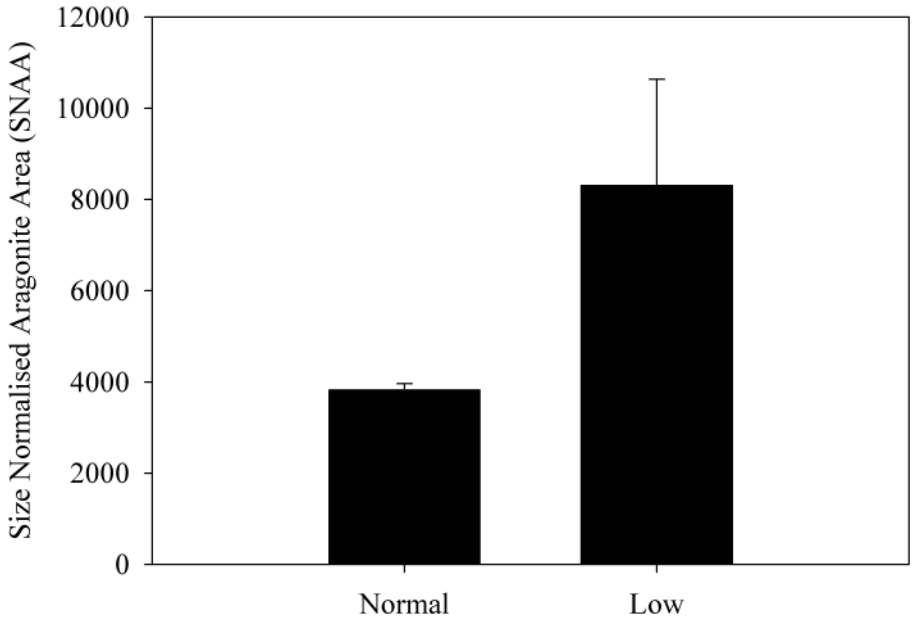

Figure 8. Size normalised aragonite area (SNAA). Normal = pH_n-shells, Low = pH_{low}-shells.

BGD
11, 12571–12590, 2014

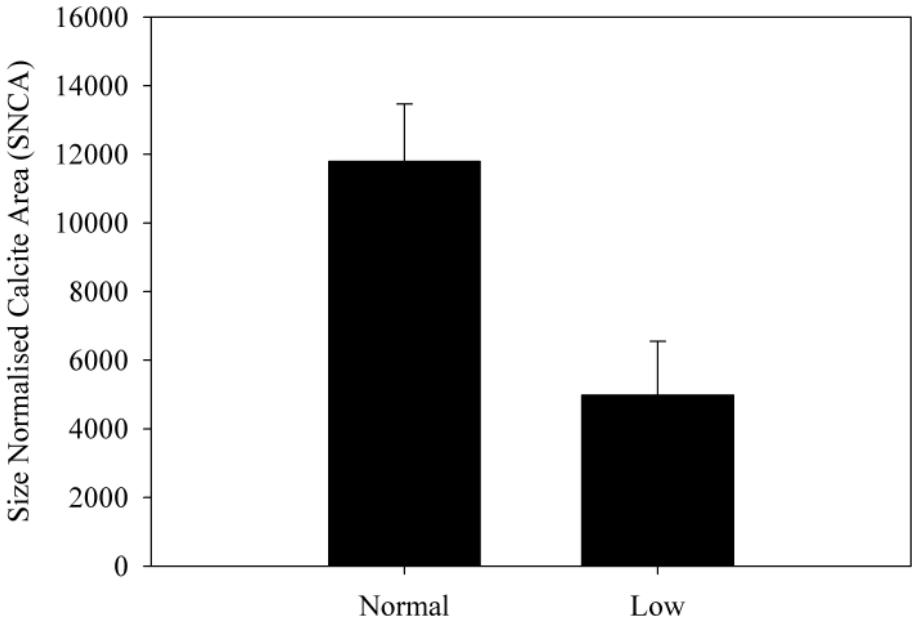

Figure 9. Size normalised calcite area (SNCA). Normal = pH_n-shells, Low = pH_{low}-shells.

BGD
11, 12571–12590, 2014

Appendix E4:

P. Calosi, S.P.S. Rastrick, M. Graziano, S.C. Thomas, **C. Baggini**, H.A. Carter, J. Hall-Spencer, M. Milazzo, J.I. Spicer (2013). Ecophysiology of sea urchins living near shallow water CO_2 vents: Investigations of acid-base balance and ionic regulation using *in-situ* transplantation. *Marine Pollution Bulletin*, 73: 470-484.

ARTICLE IN PRESS

Marine Pollution Bulletin xxx (2013) xxx–xxx

Contents lists available at SciVerse ScienceDirect

Marine Pollution Bulletin

journal homepage: www.elsevier.com/locate/marpolbul

Distribution of sea urchins living near shallow water CO_2 vents is dependent upon species acid–base and ion-regulatory abilities

P. Calosi [a,*], S.P.S. Rastrick [a], M. Graziano [b,c], S.C. Thomas [a], C. Baggini [a], H.A. Carter [d], J.M. Hall-Spencer [a], M. Milazzo [c], J.I. Spicer [a]

[a] Marine Biology and Ecology Research Centre, School of Marine Science & Engineering, University of Plymouth, Drake Circus, Plymouth PL4 8AA, UK
[b] CNR-Institute of Atmospheric Pollution Research, UNICAL-Polifunzionale, 87036 Rende, Italy
[c] Dipartimento di Scienze della Terra e del Mare, CoNISMa, University of Palermo, via Archirafi 28, 90123 Palermo, Italy
[d] Romberg Tiburon Center for Environmental Studies, San Francisco State University, Tiburon, CA 94920, USA

ARTICLE INFO

Keywords:
Carbon capture and storage (CCS)
Ocean acidification
Arbacia lixula
Paracentrotus lividus
Acid–base and ionic regulation
Distribution

ABSTRACT

To reduce the negative effect of climate change on Biodiversity, the use of geological CO_2 sequestration has been proposed; however leakage from underwater storages may represent a risk to marine life. As extracellular homeostasis is important in determining species' ability to cope with elevated CO_2, we investigated the acid–base and ion regulatory responses, as well as the density, of sea urchins living around CO_2 vents at Vulcano, Italy. We conducted *in situ* transplantation and field-based laboratory exposures to different pCO_2/pH regimes. Our results confirm that sea urchins have some ability to regulate their extracellular fluid under elevated pCO_2. Furthermore, we show that even in closely-related taxa divergent physiological capabilities underlie differences in taxa distribution around the CO_2 vent. It is concluded that species distribution under the sort of elevated CO_2 conditions occurring with leakages from geological storages and future ocean acidification scenarios, may partly be determined by quite subtle physiological differentiation.

1. Introduction

Increased anthropogenic CO_2 emissions accompanied the advent of industrialisation and have resulted over the past two centuries in a net increase in atmospheric CO_2 (Solomon et al., 2007). This in turn increased oceanic CO_2 levels, resulting in a reduction in both pH and carbonate ion (CO_3^{2-}) concentration (Zeebe and Wolf-Gladrow, 2001). This phenomenon is termed ocean acidification (OA) (Caldeira and Wickett, 2003; Orr et al., 2005; Raven et al., 2005) and is considered a threat to marine life. The use of geological CO_2 sequestration (so called Carbon Capture and Storage – CCS) has been proposed to reduce (or slow down) the impact of global climate change on global biodiversity (Gibbins et al., 2006; Blackford et al., 2009). However, leakages from CCS represent a potential risk to marine life, as they may lead to localized acute and extreme CO_2 release events, with potentially negative biological consequences (Seibel and Walsh, 2003; Barry et al., 2004; Blackford et al., 2009; Small et al., 2010; Christen et al., 2012; Donohue et al., 2012). There is evidence that increased CO_2 levels in sea water and the resultant reduction in pH may impair physiological, ecological and behavioural functions of marine animals (Widdicombe and Spicer, 2008; Melzner et al., 2009; Munday et al., 2009). The capacity for extracellular acid–base regulation is thought to be important in determining a species' ability to cope with elevated CO_2 (Pörtner et al., 1998; Widdicombe and Spicer, 2008; Melzner et al., 2009; Whiteley, 2011), with echinoderms and molluscs being amongst the phyla exhibiting the poorest regulatory abilities, and thus being amongst the most vulnerable. The vulnerability of echinoderms and molluscs to OA is highlighted by the results of a series of multispecies mesocosm laboratory experiments (Widdicombe et al., 2009; Hale et al., 2011; Christen et al., 2012) and observations made on assemblages associated with natural CO_2 vents (Hall-Spencer et al., 2008; Cigliano et al., 2010; Kroeker et al., 2011; Johnson et al., 2012). The abundance of echinoids and bivalves, in particular, is negatively related to increased seawater pCO_2 (or reduced pH), indicating that in a future high-CO_2 world taxa distribution may in part be determined by their homeostatic abilities and associated energy costs.

Most studies investigating how elevated CO_2 conditions will impact the function of marine organisms are laboratory-based (although cf. Thomsen et al., 2010; Lombardi et al., 2011; Rodolfo-Metalpa et al., 2011), making it difficult to directly relate laboratory results to the effect that elevated CO_2 (i.e. OA and CCS leakages) will have on marine biota *in situ*. Field experiments, at sites with naturally-elevated CO_2 conditions, such as shallow-water

* Corresponding author. Tel.: +44 (0)1752 586125; fax: +44 (0)1752 584605.
E-mail address: piero.calosi@plymouth.ac.uk (P. Calosi).

0025-326X/$ - see front matter Crown Copyright © 2012 Published by Elsevier Ltd. All rights reserved.
http://dx.doi.org/10.1016/j.marpolbul.2012.11.040

CO_2 vents, are potentially useful analogues for investigating the effect of future dissolved CO_2 levels on marine organisms and ecosystems (Hall-Spencer et al., 2008; Cigliano et al., 2010; Thomsen et al., 2010; Lombardi et al., 2011; Rodolfo-Metalpa et al., 2011; Kroeker et al., 2011, 2012).

As mentioned previously, echinoderms, and echinoids in particular, are considered particularly vulnerable to low pH and carbonate saturation status (e.g. Kurihara and Shirayama, 2004a, 2004b; Miles et al., 2007; Widdicombe and Spicer, 2008; Melzner et al., 2009; Todgham and Hofmann, 2009; Dupont et al., 2010; Spicer et al., 2011; Stumpp et al., 2011; Catarino et al., 2012). However, contrary to the prevailing view that echinoids possess limited (or no) extracellular regulatory ability, recent studies seem to indicate the presence of a diverse suite of acid–base and osmo–iono responses to elevated CO_2 (low pH) in some sea urchin species (Miles et al., 2007; Vidolin et al., 2007; Spicer et al., 2011; Stumpp et al., 2011; see also Spicer et al., 1988), For example, values of the non-bicarbonate buffer line slope (β_{NB}, expressed here as mmol l^{-1} pH^{-1}, Stumpp et al., 2012) for the species of sea urchins investigated to date appear to vary between 0.4 and 5.6 (see Spicer et al., 1988, 2011; Miles et al., 2007; Stumpp et al., 2011), suggesting considerable variation in aspects of the acid–base regulatory ability within this group, perhaps as extreme as the comparison between gastropod and bivalves with cephalopods (i.e. both ends of the range of homeostatic properties of the acid–base status for invertebrates, see Melzner et al., 2009 for review). Clearly we do not yet have a good working knowledge of acid–base regulation in echinoids, let alone understand the physiological responses closely-related species will show to elevated CO_2, and the importance of such responses to species' ecology.

This aim of this study is to better understand the physiological responses of vulnerable shallow-water marine organisms *in situ* to the exposure to elevated CO_2 (low pH) predicted to occur under future OA, and potential CCS leakage scenarios. Consequently, we investigated the extracellular acid–base balance and ionic regulation of two sea urchin species both *in situ*, and after transplantation around shallow water CO_2 vents at Vulcano Island, Italy. First, we determined the distribution and density of both species at key points along the CO_2/pH gradient at the vent, selecting comparable habitats suitable for sea urchins settling. We then characterised baseline extracellular acid–base and ionic values in untreated, field-collected individuals as a back-drop to investigating the acid–base and ionic regulatory responses of sea urchins exposed in *in situ* transplantation (2–4 d) and in a short-term field-laboratory experiments (0–24 h) to different pCO_2/pH conditions.

2. Materials and methods

2.1. Species studied

Only two echinoid species are common around the shallow water CO_2 vents of Vulcano Island; the black sea urchin, *Arbacia lixula* (Linnaeus 1758) and the purple sea urchin, *Paracentrotus lividus* (Lamarck 1816). Both species regularly co-occur in the infralittoral zone along the Mediterranean and north-east Atlantic coasts (Privitera et al., 2008). Although both species are found in coralline algal barrens, macroalgae and seagrass habitats (Privitera et al., 2008; Bonaviri et al., 2011; Pinna et al., 2012), *A. lixula* preferentially feeds on encrusting coralline algae (Privitera et al., 2008), and at least partially on sessile animals (Wangensteen et al., 2011), whilst *P. lividus* favours erect fleshy algae (Privitera et al., 2008; Bonaviri et al., 2011). Sparid fishes and starfish are natural predators of both sea urchins, as are some labrid fishes which prey on their juvenile forms (Hereu et al., 2005; Bonaviri et al., 2009). Of the two species only *P. lividus* is harvested, although no harvesting was recorded in the study area, which is private property inaccessible to bathers.

2.2. Study site and sea urchin survey

The study area is Levante Bay (38°25'N, 14°57'E) located on the north-east side of the volcanic island, Vulcano (Italy), where an active shallow-water CO_2 vent creates a natural pH and pCO_2 gradient along the north-westerly side of the bay (Johnson et al., 2011; Arnold et al., 2012; Lidbury et al., 2012; Boatta et al., in press, see Fig. 1). The stations identified for the experiment were characterised by different concentrations of CO_2 and thus different levels of pH (A: non-acidified water, B and C: acidified water; see Table 1, Fig. 1), but were similar in depth (approx. 2–3 m). The densities of sea urchins (*A. lixula* and *P. lividus*) were estimated at stations A and B, whilst at station C there was no suitable habitat for sea urchins to settle on and so, unsurprisingly, no sea urchins were found. Counts of both sea urchin species were obtained from a visual census and density expressed as numbers of individuals encountered while snorkelling a 2×5 m transect over comparable rocky substrata with macroalgal coverage (Kingsford and Battershill, 1998; Edgar and Barret, 1997). Three transects (in total 12 replicates at 1–3 m water depth) were surveyed in two areas chosen haphazardly within stations A and B.

2.3. Environmental monitoring

Seawater pH, temperature and salinity were measured at different stations and on numerous occasions throughout the duration of the observations and experiments described below (approx. three weeks). These values are compared with a monitoring programme carried out at this same site by Boatta et al. (in press), which took place from September 2009 to July 2011. This was a good cross-check on whether the environmental conditions to which we exposed the sea urchins during the experiments, described below, were representative of the mean and variation characterising the pH gradient. For the *in situ* transplantation and field-laboratory experiments the environmental monitoring was carried out as follows. pH_{NSB} was measured using a pH electrode, always maintained at ambient seawater temperature (Seven Easy pH InLab micro-electrode, Mettler-Toledo Ltd., Beaumont Leys, UK), coupled to a pH meter (Sevengo, Mettler-Toledo Ltd., Beaumont Leys, UK) and calibrated using Mettler-Toledo pH standards (pH 4.01, 7.00, 9.21 at 25 °C) also maintained at seawater temperature. Temperature was measured using a digital thermometer (HH806AU, OMEGA Eng. Ltd., Manchester, UK). Salinity was measured using a hand-held conductivity meter (TA 197 LFMulti350, WTW, Weilheim, Germany). Mean total alkalinity values given here were taken from Johnson et al. (2011). Additional carbonate system parameters (dissolved inorganic carbon (DIC), pCO_2, calcite and aragonite saturation, [HCO_3^-] and [CO_3^{2-}]) were calculated from pH and TA measurements using the software program CO2SYS (Pierrot et al., 2006) with dissociation constants from Mehrbach et al. (1973) refit by Dickson and Millero (1987) and [KSO_4] using Dickson (1990).

Our results for the carbonate system along the pCO_2/pH gradient of the vent (Table 1) indicate that the mean values for water chemistry parameters recorded during the *in situ* transplantations and the field-laboratory experiments were broadly comparable (see Table 1) to those of Boatta et al. (in press) with one important exception, as a shift in pCO_2/pH during our study resulted in the seawater chemistry of station C resembling more closely the profile of station B. So sea urchins were transplanted to station C to carry out the 2–4 d *in situ* exposure. Also seawater was pumped from station C to the field-laboratory for use in the 0–24 h experiment, field-laboratory experiments.

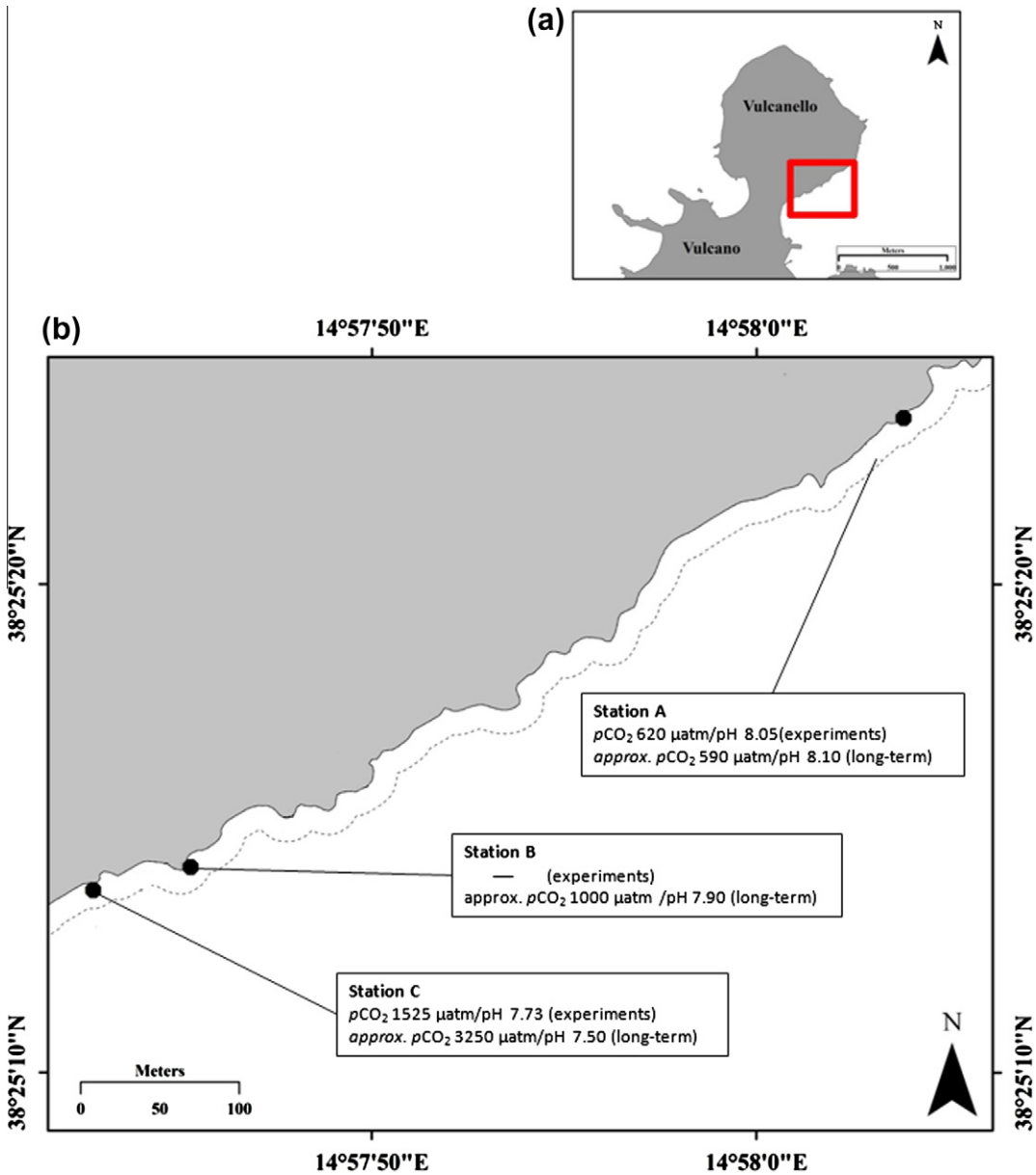

Fig. 1. Maps of the study area showing the (a) northern region of the island of Vulcano (Sicily, Italy), the red square indicates the study area in Cala di Levante; and (b) pCO_2/pH gradient around the CO_2 vent; the grey shaded area represents land, the continuous line represents the coastline, and the dashed line defines the 5 m seawater belt parallel to the coastline were the pCO_2/pH gradient is present. Station A: Caging experiment and sea-urchin density visual census site with normal pH; station B: Sea-urchin density visual census site in acidified waters; station C: Caging experiment site in acidified waters. In the boxes for each station, mean values for pCO_2 and pH are reported for measurements obtained *in situ* throughout the duration of the 'experiments' (approx. three weeks), and from a 'long-term' monitoring programme carried out at this same site (see Boatta et al. (in press) in this special issue).

2.4. Sea urchins collection and experimental set-up

Sea urchins were collected by hand from station A by snorkelers, and immediately transferred to a bucket (vol. = 12 l) whilst still underwater to avoid any negative effects of the exposure to air on sea urchin physiology (see Spicer et al., 1988; Burnett et al., 2002). Buckets containing sea urchins were kept immersed for <5 min before removal to the experimental field laboratory (near station C) which minimised potential thermal fluctuations. Upon arrival sea urchins were used in one of three different ways:

(i) To characterise the physiological parameters to establish baseline levels for untreated, field-collected individuals as described below, *A. lixula* ($N = 23$) and *P. lividus* ($N = 34$). Immediately upon arrival at the field laboratory coelomic fluid was collected, physiological and morphometric measurements made, and sampling of calcified structures was carried out (all as described in detail below).

(ii) For a transplantation caging experiment to investigate sea urchins *in situ* physiological responses over 2 and 4 d exposure to either control or elevated pCO_2. After collection from station A two groups of approx. 10 individuals *per* species, *per* treatment were haphazardly selected and placed individually in cages (20 × 20 × 20 cm, wooden framed with plastic garden mesh ∅ = 0.5 cm). Five or six stones of comparable size were placed in each cage; stones were collected from the same area were sea urchins were collected and were covered by a natural film of bacteria/microalgae. This

Table 1
Mean ± SD of seawater physico-chemical parameters measured in, or calculated for, the field and field-laboratory control and acidified areas. Seawater chemistry parameters, dissolve inorganic carbon (DIC), CO_2 partial pressure (pCO_2), calcite and aragonite saturation (Ω_{calc} and Ω_{ara}), bicarbonate and carbonate ions concentration ([HCO_3^-] and [CO_3^{2-}]), were calculated from pH and total alkalinity (TA) using CO2SYS (Pierrot et al., 2006) with dissociation constants from Mehrbach et al. (1973) refit by Dickson and Millero (1987) and [KSO_4] using Dickson (1990) are indicated by an asterisk (*). TA values are from Johnson et al., 2011 (†).

Parameter	Field		Field-laboratory	
	Station A – control (*in situ* transplantation experiment)	Station C – acidified (*in situ* transplantation experiment)	Control (0–24 h experiment)	Acidified (0–24 h experiment)
Salinity	38	38	38	38
Temperature (°C)	19.51 ± 0.24	19.85 ± 0.91	22.12 ± 0.20	23.01 ± 1.11
TA (μEq kg^{-1})†	2625	2736	2625	2736
pH	8.05 ± 0.04	7.73 ± 0.09	8.06 ± 0.05	7.69 ± 0.12
DIC (μmol kg^{-1})*	2391.66 ± 22.87	2646.40 ± 36.09	2369.41 ± 28.95	2646.95 ± 45.15
pCO_2 (μatm)*	620.09 ± 68.83	1525.76 ± 397.40	619.26 ± 8212	1754.60 ± 583.18
Ω_{calc}*	4.14 ± 0.34	2.29 ± 0.40	4.50 ± 0.43	2.34 ± 0.49
Ω_{ara}*	2.70 ± 0.21	1.50 ± 0.26	2.96 ± 0.28	1.54 ± 0.32
HCO_3^- (μmol kg^{-1})*	2194.44 ± 35.13	2499.65 ± 41.43	2158.26 ± 44.93	2495.88 ± 50.53
CO_3^{2-} (μmol kg^{-1})*	177.25 ± 14.40	96.13 ± 17.18	192.56 ± 16.48	99.99 ± 20.94

provided both a suitable substrata for the sea urchins to attach onto and a source of food to graze on. After 2 or 4 d of exposure to either control or acidified conditions (station A and C respectively), eight individuals *per* species, *per* treatment were haphazardly recovered by snorkelling, immediately transported to the field laboratory in a bucket of sea water. Upon arrival, extracellular (coelomic) fluid was collected and physiological, morphometric and body mass measurements were obtained (as described below).

(iii) To investigate more acute physiological responses in the sea urchins to aid interpretation of the trajectory observed at 2 and 4 d, a field-laboratory was constructed to conduct repeated measures at different times over a 24 h period of sea urchins exposed to either control or elevated pCO_2. On arrival at the field laboratory eight specimens *per* species, *per* treatment were immediately transferred to individually-identifiable open containers (vol. = 1 l) nested within an opaque experimental aquaria (vol. = 80 l), fitted with a lid. This small set-up was coupled to an electrical water pump (2CPM80E HP 0.5, Pedrollo, Verona, Italy) for the continuous circulation of sea water within the aquaria (flow rate: max 130 ± 5 l min^{-1}). Sea water was supplied from either the control or acidified area, *via* an adjustable-length hose, for the entire duration of the trials, thus maintaining pH, temperature and salinity conditions near-identical to that of the relative field stations. Coelomic fluid from individual sea urchins exposed to low or elevated pCO_2 conditions was sampled at 0, 1.5, 3, 6, 12 and 24 h for the determination of acid–base balance parameters (see Section 2.5), and at 0, 3, 6, 12 and 24 h for the determination of ions concentrations (see Section 2.5). All sampling took place on partly immersed individuals. Morphometric measurements, detailed below, were undertaken at the end of the experiment. All experiments were run in parallel, but separately, for the two species investigated.

2.5. Sampling and analysis of coelomic fluid

Upon arrival at the field laboratory, sea urchins were either sampled immediately or after exposure, always within 3 s of being handled under water. A clean, clear and anaerobically-obtained, coelomic fluid sample (vol. = 100 μl) was obtained from each individual by inserting the needle of a gas-tight syringe (Hamilton, gas-tight 1710RN, Bonaduz, Switzerland, vol. = 100 μl), to a depth of about 1 cm through the peristomial membrane and the peripharyngeal peritoneum, into the perivisceral coelom. The residence time of samples within the syringe was <10 s, before use in the determination of acid–base parameters or storage for subsequent analysis (see below).

To measure coelomic fluid pH (pH_{cf}), total CO_2 [TCO_2] and major cations the following procedure was carried out. To determine TCO_2, a 50 μl subsample was immediately introduced anaerobically into a previously calibrated carbon dioxide analyser (965D, Ciba Corning Diagnostics Cor., Cambridge, USA). The remaining fluid (vol. = 50 μl) was transferred immediately to a 0.5 ml microcentrifuge tube (polyethylene Beckman type, Fisher Scientific, Loughborough, UK) and pH_{cf} measured (< 10 s after extraction) by immersing a micro-pH probe (Micro-InLab pH combination electrode, Mettler Toledo) in the fluid creating an anaerobic sealed area between the bottom of the tube and the tip of the pH probe (see also Miles et al., 2007; Spicer et al., 2007; Marchant et al., 2010; Small et al., 2010; Donohue et al., 2012). The micro-pH probe was coupled to a pH meter (Seven Easy pH Meter, Mettler Toledo), calibrated as described above. The remaining coelomic fluid (vol. = 50 μl, min 10 μl) was sealed in the microcentrifuge tube, stored for 2 weeks at ambient temperature and subsequently used for cation analysis upon return to Plymouth, UK. These samples of coelomic fluid (10 μl) were carefully diluted to a final volume of 2 ml using ultra-pure water. The resultant dilutions were then analysed for [Ca^{2+}], [Mg^{2+}], [Sr^{2+}], [Na^+] and [K^+], using an ICP optical emission spectrometer (725-ES, Varian Medical Systems Inc., Palo Alto, USA). Values were expressed as mmol l^{-1}. To execute these measurements as rapidly as possible two operators always worked together.

2.6. Calculation of coelomic fluid pCO_2 and [HCO_3^-]

Coelomic fluid pCO_2 and [HCO_3^-] were calculated using the Henderson–Hasselbach equation in the following forms (see Spicer et al., 2007):

$$pCO_2 = TCO_2/\alpha(10^{(pHcf-pK'1)} + 1) \quad (1)$$

$$[HCO_3^-] = TCO_2 - \alpha pCO_2 \quad (2)$$

where α is the solubility coefficient of CO_2 of sea water taken as 0.337 mmol l^{-1} kPa^{-1} at 15 °C approx. 35 salinity, and pK'_1 is the negative log of the first apparent dissociation constant of carbonic acid taken as 6.04 at 15 °C (Truchot, 1976). Truchot's pK_1 for haemolymph for the crab, *Carcinus maenas* was chosen because: (i) the pK_1 for *A. lixula* could not be determined at the time of this experiment due to logistic difficulties and it is not available in the literature, (ii) pK_1 for *P. lividus* whilst available in the literature was determined in an Atlantic population and under a different salinity-temperature regime than used here, (iii) Truchot

determined values over a salinity-temperature range similar to that of this present study.

2.7. Measurement of echinoid mass, morphometrics and mineralisation of calcified structures

Immediately post-sampling, individual sea urchins were weighed with a digital high-precision scale (BA 210-S, Sartorius Mechatronics, Göttingen, Germany, to 0.1 mg accuracy), taking great care to avoid loss of coelomic fluid from the wound created by the sampling described above.

The height and diameter of the test were then measured using precision callipers. Finally, individuals were sacrificed and the entire test, all undamaged primary spines (not from the ambulacral region) and entire Aristotle's lanterns samples were collected for cations analyses upon return to Plymouth, UK. Upon arrival, individual tissue samples were scrubbed clean of all organic material using a plastic soft brush and plastic dissection tools before being freeze-dried at −50 °C for 48 h with a freeze-drier apparatus (Edwards Super Modulyo, Edwards Vacuum, Crawley, UK). Samples were weighed with a high precision digital scale (PS-200, Fisher Scientific Ltd., Corby, UK, to 0.1 mg accuracy) before being digested individually in a glass beaker (vol. = 50 ml) containing 3 ml of nitric acid (70% concentration, trace analysis grade, Fisher Scientific UK Ltd., Loughborough, UK). The beaker was covered with a watch glass and left at room temperature for 60 min to allow readily oxidised material to be digested. The beaker containing the digestant was then placed in a high-Throughput Microwave Reaction System Run (MARSXpress, CEM Corporation, Matthews, USA) and gently heated to boiling for at least 1 h to ensure full digestion. The sample was then transferred to an acid-washed 25 ml volumetric flask and diluted to 25 ml with ultra-pure water to obtain solutions with concentration of the cations of interests within the range detectable by an atomic absorption spectrometer. The sample was then analysed for [Ca^{2+}], [Mg^{2+}] and [Sr^{2+}] using an ICP optical emission spectrometer (725-ES, Varian Medical Systems Inc., Palo Alto, USA). Data were expressed as mmol of ion kg^{-1}.

2.8. Statistical analysis

Differences in the density and distribution of *A. lixula* and *P. lividus*, separately were tested using two univariate PERMANOVA applying the following two factorial experimental design with 'pH station' (two levels, fixed) and 'Area' (two levels, random, nested in pH) (Anderson, 2001).

Two different statistical approaches were employed to analyse the short-term laboratory (0–24 h) and longer-term *in situ* (2–4 d) exposure experiments. For the short-term exposure experiment, as measurements were repeated on the same individuals at each time interval, a two-way nested orthogonal experimental design was employed to investigate the relationship between pCO_2/pH exposure and duration of exposure and the physiological parameters measured, with individuals set as random factors nested in the pCO_2/pH treatment. For the long-term exposure experiment a two-way orthogonal experimental design was employed to investigate the relationship between pCO_2/pH exposure and duration of exposure and the physiological parameters measured. For both experimental designs, relationships were explored using GLM with the spheroid volume of the main body of the sea urchin or mass as a covariate. We included spheroid volume, as a proxy for coelomic fluid volume, as potentially more relevant to the investigation of acid–base and ionic regulation. When mass and volume as the covariate were found not to have a significant effect on acid–base and ionic regulation traits, they were removed from analysis. In addition, where a significant relationship between pCO_2/pH and duration of exposure was detected comparisons amongst treatments for any given life-history and physiological parameter were conducted using Estimate Marginal Mean tests with Bonferroni adjustment for multiple comparisons.

Data met assumption for normality of distribution for most parameters (minimum $Z_{32} = 1.309$, $P = 0.065$, Kolmogorov–Smirnov test), with the following exceptions: in *P. lividus* TCO_2/pCO_2/[HCO_3^-] for the 0–24 h exp., in *A. lixula* TCO_2 and pCO_2 for the 2–4 d exp., and finally in untreated field-collected individuals pCO_2 (maximum $Z_{96} = 1.813$, $P < 0.0001$, Kolmogorov–Smirnov test). Assumption of homogeneity of variance was met for all traits investigated (minimum $F_{3,28} = 2.657$, $P = 0.068$, Levene's test), with the following exceptions: in *P. lividus* pH for the 2–4 d exp., TCO_2/pCO_2/[HCO_3^-] for the 0–24 h exp., in *A. lixula* pCO_2 for the 2–4 d exp., pH/TCO_2/pCO_2/[HCO_3^-] for the 24 h exp., and finally for untreated field-collected individuals TCO_2 and HCO_3^- (maximum $F_{1,56} = 6.218$, $P = 0.016$, Levene's test). However, our experimental designs included between 4 and 12 treatment combinations for the short-term field laboratory and long-term *in situ* experiments with a minimum of seven replicates *per* pCO_2/pH ∗ duration combination. Thus we assume that our test should be tolerant to deviation from the assumption of normality and homogeneity (Sokal and Rohlf, 1995; Underwood, 1997). For the testing of physiological parameters in untreated field-collected individuals, where assumptions of the test used were not met, a Kruskal–Wallis test or a Welch ANOVA test as appropriate were run to validate the results of the *t*-test. All statistical analyses were conducted using SPSS v.19.

3. Results

No mortality was recorded for any of the collections and experiments undertaken, with all sea urchins appearing to be in a good health (actively moving spines and tubular feet, and showing no spine loss) throughout the duration of the experiments.

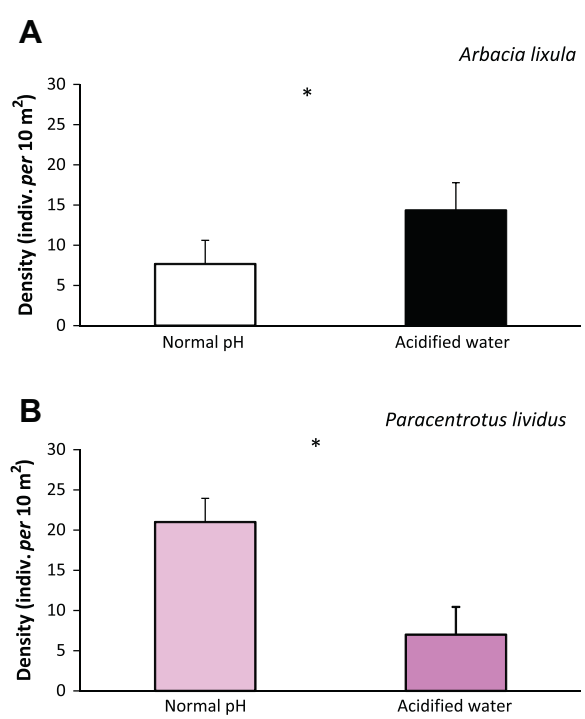

Fig. 2. The densities of (A) the black sea urchin, *Arbacia lixula* and, (B) the purple sea urchin, *Paracentrous lividus* separately for each species under control (white and pink respectively) and acidified conditions (black and purple respectively). ∗ indicate significant differences ($P < 0.05$) in the densities recorded at each pCO_2/pH area. (For interpretation of the references to color in this figure legend, the reader is referred to the web version of this article.)

3.1. Sea urchins' density along the pCO_2/pH gradient

Mean density of *Arbacia lixula* was approx. eight indiv. *per* 10 m^2 in the control area (station A) and 14 indiv. *per* 10 m^2 inside the acidified area (station B) (Fig. 2A). This difference in density between the two sites characterised by different pH levels, was significant (Pseudo-$F_{1,11}$ = 200.00, P = 0.005). In *Paracentrotus lividus*, however, mean density was approx. 21 indiv. *per* 10 m^2 in the control area (station A) and seven indiv. *per* 10 m^2 inside the acidified area (station B) (Fig. 2B). Again, the difference in density between the sites was significant (Pseudo-$F_{1,11}$ = 21.51, P = 0.046) but where *A. lixula* was most abundant in the acidified area, *P. lividus* was more abundant in the control area. For both species, the term 'Area (pH)' had no significant effect (maximum Pseudo-$F_{2,11}$ = 2.12, P = 0.174).

3.2. Acid–base balance and cation status in field-collected, untreated individuals

Baseline parameters for extracellular fluid acid–base status in field-collected untreated individuals of the sea urchin *A. lixula* and *P. lividus* are presented in Fig. 3, and those for extracellular fluid ionic status are presented in Table 2. In summary, *A. lixula* showed lower mean coelomic fluid pH, TCO_2 and bicarbonate

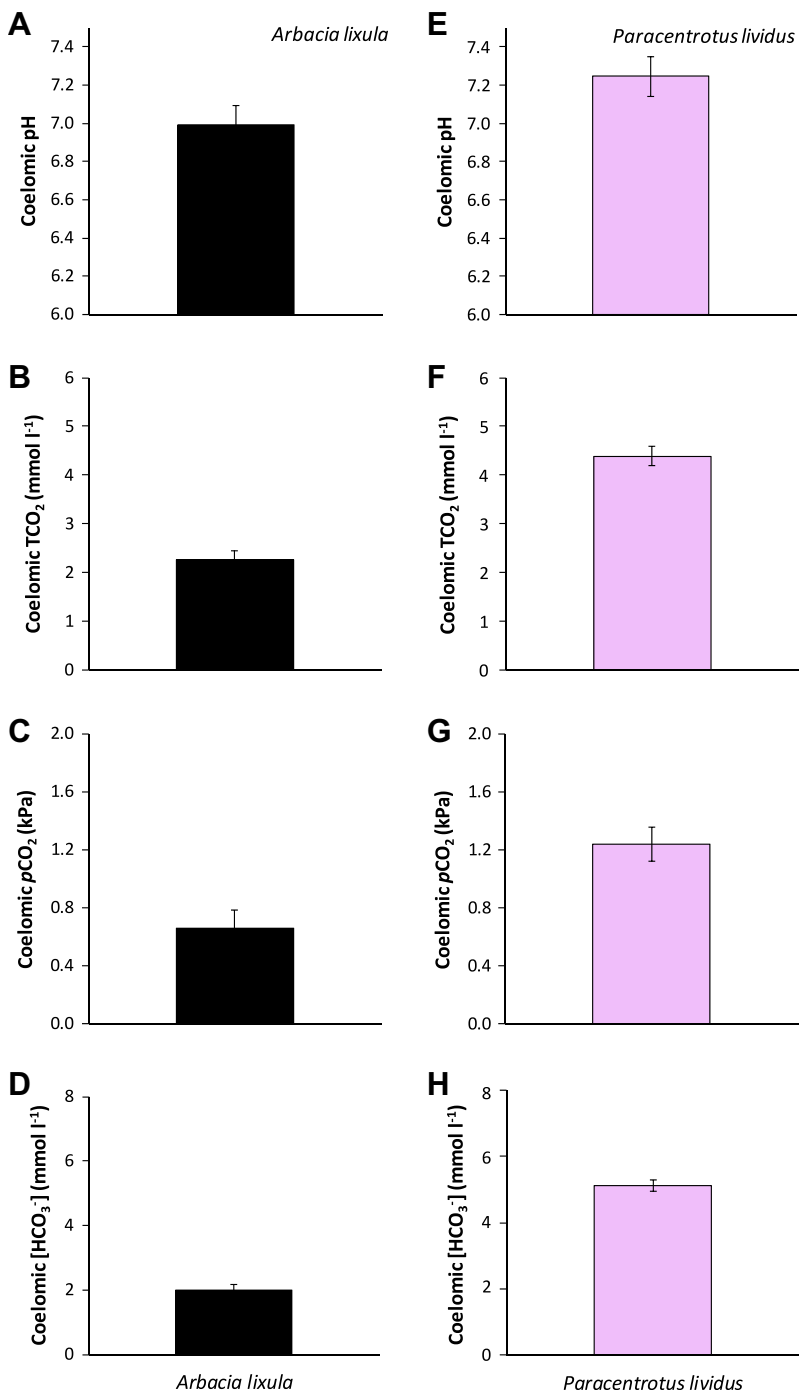

Fig. 3. Baseline parameters for extracellular fluid acid–base status (pH, TCO_2, pCO_2, [HCO_3^-]) in untreated field-collected sea urchins of *A. lixula* (A–D in black) and *P. lividus* (E–H in pink). Histograms are means ± SE. (For interpretation of the references to color in this figure legend, the reader is referred to the web version of this article.)

Please cite this article in press as: Calosi, P., et al. Distribution of sea urchins living near shallow water CO_2 vents is dependent upon species acid–base and ion-regulatory abilities. Mar. Pollut. Bull. (2013), http://dx.doi.org/10.1016/j.marpolbul.2012.11.040

Table 2
Ionic content of the coelomic fluid and calcified tissues of field-collected untreated individuals of the black sea urchin, *Arbacia lixula* (Linnaeus 1758) and the purple sea urchin, *Paracentrotus lividus* (Lamarck 1816). Values are mean ± SE. Data are expressed as mmol l^{-1} for coelomic fluid and mmol kg^{-1} for the other parameters.

Structure	Inn	*Arbacia lixula*	*Paracentrotus lividus*
Coelomic			
	Ca^{2+}	14.52 ± 0.49	8.74 ± 0.24
	Mg^{2+}	65.22 ± 4.3	53.94 ± 1.30
	Sr^{2+}	0.19 ± 0.01	0.09 ± 0.002
	Na^{+}	558 ± 20	462 ± 11
	K^{+}	14.29 ± 0.69	1319 ± 0.34
Test			
	Ca^{2+}	6435 ± 205	6345 ± 115
	Mg^{2+}	636 ± 18	678 ± 16
	Sr^{2+}	16.55 ± 0.53	17.95 ± 0.38
Lantern			
	Ca^{2+}	6326 ± 118	6475 ± 83
	Mg^{2+}	641 ± 15	725 ± 19
	Sr^{2+}	16.37 ± 0.32	18.14 ± 0.35
Spines			
	Ca^{2+}	6644 ± 608	7550 ± 51
	Mg^{2+}	400 ± 46	279 ± 6.88
	Sr^{2+}	15.17 ± 1.54	16.77 ± 0.25

levels, as well as higher ionic concentrations in the coelomic fluid and largely lower concentrations of ions in the exoskeleton compared to *P. lividus*.

3.3. Coelomic fluid acid–base balance and cation status of individuals exposed in situ to elevated pCO_2 conditions

After 2 and 4 d of exposure to elevated pCO_2 and low pH conditions *in situ* the mean coelomic fluid pH (pH_{cf}) of *A. lixula* ranged between 6.80 and 6.87, and between 7.18 and 7.34 for *P. lividus*. In both species, pH_{cf} measured across all treatments were comparable (see Fig. 4A and E). In fact there was no significant effect of exposure to different pCO_2, exposure duration or their interaction for pH_{cf} of either species (max $F_{1,32} = 1.252$, $P = 0.272$). In addition, mean pH_{cf} values from the *in situ* exposure were broadly comparable to those for field-collected untreated individuals (see Fig. 3). Furthermore, in *A. lixula* after 4 d exposure to elevated pCO_2/low pH, mean coelomic TCO_2 and [HCO_3^-] was 4.11 mmol l^{-1} and 3.42 mmol l^{-1} respectively (Fig. 4B and C), which was significantly greater than values measured at all other treatments (approx. 1.93 mmol $l^{-1}$and 1.61 mmol l^{-1} respectively) (min $F_{1,32} = 17.986$, $P < 0.0001$). Mean coelomic pCO_2 (0.61–1.84 kPa) was significantly greater in individuals kept in elevated pCO_2/low pH conditions after 4 d exposure when compared to individuals kept for 2 d to elevated pCO_2/low pH and 4 d under control pCO_2/pH conditions (Fig. 4C), as indicated by significant interactions between exposure to pCO_2 and exposure duration (min $F_{1,32} = 9.514$, $P = 0.005$). No effect of spheroid volume on any parameters investigated was detected ($P > 0.05$). In *P. lividus*, mean coelomic TCO_2 and [HCO_3^-] ranged between 2.51 and 6.91 mmol l^{-1} and 2.29 and 4.99 mmol l^{-1} respectively (Fig. 4F and H), and increased with exposure duration only in individuals in elevated pCO_2/low pH conditions (Fig. 4F and H), as indicated by the presence of significant interactions between exposure to elevated pCO_2 and exposure duration (minimum $F_{1,32} = 23.152$, $P < 0.0001$). No significant effect of exposure to elevated pCO_2 and exposure duration on coelomic pCO_2 and spheroid volume on any parameter investigated was detected (Fig. 4G, $P > 0.05$).

Ion concentrations for coelomic fluid and calcified tissues are summarised in Table 3. In *A. lixula*, no significant differences in coelomic fluid, test, Aristotle's lantern or spines ion content were detected as a result of exposure to different pCO_2/pH levels, exposure duration or their interaction. In fact there was no significant effect at all (maximum $F_{1,29} = 4.008$, $P = 0.055$). In *P. lividus*, after 2 and 4 d of exposure to elevated pCO_2/low pH conditions, mean [Na^+] in the coelomic fluid increased from approx. 472 to approx. 535 mmol l^{-1}, with exposure having a significant effect on this parameter ($F_{1,29} = 4.458$, $P = 0.043$, see Table 3). In addition, exposure to elevated pCO_2/low pH conditions was accompanied by a significant increase in mean [Ca^{2+}] of the test (from approx. 6094 mmol kg^{-1} to approx. 6545 mmol kg^{-1}) and mean [Mg^{2+}] (from approx. 664 mmol $kg^{-1}$to approx. 695 mmol kg^{-1}) (min $F_{1,29} = 7.888$, $P = 0.009$, see Table 3). Finally, mean [Sr^{2+}] in the spines of *P. lividus* ranged between 16.88 and 20.81 mmol kg^{-1}, with the mean value at 2 d of exposure under control pCO_2/pH conditions being significantly greater than those measured at the other treatments ($F_{2,39} = 34.066$, $P < 0.001$, see Table 3). There was no significant difference in any of the other comparisons for *P. lividus* ($P > 0.05$).

3.4. Coelomic fluid acid–base balance and cation status of individuals exposed in the field-laboratory set-up to elevated pCO_2 conditions

The effects of exposure to elevated pCO_2 and low pH at 0, 1.5, 3, 6, 12, and 24 h are presented in Fig. 5. In summary, *A. lixula* coelomic acid–base parameters largely did not vary between pCO_2 treatments throughout the entire duration of the exposure, with the exception of coelomic TCO_2 and [HCO_3^-] at 3 and 12 h, which increased from an average of 2.04 to 3.36 mmol l^{-1} and from an average of 1.83 to 3.03 mmol l^{-1} respectively (Fig. 5B and C). The differences among these values were significant, as indicated by the presence of interactions between exposure to elevated pCO_2/low pH and exposure duration (min $F_{5,84} = 3.937$, $P = 0.003$). Individuals of *P. lividus* kept under elevated pCO_2/low pH conditions, however, exhibited a significant decrease in pH at 1.5, 12 and 24 h, from a mean of pH 7.23 to 6.94 (Fig. 5E). There was also a significant increase in coelomic TCO_2 and [HCO_3^-] at 3, 6, 12 and 24 h of exposure (Fig. 5F and H), as well as pCO_2 at 1.5, 12 and 24 h (Fig. 5G), as indicated by the presence of significant interactions between exposure to elevated pCO_2/low pH and exposure duration for all these parameters (min $F_{1,84} = 3.665$, $P = 0.005$). Finally spheroid volume had a significant positive effect on *A. lixula* pH_{cf}, ($F_{1,84} = 6.224$, $P = 0.015$).

Values for the coelomic fluid ion concentration are presented in Table 4. Mean [Mg^{2+}] of coelomic fluid of *A. lixula* decreased from 72 to 62 mmol l^{-1} and [Na^+] decreased from 567 to 537 mmol l^{-1} upon exposure to elevated pCO_2/low pH conditions. These differences were significant (Table 4, min $F_{1,64} = 4.17$, $P = 0.045$). Mean [Ca^{2+}], [Sr^{2+}] and [K^+] were not affected by elevated pCO_2/low pH, duration of exposure or their interaction. In *P. lividus*, mean concentrations for all ions measured were significantly greater under elevated pCO_2/low pH conditions (Table 4, minimum $F_{1,65} = 9.266$, $P < 0.0001$). Finally, duration of exposure had a negative effect on coelomic [Mg^{2+}] decreasing from 73 to 60 mmol l^{-1} between 3 and 24 h under elevated pCO_2/low pH (Table 4, minimum $F_{4,65} = 4.638$, $P = 0.004$). No other comparisons were significantly different ($P > 0.05$).

4. Discussion

4.1. Sea urchins density under different pCO_2/pH regimes

Around the area of the shallow-water CO_2 vent of Vulcano Island, the black sea urchin, *A. lixula* and the purple sea urchin, *P. lividus* both show significant differences in their distributional patterns in relation to the spatial difference in seawater pCO_2. Whilst there is a reduction in density of *P. lividus* as one gets closer

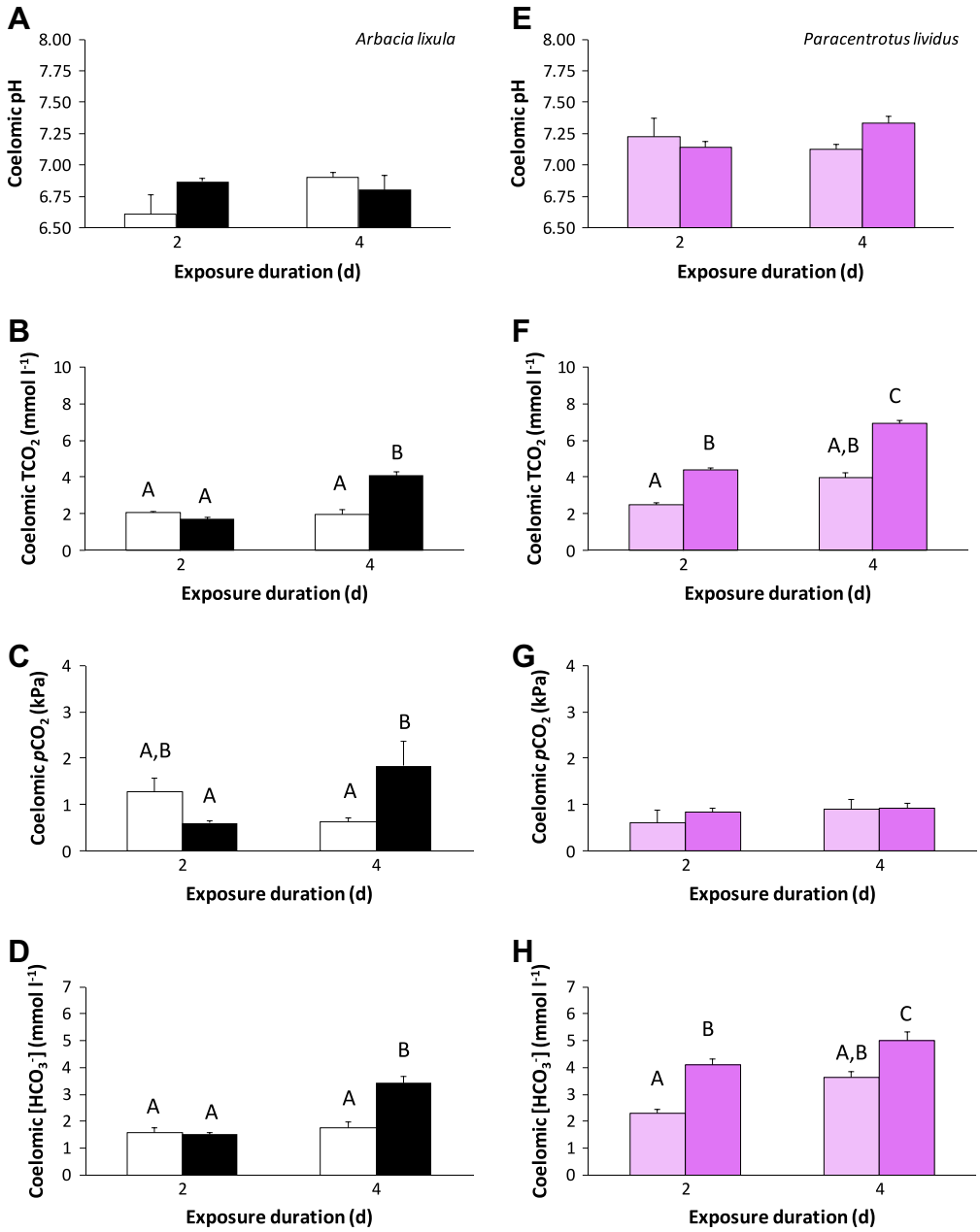

Fig. 4. Extracellular fluid acid–base status (pH, TCO_2, pCO_2, [HCO_3^-]) in sea urchins of *A. lixula* (A–D) and *P. lividus* (E–H) sampled at 2 d or 4 d of exposure to *in situ* control (white and pink respectively) and acidified conditions (black and purple respectively). Values are mean ± SE. (For interpretation of the references to color in this figure legend, the reader is referred to the web version of this article.)

to the CO_2 vents (−67%), a pattern already documented for other vents (Hall-Spencer et al., 2008; see also Johnson et al., 2012; Suggett et al., 2012 for the Vulcano CO_2 vents although it is difficult to directly compare our results to these studies as they included unsuitable habitats for sea urchins in their investigation, see Johnson, 2012), *A. lixula* occurs at greatest densities in areas characterised by higher pCO_2/lower pH (+87%). Increasing abundance with increasing pCO_2/decreasing pH has been documented previously for species of 'tolerant' phyla, such as crustaceans, polychaetes, and nematodes (e.g. Cigliano et al., 2010 for field observations, e.g. Hale et al., 2011; Christen et al., 2012 for laboratory mesocosm experiments). To our knowledge, however, this is the first time it has been recorded for echinoids, which contains species that were previously reported to be more sensitive. Increases in density of a given taxa/group across a pH gradient have been thought to be generated directly by their ability to respond physiologically to elevated CO_2 conditions, and/or indirectly colonisation of new 'ecological space' due to the loss of less tolerant taxa or changes to species interactions (Hale et al., 2011; Christen et al., 2012; Johnson et al., 2012; Kroeker et al., 2012), indirect effects likely caused by species different level of physiological vulnerability to elevated CO_2 and low pH. Physiological impairment due to elevated pCO_2/low pH is attributed to alteration of cellular homeostasis (e.g. Reipschläger et al., 1997; Pörtner et al., 1998) and energy metabolism (Pörtner et al., 1998; Beniash et al., 2010; Lannig et al., 2010; Melatunan et al., 2011; Dickinson et al., 2012) leading to altered energy budgets (see Wood et al., 2008; Findlay et al., 2010; Stumpp et al., 2011; Melatunan et al., 2012), ultimately determining taxon distribution in response to elevated pCO_2 conditions (see Bozinovic et al., 2011). We now explore the relationship between changes in sea urchin distribution along the pCO_2/pH gradient and the different physiological responses of these two species. However,

Table 3
Ionic content of the coelomic fluid and calcified tissues of the sea urchins, (A) *A. lixula* and, (B) *P. lividus* exposed *insitu* to different pCO_2/pH conditions. Values are mean ± SE. Data are expressed as mmol l^{-1} for coelomic fluid and mmol kg^{-1} for the other parameters. Different letters show significant differences ($P < 0.05$) among means of a same trait measured under different treatments.

Duration of exposure (d)	Tissue							
	Coelomic fluid		Test		Lantern		Spine	
	2	4	2	4	2	4	2	4
A								
Control								
Ca^{2+}	15.46 ± 0.69	14.92 ± 0.28	5757 ± 508	3701 ± 242	6861 ± 140	7750 ± 1134	7278 ± 167	7069 ± 93
Mg^{2+}	63.88 ± 4.94	68.45 ± 4.26	573.60 ± 51.90	549.00 ± 19.20	705.80 ± 21.2	774.00 ± 113.00	453.7 ± 11.10	452.96 ± 9.16
Sr^{3+}	0.14 ± 0.009	0.12 ± 0.009	14,95 ± 1.33	14.52 ± 0.69	16.52 ± 1.42	20.13 ± 2.91	16.83 ± 0.37	16.56 ± 0.23
Na^{+}	549.62 ± 8.25	565.7 ± 11.9	–	–	–	–	–	–
K^{+}	14.51 ± 0.55	13.81 ± 0.64	–	–	–	–	–	–
Acidified								
Ca^{2+}	11.98 ± 2.69	13.97 ± 2.70	6221 ± 220	6361 ± 107	6904 ± 102	6908 ± 223	7247 ± 98	7326 ± 67
Mg^{2+}	54.12 ± 5.53	61.16 ± 8.42	619.80 ± 24.90	643.80 ± 17.00	686.1 ± 10.3	699.20 ± 24,20	470.75 ± 7.26	470.96 ± 9.35
Sr^{2+}	0.10 ± 0.016	0.11 ± 0.02	15.80 ± 0.54	16.00 ± 0.65	17.93 ± 0.28	27.76 ± 0.59	26.97 ± 0.23	17.15 ± 0.20
Na^{+}	467.70 ± 47.30	502.10 ± 56.80	–	–	–	–	–	–
K^{+}	12.02 ± 1.25	16.63 ± 2.16						
B								
Control								
	9.48 ± 0.22	9.33 ± 0.20	6148 ± 131^{A}	6039 ± 172^{A}	6477 ± 190	6364 ± 196	9090 ± 1398	7404 ± 371
Mg^{2+}	55.72 ± 1.34	54.46 ± 2.42	677.70 ± 15.60^{A}	652.228.5^{A}	709.50 ± 24.80	727.30 ± 34.60	336.80 ± 57.80	272.75 ± 7.03
Sr^{2+}	0.08 ± 0.013	0.09 ± 0.001	17.12 ± 0.57	16.98 ± 0.46	17.13 ± 0.36	18.22 ± 0.79	20.81 ± 3.29^{A}	16.88 ± 0.20^{B}
Na^{+}	471.33 ± 6.72^{A}	472.67 ± 9.16^{A}	–	–	–	–	–	–
K^{+}	11.63 ± 0.33	12.55 ± 0.15	–	–	–	–	–	–
Acidified								
Ca^{2+}	15.09 ± 3.10	10.23 ± 0.56	6571 ± 103^{B}	6518 ± 234^{B}	6425 ± 263	6514 ± 268	74570 ± 93	7462 ± 107
Mg^{2+}	61.78 ± 6.04	59.94 ± 3.04	707.70 ± 10.80^{B}	682.30 ± 23.70^{B}	713.00 ± 25.90	747.90 ± 10.38	289.01 ± 8.59	287.60 ± 8.78
Sr^{2+}	0.11 ± 0.019	0.10 ± 0.006	18.23 ± 0.34	18.03 ± 0.68	17.73 ± 0.68	18.55 ± 0.814	17.28 ± 0.27^{B}	17.20 ± 0.42^{B}
Na^{+}	541.90 ± 52.40^{B}	527.90 ± 28.20^{B}	–	–	–	–	–	–
K^{+}	13.65 ± 1.49	13.76 ± 0.83						

first we must consider some ecological factors that could determine sea urchins' distribution.

4.2. Rejection of feeding biology and predators as determinants of sea urchin distribution around CO_2 vents

Differences in the distribution of the two sea urchins investigated here may be related to different feeding preferences. Gut contents analyses suggest that *A. lixula* preferentially feeds on calcitic algae (Privitera et al., 2008), although a recent study using stable isotopes has shown that its feeding niche may be broader including sessile animals (Wangensteen et al., 2011). On the contrary, *P. lividus* more strictly favours erect fleshy algae (Privitera et al., 2008; Bonaviri et al., 2011; Wangensteen et al., 2011). Along the pCO_2/pH gradient created by the CO_2 vent of Vulcano, Johnson et al. (2012) reported that calcified algae are most abundant in the control pCO_2/pH areas, whilst fleshy macroalgae (in particular brown macroalgae) become progressively more abundant in the acidified areas. This pattern is similar to that reported from other CO_2 vents (e.g. Porzio et al., 2011; Fabricius et al., 2011). Based on their different feeding ecology, we might have predicted *A. lixula* to be most abundant in the control pCO_2 areas where calcified algae are most abundant, and *P. lividus* to be most abundant in the more acidified areas where macroalgae are dominant and productivity enhanced (see Johnson et al., 2012; Russell et al., in press). However, the opposite is true. Although we cannot completely exclude that *A. lixula* could also be able to exploit non-calcifying invertebrates in acidified waters, as could do in control areas, current evidence to date support the idea that feeding biology can be rejected as a major determinant of sea urchins' distribution in the area around the CO_2 vent of Vulcano.

We may also reject the idea that differences in the activity levels of natural predators shaped sea urchins' local distribution. There are no changes in distribution or behaviour of natural predators in the areas around the vent compared with the vent area (Milazzo and Azzurro, *pers. obs.*), and human harvesting of *P. lividus* does not occur here. Furthermore, it is important to consider that the Vulcano CO_2 vent system does not allow for replication (being one pCO_2/pH gradient only) and that despite in this work we measured sea urchins density in comparable habitats, suitable for sea urchins settling across the CO_2 gradient, the habitat structure in Vulcano is relatively patchy. Despite these limitations, and although we advise this type of investigations are conducted in multiple sites to verify their consistency, the distribution of these sea urchin species around this natural CO_2 vent appear to be influenced (and possibly determined), as with other species, by their respective physiologies (e.g. Stillman, 2002; Calosi et al., 2007, 2008, 2010; Bozinovic et al., 2011; Lai et al., 2011; Rastrick and Whiteley, 2011; Whiteley et al., 2011).

4.3. Acid–base and ionic status of field-collected untreated sea urchins

Field-collected individuals of *A. lixula* and *P. lividus* have different physiologies. The coelomic fluid of field-collected *A. lixula* is more acidic (mean = 6.99) than *P. lividus*, being approx. 0.3 units lower. Indeed it is the lowest echinoid extracellular pH recorded under control seawater pCO_2/pH conditions (cf. Spicer et al., 1988, 2011; Spicer, 1995; Burnett et al., 2002; Catarino et al., 2012; Stumpp et al., 2012), with the exception of the sand dollar, *Echinarachnius parma* (Cole, 1940). The pH of sea urchin coelomic fluid is usually well below that of sea water, due to the accumulation of CO_2 and organic acid metabolites, as aerobic and anaerobic pathways operate even in normoxic echinoids (Farmanfarmaian, 1966; Ellington, 1982; Shick, 1983; Bookbinder and Shick, 1986). In addition, the CO_2 capacity of the coelomic fluid of *P. lividus* is amongst the highest ever recorded in a sea urchin (see Spicer et al. 1988, 1995, 2011; Miles et al., 2007; Stumpp et al., 2011), and comparable to that of a population of the green sea urchin,

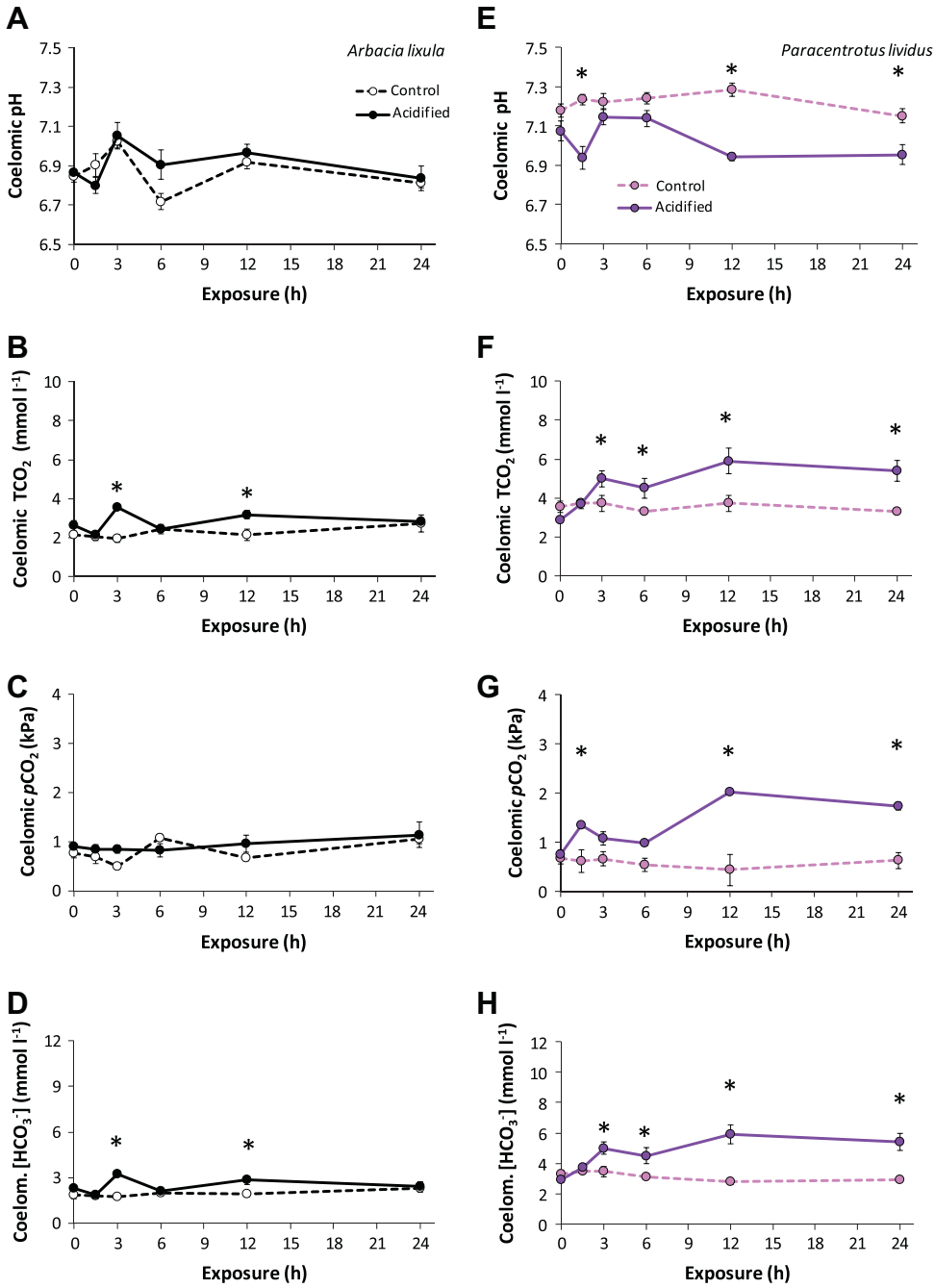

Fig. 5. Coelomic fluid acid–base status (pH, TCO_2, pCO_2, $[HCO_3^-]$) in sea urchins of *A. lixula* (A–D) and *P. lividus* (E–H) exposed for 24 h to control (white and pink respectively, dotted line) and acidified conditions (black and purple respectively, full line) under field-laboratory conditions. Repeated coelomic fluid sampling of the same individuals was undertaken at 0, 3, 6, 12, 24 h from the starting of the exposure. Values are mean ± SE. (For interpretation of the references to color in this figure legend, the reader is referred to the web version of this article.)

Strongylocentrotus droebachiensis from Maine (USA) (6.00 mmol l^{-1} – Cole, 1940). Also the CO_2 capacity of the coelomic fluid of *P. lividus* is about double that of *A. lixula*, the latter being more comparable to that recorded in the purple-tipped sea urchin, *Psammechinus miliaris* by Spicer et al. (1988). Mean coelomic $[HCO_3^-]$ and pCO_2 of *P. lividus* are, to date, amongst the highest measured in a sea urchin under control seawater pCO_2/pH conditions (Spicer, 1995, 2011; Miles et al., 2007; Stumpp et al., 2011), whilst mean coelomic $[HCO_3^-]$ and pCO_2 in *A. lixula* were less than half of those measured in *P. lividus*. Nonetheless mean pCO_2 values in *P. lividus* were at the higher end of those reported to date for other echinoids. Our data being the first on the acid-base regulation of *P. lividus* and *A. lixula,* differences in coelomic pCO_2 may be explained by differences in the experimental regime we used when compared to those of other studies (i.e. semi-natural conditions *vs.* laboratory maintenance and experiments), as well as by the natural variability among different species of echinoids. This may mean that *P. lividus* may incur greater regulatory costs. *Arbacia lixula* may instead have evolved low coelomic fluid pH, thus possibly keeping regulatory cost lower in area with fluctuating pH and CO_2.

A. lixula displays a greater capacity to control tissue water than other sea urchins for which we have data, namely the rock boring sea urchin, *Echinometra lucunter* and the variegated sea urchin,

Table 4
Ionic content of the coelomic fluid of sea urchins, (A) *A. lixula* and, (B) *P. lividus* exposed to different pCO_2/pH conditions in the laboratory. Values are mean ± SE. Data are expressed as mmol l^{-1} for coelomic fluid and mmol kg^{-1} for the other parameters. (†) Mean values for *P. lividus* of the group of individuals used for the acidified treatment could not be taken at time 0 under, therefore here we give mean values for those individuals of *P. lividus* subsequently kept at control conditions.

Duration *of* exposure (d)	0	3	6	12	24
A					
Control					
Ca^{2+}	14.52 ± 0.49	13.84 ± 1.32	15.09 ± 0.68	14.58 ± 1.28	15.86 ± 0.63
Mg^{2+}	65.22 ± 4.3	69.36 ± 7.01	82.19 ± 4.75	76.42 ± 6.58	70.33 ± 4.67
Sr^{2+}	0.19 ± 0.01	0.11 ± 0.01	0.13 ± 0.006	0.12 ± 0.01	0.12 ± 0.007
Na^{+}	558.3 ± 19.7	525.1 ± 49.1	598 ± 19	567.3 ± 45.3	586.83 ± 9.45
K^{+}	14.29 ± 0.69	12.89 ± 1.03	14.35 ± 0.41	14.2 ± 1.13	14.29 ± 1.01
Acidified					
Ca^{2+}	16.83 ± 2.44	11.21 ± 0.73	15.3 ± 2.22	10.47 ± 1.39	15.98 ± 2.57
Mg^{2+}	61.15 ± 0.76	61.91 ± 2.92	61.12 ± 0.72	61.08 ± 1.91	63.09 ± 2.2
Sr^{3+}	0.13 ± 0.01	0.1 ± 0.006	0.12 ± 0.01	0.09 ± 0.006	0.13 ± 0.012
Na^{+}	533.12 ± 6.01	537 ± 26.7	534.7 ± 11.6	533.7 ± 1.69	547.1 ± 16.5
K^{+}	13.69 ± 0.22	13.57 ± 0.86	12.84 ± 0.21	12.91 ± 0.50	14.31 ± 0.44
B					
Control					
Ca^{2+}	8.74 ± 0.24	9.51 ± 0.25	9.47 ± 0.135	10.14 ± 0.77	8.75 ± 0.24
Mg^{2+}	53.94 ± 1.30	57.01 ± 0.88	57.88 ± 0.231	59.12 ± 3.78	53.26 ± 1.06
Sr^{2+}	0.09 ± 0.002	0.10 ± 0.01	0.09 ± 0.001	0.10 ± 0.008	0.09 ± 0.002
Na^{+}	461.7 ± 11	485.08 ± 7.56	503.84 ± 2.97	511.2 ± 32.8	463.08 ± 9.48
K^{+}	13.19 ± 0.34	12.08 ± 0.27	13.06 ± 0.22	12.83 ± 0.83	11.97 ± 0.3
Acidified					
Ca^{2+}	8.74 ± 0.24†	22.25 ± 2.53	30.98 ± 8.62	24.35 ± 8.35	14.43 ± 0.35
Mg^{2+}	53.94 ± 1.30†	72.88 ± 0.95	70.53 ± 1.63	65.89 ± 0.76	65.17 ± 0.47
Sr^{2+}	0.09 ± 0.002†	016 ± 0.01	0.21 ± 0.04	0.16 ± 0.04	0.11 ± 0.002
Na^{+}	461.7 ± 11†	573.53 ± 9.48	575.3 ± 13.3	541.15 ± 4.51	546.48 ± 3.84
K^{+}	13.19 ± 0.34†	15.73 ± 0.47	15.50 ± 0.55	14.45 ± 0.15	15.33 ± 0.53

Lytechinus variegatus (Freire pers. obs.) and displayed a greater coelomic fluid Ca^{2+}, Mg^{2+}, Sr^{2+} and Na^{+} content when compared *to P. lividus*, however, details as to why this occurs remains unclear. Strong iono-regulatory capacity is generally coupled with capacity for acid–base regulation (Seibel and Walsh, 2003; Pörtner et al., 2004; Widdicombe and Spicer, 2008; Melzner et al., 2009; Whiteley, 2011). Thus *A. lixula*'s ability to maintain ionic gradients for major cations may indicate better developed acid–base regulatory ability compared to *P. lividus*. These differences in baseline acid–base and ionic status support the idea that the sea urchins investigated here may be differently equipped to respond to elevated environmental pCO_2 that occur with CO_2 leakages. However, the capacity for regulation of acid–base and ionic status, rather than the status *per se*, is more important when understanding differences taxa homeostatic ability.

4.4. In-situ mid-term acid–base and ionic regulation following acclimatisation to elevated pCO_2/low pH

After 2 and 4 d exposure *in situ* to elevated pCO_2/low pH, both sea urchin species fully compensated their coelomic fluid pH. However, in *P. lividus* buffering is achieved, *via* an increase in extracellular [HCO_3^-] (see Fig. 6B), with no significant changes observed in coelomic pCO_2. This suggests a metabolic component to the compensation. In *A. lixula*, complete compensation at day 2 cannot be attributed to changes in [HCO_3^-] or metabolic alkalosis. Full non-bicarbonate compensation of extracellular-fluid pH was recently described in the velvet fiddler crab, *Necora puber* (Small et al., 2010) and the burrowing shrimp, *Upogebia deltaura* (Donohue et al., 2012) under comparable pCO_2/pH conditions after 30 d of exposure. In these crustaceans, non-bicarbonate full compensation of haemolymph pH was suggested to be linked to an increase in protein content and represent a longer-term compensatory mechanism, as crustaceans are known at least in the short-term to rely on the HCO_3^- buffering (Truchot et al., 1976; Cameron and Iwama, 1987; Whiteley, 1999, 2011; Spicer et al., 2007). In *A. lixula*, the situation is reversed as non-bicarbonate buffering is observed at day 4 when the sea urchin switches to HCO_3^- compensation, despite [HCO_3^-] in this species being lower than that of *P. lividus*. Considering the low protein and lipid content of sea urchin coelomic fluid (see Boolootian, 1966; Binyon, 1972), it is unlikely that increases in these parameters explain the initial buffering capacity of *A. lixula*, although at this stage there is no plausible alternative. Furthermore, at day 4 *A. lixula* also experienced an increase in coelomic fluid pCO_2 whilst maintaining its coelomic fluid pH constant, which is caused by a significant increase in [HCO_3^-] but also partially by a possible metabolic compensation (Fig. 6A). In addition, in *A. lixula* there were no significant changes in ions in coelomic fluid or carbonated tissues. Since coelomic [Ca^{2+}], [Mg^{2+}] and [Sr^{2+}] does not increase, and test concentrations for these ions did not change significantly, it is likely that sea urchins do not incur dissolution of their carbonate structures (test and lantern in particular). Thus the HCO_3^- increase observed (approx. 1.7 mmol l^{-1}) at day 4 may be due to the uptake of this ion from sea water as proposed for other species (e.g. Cameron, 1985; Small et al., 2010; Donohue et al., 2012). An alternative explanation could be that [HCO_3^-] increases as the consequence of an increase in activity of the enzyme carbonic anhydrase (CA), but no direct measure of CA activity is available for this study. In *P. lividus* the increase in HCO_3^- is approx. 1.8 and 1.4 mmol l^{-1} at 2 and 4 d respectively. The significant increase in test's [Ca^{2+}] and [Mg^{2+}] suggests that not only does this species not experience test dissolution (confirming Catarino et al., 2012 results) but possibly net calcification may increase. This is the first time that both the carbonated compartments of a sea urchin that can contribute to internal HCO_3^- buffering *via* dissolution (test and Aristotle's lantern) and its coelomic fluids are sampled in order to establish the origin of the HCO_3^- used for buffering. Furthermore, increased calcification in organisms exposed to elevated pCO_2/low pH has already been documented in various taxa of marine organisms (see Ries et al., 2009; Findlay et al., 2011), including the sea urchin, *Arbacia punctulata* (Ries et al., 2009) which was exposed at pCO_2/pH/Ω_{ara} values comparable to that

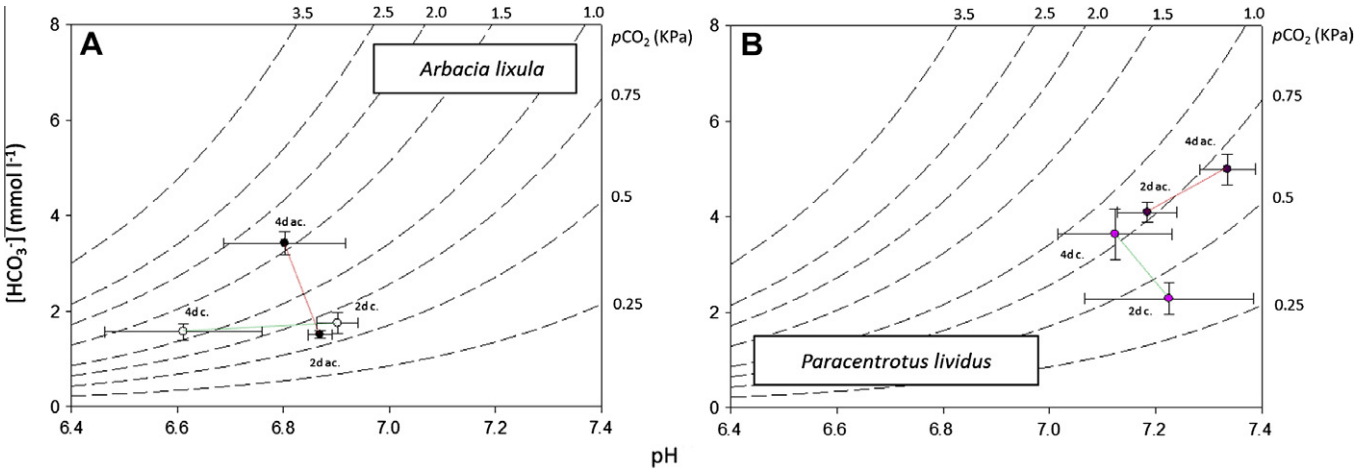

Fig. 6. Davenport diagram showing the effects of elevated pCO_2/pH on the acid base status of coelomic fluid from the sea urchins *A. lixula* and *P. lividus* measured *in situ* at 2 d and 4 d from the beginning of exposure to control (white and pink respectively) and acidified conditions (black and purple respectively). Points are means ± SE for each time point. Full isopleths show calculated pCO_2 values for each [HCO_3^-] and pH combination. (For interpretation of the references to color in this figure legend, the reader is referred to the web version of this article.)

measured in the acidified site during our experiments and those from the long-term monitoring by Boatta et al. (in press). If chronic hyper-calcification does occur in *P. lividus*, the high energetic cost of this process may not be a sustainable strategy, altering trade-offs between maintenance and growth/reproduction (see Wood et al., 2008; Stumpp et al., 2012; but cf. Findlay et al., 2010). The small changes in HCO_3^- buffering observed here indicate that other compensatory mechanisms may be operating, e.g. the electroneutral Na^+/H^+ exchangers. The observed increase in coelomic [Na^+] is normally established by the Na^+/K^+ ATPase pumps, but here can be considered as another evidence of increased sea water uptake in sea urchins kept under elevated pCO_2/low pH conditions, this indicating that also *P. lividus* can concentrate its coelomic fluid. Our results corroborate Freire et al. (2011)'s conclusion that echinoderms may be able to up-regulate Na^+ uptake.

4.5. Acid–base and ionic-regulatory acclimation in sea urchins exposed to elevated pCO_2/low pH conditions

The difference in the acid–base balance abilities in *A. lixula* and *P. lividus* after 2 and 4 d *in situ* were more pronounced in the laboratory experiments. These experiment are particularly useful (due to the fine time resolution) for helping us understand the different physiological pathways species follow to acclimatise to elevated pCO_2 before reaching at 2 and 4 d full pH_{cf} compensation.

A. lixula again displays the capacity to compensate extracellular pH at each time point of observation during the 24 h of exposure to elevated pCO_2/low pH conditions. Respiratory acidosis appears to occur in this species at 1.5 and 6 h (see Fig. 7A) of exposure to elevated pCO_2 but is immediately compensated by a metabolic alkalosis at 3 and 12 h, as indicated in the Davenport diagram (at these time points there is an approx. 1.7 mmol l^{-1} increase in coelomic [HCO_3^-] with no significant increase in coelomic pCO_2 (see Fig. 7A). Then there is no change between 24 h and 2–4 d of exposure to elevated pCO_2 in this species, apart from a small increase in [HCO_3^-] between 2 and 4 d. However, caution is necessary when comparing data from the *in situ* and field laboratory experiment together due to the different experimental approaches employed. In addition, coelomic fluid [Mg^{2+}] and [Na^+] were significantly lower under elevated pCO_2/low pH conditions, which may indicate either a partial loss of the ionic regulatory ability or an attempt to lower the concentration of this cation in the coelomic fluid in hypercap-

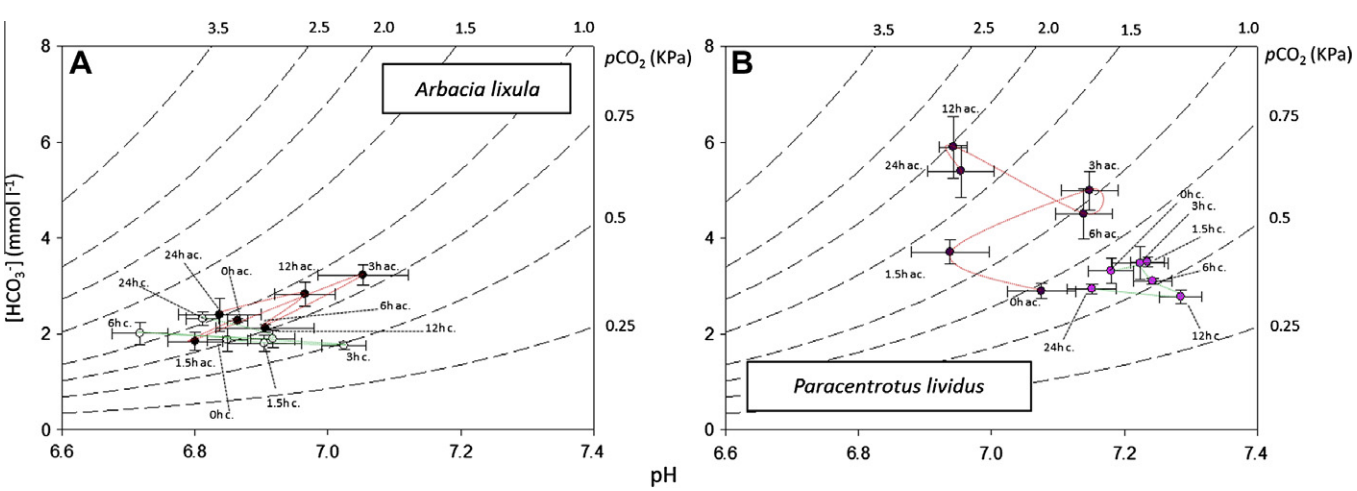

Fig. 7. Davenport diagrams showing the effects of elevated pCO_2/pH on the acid base status of the coelomic fluid from sea urchins *A. lixula* (A) and *P. lividus* (B) measured at the field laboratory at 0, 1.5, 3, 6, 12, 24 h from the beginning of exposure control (white and pink respectively) and acidified conditions (black and purple respectively). Points are means ± SE for each time point. Full isopleths show calculated pCO_2 values for each [HCO_3^-] and pH combination. Note the difference in scale of the *Y*-axis for *A. lixula* and *P. lividus*. (For interpretation of the references to color in this figure legend, the reader is referred to the web version of this article.)

Please cite this article in press as: Calosi, P., et al. Distribution of sea urchins living near shallow water CO_2 vents is dependent upon species acid–base and ion-regulatory abilities. Mar. Pollut. Bull. (2013), http://dx.doi.org/10.1016/j.marpolbul.2012.11.040

nic sea urchins. In any case, *A. lixula* does not appear to undergo any dissolution of the carbonated tissues during the first 24 h of exposure to elevated pCO_2.

On the other hand *P. lividus* displays a severe respiratory acidosis at 1.5 h which is compensated, *via* a possible respiratory alkalosis at 3–6 h (Fig. 7B). This is followed by a second respiratory acidosis at 12–24 h which is further compensated by another respiratory alkalosis occurring between 24 h and 2 d (Figs. 7B and 6B). The levels of bicarbonate observed in the coelomic fluid of *P. lividus* under these conditions are among the highest so far recorded for any species of echinoid, although we should remember that they are transient. In fact, at 2 and 4 d of exposure *in situ*, extracellular $[HCO_3^-]$ returns to values comparable to those recorded in field-collected individuals. We suggest that between 24 h and 2–4 d, *P. lividus* potentially undergoes a switch in its buffering mode, as it stops relying on bicarbonate buffering with $[HCO_3^-]$ (probably too energetically expensive to sustain long-term), reducing from approx. 5.99 mmol l^{-1} (at 12 h, see Fig. 7B) to approx. 4.54 mmol l^{-1} (at 2 and 4 d, see Fig. 6B). This further corroborates the idea that also sea urchins may switch between buffering modes, as seen in crustaceans (Spicer et al., 2007; Small et al., 2010; Donohue et al., 2012).

5. Conclusions

The decrease in density in the high CO_2 areas in *P. lividus* could be interpreted as the long-term consequence of its relatively poorer ability to regulate extracellular acid–base balance. Despite a greater capacity for bicarbonate buffering, *P. lividus* is more at risk from the negative effects of elevated pCO_2 due to the possible long-term costs of maintaining high $[HCO_3^-]$. This may have repercussions for the functioning of the marine ecosystems to which this species belongs, as well as for its fisheries and aquaculture industries. On the other hand, *A. lixula* possesses low pH_{cf} and (in the short term) the ability for full pH compensation, *via* an unidentified non-bicarbonate mechanism: possibly linked to lower metabolic rate function. Its ability to regulate extracellular ions may also bestow on *A. lixula* a greater resilience to high CO_2. We should highlight that in our experiments Ω_{calc} and Ω_{ara} were not undersaturated, and so our results can be considered to be solely related to the level of environmental pCO_2 and pH reported. Furthermore, our findings lend further support to the idea that echinoids do possess a certain degree for extracellular acid–base and ionic regulatory ability, but also that a considerable degree of variation exists in these traits (Spicer et al., 1988; Spicer, 1995; Miles et al., 2007; Vidolin et al., 2007; Freire et al., 2011; Stumpp et al., 2012). Thus differences in the ecophysiology of individual species (as with the sea urchins in this study) will likely play an important role in defining the ability of assemblages to cope with elevated pCO_2/low pH. It is likely that such differences will be due to changes in energy budgets, with follow-on constrains on species future abundance and distribution.

Acknowledgments

We thank R. Haslam, M. Hawkins, A. Fisher, A. Savona and Bartolo for advice and technical support. We also thank V. Johnson for sharing information on the structure of algal communities at CO_2 vents. P.C. personally wishes to thank K. Kroeker for a stimulating discussion on how experimental limitations and alternative factors play a role in organisms' distribution within CO_2 vents. This work was undertaken whilst P.C. was in receipt of a Research Council UK Research Fellowship to investigate ocean acidification at Plymouth University. J.I.S. was in receipt of a RCUK research fund. This project is a joint contribution to the Task 1.4 'Identify the potential for organism resistance and adaptation to prolonged CO_2 exposure' of the NERC Consortium Grant 'Impacts of ocean acidification on key benthic ecosystems, communities, habitats, species and life cycles' grant NE/H017127/1 to J.I.S. and P.C. and the Task 4.1.4 'Assessment of the abundance and physiology of selected molluscs, crustaceans, echinoderms and fish along gradients of CO_2 at Vulcano (Italy) and Methana (Greece)' of the EU FP7 project 'Mediterranean Sea Acidicification in a changing climate' (MedSeA project)' Grant 265103 to J.M. H.-S., J.I.S., M.M. and P.C., H.A.C. visited the Marine Biology and Ecology Research Centre with support from a National Science Foundation, PI: J. H. Stillman Ocean Acidification Category 1 Collaborative Research: RUI: Synergistic Effects of Temperature and pH Variability on Physiology, Transcriptome and Proteome of Porcelain Crabs. BIO-MCB-1041225. Multivariate analyses were carried out using PRIMER with the add-on PERMANOVA (licenced to Mariagrazia Graziano).

References

Anderson, M.J., 2001. Permutation tests for univariate or multivariate analysis of variance and regression. Can. J. Fish. Aquat. Sci. 58, 626–639.

Arnold, T., Mealey, C., Leahey, H., Miller, A.W., Hall-Spencer, J.M., Milazzo, M., Maers, K., 2012. Ocean acidification and the loss of protective phenolics in seagrasses. PLoS ONE 7, e35107.

Barry, J.P., Buck, K.R., Lovera, C.F., Kuhnz, L., Whaling, J.P., Peltzer, E.T., Walz, P., Brewer, P.G., 2004. Effects of direct ocean CO_2 injection on deep-sea meiofauna. J. Oceanogr. 60, 759–766.

Beniash, E., Ivanina, A., Lieb, N.S., Kurochkin, I., Sokolova, I.M., 2010. Elevated level of carbon dioxide affects metabolism and shell formation in oysters *Crassostrea virginica*. Mar. Ecol. – Prog. Ser. 419, 95–108.

Binyon, J., 1972. Physiology of Echinoderms. Pergamon Press, Oxford.

Blackford, J.C., Jones, N., Proctor, R., Holt, J., Widdicombe, S., Lowe, D., Rees, A., 2009. An initial assessment of the potential environmental impact of CO_2 escape from marine carbon capture and storage systems. Proc. ImechE Part A: J. Power Energy 223, 269–282.

Boatta, F., D'Alessandro, W., Gagliano, A.L., Liotta, M., Milazzo, M., Rodolfo-Metalpa, R., Hall-Spencer, J.M., Parello, F., in press. Geochemical survey of Levante Bay, Vulcano Island (Italy), a natural laboratory for the study of ocean acidification. Marine Pollution Bulletin.

Bonaviri, C., Vega-Fernández, T., Badalamenti, F., Gianguzza, P., Di Lorenzo, M., Raggio, S., 2009. Relative role of fish vs. starfish predation in controlling sea urchin populations in Mediterranean rocky shores. Mar. Ecol. – Prog. Ser. 382, 129–138.

Bonaviri, C., Fernandez, T.V., Fanelli, G., Badalamenti, F., Gianguzza, P., 2011. Leading role of the sea urchin *Arbacia lixula* in maintaining the barren state in southwestern Mediterranean. Mar. Biol. 158, 2505–2513.

Bookbinder, L.H., Shick, J.M., 1986. Anaerobic and aerobic energy metabolism in ovaries of the sea urchin *Strongylocentrotus droebachiensis*. Mar. Biol. 93, 103–110.

Boolootian, R.A., 1966. Physiology of Echinodermata. John Wiley & Sons Inc., New York.

Bozinovic, F., Calosi, P., Spicer, J.I., 2011. Physiological correlates of geographical range in animals. Annu. Rev. Ecol. Evol. Syst. 42, 155–179.

Burnett, L., Terwilliger, N., Carroll, A., Jorgensen, D., Scholnick, D., 2002. Respiratory and acid–base physiology of the purple sea urchin, *Strongylocentrotus purpuratus*, during air exposure: presence and function of a facultative lung. Biol. Bull. 203, 42–50.

Caldeira, K., Wickett, M.E., 2003. Anthropogenic carbon and ocean pH. Nature 425, 365–372.

Calosi, P., Bilton, D.T., Spicer, J.I., 2008. Thermal tolerance, acclimatory capacity and vulnerability to global climate change. Biol. Lett. 4, 99–102.

Calosi, P., Bilton, D.T., Spicer, J.I., Votier, S.C., Atfield, A., 2010. What determines a species' geographical range? Thermal biology and latitudinal range size relationships in European diving beetles (Coleoptera: Dytiscidae). J. Anim. Ecol. 79, 194–204.

Calosi, P., Morritt, D., Chelazzi, G., Ugolini, A., 2007. Physiological capacity and environmental tolerance in two sandhopper species with contrasting geographical ranges: *Talitrus saltator* and *Talorchestia ugolinii*. Mar. Biol. 151, 1647–1655.

Cameron, J.N., 1985. Compensation of hypercapnic acidosis in the aquatic blue crab, *Callinectes sapidus*: the predominance of external sea water over carapace carbonate as the proton sink. J. Exp. Biol. 114, 197–206.

Cameron, J.N., Iwama, G.K., 1987. Compensation of progressive hypercapnia in channel catfish and blue crabs. J. Exp. Biol. 133, 183–197.

Catarino, A., Bauwens, M., Dubois, P., 2012. Acid–base balance and metabolic response of the sea urchin *Paracentrotus lividus*; to different seawater pH and temperatures. Environ. Sci. Pollut. Res. 196, 2344–2353.

Christen, N., Calosi, P., McNeill, C.L., Widdicombe, S., 2012. Structural and functional vulnerability to elevated pCO_2 in marine benthic communities. Marine Biology. http://dx.doi.org/ 10.1007/s00227-012-2097-0.

Cigliano, M.C., Gambi, R., Rodolfo-Metalpa, R., Patti, F.P., Hall-Spencer, J.M., 2010. Effects of ocean acidification on invertebrate settlement at volcanic CO_2 vents. Mar. Biol. 157, 2489–2502.

Cole, W.H., 1940. Composition of fluids and sera of some marine animals and of the sea water in which they live. J. Gen. Physiol. 23, 575–584.

Dickinson, G.H., Ivanina, A., Matoo, O.B., Pörtner, H.-O., Lannig, G., Bock, C., Beniash, E., Sokolova, A.P., 2012. Interactive effects of salinity and elevated CO_2 levels on juvenile eastern oysters, *Crassostrea virginica*. J. Exp. Biol. 215, 29–43.

Dickson, A.G., 1990. Thermodynamics of the dissociation of boric acid in synthetic seawater from 273.15 to 318.15 K. Deep-Sea Res. 37, 755–766.

Dickson, A.G., Millero, F.J., 1987. A comparison of the equilibrium constants for the dissociation of carbonic acid in seawater media. Deep-Sea Res. 34, 1733–1743.

Donohue, P., Calosi, P., Bates, A., Laverock, A.H., Rastrick, S., Mark, F.C., Stroble, A., Widdicombe, S., 2012. Physiological and behavioural impacts of exposure to elevated pCO_2 on an important ecosystem engineer, the burrowing shrimp *Upogebia deltaura*. Aquat. Biol. 15, 73–86.

Dupont, S., Ortega-Martínez, O., Thorndyke, M., 2010. Impact of near-future ocean acidification on echinoderms. Ecotoxicology 19, 449–462.

Edgar, G.J., Barret, N.S., 1997. Short term monitoring of biotic change in Tasmanian marine reserves. J. Exp. Mar. Biol. Ecol. 213, 261–279.

Ellington, W.R., 1982. Intermediary metabolism. In: Jangoux, M., Lawrence, J.M. (Eds.), Echinoderm Nutrition. Balkema, A.A., Rotterdam, The Netherland.

Fabricius, K.E., Langdon, C., Uthicke, S., Humphrey, C., Noonan, S., De'ath, G., Okazaki, R., Muehllehner, N., Glas, M.S., Lough, J.M., 2011. Losers and winners in coral reefs acclimatized to elevated carbon dioxide concentrations. Nat. Climate Change 1, 165–169.

Farmanfarmaian, A., 1966. The respiratory physiology of the echinoderms. In: Boolootian, R.A. (Ed.), Physiology of Echinodermata. Interscience Publishers, USA, New York, USA.

Findlay, H.S., Kendall, M.A., Spicer, J.I., Widdicombe, S., 2010. Relative influences of ocean acidification and temperature on intertidal barnacle post-larvae at the northern edge of their geographic distribution. Estuar. Coast. Shelf Sci. 86, 675–682.

Findlay, H.S., Wood, H.L., Kendall, M.A., Spicer, J.I., Twitchett, R.J., Widdicombe, S., 2011. Comparing the impact of high CO_2 on calcium carbonate structures in different marine organisms. Mar. Biol. Res. 7, 565–575.

Freire, C.A., Santos, I.A., Vidolin, D., 2011. Osmolality and ions of the perivisceral coelomic fluid of the intertidal sea urchin *Echinometra lucunter* (Echinodermata: Echinoidea) upon salinity and ionic challenges. Zoologia 28, 479–487.

Gibbins, J., Haszeldine, S., Holloway, S., Pearce, J., Oakey, J., Shackley, S., Cockerill, T., 2006. Scope for future CO_2 emission reductions from electricity generation through the deployment of carbon capture and storage technologies. In: Schellnhuber, H.J., Cramer, W., Nakicenovic, N., Wigley, T., Yohe, G. (Eds.), Avoiding Dangerous Climate Change. Cambridge University Press, Cambridge, pp. 379–383.

Hale, R., Calosi, P., McNeill, L., Mieszkowska, N., Widdicombe, S., 2011. Predicted levels of future ocean acidification and temperature rise could alter community structure and biodiversity in marine benthic communities. Oikos 120, 661–674.

Hall-Spencer, J.M., Rodolfo-Metalpa, R., Martin, S., Ransome, E., Fine, M., Turner, S.M., Rowley, S.J., Tedesco, D., Buia, M.-C., 2008. Volcanic carbon dioxide vents show ecosystem effects of ocean acidification. Nature 454, 96–99.

Hereu, B., Zabala, M., Linares, C., Sala, E., 2005. The effects of predator abundance and habitat structural complexity on survival of juvenile sea urchins. Mar. Biol. 146, 293–299.

Johnson, V., 2012. A study of marine benthic algae along a natural carbon dioxide gradient. PhD thesis. Plymouth University, UK. 274p.

Johnson, V., Brownlee, C., Rickaby, R., Graziano, M., Milazzo, M., Hall-Spencer, J., 2011. Responses of marine benthic microalgae to elevated CO_2. Mar. Biol.. http://dx.doi.org/10.1007/s00227-011-1840-2, published online.

Johnson, V., Russell, B.D., Fabricius, K.E., Brownlee, C., Hall-Spencer, J., 2012. Temperate and tropical brown macroalgae thrive, despite decalcification, along natural CO_2 gradients. Glob. Change Biol. 18, 2792–2803.

Kingsford, M., Battershill, E., 1998. Studying Temperate Marine Environments. Canterbury University Press, Canterbury, New Zealand, p. 334.

Kroeker, K.J., Micheli, F., Gambi, M.C., Martz, T.R., 2011. Divergent ecosystem responses within a benthic marine community to ocean acidification. Proc. Natl. Acad. Sci. USA 108, 14515–14520.

Kroeker, K.J., Micheli, F., Gambi, M.C., 2012. Ocean acidification causes ecosystem shifts *via* altered competitive interactions. Nat. Climate Change. http://dx.doi.org/10.1038/NCLIMATE1680.

Kurihara, H., Shirayama, Y., 2004a. Effects of increased atmospheric CO_2 and decreased pH on sea urchin embryos and gametes. In: München-Heinzeller, N. (Ed.), Echinoderms. Taylor and Francis, London, pp. 31–36.

Kurihara, H., Shirayama, Y., 2004b. Effects of increased atmospheric CO_2 on sea urchin early development. Mar. Ecol. – Prog. Ser. 274, 161–169.

Lai, C.H., Morley, S.A., Tan, K.S., Peck, L.S., 2011. Thermal niche separation in two sympatric tropical intertidal *Laternula* (Bivalvia: Anomalodesmata). J. Exp. Mar. Biol. Ecol. 405, 68–72.

Lannig, G., Eilers, S., Pörtner, H.-O., Sokolova, A.P., Bock, C., 2010. Impact of ocean acidification on energy metabolism of oyster, *Crassostrea gigas* — changes in metabolic pathways and thermal response. Mar. Drugs 8, 2318–2339.

Lidbury, I., Johnson, V., Hall-Spencer, J.M., Munn, C.B., Cunliffe, M., 2012. Community-level response of coastal microbial biofilms to ocean acidification in a natural carbon dioxide vent ecosystem. Mar. Pollut. Bull. 64, 1063–1066.

Lombardi, C., Rodolfo-Metalpa, R., Cocito, S., Gambi, M.C., Taylor, P.D., 2011. Structural and geochemical alterations in the Mg calcite bryozoan *Myriapora truncata* under elevated seawater pCO_2 simulating ocean acidification. Mar. Ecol. 32, 211–221.

Marchant, H.K., Calosi, P., Spicer, J.I., 2010. Short-term exposure to hypercapnia does not compromise feeding, acid-base balance or respiration of *Patella vulgata* but surprisingly is accompanied by radula damage. J. Mar. Biol. Assoc. UK 90, 1379–1384.

Mehrbach, C., Culberson, C.H., Hawley, J.E., Pytkowicz, R.M., 1973. Measurement of the apparent dissociation constants of carbonic acid in seawater at atmospheric pressure. Limnol. Oceanogr. 18, 897–907.

Melatunan, S., Calosi, P., Rundle, S.D., Moody, J.A., Widdicombe, S., 2011. Exposure to elevated temperature and pCO_2 reduces respiration rate and energy status in the periwinkle *Littorina littorea*. Physiol. Biochem. Zool. 84, 583–594.

Melatunan, S., Calosi, P., Rundle, S.D., Widdicombe, S., Moody, J.A., 2012. The effects of ocean acidification and elevated temperature on shell plasticity and its energetic basis in an intertidal gastropod. Mar. Ecol. – Prog. Ser., doi: 10.3354/meps10046.

Melzner, F., Gutowska, M., Langebuch, M., Dupont, S., Lucassen, M., Thorndyke, M., Bleich, M., Pörtner, H.-O., 2009. Physiological basis for high CO_2 tolerance in marine ecothermic animals: pre-adaptation through lifestyle and ontogeny? Biogeosci. Discuss. 6, 4693–4738.

Miles, H., Widdicombe, S., Spicer, J.I., Hall-Spencer, J., 2007. Effects of anthropogenic seawater acidification on acid–base balance in the sea urchin *Psammechinus miliaris*. Mar. Pollut. Bull. 54, 89–96.

Munday, P.L., Dixson, D.L., Donelson, J.M., Jones, G.P., Pratchett, M.S., Devitsina, G.V., Døving, K.B., 2009. Ocean acidification impairs olfactory discrimination and homing ability of a marine fish. Proc. Natl. Acad. Sci. USA 106, 1848–1852.

Orr, J.C., Fabry, V.J., Aumont, O., Bopp, L., Doney, S.C., Feely, R.A., Gnanadesikan, A., Gruber, N., Ishida, A., Joos, F., Key, R.M., Lindsay, K., Maier-Reimer, E., Matear, R., Monfray, P., Mouchet, A., Najjar, R.G., Plattner, G.-K., Rodgers, K.B., Sabine, C.L., Sarmiento, J.L., Schlitzer, R., Slater, R.D., Totterdell, I.J., Weirig, M.-F., Yamanaka, Y., Yool, A., 2005. Anthropogenic ocean acidification over the twenty-first century and its impact on calcifying organisms. Nature 437, 681–686.

Pierrot, D., Lewis, E., Wallace, D.W.R., 2006. MS Excel Program Developed for CO_2 System Calculations, ORNL/CDIAC-105. Carbon Dioxide Information Analysis Center, Oak Ridge National Laboratory, U.S. Department of Energy, Oak Ridge, Tennessee.

Pinna, S., Pais, A., Campus, P., Sechi, N., Ceccherelli, G., 2012. Habitat preferences of the sea urchin *Paracentrotus lividus*. Mar. Ecol. – Prog. Ser. 445, 173–180.

Pörtner, H.-O., Langebuch, M., Reipschläger, A., 2004. Biological impact of elevated ocean CO_2 concentrations: lessons from animal physiology and Earth history. J. Oceanogr. 60, 705–718.

Pörtner, H.-O., Reipschläger, A., Heisler, N., 1998. Acid-base regulation, metabolism and energetics in *Sipunculus nudus* as a function of ambient carbon dioxide level. J. Exp. Biol. 201, 43–55.

Porzio, L., Buia, M.C., Hall-Spencer, J.M., 2011. Effects of ocean acidification on macroalgal communities. J. Exp. Mar. Biol. Ecol. 400, 278–287.

Privitera, D., Chiantore, M., Mangialajo, L., Glavic, N., Kozul, W., Cattaneo-Vietti, R., 2008. Inter- and intra-specific competition between *Paracentrotus lividus* and *Arbacia lixula* in resource-limited barren areas. J. Sea Res. 60, 184–192.

Rastrick, S.P.S., Whiteley, N.M., 2011. Congeneric amphipods show differing abilities to maintain metabolic rates with latitude. Physiol. Biochem. Zool. 84, 154–165.

Raven, J., Caldeira, K., Elderfield, H., Hoegh-Guldberg, O., Liss, P., Riebesell, U., Shepherd, J., Turley, C., Watson, A., 2005. Ocean acidification due to increasing atmospheric carbon dioxide. The Royal Society policy document 12:05. Clyvedon Press, Cardiff, UK.

Ries, J.B., Cohen, A.L., McCorkle, D.C., 2009. Marine calcifiers exhibit mixed responses to CO_2-induced ocean acidification. Geology 37, 1131–1134.

Reipschläger, A., Nilsson, G.E., Pörtner, H.-O., 1997. A role for adenosine in metabolic depression in the marine invertebrate *Sipunculus nudus*. Am. J. Physiol. Regul. Integr. Comp. Physiol. 272, 350–356.

Rodolfo-Metalpa, R., Houlbreque, F., Tambutte, E., Boisson, F., Baggini, C., Patti, F.P., Jeffree, R., Fine, M., Foggo, A., Gattuso, J.P., Hall-Spencer, J.M., 2011. Coral and mollusc resistance to ocean acidification adversely affected by warming. Nat. Climate Change 1, 308–312.

Russell, B.D., Connell, S.D., Uthicke, S., Muehllehner, N., Fabricius, K.E., Hall-Spencer, J.M., in press. Future seagrass beds: increased productivity leading to carbon storage? Marine Pollution Bulletin.

Seibel, B.A., Walsh, P.J., 2003. Biological impacts of deep-sea carbon dioxide injection inferred from indices of physiological performance. J. Exp. Biol. 206, 641–650.

Shick, J.M., 1983. Respiratory gas exchange in echinoderms. In: Jangoux, M., Lawrence, J.M. (Eds.), Echinoderms Studies, vol. 1. Balkema, Rotterdam, The Netherland.

Small, D., Calosi, P., Widdicombe, S., White, D., Spicer, J.I., 2010. Impact of long-term exposure to hypercapnia on physiological functions of the velvet swimming crab, *Necora puber*. Aquat. Biol. 10, 11–21.

Sokal, R., Rohlf, F.J., 1995. Biometry: the Principles and Practice of Statistics in Biological Research, third ed. W.H. Freeman and Company, New York.

Solomon, S., Qin, D., Manning, M., Chen, Z., Marquis, M., Averyt, K.B., Tignor, M., Miller, H.L.J., 2007. Contribution of Working Group I to the Fourth Assessment Report of the Intergovernmental Panel on Climate Change. Cambridge University Press, Cambridge, UK.

Spicer, J.I., 1995. Oxygen and acid-base status of the sea-urchin *Psammechinus miliaris* during environmental hypoxia. Mar. Biol. 124, 71–76.

Spicer, J.I., Raffo, A., Widdicombe, S., 2007. Influence of CO_2-related seawater acidification on extracellular acid–base balance in the velvet swimming crab *Necora puber*. Mar. Biol. 151, 1117–1125.

Spicer, J.I., Taylor, A.C., Hill, A.D., 1988. Acid–base status in the sea urchins *Psammechinus miliaris* and *Echinus esculentus* (Echinodermata: Echinoidea) during emersion. Mar. Biol. 99, 527–534.

Spicer, J.I., Widdicombe, S., Needham, H.R., Berge, J.A., 2011. Impact of CO_2-acidified seawater on the extracellular acid–base balance of the northern sea urchin *Strongylocentrotus dröebachiensis*. J. Exp. Mar. Biol. Ecol. 407, 19–25.

Stillman, J.H., 2002. Causes and consequences of thermal tolerance limits in rocky intertidal porcelain crabs, genus *Petrolisthes*. Integr. Comp. Biol. 42, 790–796.

Stumpp, M., Trübenbach, K., Brennecke, D., Hu, M.Y., Melzner, F., 2012. Resource allocation and extracellular acid–base status in the sea urchin *Strongylocentrotus droebachiensis* in response to CO_2 induced seawater acidification. Aquat. Toxicol. 110–111, 194–207.

Stumpp, M., Wren, J., Melzner, F., Thorndyke, M.C., Dupont, S.T., 2011. CO_2 induced seawater acidification impacts sea urchin larval development. I: elevated metabolic rates decrease scope for growth and induce developmental delay. Comp. Biochem. Physiol. 160A, 331–340.

Suggett, D.J., Hall-Spencer, J.M., Rodolfo-Metalpa, R., Boatman, T.G., Payton, R., Tye Pettay, D., Johnson, V.R., Warner, M.E., Lawson, T., 2012. Sea anemones may thrive in a high CO_2 world. Glob. Change Biol. 18, 3015–3025.

Todgham, A.E., Hofmann, G.E., 2009. Transcriptomic response of sea urchin larvae *Strongylocentrotus purpuratus* to CO_2-driven seawater acidification. J. Exp. Biol. 212, 2579–2594.

Thomsen, J., Gutowska, M.A., Saphörster, J., Heinemann, A., Trübenbach, K., Fietzke, J., Hiebenthal, C., Eisenhauer, A., Körtzinger, A., Wahl, M., Melzner, F., 2010. Calcifying invertebrates succeed in a naturally CO_2-rich coastal habitat but are threatened by high levels of future acidification. Biogeosciences 7, 3879–3891.

Truchot, J.P., 1976. Carbon dioxide combining properties of the blood of the shore crab *Carcinus maenas* (L): carbon dioxide solubility coefficient and carbonic acid dissociation constants. J. Exp. Biol. 64, 45–57.

Underwood, A.J., 1997. Experiments in Ecology: their Logical Design and Interpretation Using Analysis of Variance. Cambridge University Press, Cambridge, UK.

Vidolin, D., Santos-Gouvea, I.A., Freire, C.A., 2007. Differences in ion regulation in the sea urchins *Lytechinus variegatus* and *Arbacia lixula* (Echinodermata: Echinoidea). J. Mar. Biol. Assoc. UK 87, 769–775.

Wangensteen, O.S., Turon, X., García-Cisneros, A., Recasens, M., Romero, J., Palacín, C., 2011. A wolf in sheep's clothing: carnivory in dominant sea urchins in the Mediterranean. Mar. Ecol. – Prog. Ser. 441, 117–128.

Widdicombe, S., Dashfield, S.L., McNeil, C.L., Needham, H.R., Beesley, A., McEvoy, A., Øxnevad, S., Clarke, K.R., Berge, J.A., 2009. Effects of CO_2 induced seawater acidification on infaunal diversity and sediment nutrient fluxes. Mar. Ecol. – Prog. Ser. 379, 59–75.

Widdicombe, S., Spicer, J.I., 2008. Predicting the impact of ocean acidification on benthic biodiversity: what can animal physiology tell us? J. Exp. Mar. Biol. Ecol. 366, 187–197.

Whiteley, N.M., 1999. Acid–base regulation in crustaceans: the role of bicarbonate ions. In: Egginton, S., Taylor, A.C., Raven, J. (Eds.), Regulation of Acid-Base Status in Animals and Plants. Cambridge University Press, pp. 233–256.

Whiteley, N.M., 2011. Physiological and ecological responses of crustaceans to ocean acidification. Mar. Ecol. – Prog. Ser. 430, 257–271.

Whiteley, N.M., Rastrick, S.P.S., Lunt, D.H., Rock, J., 2011. Latitudinal variations in the physiology of marine gammarid amphipods. J. Exp. Mar. Biol. Ecol. 400, 70–77.

Wood, H.L., Spicer, J.I., Widdicombe, S., 2008. Ocean acidification may increase calcification rates, but at a cost. Proc. R. Soc. Lond. B 275, 1767–1773.

Zeebe, R.E., Wolf-Gladrow, D., 2001. CO_2 in Seawater: Equilibrium, Kinetics, Isotopes, Oceanography Series. Elsevier, Amsterdam, The Netherlands, pp. 1–346.

Please cite this article in press as: Calosi, P., et al. Distribution of sea urchins living near shallow water CO_2 vents is dependent upon species acid–base and ion-regulatory abilities. Mar. Pollut. Bull. (2013), http://dx.doi.org/10.1016/j.marpolbul.2012.11.040

Appendix E5:

S. Hahn, R. Rodolfo-Metalpa, E. Griesshaber, W.W. Schmahl, D. Buhl, J.M. Hall-Spencer, **C. Baggini**, K.T. Fehr, A. Immenhauser (2012). Marine bivalve shell geochemistry and ultrastructure from modern low pH environments: environmental effect versus experimental bias. *Biogeosciences*, 9: 1897-1914.

Biogeosciences, 9, 1897–1914, 2012
www.biogeosciences.net/9/1897/2012/
doi:10.5194/bg-9-1897-2012

Biogeosciences

Marine bivalve shell geochemistry and ultrastructure from modern low pH environments: environmental effect versus experimental bias

S. Hahn[1], R. Rodolfo-Metalpa[2], E. Griesshaber[3], W. W. Schmahl[3], D. Buhl[1], J. M. Hall-Spencer[2], C. Baggini[2], K. T. Fehr[3], and A. Immenhauser[1]

[1]Inst. of Geology, Mineralogy and Geophysics, Ruhr-University Bochum, Universitätsstraße 150, 44801 Bochum, Germany
[2]Marine Institute, Marine Biology and Ecology Research Centre, University of Plymouth, A428, Portland Square, Drake Circus, Plymouth, Devon, PL4 8AA, UK
[3]Dept. of Earth and Environmental Science, Ludwig Maximilian University, Theresienstraße 41, 80333 Munich, Germany

Correspondence to: S. Hahn (sabine.hahn@rub.de)

Received: 20 September 2011 – Published in Biogeosciences Discuss.: 24 October 2011
Revised: 12 April 2012 – Accepted: 29 April 2012 – Published: 29 May 2012

Abstract. Bivalve shells can provide excellent archives of past environmental change but have not been used to interpret ocean acidification events. We investigated carbon, oxygen and trace element records from different shell layers in the mussels *Mytilus galloprovincialis* combined with detailed investigations of the shell ultrastructure. Mussels from the harbour of Ischia (Mediterranean, Italy) were transplanted and grown in water with mean pH_T 7.3 and mean pH_T 8.1 near CO_2 vents on the east coast of the island. Most prominently, the shells recorded the shock of transplantation, both in their shell ultrastructure, textural and geochemical record. Shell calcite, precipitated subsequently under acidified seawater responded to the pH gradient by an in part disturbed ultrastructure. Geochemical data from all test sites show a strong metabolic effect that exceeds the influence of the low-pH environment. These field experiments showed that care is needed when interpreting potential ocean acidification signals because various parameters affect shell chemistry and ultrastructure. Besides metabolic processes, seawater pH, factors such as salinity, water temperature, food availability and population density all affect the biogenic carbonate shell archive.

1 Introduction

Over the last two centuries, human activities have increased the atmospheric CO_2 concentration by about 31 % (Lüthi et al., 2008; Solomon et al., 2009). Approximately one third of the anthropogenic carbon added to the atmosphere is absorbed by the oceans. Uptake of atmospheric CO_2 results in a decrease in ocean water pH, an effect referred to as "ocean acidification" (Caldeira and Wickett, 2003). As a consequence, marine calcareous organisms are increasingly stressed. This is because net calcification rates are affected by decreased calcium carbonate saturation and carbonate ion availability (Fabry et al., 2008; Guinotte and Fabry, 2008; Hall-Spencer et al., 2008).

Previous studies focused on the response of marine calcified organisms to increased CO_2 levels to predict the combined impact of future ocean acidification and increasingly elevated seawater temperatures (Orr et al., 2005; Davies et al., 2007; Fine and Tchernov, 2007; Hoegh-Guldberg et al., 2007; Carroll et al., 2009; Cigliano et al., 2010; Dias et al., 2010; Gutowska et al., 2010; Rodolfo-Metalpa et al., 2010, 2011). Other approaches focussed on past acidification events (Kump et al., 2009; Zeebe and Ridgwell, 2011), such as the Paleocene-Eocene Thermal Maximum 55 million years ago (PETM; Zachos et al., 2005; Sluijs et al., 2007; Iglesias-Rodriguez et al., 2008; Gibbs et al., 2010). Previously applied methods include model organisms cultured under laboratory conditions (e.g. Russell et al., 2004; Kisakürek et al., 2011), mesocom experiments (e.g. Engel

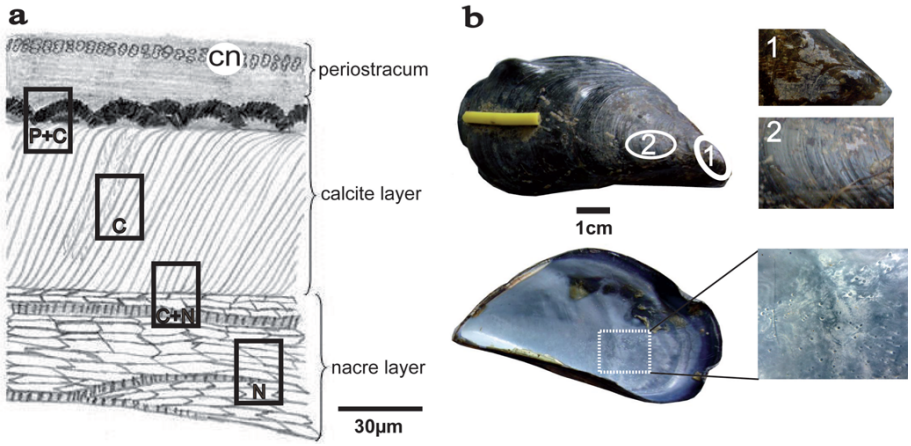

Fig. 1. (a) Sketch of tripartite shell structure of *M. galloprovincialis*. Note periostracum, calcite and aragonitic nacreous layers. The sketch shows the general structure of the shell without a scale. Black boxes indicate sampling sites for isotope analysis. P+C = periostracum and calcite layer; C = calcite layer; C+N = calcite and nacreous layer; N = nacreous layer. "Cn" indicates channel network ("pipe system") in the upper part of the periostracum. **(b)** *Mytilus galloprovincialis* from experimental site B1. Note partial lack of periostracum and absence of encrusting or colonizing marine biota in upper image (white circles, labelled 1 and 2, corresponding to close up images to the right) and incomplete nacreous layer with small holes (white rectangle, corresponding to close up image to the right) in lower image. On 26 September 2009, i.e. prior to transplantation, specimens were labelled with a yellow marker in order to differentiate pre- and post-transplantation shell material.

et al., 2005; Riebesell et al., 2007), studies using naturally acidified sites (e.g. Hall-Spencer et al., 2008; Manzello et al., 2008; Kroeker et al., 2011) and the investigation of geological archives (e.g. Mutterlose et al., 2007; Kump et al., 2009; Gibbs et al., 2010). Brief monitoring and culturing experiments (several months to few years; Klein et al., 1996b; Berge et al., 2006; Thomsen et al., 2010) have shortcomings as they provide only limited evidence for longer term adaptation strategies of marine ecosystems (e.g. Guinotte and Fabry, 2008; Ellis et al., 2009; Gutowska et al., 2010). Studies dealing with geological archives suffer from the lack of biological information and are limited by problems of time control (e.g. Ragland et al., 1979; Gomez-Alday and Elorza, 2003; Aubry et al., 2007; Röhl et al., 2007). The majority of geological archive work deals with planktonic organisms from pelagic core material (Raffi et al., 2005; Gibbs et al., 2006; Giusberti et al., 2007; Mutterlose et al., 2007; Westerhold et al., 2007). In contrast, studies with focus on the impact of past acidification events on fossil coastal neritic settings are scarce (Scheibner and Speijer, 2008).

One of the most promising archives of past coastal seawater properties are bivalves (Buick and Ivany, 2004; Lopez Correa et al., 2005; Latal et al., 2006; Foster et al., 2009). Bivalves are sessile organisms that over time record environmental changes in their aragonitic and calcitic shells (Witbaard et al., 1994; Vander Putten et al., 2000; Elliot et al., 2003; Immenhauser et al., 2005; Hippler et al., 2009) and at least their calcitic shells hardparts have, under favourable conditions, a high fossilization potential (Elorza and GarciaGarmilla, 1996; Gomez-Alday and Elorza, 2003; Immenhauser et al., 2005).

The effects of ocean seawater acidification on the bioperformance of the blue mussel *Mytilus edulis* has previously been the topic of mainly biological research (Bamber, 1987; Michaelidis et al., 2005; Berge et al., 2006; Gazeau et al., 2007). The *M. edulis* group, involving the three species *M. edulis*, *M. galloprovincialis* and *M. trossulus* (Koehn, 1991; Aguirre et al., 2006) was investigated for growth patterns (shell length), tissue weight and overall activity and health of these organisms (Bamber, 1987; Berge et al., 2006; Beesley et al., 2008). *Mytilus edulis* has a very wide geographical distribution from the subtropics to the Arctic regions, while *M. trossulus* and *M. galloprovincialis* are more environmentally restricted (Gosling, 2003), but tolerate a wide temperature range (Aral, 1999). The environmental adaptability of *M. edulis* with respect to its wide distribution range including freshwater (Shumway, 1977; Gillikin et al., 2006a, b; Tynan et al., 2006), brackish (Hietanen et al., 1988) and marine settings qualifies the blue mussel as an adaptable and widely used test organism.

Generally, bivalve shells have three layers: the periostracum and two calcium carbonate layers (Fig. 1a). The periostracum forms a quinone-tanned protein layer on the outside of the shell (Fig. 1a; Kennedy et al., 1969), protects the shell, serves as a seal of the extrapallial space for the achievement of supersaturation conditions (Marin and Luquet, 2004) and provides the site of nucleation for calcium carbonate (Checa, 2000). Carbonate shell layers can be distinguished optically as well as by means of their microstructure and mineralogy. The inner layer consists of iridescent, nacreous aragonite (Fig. 1b; Marin and Luquet, 2004) and is composed of 10–20 µm wide tablets that form parallel arranged 0.5 µm

thick lamellae (Fig. 1a). The outer shell layer has a prismatic structure and is composed of calcite prisms (Fig. 1a).

Here we report on the outcome of a study with focus on *M. galloprovincialis* exposed to different seawater pH along a natural gradient in CO_2 levels near volcanic vents (pH_T range 6.6–7.1) off Ischia. We explore and combine the potential of three different proxies within the same carbonate archive: (i) shell isotope and major and trace element geochemistry; (ii) shell ultra- and microstructure imaging, and (iii) crystallographic texture analysis. The aims of this work are twofold. Firstly, we test, the potential of bivalve shell geochemistry and ultrastructure as recorders of environmental change and particularly seawater acidification. Secondly, we assess the sensitivity of the bivalve metabolism to experimental transplantation shock. This work has significance for those concerned in future effects of ocean acidification, paleo-environmental analysis and carbonate archive research in general.

2 Materials and methods

2.1 Field study

The field site lies on the east coast of Ischia (40°43.81′ N, 13°57.98′ E), south of Castello Aragonese where vents acidify the seawater (Fig. 2). The vents emit gas composed of 90–95 % CO_2, 3–6 % N_2, 0.6–0.8 % O_2, 0.2–0.8 % CH_4 and 0.08–0.1 % Ar and lacked toxic sulphur compounds (Hall-Spencer et al., 2008). Published data of $\delta^{13}C_{(CO_2)}$ from gas vents along the eastern margin of Ischia indicate ^{13}C-enriched values of +0.5 to −0.8 % (Tedesco, 1996). The seawater pH_T range is 6.6 to 8.1 depending on distance from the vents. Seawater carbon (DIC) isotope values measured during late fall and early winter, i.e. the time interval when the transplantation experiment was undertaken, range from 0.2 ‰ (Ischia harbour, IP, Fig. 2c) to 0.8 ‰ seawater off Ischia (C and OS Fig. 2c, d), whilst a $\delta^{13}C_{DIC}$ of 0.9 ‰ was found for vent areas (B1 and ES Fig. 2d; Table 1). During spring and summer months, when plankton bloom removes isotopically light carbon from seawater, seawater $\delta^{13}C_{DIC}$ is more positive (1–1.4 ‰) and differences between harbour, experimental site B1 and control site C are more reduced. During this time, seawater $\delta^{13}C_{DIC}$ approaches regional values as reported in Pierre (1999).

Ischia seawater oxygen isotope values measured during late fall and early winter, i.e. the time interval when the transplantation experiment was undertaken, range from 1.1 ‰ SMOW (Ischia harbour, IP, Fig. 2c; Table 1) to 1.2 ‰ SMOW seawater at the vent areas (B1 and ES Fig. 2d; Table 1) and off Ischia (C and OS Fig. 2c, d; Table 1). These data are in agreement with regional seawater oxygen isotope values (1.2–1.3 ‰ SMOW) representing April water samples (Pierre, 1999).

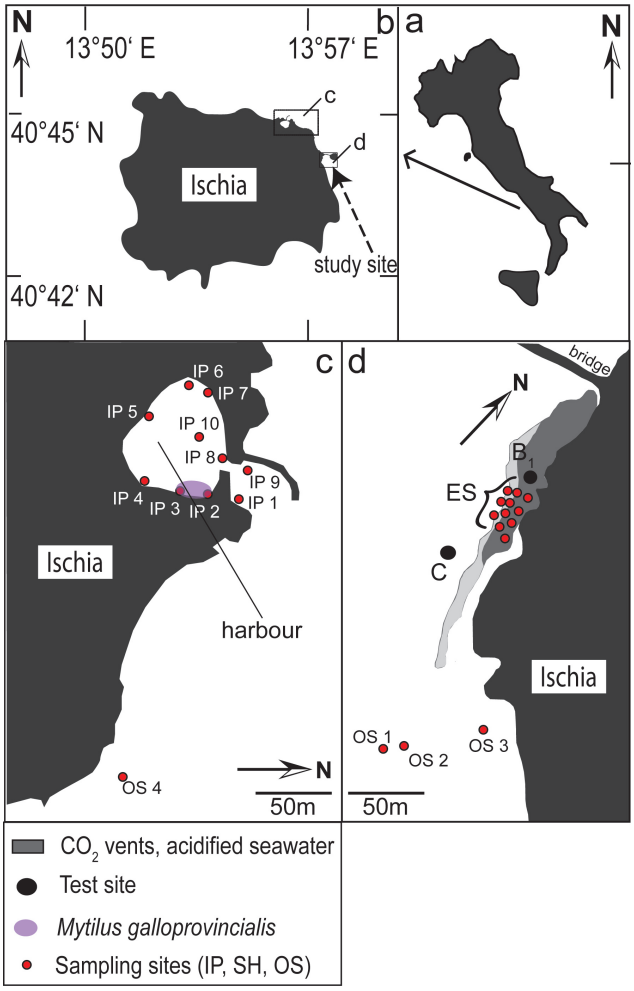

Fig. 2. Map of Italy **(a)** and the Island of Ischia **(b)**. **(c)** Schematic map of Ischia harbour with location of the seawater sampling points IP (Ischia Port) and OS (oceanic seawater), as well the location of *M. galloprovincialis*, marked by the purple dot. **(d)** Schematic map of the natural experiment sites off Ischia in the vicinity of CO_2 vents. Specimens of *M. galloprovincialis* were transplanted in September 2009 from the harbour (pH 8.07) to control site C (mean pH_T 8.07) and experimental site B1 (mean pH_T of 7.25, minimum pH_T 6.83) where they were kept until December 2009 (modified after Hall-Spencer et al., 2008). Seawater sampling sites are labelled OS and ES.

Several adult *M. galloprovincialis* (>40 mm length) collected from the Ischia port (pH_T 8.07) (Fig. 2b, c) were transplanted to a control site with normal pH_T (C in Fig. 2b, d; mean pH_T 8.07) and to an experimental site with acidified seawater (B1 in Fig. 2b, d; mean pH_T 7.25, minimum pH_T 6.83). Samples were labelled with a yellow marker glued onto the shell edge (Fig. 1b) to differentiate between shell precipitated before and after transplantation. The mussels were kept at the test sites for 68 days (28 September to 2 December 2009). Seawater temperature, pH_T and total alkalinity (At) were monitored for the duration of the experiment

Table 1. Parameters of harbour and field experimental sites. Mean ± S.D. seawater chemistry calculated over the experiment period at the experimental site B1 and control site C. pH_T is in total scale; pCO_2 in µatm; HCO_3^-, CO_3^{2-}, CO_2 and DIC (dissolved inorganic carbon) are in µmol kg^{-1}; saturation state (Ω) of aragonite and calcite. IP = Ischia port (harbour); OS = ocean seawater off Ischia; ES = experimental site.

	mean T (°C) late summer to early winter	pH_T	pCO_2 (µatm)	HCO_3^- (µmol kg^{-1})	CO_3^{2-} (µmol kg^{-1})	CO_2 (µmol kg^{-1})	DIC (µmol kg^{-1})	Ω calcite	Ω aragonite	$\delta^{18}O$ (‰ SMOW) late fall/ early winter	$\delta^{13}C$ (‰ VPDB) late fall/ early winter	$\delta^{18}O$ (‰ SMOW) spring	$\delta^{13}C$ (‰ VPDB) spring
Harbour (IP)	18.9 (±0.98)	8.07 (±0.07)	n.d.	2993 (±136)	n.d.	n.d.	n.d.	n.d.	n.d.	1.1 (±0.02)	0.2 (±0.02)	1.2–1.3 (±0.02)	1.4 (±0.02)
Site C (OS)	21 (±4.2)	8.07 (±0.04)	474 (±58)	2015 (±74)	235 (±35)	15 (±2)	2265 (±43)	5.42 (±0.74)	3.55 (±0.52)	1.2 (±0.02)	0.8 (±0.02)	1.2–1.3 (±0.02)	1.4 (±0.02)
Site B1 (ES)	20.7 (±4.2)	7.25 (±0.44)	5494 (±5520)	2428 (±108)	61 (±45)	173 (±175)	2661 (±226)	1.37 (±0.95)	0.98 (±0.69)	1.2 (±0.02)	0.9 (±0.02)	1.2–1.3 (±0.02)	1.4 (±0.02)

(Table 1). Refer to Hall-Spencer et al. (2008), Martin et al. (2008), Cigliano et al. (2010) and Rodolfo-Metalpa et al. (2010) for details of the experimental and analytical approach.

2.2 Methods: carbon and oxygen isotope and elemental geochemistry

Carbon and oxygen-isotope analyses of 170 powder samples of *M. galloprovincialis*$_{\text{B1 and C}}$ (Table S1, Supplement) extracted from mussel shells and 28 seawater samples were performed with a ThermoFinnigan MAT 253 ratio mass spectrometer equipped with a Gasbench II at the isotope laboratory of the Institute for Geology, Mineralogy and Geophysics (Ruhr-University Bochum, Germany). Repeated analyses of certified carbonate standards (NBS 19, IAEA CO-1 and CO-8) and internal standards show an external reproducibility of ≤0.02 ‰ for $\delta^{13}C$ and ≤0.06 ‰ for $\delta^{18}O$ for the powder samples. An internal laboratory standard (Na_2CO_3) was used for the seawater $\delta^{13}C_{DIC}$ samples. The 1σ-reproducibility of the measured values is 0.19 ‰ $\delta^{13}C_{DIC}$. All isotope results are reported in per mil (‰) relative to the V-PDB standard in the conventional manner. For analyses of the seawater $\delta^{13}C_{DIC}$ vials were treated with 85 % phosphoric acid and then flushed with helium. Subsequently, carbonate hardness was determined and the required amount of sample material was added into the prepared vials. Seawater $\delta^{18}O$ was analyzed in the laboratories of Johanneum Research Centre in Graz (Austria). Seawater $\delta^{13}C_{DIC}$ and $\delta^{18}O$ from Ischia harbour, control and experimental sites are given in Table 1.

In total two different sampling approaches were applied for powder samples. One approach used bulk shell samples (including all shell layers and shell layers in variable admixtures; Fig. 1a) following a transect along the maximum growth axis of the shell. For the second approach, shells were cut perpendicularly to the maximum growth axis and calcite samples were extracted using a micro drilling system (MicroMill, Mechantek (esi/New Wave); Dettman and Lohmann, 1995). For detailed information of the analytical procedure refer to Immenhauser et al. (2005). For the sake of data comparability, aragonitic (nacreous) layer isotope data were normalized against calcite isotope values using the equation of Rubinson and Clayton (1969) for $\delta^{13}C$ and that of Tarutani et al. (1969) for $\delta^{18}O$.

Elemental geochemistry analysis was performed on a *M. galloprovincialis* shell from experimental locality B1 (Fig. 2b, d) using a Cameca SX50 electron microprobe at the Department of Earth and Environmental Sciences of the LMU Munich; Germany. The probe was operated at 15 keV acceleration and 20 nA beam current. Barium (Ba), calcium (Ca), chlorine (Cl), iron (Fe), magnesium (Mg), manganese (Mn), phosphorus (P), silicon (Si), sodium (Na) and strontium (Sr) were measured. Albite (Na), apatite (Ca and P), baryte ($BaSO_4$) (Ba), Fe_2O_3 (Fe), ilmenite ($MnTiO_3$) (Mn), periclase (Mg), $SrSO_4$ (Sr), vanadite (Cl) and wollastonite (Si) were used as standards. Matrix correction was performed by the PAP procedure (Pouchou and Pichoir, 1984). The reproducibility of standard analyses was <1 % for each routinely analysed element. The PAP corrected data were stoichiometrically calculated as carbonate. Samples were taken over the entire shell, but emphasis was placed on the shell formed directly before and after the transplantation (Fig. 1b).

2.3 Methods: shell microstructure and texture analysis

The microstructure and texture of *M. galloprovincialis* shells were investigated under a scanning electron microscope (SEM) using polished thin sections and fragments of surface samples as well as under electron backscattered diffraction (EBSD). We use the following macroscopic reference frame: all sample wafers were obtained from a longitudinal cut through the shell that ranged from the hinge to the commissure of the valve. The sample wafers were ∼200 micrometer thick and placed 90 degrees to the plane of cut onto a glass holder. Samples were subsequently prepared on both sides of the shell as highly polished, 150 µm thick sections. The surface of the thin sections was subsequently etched for 45 s with a suspension of alumina nanoparticles. The samples were then cleaned, dried, and coated with the thinnest possible conducting carbon coating (SEM: 4–6 µm and EBSD: 15 µm). Scanning electron micrographs and EBSD patterns were obtained on a LEO Gemini 1530 SEM and a JEOL

Table 2. Thickness characteristics of different shell layers of *M. galloprovincialis*$_{\text{B1 and C}}$ in µm. Shell thickness was measured before and after transplantation. N.d. = no data; n.f. = not formed, i.e. shell was not precipitated.

	Mytilus galloprovincialis from site C pH_T 8.07 in µm	*Mytilus galloprovincialis* from site B1 pH_T 7.25 in µm
Calcite layer	130–500	215–820
– commissure	200–250	215–230
– near commissure (after transplantation, C and B1)	200–250	340–430
– transition from harbour site to experimental site	n.d.	620
– near commissure (before transplantation, C and B1)	500	760–820
– middle of the shell	130	430–520
Nacreous layer	5–440	10–150
– commissure	0–10	n.f.
– near commissure (after transplantation, C and B1)	0–10	n.f.
– transition from the harbour site to experimental site	n.d.	n.f.
– near commissure (before transplantation, C and B1)	40	10–150
– middle of the shell	440	10–100
Total shell (calcite and nacreous layer)	135–570	225–970
– commissure	200–260	215–230
– near commissure (after transplantation, C and B1)	200–260	340–430
– transition from the harbour site to experimental site	n.d.	620
– near commissure (before transplantation, C and B1)	540	770–970
– middle of the shell	570	440–620

JSM 6500F SEM each equipped with the HKL Technology "Channel 5" EBSD system. Images and EBSD patterns were generated using an accelerating voltage of 20 kV and a beam current of 3.0 nA. The lattice orientation of grains was determined with a spatial resolution of 2–3 µm and an absolute angular resolution of ±0.5 degrees. Electron backscattered diffraction patterns with a mean angular uncertainty of 1 degree and above were discarded. Several EBSD maps were conducted from each wafer, starting at the commissure and moving towards the hinge. Calcite c-axes of the pole figures always point to the outer rim of the shell and rotate (for the calcitic shell portion) with the curvature of the shell.

3 Results

3.1 Macroscopic observations

Macroscopic examination of *M. galloprovincialis*$_{\text{B1}}$ samples transplanted to the acidified experimental site (pH_T 7.25, Fig. 2d) developed characteristic features of the periostracum, the calcitic and the aragonitic shell layers: (i) Mussels lacked encrusting or colonizing marine biota (Fig. 1b); (ii) near the umbo, the oldest part of the shell, the periostracum was abraded while (iii) the nacreous layer lacked its normal lustre and was pitted with small holes (∼0.1 mm) and scattered with white spots (Fig. 1b). In contrast, *M. galloprovincialis*$_{\text{C}}$ from the control site C (pH_T 8.07) were characterized by shells encrusted by marine biota and displayed a lustrous nacreous layer.

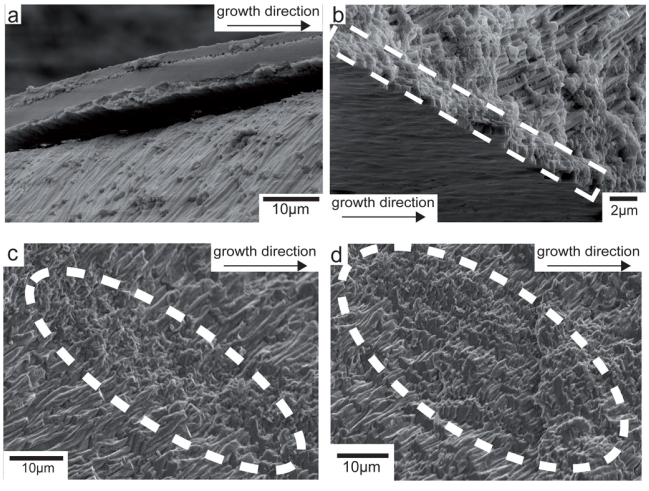

Fig. 3. Calcite layer SEM images from *Mytilus galloprovincialis*$_{\text{B1 and C}}$ fragments of the surface. Images are from outer margin precipitated from normal marine seawater pH **(a, b)** and from shells precipitated from acidified seawater **(c, d)**. (**a** and **b**) Calcite layer of *M. galloprovincialis* from control site C (pH_T = 8.07). Note well structured calcite layer. White stippled box indicates aragonite layer. (**c** and **d**) Calcite layer of *M. galloprovincialis* from acidified experimental site B1. Note portions of calcite layer with disorganized shell structure (white stippled oval) within otherwise well organized calcite shell.

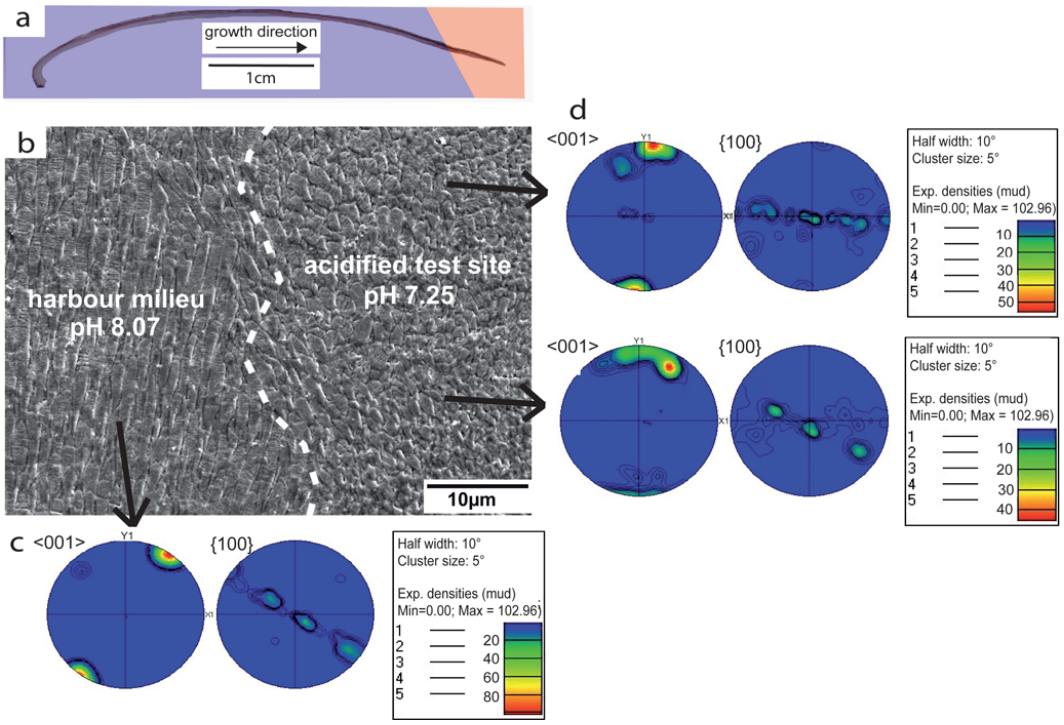

Fig. 4. Thin section view of calcite layer of *M. galloprovincialis* from acidified seawater site B1. **(a)** Blue colour indicates shell precipitated prior to transplantation and red colour indicates shell precipitated after transplantation to acidified test site B1. **(b)** SEM image of shell precipitated parallel to the longest growth axis and directly before and after transplantation. Note pronounced differences in the orientation of the calcite layer across transplantation event (white, stippled line). Locations of respective pole figures **(c)** and **(d)** are indicated. (**c** and **d**) Pole figures representing stereographic projections of crystallographic axes and planes. The strength of clustering is specified with the MUD (multiples of uniform density) value that gives the distribution pattern of EBSD data relative to that of a random distribution.

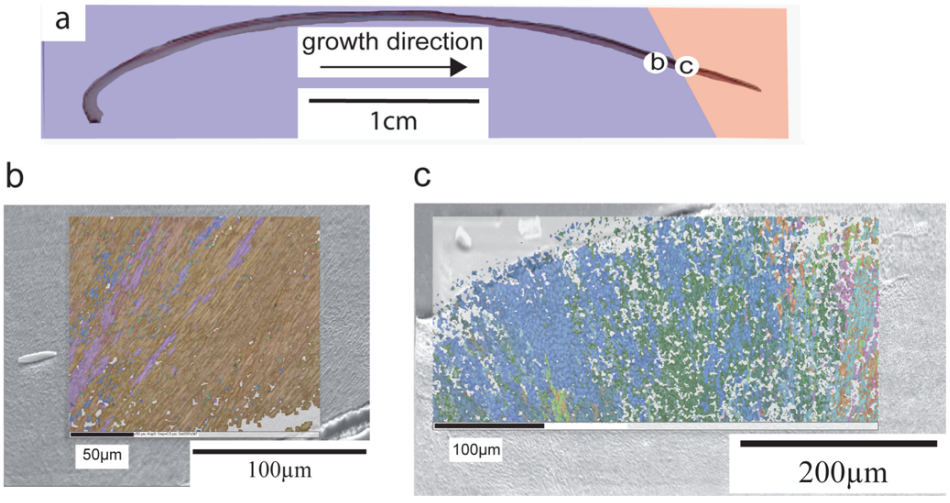

Fig. 5. Thin-section view of *M. galloprovincialis* from experimental site B1. **(a)** Blue colour indicates shell precipitated prior to transplantation and red colour indicates shell precipitated after transplantation to acidified experimental site. (**b** and **c**) Electron backscattered diffraction (EBSD) maps. Note location of b and c in Fig. 5a. Different colours indicate different orientations of calcite prisms. White points denote those regions within the shell where Kikuchi patterns could not be indexed. The three RGB colour components code for the three Euler angles of crystal orientation. In order to visualize all patterns the whole range of Euler angles are plotted (Euler 1 between 0–180°, Euler 2 between 0–180° and Euler 3 between 0–120°). Note rather homogenous (brown to lilac, **b**) colours in well structured calcite shell prior to transplantation. The EBSD map of shell portions precipitated after the transplantation indicates a wider range of colours and spatially disorganized calcite prisms indicating shell precipitation under acidified environments.

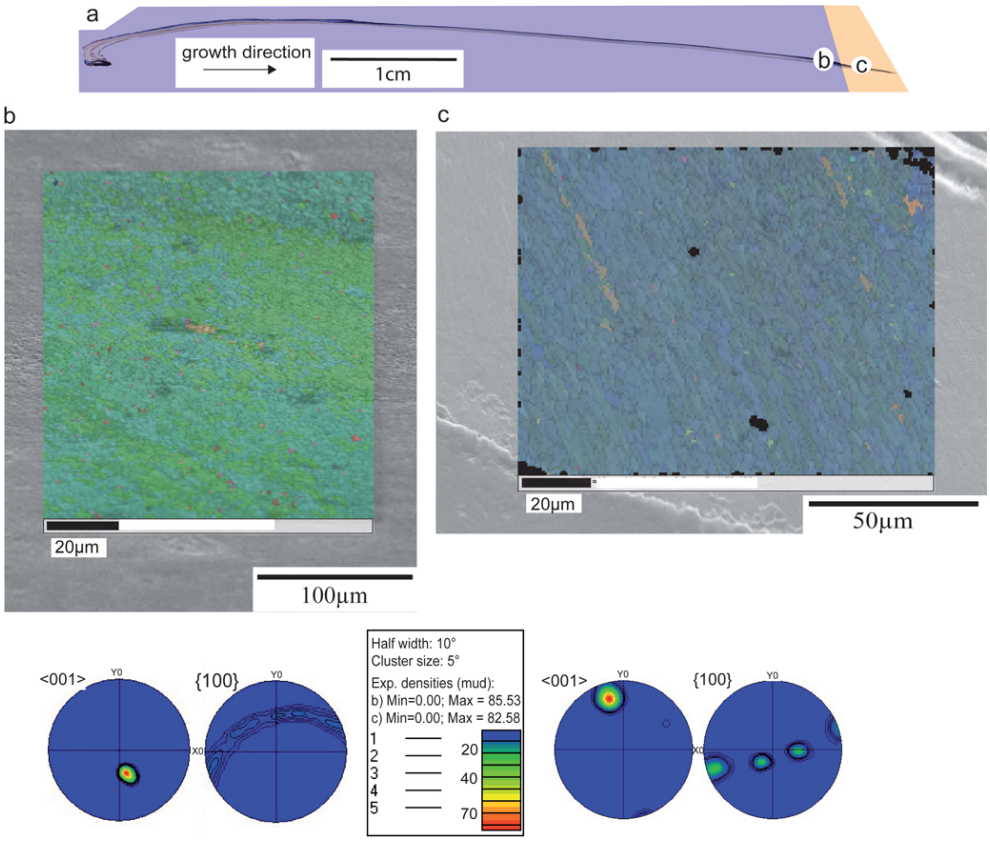

Fig. 6. Thin-section view of *M. galloprovincialis* from control site C. **(a)** Blue colour indicates shell precipitated prior to transplantation and orange colour indicates shell precipitated after transplantation to control site. (**b** and **c**) Electron backscattered diffraction (EBSD) maps and pole figures. Note location of b and c in Fig. 6a. Different colours indicate different orientations of calcite prisms. Black points denote those regions within the shell where Kikuchi patterns could not be indexed. The three RGB colour components code for the three Euler angles of crystal orientation. In order to visualize all patterns the whole range of Euler angles are plotted (Euler 1 between 0–180°, Euler 2 between 0–180° and Euler 3 between 0–120°). Note homogenous (green to blue) colours in well structured calcite shell prior to and after transplantation. The differences between the maps are due to different step sizes. Pole figures representing stereographic projections of crystallographic axes and planes. MUD = Multiples of Uniform Density.

3.2 Shell ultrastructure, microstructure and texture

Figure 1a displays a sketch of the major structural units of the shell's ultrastructure based on SEM observations of transplanted *M. galloprovincialis*$_{\text{B1 and C}}$. In the following, differences and similarities of shell portions that represent the pre-transplantation growth period and such that represent the post-transplantation growth period are compared.

The thickness of the calcite and aragonite layers varies significantly over the life time of individual specimen whilst the thickness of the periostracum remains more constant. The calcite shell ranges from 120 to 830 µm and the nacreous layer ranges from 5 to 1520 µm in thickness (Table 2). The calcite shell layer formed from seawater at sites B1 and C has thinned to about 70 % in the case of experimental site *M. galloprovincialis*$_{\text{B1}}$ and to about 55 % of its former thickness in the case of control site *M. galloprovincialis*$_{\text{C}}$ (Table 2). In *M. galloprovincialis* $_{\text{B1}}$ the nacreous shell layer was not formed, while it is present in samples from site C as a 5–10 µm thick layer (Table 2).

Figure 3 depicts comparable portions of *M. galloprovincialis*$_{\text{B1 and C}}$ shells formed after the transplantation. The calcite layer of samples from control site seawater pH environments (Site C, pH_T 8) is well ordered (Fig. 3a to b), while, in contrast, the calcitic layer of the *M. galloprovincialis* $_{\text{B1}}$ specimen from the acidified experimental site (pH_T of 7.25) is unordered. This effect is most pronounced in the portion of the shell formed directly after the transplantation into the acidified environment (Fig. 4b). With time, the shell structure formed under acidified seawater conditions takes up the formerly structured organization, albeit with localized patches of disordered shell calcite prisms (Fig. 3c and d). The later observation is considered significant.

Electron backscattered diffraction measurements from *M. galloprovincialis*$_{\text{B1}}$ are displayed in Figs. 4 and 5. The SEM image in Fig. 4b shows the shell's microstructure across the

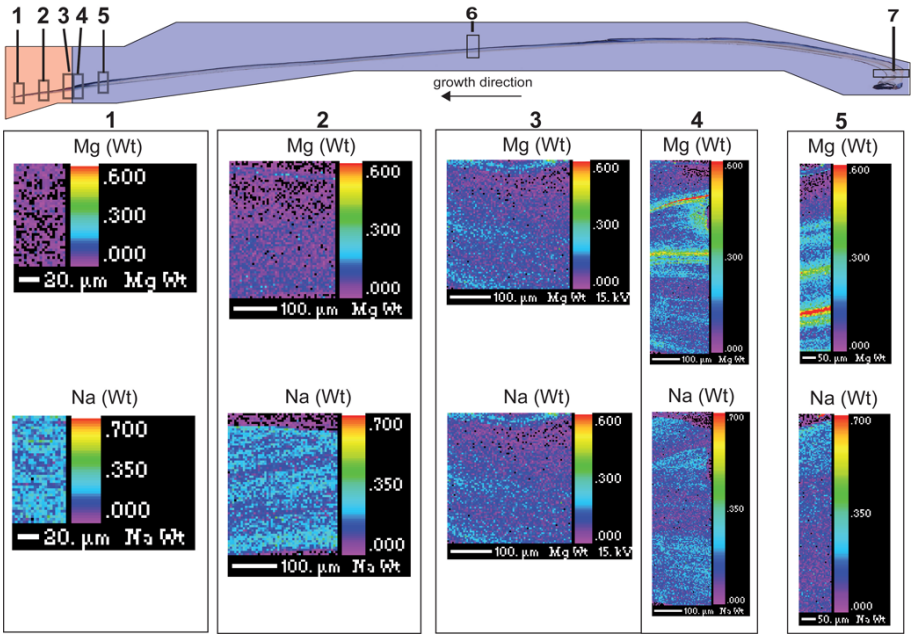

Fig. 7. Thin section view of *M. galloprovincialis* from acidified experimental site B1. Blue colour indicates shell precipitated prior to transplantation and red colour indicates shell precipitated after transplantation. Gray boxes numbered 1 through 7 indicate the position of the microprobe maps. The maps 1 to 5 were measured across the calcitic shell layer only. Maps 6 and 7 are shown in Fig. 8 and are located at the mid-shell and the hinge. Map 6 was measured across the calcitic and aragonitic layers, map 7 was measured across the aragonitic layer. Magnesium and sodium microprobe maps 1 through 5 are numbered in ascending order from the commissure to the hinge (corresponding to the boxes with the microprobe maps). Due to the incisive difference between the element magnesium (Mg) and sodium (Na), these elements are illustrated. The concentration of elements is given in weight percent (Wt). The element distribution in the shell displays no discernible pattern while concentrations of Mg and Na follow opposite trends.

transition from normal to acidified seawater. Calcite prisms formed prior to the transplantation are aligned in parallel (Fig. 4b) and the corresponding electron backscattered diffraction pattern shows a unimodal distribution (Fig. 4c). After the transplantation, a microstructural disarrangement of the shell fabric is observed (Fig. 4b). This feature is perhaps best explained as an adaptation shock of the mussel to the transplantation. After adaptation to the new environment, *M. galloprovincialis*$_{B1}$ precipitates an ordered but thinner calcite shell layer with prisms arranged in parallel (Fig. 3c, d). The electron backscattered diffraction projection patterns in Fig. 4d, documenting post-transplantation shell growth, display bimodal, or more distribution.

The shell texture, specifically the 3-D orientation of calcite fibre c-axes, displays a similar transplantation effect (Fig. 5). A well ordered array of calcite fibre c-axes is precipitated prior to the transplantation (Fig. 5b). Less ordered fibre c-axes characterize the portion of the shell formed directly after the transplantation (Fig. 5c).

Electron backscattered diffraction analyses of control site *M. galloprovincialis*$_{C}$ are displayed in Fig. 6. The shell texture, specifically the 3-D orientation of calcite fibre c-axes, displays a well ordered array precipitated prior and after transplantation (Fig. 6b and c). Electron backscattered diffraction projection patterns in Fig. 6b and c show a unimodal distribution.

3.3 Shell geochemistry

3.3.1 Elemental abundances

Microprobe analysis results of samples obtained from *M. galloprovincialis*$_{B1}$ are listed in Table S2 (Supplement). Magnesium and sodium abundances are summarized in seven distribution pattern maps shown in Figs. 7 and 8. Clear differences in Ca, Mg, Na and P elemental composition between shell portions representing normal control site and such representing acidified experimental site seawater are recognized. All other elements were either evenly distributed or below detection limit.

While Ca values are around 390 000 ppm (39 wt %) in all measured maps, P shows a highly variable concentration distribution pattern of 1510 (0.151 wt %) to 4680 ppm (0.468 wt %). Both elements, however, are enriched in the calcite in comparison to the aragonite layer. Magnesium and sodium show opposing distribution patterns. While magnesium is only present in the calcite layer, sodium is present in both layers. In contrast to magnesium, however, sodium is more abundant in the nacreous layer (10 600 ppm or

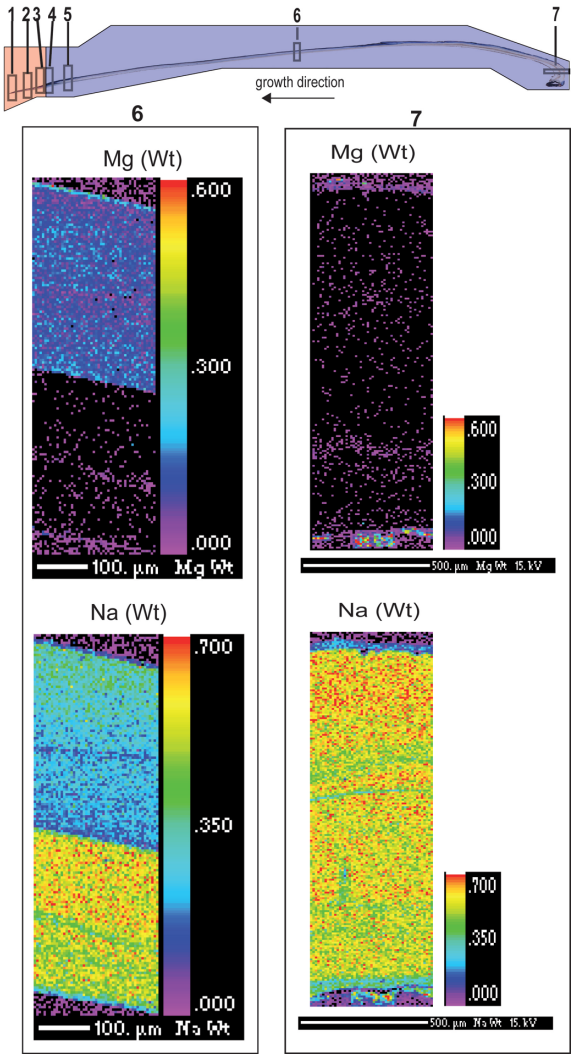

Fig. 8. Thin section view of *M. galloprovincialis* from acidified experimental site B1. Blue colour indicates shell precipitated prior to transplantation and red colour indicates shell precipitated after transplantation to acidified test site. Gray boxes numbered 1 to 7 indicate the position of the microprobe maps. The maps 1 to 5 are shown in Fig. 7. Magnesium and sodium concentration is given in weight percent. Differences in element concentrations in map 6 reflect differences between calcite and aragonite layer. Magnesium and sodium are incorporated in calcite layer. Nacreous layer displays considerably higher concentrations of sodium. Judging from elemental maps, the shell hinge is composed almost entirely of aragonite.

1.060 wt %) compared to the calcite layer (about 4500 ppm or 0.450 wt %; Table S2). The sodium content decreases gradually from the shell hinge to the most recent portions of the shell.

Magnesium shows a different distribution pattern with increasing and decreasing trends between shell hinge and commissure. In part, this distribution is related to the thickness of the aragonite versus the calcite layer with Mg incorporated far more substantially into calcite. Initially, Mg increases in abundance from the shell hinge towards the commissure, this as the nacreous shell layer thins whilst the calcitic layer thickens (Table S2). At the commissural end of the shell (i.e. in the youngest portions of the shell), Mg abundances within the calcite layer first increase and then decrease.

3.3.2 Carbon and oxygen isotope ratios from specific shell layers

In order to assess the relative significance of each individual shell layer (periostracum, calcite layer, nacreous/aragonite layer) on bulk δ^{13}C and δ^{18}O isotope data and in order to capture the internal variability, sub-samples were drilled from individual layers in selected shells (Fig. 1a). Isotope data are listed in Table S1 (Supplement) and shown in Fig. 9 whilst seawater isotope values are given in Table 1. Due to the complexity of the data set, the main features are summarized below. Previous work by Rubinson and Clayton (1969; δ^{13}C) and Tarutani et al. (1969; δ^{18}O) reported on the crystallographical effects of isotope fractionation in inorganic aragonite and calcite precipitates. Therefore, $\delta^{13}C_{Aragonite}$ values in Fig. 9a and c were normalized for calcite. In a comprehensive study, however, Lecuyer et al. (2004) found no evidence that oxygen isotope fractionation between mollusc aragonite and water differs from that of mollusc calcite and water. Aragonite oxygen-isotope values in Fig. 9b and d were normalized by the much smaller factor of 0.06 ‰ as proposed in Tarutani et al. (1969) but it seems unclear if this step is justified for biogenic carbonates.

Bulk carbon isotope values from *M. galloprovincialis*$_{B1}$ shells prior to transplantation range from −1.6 to −0.2 ‰ (standard deviation (σ) = 0.02 ‰). Calcite and aragonite δ^{13}C ratios scatter between 1.3 and −0.3 ‰ (σ = 0.02 ‰). Shell material from experimental site B1 (pH$_T$ 7.25) has δ^{13}C values of 2.4 ‰ (σ = 0.02 ‰) (with periostracum) and around 2.0 ‰ (σ = 0.02 ‰) (without periostracum), i.e. a difference of less than 0.5 ‰.

Furthermore, *M. galloprovincialis*$_{B1\ and\ C}$ values reveal differences between the three layers (Fig. 9 and Table S1). The lightest $\delta^{13}C_{shell}$ values were recorded in the nacre-layer. Samples combining calcite and nacreous layer are enriched in ^{13}C. The values combining periostracum and calcite layer and such data from the calcite layer alone are intermediate in isotopic composition. This pattern is not always detectable in *M. galloprovincialis* from sites B and C. Furthermore, sub-samples combining (i) periostracum and calcite layer and (ii) calcite and nacreous layer show an ontogenetic trend to higher values from the hinge to the commissure, i.e. in growth direction.

Oxygen isotope ratios were analyzed from sub-samples drilled from individual layers in selected shells (Fig. 1a) as well as from bulk samples. Results are shown in Table S1 and summarized in Fig. 9. Bulk δ^{18}O data from *M. galloprovincialis*$_{B1}$ formed prior to transplantation range from

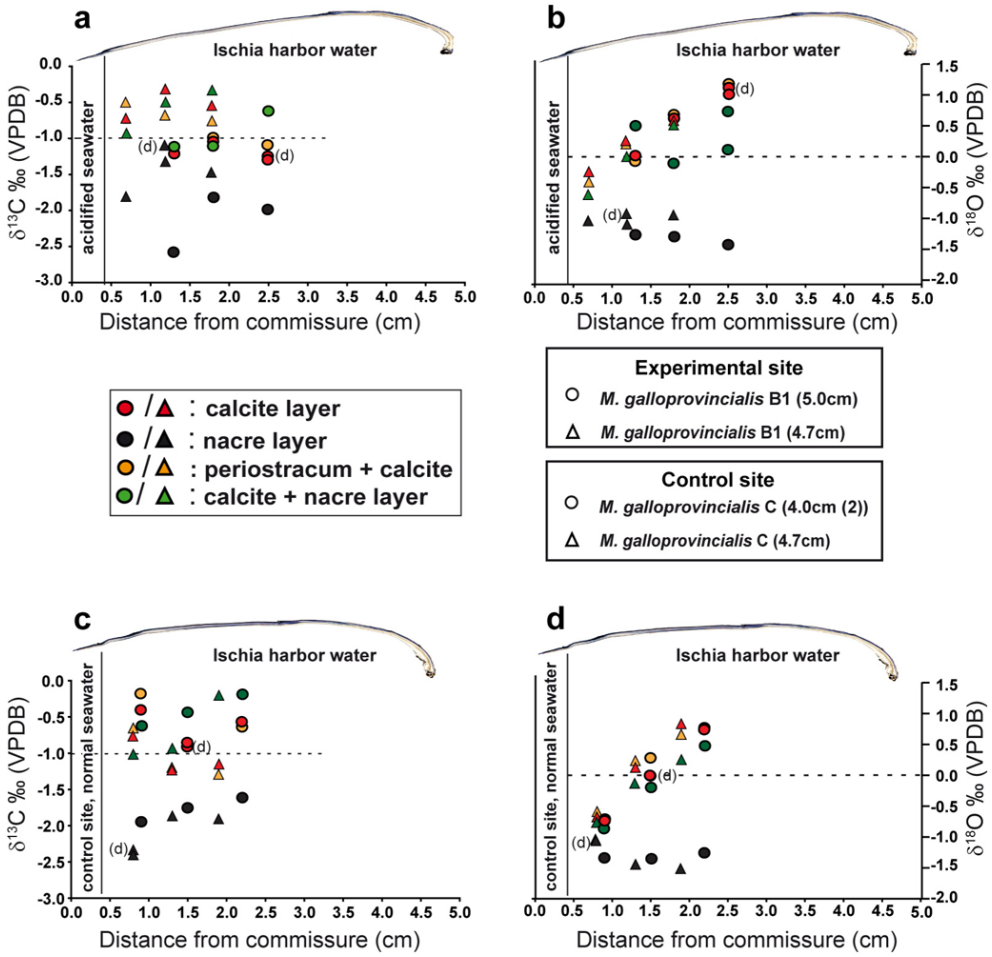

Fig. 9. Differential carbon and oxygen isotope ratios representing shell layer and mixed samples (legend and Fig. 1a) of four specimens of *M. galloprovincialis* $_{\text{B1 and C}}$ **(a–d)** plotted against distance from commissure. Different specimen are characterized by their different shell length and experimental site, e.g. *M. galloprovincialis* C (4.0 cm, 2) refers to a specimen with a shell length of 4 cm that was dislocated to control site C. Isotope values from two specimen from the same site, differentiated by their length, are labelled by a circle and a triangle, respectively. (**a** through **d**) *Mytilus galloprovincialis* shell isotope values from experimental site B1 **(a, b)** and control site C **(c, d)**. Colour code represents different layers analyzed. Note considerable differences in isotope values from different shell layers. Aragonitic (nacreous) layer isotope data were normalized against calcite isotope values using the equation of Rubinson and Clayton (1969) for δ^{13}C and that of Tarutani et al. (1969) for δ^{18}O.

-0.4 to 0.6 ‰ ($\sigma = 0.02$ ‰). Without periostracum material, data range from -0.3 to 0.6 ‰ ($\sigma = 0.02$ ‰). In shell material precipitated under acidified seawater conditions, δ^{18}O bulk ratios are in the order of 0.8 ‰ ($\sigma = 0.01$ ‰). In samples lacking periostracum material, lower values of 0.6 ‰ ($\sigma = 0.02$ ‰) are found. All of these values are depleted in ^{18}O relative to the $\delta^{18}O_{\text{seawater}}$ of 1.2 ‰ SMOW.

Furthermore, *M. galloprovincialis*$_{\text{B1 and C}}$ values reveal isotopic differences between shell layers (Fig. 9 and Table S1), with the nacreous layer being depleted. From the oldest shell portions (hinge) to the youngest shell portions (commissure) δ^{18}O values decrease. This includes samples taken from (i) the periostracum and the calcite layers, (ii) samples from the calcite layer and (iii) samples drilled from the calcite and nacreous layers (Fig. 9). In contrast, samples drilled within the transect in the nacreous layer remain invariant.

3.3.3 Isotope time series analysis of calcite shell samples: acidified versus normal seawater environments

In order to capture the geochemical pattern contained in shell material across the transplantation interval, a high resolution isotope record focusing on the calcite layer of *M. galloprovincialis*$_{\text{B1}}$ and *M. galloprovincialis*$_{\text{C}}$ was analyzed. Data are listed in Table S1 (Supplement) and results are displayed in Fig. 10. The data set is complex but clearly indicates that fractionation patterns in different shell layers of the same mussel differ considerably. The main features are

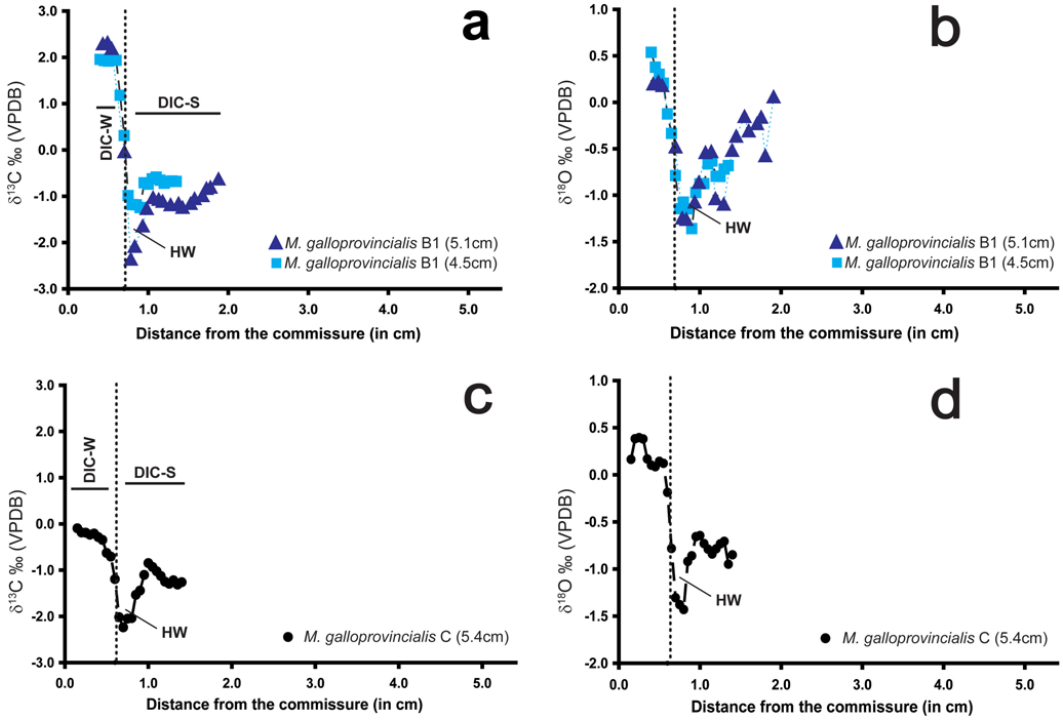

Fig. 10. Times series δ^{13}C and δ^{18}O ratios plotted against distance from shell commissure. Different specimens/shells are labelled according to shell length. *Mytilus galloprovincialis*$_{C}$ (5.4 cm) refers, for example, to a specimen with shell length of 5.4 cm transplanted from the harbour to the control site C. (**a** and **b**) Horizontal, black stippled line separates data from shell material precipitated before (right) and after (left) transplantation. Note considerable negative excursion in both carbon and oxygen data in August 2009 followed by marked positive trend until December 2009. Negative δ^{18}O shift is probably best interpreted as effect of an anomalous warm and long heat-wave (HW). Positive shift is only in part related to temperature alone and is probably related to seawater pH change and metabolic effects. DIC-S refers to seawater $\delta^{13}C_{DIC}$ value during summer 2009 and DIC-W the $\delta^{13}C_{DIC}$ value of seawater during winter 2009. (**c** and **d**) Data from *M. galloprovincialis*$_{C}$ showing transition from Ischia harbour to normal pH control site C. Near identical isotope pattern as recorded at site B1 is found albeit with smaller amplitudes.

summarized below and are placed against seawater values as shown in Table 1.

Calcite layer carbon and oxygen isotope ratios of *M. galloprovincialis*$_{B1}$ prior to transplantation range from −2.4 to −0.6 ‰ ($\delta^{13}C_{shell;}\sigma = 0.02$ ‰) and −1.4 to 0.1 ‰ ($\delta^{18}O_{shell;}\sigma = 0.03$ ‰). Isotope ratios of shell material precipitated directly after the transplantation, are enriched in ^{13}C and range between 0 and 0.3 ‰ ($\sigma = 0.02$ ‰) and ^{18}O (−0.1 and −0.5 ‰; $\sigma = 0.03$ ‰). In calcite precipitated after the adaptation of the shell to acidified seawater at experimental site B1 (Fig. 2b, d), strongly elevated δ^{13}C ratios of 1.9 to 2.4 ‰ ($\sigma = 0.02$ ‰) and δ^{18}O ratios of 0.2 to 0.5 ‰ ($\sigma = 0.03$ ‰) are found. The maximum difference in pre- and post-transplantation δ^{13}C calcite layer is in the order of 4 ‰ and around 1.9 ‰ for δ^{18}O. This difference is considerable. The maximum difference in pre- and post-transplantation δ^{13}C bulk shell materials is smaller, i.e. up to 2.5 ‰ and about 1.0 ‰ for δ^{18}O.

Carbon and oxygen isotope ratios of *M. galloprovincialis*$_{C}$ prior to transplantation range from −2.2 to −0.9 ‰ ($\delta^{13}C_{shell}$; $\sigma = 0.02$ ‰) and −1.4 to −0.9 ‰ ($\delta^{18}O_{shell}$; $\sigma = 0.03$ ‰). Shell material precipitated after the adaptation to the normal seawater conditions at control site C (Fig. 2b, d) ranges between −0.7 to −0.1 ‰ ($\delta^{13}C_{shell}$; $\sigma = 0.02$ ‰) and δ^{18}O ratios of 0.1 to 0.4 ‰ ($\sigma = 0.03$ ‰). The maximum difference in pre- and post-transplantation δ^{18}O calcite layer is around 1.8 ‰ (2 ‰ for $\delta^{13}C_{calcite}$), i.e. about 50 % of the difference found in shells kept under acidified conditions. For bulk samples, the maximum difference in pre- and post-transplantation $\delta^{13}C_{shell}$ is 1.4 ‰ and around ∼1.6 ‰ for $\delta^{18}O_{shell}$.

4 Interpretation and discussion

4.1 Sensitivity of *Mytilus* shell geochemistry and ultrastructure to environmental change

All mussels of the *M. edulis* group show a distinct biological control on biomineralization (Heinemann et al., 2008) and, in their rather complex, tripartite shell structure (Fig. 1), a high level of mineralogical and geochemical complexity. The data shown here are clear evidence that this internal complexity is

underexplored from the viewpoint of geochemistry and crystallography and represents a significant obstacle for those dealing with the paleo-environmental analysis of fossil material.

Additional complexity comes from the metabolic effects active during the incorporation of carbonate ions from seawater and organic matter taken up as food and incorporated as bicarbonate ions into the bivalve shells (Lorens and Bender, 1977; Klein et al., 1996a, b; Vander Putten et al., 2000; Lecuyer et al., 2004; Dalbeck et al., 2006; Wanamaker et al., 2007; Heinemann et al., 2008). During winter months, Ischia harbour seawater $\delta^{13}C_{DIC}$ is considerably depleted (mean of 0.2 ‰) due to sewage water from Ischia Porto village. Lowest DIC carbon isotope values of −0.5 ‰ (and $\delta^{18}O_{seawater}$ of 0.8 ‰ SMOW) were measured from a water sample taken directly beside one of the sewage pipes in the harbour. During much of spring to early fall, when biogenic carbonate secretion preferentially removes ^{12}C from seawater, mean harbour DIC values reach 1 ‰ and more (DIC-S in Fig. 10a, c). In late fall and winter months, seawater $\delta^{13}C_{DIC}$ of the control site C is in the order of 0.8 ‰ (DIC-W in Fig. 10c), whilst it is 0.9 ‰ near the vent areas (DIC-W in Fig. 10a; cf. Fig. 2d and Table 1). The slightly more positive seawater $\delta^{13}C_{DIC}$ at the acidified experimental site B1 (Fig. 10a) is probably due to the ^{13}C-enriched values of the volcanic CO_2 (Tedesco, 1996). During spring and summer months control (C) and experimental site (B1) seawater values approach the regional values of 1.2 to 1.4 ‰ reported in Pierre (1999).

Mussels were transplanted near end of September and moved to the control and the experimental sites (Fig. 2d). Bivalves experienced an approximate $\Delta^{13}C_{DIC}$ of about 0.4 ‰ from Ischia harbour (spring and summer, ^{12}C-depleted) to the test and experimental site (late fall to winter months, ^{12}C-enriched). Shell $\delta^{13}C_{calcite}$ values are depleted by about 1.5 to 2 ‰ relative to pre-transplantation harbour seawater $\delta^{13}C_{DIC}$ conditions of 0.8 to 1 ‰ (Fig. 10a, c). Following previous work (Vander Putten et al., 2000; Wanamaker et al., 2007; Immenhauser et al., 2008), this depletion is indicative of metabolic processes and an organic carbon source. Directly prior to the transplantation event, shell $\delta^{13}C_{calcite}$ shifts to even more depleted values (HW in Fig. 10). We propose that mussels suffered from an anomalous warm and long heat-wave during the summer 2009, which caused massive mortalities of corals, gorgonians, sponges and bivalves around Ischia (Rodolfo-Metalpa et al., 2011). This heat wave is equally recorded in the negative shift in shell $\delta^{18}O$ values directly prior to the transplantation (Fig. 10b, d).

Post-transplantation $\delta^{13}C_{calcite}$ becomes increasingly more positive. Towards the end of the transplantation experiment, $\delta^{13}C_{calcite}$ from the control site C is depleted by about 1 ‰ relative to seawater DIC (Fig. 10c), whilst it is enriched by more than 1 ‰ relative to seawater DIC at the experimental site B (Fig. 10a and Table 1). The conspicuous $\delta^{13}C$ shift is probably best understood in the context of sudden, transplantation-related changes in food availability and population density as well as seasonal changes in seawater DIC between harbour and experimental sites seawater. The offset between harbour seawater $\delta^{13}C_{DIC}$ and shell $\delta^{13}C_{aragonite}$ and $\delta^{13}C_{calcite}$ lie in the same overall range (0.2 to 1.5 ‰ for aragonite) as reported in Grossman and Ku (1986).

The maximum $\Delta^{18}O_{shell}$ in pre- and post-transplantation is 1.9 ‰. The shift from lighter to heavier $\delta^{18}O_{shell}$ ratios (Fig. 10b, d), reflects, in the view of the authors, only in part the abrupt transplantation change from warmer harbour temperatures to gradually cooler water masses at the test and control site (Fig. 2d). A heat wave in July and August 2009 with peak water temperatures of 26 °C stressed bivalves in Ischia harbour. Conspicuously, depleted $\delta^{18}O_{shell}$ ratios in pre-transplantation shell material (Fig. 10b and d) are evidence for this event. Applying the temperature equation of Anderson and Arthur (1983) for calcite to the *M. galloprovincialis* shell data, a pre-transplantation shell $\delta^{18}O$ ratio of −1.5 ‰ ($\delta^{18}O_{seawater}$ of 1.1 ‰ SMOW) corresponds to a seawater temperature of 27.6 °C, a value that is in reasonable agreement (+1.6 °C) with average august harbour water temperatures of 26 °C. After the transplantation in September, seawater temperatures at the control and the experimental site were still at 24 °C but fell to 20 °C during October. Peak December oxygen isotope values of 0.5 ‰ (Fig. 10b and d), in contrast, measured from shell calcite precipitated after the transplantation to control and experimental sites ($\delta^{18}O_{seawater}$ of 1.2 ‰ SMOW), correspond to calculated seawater temperature of 19 °C. This calculated value disagrees by 3 °C with measured seawater temperatures of 16 °C for December.

On the level of a working hypothesis, it seems likely, that changes in seawater pH (Bamber, 1987; Michaelidis et al., 2005; Berge et al., 2006; Beesley et al., 2008) influenced the shell oxygen isotope values, perhaps via calcification rates (Kleypas et al., 1999; Fabry et al., 2008) to some degree. Seawater pH, however, does not explain the observed isotope shifts in shells dislocated to the control site C that is characterized by a normal seawater pH. This is considered evidence that, under environmental stress such as the summer heat wave and the transplantation shock, *M. galloprovincialis* shell $\delta^{18}O$ is in disequilibrium with ambient seawater. The later observation is significant for shell calcite $\delta^{18}O$ seawater temperature reconstructions. In essence, shell $\delta^{18}O$ values overestimate seawater temperatures by approximately 1.5 to 3 °C.

Shell elemental compositions as shown in Figs. 7 and 8 are difficult to interpret. Differences in for example Mg abundance between calcite and aragonite are strongly controlled by the crystallographic properties of these carbonate materials (e.g. Okumura and Kitano, 1986; Dalbeck et al., 2006). In contrast to magnesium and calcium, however, sodium is more abundant in the nacreous layer compared to the calcite layer. Our results confirm the experiment of Okumura and Kitano (1986), which co-precipitated alkali ions with aragonite and calcite. They showed that sodium ions substitute for calcium in the aragonite lattice. The spatial differences

in Ca, Mg, Na and P elemental composition within either aragonite or calcite layers are probably meaningful on the level of biomineralization, i.e. the effect of acidified seawater, temperature and other environmental factors on element incorporation. Previous work has documented that Ca^{2+} and Mg^{2+} are transported across the epithelium via inter- and/or intra-cellular pathways (Watabe et al., 1990). Cations are either actively pumped across the cell membrane or move by passive diffusion through extracellular fluids to the site of calcification (Weiner and Dove, 2003; Addadi et al., 2006). At present, the authors accept that a detailed level of knowledge regarding the biologically controlled incorporation of elements in the shell of *M. galloprovincialis* is not reached and an in-depth interpretation of these data is beyond the scope of this paper.

The observed differences in the shell ultrastructure in specimen dislocated to experimental site B1 and control site C are significant and document the sensitivity of this previously underexplored proxy to environmental change. While the portions of the shell, that were biomineralized under normal seawater pH_T of 8.07 (control site C in Figs. 2d, 3a, b and 6c) are well ordered, the shell portions that precipitated under acidified seawater conditions (site B1; Fig. 2d, 4b and 5c) directly after the transplantation show a more unstructured shell microstructure than the control. Shell portions precipitated some weeks after the transplantation are rather well structured but contain spatially irregular shell portions with disordered calcite prisms (Fig. 3c, d). These detailed insights into the shell ultrastructure are equally encouraging and illustrated through the measured EBSD maps (Figs. 4 and 5).

Another important macroscopic feature refers to the aragonite or nacreous layer. In shell material from the acidified test environment B1, the aragonite layer is characterized by small, spatially isolated holes (diameters of ∼0.1 mm), an overall reduced thickness and a dull surface (Fig. 1b). These dissolution effects may be caused by the acid base balance regulation of the mussel in acidified conditions (Michaelidis et al., 2005). Mussels that were transported to control C (pH_T 8.07) lack these features but are in contrast characterized by a highly lustrous nacreous layer.

M. galloprovincialis$_{\text{B1 and C}}$ show both a distinct thinning of the calcite shell layer directly after the transplantation. A connection with the implementation process itself can not be excluded but the shells remain relatively thin after their adaptation to the new environment. Many independent factors, however, influence bivalve shell formation and thickness. Given that a shell thinning is present at sites with acidified and at sites with normal seawater pH, the relation between shell thickness and environmental factors is probably complex. All of these above features, structured versus unstructured shell organization, differences in the appearance of the nacreous layer, calcite layer thinning and marked changes in geochemical signature, have a considerable fossilization potential. These results are considered encouraging.

4.2 Environmental impact versus experimental bias

Mytilus shells are complex biomineral structures (Lowenstam and Weiner, 1989) precipitated under controlled extracellular processes (Crenshaw, 1980; Falini et al., 1996; Gotliv et al., 2003; Gaspard et al., 2008). Factors that affect the complex metabolic processes that in turn govern biomineralization include: (i) environment (Vander Putten et al., 2000) and here particularly seawater temperature (Grossman and Ku, 1986; Klein et al., 1996a; Bauwens et al., 2010), $\delta^{13}C$ of different carbon species in seawater (Dietzel and Kirchhoff, 2002; Hoefs, 2009 and references therein), salinity (Epstein and Mayeda, 1953; Bayne, 1976) and pH (Bamber, 1987; Michaelidis et al., 2005; Berge et al., 2006; Beesley et al., 2008); (ii) food availability (Gosling, 2003); and (iii) the degree of competition and population density (Gosling, 2003).

The potentially intricate combination of the above factors complicates the interpretation of geochemical and ultrastructural data shown here. This is because specimen of *M. galloprovincialis* were dislocated to environments not only characterized by different seawater temperatures and pH (Table 1) but where also exposed to sites with, in respect to their former harbour environment, different nutrient levels and seawater $\delta^{13}C_{DIC}$ and mussels experienced an abrupt change in population density. The abrupt change in the spatial orientation of calcite fibres c-axes across the transplantation suture shown in Fig. 4b is perhaps best explained by the transplantation shock because this suture line is present in samples dislocated to experimental (acidified) seawater site B1 as well as in such brought to control site C with normal pH. The transplantation shock therefore resulted in artefact features that are not expected in natural settings where environmental changes tend to be more gradual. This includes for example seasonal changes in seawater temperature, food availability but also gradual changes in population density.

The above consideration document the potential limitations of the field experimental setup applied here. First, our experiment was too short (68 days) to allow specimens to recover from the transplantation shock and to fully adapt to normal grow rates. Second, bivalves might have been stressed due to abnormally high seawater temperatures prior to the transplantation. Third, natural settings are by definition complex multi-factor systems. This background level of complexity, combined with experimental artefacts such as transplantation shock features limits the interpretation of geochemical and structural features observed to some degree. Culturing experiments, performed under constant environmental parameters and food availability (Thomsen and Melzner, 2010; Thomsen et al., 2010; Heinemann et al., 2011) are poor analogues of naturally complex environments but allow for a precise relation of specific environmental factors to textural or geochemical features observed in the test shells. In this sense, the outcome of the experiment shown here is considered a successful failure. Successful, as the data

clearly document the potential of combined geochemical and shell ultrastructure proxy analysis. A failure, as it is at present not possible to precisely allocate specific environmental parameters to specific geochemical or structural features.

5 Conclusions

Based on the data shown here, the following conclusions are drawn:

1. Live specimen of *M. galloprovincialis* were transplanted from Ischia harbour to nearby CO_2 vents and exposed to mean seawater pH_T 8.07 and 7.25. The shells responded with differential changes in shell carbon, oxygen and elemental composition, by a marked thinning of the calcite layer and by an – at least partial – lack of structure in the orientation of calcite prisms. In addition, the nacreous layer of mussels grown in experimental sites under acidified seawater was thin, dull and partially dissolved.

2. The marked trends in $\delta^{18}O$ across mussel shells grown after transplantation cannot be explained by seawater temperatures and pH differences alone. Oxygen-based seawater temperature calculations overestimate measured seawater temperatures by 1.5 to 3 °C. Pending more data, we suspect that environmental stress, and most dominantly seawater temperature and transplantation shock, affected mussel metabolism which in turn influenced the shell $\delta^{18}O$ ratios.

3. Pronounced shifts in $\delta^{13}C$ may reflect abrupt changes in food availability and population density when the mussels were transplanted to the CO_2 vent area. Remarkably, the pre- to post-transplantation $\Delta^{13}C_{calcite}$ of shells exposed to acidified experimental site seawater was about twice (4 ‰) that (2 ‰) found in shells precipitated from control site normal seawater pH. This point to an influence of seawater pH on bivalve metabolism and probably food availability that is again influenced by seawater pH.

4. Different shell layers, i.e. periostracum, aragonite and calcite layers show remarkable differences in both carbon and oxygen isotope values even when aragonite is normalized to calcite values. This notion questions the value of bulk data from bivalve shells.

5. Differences in shell elemental abundances in mussels exposed to acidified seawater at experimental site compared to normal conditions at control site are difficult to interpret. First order elemental differences are related to crystallographical differences between calcite and aragonite. Nevertheless, the spatial differences in Ca, Mg, Na and P elemental composition within one shell layer are highly complex and probably meaningful on the level of metabolic controls during biomineralization.

6. We have documented the successful application of a combined geochemical and shell ultrastructural/textural proxy analysis from complex natural archives. The transplantation shock clearly recorded in the mussel shells is a problem and suggests that specimen must be kept several months at test sites before they adapt to the new environment. Our field experiments show that caution is required when using bivalve shells to interpret past ocean acidification evens as shells can respond to a range of factors along with the effects of high CO_2.

7. It is proposed that the combination of field experiments and laboratory cultures will lead to an improved understanding of factors affecting shell growth and its use in interpretations of ocean acidification events.

Supplementary material related to this article is available online at: http://www.biogeosciences.net/9/1897/2012/bg-9-1897-2012-supplement.pdf.

Acknowledgements. This is a contribution to BioAcid. We wish to thank R. Enders (LMU Munich) and the laboratory staff at the Ruhr University for analytical support. We thank Andreas Götz for his support and image analysis program. We especially thank Dorothee Hippler for the discussions and insights into the topic. The project has been supported by FP7 EU MedSeA (265103) and EU MARES. We thankfully acknowledge the support of Federal Ministry of Education and Research (BMBF; FKZ 03F0608H).

Edited by: C. P. Slomp

References

Addadi, L., Joester, D., Nudelman, F., and Weiner, S.: Mollusk shell formation: A source of new concepts for understanding biomineralization processes, Chemistry, 12, 980–987, doi:10.1002/chem.200500980, 2006.

Aguirre, M. L., Perez, S. I., and Sirch, Y. N.: Morphological variability of *brachidontes swainson* (bivalvia, *Mytilidae*) in the marine Quaternary of Argentina (SW Atlantic), Palaeogeogr. Palaeocl., 239, 100–125, doi:10.1016/j.palaeo.2006.01.019, 2006.

Anderson, T. F. and Arthur, M. A.: Stable isotopes of oxygen and carbon and their application to sedimentologic and paleoenvironmental problems, 10. Society of Sedimentary Geology, 151 pp., 1983.

Aral, O.: Growth of the Mediterranean mussel (*Mytilus galloprovincialis* lam., 1819) on ropers in the Black Sea, Turkey, Turk. J. Vet. Anim. Sci., 23, 183–189, 1999.

Aubry, M. P., Ouda, K., Dupuis, C., Berggren, W. A., and Van Couvering, J. A.: The Global Standard Stratotype-section and Point (GSSP) for the base of the Eocene series in the Dababiya section (Egypt), Episodes, 30, 271–286, 2007.

Bamber, R. N.: The effects of acidic sea-water on young carpet-shell clams *Venerupis-decussata* (l) (mollusca, *Veneracea*), J. Exp. Mar. Biol. Ecol., 108, 241–260, doi:10.1016/0022-0981(87)90088-8, 1987.

Bauwens, M., Ohlsson, H., Barbé, K., Beelaerts, V., Schoukens, J., and Dehairs, F.: A nonlinear multi-proxy model based on manifold learning to reconstruct water temperature from high resolution trace element profiles in biogenic carbonates, Geosci. Model Dev., 3, 653–667, doi:10.5194/gmd-3-653-2010, 2010.

Bayne, B. L.: Marine mussels, their ecology and physiology, in: International Biological Programme Synthesis Series, Cambridge University Press, Cambridge, UK, 523, 47–48, 200–205, 1976.

Beesley, A., Lowe, D. M., Pascoe, C. K., and Widdicombe, S.: Effects of CO_2-induced seawater acidification on the health of *Mytilus edulis*, Clim. Res., 37, 215–225, doi:10.3354/cr00765, 2008.

Berge, J. A., Bjerkeng, B., Pettersen, O., Schaanning, M. T., and Oxnevad, S.: Effects of increased sea water concentrations of CO_2 on growth of the bivalve *Mytilus edulis* l, Chemosphere, 62, 681–687, doi:10.1016/j.chemosphere.2005.04.111, 2006.

Buick, D. P. and Ivany, L. C.: 100 years in the dark: Extreme longevity of Eocene bivalves from Antarctica, Geology, 32, 921–924, doi:10.1130/g20796.1, 2004.

Caldeira, K. and Wickett, M. E.: Anthropogenic carbon and ocean pH, Nature, 425, 365–365, doi:10.1038/425365a, 2003.

Carroll, M. L., Johnson, B. J., Henkes, G. A., McMahon, K. W., Voronkov, A., Ambrose, W. G., and Denisenko, S. G.: Bivalves as indicators of environmental variation and potential anthropogenic impacts in the southern Barents Sea, Mar. Pollut. Bull., 59, 193–206, doi:10.1016/j.marpolbul.2009.02.022, 2009.

Checa, A.: A new model for periostracum and shell formation in *Unionidae* (bivalvia, mollusca), Tissue Cell, 32, 405–416, doi:10.1054/tice.2000.0129, 2000.

Cigliano, M., Gambi, M. C., Rodolfo-Metalpa, R., Patti, F. P., and Hall-Spencer, J. M.: Effects of ocean acidification on invertebrate settlement at volcanic CO_2 vents, Mar. Biol., 157, 2489–2502, doi:10.1007/s00227-010-1513-6, 2010.

Crenshaw, M. A.: Mechanisms of shell formation and dissolution, in: Skeletal growth of aquatic organisms, edited by: Rhods, D. C. and Lutz, R. A., Plenum Publishing Corporation, New York, 115–132, 1980.

Dalbeck, P., England, J., Cusack, M., Lee, M. R., and Fallick, A. E.: Crystallography and chemistry of the calcium carbonate polymorph switch in *M. edulis* shells, Eur. J. Mineral., 18, 601–609, doi:10.1127/0935-1221/2006/0018-0601, 2006.

Davies, A. J., Roberts, J. M., and Hall-Spencer, J.: Preserving deep-sea natural heritage: Emerging issues in offshore conservation and management, Biol. Conserv., 138, 299–312, doi:10.1016/j.biocon.2007.05.011, 2007.

Dettman, D. L. and Lohmann, K. C.: Microsampling carbonates for stable isotope and minor element analysis – physical separation of samples on a 20 µm scale, J. Sediment. Res. A, 65, 566–569, 1995.

Dias, B. B., Hart, B., Smart, C. W., and Hall-Spencer, J. M.: Modern seawater acidification: The response of foraminifera to high-CO_2 conditions in the Mediterranean Sea, J. Geol. Soc. London, 167, 843–846, doi:10.1144/0016-76492010-050, 2010.

Dietzel, M. and Kirchhoff, T.: Stable isotope ratios and the evolution of acidulous ground water, Aquat. Geochem., 8, 229–254, doi:10.1023/B:AQUA.0000003724.43004.1e, 2002.

Elliot, M., deMenocal, P. B., Linsley, B. K., and Howe, S. S.: Environmental controls on the stable isotopic composition of *Mercenaria mercenaria*: Potential application to paleoenvironmental studies, Geochem. Geophy. Geosy., 4, 1–16, doi:10.1029/2002gc000425, 2003.

Ellis, R. P., Bersey, J., Rundle, S. D., Hall-Spencer, J. M., and Spicer, J. I.: Subtle but significant effects of CO_2 acidified seawater on embryos of the intertidal snail, *Littorina obtusata*, Aquat. Biol., 5, 41–48, doi:10.3354/ab00118, 2009.

Elorza, J. and GarciaGarmilla, F.: Petrological and geochemical evidence for diagenesis of inoceramid bivalve shells in the Plentzia formation (Upper Cretaceous, Basque-Cantabrian region, Northern Spain), Cretaceous Res., 17, 479–503, doi:10.1006/cres.1996.0029, 1996.

Engel, A., Zondervan, I., Aerts, K., Beaufort, L., Benthien, A., Chou, L., Delille, B., Gattuso, J. P., Harlay, J., Heemann, C., Hoffmann, L., Jacquet, S., Nejstgaard, J., Pizay, M. D., Rochelle-Newall, E., Schneider, U., Terbrueggen, A., and Riebesell, U.: Testing the direct effect of CO_2 concentration on a bloom of the coccolithophorid *Emiliania huxleyi* in mesocosm experiments, Limnol. Oceanogr., 50, 493–507, doi:10.4319/lo.2005.50.2.0493, 2005.

Epstein, S. and Mayeda, T.: Variation of o-18 content of waters from natural sources, Geochim. Cosmochim. Ac., 4, 213–224, doi:10.1016/0016-7037(53)90051-9, 1953.

Fabry, V. J., Seibel, B. A., Feely, R. A., and Orr, J. C.: Impacts of ocean acidification on marine fauna and ecosystem processes, Ices J. Mar. Sci., 65, 414–432, doi:10.1093/icesjms/fsn048, 2008.

Falini, G., Albeck, S., Weiner, S., and Addadi, L.: Control of aragonite or calcite polymorphism by mollusk shell macromolecules, Science, 271, 67–69, doi:10.1126/science.271.5245.67, 1996.

Fine, M. and Tchernov, D.: Ocean acidification and Scleractinian corals, Science, 317, 1032–1033, 2007.

Foster, L. C., Allison, N., Finch, A. A., Andersson, C., and Ninnemann, U. S.: Controls on delta δ^{18}O and delta δ^{13}C profiles within the aragonite bivalve *Arctica islandica*, Holocene, 19, 549–558, doi:10.1177/0959683609104028, 2009.

Gaspard, D., Marin, F., Guichard, N., Morel, S., Alcaraz, G., and Luquet, G.: Shell matrices of recent rhynchonelliform brachiopods: Microstructures and glycosylation studies, Earth Env. Sci. T. R. So., 98, 415–424, doi:10.1017/s1755691007078401, 2008.

Gazeau, F., Quiblier, C., Jansen, J. M., Gattuso, J. P., Middelburg, J. J., and Heip, C. H. R.: Impact of elevated CO_2 on shellfish calcification, Geophys. Res. Lett., 34, 1–5, doi:10.1029/2006GL028554, 2007.

Gibbs, S. J., Bown, P. R., Sessa, J. A., Bralower, T. J., and Wilson, P. A.: Nannoplankton extinction and origination across the Paleocene-Eocene Thermal Maximum, Science, 314, 1770–1773, doi:10.1126/science.1133902, 2006.

Gibbs, S. J., Stoll, H. M., Bown, P. R., and Bralower, T. J.: Ocean acidification and surface water carbonate production across the Paleocene-Eocene Thermal Maximum, Earth Planet. Sc. Lett., 295, 583–592, doi:10.1016/j.epsl.2010.04.044, 2010.

Gillikin, D. P., Dehairs, F., Lorrain, A., Steenmans, D., Baeyens, W., and Andre, L.: Barium uptake into the shells of the common mussel (*Mytilus edulis*) and the potential for estuarine

paleo-chemistry reconstruction, Geochim. Cosmochim. Ac., 70, 395–407, doi:10.1016/j.gca.2005.09.015, 2006a.

Gillikin, D. P., Lorrain, A., Bouillon, S., Willenz, P., and Dehairs, F.: Stable carbon isotopic composition of *Mytilus edulis* shells: Relation to metabolism, salinity, delta C-13(dic) and phytoplankton, Org. Geochem., 37, 1371–1382, doi:10.1016/j.orggeochem.2006.03.008, 2006b.

Giusberti, L., Rio, D., Agnini, C., Backman, J., Fornaciari, E., Tateo, F., and Oddone, M.: Mode and tempo of the Paleocene-Eocene Thermal Maximum in an expanded section from the Venetian pre-Alps, Geol. Soc. Am. Bull., 119, 391–412, doi:10.1130/b25994.1, 2007.

Gomez-Alday, J. J. and Elorza, J.: Diagenesis, regular growth and records of seasonality in inoceramid bivalve shells from mid-Maastrichtian hemipelagic beds of the Bay of Biscay, Neth. J. Geosci., 82, 289–301, 2003.

Gosling, E.: Bivalve molluscs – biology, ecology and culture, Fishing News Books, Blackwell Publishers, 44–50, 182–184, 188–189, 2003.

Gotliv, B. A., Addadi, L., and Weiner, S.: Mollusk shell acidic proteins, in: Search of individual functions, Chembiochem, 4, 522–529, doi:10.1002/cbic.200200548, 2003.

Grossman, E. L. and Ku, T. L.: Oxygen and carbon isotope fractionation in biogenic aragonite: Temperature effects, Chem. Geol., 59, 59–74, doi:10.1016/0009-2541(86)90044-6, 1986.

Guinotte, J. M. and Fabry, V. J.: Ocean acidification and its potential effects on marine ecosystems, Ann. Ny. Acad. Sci., 1134, 320–342, doi:10.1196/annals.1439.013, 2008.

Gutowska, M. A., Melzner, F., Portner, H. O., and Meier, S.: Cuttlebone calcification increases during exposure to elevated seawater pCO(2) in the cephalopod *Sepia officinalis*, Mar. Biol., 157, 1653–1663, doi:10.1007/s00227-010-1438-0, 2010.

Hall-Spencer, J. M., Rodolfo-Metalpa, R., Martin, S., Ransome, E., Fine, M., Turner, S. M., Rowley, S. J., Tedesco, D., and Buia, M. C.: Volcanic carbon dioxide vents show ecosystem effects of ocean acidification, Nature, 454, 96–99, doi:10.1038/nature07051, 2008.

Heinemann, A., Fietzke, J., Eisenhauer, A., and Zumholz, K.: Modification of Ca isotope and trace metal composition of the major matrices involved in shell formation of *Mytilus edulis*, Geochem. Geophy. Geosy., 9, 1–8, doi:10.1029/2007gc001777, 2008.

Heinemann, A., Hiebenthal, C., Fietzke, J., Eisenhauer, A., and Wahl, M.: Disentangling the biological and environmental control of *M. edulis* shell chemistry, Geochem. Geophy. Geosy., 12, Q05012, doi:10.1029/2011GC003673, 2011.

Hietanen, B., Sunila, I., and Kristoffersson, R.: Toxic effects of zinc on the common mussel *Mytilus edulis* l. (bivalvia) in brackish water. 1. Physiological and histopathological studies, Ann. Zool. Fenn., 25, 341–347, 1988.

Hippler, D., Buhl, D., Witbaard, R., Richter, D. K., and Immenhauser, A.: Towards a better understanding of magnesium-isotope ratios from marine skeletal carbonates, Geochim. Cosmochim. Ac., 73, 6134–6146, doi:10.1016/j.gca.2009.07.031, 2009.

Hoefs, J.: Stable isotope geochemistry (6th Edn.), Springer, New York, Heidelberg & Berlin, 2009.

Hoegh-Guldberg, O., Mumby, P. J., Hooten, A. J., Steneck, R. S., Greenfield, P., Gomez, E., Harvell, C. D., Sale, P. F., Edwards, A. J., Caldeira, K., Knowlton, N., Eakin, C. M., Iglesias-Prieto, R., Muthiga, N., Bradbury, R. H., Dubi, A., and Hatziolos, M. E.: Coral reefs under rapid climate change and ocean acidification, Science, 318, 1737–1742, doi:10.1126/science.1152509, 2007.

Iglesias-Rodriguez, M. D., Halloran, P. R., Rickaby, R. E. M., Hall, I. R., Colmenero-Hidalgo, E., Gittins, J. R., Green, D. R. H., Tyrrell, T., Gibbs, S. J., von Dassow, P., Rehm, E., Armbrust, E. V., and Boessenkool, K. P.: Phytoplankton calcification in a high-CO_2 world, Science, 320, 336–340, doi:10.1126/science.1154122, 2008.

Immenhauser, A., Nägler, T. F., Steuber, T., and Hippler, D.: A critical assessment of mollusk O-18/O-16, Mg/Ca, and Ca-44/Ca-40 ratios as proxies for cretaceous seawater temperature seasonality, Palaeogeogr. Palaeocl., 215, 221–237, doi:10.1016/j.palaeo.2004.09.005, 2005.

Immenhauser, A., Holmden, C., and Patterson, W. P.: Interpreting the carbon-isotope record of ancient shallow epeiric seas: Lessons from the recent, in: Dynamics of epeiric seas, edited by: Pratt, B. R. and Holmden, C., Geological Association of Canada Special Publication, 135–174, 2008.

Kennedy, W. J., Taylor, J. D., and Hall, A.: Environmental and biological controls on bivalve shell mineralogy, Biological Review of the Cambridge Philosophical Society, 44, 499–530, doi:10.1111/j.1469-185X.1969.tb00610.x, 1969.

Kisakürek, B., Eisenhauer, A., Böhm, F., Hathorne, E. C., and Erez, J.: Controls on calcium isotope fractionation in cultured planktic foraminifera, *Globigerinoides ruber* and *Globigerinella siphonifera*, Geochim. Cosmochim. Ac., 75, 427–443, doi:10.1016/j.gca.2010.10.015, 2011.

Klein, R. T., Lohmann, K. C., and Thayer, C. W.: Bivalve skeletons record sea-surface temperature and delta O-18 via Mg/Ca and O-18/O-16 ratios, Geology, 24, 415–418, doi:10.1130/0091-7613(1996)024<0415:BSRSST>2.3.CO;2, 1996a.

Klein, R. T., Lohmann, K. C., and Thayer, C. W.: Sr/Ca and C-13/C-12 ratios in skeletal calcite of *Mytilus trossulus*: Covariation with metabolic rate, salinity, and carbon isotopic composition of seawater, Geochim. Cosmochim. Ac., 60, 4207–4221, doi:10.1016/S0016-7037(96)00232-3, 1996b.

Kleypas, J. A., Buddemeier, R. W., Archer, D., Gattuso, J. P., Langdon, C., and Opdyke, B. N.: Geochemical consequences of increased atmospheric carbon dioxide on coral reefs, Science, 284, 118–120, doi:10.1126/science.284.5411.118, 1999.

Koehn, R. K.: The genetics and taxonomy of species in the genus mytilus, Aquaculture, 94, 125–145, 1991.

Kroeker, K. J., Micheli, F., Gambi, M. C., and Martz, T. R.: Divergent ecosystem responses within a benthic marine community to ocean acidification, PNAS, 108, 14515–14520, doi:10.1073/pnas.1107789108, 2011.

Kump, L. R., Bralower, T. J., and Ridgwell, A.: Ocean acidification in deep time, Oceanography, 22, 94–107, doi:10.5670/oceanog.2009.100, 2009.

Latal, C., Piller, W. E., and Harzhauser, M.: Shifts in oxygen and carbon isotope signals in marine molluscs from the central Paratethys (Europe) around the lower/middle Miocene transition, Palaeogeogr. Palaeocl., 231, 347–360, doi:10.1016/j.palaeo.2005.08.008, 2006.

Lecuyer, C., Reynard, B., and Martineaua, F.: Stable isotope fractionation between mollusc shells and marine waters from Martinique island, Chem. Geol., 213, 293–305, doi:10.1016/j.chemgeo.2004.02.001, 2004.

Lopez Correa, M., Freiwald, A., Hall-Spencer, J., Taviani, M., and Roberts, J. M.: Distribution and habitats of *Acesta excavata* (bivalvia: Limidae) with new data on its shell ultrastructure, Cold-water corals and ecosystems [Erlangen Earth Conference Series], 173–205, doi:10.1007/3-540-27673-4_9, 2005.

Lorens, R. B. and Bender, M. L.: Physiological exclusion of magnesium from *Mytilus edulis* calcite, Nature, 269, 793–794, doi:10.1038/269793a0, 1977.

Lowenstam, H. A. and Weiner, S.: On biomineralization, in Biomineralization: Chemical and Biochemical Perspectives, Oxford University Press, Inc., New York, 27–49, 99–110, 1989.

Lüthi, D., Le Floch, M., Bereiter, B., Blunier, T., Barnola, J. M., Siegenthaler, U., Raynaud, D., Jouzel, J., Fischer, H., Kawamura, K., and Stocker, T. F.: High-resolution carbon dioxide concentration record 650,000-800,000 years before present, Nature, 453, 379–382, doi:10.1038/nature06949, 2008.

Manzello, D. P., Kleypas, J. A., Budd, D. A., Eakin, C. M., Glynn, P. W., and Langdon, C.: Poorly cemented coral reefs of the eastern tropical pacific: Possible insights into reef development in a high-CO_2 world, P. Natl. Acad. Sci. USA, 105, 10450–10455, doi:10.1073/pnas.0712167105, 2008.

Marin, F. and Luquet, G.: Molluscan shell proteins, C. R. Palevol, 3, 469–492, 2004.

Martin, S., Rodolfo-Metalpa, R., Ransome, E., Rowley, S., Buia, M. C., Gattuso, J. P., and Hall-Spencer, J.: Effects of naturally acidified seawater on seagrass calcareous epibionts, Biol. Letters, 4, 689–692, doi:10.1098/rsbl.2008.0412, 2008.

Michaelidis, B., Ouzounis, C., Paleras, A., and Portner, H. O.: Effects of long-term moderate hypercapnia on acid-base balance and growth rate in marine mussels *Mytilus galloprovincialis*, Mar. Ecol.-Prog. Ser., 293, 109–118, doi:10.3354/meps293109, 2005.

Mutterlose, J., Linnert, C., and Norris, R.: Calcareous nannofossils from the Paleocene-Eocene Thermal Maximum of the equatorial Atlantic (ODP site 1260b): Evidence for tropical warming, Mar. Micropaleontol., 65, 13–31, doi:10.1016/j.marmicro.2007.05.004, 2007.

Okumura, M. and Kitano, Y.: Coprecipitation of alkali metal ions with calcium carbonate, Geochim. Cosmochim. Ac., 50, 49–58, doi:10.1016/0016-7037(86)90047-5, 1986.

Orr, J. C., Fabry, V. J., Aumont, O., Bopp, L., Doney, S. C., Feely, R. A., Gnanadesikan, A., Gruber, N., Ishida, A., Joos, F., Key, R. M., Lindsay, K., Maier-Reimer, E., Matear, R., Monfray, P., Mouchet, A., Najjar, R. G., Plattner, G. K., Rodgers, K. B., Sabine, C. L., Sarmiento, J. L., Schlitzer, R., Slater, R. D., Totterdell, I. J., Weirig, M. F., Yamanaka, Y., and Yool, A.: Anthropogenic ocean acidification over the twenty-first century and its impact on calcifying organisms, Nature, 437, 681–686, doi:10.1038/nature04095, 2005.

Pierre, C.: The oxygen and carbon isotope distribution in the Mediterranean water masses, Mar. Geol., 153, 41–55, doi:10.1016/s0025-3227(98)00090-5, 1999.

Pouchou, J. L. and Pichoir, F.: A new model for quantitative x-ray-microanalysis. 2. Application to in-depth analysis of heterogeneous samples, Rech. Aerospatiale, 5, 349–367, 1984.

Raffi, I., Backman, J., and Palike, H.: Changes in calcareous nannofossil assemblages across the Paleocene/Eocene transition from the paleo-equatorial Pacific Ocean, Palaeogeogr. Palaeocl., 226, 93–126, doi:10.1016/j.palaeo.2005.05.006, 2005.

Ragland, P. C., Pilkey, O. H., and Blackwelder, B. W.: Diagenetic changes in the elemental composition of uncrystallized mollusk shells, Chem. Geol., 25, 123–134, doi:10.1016/0009-2541(79)90088-3, 1979.

Riebesell, U., Schulz, K. G., Bellerby, R. G. J., Botros, M., Fritsche, P., Meyerhofer, M., Neill, C., Nondal, G., Oschlies, A., Wohlers, J., and Zollner, E.: Enhanced biological carbon consumption in a high CO_2 ocean, Nature, 450, 545–510, doi:10.1038/nature06267, 2007.

Rodolfo-Metalpa, R., Lombardi, C., Cocito, S., Hall-Spencer, J., and Gambi, M. C.: Effects of ocean acidification and high temperatures on the bryozoan *Myriapora truncata* and natural CO_2 vents, Mar. Ecol., 31, 447–456, doi:10.1111/j.1439-0485.2009.00354.x, 2010.

Rodolfo-Metalpa, R., Houlbrèque, F., Tambutté, E., Boisson, F., Baggini, C., Patti, F. P., Jeffree, R., Fine, M., Foggo, A., Gattuso, J.-P., and Hall-Spencer, J. M.: Coral and mollusc resistance to ocean acidification adversely affected by warming, Nature Climate Change Letters, 1, 308–312, doi:10.1038/NCLIMATE1200, 2011.

Röhl, U., Westerhold, T., Bralower, T. J., and Zachos, J. C.: On the duration of the Paleocene-Eocene Thermal Maximum (PETM), Geochem. Geophy. Geosy., 8, 1–13, doi:10.1029/2007GC001784, 2007.

Rubinson, M. and Clayton, R. N.: Carbon-13 fractionation between aragonite and calcite, Geochim. Cosmochim. Ac., 33, 997–1002, 1969.

Russell, A. D., Honisch, B., Spero, H. J., and Lea, D. W.: Effects of seawater carbonate ion concentration and temperature on shell U, Mg, and Sr in cultured planktonic foraminifera, Geochim. Cosmochim. Ac., 68, 4347–4361, doi:10.1016/j.gca.2004.03.013, 2004.

Scheibner, C. and Speijer, R. P.: Late Paleocene-early Eocene tethyan carbonate platform evolution – a response to long- and short-term paleoclimatic change, Earth-Sci. Rev., 90, 71–102, doi:10.1016/j.earscirev.2008.07.002, 2008.

Shumway, S. E.: Effect of salinity fluctuation on osmotic-pressure and Na^+, Ca^{2+} and Mg^{2+} ion concentrations in hemolymph of bivalve mollusks, Mar. Biol., 41, 153–177, doi:10.1007/BF00394023, 1977.

Sluijs, A., Brinkhuis, H., Schouten, S., Bohaty, S. M., John, C. M., Zachos, J. C., Reichart, G. J., Damste, J. S. S., Crouch, E. M., and Dickens, G. R.: Environmental precursors to rapid light carbon injection at the Palaeocene/Eocene boundary, Nature, 450, 1218–1215, doi:10.1038/nature06400, 2007.

Solomon, S., Plattner, G. K., Knutti, R., and Friedlingstein, P.: Irreversible climate change due to carbon dioxide emissions, P. Natl. Acad. Sci. USA, 106, 1704–1709, doi:10.1073/pnas.0812721106, 2009.

Tarutani, T., Clayton, R. N., and Mayeda, T. K.: The effect of polymorphism and magnesium substitution on oxygen isotope fractionation between calcium carbonate and water, Geochim. Cosmochim. Ac., 33, 987–996, 1969.

Tedesco, D.: Chemical and isotopic investigations of fumarolic gases from Ischia Island (Southern Italy): Evidences of magmatic and crustal contribution, J. Volcanol. Geoth. Res., 74, 233–242, doi:10.1016/S0377-0273(96)00030-3, 1996.

Thomsen, J. and Melzner, F.: Moderate seawater acidification does not elicit long-term metabolic depression in the blue mussel

Mytilus edulis, Mar. Biol., 157, 2667–2676, doi:10.1007/s00227-010-1527-0, 2010.

Thomsen, J., Gutowska, M. A., Saphörster, J., Heinemann, A., Trübenbach, K., Fietzke, J., Hiebenthal, C., Eisenhauer, A., Körtzinger, A., Wahl, M., and Melzner, F.: Calcifying invertebrates succeed in a naturally CO_2-rich coastal habitat but are threatened by high levels of future acidification, Biogeosciences, 7, 3879–3891, doi:10.5194/bg-7-3879-2010, 2010.

Tynan, S., Opkyke, B. N., Ellis, D., and Beavis, S.: A history of heavy metal pollution recorded in the shell of *Mytilus edulis*, Geochim. Cosmochim. Ac., 70, A662–A662, doi:10.1016/j.gca.2006.06.1235, 2006.

Vander Putten, E., Dehairs, F., Keppens, E., and Baeyens, W.: High resolution distribution of trace elements in the calcite shell layer of modern *Mytilus edulis*: Environmental and biological controls, Geochim. Cosmochim. Ac., 64, 997–1011, doi:10.1016/S0016-7037(99)00380-4, 2000.

Wanamaker, A. D., Kreutz, K. J., Borns, H. W., Introne, D. S., Feindel, S., Funder, S., Rawson, P. D., and Barber, B. J.: Experimental determination of salinity, temperature, growth, and metabolic effects on shell isotope chemistry of *Mytilus edulis* collected from Maine and Greenland, Paleoceanography, 22, 1–12, doi:10.1029/2006pa001352, 2007.

Watabe, N., Kingsley, R. J., and Crick, R. E.: Extra-, inter-, and intracellular mineralization in invertebrates and algae, Origin, evolution and modern aspects of biomineralization in plants and animals, 209–223, 1990.

Weiner, S. and Dove, P. M.: An overview of biomineralization processes and the problem of the vital effect, Biomineralization, 54, 1–29, doi:10.2113/0540001, 2003.

Westerhold, T., Rohl, U., Laskar, J., Raffi, I., Bowles, J., Lourens, L. J., and Zachos, J. C.: On the duration of magnetochrons C24r and C25n and the timing of early Eocene global warming events: Implications from the ocean drilling program leg 208 Walvis Ridge depth transect, Paleoceanography, 22, 1–19, doi:10.1029/2006pa001322, 2007.

Witbaard, R., Jenness, M. I., Vanderborg, K., and Ganssen, G.: Verification of annual growth increments in *Arctica islandica* l. From the North Sea by means of oxygen and carbon isotopes, Neth. J. Sea Res., 33, 91–101, doi:10.1016/0077-7579(94)90054-X, 1994.

Zachos, J. C., Rohl, U., Schellenberg, S. A., Sluijs, A., Hodell, D. A., Kelly, D. C., Thomas, E., Nicolo, M., Raffi, I., Lourens, L. J., McCarren, H., and Kroon, D.: Rapid acidification of the ocean during the Paleocene-Eocene Thermal Maximum, Science, 308, 1611–1615, doi:10.1126/science.1109004, 2005.

Zeebe, R. E. and Ridgwell, A.: Past changes in ocean carbonate chemistry, in: Ocean acidification, edited by: Gattuso, J.-P. and Hansson, L., Oxford University Press, Oxford, 21–40, 2011.

Appendix E6:

C. Baggini, Y. Issaris, M. Salomidi, J.M. Hall-Spencer (2014). Herbivore diversity improves benthic community resilience to ocean acidification. *Journal of Experimental Marine Biology and Ecology* (accepted pending revisions).

Elsevier Editorial System(tm) for Journal of Experimental Marine Biology and Ecology
Manuscript Draft

Manuscript Number: JEMBE-D-14-00340

Title: Herbivore diversity improves benthic community resilience to ocean acidification.

Article Type: Full Length Article

Keywords: ocean acidification; species interactions; functional redundancy

Corresponding Author: Mrs. Cecilia Baggini,

Corresponding Author's Institution:

First Author: Cecilia Baggini

Order of Authors: Cecilia Baggini; Yiannis Issaris; Maria Salomidi; Jason M Hall-Spencer

Abstract: Ocean acidification is expected to alter a wide range of marine systems, but there is great uncertainty about its indirect effects. Responses of biological communities to increases in carbon dioxide can be assessed at volcanic seeps that cause chronic exposure to acidified seawater. Subtidal benthic communities at seeps exhibit profound changes along gradients of increasing pCO2. Changes in herbivore densities due to intolerance to high CO2 conditions may interact with direct CO2 effects to determine benthic community structure as oceans acidify. Here, an exclusion experiment was used to test effects of herbivory in benthic communities along a pCO2 gradient off Methana (Greece). A manipulative experiment was used to examine how large herbivores affect sublittoral algal communities as carbon dioxide levels increase. Our data show that sea urchins and herbivorous fish dramatically reduced macroalgal biomass at background carbon dioxide levels; this effect was not hampered by increased pCO2 despite lower sea urchin densities near the seeps, since fish abundances concurrently increased. We found that carbon dioxide levels up to about 2000 μatm are unlikely to significantly reduce the role of herbivory in structuring Mediterranean benthic communities, even in areas where top-down control by herbivores is strong. A shift from sea urchins to fish as main grazers highlights that ocean acidification will likely cause complex responses at the community level, and that maintaining high functional redundancy in marine ecosystems is key to improving their resilience.

***Cover Letter**

Dear Editor,

I wish to submit the full length article entitled “Herbivore diversity improves benthic community resilience to ocean acidification” to be considered for publication in *Journal of Experimental Marine Biology and Ecology.*

The article has not been published or submitted to any other journal; all authors have read and approved the final version of the manuscript.

Community responses to ocean acidification are still poorly understood, but recent studies at volcanic CO_2 seeps have shown that macroalgal communities undergo profound changes as carbon dioxide increases. Here we experimentally test the hypothesis that decreased sea urchin abundances at elevated CO_2 levels alter top-down control on benthic communities. We found that macroalgal biomass is similarly controlled by herbivores regardless of pCO_2 thanks to a change from sea urchin to fish as the main herbivore guild. Our results highlight that ocean acidification will not always have predictable effects at the community level, and that functional diversity can be important to reduce ocean acidification impacts.

I think this study has broad implications in the field of marine climate change ecology, and is thus suitable for publication in a journal with a marine ecology audience such as JEMBE.

I look forward to working with you and the reviewers.

Yours sincerely,

Cecilia Baggini

Highlights:

- Macroalgal biomass is still controlled by herbivores at elevated CO_2 levels
- Main herbivores change from sea urchins to fish at high CO_2
- Functional redundancy can improve benthic community resilience to ocean acidification

Herbivore diversity improves benthic community resilience to ocean acidification.

Cecilia Baggini[a*], Yannis Issaris[b], Maria Salomidi[c], Jason Hall-Spencer[a]

[a] Marine Biology and Ecology Research Centre, Plymouth University, Plymouth PL4 8AA, United Kingdom.

[b] Institute of Marine Biology, Biotechnology and Aquaculture, Hellenic Centre for Marine Research, Heraklion, Crete, Greece.

[c] Institute of Oceanography, Hellenic Centre for Marine Research, Anavissos, Attica, Greece.

* Corresponding author: cecilia.baggini@plymouth.ac.uk, +447774958982

Abstract

Ocean acidification is expected to alter a wide range of marine systems, but there is great uncertainty about its indirect effects. Responses of biological communities to increases in carbon dioxide can be assessed at volcanic seeps that cause chronic exposure to acidified seawater. Subtidal benthic communities at seeps exhibit profound changes along gradients of increasing pCO_2. Changes in herbivore densities due to intolerance to high CO_2 conditions may interact with direct CO_2 effects to determine benthic community structure as oceans acidify. Here, an exclusion experiment was used to test effects of herbivory in benthic communities along a pCO_2 gradient off Methana (Greece). A manipulative experiment was used to examine how large herbivores affect sublittoral algal communities as carbon dioxide levels increase. Our data show that sea urchins and herbivorous fish dramatically reduced macroalgal biomass at background carbon dioxide levels; this effect was not hampered by increased pCO_2 despite lower sea urchin densities near the seeps, since fish abundances concurrently increased. We found that carbon dioxide levels up to about 2000 µatm are unlikely to significantly reduce the role of herbivory in structuring Mediterranean benthic communities, even in areas where top-down control by herbivores is strong. A shift from sea urchins to fish as main grazers highlights that ocean acidification will likely cause complex responses at the community level, and that maintaining high functional redundancy in marine ecosystems is key to improving their resilience.

1. Introduction

Increasing anthropogenic atmospheric CO_2 is altering the chemistry of surface seawater worldwide, resulting in ocean acidification (Caldeira and Wickett, 2003). Mean surface ocean pH has already decreased by 0.1 units (a 30% increase in H^+ concentration) compared to pre-industrial times, and is falling rapidly (Doney et al., 2009). Studies at volcanic seeps have shown that chronic exposure to increased CO_2 reduces diversity and causes changes in benthic macroalgal and invertebrate communities (Kroeker et al., 2011; Porzio et al., 2011; Fabricius et al., 2014). These changes could be caused by physiological effects of CO_2 on macroalgae, altered competitive interactions between algal species and changes in chemical plant defences (Arnold et al., 2012; Kroeker et al., 2013). In addition, grazers may have a determining role in community changes (Poore et al., 2012). Some herbivores, such as amphipods, can become more abundant as CO_2 increases at volcanic seeps (Cigliano et al., 2010; Kroeker et al., 2011). Conversely, key grazers such as sea urchins decrease in abundance with increased CO_2 (Hall-Spencer et al., 2008; Johnson et al., 2012), but their contribution to community changes along pCO_2 gradients has not previously been tested experimentally.

Coastal environments have low functional redundancy, even when diversity is relatively high (Micheli et al., 2014). Decrease of sea urchin densities as seawater CO_2 increases thus leave marine ecosystem vulnerable to phase shifts, especially in the absence of herbivorous fish (Hughes, 1994). Numerous dramatic changes to benthic communities due to reduction in grazing rates have been reported; for instance, tropical coral reefs can be overgrown by macroalgae if grazing pressure is removed (Hughes et al., 2007).

In Mediterranean sublittoral environments, high densities of the sea urchins *Paracentrotus lividus* (Lamarck, 1816) and *Arbacia lixula* (Linnaeus, 1758) can cause a shift from photophilic algal assemblages to “barren grounds”, which are impoverished assemblages dominated by encrusting algae (Guidetti and Dulcic, 2007). Sea urchin grazing can cause a shift to barren grounds in temperate rocky reefs worldwide, and they are considered an alternative stable state to kelp beds (Filbee-Dexter and Scheibling, 2014). Once established, barren grounds can be maintained by relatively low sea urchin densities (Chiantore et al., 2008).

Herbivorous fish are normally thought to exert weaker top-down control on temperate macroalgal communities than sea urchins (Floeter et al., 2005). However, in the warm-temperate Mediterranean Sea herbivorous fish limit the distribution of many macroalgae (Vergés et al., 2009) and can also produce and maintain barren grounds in the Eastern Mediterranean Sea (Sala et al., 2011). Here, the main herbivorous fish are the sparid *Sarpa salpa* (Linnaeus, 1758) and the scarid *Sparisoma cretense* (Linnaeus, 1758), as well as the lessepsian migrant *Siganus luridus* (Rüppell, 1829) and *Siganus rivulatus* (Forsskål and Niebuhr, 1775); the latter two species can account for over 90% of herbivorous fish biomass in Greek southern seas (Kalogirou et al., 2012).

Ocean acidification has a detrimental effect on the physiology of many sea urchin species and their densities often decrease as seawater pCO_2 increases (Calosi et al., 2013; Bray et al., 2014). On the other hand, many fish seem to tolerate carbon dioxide levels predicted for the end of this century (Melzner et al., 2009). In some fish species, neuroreception changes with increasing CO_2 affect their behaviour, making them less alert to predators after prolonged exposure to elevated CO_2 at volcanic seeps (McCormick et al., 2013; Munday et al., 2014). Herbivorous fish could

benefit from ocean acidification because of increased food availability following decreased competition with sea urchins (Pinnegar and Polunin, 2004; Johnson et al., 2012) and because of increased food palatability due to the loss of plant chemical defences (Arnold et al., 2012).

Our understanding of ecosystem shifts due to elevated CO_2 has evolved through a series of studies at volcanic seeps. Initial work led researchers to conclude that a shift from coralline algae dominated to fleshy algal communities was driven by dissolution effects on calcified algae (Hall-Spencer et al., 2008; Martin et al., 2008). Subsequent work investigating macroalgal succession indicated that certain coralline algae were able to withstand dissolution at CO_2 levels predicted for the end of this century, but fleshy algae were able to outcompete them at high CO_2 (Kroeker et al., 2013). In a comparison of tropical and temperate CO_2 seep systems, Johnson et al. (2012) found that *Padina* spp. thrived at high CO_2 levels despite dissolution of their carbonate layer and postulated that this was possible since sea urchins, their main grazers, were unable to tolerate high CO_2 conditions. There is now a growing realisation that major ecological effects of ocean acidification are likely to be indirect and mediated through changes in trophic interactions, and that functional redundancy may have a role in ecosystems resilience to increased CO_2 (Alsterberg et al., 2013). Here we test the indirect and direct effects of ocean acidification in an experiment at sites with reference and elevated pCO_2 on rocky Mediterranean shores with and without grazers present.

2. Methods

2.1 Study site and environmental parameters monitoring

Volcanic seeps off Methana influence carbonate chemistry along a wide stretch of rocky shore, and can be used to study the effects of elevated CO_2 on biological communities as there are no confounding gradients in temperature, salinity, total alkalinity, nutrients and heavy metals (Baggini et al., accepted). At this site, macroalgal communities change consistently between pCO_2 levels, so carbon dioxide is the main determinant of benthic community structure (Baggini et al., accepted). For this study, a site with high and variable pCO_2 (SEEP) and a reference site (REF) were used (Figure 1). Environmental variables were measured in September 2012 and June 2013. Seawater pH, temperature and salinity were measured using a multiprobe (YSI 63) from the shore. The probe was calibrated before use with pH 4.01, 7.01 and 10.01 NBS standards. Since variations of up to 1 pH unit were detected over a few hours at the low pH site, the lack of precision in using the NBS scale for seawater measurements (approximately 0.05 pH, Riebesell et al., 2010) was considered acceptable for this study. For pH, medians and interquartile ranges (IQ) were calculated from hydrogen ion concentrations before re-converting back to pH values following seep monitoring methods provided by Kerrison et al. (2011). Seawater samples for total alkalinity determination were collected in 125 ml borosilicate glass bottles with Teflon caps. Three independent samples per site were collected twice per visit, immediately poisoned with $HgCl_2$ and stored in the dark until analysis. Samples were analysed by Gran titration (AS-ALK 2, Apollo SciTech) and the reliability of the measurements was checked against standard seawater samples provided by A. Dickson (batches 112 and 121). The average total alkalinity value per site and individual pH measurements were used to

calculate pCO_2, HCO_3^-, CO_3^{2-}, Ω_{Ar} and Ω_{Ca} using CO2Sys software (Lewis and Wallace, 1998).

2.2 Herbivore surveys

Herbivore densities were determined at both sites. Densities of *Paracentrotus lividus* and *Arbacia lixula* were determined separately using transects: individuals present between 1 and 2 m depth were counted by snorkelers along five transects (5 m long and 1 m wide) per site per species in September 2012 and June 2013. Fish community composition and biomass were quantified in September 2013 using a standard visual census technique (while SCUBA diving) within belt transects of 25 m length and 5 m width placed at 3m depth (three replicates, 125 m^2 surface each). The observer conducting the fish survey moved at constant speed identifying, counting and attributing all individuals to 5 cm size classes within 2.5 m on either side of the 25 m transect line (La Messa and Vacchi, 1999; Giakoumi et al., 2012). Length estimates of fish from the visual surveys were converted to wet weight by using the allometric length-weight conversion: $W = a L^b$, where W is weight in grams and L is total length in cm. The constant parameters a and b corresponding to the closest geographical area were obtained from Morey et al. (2003).

2.3 Herbivore exclusions

Four sterile 10 x 10 cm ceramic tiles were attached to rocks using epoxy putty and deployed at the two Methana study sites by snorkelers as controls; four tiles per site were enclosed in a 1 cm mesh cage to exclude herbivores, and four additional tiles per site were enclosed in a three-sided cage acting as procedural controls (Figure S1). The cages were painted using non-toxic antifouling paint (EP-2000, ePaint, Florida) to prevent epiphytes from growing and shading the tiles. Tiles were deployed in September 2012 and recovered in June 2013, when Mediterranean

seaweed biomass reaches its annual peak. All tiles were recovered, except for one procedural control at both sites and one exclusion tile at the high CO_2 site.

After recovery, tiles were detached from the rock, put in individual zip-lock bags and stored frozen. In the laboratory, their cover was visually assessed and quantified as percent cover of functional groups. The functional groups used were: fucoid algae (mostly *Cystoseira* sp.; C.Agardh, 1820), erect brown algae, fleshy brown algae (mostly *Dictyota* sp.; J.V.Lamouroux, 1809), calcifying brown algae (mostly *Padina pavonica*; (Linnaeus) Thivy, 1960), turf algae (mat-forming algae shorter than 2 cm, mostly juvenile *Halopteris scoparia*; (Linnaeus) Sauvageau, 1904), encrusting black sponge, encrusting green algae, filamentous green algae, articulated coralline algae, coralline crustose algae (CCA), serpulid worms, biofilm, bare substratum. The biomass of turf and erect algae was measured by scraping the algae from the tiles, drying them at 60°C for 72 h and weighing them to obtain dry weight (DW).

2.4 Statistical analyses

Sea urchin data were analysed with a three-way ANOVA (fixed factors: species, season and site) after transforming them (fourth root) to comply with the normality and variance homogeneity requirements of ANOVA. Log-transformed biomass of the three recorded herbivorous fish was also analysed using an ANOVA with site and species as fixed factors. All the analyses above were performed using SPSS v19 (IBM, USA).

Structure of communities grown on tiles quantified using visual census was tested using a two-factor PERMANOVA with “site” and “treatment” as fixed factors. A square-root transformation was used to reduce the influence of abundant taxa in the community and a Bray-Curtis dissimilarity matrix was used. Type III sum of squares with 9,999 unrestricted permutations of the raw data was used to account for small

sample sizes. Pairwise tests were performed when a factor with more than two levels was significant. A nMDS plot was used to visually inspect the similarities among samples. The same procedure was used to analyse biomass of communities grown on tiles.

Percent cover or biomass changes in key groups of macroalgae were analysed using the experimental design described above, but using dissimilarity matrices based on Euclidean distances. Percent cover was used for those functional groups that could not be reliably scraped from the tile (i.e. CCA, encrusting green algae, encrusting black sponge, biofilm and bare substratum). All analyses above were performed using PRIMER 6 with PERMANOVA+ extension (Plymouth Routines In Multivariate Ecological Research, version 6).

3. Results

3.1 Environmental parameters

Measured and calculated carbonate chemistry parameters are shown in Table 1. The mean pH near the seeps was approximately 7.7, more than 0.3 points lower than the reference sites. On the other hand, temperature and salinity were not significantly different between the two sites. At the high CO_2 site, seawater pCO_2 was double that of the reference site, even though on average seawater was still saturated with respect to both calcite and aragonite.

3.2 Herbivore surveys

Sea urchin densities significantly differed both between sites and between species. On the other hand, no effect of season was detected, and the lack of significant interactions indicates that both *A.lixula* and *P.lividus* densities changed consistently between sites. As no significant effect of season was detected, sea urchin densities were pooled between seasons for easier representation. Densities of *A. lixula* were

consistently higher than those of *P. lividus* (Figure 2A), with average densities of the former species ranging from 1.9 to 7.5 individuals in a five-metre transect. On the other hand, *P. lividus* densities ranged from 0.2 to 1.6 individuals. There was also a clear reduction in the densities of both species near the seeps, with *P. lividus* being almost absent at the high CO_2 site.

Three herbivorous fish species were recorded at the study sites: *Sarpa salpa*, *Siganus luridus* and *Sparisoma cretense*. Results from ANOVA (Table S2) show that, just as with sea urchins, both site and species had a significant effect on fish biomass. No significant interactions were found, meaning that changes in all species' biomass between sites followed a similar pattern. All species increased in biomass near the seeps (Figure 2B), but the magnitude of the change was very different among species: while *S. cretense* had a low biomass that changed very little between sites, the two other species had very marked changes in biomass between sites. *S. luridus* was present at both sites and its mean biomass increased from 65 to 1565 g from REF to SEEP. *S. salpa* was absent from REF, while at SEEP it was the dominant species in terms of biomass.

3.3 Herbivore exclusion

Statistical analysis of tiles macroalgal cover (Table 2) showed that both sites and treatment had significant effects on assemblages, but there was no interaction between the two factors. Since the factor 'treatment' was significant, pairwise comparisons were performed among treatment levels to detect which pairs were significantly different. The results (Table 2, lower part) show that exclusions were significantly different from both control and procedural control, which did not differ between each other.

Figure 3 shows that SEEP and REF were clearly different for all treatments. Controls and procedural controls were closely grouped whereas exclusion tiles were very different. Tiles where herbivores were excluded showed a more marked difference between sites compared to the other treatments, and they were more dispersed. This was particularly evident at the SEEP site, where a different group of algae (erect brown algae, fleshy brown algae, calcifying brown algae) was dominant in each exclusion tile, whereas in the reference site there was mostly an increase in calcifying brown algal cover when herbivores were excluded.

Statistical analysis of the fleshy and erect algal biomass produced results analogous to the percent cover data, so only the latter are reported as they are more comprehensive (i.e. they also include encrusting forms). Total biomass clearly increased in the exclusion treatment, ranging from about 0.1 g in the control to approximately 3 g in the exclosures (Figure 4). However, at the reference site procedural controls had values intermediate between controls and exclusions.

Eight functional groups were significantly different between treatments or sites, four turf or erect and four encrusting forms. Overall, turf and erect algae increased in herbivore exclusions (Table 3a), whereas encrusting forms showed the opposite trend (Table 3b). Biofilm percent cover did not show any clear effect of herbivore exclusion, but it significantly increased at the high CO_2 site. The effect of herbivore exclusion was always clear at SEEP, while at REF some functional groups (turf algae, CCA and bare substratum) had biomass or cover values similar between exclusion and procedural control. There were significant differences between sites as well, with turf algae, calcifying brown algae and CCA decreasing as CO_2 increased and fucoid algae, fleshy brown algae, biofilm and bare substratum showing the opposite trend.

4. Discussion

Coastal assemblages often have low functional redundancy, and the loss of a few species can negatively affect ecosystem functioning (Micheli and Halpern, 2005). Taxonomic diversity can help marine community resilience to increased temperatures (Allison, 2004), but there is no evidence this applies to community responses to ocean acidification. Here we show that high taxonomic diversity helps improving resilience to ocean acidification: herbivorous fish kept grazing pressure high at elevated CO_2, even though sea urchin densities decreased near the seeps. Overfishing of apex predators has led to higher abundances of Mediterranean sea urchins and herbivorous fish, as they are usually not targeted by commercial fisheries (Guidetti and Dulčić, 2007; Guidetti and Sala, 2007). High herbivore densities can often lead to impoverished macroalgal communities, very different from unexploited Mediterranean coastal ecosystems (Sala et al., 2012). Thus, unvaried grazing pressure at different CO_2 levels may maintain suboptimal community structure. However, at a global level herbivorous fish abundance is strongly reduced by overfishing (Micheli and Halpern, 2005), and when this is combined with other herbivores disappearing (e.g. sea urchin mass mortality in Jamaica) benthic habitat can experience dramatic phase shifts (Hughes, 1994).

The relative role of bottom-up and top-down processes in shaping marine ecosystems has long been a critical issue in marine ecology research. Previous research has shown that the relative importance of these two types of processes is highly context-dependant (Burkepile and Hay, 2006). This study shows that in Mediterranean sublittoral rocky reefs increased pCO_2 (bottom-up) has a significant effect on benthic communities. We found that herbivory strongly controlled seaweed biomass and community structure in benthic habitats off Methana (Greece)

regardless of pCO_2 levels, even though herbivore community composition changed dramatically at the high CO_2 site.

Crustose coralline algal cover significantly decreased at high CO_2 as expected, since this group is sensitive to ocean acidification, and even tolerant species become outcompeted by non-calcifying algae at elevated CO_2 levels (Kroeker et al., 2013; Brodie et al., 2014). Fleshy brown and fucoid algae significantly increased near the seeps, which aligns with observations at other Mediterranean CO_2 seeps (Porzio et al., 2011). Recently, Johnson et al. (2012) reported increasing *P. pavonica* densities as CO_2 increased in shallow waters off Vulcano, possibly because of lower consumption by sea urchins. In this study, *P. pavonica* biomass decreased with increasing CO_2 when herbivores were excluded due to increased competition with the fleshy brown alga *Dictyota* sp..

Turf algal biomass decreased near the Methana seeps, in line with surveys off Ischia (Porzio et al., 2011). This is in contrast to many laboratory experiments, where turf algae can be advantaged by increased CO_2 due to fast growth rates and carbon limitation (Connell et al., 2013). However, many turf algae are palatable to grazers (Falkenberg et al., 2014), and therefore may exhibit different responses to ocean acidification. Conversely, biofilm percent cover increased near the seeps, in accord with findings at CO_2 seeps off Vulcano (Italy), where benthic diatoms and biofilm production increase at elevated CO_2 (Lidbury et al., 2012; Johnson et al., 2013).

Herbivore exclusion at Methana dramatically changed macroalgal communities grown on tiles. Herbivore exclusion caused an increase in algal biomass regardless of site, but at the reference site only the calcifying brown algae *Padina pavonica* colonised the caged tiles. On the other hand, caged tiles at the high CO_2 site was colonised by a variety of taxa (*Padina pavonica*, *Dictyota* sp. and erect brown algae).

This confirms that non-calcifying algae increase in abundance as pCO_2 increases, likely because they can outcompete calcifying species at elevated CO_2 levels (Porzio et al., 2011; Kroeker et al., 2013).

Herbivory is known to alter outcomes of macroalgal competition, favouring less palatable macroalgal species or extremely fast-growing opportunistic algae (Hereu et al., 2008). At Methana, herbivore-resistant encrusting algae became more abundant at both CO_2 levels when herbivores were present. In addition, benthic communities at Methana showed smaller differences between CO_2 levels when herbivores were present (Figure 4). Recent evidence shows that grazers can indeed dampen the effects of climate change on primary producers, both in terrestrial and in marine ecosystems (Post and Pedersen, 2008; Anthony et al., 2011; Falkenberg et al., 2014).

Both sea urchin species had reduced densities near the seeps regardless of season, which is in accord with their predicted sensitivity to high CO_2 resulting from laboratory experiments (Dupont et al., 2010). Sea urchins were replaced by herbivorous fish at the high CO_2 site; functional redundancy of herbivores can maintain top-down control on macroalgal biomass and reduce the effects of multiple stressors on benthic communities (Blake and Duffy, 2010; Eriksson et al., 2011). It should be noted, however, that fish are highly mobile and could swim in and out of the high CO_2 area (Riebesell, 2008), masking potential negative effects of ocean acidification such as those on many species' neuroreceptors (Shaw et al., 2013).

Recent research has shown that indirect effects can be as important as the direct effects of CO_2 in shaping community responses to ocean acidification (Kroeker et al., 2013). Herbivores have a very strong effect and when they are present other indirect effects are reduced or disappear altogether (Alsterberg et al., 2013). Here we show

that carbon dioxide still affects the specific composition of macroalgal communities in sublittoral habitats even when herbivore pressure is strong; grazing, however, reduced community structure variability. The most striking finding of this study is that herbivore functional redundancy can offset indirect effects of ocean acidification; this is only possible in diverse ecosystems, highlighting the necessity of managing local stressors to maintain high diversity and increase ecosystem resilience to environmental change (Ghedini et al., 2013).

Acknowledgements:

We thank A. Deidda for his invaluable help during sampling and K. Bischof, A. Pancucci-Papadopoulou and M. Milazzo for supervising CB doctoral studies. This work was funded through a MARES Grant to CB. MARES is a Joint Doctorate programme selected under Erasmus Mundus coordinated by Ghent University (FPA 2011-0016). Check www.mares-eu.org for extra information. This work contributes to the EU FP7 project 'Mediterranean Sea Acidification under a changing climate' (grant agreement no. 265103).

References:

Allison, G., 2004. The influence of species diversity and stress intensity on community resistance and resilience. Ecological Monographs 74(1), 117-134.

Alsterberg, C., Eklof, J.S., Gamfeldt, L., Havenhand, J.N., Sundback, K., 2013. Consumers mediate the effects of experimental ocean acidification and warming on primary producers. Proceedings of the National Academy of Sciences 110(21), 8603-8608.

Anthony, K.R.N., Maynard, J.A., Diaz-Pulido, G., Mumby, P.J., Marshall, P.A., Cao, L., Hoegh-Guldberg, O.V.E., 2011. Ocean acidification and warming will lower coral reef resilience. Global Change Biology 17(5), 1798-1808.

Arnold, T., Mealey, C., Leahey, H., Miller, A.W., Hall-Spencer, J.M., Milazzo, M., Maers, K., 2012. Ocean acidification and the loss of phenolic substances in marine plants. PLoS ONE 7(4), e35107.

Baggini, C., Salomidi, M., Voutsinas, E., Bray, L., Krasakopoulou, E., Hall-Spencer, J.M., accepted. Seasonality affects macroalgal community response to increases in pCO_2. PloS ONE.

Blake, R.E., Duffy, J.E., 2010. Grazer diversity affects resistance to multiple stressors in an experimental seagrass ecosystem. Oikos 119(10), 1625-1635.

Bray, L., Pancucci-Papadopulou, M.A., Hall-Spencer, J.M., 2014. Sea urchin response to rising pCO_2 shows ocean acidification may fundamentally alter the chemistry of marine skeletons. Mediterranean Marine Science. DOI: 10.12681/mms.579.

Brodie, J., Williamson, C.J., Smale, D.A., Kamenos, N.A., Mieszkowska, N., Santos, R., Cunliffe, M., Steinke, M., Yesson, C., Anderson, K.M., Asnaghi, V., Brownlee, C., Burdett, H.L., Burrows, M.T., Collins, S., Donohue, P.J.C., Harvey, B., Foggo, A., Noisette, F., Nunes, J., Ragazzola, F., Raven, J.A., Schmidt, D.N., Suggett, D., Teichberg, M., Hall-Spencer, J.M., 2014. The future of the northeast Atlantic benthic flora in a high CO_2 world. Ecology and Evolution. DOI: 10.1002/ece1003.1105.

Burkepile, D.E., Hay, M.E., 2006. Herbivore vs nutrient control of marine primary producers: context-dependent effects. Ecology 87(12), 3128-3139.

Caldeira, K., Wickett, M.E., 2003. Oceanography: Anthropogenic carbon and ocean pH. Nature 425(6956), 365-365.

Calosi, P., Rastrick, S.P.S., Graziano, M., Thomas, S.C., Baggini, C., Carter, H.A., Hall-Spencer, J.M., Milazzo, M., Spicer, J.I., 2013. Distribution of sea urchins living

near shallow water CO_2 vents is dependent upon species acid-base and ion-regulatory abilities. Marine Pollution Bulletin 73(2), 470-484.

Chiantore, M., Vielmini, I., Privitera, D., Mangialajo, L., Cattaneo-Vietti, R., 2008. Habitat effects on the population structure of *Paracentrotus lividus* and *Arbacia lixula*. Chemistry and Ecology 24, 145-157.

Cigliano, M., Gambi, M.C., Rodolfo-Metalpa, R., Patti, F.P., Hall-Spencer, J.M., 2010. Effects of ocean acidification on invertebrate settlement at volcanic CO_2 vents. Marine Biology 157(11), 2489-2502.

Connell, S.D., Kroeker, K.J., Fabricius, K.E., Kline, D.I., Russell, B.D., 2013. The other ocean acidification problem: CO_2 as a resource among competitors for ecosystem dominance. Philosophical Transactions of the Royal Society B: Biological Sciences 368(1627), 20120442.

Doney, S.C., Fabry, V.J., Feely, R.A., Kleypas, J.A., 2009. Ocean acidification: the other CO_2 problem. Annual Review of Marine Science 1, 169-192.

Dupont, S., Dorey, N., Thorndyke, M., 2010. What meta-analysis can tell us about vulnerability of marine biodiversity to ocean acidification? Estuarine, Coastal and Shelf Science 89(2), 182-185.

Eriksson, B.K., van Sluis, C., Sieben, K., Kautsky, L., Raberg, S., 2011. Omnivory and grazer functional composition moderate cascading trophic effects in experimental *Fucus vesiculosus* habitats. Marine Biology 158(4), 747-756.

Fabricius, K.E., De'ath, G., Noonan, S., Uthicke, S., 2014. Ecological effects of ocean acidification and habitat complexity on reef-associated macroinvertebrate communities. Proceedings of the Royal Society B: Biological Sciences 281(1775), 20132479.

Falkenberg, L.J., Connell, S.D., Russell, B.D., 2014. Herbivory mediates the expansion of an algal habitat under nutrient and CO_2 enrichment. Marine Ecology Progress Series 497, 87-92.

Filbee-Dexter, K., Scheibling, R.E., 2014. Sea urchin barrens as alternative stable states of collapsed kelp ecosystems. Marine Ecology Progress Series 495, 1-25.

Floeter, S.R., Behrens, M.D., Ferreira, C.E.L., Paddack, M.J., Horn, M.H., 2005. Geographical gradients of marine herbivorous fishes: patterns and processes. Marine Biology 147(6), 1435-1447.

Gaylord, B., Kroeker, K.J., Sunday, J.M., Anderson, K.M., Barry, J.P., Brown, N.E., Connell, S.D., Dupont, S., Fabricius, K.E., Hall-Spencer, J.M., Klinger, T., Milazzo, M., Munday, P.L., Russell, B.D., Sanford, E., Schreiber, S.J., Thiyagarajan, V., Vaughan, H., Widdicombe, S., Harley, C.D.G., submitted. Ocean acidification through the lens of ecological theory. Ecology.

Ghedini, G., Russell, B., Connell, S., 2013. Managing local coastal stressors to reduce the ecological effects of ocean acidification and warming. Water 5(4), 1653-1661.

Giakoumi, S., Cebrian, E., Kokkoris, G.D., Ballesteros, E., Sala, E., 2012. Relationships between fish, sea urchins and macroalgae: The structure of shallow rocky sublittoral communities in the Cyclades, Eastern Mediterranean. Estuarine, Coastal and Shelf Science 109, 1-10.

Guidetti, P., Dulčić, J., 2007. Relationships among predatory fish, sea urchins and barrens in Mediterranean rocky reefs across a latitudinal gradient. Marine Environmental Research 63(2), 168-184.

Guidetti, P., Sala, E., 2007. Community-wide effects of marine reserves in the Mediterranean Sea. Marine Ecology Progress Series 335, 43-56.

Hall-Spencer, J.M., Rodolfo-Metalpa, R., Martin, S., Ransome, E., Fine, M., Turner, S.M., Rowley, S.J., Tedesco, D., Buia, M.-C., 2008. Volcanic carbon dioxide vents show ecosystem effects of ocean acidification. Nature 454(7200), 96-99.

Hereu, B., Zabala, M., Sala, E., 2008. Multiple controls of community structure and dynamics in a sublittoral marine environment. Ecology 89(12), 3423-3435.

Hughes, T.P., 1994. Catastrophes, phase shifts, and large-scale degradation of a Caribbean coral reef. Science 265(5178), 1547-1551.

Hughes, T.P., Rodrigues, M.J., Bellwood, D.R., Ceccarelli, D., Hoegh-Guldberg, O., McCook, L., Moltschaniwskyj, N., Pratchett, M.S., Steneck, R.S., Willis, B., 2007. Phase shifts, herbivory, and the resilience of coral reefs to climate change. Current Biology 17(4), 360-365.

Johnson, V.R., Russell, B.D., Fabricius, K.E., Brownlee, C., Hall-Spencer, J.M., 2012. Temperate and tropical brown macroalgae thrive, despite decalcification, along natural CO_2 gradients. Global Change Biology 18(9), 2792-2803.

Johnson, V., Brownlee, C., Rickaby, R., Graziano, M., Milazzo, M., Hall-Spencer, J., 2013. Responses of marine benthic microalgae to elevated CO_2. Marine Biology 160, 1813-1824.

Kalogirou, S., Wennhage, H., Pihl, L., 2012. Non-indigenous species in Mediterranean fish assemblages: Contrasting feeding guilds of *Posidonia oceanica* meadows and sandy habitats. Estuarine, Coastal and Shelf Science 96, 209-218.

Kerrison, P., Hall-Spencer, J.M., Suggett, D.J., Hepburn, L.J., Steinke, M., 2011. Assessment of pH variability at a coastal CO2 vent for ocean acidification studies. Estuarine, Coastal and Shelf Science 94(2), 129-137.

Kroeker, K.J., Micheli, F., Gambi, M.C., 2013. Ocean acidification causes ecosystem shifts via altered competitive interactions. Nature Climate Change 3, 156–159.

La Mesa, G., Vacchi, M., 1999. An analysis of the coastal fish assemblage of the Ustica Island marine reserve (Mediterranean Sea). Marine Ecology 20(2), 147-165.

Lewis, E., Wallace, W.R. (1998). Program developed for CO_2 system calculations. Carbon dioxide information analysis center, Oak Ridge National Laboratory. US Department of Energy, Oak Ridge.

Lidbury, I., Johnson, V., Hall-Spencer, J.M., Munn, C.B., Cunliffe, M., 2012. Community-level response of coastal microbial biofilms to ocean acidification in a natural carbon dioxide vent ecosystem. Marine Pollution Bulletin 64(5), 1063-1066.

Martin, S., Rodolfo-Metalpa, R., Ransome, E., Rowley, S., Buia, M.C., Gattuso, J.P., Hall-Spencer, J., 2008. Effects of naturally acidified seawater on seagrass calcareous epibionts. Biology Letters 4(6), 689-692.

McCormick, M.I., Watson, S.A., Munday, P.L., 2013. Ocean acidification reverses competition for space as habitats degrade. Scientific Reports 3, 3280.

Melzner, F., Gutowska, M.A., Langenbuch, M., Dupont, S., Lucassen, M., Thorndyke, M.C., Bleich, M., Portner, H.O., 2009. Physiological basis for high CO_2 tolerance in marine ectothermic animals: pre-adaptation through lifestyle and ontogeny? Biogeosciences 6(10), 2313-2331.

Micheli, F., Halpern, B.S., 2005. Low functional redundancy in coastal marine assemblages. Ecology Letters 8(4), 391-400.

Micheli, F., Mumby, P.J., Brumbaugh, D.R., Broad, K., Dahlgren, C.P., Harborne, A.R., Holmes, K.E., Kappel, C.V., Litvin, S.Y., Sanchirico, J.N., 2014. High vulnerability of ecosystem function and services to diversity loss in Caribbean coral reefs. Biological Conservation 171, 186-194.

Morey, G., Moranta, J., Massutí, E., Grau, A., Linde, M., Riera, F., Morales-Nin, B., 2003. Weight-length relationships of littoral to lower slope fishes from the Western Mediterranean. Fisheries Research 62(1), 89-96.

Munday, P.L., Cheal, A.J., Dixson, D.L., Rummer, J.L., Fabricius, K.E., 2014. Behavioural impairment in reef fishes caused by ocean acidification at CO_2 seeps. Nature Climate Change 4(6), 487-492.

Pinnegar, J.K., Polunin, N.V.C., 2004. Predicting indirect effects of fishing in Mediterranean rocky littoral communities using a dynamic simulation model. Ecological Modelling 172(2–4), 249-267.

Poore, A.G.B., Campbell, A.H., Coleman, R.A., Edgar, G.J., Jormalainen, V., Reynolds, P.L., Sotka, E.E., Stachowicz, J.J., Taylor, R.B., Vanderklift, M.A., Emmett Duffy, J., 2012. Global patterns in the impact of marine herbivores on benthic primary producers. Ecology Letters 15(8), 912-922.

Porzio, L., Buia, M.C., Hall-Spencer, J.M., 2011. Effects of ocean acidification on macroalgal communities. Journal of Experimental Marine Biology and Ecology 400(1-2), 278-287.

Post, E., Pedersen, C., 2008. Opposing plant community responses to warming with and without herbivores. Proceedings of the National Academy of Sciences 105(34), 12353-12358.

Riebesell, U., 2008. Climate change: Acid test for marine biodiversity. Nature 454(7200), 46-47.

Riebesell, U., Fabry, V.J., Hansson, L., Gattuso J.-P. (Eds.), 2010. Guide to best practices for ocean acidification research and data reporting. Luxembourg: Publications Office of the European Union.

Sala, E., Kizilkaya, Z., Yildirim, D., Ballesteros, E., 2011. Alien marine fishes deplete algal biomass in the Eastern Mediterranean. PLoS ONE 6(2), e17356.

Sala, E., Ballesteros, E., Dendrinos, P., Di Franco, A., Ferretti, F., Foley, D., Fraschetti, S., Friedlander, A., Garrabou, J., Güçlüsoy, H., Guidetti, P., Halpern, B.S., Hereu, B., Karamanlidis, A.A., Kizilkaya, Z., Macpherson, E., Mangialajo, L., Mariani, S., Micheli, F., Pais, A., Riser, K., Rosenberg, A.A., Sales, M., Selkoe, K.A., Starr, R., Tomas, F., Zabala, M., 2012. The Structure of Mediterranean Rocky Reef Ecosystems across Environmental and Human Gradients, and Conservation Implications. PLoS ONE 7(2), e32742.

Shaw, E.C., Munday, P.L., McNeil, B.I., 2013. The role of CO_2 variability and exposure time for biological impacts of ocean acidification. Geophysical Research Letters 40(17), 4685-4688.

Verges, A., Alcoverro, T., Ballesteros, E., 2009. Role of fish herbivory in structuring the vertical distribution of canopy algae *Cystoseira* spp. in the Mediterranean Sea. Marine Ecology-Progress Series 375, 1-11.

Figure 1. Study sites (points) and area where pH was more variable than at reference site (light grey).

Figure 2. Herbivores abundance. (A) Average number (± SE, n=11) of sea urchins along 5 m transects at Methana study sites pooling data from September 2012 and June 2013. (B) Average biomass (± SE, n=3) of herbivorous fish per 25 m transect at REF and SEEP in September 2013. Different letters represent significantly different groups.

Figure 3: MDS plot of the results of an herbivore exclusion experiment performed at Methana from September 2012 to June 2013; circles represent tiles placed at REF, triangles were tiles placed at SEEP. Letters above the symbols represent the treatments: C is control, P is procedural control, E is exclusion.

Figure 4. Average biomass (± SE; n = 3-4) of fleshy and erect algae grown on tiles for all three treatments of the herbivore exclusion experiment conducted at Methana from September 2012 to June 2013. Different letters represent significantly different groups.

Table 1

Table 1. Mean (± SD, n=11-24) environmental parameters: pH, temperature and salinity were measured at Methana in September 2012 and June 2013 and pCO_2, bicarbonate ions, carbonate ions, seawater saturation with respect to calcite and aragonite were calculated using CO2Sys.

	pH_{NBS}	**T** (˚C)	**S**	**pCO_2** (µatm)	**HCO_3^-** (mmol/ kgSW)	**CO_3^{2-}** (mmol/ kgSW)	**Ω_{Ca}**	**Ω_{Ar}**
SEEP	7.70 ± 0.16	25.34 ± 0.85	38.77 ± 0.93	1676.8 ± 643.5	2485.4 ± 112.4	125.0 ± 46.5	2.91 ± 1.06	1.93 ± 0.71
REF	8.09 ± 0.06	25.01 ± 1.05	38.94 ± 0.87	586.9 ± 106.7	2140.5 ± 63.3	232.1 ± 25.9	5.40 ± 0.59	3.57 ± 0.39

Table 2. PERMANOVA analyses of percentage cover of uncaged and caged tiles (square-root transformed) deployed at Methana from September 2012 to June 2013. The first table shows main factors and their interactions and degrees of freedom (df), sum of squares (SS), Mean Square (MS), pseudo-F, permutational p and unique permutations for each of them. The second table shows pair-wise comparisons between treatments pooling sites; for each comparison the t value, p value and number of unique permutations are shown.

Source	**df**	**SS**	**MS**	**Pseudo-F**	**P(perm)**	**Unique perms**
Site	1	5380.7	5380.7	5.3584	**0.0003**	9938
Treatment	2	11675	5837.4	5.8133	**0.0001**	9937
Site x Treatment	2	2318.5	1159.2	1.1544	0.3204	9945
Residual	15	15062	1004.2			
Total	20	34487				

Groups	**t**	**P(perm)**	**Unique perms**
Control, Exclusion	2.7397	**0.0001**	9937
Control, Proc control	1.2182	0.2271	9918
Exclusion, Proc control	2.3722	**0.0009**	9878

Table 3

Table 3. Mean (± SE, n=3-4) biomass (A) and percent cover (B) of functional groups that showed significant differences between sites (REF and SEEP) or treatments (C=controls; P=procedural controls; E=herbivore exclusions). Different letters indicate significantly different sub-groups within functional groups.

		REF			**SEEP**		
		C	**P**	**E**	**C**	**P**	**E**
A)	Turf algae	0.114 ± 0.112[a]	1.010 ± 0.353[b]	1.595 ± 0.366[b]	0.001 ± 0.001[c]	0.008 ± 0.008[c]	0.200 ± 0.062[a]
	Fucoid algae	0.000[a]	0.000[a]	0.060 ± 0.030[b]	0.143 ± 0.065[b]	0.219 ± 0.061[b]	0.406 ± 0.054[c]
	Fleshy brown algae	0.001 ± 0.001[a]	0.000[a]	0.351 ± 0.346[b]	0.001 ± 0.001[a]	0.005 ± 0.005[a]	1.867 ± 1.841[b]
	Calcifying brown algae	0.000[a]	0.000[a]	1.697 ± 0.605[b]	0.000[a]	0.000[a]	0.485 ± 0.474[b]
B)	Encrusting green algae	14.50 ± 10.27[a]	8.33 ± 4.91[a]	0.25 ± 0.25[b]	27.25 ± 4.61[a]	14.33 ± 9.77[a]	0.00[b]
	Biofilm	0.00[a]	0.00[a]	0.25 ± 0.25[a]	5.00 ± 2.68[b]	1.00 ± 0.58[b]	4.00 ± 4.00[b]
	CCA	12.50 ± 2.90[a]	8.00 ± 3.61[a,b]	3.75 ± 2.25[b]	1.25 ± 0.48[c]	0.67 ± 0.67[c]	0.00[d]
	Bare substratum	23.25 ± 4.80[a,b]	48.00 ± 9.17[a]	13.25 ± 6.17[b]	49.00 ± 5.35[a]	48.67 ± 11.67[a]	5.33 ± 3.53[b]

Figure 1
Click here to download high resolution image

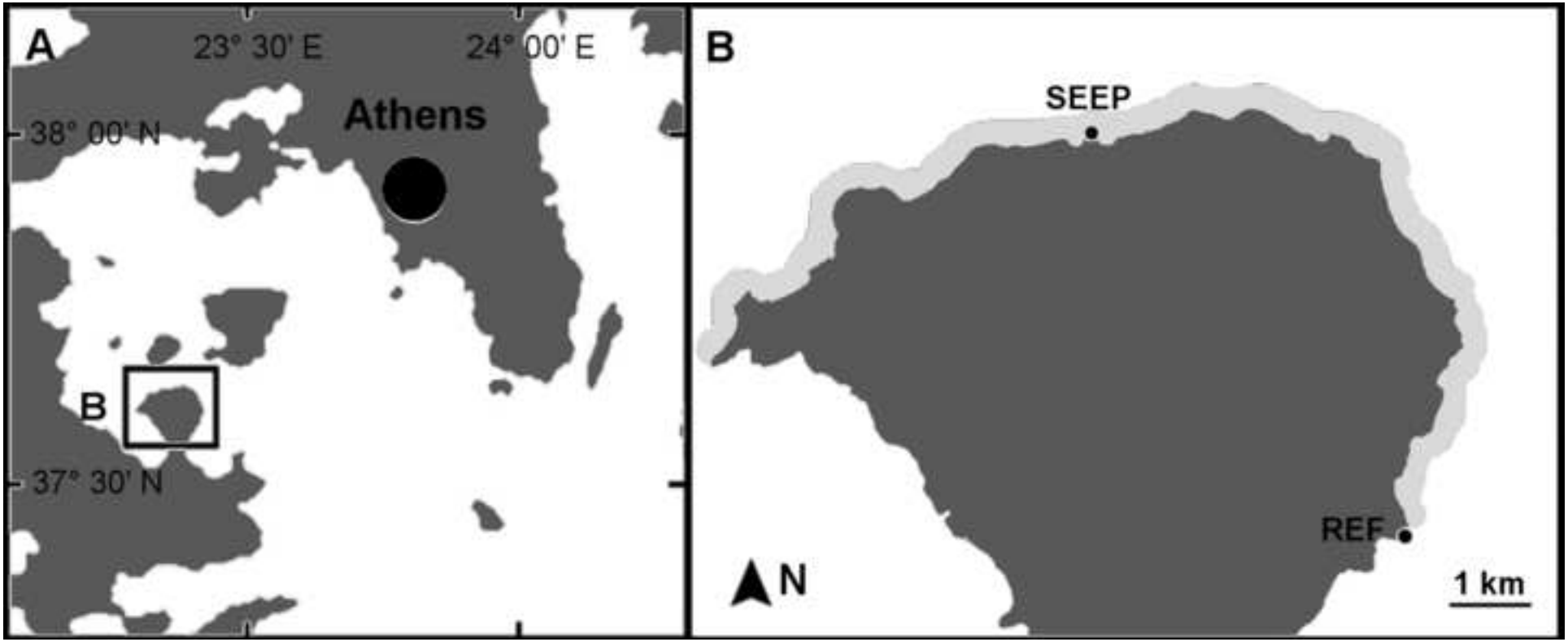

Figure 2
Click here to download high resolution image

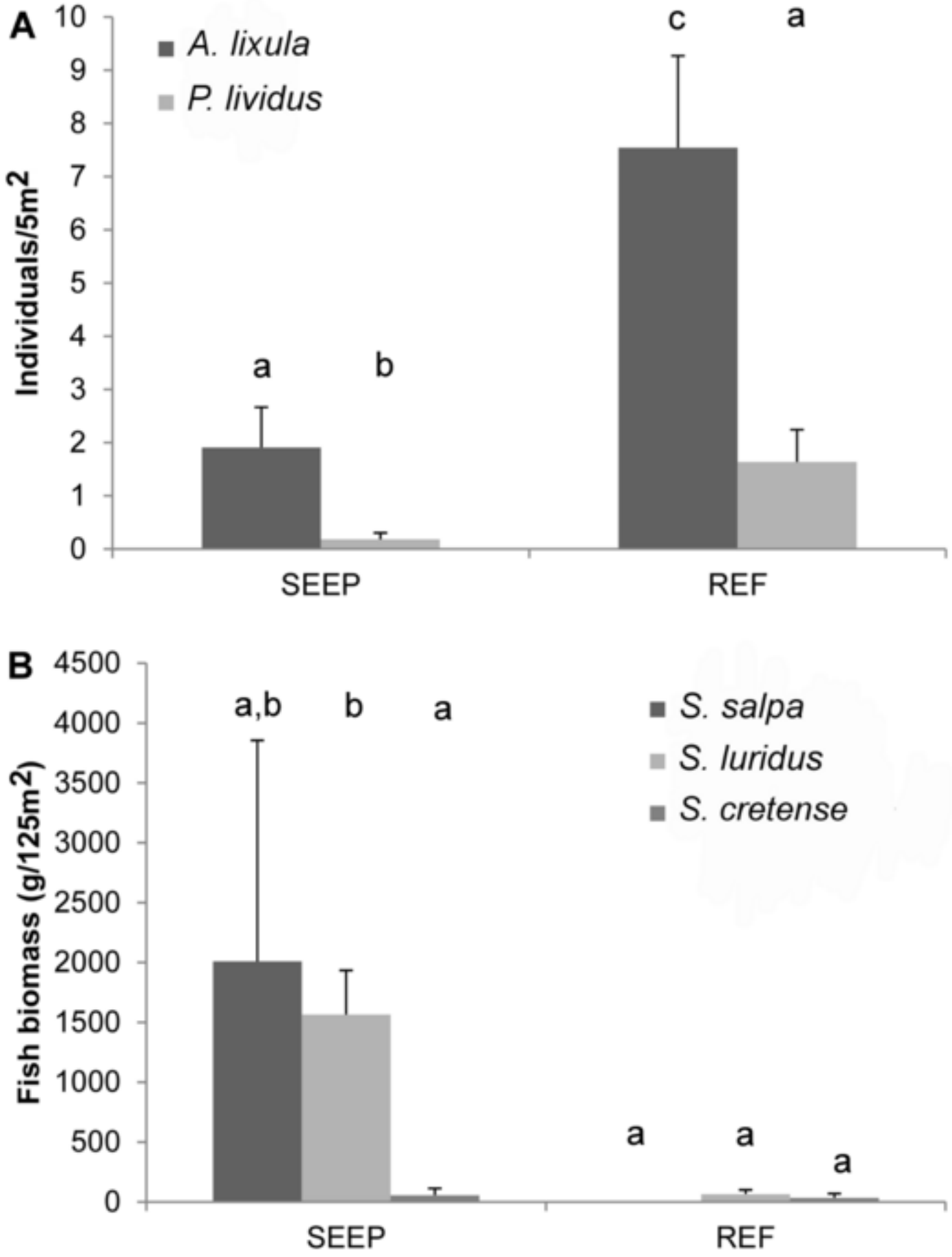

Figure 3
Click here to download high resolution image

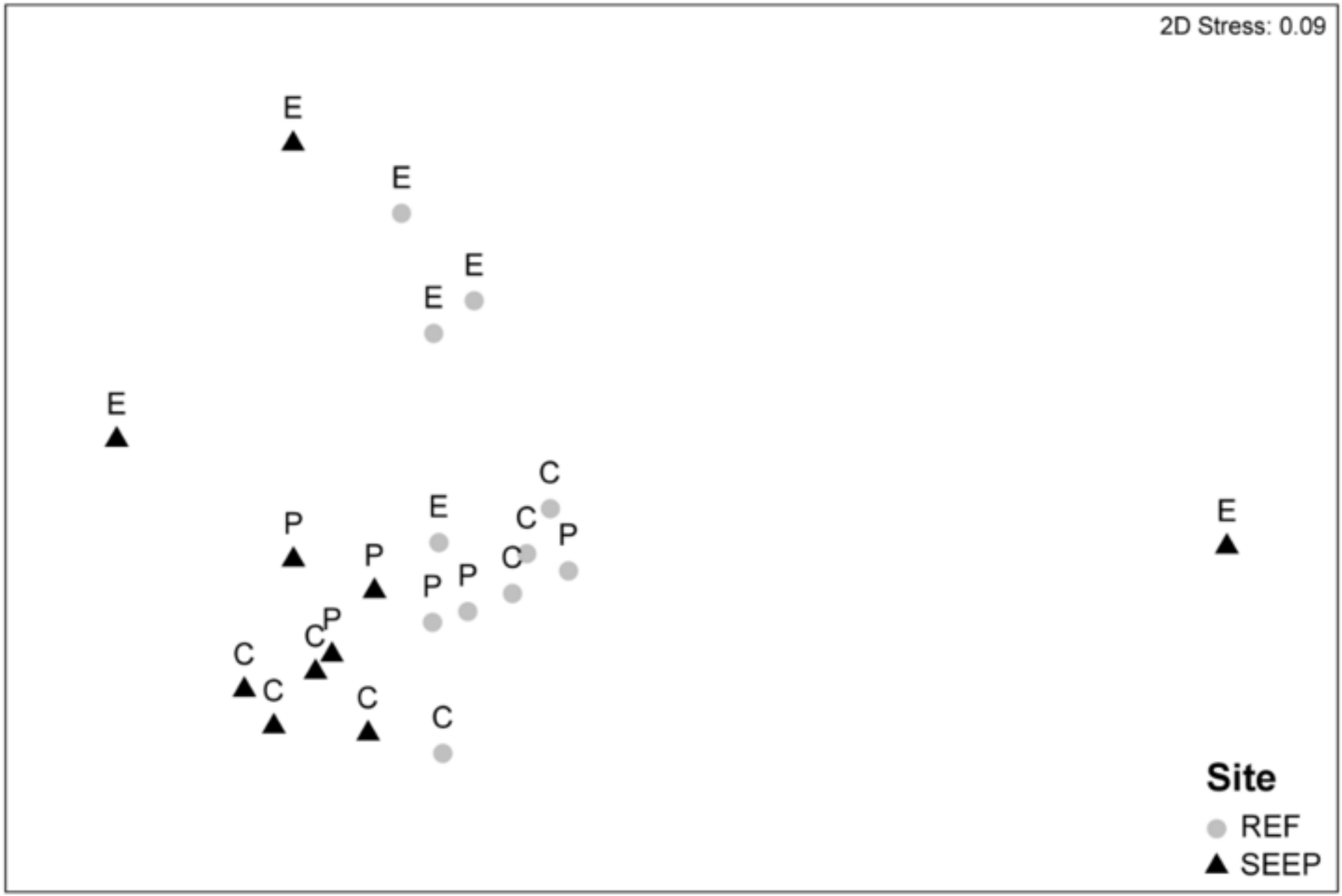

Figure 4
Click here to download high resolution image

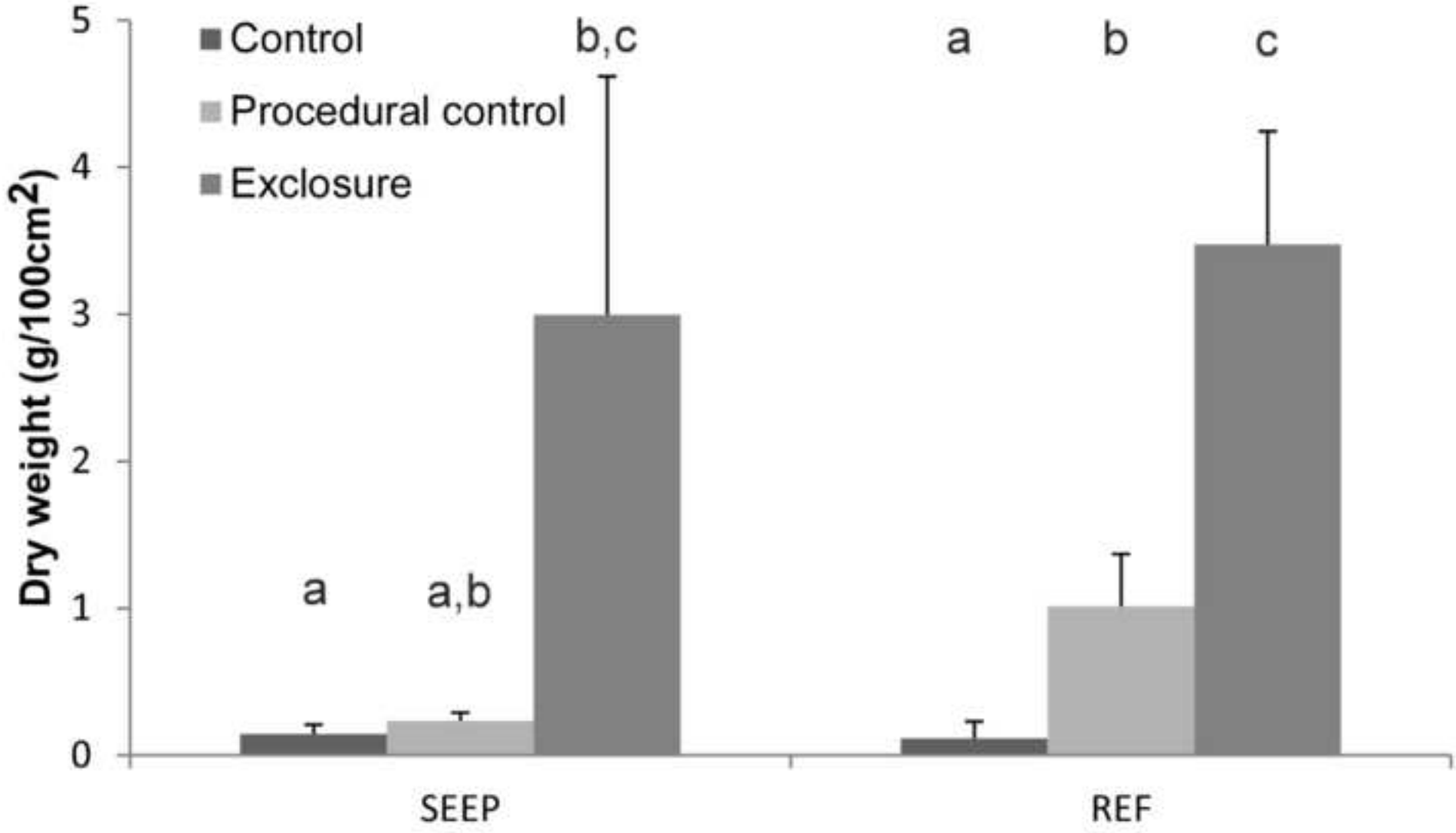

Supplementary Material

Click here to download Supplementary Material: Supplementary material.docx